

Enantioselective Total Syntheses of Acylfulvene, Irofulven, and the Agelastatins

by

Dustin S. Siegel

B.S., Chemistry
University of California, San Diego, 2003

Submitted to the Department of Chemistry
In Partial Fulfillment of the Requirements for the Degree of

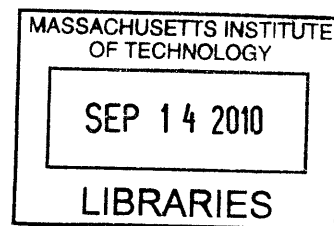
DOCTOR OF PHILOSOPHY
IN ORGANIC CHEMISTRY

at the

Massachusetts Institute of Technology

June 2010

ARCHIVES



© 2010 Massachusetts Institute of Technology
All rights reserved

Signature of Author

Dustin S. Siegel
Department of Chemistry
May 12th, 2010

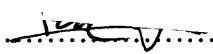
Certified by.....

Mohammad Movassaghi
Professor Mohammad Movassaghi
Associate Professor of Chemistry
Thesis Supervisor

Accepted by.....

Robert W. Field
Professor Robert W. Field
Chairman, Department Committee on Graduate Students

This doctoral thesis has been examined by a committee in the Department of Chemistry as follows:

Professor Rick L. Danheiser..........
Chairman

Professor Mohammad Movassaghi..........
Thesis Supervisor

Professor Gregory C. Fu.....
.....

To my parents, Phil and Nancy Siegel

To my twin sister, Emily Siegel

Acknowledgements

First, I would like to thank my advisor Professor Mohammad Movassaghi. It has truly been a privilege and an honor for me to work under his guidance. His passion and dedication for chemistry are inspirational. His leadership and counsel have been instrumental in my pursuit of excellence as a scientist. It gives me great delight to have been a part of his group. I would also like to thank my thesis committee, Professors Rick Danheiser and Greg Fu, for their thoughtful discussions. Furthermore, I am thankful for my experiences as a teaching assistant with Professors Steve Buchwald and Sarah O'Connor.

I have enormous gratitude for my colleagues with whom I have had the pleasure of working alongside over the years. I would especially like to thank Sunkyu Han, whom I collaborated with on the agelastatin project. His cheer, goodwill, and friendship have carried me through many challenging times. I would also like to thank my collaborators on the irofulven project, Dr. Grazia Piizzi and Dr. Giovanni Piersanti. Furthermore, I am indebted to all the members of the Movassaghi group. I give special thanks to Meiliana Tjandra, who started her graduate career alongside me, to Mike Schmidt for the shared meals and friendship, to Justin Kim for his friendship and thought provoking discussions, and to James Ashenhurst, Alison Ondrus, Umit Kaniskan, Fan Liu, and Jon Medley for their friendship as well. I would also like to express my appreciation for my good friend Matt Hill not only for his support over the years, but also for the many good times we have shared together.

Those individuals who have enriched my life outside of MIT also deserve special recognition. I am greatly indebted to Professor Clifford Kubiak, Professor Michael VanNieuwenhze, and John Stires, for their support and guidance at UCSD. I will always have fond memories of the improvisational jam sessions with Erik Willecke and Brian Arnold, the frigid northeastern surf sessions with Soren Harrison and Adam Swenson, and the wine tasting adventures with Kate and Matt Copeland, Aaron Van Dyke, and Victor Gehling. I would also like to acknowledge my roommates James Poplaski and Jenna Barrows who have uplifted my life at home.

I have the greatest thanks and praise for my family. Included in this list is Rory Spence, whose friendship I have cherished throughout my life, and who is like a brother to me. I greatly appreciate my relatives Mike, Kristy, Dave, Connor, and Peter Phillips for their visitations, and for the enormous amount of support they and the rest of the Phillips family have provided over the years. Finally, I would most of all like to thank my parents, Phil and Nancy, and my sister, Emily. I am extremely blessed and proud to have such a loving and close family. They have instilled in me the values that have made these studies possible, and I am honored to dedicate this work to them.

Preface

Portions of this work have been adapted from the following articles that were co-written by the author and are reproduced in part with permission from:

Movassaghi, M.; Piizzi, G.; Siegel, D. S.; Piersanti, G. "Enantioselective Total Synthesis of (-)-Acylfulvene and (-)-Irofulven." *Angew. Chem. Int. Ed.* **2006**, *45*, 5859-5863. Copyright 2006 Wiley-VCH Verlag GmbH & Co. KgaA.

Movassaghi, M.; Piizzi, G.; Siegel, D. S.; Piersanti, G. "Observations in the Synthesis of the Core of the Antitumor Illudins via an Enyne Ring Closing Metathesis Cascade." *Tetrahedron Lett.* **2009**, *50*, 5489-5492. Copyright 2009 Elsevier Limited.

Siegel, D. S.; Piizzi, G.; Piersanti, G.; Movassaghi, M. "Enantioselective Total Synthesis of (-)-Acylfulvene and (-)-Irofulven." *J. Org. Chem.* **2009**, *74*, 9292-9304. Copyright 2009 American Chemical Society.

Enantioselective Total Syntheses of Acylfulvene, Irofulven, and the Agelastatins

by

Dustin S. Siegel

Submitted to the Department of Chemistry
on May 12th, 2010 in Partial Fulfillment of the
Requirements for the Degree of Doctor of Philosophy in
Organic Chemistry

ABSTRACT

I. Enantioselective Total Synthesis of (–)-Acylfulvene, and (–)-Irofulven

We report the enantioselective total synthesis of (–)-acylfulvene and (–)-irofulven, which features metathesis reactions for the rapid assembly of the molecular framework of these antitumor agents. We discuss (1) the application of an Evans Cu-catalyzed aldol addition reaction using a strained cyclopropyl ketene thioacetal, (2) an efficient enyne ring-closing metathesis cascade reaction in a challenging setting, (3) the reagent, IPNBSH, for a late stage reductive allylic transposition reaction, and (4) the final ring-closing metathesis/dehydrogenation sequence for the formation of (–)-acylfulvene and (–)-irofulven.

II. Total Synthesis of the (–)-Agelastatin Alkaloids

The pyrrole-imidazole super-family of marine alkaloids, derived from linear clathrodin-like precursors, constitutes a diverse array of structurally complex natural products. The bioactive agelastatins are members of this family that have a tetracyclic molecular framework incorporating C4–C8 and C7–N12 bond connectivities. We provide a hypothesis for the formation of the unique agelastatin architecture that maximally exploits the intrinsic chemistry of plausible biosynthetic precursors. We report the concise enantioselective total syntheses of the agelastatin alkaloids, including the first total syntheses of agelastatins C and E. Our gram-scale chemical synthesis of agelastatin A was inspired by our hypothesis for the biogenesis of the cyclopentane C-ring and required the development of new transformations including an imidazolone-forming annulation reaction and a carbohydroxylative trapping of imidazolones.

Thesis Supervisor: Professor Mohammad Movassaghi
Title: Associate Professor of Chemistry

Table of Contents

I. Enantioselective Total Synthesis of (-)-Acylfulvene, and (-)-Irofulven

Introduction and Background	12
Review of Prior Enantioselective Syntheses of Acylfulvene and Irofulven	14
Results and Discussion	17
Synthesis of the Key Aldehyde Intermediate	18
Evaluation of the Enyne Ring-Closing Metathesis Cascade Reaction	25
Completion of the Synthesis of (-)-Acylfulvene and (-)-Irofulven	29
Conclusion	32
Experimental Section	39

II. Total Synthesis of the (-)-Agelastatin Alkaloids

Introduction and Background	76
Review of Prior Syntheses of the Agelastatin Alkaloids	78
Results and Discussion	85
Conclusion	92
Experimental Section	97

Appendix A: Spectra for Chapter I	143
--	-----

Appendix B: Spectra for Chapter II	215
---	-----

Curriculum Vitae	284
-------------------------	-----

Abbreviations

Å	angstrom
[α]	specific rotation
Ac	acetyl
Ad-mix α	reagent mixture for Sharpless' asymmetric dihydroxylation
Anis	anisaldehyde
app	apparent
aq	aqueous
AQN	anthraquinone
atm	atmosphere
Boc	<i>tert</i> -butyloxycarbonyl
Box	bisoxazoline
br	broad
Bn	benzyl
Bu	butyl
°C	degree Celsius
<i>c</i>	cyclo
CAM	ceric ammonium molybdate
cat.	catalytic
CBS	Corey-Bakashi-Shibata
cm	centimeter
cm ⁻¹	wavenumber
COSY	correlation spectroscopy
d	days
d	doublet
<i>d</i>	deuterium
δ	parts per million
DART	direct analysis in real time
DBU	1,8-diazabicyclo[5.4.0]undec-7-ene
DDQ	2,3-dichloro-5,6-dicyanobenzoquinone
DEAD	diethyl azodicarboxylate
DET	diethyl tartrate
DHQD	dihydroquinidine
diam	diameter
DIBAL-H	diisobutylaluminium hydride
DMAP	4-dimethylaminopyridine
DMDO	dimethyldioxirane
DMF	<i>N,N</i> -dimethylformamide
DMP	Dess-Martin periodinane
DMSO	dimethylsulfoxide
DNA	deoxyribonucleic acid
DTBMP	2,6-di- <i>tert</i> -butyl-4-methylpyridine
dr	diastereomeric ratio
ee	enantiomeric excess
EI	electron ionization
equiv	equivalent

ESI	electrospray ionization
Et	ethyl
EYRCM	enyne ring-closing metathesis
FT	Fourier transform
g	gram
G1	Grubbs' 1 st generation catalyst
G2	Grubbs' 2 nd generation catalyst
GC	gas chromatography
h	hour
ht	height
HBTU	<i>O</i> -benzotriazole- <i>N,N,N',N'</i> -tetramethyl-uronium-hexafluoro-phosphate
HMBC	heteronuclear multiple bond correlation
HMDS	hexamethyldisylamide
HPLC	high performance liquid chromatography
HRMS	high resolution mass spectroscopy
HSQC	heteronuclear single quantum correlation
Hx	hexyl
Hz	Hertz
<i>i</i>	iso
IBX	2-iodoxybenzoic acid
IR	infrared
IPNBSH	<i>N</i> -isopropylidene- <i>N'</i> -2-nitrobenzenesulfonyl hydrazine
<i>J</i>	coupling constant
L	liter
LDA	lithium diisopropylamide
LRMS	low resolution mass spectroscopy
m	medium
<i>m</i>	meta
m	multiplet
m	milli
M	molar
μ	micro
<i>m</i> CPBA	<i>meta</i> -chloroperoxybenzoic acid
Me	methyl
Mes	mesityl
MHz	megahertz
min	minute
mol	mole
MS	mass spectrometry
<i>m/z</i>	mass to charge ratio
N	normal
NADP	nicotinamide adenine dinucleotide phosphate
NaHMDS	sodium hexamethyldisylamide
NB	nitrobenzyl
NBS	<i>N</i> -bromosuccinimide
NBSH	<i>ortho</i> -nitrobenzenesulfonylhydrazide

NME	<i>N</i> -methylephedrin
NMM	<i>N</i> -methylnorpholine
NMP	<i>N</i> -methyl-2-pyrrolidone
NMR	nuclear magnetic resonance
nOe	nuclear Overhauser effect
Nuc	nucleophile
<i>o</i>	ortho
<i>p</i>	para
PCC	pyridinium chlorochromate
Ph	phenyl
PMA	phosphomolybdic acid
ppm	parts per million
Pr	propyl
PTSA	<i>para</i> -toluenesulfonic acid
Pybox	2,6-Bis[(4 <i>R</i>)-4-phenyl-2-oxazoliny]pyridine
pyr	pyridine
PYR	pyrimidine
q	quartet
ref	reference
RCM	ring-closing metathesis
<i>R_f</i>	retention factor
RT	room temperature
RuPhos	2-dicyclohexylphosphino-2',6'-di- <i>i</i> -propoxy-1,1'-biphenyl
<i>s</i>	sec
<i>s</i>	singlet
<i>s</i>	strong
SES	2-trimethylsilylethanesulfonyl
SPhos	2-dicyclohexylphosphino-2',6'-dimethoxybiphenyl
str	stretch
<i>t</i>	tert
<i>t</i>	triplet
TBAF	tetra- <i>n</i> -butylammonium fluoride
TBS	<i>tert</i> -butyldimethylsilyl
TC	thiophene-2-carboxylate
Tf	trifluoromethylsulfonate
TFA	trifluoroacetic acid
TFE	trifluoroethanol
THF	tetrahydrofuran
TLC	thin layer chromatography
TMEDA	tetramethylethylenediamine
TMS	trimethyl silyl
Tris	triphenylmethyl
Ts	toluenesulfonic
UV	ultraviolet
w	weak
XPhos	2-dicyclohexylphosphino-2',4',6'-triisopropylbiphenyl

Chapter I.

Enantioselective Total Synthesis of (-)-Acylfulvene and (-)-Irofulven

Introduction and Background

The illudins are a family of highly cytotoxic sesquiterpenes isolated from the bioluminescent mushroom *Omphalotus illudens* (Jack O'Lantern mushroom) and other related fungi.¹ The illudins exhibit a unique tricyclic core featuring a spiro-cyclopropane A-ring and 6,5-fused BC-ring system. Illudin M (**3**) and illudin S (**4**, Figure 1) are among the most cytotoxic members of this family and have been studied extensively for their promising antitumor activity.²

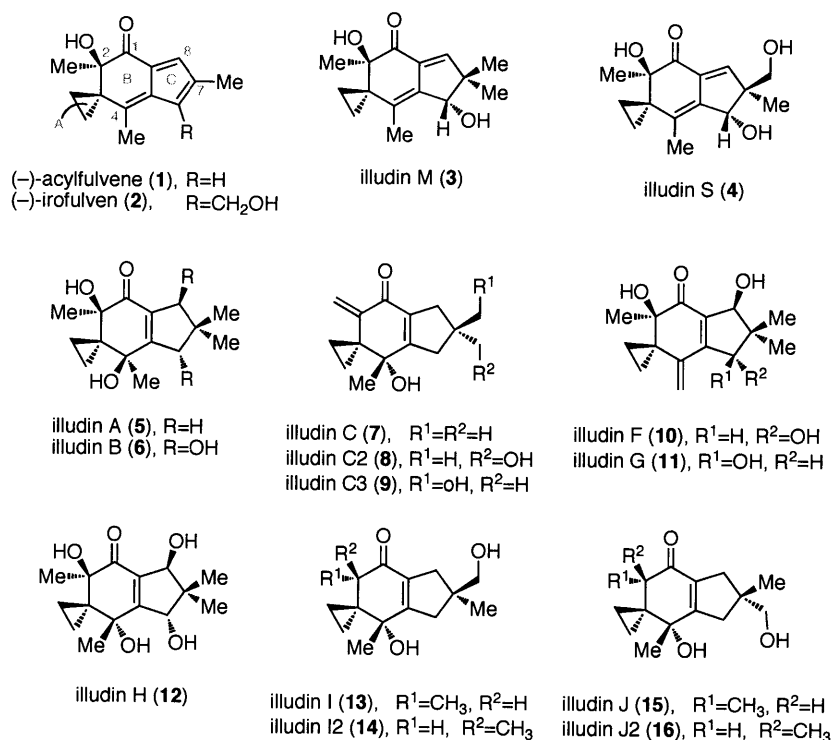
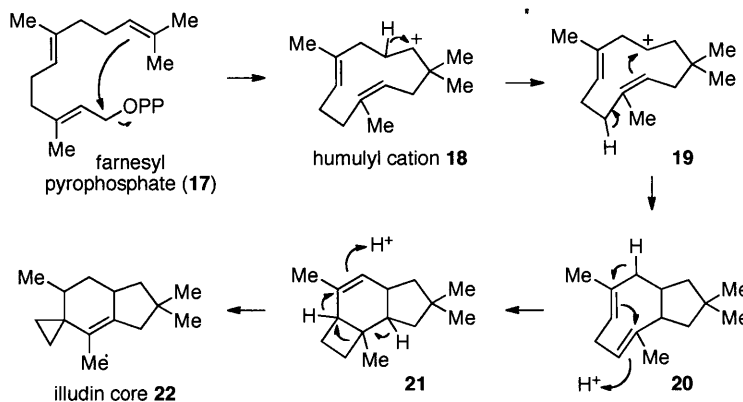


Figure 1. The illudin family of sesquiterpenes.

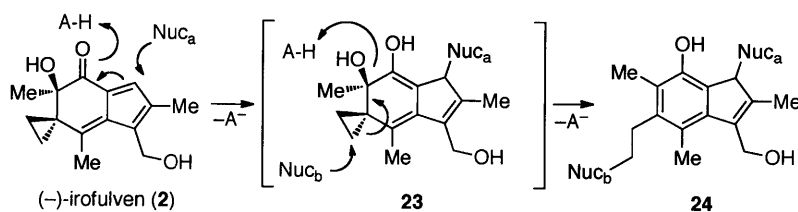
Several studies have been directed at elucidating the biogenesis of the illudin fungal metabolites.³ Feeding studies involving the addition of carbon-13 and deuterium labeled acetate and mevalonate precursors to cultures of the mushroom *Clitocybe illudens* followed by NMR spectroscopic analysis of the radiolabel enrichment in Illudin M (**3**) and illudin S (**4**) revealed that the biosynthetic sequence likely proceeds according to Scheme 1. The fundamental sesquiterpene precursor farnesyl pyrophosphate (**17**) undergoes ionization followed by cyclization to afford humulyl cation **18**. 1,2-Hydride migration followed by cyclopentane ring formation leads to **20**. Protonation followed by cyclization forms the cyclobutane intermediate

21, which then undergoes a 1,2-hydride migration and ring contraction to afford the tricyclic illudin core **22**.



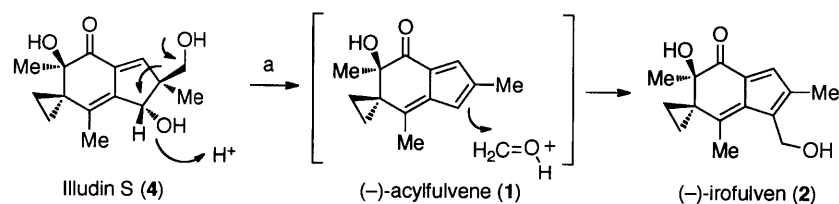
Scheme 1. The biosynthesis of the tricyclic illudin core.

Despite their high cytotoxicity, the natural illudins exhibit low therapeutic indices in solid-tumor systems.⁴ Consequently, several analogs of the natural illudins have been prepared and evaluated for the treatment of various cancers.⁵ Two such semi-synthetic derivatives, (–)-acylfulvene (**1**) and (–)-irofulven (**2**), were prepared from illudin S and have demonstrated greatly enhanced therapeutic potential against several solid tumor systems.⁶ The superior pharmacological properties of (–)-acylfulvene (**1**) and (–)-irofulven (**2**) are accompanied by a markedly lower cytotoxicity than that of illudin S (**4**).⁷ Several studies have been directed toward elucidating the mechanism of biological activity of the illudins, acylfulvene (**1**), and irofulven (**2**) in order to understand the nature of this selective toxicity.⁸ The mechanism is believed to involve an initial activation step by conjugate addition of a hydride (NADPH) or thiol (glutathione or cysteine) nucleophile into the enone moiety followed by nucleophilic addition of DNA to the strained cyclopropane ring to generate a stable aromatic DNA adduct **24** (Scheme 2). The observed onset of apoptosis is believed to be a result of DNA alkylation followed by strand cleavage through this general mechanism. (–)-Irofulven (**2**) is currently undergoing clinical trials for the treatment of various cancers as both a monotherapy and in combination with other chemotherapeutics.⁹ The promising antitumor properties and the highly reactive molecular framework of (–)-irofulven (**2**) and other illudins have rendered them interesting synthetic targets.¹⁰



Scheme 2. Proposed mechanism of biological activity of (-)-irofulven (**2**). Nuc_a = glutathione, cysteine, or hydride (NADPH). Nuc_b = DNA.

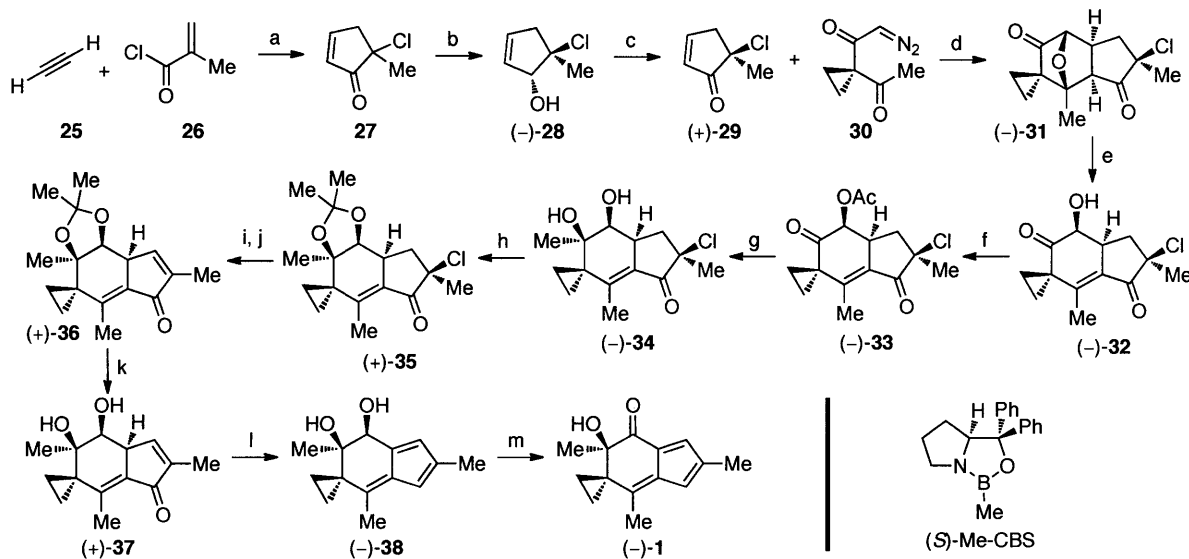
Review of Prior Enantioselective Syntheses of Acylfulvene and Irofulven. (-)-Irofulven (**2**) was initially prepared by McMorris in 1996 via a semi-synthesis from illudin S (**4**), which is readily obtained from fermentation of *Omphalotus illudens* (Scheme 3).⁶ Treatment of illudin S (**4**) with dilute H₂SO₄ in the presence of excess paraformaldehyde afforded (-)-irofulven (**2**) in 38% yield on 353 mg scale along with (-)-acylfulvene (**1**, 17%). Interestingly, (-)-irofulven (**2**) and (-)-acylfulvene (**1**) were shown to be significantly more toxic than their enantiomers, (+)-**2** and (+)-**1** respectively,^{10i,10j} which highlights the importance of establishing efficient enantioselective syntheses of these compounds.



Scheme 3. Semi-synthesis of (-)-acylfulvene (**1**) and (-)-irofulven (**2**). Conditions: a) (CH₂O)_n, H₂SO₄, H₂O, Me₂CO, RT, 72 h, 38%.

In a continuation of his studies of these anticancer agents, McMorris developed the first synthesis of racemic irofulven (**2**) in 1997 via a Padwa carbonyl ylide 1,3-dipolar cycloaddition strategy.^{10f} In 2004, McMorris reported a second generation approach for the enantioselective total synthesis of (-)-irofulven (**2**, Scheme 4).¹⁰ⁱ In this approach, the optically active cyclopentenone (+)-**29** was readily prepared from acetylene (**25**) and methacryloyl chloride (**26**). Treatment of **25** and **26** with aluminum trichloride afforded racemic cyclopentenone **27** via a Nazarov cyclization. The enantiomers of cyclopentenone **27** were resolved through a reduction with BH₃•THF in the presence of catalytic (*S*)-2-methyl-CBS-oxazaborolidine ((*S*)-Me-CBS),

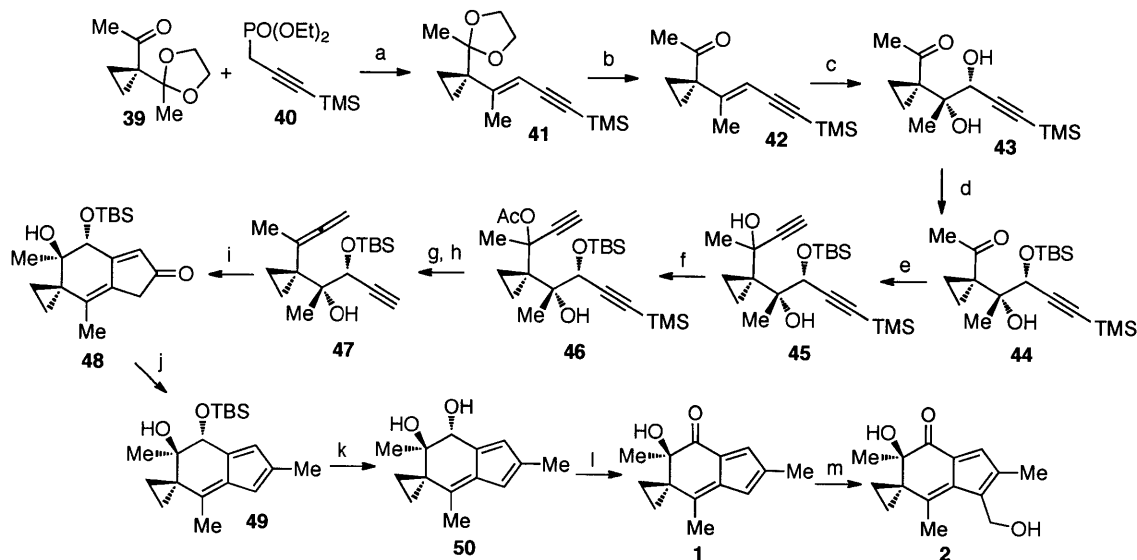
followed by oxidation to afford (+)-5-chloro-5-methyl-2-cyclopentenone (**29**) in 98% ee. The key cycloaddition reaction of (+)-**29** with diazoketone **30** in the presence of catalytic $\text{Rh}_2(\text{OAc})_4$ in refluxing dichloromethane afforded cyclohexane (–)-**31** in 54% yield. Cleavage of the oxo bridge under mild basic conditions followed by acylation and a Grignard addition with methylmagnesium chloride afforded the C2-tertiary alcohol stereocenter (–)-**34**. Ketal formation followed by elimination of the chloride and isomerization of the double bond then afforded the thermodynamically favored cyclopentenone isomer (+)-**36**. After removal of the ketal protecting group, cyclopentenone (+)-**37** was reduced to the fulvene diol (–)-**38** with DIBAL-H in 49% yield. 2-Iodoxybenzoic acid (IBX) oxidation then afforded (–)-acylfulvene (**1**) in 53% yield, which was readily converted to (–)-irofulven (**2**) using their previously reported Prins reaction.⁶



Scheme 4. McMorris' enantioselective synthesis of (–)-acylfulvene (**1**). Conditions: a) AlCl_3 , $(\text{CH}_2\text{Cl}_2)_2$, 35 °C, 8 h, 67%. b) (*S*)-Me-CBS, BH_3 , THF, RT, 5 min, 27%, 98% ee. c) PCC, CH_2Cl_2 , RT, 8 h, 73%. d) $\text{Rh}_2(\text{OAc})_4$, CH_2Cl_2 , Reflux, 1 h, 54%. e) K_2CO_3 , $i\text{PrOH}$, H_2O , RT, 6 h, 70%. f) Ac_2O , pyr, RT, 2 h, 90%. g) MeMgCl , THF, –78 °C, 2 h, 87%. h) 2,2-dimethoxypropane, TsOH, DMF, RT, 24 h, 83%. i) DBU, PhH, RT, 1.5 h. j) $\text{RhCl}_3 \cdot 3\text{H}_2\text{O}$, EtOH, Reflux, 20 min, 62% (2 steps). k) AcOH, H_2O , 90 °C, 2 h, 78%. l) DIBAL-H, CH_2Cl_2 , –78 °C, 30 min, 49%. m) IBX, DMSO, RT, 2 h, 53%.

A formal enantioselective synthesis of irofulven (**2**) was reported by Brummond in 2000 employing a key allenic Pauson-Khand reaction to secure the tricyclic core (Scheme 5).^{10h} Their synthesis commenced with a Horner-Wadsworth-Emmons reaction involving the treatment of ketone **39**, available in two steps from commercial material, with diethyl 3-trimethylsilylpropynyl phosphate (**40**) to selectively afford the *E*-enyne **41** in 86% yield. The

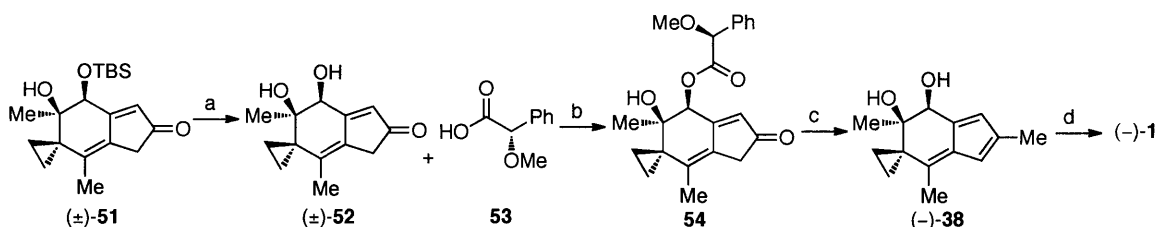
C2-stereocenter was then generated via a Sharpless dihydroxylation to afford diol **43** in 49% yield and >95% ee. Selective silylation of the propargylic alcohol afforded **44** in 76% yield and furnished a formal enantioselective synthesis of (–)-irofulven (**2**). Using racemic material, they prepared the key intermediate **47** via acetylide addition to the ketone, acylation, and allene formation. Their key Pauson-Khand reaction was then carried out via treatment of the alkynyl allene **47** with Mo(CO)₆ in dimethylsulfoxide (DMSO) and toluene at 110 °C to afford tricycle **48** in 69% yield. Methyl lithium addition to the ketone in the presence of cerium trichloride followed by dehydration then afforded **49** in 96% yield. Their synthesis of (–)-irofulven (**2**) was then completed through desilylation, Dess-Martin periodinane (DMP) oxidation, and treatment with formaldehyde in the presence of acid. Notably, this formal enantioselective synthesis was validated by Sturla in 2006, who prepared optically enriched samples of (–)-acylfulvene (**1**) and (–)-irofulven (**2**) via this strategy.^{10j}



Scheme 5. Brummond's formal enantioselective synthesis of (–)-irofulven (**2**) validated by Sturla. Conditions: a) NaHMDS, THF, –78 °C, 86%. b) PTSA, acetone, H₂O, 95%. c) (DHQD)₂PYR, K₂OsO₂(OH)₄, K₃F₃(CN)₆, K₂CO₃, CH₃SO₂NH₂, *t*-BuOH, H₂O, 49%, >95% ee. d) TBSOTf, 2,6-lutidine, CH₂Cl₂, 76%. e) HCCMgBr, CeCl₃, 97% f) Ac₂O, DMAP, Et₃N, 98%. g) [(PPh₃)CuH]₆, 54%. h) K₂CO₃, CH₃OH, H₂O, 95%. i) Mo(CO)₆, DMSO, PhMe, 110 °C, 10 min, 69%. j) MeLi (10 eq), CeCl₃; 0.1 M HCl, 96%. k) TBAF, 97%. l) DMP, 78%. m) H₂CO, H₂SO₄, acetone, H₂O, 68%.

In addition to validating the formal enantioselective synthesis of (–)-irofulven (**2**) via the strategy reported by Brummond (vide supra, Scheme 5), Sturla also developed a chiral-resolution method for the preparation of these compounds in optically enriched form.^{10j} This strategy utilized racemic cyclopentenone (±)-**51**, which was prepared according to Brummond's asymmetric synthesis of **2** (Scheme 6).^{10g} Removal of the silyl protecting group furnished *cis*-diol

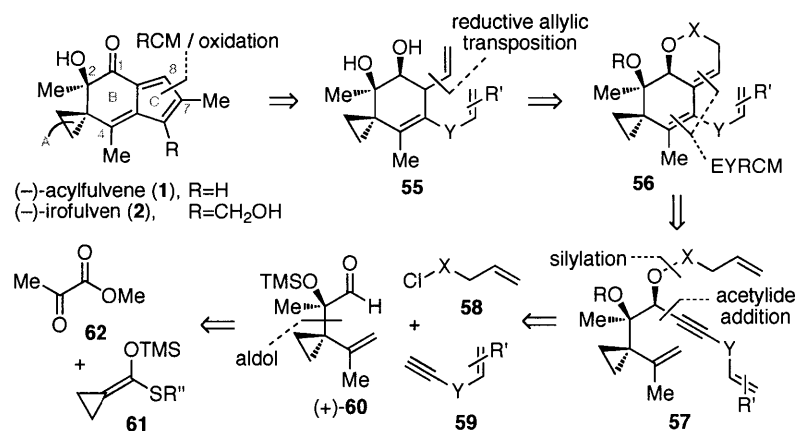
(±)-**52** that was coupled to chiral acid **53**. The two diastereomers of ester **54** were resolved by preparative HPLC to afford samples of **54** in >98 % ee. Treatment of the optically enriched ester **54** with methyllithium and cerium trichloride in THF then afforded the fulvene diol (–)-**38** in 90%, which was readily converted to (–)-acylfulvene (**1**) through IBX oxidation in 88% yield.



Scheme 6. Sturla's chiral resolution strategy. Conditions: a) TBAF, THF, 97%. b) HBTU, DMAP, Et₃N, THF, 70%. c) CeCl₃, MeLi, THF, 90%. d) IBX, DMSO, 88%.

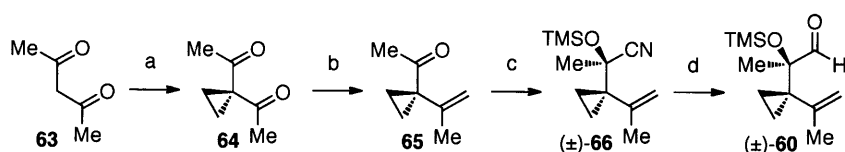
Results and Discussion

The promising antitumor properties and the interesting molecular architecture of (–)-acylfulvene (**1**) and (–)-irofulven (**2**) have rendered them interesting synthetic targets to us. We have disclosed the concise enantioselective syntheses of (–)-acylfulvene (**1**) and (–)-irofulven (**2**) and related derivatives.¹¹ Key features of our approach include a stereoselective aldol addition of a strained ketene hemithioacetal **61**, which secures the C2-stereocenter and enables ready access to aldehyde (+)-**60** (Scheme 7). A key enyne ring-closing metathesis (EYRCM)¹² cascade reaction of trienene **57** generates the B-ring **56**. A reductive allylic transposition then sets the stage for the final ring-closing olefin metathesis (RCM) to build the C-ring and complete the syntheses of (–)-acylfulvene (**1**) and (–)-irofulven (**2**). Herein, we describe the development of our synthetic strategy to these fascinating molecules.



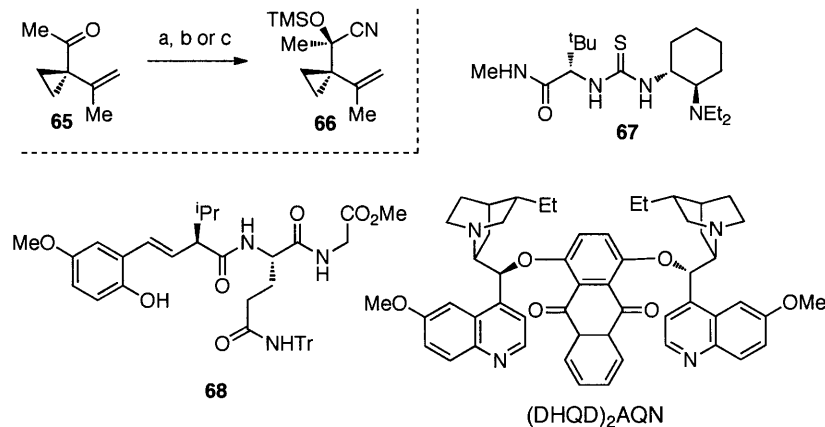
Scheme 7. Retrosynthetic analysis of (–)-acylfulvene (**1**) and (–)-irofulven (**2**).

Synthesis of the Key Aldehyde Intermediate. Since aldehyde **60** contains the reactive cyclopropane and tertiary alcohol substructure common to acylfulvene (**1**), irofulven (**2**), and most members of the illudin family, its efficient synthesis was of critical importance.¹³ Initially, we developed a synthetic route that enabled us to rapidly generate large quantities of racemic aldehyde **60** for evaluation of our synthetic strategy (Scheme 8). This route involved treatment of pentane-2,4-dione (**63**) with 1,2-dibromoethane and potassium carbonate in DMSO to afford cyclopropyl diketone **64** in 61% yield. Mono-olefination using the Wittig reaction afforded intermediate **65** in 56% yield. Silylcyanation with stoichiometric trimethylsilyl cyanide (TMSCN) in the presence of catalytic InBr₃¹⁴ then afforded cyanohydrin **66** in 81% yield, and DIBAL-H reduction afforded racemic aldehyde **60** in multi-gram quantities.



Scheme 8. Synthesis of aldehyde (±)-**60**. Conditions: a) (CH₂Br)₂, K₂CO₃, DMSO, 61%. b) MePh₃PBr, ^tBuOK, Et₂O, 56%. c) TMSCN, InBr₃ (5 mol%), CH₂Cl₂, 81%. d) DIBAL-H, Et₂O, -78 °C, 69%.

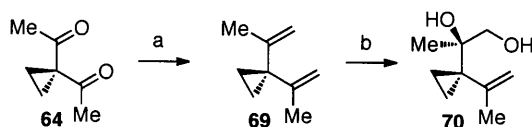
The enantioselective total synthesis of the target compounds, (–)-**1** and (–)-**2**, required an enantioselective synthesis of aldehyde **60**. Initially, we considered an asymmetric silylcyanation strategy to generate the tertiary alcohol stereocenter (Scheme 9) based on the route to racemic aldehyde **60**. Examination of Jacobsen's thiourea catalyst **67**¹⁵ provided the desired optically enriched cyanohydrin **66**; however, the conversion and level of stereoselection with ketone **65** was non-ideal (50 h, 13%, 53% ee).¹⁶ Furthermore, the selectivity was detrimentally affected by the long reaction times that were required for full conversion of the starting material (8 d, 71%, 34% ee). The use of ketone **65** as a substrate with Hoveyda's catalyst **68**¹⁷ in the presence of Al(O^{*i*}Pr)₃ and Ph₃PO afforded the desired compound in good yields (79%), but unfortunately without enantioselection.¹⁶ Likewise, the use of Deng's silylcyanation reaction conditions¹⁸ employing a cinchona alkaloid based catalyst ((DHQD)₂AQN) also proved problematic, highlighting the challenge in developing a solution strictly based on the proven route to racemic **60**.



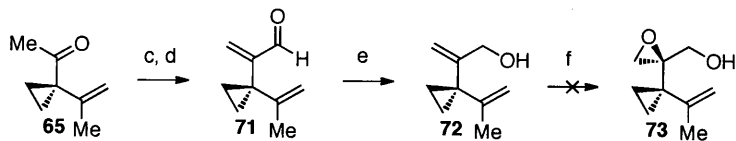
Scheme 9. Attempted asymmetric silylcyanation reactions with ketone **65**. Conditions: a) TMSCN, **67**, TFE, CH₂Cl₂, 50 h, 13%, 53% ee; 8 d, 71%, 34% ee.¹⁶ b) TMSCN, Al(OⁱPr)₃, **68**, MeOH, PhMe, 3Å MS, 79%, 0% ee.¹⁶ c) TMSCN, (DHQD)₂AQN, CH₂Cl₂, 7 d, 11%, 0% ee.

We investigated several asymmetric oxidation reactions as a means of accessing the tertiary alcohol stereocenter including a Sharpless dihydroxylation, a Sharpless epoxidation, and a substrate directed epoxidation relying on a stereocenter set by a Carreira alkylation reaction (Scheme 10). Double olefination of diketone **64** afforded the volatile diene **69**, which was subjected to Sharpless' dihydroxylation conditions.¹⁹ While the desired diol **70** was generated in 50% yield, the diene **69** proved to be a poor substrate for enantioselective dihydroxylation.¹⁶ We proceeded to explore the Sharpless asymmetric epoxidation²⁰ reaction with alcohol **72**, which was prepared from ketone **65** through a Shapiro reaction with dimethylformamide (DMF) followed by a Luche reduction. Unfortunately, the Sharpless epoxidation of diene **72** provided a complex mixture of products likely resulting from the oxidation of the undesired olefin. Also, an alternative synthesis of racemic **73** highlighted its undesired propensity to undergo a Lewis acid catalyzed rearrangement to aldehyde **71**. An approach based on asymmetric alkylation of aldehyde **71** followed by substrate directed epoxidation also did not provide the desired C2-stereocenter.²¹ While Carreira's alkylation reaction provided the desired product **74** with excellent stereoselectivity (99% ee) using superstoichiometric Zn(OTf)₂ and *N*-methylephedrine (NME), the subsequent epoxidation of the allylic alcohol **74** using *meta*-chloroperbenzoic acid (*m*CPBA) resulted in the formation of a complex mixture of products. Since oxidation reactions aimed at forming the stereocenter adjacent to the cyclopropane proved to be problematic, we pursued an alternative route.

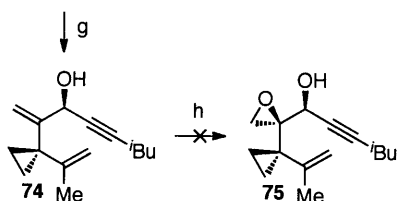
Sharpless' Asymmetric Dihydroxylation



Sharpless' Asymmetric Epoxidation

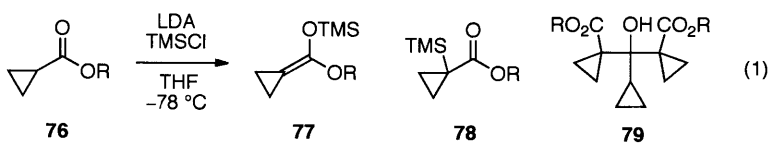


Carreira's Asymmetric Alkylation and directed epoxidation.

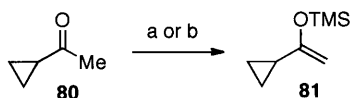


Scheme 10. Asymmetric oxidation approaches to secure the tertiary alcohol stereocenter. Conditions: a) MePh_3PBr , $t\text{BuOK}$, Et_2O , 8%. b) AD-mix α , MeSO_2NH_2 , $t\text{BuOH}$, H_2O , 50%, 0% ee.¹⁶ c) TrisNHNH_2 , cat. TsOH , MeCN , 73%. d) $t\text{BuLi}$, TMEDA , hexanes; DMF , 86%. e) NaBH_4 , CeCl_3 , CH_2Cl_2 , MeOH , 75%. f) $\text{Ti}(\text{O}^i\text{Pr})_4$, (-)-DET, $t\text{BuOOH}$, CH_2Cl_2 . g) HCC^tBu , $\text{Zn}(\text{OTf})_2$, (-)-NME, Et_3N , PhMe , 25%, 99% ee. h) *m*CPBA, CH_2Cl_2 .

We sought to use Evans' copper catalyzed aldol reaction for the formation of the desired tertiary alcohol stereocenter,²² in which we needed to generate a highly strained cyclopropyl ketene hemithioacetal nucleophile **61** (vide supra, Scheme 7). Initial studies by Ainsworth and coworkers aimed at generating the *O*-silylated cyclopropyl ketene acetal **77** revealed that formation of this strained exocyclic double bond was problematic. They reported that the product **77** was generated in at most 10% yield ($\text{R} = \text{Me}$, Equation 1).²³ Instead, the *C*-silylated product **78** was formed as the major product (40%, $\text{R} = \text{Me}$, Equation 1). Following this report, Pinnick and coworkers observed the formation of trimer **79** in addition to the *C*- and *O*-silylated products **77** and **78** ($\text{R} = \text{Et}$, Equation 1).²⁴ These cyclopropyl ester enolate anions are generally regarded as pyramidalized carbanion centers rather than the *O*-lithiated planar methylene cyclopropane species.²⁵

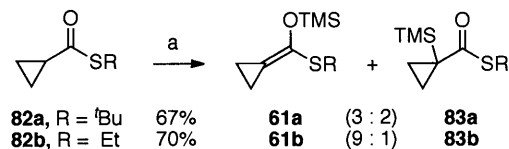


Our studies revealed that enolization of 1-cyclopropylethanone (**80**) at the cyclopropyl carbon is problematic if competing enolization pathways are accessible. Both hard and soft enolization conditions afforded the undesired silyl enol ether **81** exclusively (Scheme 11).²⁶



Scheme 11. Enolization of 1-cyclopropylethanone (**80**). Conditions: a) LDA, TMSCl, THF, $-78\text{ }^{\circ}\text{C}$, 84%. b) TMSOTf, Et₃N, CH₂Cl₂, $-78\text{ }^{\circ}\text{C}$, 87%.

Interestingly, Seebach and coworkers were able to generate a lithium cyclopropanecarbothioate anion from the corresponding thioester and characterize it through X-Ray crystallographic analysis.²⁷ This structure exhibited features characteristic of a normal planar *O*-lithiated enolate, as opposed to a pyramidal *C*-lithiated center. Guided by this observation, we reasoned that the enolate of cyclopropyl thioesters might prefer the formation of the *O*-silylated ketene hemithioacetal rather than the *C*-silylated product. To our delight, the *O*-silylated ketene hemithioacetals **61a** and **61b** were generated as the major products through treatment of cyclopropyl thioesters **82a** and **82b** with lithium diisopropylamide (LDA) and trimethylsilyl chloride (TMSCl) in THF at $-78\text{ }^{\circ}\text{C}$ (Scheme 12). This reaction afforded an inseparable mixture of *O*- and *C*-silylated products **61** and **83**. The highest selectivity was achieved with ethyl thioester **61b** to generate a 9:1 mixture of **61b** and **83b** in 70% yield; whereas, *tert*-butyl thioester **82a** led to a 3:2 mixture of **61a** and **83a** in 67% yield. Fortunately, the undesired *C*-silylated products **83a** and **83b** did not interfere with the planned aldol reaction. The mixture of compounds **61b/83b** (9:1) could be generated on multi-gram scale and could be stored under an argon atmosphere at $-10\text{ }^{\circ}\text{C}$ for greater than a month without any decomposition or *O*- to *C*-silyl transfer. To the best of our knowledge, this is the first example of the formation of a cyclopropyl silylketene hemithioacetal that can be applied in a Mukaiyama aldol reaction.²⁸



Scheme 12. Synthesis of ketene hemithioacetals **61a** and **61b**. Conditions: a) LDA, TMSCl, THF, $-78\text{ }^{\circ}\text{C}$.

Table 1. The use of cyclopropyl ketene hemithioacetal in Evans' asymmetric aldol addition reaction.^a

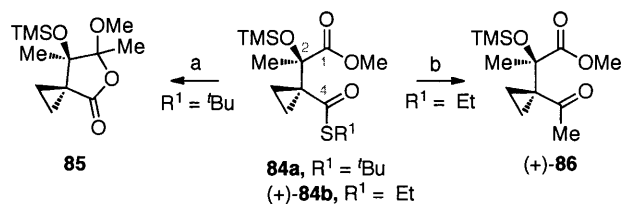
Entry	Substrate	Catalyst	Solvent	Temp (°C)	Time (h)	Yield (%) R ² = TMS : H	% ee
1	61a	Cu(OTf) ₂	CH ₂ Cl ₂	-78	2	- : 51	-
2	61a	<i>R,R</i> -CuPybox	CH ₂ Cl ₂	-78	48	- : 20	0
3 ^b	61a	<i>R,R</i> -CuPybox	CH ₂ Cl ₂	-78	18	- : 19	0
4	61a	<i>S,S</i> -CuBox	CH ₂ Cl ₂	-78	6.5	- : 73	-90
5	61a	<i>S,S</i> -CuBox	CH ₂ Cl ₂	23	2	- : 77	-85
6	61a	<i>S,S</i> -CuBox	THF	-78	2	- : 92	-95
7 ^c	61b	<i>S,S</i> -CuBox	THF	-78	8	71 : 8	-99
8 ^{b,c}	61b	<i>S,S</i> -CuBox	THF	-78	1	76 : 19	-95
9	61b	<i>R,R</i> -CuBox	THF	-78	12	- : 93	93
10 ^c	61b	<i>R,R</i> -CuBox	THF	-78	12	95 : 0	92

^a Reactions were run at [62] = 0.25M, with 10 mol% catalyst loading, and were quenched with TBAF followed by filtration through a plug of silica gel. Enantiomeric excess (ee) was determined by HPLC using a chiralcel AD-H column with the corresponding free alcohol **84** (R² = H) after desilylation. ^b Reactions were run in the presence of TMSOTf (1 equiv). ^c Reactions were directly filtered through a plug of silica gel without TBAF treatment.

Due to the strain associated with the exocyclic double bond, the cyclopropyl ketene hemithioacetals **61a** and **61b** are highly reactive and are excellent substrates for Evans' copper catalyzed aldol reaction²² (Table 1). Under optimal conditions, treatment of silylketene hemithioacetal **61b** (1.1 equiv, mixture of **61b**:**83b** = 9:1) with methyl pyruvate (**62**) in the presence of 10 mol% of (*R,R*)-CuBox²⁹ provided the enantiomerically enriched thioester (+)-**84b** (R² = TMS) in 95% yield and 92% ee (entry 10, Table 1).³⁰ This reaction was performed on large scale to generate a 19.8 gram batch of the desired product (+)-**84b**, and the (*R,R*)-Box ligand was recovered in approximately 85% yield from the reaction mixture. As a part of these studies, we also evaluated the (*R,R*)-CuPybox catalyst, but it proved to be inferior to the CuBox system for this transformation (entries 2 and 3, Table 1). While the *tert*-butyl substrate **61a** was competent

for this transformation under the optimized conditions (entry 6, Table 1), attempts to derivatize the resulting *tert*-butyl thioester **84a** proved to be ineffective (*vide infra*, Scheme 13).

With esters **84a** and (+)-**84b** in hand, we proceeded to derivatize the thioester moiety selectively. Initially, we investigated methyl cuprate addition into the C4-thioester.³¹ Attempts to functionalize *tert*-butyl thioester **84a** proved to be inefficient (Scheme 13). Surprisingly, using a large excess of methyl cuprate (10 equiv), methyl addition occurred exclusively at the C1-methyl ester to afford the lactone **85** in 45% yield. In contrast, addition of one equivalent of methyl cuprate to the more reactive ethyl thioester (+)-**84b** afforded the desired product (+)-**86** in 25% yield. However, this reaction was complicated by significant decomposition of the sensitive cyclopropyl ketone (+)-**86** under the reaction conditions.



Scheme 13. Cuprate addition to the thioesters **84a** and (+)-**84b**. Conditions: a) **84a**, Me₂CuLi (10 equiv), Et₂O, 0 °C, 2 h, 45%. b) (+)-**84b** Me₂CuLi (1 equiv), Et₂O, 23 °C, 30 min, 25%.

We found that the ethyl thioester (+)-**84b** could be efficiently derivatized through a modified Fukuyama cross-coupling protocol.³² Using the reported reaction conditions,^{32a} we obtained the desired product (+)-**86** in 42% yield (entry 1, Table 2). Under these conditions, the reaction suffered from incomplete conversion of the starting material (27% recovered (+)-**84b**) and the instability of the catalyst, which was evident from the precipitation of palladium black over the course of the reaction. We developed the optimal conditions for the substrates of interest by evaluating various ligands, reaction temperatures, and solvents (Table 2). Using the optimal conditions, multi-gram quantities of methyl ketone (+)-**86** were efficiently prepared in 83% yield via the cross-coupling of thioester (+)-**84b** with iodomethylzinc using 2-dicyclohexylphosphino-2',6'-dimethoxy-1,1'-biphenyl (SPhos)^{32b} as a supporting ligand in a 1:1.5 THF:NMP^{32c} solvent mixture (entry 7, Table 2). SPhos proved to be the ideal ligand for this difficult transformation, providing improved stability for the palladium metal center and high overall efficiency.

Table 2. Thioester cross-coupling.^a

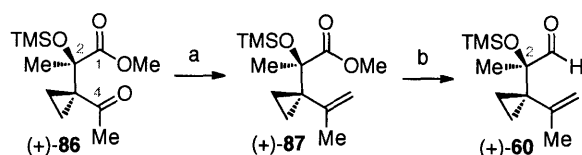
ligand:

SPhos: R¹=OMe, R²=H
 XPhos: R¹=R²=iPr
 RuPhos: R¹=O*i*Pr, R²=H

Entry	Catalyst	Ligand	Solvent ^b	Temp (°C)	Time (h)	Yield (%)
1	PdCl ₂ (PPh ₃) ₂	-	PhMe	23	11	42
2	PdCl ₂ (PPh ₃) ₂	-	THF, NMP	65	15	66
3	Pd ₂ (dba) ₃	SPhos	PhMe	23	11	0
4	Pd ₂ (dba) ₃	SPhos	THF	23	11	0
5	Pd ₂ (dba) ₃	SPhos	PhMe	65	11	19
6	Pd ₂ (dba) ₃	SPhos	THF	65	11	42
7	Pd₂(dba)₃	SPhos	THF, NMP	65	2	83
8	Pd ₂ (dba) ₃	XPhos	THF, NMP	65	2	70
9	Pd ₂ (dba) ₃	RuPhos	THF, NMP	65	2	66

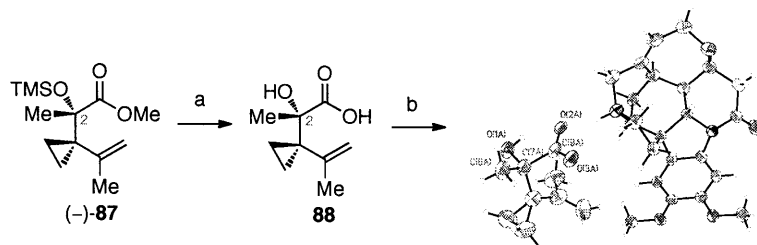
^a Reactions were run with PdL_n (5 mol%), ligand (20 mol%), MeZnI (5 equiv), [(+)-84b] = 0.3M. ^b THF, NMP (1:1.5).

Methylenation of the sensitive and sterically hindered ketone (+)-86 was achieved through a Takai olefination (Scheme 14).³³ Treatment of ketone (+)-86 with CH₂I₂, Zn dust, TiCl₄, and catalytic PbCl₂ afforded olefin (+)-87 in 89% yield.³⁴ The ester (+)-87 was then treated with DIBAL-H to afford a mixture of the desired aldehyde (+)-60 and the corresponding fully reduced primary alcohol (1:2.5 respectively). Without purification, this mixture was immediately oxidized with DMP to give aldehyde (+)-60 exclusively in 91% yield over the two steps.



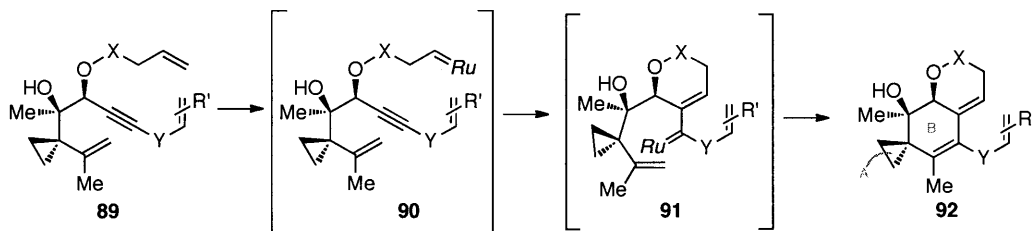
Scheme 14. Synthesis of aldehyde (+)-60. Conditions: a) CH₂I₂, Zn, TiCl₄, PbCl₂, THF, 89%. b) DIBAL-H, Et₂O; DMP, CH₂Cl₂, 91%.

The configuration of C2 in aldehyde (+)-**60** was verified through X-ray crystallographic analysis of a corresponding carboxylate derivative **88** with (-)-brucine (Scheme 15).³⁵ This efficient aldol-based approach for securing the C2-stereochemistry enabled us to generate multi-gram quantities of the key aldehyde (+)-**60**. Notably, aldehyde (+)-**60** possesses a substructure that can be mapped on to most of the illudin sesquiterpenes and provides a platform for the rapid and convergent synthesis of a broad range of derivatives of the functional illudin core structure.¹¹



Scheme 15. Thermal ellipsoid representation of the carboxylic acid **88** salt with (-)-brucine. Conditions: a) LiOH, THF, 82%. b) (-)-brucine.

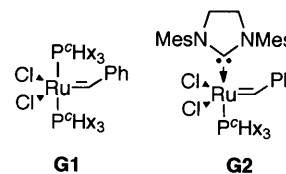
Evaluation of the Enyne Ring-Closing Metathesis Cascade Reaction. The EYRCM sequence described in Scheme 16 represented our planned approach toward the synthesis of the functional AB-ring system common to the illudins. The enyne metathesis between the tethered olefin and the alkyne of **89** would generate a ruthenium alkylidene **90**³⁶ that would undergo a ring-closing olefin metathesis to afford a tetrasubstituted alkene on a highly substituted B-ring **92**.³⁷ We envisioned that elaboration of the functionalized side chain of **92** would potentially allow rapid access to various members of the illudin family.



Scheme 16. Our planned EYRCM cascade for the formation of the AB-ring system.

We evaluated several olefin tethers for the key EYRCM using model substrate **93** in order to identify optimal tethers that were both stable to the EYRCM reaction conditions and

readily removable (Table 3). Both Grubbs' first- and second-generation metathesis catalysts (**G1** and **G2**, respectively)³⁸ were evaluated, with **G2** generally providing the desired product **94** with greater efficiency compared to **G1**. Under optimal EYRCM reaction



conditions, neither the carbonate nor the carbamate tethers (entries 1 and 2, Table 3) provided the desired EYRCM product **94**. Instead, the carbonate tether fragmented to afford the corresponding propargylic alcohol,³⁹ and the Lewis basic carbamate likely reduced the activity of the **G2** metathesis catalyst through an unproductive coordination event.

Table 3. Evaluation of olefin tethers for the EYRCM.

Entry	Tether	Solvent	Temp (°C)	Time	Yield ^a
1		PhH	65	1.5 h	0%
2		PhMe	110	1.5 h	0%
3		PhMe	110	1.5 h	47%
4		PhH	80	6 h	15% ^b
5		PhH	65	30 min	91%
6		PhH	65	3 h	92%

^a Isolated yields. ^b Isolated yield of free amide after TBS deprotection with TBAF.

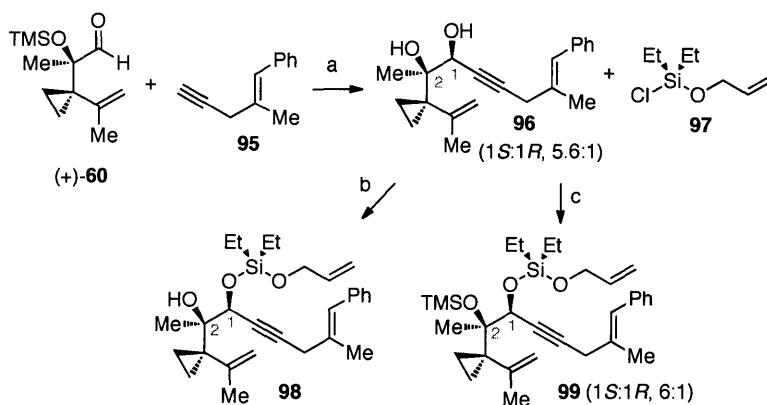
Interestingly, when the cyclohexyl (^cHx) carbamate (entry 3, Table 3) was submitted to the EYRCM conditions, the product **94** was generated in 47% yield. We attribute this enhanced reactivity to the expected substrate preference to adopt the carbamate rotamer that positions the

allyl substituent trans to the carbonyl. In this conformation the olefin is oriented in close proximity to the alkyne and is poised for the ensuing EYRCM with minimal interference by the Lewis basic carbonyl. In light of this, we also prepared the *tert*-butyldimethylsilyl allylamide (entry 4, Table 3), which would enable access to a more hydrolytically labile cyclic-carbonate by treatment with tetra-*n*-butylammonium fluoride (TBAF). However, the tandem EYRCM-TBAF treatment provided the desired product in only 15% yield, due to the lability of the silylcarbamate under the EYRCM conditions.

None of the carbonate or carbamate based tethers proved superior to silicon based olefin tethers examined for this transformation. When the allylsilane tether, first reported by Grubbs and Yao,⁴⁰ was subjected to the EYRCM conditions, the desired product **94** was afforded in 91% yield (entry 5, Table 3) within 30 min. Furthermore, the allyloxysilane tether (entry 6, Table 3)⁴¹ also provided the desired enyne metathesis product in 92% yield, albeit requiring a longer reaction time. Interestingly, in related systems we observed that the diethylallyloxysilane tether (entry 6, Table 3) was optimal as compared to the corresponding dimethyl and diisopropyl variants. The diethylallyloxysilane tether provided the best balance between stability and reactivity. The dimethylallyloxysilane tether was too labile under the EYRCM reactions conditions leading to premature desilylation, while the diisopropylallyloxysilane was both more difficult to prepare due to lower rate of etherification and also gave the desired metathesis products in low yields. Due to the difficulty in elaborating the allylsilane tether to the desired allylic alcohol via oxidation protocols,⁴² we focused on applying the allyloxysilane tethers toward the synthesis of (–)-acylfulvene (**1**) and (–)-irofulven (**2**). This tether would allow for direct access to the stable allylic alcohol product from the EYRCM reaction via *in situ* removal of the tether.

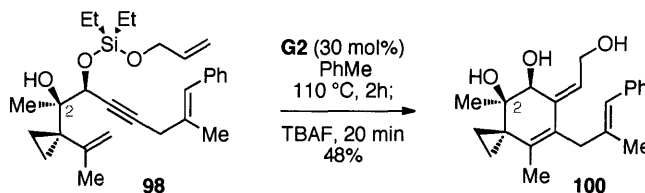
The successful synthesis of (–)-acylfulvene (**1**) and (–)-irofulven (**2**) using the EYRCM strategy began with the rapid assembly of key trienyne **98** and **99** via the coupling of readily available aldehyde (+)-**60**, enyne **95**, and allyloxydiethylchlorosilane⁴³ (**97**, Scheme 17). Addition of the corresponding lithium acetylide of enyne **95** to aldehyde (+)-**60** provided diol **96** (72%) after desilylation of the immediate silyl-migration (C1→C2) product as a mixture of C1-diastereomers (1*S*:1*R*, 5.6:1) favoring the Felkin-Ahn mode of carbonyl addition (Scheme 17). Given the final stage oxidation of the C1-hydroxyl group to the corresponding C1-carbonyl of the target compounds, both diastereomers were moved forward without chromatographic

separation. The diastereomeric mixture of diols **96** were subjected to selective secondary alcohol allyloxydiethylsilylation to afford **98** (65%). Additionally, we developed a one-pot procedure for the formation of the C2-silyl ether substrate **99** in 83% yield directly from **96**, which involved sequential addition of allyloxydiethylchlorosilane (**97**) followed by trimethylsilyl trifluoromethanesulfonate (TMSOTf, Scheme 17).



Scheme 17. Synthesis of the trienyne **98** and **99**. For clarity, only the major diastereomers are shown. Conditions: a) LiHMDS, THF, $-78 \rightarrow 40$ °C; TBAF, AcOH, 72%. b) $(\text{Et})_2\text{Si}(\text{Cl})\text{OCH}_2\text{CH}=\text{CH}_2$, 2,6-lutidine, CH_2Cl_2 , 65%. c) $(\text{Et})_2\text{Si}(\text{Cl})\text{OCH}_2\text{CH}=\text{CH}_2$, 2,6-lutidine, CH_2Cl_2 , -78 °C; TMSOTf, 83%.

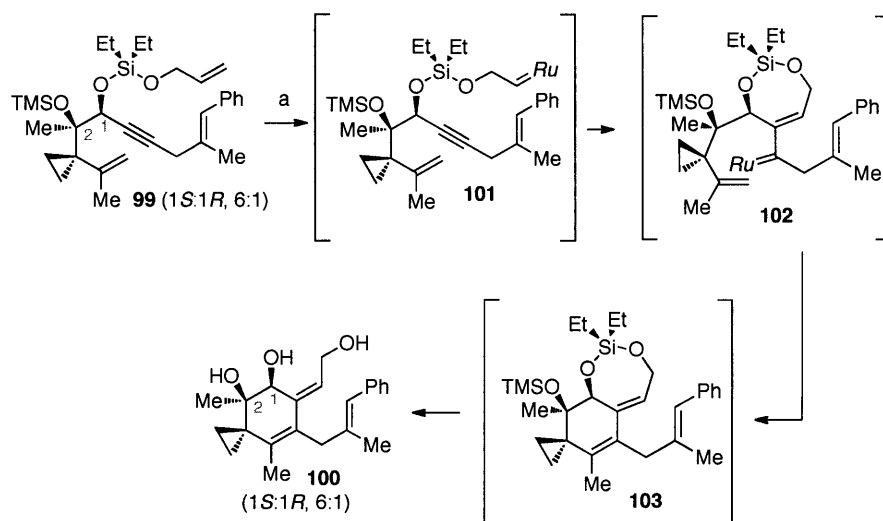
We first evaluated the tandem EYRCM sequence with the C2-hydroxyl substrate **98**; however, this substrate exhibited low efficiency for this transformation. The EYRCM with the C2-hydroxyl trienyne **98** afforded the desired triol in 48% isolated yield, and required a high temperature (110 °C), a long reaction time (2 h), and a high catalyst loading (30 mol%, Scheme 18). We speculated that at high temperature, partial loss of the allyloxydiethylsilyl tether, promoted by the vicinal C2-hydroxyl group, was responsible for the low efficiency of the reaction.



Scheme 18. EYRCM with the C2-hydroxyl substrate **98**. For clarity, only the major diastereomers are shown.

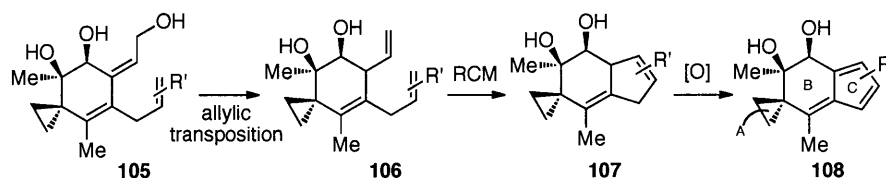
Importantly, the reactivity of the C2-silyl ether substrate **99** was significantly enhanced under the EYRCM conditions and required only 15 mol% catalyst loading of **G2** at 90 °C in only

30 min for the reaction to proceed to full conversion (Scheme 19). In the event, the C2-silyl ether substrate **99**, containing the trisubstituted styrenyl alkene, underwent the EYRCM cascade and desilylation reaction smoothly to afford the desired triol **100** in 74% yield (Scheme 19). Interestingly, we observed no byproducts associated with metathesis of the trisubstituted styrenyl olefin under the EYRCM conditions. Both C1-diastereomers of trienyne **99** were equally effective substrates for this key EYRCM cascade to generate triol **100** (1*S*:1*R*, 6:1). Triol **100** contained all the necessary functional groups and the carbon skeleton needed for completion of the synthesis.



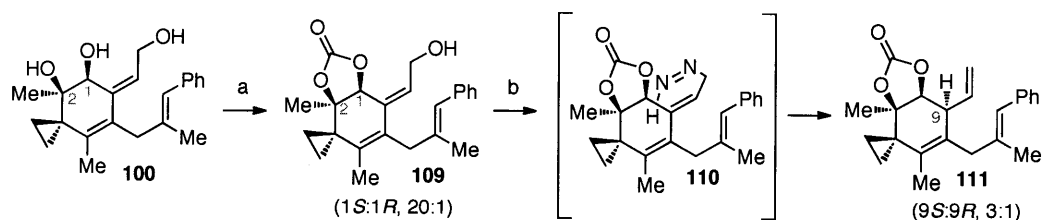
Scheme 19. EYRCM cascade. For clarity, only the major diastereomers are shown. Conditions: a) **G2** (15 mol%), PhMe (0.01M), 90 °C, 30 min; TBAF, AcOH, THF, 23 °C, 10 min, 74%.

Completion of the Synthesis of (–)-Acyfulvene and (–)-Irofulven. Accordingly, we advanced our synthesis based on a reductive allylic transposition strategy (Scheme 20). Through this strategy, alcohol **105** would be elaborated to the terminal olefin **106**, which would then be converted to tricycle **107** via a RCM reaction. Oxidative dehydrogenation would then provide the fulvene **108**.



Scheme 20. Reductive allylic transposition and C-ring synthesis strategy.

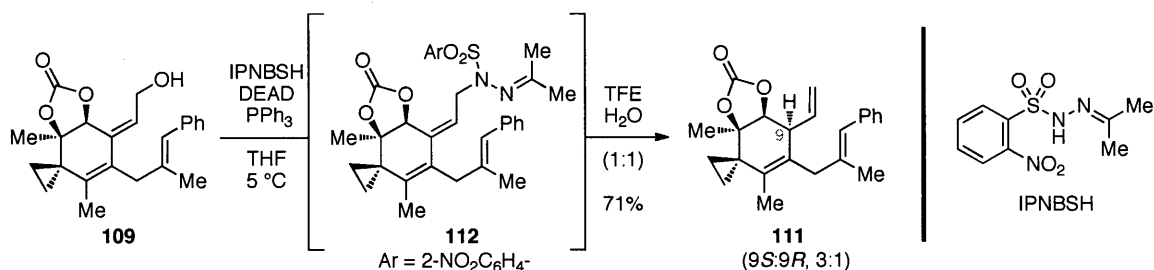
With triol **100** in hand, we evaluated the reductive allylic transposition reaction and RCM reaction for the completion of the synthesis of (-)-acylfulvene (**1**) and (-)-irofulven (**2**). We found it necessary to mask the tertiary and secondary alcohols, and developed a tandem process to generate carbonate **109** (Scheme 21). Monosilylation of allylic alcohol **100** with *tert*-butyldimethylsilyl trifluoromethanesulfonate (TBSOTf, 1 equiv) selectively protected the primary alcohol. Sequential treatment with triphosgene and TBAF afforded the desired carbonate **109** (1*S*:1*R*, 20:1) in 67% yield in a single flask. Enrichment of the major diastereomer was observed as a result of the difficulty in forming the *trans*-fused cyclic carbonate. Substrate **109** was then subjected to Myers' reductive allylic transposition reaction to give the desired triene **111**.⁴⁴ In the event, the Mitsunobu displacement of alcohol **109** with 2-nitrobenzene-sulfonylhydrazide (NBSH) in *N*-methylmorpholine (NMM, -30→23 °C) gave triene **111** (9*S*:9*R*, 3:1) via a sigmatropic loss of dinitrogen from the intermediate monoalkyl diazene **110**. Due to the insolubility of the substrate **109** in the optimal reaction media at low temperature and at high concentration, variable yields of the desired product were obtained (35-54%).



Scheme 21. Synthesis of carbonate **109** and the reductive allylic transposition using NBSH. For clarity, only the major diastereomers are shown. Conditions: a) TBSOTf, 2,6-lutidine, CH₂Cl₂, -78 °C; triphosgene, 23 °C; TBAF, 67%. b) NBSH, DEAD, PMe₃, allylbenzene, NMM, -30 °C, 1 h; 23 °C, 40 min, 47%.

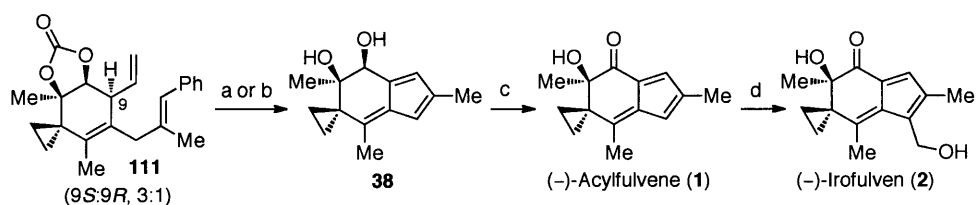
In order to address the complications associated with substrate **109**, we considered the use of a more stable derivative of NBSH that would allow us to carry out the challenging Mitsunobu displacement at higher temperatures and lower solvent concentrations. Thus, the acetone hydrazone derivative, *N*-isopropylidene-*N'*-2-nitrobenzenesulfonyl hydrazine (IPNBSH),⁴⁵ was prepared and used for the reductive allylic transposition of alcohol **109** (Scheme 22). We were pleased to find that the Mitsunobu displacement of alcohol **109** with IPNBSH proceeded smoothly at temperatures between 5-23 °C and at lower concentrations to give the stable hydrazone intermediate **112**. Under optimal conditions, the solvolysis of

hydrazone **112** using 2,2,2-trifluoroethanol (TFE) at 0 °C afforded the desired olefin **111** in 71% yield.



Scheme 22. IPNBSh mediated transposition reaction. For clarity, only the major diastereomers are shown.

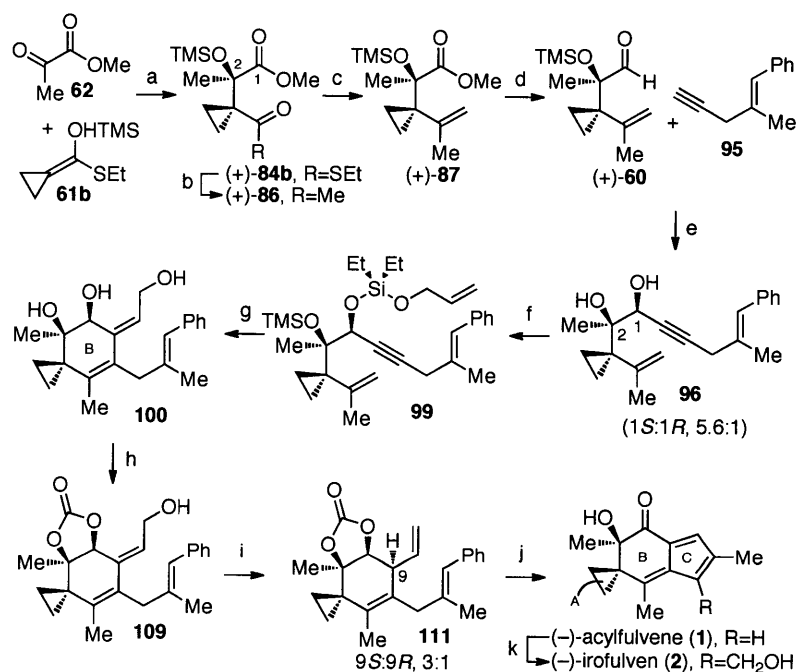
With triene **111** in hand, we focused on the final stages of the synthesis of (–)-acylfulvene (**1**) and (–)-irofulven (**2**). We established a tandem process to include the RCM, hydrolysis, and dehydrogenation in a single flask. Thus, triene **111** was subjected to a three-step sequence involving the RCM, carbonate hydrolysis, and sequential chloranil oxidation to afford the desired diol fulvene **38** directly in 70% yield (Scheme 23). IBX oxidation then afforded (–)-acylfulvene (**1**) in 80% yield. Interestingly, by replacing chloranil with DDQ, a more potent oxidant, triene **111** could be converted directly to (–)-acylfulvene (**1**) in 30% yield without isolation of any intermediates (Scheme 23). Finally, (–)-acylfulvene (**1**) was then elaborated to (–)-irofulven (**2**) in 35% yield⁴⁶ using the protocol described by McMorris and coworkers.⁶ All spectroscopic data for (–)-acylfulvene (**1**) and (–)-irofulven (**2**) matched those reported in the literature.



Scheme 23. Synthesis of (–)-acylfulvene (**1**) and (–)-irofulven (**2**). For clarity, only the major diastereomers are shown. Conditions: a) **111**→(–)-**1**: **G2** (15mol%), PhH, 80 °C, 50 min; NaOMe, MeOH, 23 °C, 18 h; AcOH; DDQ, MeCN, 14 h, 30%. b) **111**→**38**: **G2** (15mol%), PhH, 80 °C, 50 min; NaOMe, MeOH, 23 °C, 18 h; AcOH; chloranil, MeCN, 13 h, 70%. c) IBX, DMSO, 80%. d) H₂SO₄, CH₂O aq., Me₂CO, 4 d, 35%.

Conclusion

We have described the development of our synthesis of two potent antitumor agents (–)-acylfulvene (**1**) and (–)-irofulven (**2**). The optimal sequence is summarized in Scheme 24. The asymmetric copper catalyzed Evans aldol addition reaction with the strained ketene acetal secured the C2-stereocenter of the target compounds. The powerful EYRCM cascade reaction with the allyloxysilane tether was successfully employed for the B-ring construction. The reagent IPNBSH efficiently provided the necessary reductive transposition of an advanced allylic alcohol. Finally, a tandem RCM/dehydrogenation process was employed for the C-ring construction to complete the syntheses of (–)-acylfulvene (**1**) and (–)-irofulven (**2**).



Scheme 24. Summary of the enantioselective total synthesis of (–)-acylfulvene (**1**) and (–)-irofulven (**2**). For clarity, only the major diastereomers of intermediates **96**–**111** are shown. Conditions: a) (*R,R*)-2,2'-isopropylidene-bis(4-*t*-butyl-2-oxazoline), Cu(OTf)₂, THF, –78 °C, 12 h, 95%, 92% ee. b) MeZnI, Pd₂(dba)₃, SPhos, THF, NMP, 65 °C, 2 h, 83%. c) CH₂I₂, TiCl₄, Zn, PbCl₄, CH₂Cl₂, THF, 23 °C, 4 h, 89%. d) DIBAL-H, Et₂O, –78 °C; DMP, CH₂Cl₂, 23 °C, 91%. e) **95**, LiHMDS, THF, –78→–40 °C; TBAF, AcOH, 72%. f) (Et)₂Si(Cl)OCH₂CH=CH₂, 2,6-lutidine, CH₂Cl₂; TMSOTf, –78 °C, 83%. g) **G2** (15 mol%), PhMe, 90 °C, 30 min; TBAF, AcOH, 74%. h) TBSOTf, 2,6-lutidine, CH₂Cl₂, –78 °C; triphosgene; TBAF, 67%. i) IPNBSH, DEAD, Ph₃P, THF, 0→23 °C; TFE, H₂O, 71%. j) **G2** (15 mol%), PhH, 80 °C; NaOMe; AcOH; DDQ (**111**→(–)-**1**, 30%) - or use chloranil to isolate **38** (70%), then IBX, DMSO, 80%. k) H₂SO₄, CH₂O_{aq}, 35%

-
1. Isolation of Illudin M and S: (a) Anchel, M.; Hervey, A.; Robbins, W. J. *Proc. Natl. Acad. Sci. U.S.A.* **1950**, *36*, 300. (b) Anchel, M.; Hervey, A.; Robbins, W. J. *Proc. Natl. Acad. Sci. U.S.A.* **1952**, *38*, 927. (c) Nakanishi, K.; Tada, M.; Yamada, Y.; Ohashi, M.; Komatsu, N.; Terekawa, H. *Nature* **1963**, *197*, 292. (d) McMorris, T. C.; Anchel, M. *J. Am. Chem. Soc.* **1963**, *85*, 831. (e) McMorris, T. C.; Anchel, M. *J. Am. Chem. Soc.* **1965**, *87*, 1594. (f) Nakanishi, K.; Ohashi, M.; Tada, M.; Yamada, Y. *Tetrahedron* **1965**, *21*, 1231. (g) Matsumoto, T.; Shirahama, H.; Ichihara, A.; Fukuoka, Y.; Takahashi, Y.; Mori, Y.; Watanabe, M. *Tetrahedron*, **1965**, *21*, 2671. Isolation of Illudin A and B: (h) Arnone, A.; Cardillo, G.; Nasini, G.; De Rava, O. V. *J. Chem. Soc., Perkin Trans.* **1991**, *1*, 733. Isolation of Illudin C, C2, and C3: (i) Arnone, A.; Cardillo, R.; Modugno, V.; Nasin, G. *Gazz. Chim. Ital.* **1991**, *121*, 345. (j) Lee, I.-K.; Jeong, C. Y.; Cho, S. M.; Yun, B. S.; Kim, Y. S.; Yu, S. H.; Koshino, H.; Yoo, I. D. *J. Antibiot.* **1996**, *49*, 821. Isolation of Illudin F, G, and H: (k) Burgess, M. L.; Zhang, Y. L.; Barrow K. D. *J. Nat. Prod.* **1999**, *62*, 1542. Isolation of Illudin I, I2, J and J2: (l) Reina, M.; Orihuela, J. C.; Gonzales-Coloma, A.; de Ines, C.; de la Crus, M.; Gonzalez del Val, A.; Torno, J. R.; Fraga, B. M. *Phytochemistry*, **2004**, *65*, 381.
 2. Kelner, M. J.; McMorris, T. C.; Beck, W. T.; Zamora, J. M.; Taetle, R. *Cancer Res.* **1987**, *47*, 3186.
 3. (a) Anchel, M.; McMorris, T. C.; Singh, P. *Phytochemistry*, **1970**, *9*, 2339. (b) Hanson, J. R.; Marten, T.; Nyfeler, R. *J. Chem. Soc., Perkin Trans. I* **1976**, 876. (c) Bradshaw, A. P. W.; Hanson, J. R.; Sadler, I. H. *J. Chem. Soc., Perkin Trans. I* **1982**, 2445.
 4. Kelner, M. J.; McMorris, T. C.; Taetle, R. *J. Natl. Cancer Inst.* **1990**, *82*, 1562.
 5. For synthetic studies of illudin derivatives, see: (a) Kinder, F. R.; Wang, R. M.; Bauta, W. E.; Bair, K. W. *Bioorg. Med. Chem. Lett.* **1996**, *6*, 1029. (b) McMorris, T. C.; Yu, J.; Hu, Y. *J. Org. Chem.* **1997**, *62*, 3015. (c) McMorris, T. C.; Yu, J.; Lira, R.; Dawe, R.; MacDonald, J. R.; Waters, S. J.; Estes, L. A.; Kelner, M. J. *J. Org. Chem.* **2001**, *66*, 6158. (d) McMorris, T. C.; Cong, Q.; Kelner, M. J. *J. Org. Chem.* **2003**, *68*, 9648. (e) Pirrung, M. C.; Liu, H. *Org. Lett.* **2003**, *5*, 1983. (f) Gregerson, L. N.; McMorris, T. C.; Siegel, J. S.; Baldrige, K. K. *Helv. Chim. Acta* **2003**, *86*, 4133.
 6. McMorris, T. C.; Kelner, M. J.; Wang, W.; Yu, J.; Estes, L. A.; Taetle, R. *J. Nat. Prod.* **1996**, *59*, 896.

-
7. Woynarowsky, J. M.; Napier, C.; Koester, S. K.; Chen, S.-F.; Troyer, D.; Chapman, W.; MacDonald, J. R. *Biochem. Pharm.* **1997**, *54*, 1181.
8. (a) McMorris, T. C.; Kelner, M. J.; Chadha, R. K.; Siegel, J. S.; Moon, S.; Moya, M. M. *Tetrahedron* **1989**, *45*, 5433. (b) McMorris, T. C.; Kelner, M. J.; Wang, W.; Yu, J.; Estes, L. A.; Taetle, R. *Chem. Res. Toxicol.* **1990**, *3*, 574. (c) Gregerson, L. N.; McMorris, T. C.; Siegel, J. S.; Baldrige, K. K. *Helv. Chim. Acta.* **2003**, *86*, 4133. (d) Dick, R. A.; Yu, X.; Kensler, T. W. *Clin. Cancer Res.* **2004**, *10*, 1492. (e) Gong, J.; Vaidyanathan, V. G.; Yu, X.; Kensler, T. W.; Peterson, L. A.; Sturla, S. J. *J. Am. Chem. Soc.* **2007**, *129*, 2101. (f) Neels, J. F.; Gong, J.; Yu, X.; Sturla, S. J. *Chem. Res. Toxicol.* **2007**, *20*, 1513.
9. (a) Alexandre, J.; Raymond, E.; Kaci, M. O.; Brian, E. C.; Lokiec, F.; Kahatt, C.; Faivre, S.; Yovine, A.; Goldwasser, F.; Smith, S. L.; MacDonald, J. R.; Misset, J.-L.; Cvitkovic, E. *Clin. Cancer Res.* **2004**, *10*, 3377. (b) Serova, M.; Calvo, F.; Lokiec, F.; Koeppel, F.; Poindessous, V.; Larsen, A. K.; Van Laar, E. S.; Waters, S. J.; Cvitkovic, E.; Raymond, E. *Cancer Chemother. Pharmacol.* **2006**, *57*, 491. (c) Seiden, M. V.; Gordon, A. N.; Bodurka, D. C.; Matulonis, U. A.; Penson, R. T.; Reed, E.; Alberts, D. S.; Weems, G.; Cullen, M.; McGuire, W. P. III *Gynecol. Oncol.* **2006**, *101*, 55. (d) Hilgers, W.; Faivre, S.; Chieze, S.; Alexandre, J.; Lokiec, F.; Goldwasser, F.; Raymond, E.; Kahatt, C.; Taamma, A.; Weems, G.; MacDonald, J. R.; Misset, J. -L.; Cvitkovic, E. *Invest. New Drugs* **2006**, *24*, 311. (e) Paci, A.; Rezai, K.; Deroussent, A.; De Valeriola, D.; Re, M.; Weill, S.; Cvitkovic, E.; Kahatt, C.; Shah, A.; Waters, S.; Weems, G.; Vassal, G.; Lokeic, F. *Drug Metab. Dispos.* **2006**, *34*, 1918. (f) Wang, Y.; Wiltshire, T.; Senft, J.; Wenger, S. L.; Reed, E.; Wang, W. *Mol. Cancer Ther.* **2006**, *5*, 3153. (g) Yeo, W.; Boyer, M.; Chung, H. C.; Ong, S. Y. K.; Lim, R.; Zee, B.; Ma, B.; Lam, K. C.; Mo, F. K. F.; Ng, E. K. W.; Ho, R.; Clarke, S.; Roh, J. K.; Beale, P.; Rha, S. Y.; Jeung, H. C.; Soo, R.; Goh, B. C.; Chan, A. T. C. *Cancer Chemother. Pharmacol.* **2006**, *59*, 295. (h) Wiltshire, T.; Senft, J.; Wang, Y.; Konat, G. W.; Wenger, S. L.; Reed, E.; Wang, W. *Mol. Pharmacol.* **2007**, *71*, 1051. (i) Alexandre, J.; Kahatt, C.; Berthault-Cvitkovic, F.; Faivre, S.; Shibata, S.; Hilgers, W.; Goldwasser, F.; Lokiec, F.; Raymond, E.; Weems, G.; Shah, A.; MacDonald, J. R.; Cvitkovic, E. *Invest. New Drugs* **2007**, *25*, 453. (j) Escargueil, A. E.; Poindessous, V.; Soares, D. G.; Sarasin, A.; Cook, P. R.; Larsen, A. K. *J. Cell Sci.* **2008**, *121*, 1275. (k) Kelner, M. J.; McMorris, T. C.; Rojas, R. J.; Estes, L. A.;

-
- Suthipinijtham, P. *Invest. New Drugs* **2008**, *26*, 407. (l) Kelner, M. J.; McMorris, T. C.; Rojas, R. J.; Estes, L. A.; Suthipinijtham, P. *Cancer Chemother. Pharmacol.* **2008**, *63*, 19. (m) Dings, R. P. M.; Van Laar, E. S.; Webber, J.; Zhang, Y.; Griffin, R. J.; Waters, S. J.; MacDonald, J. R.; Mayo, K. H. *Cancer Lett.* **2008**, *265*, 270.
10. For total syntheses of illudin M (**3**), see: (a) Matsumoto, T.; Shirahama, H.; Ichihara, A.; Shin, H.; Kagawa, S.; Sakan, F.; Matsumoto, S.; Nishida, S. *J. Am. Chem. Soc.* **1968**, *90*, 3280. (b) Matsumoto, T.; Shirahama, H.; Ichihara, A.; Shin, H.; Kagawa, S.; Sakan, S.; Miyano, K. *Tetrahedron Lett.* **1971**, 2049. (c) Kinder, F. R.; Bair, K. W. *J. Org. Chem.* **1994**, *59*, 6965. For representative synthetic studies towards illudins, see: (d) Padwa, A.; Sandanayaka, V. P.; Curtis, E. A. *J. Am. Chem. Soc.* **1994**, *116*, 2667. (e) Primke, H.; Sarin, G. S.; Kohlstruk, S.; Adiwidjaja, G.; de Meijere, A. *Chem. Ber.* **1994**, *127*, 1051. For total syntheses of racemic acylfulvene (**1**) and irofulven (**2**), see: (f) McMorris, T. C.; Hu, Y.; Yu, J.; Kelner, M. *Chem. Commun.* **1997**, 315 (g) Brummond, K. M.; Lu, J. *J. Am. Chem. Soc.* **1999**, *121*, 5087. For enantioselective syntheses of (–)-acylfulvene (**1**) and (–)-irofulven (**2**), see: (h) Brummond, K. M.; Lu, J.; Petersen, J. *J. Am. Chem. Soc.* **2000**, *122*, 4915. (i) McMorris, T. C.; Staake, M. D.; Kelner, M. *J. Org. Chem.* **2004**, *69*, 619. (j) Gong, J.; Neels, J. F.; Yu, X.; Kensler, T. W.; Peterson, L. A.; Sturla, S. J. *J. Med. Chem.* **2006**, *49*, 2593.
11. (a) Movassaghi, M.; Piizzi, G.; Siegel, D. S.; Piersanti, G. *Angew. Chem. Int. Ed.* **2006**, *45*, 5859. (b) Movassaghi, M.; Piizzi, G.; Siegel, D. S.; Piersanti, G. *Tetrahedron Lett.* **2009**, *50*, 5489. (c) Siegel, D. S.; Piizzi, G.; Piersanti, G.; Movassaghi, M. *J. Org. Chem.* **2009**, *74*, 9292.
12. For representative examples of EYRCM reactions, see: (a) Kim, S.-H.; Bowden, N.; Grubbs, R. H. *J. Am. Chem. Soc.* **1994**, *116*, 10801. (b) Zuercher, W. J.; Scholl, M.; Grubbs, R. H. *J. Org. Chem.* **1998**, *63*, 4291. (c) Layton, M. E.; Morales, C. A.; Shair, M. D. *J. Am. Chem. Soc.* **2002**, *124*, 773. (d) Fukumoto, H.; Takanishi, K.; Ishihara, J.; Hatakeyama, S. *Angew. Chem. Int. Ed.* **2006**, *45*, 2731. For a review, see: (e) Nicolaou, K. C.; Bulger, P. G.; Sarlah, D. *Angew. Chem. Int. Ed.* **2005**, *44*, 4490
13. While the yields and results in this chapter were obtained by me unless otherwise noted they were greatly enabled through collaborative efforts with my colleagues Grazia Piizzi and Giovanni Piersanti.

-
14. (a) Bandini, M.; Cozzi, P. G.; Melchiorre, P.; Umani-Ronchi, A. *Tetrahedron Lett.* **2001**, *42*, 3041. (b) Bandini, M.; Cozzi, P. G.; Garelli, A.; Melchiorre, P.; Umani-Ronchi, A. *Eur. J. Org. Chem.* **2002**, 3243.
15. Fuerst, D. E.; Jacobsen, E. N. *J. Am. Chem. Soc.* **2005**, *127*, 8964
16. Reaction was carried out by Dr. Grazia Piizzi.
17. Deng, H.; Isler, M. P.; Snapper, M. L.; Hoveyda A. H. *Angew. Chem. Int. Ed.* **2002**, *41*, 1009.
18. Tian, S.-K.; Deng, L. *J. Am. Chem. Soc.* **2001**, *123*, 6195.
19. Kolb, H. C.; VanNieuwenhze, M. S.; Sharpless, B. *Chem. Rev.* **1994**, *94*, 2483.
20. Gao, Y.; Klunder, J. M.; Hanson, R. M.; Masamune, H.; Ko, S. Y.; Sharpless, K. B. *J. Am. Chem. Soc.* **1987**, *109*, 5765.
21. Frantz, D. E.; Fassler, R.; Carreira, E. M. *J. Am. Chem. Soc.* **2000**, *122*, 1806.
22. Evans, D. A.; Burgey, C. S.; Kozlowski, M. C.; Tregay, S. W. *J. Am. Chem. Soc.* **1999**, *121*, 686.
23. Ainsworth, C.; Chen, F.; Kuo, Y. -N. *J. Organomet. Chem.* **1972**, *46*, 59.
24. Pinnick H. W.; Chang, Y.-H.; Foster, S. C.; Govindan, M. *J. Org. Chem.* **1980**, *45*, 4505.
25. (a) Itoh, O.; Yamamoto, N.; Fujimoto, H.; Ichikawa, K. *J. Chem. Soc., Chem. Commun.* **1979**, 101. (b) Reissig, H.-U., Böhm, I. *J. Am. Chem. Soc.* **1982**, *104*, 1735. (c) Feit, B. A.; Elser, R.; Melamed, U.; Goldberg, I. *Tetrahedron* **1984**, *40*, 5177. (d) Häner, R.; Maetzke, T.; Seebach, D. *Helv. Chim. Acta* **1986**, *69*, 1655. (e) Blankenship, C.; Wells, G. J.; Paquette, L. A. *Tetrahedron* **1988**, *44*, 4023.
26. For an alternative approach using acylsilanes for the formation of cyclopropylsilyl enol ethers see: Reich, H. J.; Holtan, R. C.; Bolm, C. *J. Am. Chem. Soc.* **1990**, *112*, 5609.
27. Hahn, E.; Maetzke, T.; Plattner, D. A.; Seebach, D. *Chem. Ber.* **1990**, *123*, 2059.
28. For approaches using cyclopropyl esters as nucleophiles in the aldol reaction, see: (a) Paquette, L. A.; Blankenship, C.; Wells, G. J. *J. Am. Chem. Soc.* **1984**, *106*, 6442. (b) Danheiser, R. L.; Lee, T. W.; Menichincheri, M.; Brunelli, S.; Masaki, N. *Synlett* **1997**, 469.
29. For the preparation of (*R,R*)-2,2'-isopropylidene-bis(4-^tbutyl-2-oxazoline) see: Evans, D. A.; Peterson, G. S.; Johnson, J. S.; Barnes, D. M.; Campos, K. R.; Woerpel, K. A. *J. Org. Chem.* **1998**, *63*, 4541.

-
30. The enantiomeric excess of the desilylated C2-alcohol (+)-**48b** ($R^2 = H$) was established by chiral HPLC analysis and the absolute stereochemistry of this reaction was verified through X-ray crystallographic analysis.
31. Anderson, R. J.; Henrick, C. A.; Rosenblum, L. D. *J. Am. Chem. Soc.* **1974**, *96*, 3654.
32. (a) Tokuyama, H.; Yokoshima, S.; Yamashita, T.; Fukuyama, T. *Tetrahedron Lett.* **1998**, *39*, 3189. (b) Milne, J. E.; Buchwald, S. L. *J. Am. Chem. Soc.* **2004**, *126*, 13028. (c) Zhou, J.; Fu, G. C. *J. Am. Chem. Soc.* **2003**, *125*, 12527. Synthesis of MeZnI in NMP: (d) Huo, S. *Org. Lett.* **2003**, *5*, 423.
33. Takai, K.; Kakiuchi, T.; Kataoka, Y.; Utimoto, K. *J. Org. Chem.* **1994**, *59*, 2668.
34. Alternative olefination protocols including the Wittig, Petasis, Tebbe, Peterson, and standard Takai reactions were ineffective at carrying out this transformation. For references, see: (a) Petasis, N. A.; Lu, S.-P. *J. Am. Chem. Soc.* **1995**, *117*, 6394. (b) Tebbe, F. N.; Parshall, G. W.; Reddy, G. S. *J. Am. Chem. Soc.* **1978**, *100*, 3611. (c) Peterson, D. J. *J. Org. Chem.* **1968**, *33*, 780. (d) Okazoe, T.; Takai, K., Utimoto, k. *J. Am. Chem. Soc.* **1987**, *109*, 951.
35. Structural parameters for the carboxylic acid **88** salt with (–)-brucine are freely available from the Cambridge Crystallographic Data Center under CCDC-622286.
36. It may also be plausible that the formation of the EYRCM products occurs through initial complexation of the metathesis catalyst ($L_nRu=CH_2$) with the alkyne followed by EYRCM.
37. For examples of syntheses of cyclohexenes containing tetrasubstituted olefin via enyne metathesis see: (a) T. Kitamura, Y. Sato, M. Mori, *Chem. Comm.* **2001**, *14*, 1258. (b) T. Kitamura, Y. Sato, M. Mori, *Adv. Synth. Catal.* **2002**, *344*, 678.
38. (a) Miller, S. J.; Blackwell, H. E.; Grubbs, R. H. *J. Am. Chem. Soc.* **1996**, *118*, 9606. (b) Scholl, M.; Ding, S.; Lee, C. W.; Grubbs, R. H. *Org. Lett.* **1999**, *1*, 953.
39. The allyl carbonate fragmentation may involve a competing pathway in which catalyst decomposition products may form π -allyl complexes. For an example of ruthenium π -allyl complex formation with allyl carbonates, see: Gürbüz, N.; Özdemir, I.; Çetinkaya, B.; Renaud, J.-L.; Demerseman, B.; Bruneau, C. *Tetrahedron Lett.* **2006**, *47*, 535.
40. For representative examples of allyl dialkyl silicon tether mediated olefin metathesis reactions, see: (a) Chang, S.; Grubbs, R. H.; *Tetrahedron Lett.* **1997**, *38*, 4757. (b) Yao, Q. *Org. Lett.* **2001**, *3*, 2069.

-
41. For examples of metathesis reactions using allyloxysilane tethers, see: (a) Hoye, T. R.; Promo, M. A. *Tetrahedron Lett.* **1999**, *40*, 1429. (b) Briot, A.; Bujard, M.; Gouverneur, V.; Nolan, S. P.; Mioskowski, C. *Org. Lett.* **2000**, *2*, 1517. (c) Van de Weghe, P.; Aoun, J.-G. Boiteau, D.; Eustache, J. *Org. Lett.* **2002**, *4*, 4105. (d) Postema, M. H.; Piper, J. L. *Tetrahedron Lett.* **2002**, *43*, 7095. (e) Evans, P. E.; Cui, J.; Gharpure, S. J.; Polosukhin, A.; Zhang, H.-R. *J. Am. Chem. Soc.* **2003**, *125*, 14702.
42. Our Attempts to cleave allylsilane tethers via oxidation protocols were plagued by low yields. See ref 11c.
43. Allyloxydiethylchlorosilane (**97**) was prepared according to the procedure of Krolevets, A. A.; Antipova, V. V.; Popov, A. G.; Adamov, A. V. *Zh. Obsch. Khim.*, **1988**, *58*, 2274.
44. (a) Myers, A. G.; Zheng, B. *Tetrahedron Lett.* **1996**, *37*, 4841. (b) Myers, A. G.; Movassaghi, M.; Zheng, B. *J. Am. Chem. Soc.* **1997**, *119*, 8572.
45. For an evaluation of the scope of IPNBSH, see: (a) Movassaghi, M.; Ahmad, O. K. *J. Org. Chem.* **2007**, *72*, 1838. For use of IPNBSH in a stereospecific palladium-catalyzed route to monoalkyl diazenes, see: (b) Movassaghi, M.; Ahmad, O. K. *Angew. Chem. Int. Ed.* **2008**, *47*, 8909.
46. (–)-Irofulven (**2**) was obtained in 63% by Dr. Grazia Piizzi via treatment of (–)-acylfulvene (**1**) with acidic formalin for 6 d. See ref 11a.

Experimental Section

General Procedures. All reactions were performed in oven-dried or flame-dried round bottomed flasks or modified Schlenk (Kjeldahl shape) flasks. The flasks were fitted with rubber septa and reactions were conducted under a positive pressure of argon. Gas tight syringes equipped with stainless steel needles or cannulae were used to transfer air- and moisture-sensitive liquids. Flash column chromatography was performed as described by Still et al. using silica gel (60-Å pore size, 32–63 µm, standard grade, Sorbent Technologies) or non-activated alumina gel (80–325 mesh, chromatographic grade, EM Science).¹ Analytical thin-layer chromatography was performed using glass plates pre-coated with 0.25 mm 230–400 mesh silica gel or neutral alumina gel impregnated with a fluorescent indicator (254 nm). Thin layer chromatography plates were visualized by exposure to ultraviolet light and/or by exposure to an ethanolic phosphomolybdic acid (PMA), an acidic solution of *p*-anisaldehyde (Anis), an aqueous solution of ceric ammonium molybdate (CAM), an aqueous solution of potassium permanganate (KMnO₄) or an ethanolic solution of ninhydrin followed by heating (<1 min) on a hot plate (~250 °C). Organic solutions were concentrated on Büchi R-200 rotary evaporators at ~10 Torr (house vacuum) at 25–35 °C, then at ~0.5 Torr (vacuum pump) unless otherwise indicated.

Materials. Commercial reagents and solvents were used as received with the following exceptions: dichloromethane, diethyl ether, tetrahydrofuran, acetonitrile, and toluene were purchased from J.T. Baker (Cycletainer™) and were purified by the method of Grubbs et al. under positive argon pressure.² Benzene, triethylamine, diisopropylamine, *N*-methylmorpholine, 1-methyl-2-pyrrolidinone, 2,6-lutidine, and chlorotrimethylsilane were distilled from calcium hydride immediately before use. Methanol was distilled from anhydrous magnesium methoxide. Lithium hexamethyldisilazane was purchased from Aldrich and was stored in a glove box. Sodium hydride was purchased from Aldrich Chemicals as dispersion (60%) in oil and washed four times with hexanes and stored in a glove box. Methanolic sodium methoxide solution (1.0 N) was prepared by addition of sodium hydride to anhydrous methanol at –78 °C. The molarity of *n*-butyllithium solutions was determined by titration using diphenylacetic acid as an indicator (average of three determinations).³ Where necessary (so noted) solutions were degassed by sparging with argon for >10 minutes.

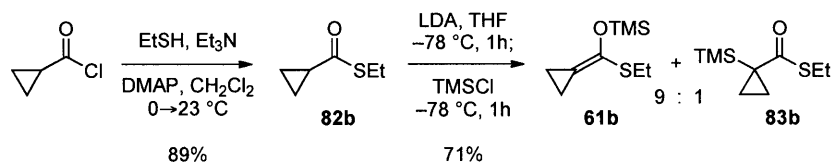
Instrumentation. Proton (¹H) and carbon (¹³C) nuclear magnetic resonance spectra were recorded on a Bruker Avance-400 (400 MHz) spectrometer with a Magnex Scientific superconducting magnet, a Bruker Avance-400 (400 MHz) spectrometer with a SpectroSpin superconducting magnet at 23 °C, or a Varian 500 INOVA (500 MHz) as noted. Proton nuclear magnetic resonance (¹H NMR) spectra are reported in parts per million from internal tetramethylsilane on the δ scale and are referenced from the residual protium in the NMR solvent (CHCl₃: δ 7.27, C₆HD₅: δ 7.16, CHD₂CN: δ 1.94). Data is reported as follows: chemical shift [multiplicity (s = singlet, d = doublet, t = triplet, q = quartet, st = sextet, sp = septet, m = multiplet, app = apparent, br = broad), coupling constant(s) in Hertz, integration, assignment]. Carbon-13 nuclear magnetic resonance spectra are reported in parts per

¹ Still, W. C.; Kahn, M.; Mitra, A. *J. Org. Chem.* **1978**, *43*, 2923–2925.

² Pangborn, A. B.; Giardello, M. A.; Grubbs, R. H.; Rosen, R. K.; Timmers, F. J. *Organometallics* **1996**, *15*, 1518–1520.

³ Kofron, W. G.; Baclawski, L. M. *J. Org. Chem.* **1976**, *41*, 1879–1880.

million from internal tetramethylsilane on the δ scale and are referenced from the carbon resonances of the solvent (CDCl₃: δ 77.2, C₆D₆: δ 128.0, CD₃CN: δ 118.7 and δ 1.39). Data is reported as follows: chemical shift [multiplicity (s = singlet, d = doublet, t = triplet, q = quartet, m = multiplet), coupling constant(s) in Hertz, assignment]. Infrared data were obtained with a Perkin-Elmer 2000 FTIR and are reported as follows: [frequency of absorption (cm⁻¹), intensity of absorption (s = strong, m = medium, w = weak, br = broad), assignment]. Gas chromatography was performed on an Agilent Technologies 6890N Network GC System with a HP-5 5% Phenyl Methyl Siloxane column (100 °C, 1 min; 30 °C/min to 250 °C; 250 °C, 2 min). The structure of **88** with (-)-brucine was obtained at the X-ray crystallography laboratory of the Department of Chemistry, Massachusetts Institute of Technology, with the assistance of Dr. Peter Mueller and Mr. Michael A. Schmidt. Gas chromatography low-resolution mass spectra (GC-LRMS) were recorded on an Agilent Technologies 6890N Network GC System with a Restek Rtx-1 100% dimethyl polysiloxane column (100 °C, 5 min; 20 °C/min to 250 °C; 250 °C, 5 min; 30 °C/min to 320 °C; 320 °C, 5 min) with a Agilent 5973*Network* mass selective detector using electron impact ion source (EI). Optical Rotation was recorded on a Jasco P-1010 Polarimeter (Chloroform, Aldrich, Chromosolv Plus 99.9%; Ethanol, Aldrich, Absolute, 200 Proof 99.5%). We are grateful to Dr. Li Li for obtaining the mass spectroscopic data at the Department of Chemistry's Instrumentation Facility, Massachusetts Institute of Technology. High-resolution mass spectra (HRMS) were recorded on a Bruker APEX 4.7 Tesler FTMS spectrometer using electrospray ion source (ESI), unless otherwise noted.



(Cyclopropylidene(ethylthio)methoxy)trimethylsilane (61b):

Ethanethiol (16.3 mL, 220 mmol, 1.10 equiv) was added slowly to a solution of cyclopropanecarbonyl chloride (18.3 mL, 200 mmol, 1 equiv), triethylamine (33.5 mL, 240 mmol, 1.20 equiv), and 4-dimethylaminopyridine (2.40 g, 20.0 mmol, 0.100 equiv) in dichloromethane (500 mL) at 0 °C, and the resulting mixture was allowed to warm to 23 °C. After 3 h, the reaction mixture was concentrated under reduced pressure, and the residue was partitioned between diethyl ether (400 mL) and water (300 mL). The organic phase was separated and was washed with brine (300 mL), was dried over anhydrous sodium sulfate, was filtered, and was concentrated under reduced pressure. The residue was purified by vacuum distillation (50 °C, 5 mmHg) to afford *S*-ethyl cyclopropanecarbothioate (**82b**, 23.1 g, 89%) as a clear colorless liquid.

n-Butyllithium (2.50 M, 33.8 mL, 1.10 equiv) was added to a solution of diisopropylamine (12.9 mL, 92.3 mmol, 1.20 equiv) in THF (192 mL) at 0 °C under argon. The mixture was cooled to -78 °C, and *S*-ethyl cyclopropanecarbothioate (**82b**, 10.0 g, 76.9 mmol, 1 equiv) was added dropwise via syringe. After 1 h, freshly distilled chlorotrimethylsilane (11.7 mL, 92.3 mmol, 1.20 equiv) was added dropwise. After an additional 1h, the reaction mixture was diluted with pentane (500 mL), and was washed with water (300 mL), phosphate buffer (pH 7, 300 mL), and brine (300 mL). The organic layer was dried over anhydrous sodium sulfate, and was concentrated under reduced pressure. The residue was purified by vacuum distillation (60 °C, 1 mmHg) to afford a mixture (9:1) of (cyclopropylidene(ethylthio)methoxy)trimethylsilane (**61b**) and 1-(trimethyl-silanyl)-cyclopropanecarbothioic acid *S*-ethyl ester (**83b**), as clear colorless oil (11.0 g, 71%).

***S*-ethyl cyclopropanecarbothioate (82b):**

¹H NMR (500 MHz, CDCl₃) δ: 2.87 (q, *J* = 7.3 Hz, 2H, SCH₂), 1.98 (tt, *J* = 7.7 Hz, 4.6 Hz, 1H, CH), 1.23 (t, *J* = 7.3, 3H, CH₃), 1.15-1.11 (m, 2H, CH₂), 0.93-0.89 (m, 2H, CH₂).

¹³C NMR (125.8 MHz, CDCl₃) δ: 199.5, 23.4, 22.7, 15.0, 10.7.

FTIR (neat) cm⁻¹: 2970 (m, C-H), 1681 (s, C=O), 1451 (m), 1419 (m), 1368 (s), 1039 (s), 993 (s).

GC-LRMS: calcd for C₆H₁₀OS [M]⁺: 130, found: 130 (7.3 min)

GC, *t*_R: 1.494 min

TLC (20% EtOAc in hexanes) *R*_f: 0.55 (UV)

(cyclopropylidene(ethylthio)methoxy)trimethylsilane (61b; containing $\leq 10\%$ 83b):

^1H NMR (500 MHz, CDCl_3) δ : 2.78 (q, $J = 7.3$ Hz, 2H, SCH_2), 1.33-1.24 (m, 4H, CH_2CH_2), 1.27 (t, $J = 7.3$ Hz, 3H, CH_3), 0.24 (s, 9H, $\text{Si}(\text{CH}_3)_3$).

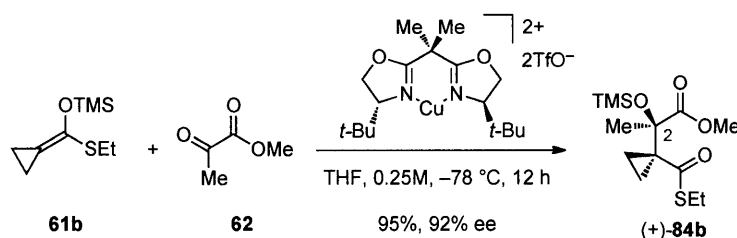
^{13}C NMR (125.8 MHz, CDCl_3) δ : 135.8, 100.5, 25.5, 15.4, 7.2, 5.1, 0.7.

FTIR (neat) cm^{-1} : 2965 (s), 1751 (s), 1449 (w), 1252 (s), 1189 (s), 1071 (m).

HRMS (ESI): calcd for $\text{C}_9\text{H}_{19}\text{OSSi}$ $[\text{M}+\text{H}]^+$: 203.0920, found: 203.0926.

GC, t_{R} : 2.499 min

TLC (10% EtOAc in hexanes) R_f : 0.5 (UV)



(+)-(R)-methyl-2-(1-((ethylthio)carbonyl)cyclopropyl)-2-((trimethylsilyl)oxy)propanoate (84b):

A flame-dried flask was charged with (*R,R*)-2,2'-isopropylidene-bis(4-*tert*-butyl-2-oxazoline) (2.03 g, 6.90 mmol, 0.10 equiv)⁴ and copper (II) trifluoromethanesulfonate (2.50 g, 6.90 mmol, 0.10 equiv) in a glove-box under a dinitrogen atmosphere. The flask was sealed with a rubber septum and removed from the glove-box. The flask containing the solids was charged with THF (304 mL) at 23 °C and was flushed with argon. After 1h, the resulting bright green solution was cooled to -78 °C, and methyl pyruvate (**62**, 7.80 g, 76.0 mmol, 1.10 equiv) was added via syringe followed by (cyclopropylidene(ethylthio)methoxy)trimethylsilane (**61b** [mixture of **61b**:**83b** = 9:1], 15.5 g, 69.0 mmol, 1 equiv **61b**) via syringe. After 19 h, the reaction mixture was diluted with diethyl ether (300 mL), and filtered through a plug of silica gel (6 × 6 cm, eluent: 1% triethylamine in diethyl ether). The filtrate was concentrated under reduced pressure and the residue was purified by flash column chromatography (silica gel: diam. 9 cm, ht. 15 cm; eluent: 1% triethylamine in [2% ethyl acetate in hexanes] to 1% triethylamine in [20% ethyl acetate in hexanes]) to afford the desired (+)-(*R*)-methyl-2-(1-((ethylthio)carbonyl)cyclopropyl)-2-((trimethylsilyl)oxy)propanoate ((+)-**84b**, 19.8 g, 95%, [α]_D²⁰ = +30.2 (*c* 2.22, CHCl₃)) as a colorless liquid. Protodesilylation of the C2-trimethylsilyloxy group of (+)-**84b** afforded samples of the corresponding C2-alcohol (**S1**) that were found to be of 92% ee by chiral HPLC analysis [Chirapak AD-H; 1.5 mL/min; 10% *i*PrOH in hexanes; *t*_R(minor) = 4.65 min, *t*_R(major) = 5.17 min]. The (*R,R*)-2,2'-isopropylidene-bis(4-*tert*-butyl-2-oxazoline) ligand was recovered from the reaction mixture (~85%) and purified by flash column chromatography (silica gel: diam. 2.5 cm, ht. 10 cm; eluent: 20% ethyl acetate in dichloromethane).

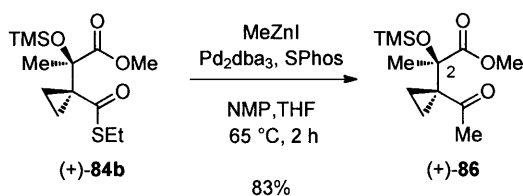
¹H NMR (500 MHz, CDCl₃) δ: 3.72 (s, 3H, OCH₃), 2.79 (q, *J* = 7.3 Hz, 2H, SCH₂), 1.58-1.54 (m, 1H, CH₂), 1.53 (s, 3H, CH₃), 1.27-1.19 (m, 2H, CH₂), 1.19 (t, *J* = 7.3 Hz, 3H, CH₂CH₃), 1.12-1.08 (m, 1H, CH₂), 0.07 (s, 9H, Si(CH₃)₃).

¹³C NMR (125.8 MHz, CDCl₃) δ: 200.9, 173.4, 75.4, 52.1, 41.8, 24.2, 23.0, 15.3, 14.8, 11.6, 1.5.

FTIR (neat) cm⁻¹: 2954 (m, C-H), 1747 (s, CO₂Me), 1666 (s, COSEt) 1456 (m), 1413 (m), 1372 (m), 1289 (m), 1263 (s).

⁴ For the preparation of (*R,R*)-2,2'-isopropylidene-bis(4-*t*-butyl-2-oxazoline) see: Evans, D. A.; Peterson, G. S.; Johnson, J. S.; Barnes, D. M.; Campos, K. R.; Woerpel, K. A. *J. Org. Chem.* **1998**, *63*, 4541-4544.

HRMS (ESI):	calcd for C ₁₃ H ₂₄ NaO ₄ SSi [M+Na] ⁺ : 327.1057, found: 327.1066.
GC, <i>t_R</i> :	4.450 min
TLC (10% EtOAc in hexanes) <i>R_f</i> :	0.4 (UV, CAM)



(+)-(2R)-2-(1-Acetyl-cyclopropyl)-2-(trimethyl-silyloxy)-propionic acid methyl ester (86):

A Schlenk flask was charged with activated Zn dust (981 mg, 15.0 mmol, 1.50 equiv)⁵, placed under reduced pressure (1 Torr), and heated to 65 °C. After 30 min, the flask was backfilled with argon and cooled to 23 °C. Anhydrous *N*-methyl pyrrolidin-2-one (NMP, 10 ml) and iodine (127 mg, 0.500 mmol, 0.050 equiv) were added and the reaction mixture was stirred vigorously for 25 min at which time the red color disappeared. Methyl iodide (619 μL , 10.0 mmol, 1 equiv) was added and the reaction mixture was stirred at 23 °C for 14 h to provide a solution of iodomethylzinc in NMP (~1 M).

A solution of iodomethylzinc (~1 M, 8.22 mL, 8.22 mmol, 5.00 equiv), prepared as described above, was added via syringe to a solution of thioester (+)-**84b** (500 mg, 1.64 mmol, 1 equiv), tris(di-benzylideneacetone)dipalladium (75.3 mg, 0.08 mmol, 0.05 equiv), and 2-dicyclohexylphosphino-2',6'-dimethoxybiphenyl (SPhos, 135 mg, 0.33 mmol, 0.20 equiv) in THF (5.5 mL) at 23 °C. The reaction mixture was heated to 65 °C and stirred under an argon atmosphere. After 2 h, the reaction mixture was cooled to 23 °C, diluted with diethyl ether (200 mL), and filtered through a plug of silica gel (diam. 5 cm, ht. 10 cm) to remove most of the NMP. The filtrate was concentrated under reduced pressure and the residue was purified by flash column chromatography (silica gel: diam. 5 cm, ht. 12 cm; hexane-EtOAc [95:5]) to afford the desired ketoester (+)-**86** as a light yellow oil (353 mg, 83%, $[\alpha]_D^{20} = +41.8$ (*c* 2.14, CHCl_3)).

¹H NMR (500 MHz, CDCl_3) δ : 3.69 (s, 3H, OCH_3), 1.84 (s, 3H, COCH_3), 1.60-1.54 (m, 1H, CH_2), 1.49 (s, 3H, CH_3), 1.19-1.09 (m, 2H, CH_2), 1.08-1.03 (m, 1H, CH_2), 0.06 (s, 9H, $\text{Si}(\text{CH}_3)_3$).

¹³C NMR (125.8 MHz, CDCl_3) δ : 207.7, 173.4, 75.1, 52.1, 41.1, 24.4, 24.2, 13.3, 10.7, 1.6.

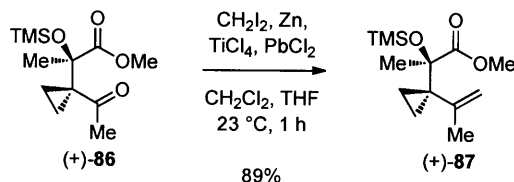
FTIR (neat) cm^{-1} : 2953 (m, C-H), 1745 (s, CO_2Me), 1685 (s, C=O), 1458 (m), 1434 (m), 1369 (s), 1327 (m), 1253 (s).

HRMS (ESI): calcd for $\text{C}_{12}\text{H}_{22}\text{NaO}_4\text{Si}$ $[\text{M}+\text{Na}]^+$: 281.1180, found: 281.1181.

GC, t_R : 3.425 min

TLC (20% EtOAc in hexanes) R_f : 0.33 (Anis)

⁵ Activated zinc dust was prepared by sequential washing of Zn dust with 1.2 N HCl in H_2O , H_2O , methanol, and diethyl ether, and drying under vacuum. Also, see: Fieser, L.; Fieser, M. "Reagents for Organic Synthesis"; Wiley: New York, 1967, Vol. 1, p. 1267.



(+)-(2*R*)-2-(1-Isopropenyl-cyclopropyl)-2-(trimethyl-silyloxy)-propionic acid methyl ester (87):

Diiodomethane (3.93 mL, 48.8 mmol, 6.00 equiv) was added to a vigorously stirred suspension of activated zinc dust (5.3 g, 81.0 mmol, 10.8 equiv)⁶ and lead (II) chloride (114.0 mg, 0.410 mmol, 0.05 equiv) in THF (60.0 mL) at 23 °C under an argon atmosphere. After 30 min, the reaction mixture was cooled to 0 °C, and titanium tetrachloride (1M in dichloromethane, 9.72 mL, 9.72 mmol, 1.20 equiv) was added dropwise via syringe. The resulting brown reaction mixture was warmed to 23 °C with continued stirring. After 30 min, the reaction mixture was cooled to 0 °C and a solution of ketoester (+)-**86** (2.10 mg, 8.10 mmol, 1 equiv) in THF (20.0 mL) was added via cannula. After 1 h, the excess reagent was quenched by the addition of saturated aqueous sodium bicarbonate solution (200 mL). The mixture was extracted with diethyl ether (3 × 200 mL), and the combined organic layers were dried over sodium sulfate, and were concentrated under reduced pressure. Purification by flash column chromatography (silica gel: diam. 4 cm, ht. 8 cm; pentane-diethyl ether [9:1]) afforded the desired (+)-(2*R*)-2-(1-isopropenyl-cyclopropyl)-2-(trimethyl-silyloxy)-propionic acid methyl ester (**87**, 1.86 g, 89%, $[\alpha]_D^{20} = +25.4$ (c 0.763, CHCl_3)) as a clear colorless liquid.

¹H NMR (500 MHz, CDCl_3) δ : 4.92 (s, 1H, C=CH₂), 4.87 (s, 1H, C=CH₂), 3.68 (s, 3H, OCH₃), 1.71 (s, 3H, C=CCH₃), 1.42 (s, 3H, CH₃), 1.05 (ddd, $J = 3.9, 5.9, 9.7$ Hz, 1H, CH₂), 0.83 (ddd, $J = 3.9, 5.9, 9.7$ Hz, 1H, CH₂), 0.47 (ddd, $J = 3.9, 5.9, 9.7$ Hz, 1H, CH₂), 0.38 (ddd, $J = 3.9, 5.9, 9.7$ Hz, 1H, CH₂), 0.06 (s, 9H, Si(CH₃)₃).

¹³C NMR (125.8 MHz, CDCl_3) δ : 175.6, 146.5, 117.3, 78.0, 51.7, 35.0, 24.6, 22.5, 9.7, 9.5, 1.7.

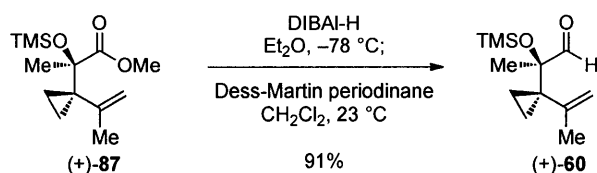
FTIR (neat) cm^{-1} : 2954 (m, C-H), 1743 (s, CO₂Me), 1639 (w), 1450 (m), 1373 (m), 1252 (s), 1154 (s), 1126 (s), 1019 (m).

HRMS (ESI): calcd for C₁₃H₂₄NaO₃Si [M+Na]⁺: 279.1387, found: 279.1384.

GC, t_R : 2.933 min

TLC (20% EtOAc in hexanes) R_f : 0.60 (Anis)

⁶ Activated zinc dust was prepared by sequential washing of Zn dust with 1.2 N HCl in H₂O, H₂O, methanol, and diethyl ether, and drying under vacuum. Also, see: Fieser, L.; Fieser, M. "Reagents for Organic Synthesis"; Wiley: New York, 1967, Vol. 1, p. 1267.



(+)-(2*R*)-2-(1-Isopropenyl-cyclopropyl)-2-(trimethyl-silyloxy)-propionaldehyde (60):

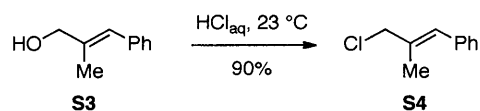
Diisobutylaluminum hydride (DIBAL-H, 1.5M in Toluene, 11.7 mL, 17.6 mmol, 3.00 equiv) was added dropwise down the side of the flask into a solution of (+)-(2*R*)-2-(1-isopropenyl-cyclopropyl)-2-(trimethyl-silyloxy)-propionic acid methyl ester (**87**, 1.5 g, 5.80 mmol, 1 equiv) in diethyl ether (29 mL) at $-78\text{ }^\circ\text{C}$ under argon. The reaction mixture was stirred and maintained at $-78\text{ }^\circ\text{C}$. After 1 h, excess hydride was quenched by the slow addition of methanol (17.6 mmol, 713 μL , 3.00 equiv). The mixture was diluted first with diethyl ether (300 mL), and then with a saturated aqueous solution of Rochelle's salt (200 mL). The mixture was allowed to warm to $23\text{ }^\circ\text{C}$, and the layers were separated. The organic layer was washed with brine (200 mL), dried over anhydrous sodium sulfate, and concentrated under reduced pressure to afford a mixture of (2*R*)-2-(1-isopropenyl-cyclopropyl)-2-(trimethyl-silyloxy)-propan-1-ol (**S2**) and (2*R*)-2-(1-isopropenyl-cyclopropyl)-2-(trimethyl-silyloxy)-propionaldehyde (**60**) as a colorless oil (**S2**:**60**, 2.5:1). Dess-Martin periodinane (2.71 g, 6.38 mmol, 1.10 equiv) was added to the mixture of (2*R*)-2-(1-isopropenyl-cyclopropyl)-2-(trimethyl-silyloxy)-propan-1-ol (**S2**) and (2*R*)-2-(1-isopropenyl-cyclopropyl)-2-(trimethyl-silyloxy)-propionaldehyde (**60**) in dichloromethane (29 mL) at $23\text{ }^\circ\text{C}$ under argon. After 1 h, the reaction mixture was filtered through a plug of silica gel (diam. 3 cm, ht. 3 cm; eluent: pentane), and was concentrated to afford (2*R*)-2-(1-isopropenyl-cyclopropyl)-2-(trimethyl-silyloxy)-propionaldehyde (**60**, 1.22 g, 91%, $[\alpha]_{\text{D}}^{20} = +63.0$ (c 0.564, CHCl_3)) as a colorless oil.

(2*R*)-2-(1-isopropenyl-cyclopropyl)-2-(trimethyl-silyloxy)-propan-1-ol (S2):

$^1\text{H NMR}$ (500 MHz, CDCl_3) δ :	4.99 (m, 2H, $\text{C}=\text{CH}_2$), 3.57 (dd, $J = 7.5, 11.0$ Hz, 1H, CH_2OH), 3.46 (dd, $J = 5.3, 11.0$ Hz, 1H, CH_2OH), 1.83 (t, $J = 1.0$ Hz, 3H, $\text{CH}_3\text{C}=\text{CH}_2$), 1.81 (dd, $J = 5.3, 7.5$ Hz, 1H, OH), 1.27 (s, 3H, CH_3), 0.91-0.88 (m, 1H, CH_2CH_2), 0.65-0.60 (m, 1H, CH_2CH_2), 0.43-0.35 (m, 2H, CH_2), 0.14 (s, 9H, $\text{Si}(\text{CH}_3)_3$).
$^{13}\text{C NMR}$ (125.8 MHz, CDCl_3) δ :	147.7, 117.6, 69.9, 46.4, 33.2, 23.5, 23.2, 9.2, 8.4, 2.6.
FTIR (neat) cm^{-1} :	3465 (br, O-H), 3078 (w, C-H), 2956 (s, C-H), 1637 (w), 1450 (m), 1413 (m), 1374 (m), 1252 (s).
HRMS (ESI):	calcd for $\text{C}_{12}\text{H}_{24}\text{NaO}_2\text{Si}$ $[\text{M}+\text{Na}]^+$: 251.1438, found: 251.1442.
GC, t_{R} :	3.013 min.
TLC (5% EtOAc in hexanes) R_f :	0.19 (Anis).

(+)-(2R)-2-(1-isopropenyl-cyclopropyl)-2-(trimethyl-silyloxy)-propionaldehyde (60):

¹ H NMR (500 MHz, CDCl ₃) δ:	9.50 (s, 1H, CHO), 4.95 (br-s, 1H, C=CH ₂), 4.87 (br-s, 1H, C=CH ₂), 1.71 (br-s, 3H, CH ₃ C=CH ₂), 1.29 (s, 3H, CH ₃ COTMS), 0.97 (ddd, <i>J</i> = 3.8, 5.8, 9.6 Hz, 1H, CH ₂ CH ₂), 0.78 (ddd, <i>J</i> = 3.9, 5.8, 9.6 Hz, 1H, CH ₂ CH ₂), 0.48 (ddd, <i>J</i> = 4.0, 5.8, 9.6 Hz, 1H, CH ₂ CH ₂), 0.41 (ddd, <i>J</i> = 3.8, 5.8, 9.6 Hz, 1H, CH ₂ CH ₂), 0.09 (s, 9H, Si(CH ₃) ₃).
¹³ C NMR (125.8 MHz, CDCl ₃) δ:	203.0, 145.6, 118.0, 79.7, 32.6, 23.2, 20.8, 8.5, 7.5, 2.2.
FTIR (neat) cm ⁻¹ :	2958 (m, C-H), 1735 (s, C=O), 1639 (w), 1448 (w), 1377 (w), 1252 (s).
HRMS (ESI):	calcd for C ₁₂ H ₂₂ NaO ₂ Si [M+Na] ⁺ : 249.1281, found: 249.1293.
TLC (100% hexanes) R _f :	0.17 (Anis).



E-(3-Chloro-2-methyl-prop-1-enyl)-benzene (S4):

Aqueous hydrochloric acid solution (12 N, 51.7 mL, 620 mmol, 3.00 equiv) was slowly added to 2-methyl-3-phenyl-prop-2-en-1-ol (30.6 g, 207 mmol, 1 equiv), and the reaction mixture was stirred and maintained at 23 °C. After 12 h, the reaction mixture was diluted with diethyl ether (50 mL), the layers were separated, and the aqueous layer was further extracted with additional diethyl ether (2 × 50 mL). The combined organic layers were washed with brine (100 mL), were dried over anhydrous sodium sulfate, and were concentrated under reduced pressure (30 °C, 100 mmHg). The residue was purified by vacuum distillation (120 °C, 12 mmHg) to afford 5-chloro-4-methyl-pent-3-enyl)-benzene (**S4**, 31.0 g, 90%) as a clear colorless oil.

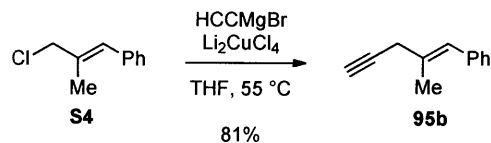
$^1\text{H NMR}$ (500 MHz, CDCl_3) δ : 8.05-8.0 (m, 2H, ArH), 7.98-7.90 (m, 3H, ArH), 7.27 (br-s, 1H, C=CH), 4.87 (s, 2H, CH_2Cl), 2.67 (d, $J = 1.5$ Hz, 3H, CH_3).

$^{13}\text{C NMR}$ (125.8 MHz, CDCl_3) δ : 136.9, 134.3, 130.0, 129.1, 128.4, 127.2, 53.1, 16.1.

FTIR (neat) cm^{-1} : 2985 (m, C-H), 1950 (w), 1885 (w), 1808 (w), 1599 (m), 1492 (s), 1442 (s), 1261 (s).

HRMS (ESI): calcd for $\text{C}_{10}\text{H}_{11}\text{Cl}$ $[\text{M}]^+$: 166.0544, found: 166.0538.

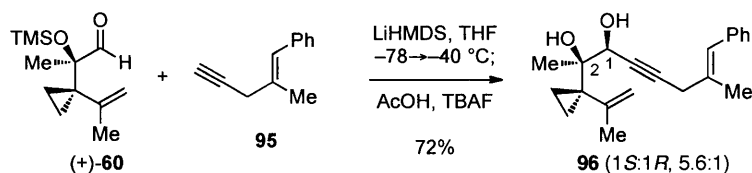
TLC (20% EtOAc in hexane) R_f : 0.70 (KMnO_4).



E-(2-Methyl-pent-1-en-4-ynyl)-benzene (95b):

A flame-dried 200-mL round-bottom flask was sequentially charged with a solution of ethynyl magnesium bromide (0.5M in THF, 448 mL, 224 mmol, 2.60 equiv) and a solution of dilithium tetrachlorocuprate (0.1 M in THF, 86.2 mL, 8.62 mmol, 0.10 equiv), and the resulting mixture was stirred at 23 °C. After 15 min, a solution of the allylic chloride **S4** (14.4 g, 86.2 mmol, 1 equiv) in THF (20 mL) was added via cannula and the resulting brown solution was heated to 55 °C. After 50 h, the reaction mixture was cooled to 23 °C and partitioned between diethyl ether (300 mL) and saturated aqueous ammonium chloride solution (150 mL). The aqueous layer was extracted with diethyl ether (2 × 300 mL) and the combined organic layers were washed with brine (150 mL), were dried over anhydrous magnesium sulfate, and were filtered. The dark solution of the crude alkyne **95b** was concentrated (to approximately 300 mL) under reduced pressure (~350 Torr, 28 °C) and was passed through silica gel (diam. 7.5 cm, ht. 30.0 cm; eluent: *n*-pentane) to give the crude alkyne **95b** as a dark yellow oil after removal of volatiles under reduced pressure. Purification of the residue by flash column chromatography (silica gel: diam. 7.5 cm, ht. 32 cm; *n*-pentane:CH₂Cl₂, [20:1]) afforded the alkyne **95b** (10.9 g, 81%) as a pale yellow oil.

¹ H NMR (500 MHz, CDCl ₃) δ:	7.38-7.33 (m, 2H, ArH), 7.30-7.21 (m, 3H, ArH), 6.61 (br-s, 1H, C=CHPh), 3.10 (br-s, 2H, CH ₂), 2.21 (t, <i>J</i> = 2.4 Hz, 1H, C≡C-H), 1.94 (br-s, 3H, CH ₃).
¹³ C NMR (125.8 MHz, CDCl ₃) δ:	138.0, 133.1, 129.0, 128.3, 126.5, 81.6, 71.2, 65.7, 29.5, 17.4.
FTIR (neat) cm ⁻¹ :	3298 (s, C≡C-H), 2984 (m, C-H), 2117 (w, C≡C), 1658 (w), 1599 (w), 1490 (m), 1442 (m), 1294 (w), 1155 (w).
HRMS (ESI):	calcd for C ₁₂ H ₁₂ Na [M+Na] ⁺ : 156.0939, found: 156.0937.
TLC (5% CH ₂ Cl ₂ in hexane) R _f :	0.22 (KMnO ₄).



E-(2*R*,3*S*)-2-(1-Isopropenyl-cyclopropyl)-7-methyl-8-phenyl-oct-7-en-4-yne-2,3-diol (96):

A solution of the alkyne **95** (1.47 g, 9.40 mmol, 1.25 equiv) in THF (50 mL) was added dropwise to a solution of lithium bis(trimethylsilyl)amide (LiHMDS, 1.68 g, 9.77 mmol, 1.30 equiv) in THF (50 mL) at -78 °C. After 5 min, a solution of the aldehyde (+)-**60** (1.70 g, 7.52 mmol, 1 equiv) in THF (12 mL) was added slowly via cannula, and the mixture was warmed to -40 °C. After 40 min, the excess base was quenched by the addition of a saturated aqueous ammonium chloride solution (5 mL) and the resulting mixture was warmed to 23 °C. The reaction mixture was diluted with H₂O (150 mL) and was extracted with ethyl acetate (3 × 150 mL). The combined organic layers were dried over anhydrous sodium sulfate and were partially concentrated under reduced pressure (to ~10 mL). The flask was charged with additional THF (40 mL) and a mixture of tetrabutylammonium fluoride (TBAF, 1.0 M in THF, 15.0 mL, 15.0 mmol, 2.00 equiv) and acetic acid (0.430 mL, 7.52 mmol, 1.00 equiv) was added to this crude mixture. After 40 min, a saturated aqueous ammonium chloride solution (150 mL) was added, and the mixture was extracted with ethyl acetate (3 × 150 mL). The combined organic extracts were dried over anhydrous sodium sulfate, were filtered, and the volatiles were removed under reduced pressure. The resulting yellow oil was purified by flash column chromatography (silica gel: diam. 5 cm, ht. 30 cm; eluent: hexanes:EtOAc, [4:1]) to give the propargylic alcohol **96** (1.80 g, 72%) as a mixture of C1-diastereomers favoring the *anti*-isomer (1*S*:1*R*, 5.6:1). The C1-stereochemistry of the major diastereomer of **96b** was secured using nOe data for a more advanced intermediate (vide infra, alcohol **109**).

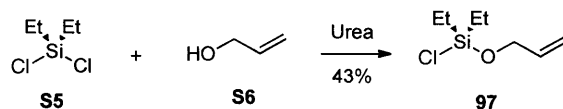
¹H NMR (500 MHz, C₆D₆, 5.6:1 mixture of (1*S*)- and (1*R*)-diastereomers; minor (1*R*)-isomer denoted by *) δ: 7.40-7.00 (m, 5H, ArH*), 7.24-7.14 (m, 4H, ArH), 7.08-7.03 (m, 1H, ArH), 6.65 (br-s, 1H, C=CHPh), 6.65 (br-s, 1H, C=CHPh*), 5.16 (br-s, 1H, C=CH₂), 5.12 (br-s, 1H, C=CH₂*), 4.95 (br-s, 1H, C=CH₂*), 4.91 (br-s, 1H, C=CH₂), 4.54 (br-s, 1H, CHOH*), 4.48 (br-s, 1H, CHOH), 2.97 (s, 2H, CH₂*), 2.82 (s, 2H, CH₂), 1.93 (s, 1H, CHOH), 1.93 (s, 1H, CHOH*), 1.87 (s, 3H, CH₃*), 1.82 (s, 3H, CH₃*), 1.77 (s, 3H, CH₃), 1.71 (s, 3H, CH₃), 1.64 (s, 1H, OH), 1.64 (s, 1H, OH*), 1.30 (s, 3H, CH₃), 1.29 (s, 3H, CH₃*), 1.26 (ddd, *J* = 4.6, 6.0, 10.0 Hz, 1H, CH₂CH₂), 1.02 (ddd, *J* = 10.0, 6.0, 4.6 Hz, 1H, CH₂CH₂*), 0.93 (ddd, *J* = 4.0, 6.1, 9.8 Hz, 1H, CH₂CH₂), 0.89 (ddd, *J* = 9.8, 6.1, 4.0 Hz, 1H, CH₂CH₂*), 0.56 (ddd, *J* = 4.6, 6.1, 10.0 Hz, 1H, CH₂CH₂), 0.52-0.45 (m, 2H, CH₂CH₂*), 0.44 (ddd, *J* = 4.0, 6.0, 9.8 Hz, 1H, CH₂CH₂).

^{13}C NMR (125.8 MHz, C_6D_6 , 5.6:1 mixture of (1*S*)- and (1*R*)-diastereomers; minor (1*R*)-isomer denoted by *) δ : 147.9, 147.9*, 138.7, 138.3*, 133.9*, 133.8, 129.5, 129.3*, 128.9*, 128.8, 127.2*, 127.1, 127.0, 127.0*, 118.4, 118.2*, 84.9, 84.1*, 83.1, 83.0*, 75.6*, 75.1, 69.9, 69.9*, 33.5, 32.6*, 30.2, 30.1*, 23.6*, 23.5, 23.4, 22.4*, 18.1, 18.1*, 11.2, 10.2*, 10.1*, 9.6.

FTIR (neat) cm^{-1} : 3440 (br-s, O–H), 2923 (m, C–H), 2227 (w, $\text{C}\equiv\text{C}$), 1635 (w), 1491 (w), 1447 (m), 1375 (m), 1105 (m), 1024 (s).

HRMS (ESI): calcd for $\text{C}_{21}\text{H}_{26}\text{NaO}_2$ $[\text{M}+\text{Na}]^+$: 333.1825, found: 333.1829.

TLC (20% EtOAc in hexanes), R_f : 0.20 (CAM)



Allyloxchlorodiethylsilane (97):⁷

Allyl alcohol (**S6**, 5.8 g, 100 mmol, 1.00 equiv) was added slowly via syringe over a 6 h period to a stirring mixture of dichlorodiethylsilane (**S5**, 15.8 g, 100 mmol, 1 equiv), and urea (7.2 g, 120 mmol, 1.20 equiv) at 23 °C under argon. The reaction mixture was transferred via cannula to a distillation apparatus, and the residue was purified by vacuum distillation (65 °C, 15 mmHg) to afford allyloxchlorodiethylsilane (**97**, 7.52 g, 43%) as a clear colorless oil.

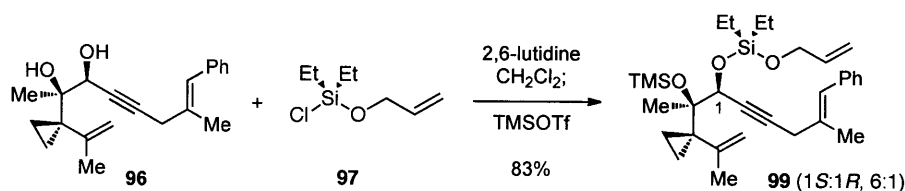
¹H NMR (500 MHz, C₆D₆) δ: 5.82-5.72 (m, 1H, CH), 5.23 (d, *J* = 17.1 Hz, 1H, CH), 4.99 (d, *J* = 10.4 Hz, 1H, CH), 4.12 (br-s, 2H, CH₂), 0.95 (t, *J* = 7.6 Hz, 6H, CH₃), 0.76-0.62 (m, 4H, CH₂).

¹³C NMR (125.8 MHz, C₆D₆) δ: 136.7, 115.1, 64.7, 8.9, 6.8.

FTIR (neat) cm⁻¹: 3331.2 (br-w), 2959 (s), 1460 (m), 1414 (w), 1243 (m), 1086 (s), 1008 (s).

GC-LRMS: calcd for C₇H₁₅ClOSi [M]⁺: 178
found: 178 (6.4 min)

⁷ Prepared according to the procedure of Krolevets, A. A.; Antipova, V. V.; Popov, A. G.; Adamov, A. V. *Zhurnal Obshchei Khimii*, **1988**, *58*, 2274-2281.



***E*-(2*R*,3*S*)-2-(1-Isopropenyl-cyclopropyl)-2-(trimethylsilyloxy)-3-(allyloxy-diethyl-silanyloxy)-7-methyl-8-phenyl-oct-7-en-4-yne (99):**

Allyloxychlorodiethylsilane (**97**, 347 mg, 2.00 mmol, 2.00 equiv) was added dropwise to a stirring solution of diol **96** (310 mg, 1.00 mmol, 1 equiv, [1*S*:1*R*, 5.6:1]), and 2,6-lutidine (674 μ L, 6.00 mmol, 6.00 equiv) in dichloromethane (5 mL) at 23 °C under argon. After 2 h, the reaction mixture was cooled to -78 °C, and trimethylsilyl trifluoromethanesulfonate (550 μ L, 3.00 mmol, 3.00 equiv) was added. After an additional 3 h, excess silylating reagent was quenched by the addition of saturated aqueous sodium bicarbonate solution (5 mL), the layers were separated, and the aqueous layer was extracted with ethyl acetate (3 \times 5 mL). The combined organic layers were dried over anhydrous sodium sulfate, and were concentrated under reduced pressure. Purification of the residue by flash column chromatography (silica gel: diam. 2.5 cm, ht. 5 cm; hexanes–EtOAc [98:2]) afforded the sensitive (hydrolysis of allyloxydiethylsilyl ether) compound **99** (435 mg, 83%, [1*S*:1*R*, 6:1]) as a light yellow oil containing residual diallyloxydiethylsilane and were used directly in the next step. Samples of metathesis substrate **99** lacking diallyloxydiethylsilane were obtained by further chromatographic purification, at the expense of additional loss of **99**. The presence of residual diallyloxydiethylsilane does not interfere with the following metathesis reaction.

^1H NMR (500 MHz, C_6D_6 , 6:1 mixture of (1*S*)- and (1*R*)-diastereomers; minor (1*R*)-isomer denoted by *) δ : 7.48–7.1 (m, 5H, ArH*), 7.40–7.36 (m, 2H, ArH), 7.31–7.27 (m, 2H, ArH), 7.18–7.13 (m, 1H, ArH), 6.81 (br-s, 1H, PhCH=CH₂), 6.79 (s, 1H, PhCH=CH₂*), 6.06–5.98 (m, 1H, OCH₂CH=CH₂), 6.06–5.98 (m, 1H, CH₂CH=CH₂*), 5.50 (dq, $J = 17.0, 2.0$ Hz, 1H, *trans*-OCH₂CH=CH₂), 5.49 (dq, $J = 17.0, 2.0$ Hz, 1H, *trans*-OCH₂CH=CH₂*), 5.42 (d, $J = 2.7$ Hz, 1H, C=CH₂), 5.40 (d, $J = 2.7$ Hz, 1H, C=CH₂*), 5.18–5.13 (m, 2H, *cis*-OCH₂CH=CH₂, C=CH₂), 5.19–5.13 (m, 2H, *cis*-OCH₂CH=CH₂*, C=CH₂*), 4.99 (t, $J = 1.8$ Hz, 1H, CHOSi), 4.95 (t, $J = 1.8$ Hz, 1H, CHOSi*), 4.49–3.98 (m, 2H, OCH₂CH=CH₂), 4.49–3.98 (m, 2H, OCH₂CH=CH₂*), 3.10 (s, 2H, CH₂C=C*), 3.02 (s, 2H, CH₂C=C), 2.05 (s, 3H, CH₃*), 2.02 (s, 3H, CH₃), 1.99 (s, 3H, CH₃*), 1.87 (s, 3H, CH₃), 1.53–1.48 (m, 7H, CH₂CH₂, CH₃, CH₃*), 1.30–1.19 (m, 6H, SiCH₂CH₃), 1.05–0.8 (m, 5H, CH₂CH₂, SiCH₂CH₃), 0.76–0.70 (m, 1H,

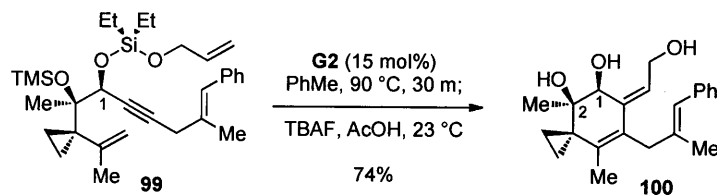
CH₂CH₂), 0.66-0.60 (m, 1H, CH₂CH₂), 0.41 (s, 9H, Si(CH₃)₃), 0.41 (s, 9H, Si(CH₃)₃*).

¹³C NMR (125.8 MHz, C₆D₆, 6:1 mixture of (1*S*)- and (1*R*)-diastereomers) δ: 148.1, 138.9, 137.9, 134.1, 129.5, 128.8, 127.1, 126.9, 118.6, 114.3, 84.0, 83.5, 79.9, 70.1, 64.2, 63.7, 34.2, 30.4, 24.1, 23.1, 18.2, 11.1, 10.3, 7.3, 7.2, 6.5, 5.6, 5.2, 3.4.

FTIR (neat) cm⁻¹: 2957 (m, C–H), 2229 (w, C≡C), 1635 (w), 1458 (w), 1415 (w), 1374 (w), 1248 (m), 1133 (m), 1064 (m), 922 (m), 839 (m).

HRMS (ESI): calcd for C₃₁H₄₈NaO₃Si₂ [M+Na]⁺: 547.3040, found: 547.3028

TLC (5% EtOAc in hexanes) R_f: 0.62 (UV, CAM, Anis)



(6Z)-(4R,5S)-6-(2-Hydroxy-ethylidene)-4,8-dimethyl-7-([E]-2-methyl-3-phenyl-allyl)-spiro[2.5]oct-7-ene-4,5-diol (100):

Trienyne **99** (435 mg, 0.830 mmol, 1 equiv, [1*S*:1*R*, 6:1]) was dried azeotropically by concentration from anhydrous benzene (3 × 1 mL). The residue was dissolved in toluene (83 mL), and the resulting solution deoxygenated by a stream of argon for 5 min. Grubbs' 1,3-dimesityl-4,5-dihydroimidazol-2-ylidene-tricyclohexylphosphine benzylidene ruthenium dichloride catalyst (**G2**, 106 mg, 0.124 mmol, 0.15 equiv) was added as a solid at 23 °C, the reaction vessel was purged quickly by a stream of argon, sealed, and the resulting dark-pink solution was stirred until complete dissolution occurred. The reaction mixture was heated to 90 °C by placement in a pre-heated oil bath. After 30 min, the metathesis catalyst was quenched by the addition of ethyl vinyl ether (4 mL). The resulting mixture was cooled to 23 °C, and was filtered through a plug of silica (diam. 4 cm, ht. 1.5 cm; hexanes-EtOAc 95:5). The filtrate was partially concentrated under reduced pressure (to ~5 mL) volume, and a mixture of TBAF (1M in THF, 3.32 mL, 3.32 mmol, 4.00 equiv) and acetic acid (95.0 μL, 1.66 mmol, 2.00 equiv) was slowly added at 23 °C under an argon atmosphere. After 2 h, the reaction mixture was diluted with saturated aqueous sodium bicarbonate solution (10 ml) and extracted with ethyl acetate (4 × 15 ml). The combined organic layers were dried over anhydrous sodium sulfate, and were concentrated under reduced pressure. Purification of the residue by flash column chromatography (silica gel: diam. 2.5 cm, ht. 2.5 cm; hexanes-EtOAc [1:1] to EtOAc-MeOH [99:1]) afforded the desired triol **100** (209 mg, 74%, [1*S*:1*R*, 6:1]) as a light brown oil.

¹H NMR (500 MHz, C₆D₆, 6:1 mixture of (1*S*)- and (1*R*)-diastereomers; minor (1*R*)-isomer denoted by *) δ: 7.27-7.22 (m, 2H, ArH), 7.26-7.00 (m, 5H, ArH*), 7.20-7.15 (m, 2H, ArH), 7.06-7.01 (m, 1H, ArH), 6.39 (s, 1H, PhCH=CH₂*), 6.31 (s, 1H, PhCH=CH₂), 5.97 (t, *J* = 7.0 Hz, 1H, C=CH*CH₂OH), 5.93 (t, *J* = 7.0 Hz, 1H, C=CHCH₂OH), 4.56 (s, 1H, CHOH*), 4.47 (s, 1H, CHOH), 4.36 (dd, *J* = 12.5, 7.6 Hz, 1H, CH₂OH), 4.22 (dd, *J* = 12.5, 7.6 Hz, 1H, CH₂OH*), 4.06 (dd, *J* = 12.8, 6.4 Hz, 1H, CH₂OH), 3.93 (dd, *J* = 12.8, 6.4 Hz, 1H, CH₂OH*), 3.40-3.28 (m, 3H, CH₂*OH), 3.12 (d, *J* = 17.7 Hz, 1H, CH₂), 3.03 (d, *J* = 17.7 Hz, 1H, CH₂), 2.96 (br-s, 1H, OH), 2.73 (br-s, 1H, OH), 1.72 (s, 3H, CH₃*), 1.79 (s, 3H, CH₃), 1.35-1.30 (m, 1H, CH₂CH₂), 1.28 (s, 3H, CH₃), 1.25 (s, 3H, CH₃), 1.16 (s, 3H, CH₃*), 1.13 (s, 3H, CH₃*), 0.96-0.90 (m, 1H, CH₂CH₂*), 0.88-0.83 (m, 1H, CH₂CH₂), 0.82-0.78 (m, 1H, CH₂CH₂*), 0.78-

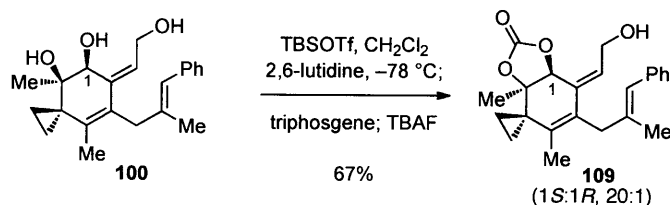
0.73 (m, 1H, CH₂CH₂), 0.72-0.65 (m, 1H, CH₂CH₂*), 0.61-0.56 (m, 1H, CH₂CH₂), 0.56-0.47 (m, 1H, CH₂CH₂*).

¹³C NMR (125.8 MHz, C₆D₆, 6:1 mixture of (1*S*)- and (1*R*)-diastereomers) δ: 141.2, 139.4, 138.8, 136.7, 129.6, 128.7, 126.7, 126.6, 126.6, 125.0, 72.9, 70.9, 58.9, 39.8, 28.4, 24.3, 18.9, 15.0, 10.2, 5.4.

FTIR (neat) cm⁻¹: 3385 (br-s, O-H), 2930 (m, C-H), 1724 (w), 1626 (w), 1597 (w), 1443 (m), 1377 (m), 1266 (m), 1173 (m).

HRMS (ESI): calcd for C₂₂H₂₈NaO₃ [M+Na]⁺: 363.1936, found: 363.1936.

TLC (1% MeOH in EtOAc) R_f: 0.40 (UV, CAM)



(6*Z*)-(4*R*,5*S*)-6-(2-Hydroxy-ethylidene)-4,8-dimethyl-7-([2*E*]-2-methyl-3-phenyl-allyl)-spiro[2.5]oct-7-ene-4,5-diol-carbonate (109):

A solution of *tert*-butyldimethylsilyl trifluoromethanesulfonate (TBSOTf, 91.9 μL , 0.40 mmol, 1.00 equiv) in dichloromethane (1 mL) was added dropwise via cannula transfer (down the side of the flask) to a solution of triol **100** (121 mg, 0.40 mmol, 1 equiv, [1*S*:1*R*, 6:1]), and 2,6-lutidine (269 μL , 2.40 mmol, 6.00 equiv) in dichloromethane (1 mL) at $-78\text{ }^\circ\text{C}$ under an argon atmosphere. During the addition, the progress of the silylation reaction was monitored by TLC analysis to ensure monosilylation of the starting triol **100**. After completion of the addition of TBSOTf, a solution of triphosgene (178 mg, 0.60 mmol, 1.50 equiv) in dichloromethane (200 μL) was added via cannula and the resulting reaction mixture was allowed to warm to $23\text{ }^\circ\text{C}$. After 3 h, the resulting dark-red mixture was cooled to $0\text{ }^\circ\text{C}$, treated with TBAF (1M in THF, 4.00 mL, 4.00 mmol, 10.0 equiv), and the resulting mixture was allowed to warm to $23\text{ }^\circ\text{C}$. After 12 h, the reaction mixture was diluted with saturated aqueous ammonium chloride solution (10 mL), and extracted with ethyl acetate ($3 \times 10\text{ mL}$). The combined organic layers were dried over anhydrous sodium sulfate, and were concentrated under reduced pressure. Purification of the residue by flash column chromatography (silica gel: diam. 3 cm, ht. 15 cm; hexanes-EtOAc [1:1]) afforded the desired carbonate **109** (98.6 mg, 67%, [1*S*:1*R*, 20:1]) as an oil. This step has not yet been optimized for the minor diastereomer, leading to enrichment of the major diastereomer in the product; this procedure has thus far been more practical rather than chromatographic separation of the diastereomers and their independent conversion to the corresponding carbonate.

$^1\text{H NMR}$ (500 MHz, C_6D_6 , 20:1 mixture of (1*S*)- and (1*R*)-diastereomers; minor (1*R*)-isomer denoted by *) δ : 7.20-7.10 (m, 4H, ArH), 7.19-7.00 (m, 5H, ArH*), 7.03-6.99 (m, 1H, ArH), 6.30 (s, 1H, PhCH=CH₂*), 6.08 (s, 1H, PhCH=CH₂), 5.95 (t, $J = 6.9\text{ Hz}$, 1H, C=CHCH₂OH), 5.67 (t, $J = 6.9\text{ Hz}$, 1H, C=CHCH₂OH*), 4.58 (s, 1H, CHO), 4.49 (s, 1H, CHOH*), 4.13-4.02 (m, 2H, CH₂OH), 3.99-3.95 (m, 2H, CH₂OH*), 3.19 (d, $J = 15.8\text{ Hz}$, 1H, CH₂*), 3.09 (d, $J = 15.8\text{ Hz}$, 1H, CH*), 2.89 (d, $J = 17.1\text{ Hz}$, 1H, CH₂), 2.80 (d, $J = 17.1\text{ Hz}$, 1H, CH₂), 1.62 (s, 3H, CH₃), 1.50 (s, 3H, CH₃*), 1.32 (br-s, 1H, OH), 1.15-1.09 (m, 1H, CH₂CH₂), 1.09 (s, 3H, CH₃), 0.99 (s, 3H, CH₃*), 0.92 (s, 3H, CH₃), 0.86 (s, 3H, CH₃*), 0.57-0.51 (m, 1H, CH₂CH₂), 0.50-0.44 (m, 1H, CH₂CH₂*), 0.41-0.35 (m, 1H, CH₂CH₂), 0.35-0.30 (m, 1H, CH₂CH₂*), 0.25-0.19 (m, 1H, CH₂CH₂), 0.18-0.12 (m, 1H, CH₂CH₂*).

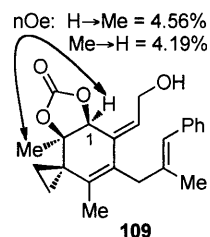
^{13}C NMR (125.8 MHz, C_6D_6 , 20:1 mixture of (1*S*)- and (1*R*)-diastereomers) δ : 154.4, 139.0, 138.8, 136.0, 135.9, 133.9, 133.5, 130.1, 129.7, 129.6, 129.5, 128.9, 128.7, 127.4, 127.1, 126.8, 125.6, 81.7, 80.3, 80.2, 59.9, 40.4, 32.9, 32.7, 30.5, 27.6, 23.5, 23.3, 22.9, 22.3, 22.2, 18.6, 16.0, 15.9, 14.7, 10.1, 9.9, 6.8, 6.7.

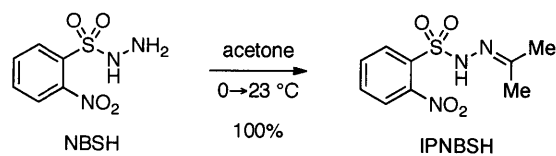
FTIR (neat) cm^{-1} : 3424 (br-m, O–H), 2923 (m, C–H), 1801 (s, C=O), 1653 (w), 1598 (w), 1444 (m), 1381 (m), 1245 (m), 1149 (m), 1024 (m).

HRMS (ESI): calcd for $\text{C}_{23}\text{H}_{26}\text{NaO}_4$ $[\text{M}+\text{Na}]^+$: 389.1723, found: 389.1732.

TLC (50% EtOAc in hexane) R_f : 0.30 (UV, Anis)

The C1-stereochemistry of the major diastereomer of **109** was secured by the following nOe data:





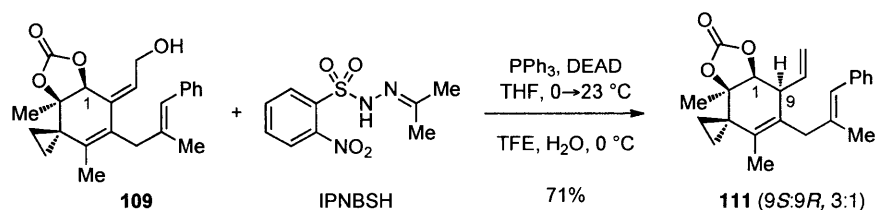
N-Isopropylidene-N'-2-nitrobenzenesulfonyl hydrazine (IPNBSH):

NBSH⁸ (601 mg, 2.77 mmol, 1 equiv) was dissolved in acetone (3.00 mL, 40.9 mmol, 14.7 equiv) and the mixture was stirred vigorously under argon at 0 °C for 1 h. The mixture was warmed to 23 °C and concentrated under reduced pressure to afford IPNBSH (712 mg, 100%)⁹ as a white solid.

¹ H NMR (500 MHz, CD ₃ CN) δ:	8.25 (br-s, 1H, NH), 8.10-8.06 (m, 1H, ArH), 7.86-7.78 (m, 3H, ArH), 1.87 (s, 3H, CH ₃), 1.86 (s, 3H, CH ₃)
¹³ C NMR (125.8 MHz, CD ₃ CN) δ:	160.3, 135.7, 133.6, 133.0, 132.1, 125.9, 120.4, 25.2, 17.7.
FTIR (neat) cm ⁻¹ :	3264 (m, N-H), 3093-2916 (w, C-H), 1550 (s, N=C), 1374 (m), 1177 (s).
HRMS (ESI):	calcd for C ₉ H ₁₂ N ₃ O ₄ S [M+H] ⁺ : 258.0543, found: 258.0546.
mp:	121-123 °C
TLC (hexanes:EtOAc 1:1) R _f :	0.50 (CAM)

⁸ For synthesis of NBSH see Myers, A. G.; Zheng, B.; Movassaghi, M. *J. Org. Chem.* **1997**, *62*, 7507.

⁹ For a prior discussion of IPNBSH, see: (a) Movassaghi, M. Ph.D. Dissertation, Harvard University (2001). For the evaluation of the scope of IPNBSH, and an updated protocol for the synthesis of IPNBSH see: (b) Movassaghi, M.; Ahmad, O. K. *J. Org. Chem.* **2007**, *72*, 1838. For use of IPNBSH in a stereospecific palladium-catalyzed route to monoalkyl diazenes, see: (c) Movassaghi, M.; Ahmad, O. K. *Angew. Chem. Int. Ed.* **2008**, *47*, 8909.



(4*R*,5*S*)-4,8-Dimethyl-7-([*2E*]-2-methyl-3-phenyl-allyl)-6-vinyl-spiro[2.5]oct-7-ene-4,5-diol-carbonate (111):

The alcohol **109** (20.0 mg, 0.054 mmol, 1 equiv, [1*S*:1*R*, 20:1]) was dried azeotropically by concentration from anhydrous benzene (3 × 1 mL). Triphenylphosphine (28.3 mg, 0.108 mmol, 2.00 equiv) and IPNBSH⁹ (27.8 mg, 0.108 mmol, 2.00 equiv) were added as solids, and the reaction vessel was sealed under an argon atmosphere. Anhydrous THF (540 μL , purged with a stream of argon for ~5 min) was added and the resulting solution was cooled to 0 °C prior to slow addition of diethyldiazocarbonylate (16.9 μL , 0.108 mmol, 2.00 equiv) via syringe. After 2 h, the reaction mixture was allowed to warm to 23 °C over 15 min. The mixture was then cooled to 0 °C and a mixture of trifluoroethanol and water (1:1, 1.08 mL, purged with a stream of argon for ~5 min) was added. After 14 h at 0 °C, the reaction mixture was warmed to 23 °C, was diluted with brine (10 mL), and the mixture was extracted with diethyl ether (3 × 5 mL). The combined organic extracts were dried over anhydrous sodium sulfate, were filtered, and were concentrated under reduced pressure. Purification of the residue by flash column chromatography (silica gel: diam. 1.5 cm, ht 5 cm; eluent: EtOAc:hexane [1:3]) provided triene **111** as a mixture of diastereomers (13.6 mg, 71%; [9*S*:9*R*, 3:1]). The C9-stereochemistry of the major diastereomer of **111** was secured using nOe data for a derivative (vide infra, carbonate **S7**).

¹H NMR (500 MHz, C₆D₆, ~3:1:0.1 mixture of three diastereomers (1*S*,9*S*:1*S*,9*R*:1*R* the minor (1*S*,9*R*)-diastereomer and the corresponding (1*R*)-diastereomer are noted as * and **, respectively) δ : 7.40-7.0 (m, 5H, ArH), 6.35 (s, 1H, PhCH**), 6.30 (s, 1H, PhCH*), 6.16 (s, 1H, PhCH), 6.03 (dt, $J = 16.9, 9.2$ Hz, 1H, CH=CH₂), 5.82 (dt, $J = 16.9, 9.2$ Hz, 1H, CH**=CH₂), 5.45 (dt, $J = 16.9, 9.2$ Hz, 1H, CH*=CH₂), 5.07-5.01 (m, 2H, CH=CH₂), 4.93-4.85 (m, 2H, CH=CH*₂), 4.84-4.62 (m, 2H, CH=CH**₂), 3.98 (d, $J = 5.3$ Hz, 1H, CHO), 3.95 (d, $J = 5.3$ Hz, 1H, CH*O), 3.86 (d, $J = 5.3$ Hz, 1H, CH**O), 3.22-3.18 (m, 1H, CH*CH=CH₂), 3.00 (dd, $J = 8.7, 6.3$ Hz, 1H, CHCH=CH₂), 2.94 (d, $J = 15.4$ Hz, 1H, CH*₂), 2.82 (d, $J = 15.4$ Hz, 1H, CH₂), 2.64 (d, $J = 15.5$ Hz, 1H, CH₂), 2.59 (d, $J = 15.5$ Hz, 1H, CH*₂), 1.81 (s, 3H, CH*₃), 1.62 (s, 3H, CH₃), 1.56 (s, 3H, CH**₃), 1.21 (s, 3H, CH*₃), 1.20 (s, 3H, CH₃), 1.10 (s, 3H, CH**₃), 0.95-0.90 (m, 1H, CH₂CH₂), 0.77 (s, 3H, CH**₃), 0.75 (s, 3H, CH₃), 0.73-0.66 (m, 2H, CH₂CH*₂), 0.64 (s, 3H,

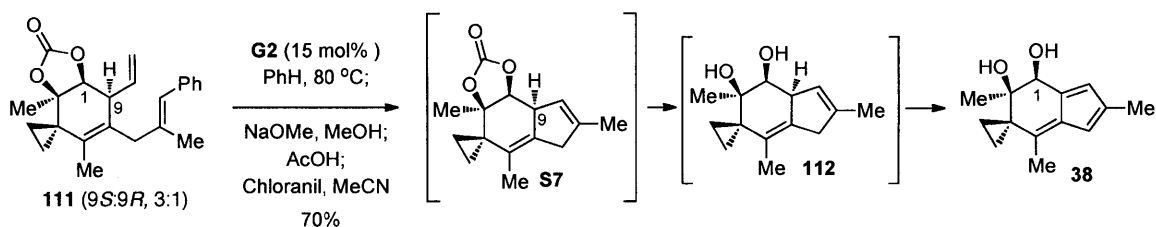
CH^{*}₃), 0.44-0.38 (m, 2H, CH₂CH₂), 0.35-0.29 (m, 1H, CH₂CH₂), 0.23-0.18 (m, 1H, CH₂CH^{**}₂), 0.10-0.04 (m, 1H, CH₂CH^{*}₂).

¹³C NMR (125.8 MHz, C₆D₆, ~3:1:0.1 mixture of three diastereomers) δ: 154.2, 154.0, 139.0, 136.4, 136.3, 134.5, 134.4, 133.3, 131.4, 130.8, 129.7, 129.6, 128.9, 128.8, 127.8, 126.9, 126.8, 118.9, 118.3, 86.1, 85.0, 83.9, 47.7, 47.5, 43.8, 42.1, 34.5, 28.4, 27.5, 25.3, 24.2, 23.8, 23.3, 18.5, 18.2, 15.7, 15.4, 11.9, 11.8, 10.8, 9.1, 8.8, 8.5.

FTIR (neat) cm⁻¹: 3080 (w, C–H), 2934 (w, C–H), 1798 (s, C=O), 1650 (w), 1598 (w), 1444 (w), 1381 (w), 1360 (w), 1238 (m), 1077 (m).

HRMS (ESI): calcd for C₂₃H₂₆NaO₃ [M+Na]⁺: 373.1780, found: 373.1776.

TLC (hexanes:EtOAc 3:1) R_f: 0.40 (Anis).

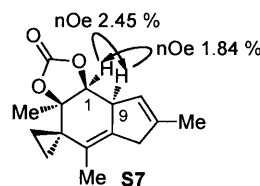


Fulvenediol 38:

The triene **111** (5.7 mg, 0.016 mmol, 1 equiv, [(1*S*,9*S*)-**111**:(1*S*,9*R*)-**111**:(1*R*)-**111**, 3:1:0.1]) was dried azeotropically by concentration from anhydrous benzene (3 × 1 mL). Benzene (320 μL) was added followed by **G2** (2.0 mg, 2.4 μmol, 0.15 equiv) at 23 °C, the mixture was sealed under an argon atmosphere, and the resulting dark-pink solution was heated to 80 °C. After 30 min, ethyl vinyl ether (0.1 mL) was introduced via a syringe, and the mixture was cooled to 23 °C. The resulting mixture was charged with a methanolic solution of sodium methoxide (1.0 M in MeOH, 33.0 μL, 0.033 mmol, 2.00 equiv) at 23 °C. After 24 h, conversion to diol **112** was complete by TLC analysis. Acetonitrile (600 μL) was added and the mixture was concentrated under reduced pressure to 30% of the total volume (ca. 300 μL). Acetic acid (1.72 μL, 0.033 mmol, 2.00 equiv) and chloranil (12.5 mg, 0.051 mmol, 3.00 equiv) were added sequentially, and the reaction mixture was stirred at 23 °C. After 13 h, saturated aqueous sodium thiosulfate solution (5 mL) was added and the reaction mixture was extracted with diethyl ether (4 × 5 mL), and the combined organic extracts were washed with saturated aqueous sodium bicarbonate solution (5 mL). The organic layer was dried over anhydrous sodium sulfate, was filtered, and was concentrated under reduced pressure. Purification of the residue by flash chromatography (silica gel: diam. 0.5 cm, ht 5 cm; eluent: EtOAc:hexane [1:3]) afforded the fulvenediol **38** (2.4 mg, 70%)¹⁰ as a yellow oil.

¹H NMR (500 MHz, CDCl₃) δ: 6.34 (br-s, 1H, CH=C), 6.08 (br-s, 1H, CH=C), 4.34 (d, *J* = 6.9 Hz, 1H, CHOH), 2.86 (br-s, 1H, OH), 2.07 (br-s, 3H, CH₃), 1.84 (s, 3H, CH₃), 1.61 (d, *J* = 7.7, 1H, OH), 1.28-1.22 (m, 1H, CH₂CH₂), 1.16 (s, 3H, CH₃), 1.05-1.00 (m, 1H, CH₂CH₂), 0.98-0.92 (m, 1H, CH₂CH₂), 0.87-0.82 (m, 1H, CH₂CH₂).

The C9-stereochemistry of the major diastereomer of substrates **111** and **112** was secured by the following nOe data with the sensitive intermediate **S7**:¹¹



¹⁰ The C1-diastereomers ((1*R*)-fulvenediol **38**) are chromatographically separable. Crude samples of fulvenediol **38** contain trace amounts of the 1*R*-diastereomer and the oxidation to acylfulvene can be performed on the mixture of these C1-diastereomers.

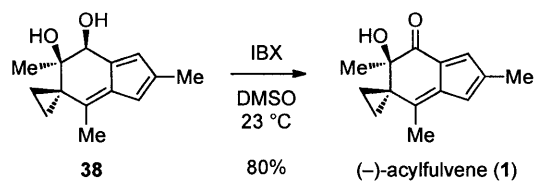
¹¹ For full characterization data see: Siegel, D. S.; Piizzi, G.; Piersanti, G.; Movassaghi, M. *J. Org. Chem.* **2009**, *74*, 9292.

^{13}C NMR (125.8 MHz, CDCl_3) δ : 151.2, 142.1, 138.8, 133.6, 131.4, 114.7, 73.5, 72.8, 30.5, 23.6, 16.6, 16.0, 13.3, 6.8.

FTIR (neat) cm^{-1} : 3421 (br-s, O-H), 2916 (s, C-H), 1630 (s), 1443 (m), 1376 (m), 1333 (m), 1114 (m).

HRMS (ESI): calcd for $\text{C}_{14}\text{H}_{18}\text{NaO}_2$ $[\text{M}+\text{Na}]^+$: 241.1199, found: 241.1206.

TLC (hexanes:EtOAc 1:1) R_f : 0.50 (CAM, UV).

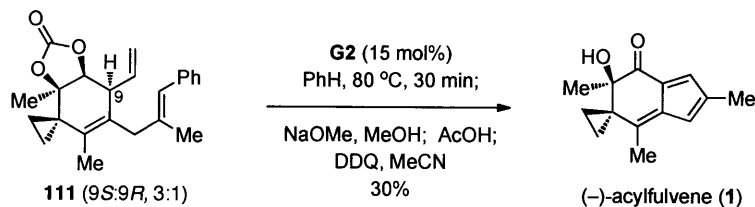


(-)-Acylfulvene (1):

The fulvenediol **38** (3.5 mg, 16 μmol , 1 equiv) was dried azeotropically by concentration from anhydrous benzene (3 \times 1 mL). Anhydrous DMSO (0.8 mL) was added followed by IBX (9.0 mg, 32 μmol , 2.0 equiv), and the resulting suspension was sealed under an argon atmosphere and stirred at 23 $^\circ\text{C}$. After 4 h, water was added (5 mL) followed by EtOAc (5 mL) and the layers were separated. The aqueous layer was extracted with EtOAc (3 \times 5 mL), and the combined organic layers were dried over anhydrous sodium sulfate, and were concentrated under reduced pressure to afford (-)-acylfulvene (**1**, 2.8 mg, 80%, 91% ee, $[\alpha]_D^{20} = -265.5$ (*c* 0.10, EtOH)) that had spectroscopic data consistent with those reported in the literature.¹² (-)-Acylfulvene (**1**) was determined to be 91% ee by chiral HPLC analysis [Chirapak AD-H; 1.0 mL/min; 10% $^i\text{PrOH}$ in hexanes; $t_R(\text{major}) = 8.30$ min, $t_R(\text{minor}) = 10.21$ min].

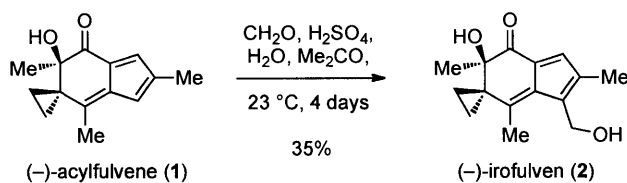
^1H NMR (400 MHz, CDCl_3) δ :	7.17 (br-s, 1H, $\text{CH}=\text{C}$), 6.43 (br-s, 1H, $\text{CH}=\text{C}$), 3.94 (br-s, 1H, OH), 2.16 (s, 3H, CH_3), 2.01 (s, 3H, CH_3), 1.57-1.52 (m, 1H, CH_2CH_2), 1.39 (s, 3H, CH_3), 1.33-1.29 (m, 1H, CH_2CH_2), 1.10-1.06 (m, 1H, CH_2CH_2), 0.75-0.71 (m, 1H, CH_2CH_2).
^{13}C NMR (100.6 MHz, CDCl_3) δ :	198.3, 159.1, 143.2, 141.2, 136.6, 127.0, 121.2, 77.0, 37.8, 28.3, 17.4, 15.7, 14.8, 10.2.
FTIR (neat) cm^{-1} :	3460 (br-m, O-H), 2918 (m, C-H), 1803 (w), 1667 (s, C=O), 1615 (s), 1490 (m), 1445 (m).
HRMS (ESI):	calcd for $\text{C}_{14}\text{H}_{16}\text{NaO}_2$ $[\text{M}+\text{Na}]^+$: 239.1043, found: 239.1044.
TLC (hexanes:EtOAc 1:1) R_f :	0.60 (CAM, UV)

¹² Our characterization data for acylfulvene was in agreement with those reported in McMorris, T. C.; Staake, M. D.; Kelner, M. J.; *J. Org. Chem.* **2004**, *69*, 619. For optical rotation values reported for (-)-acylfulvene, see: $[\alpha]_D^{25} = -493.4$ (*c* 2.1 mg/mL, EtOH) in McMorris, T. C.; Staake, M. D.; Kelner, M. J.; *J. Org. Chem.* **2004**, *69*, 619 (please see ref. 12 in this paper) and $[\alpha]_D^{25} = -606$ (*c* 0.078, EtOH) in McMorris, T. C.; Kelner, M. J.; Wang, W.; Diaz, M. A.; Estes, L. A.; Taetle, R. *Experientia*, **1996**, *52*, 75. Our measurements were conducted using absolute ethanol (Aldrich, 200 Proof 99.5%) and at 20 $^\circ\text{C}$ (pure samples, multiple readings). The enantiomeric excess of our synthetic (-)-acylfulvene was determined by HPLC analysis as described above.



(-)-Acylfulvene (1):

The triene **111** ([9S:9R, 3:1] 6.9 mg, 20 μmol , 1 equiv) was dried azeotropically by concentration from anhydrous benzene ($3 \times 1 \text{ mL}$). Benzene (400 μL) was added followed by **G2** (2.5 mg, 3.0 μmol , 0.15 equiv) at 23 °C, and the resulting dark-pink solution was sealed under an argon atmosphere and heated to 80 °C. After 30 min, the reaction ethyl vinyl ether (0.1 mL) was added via syringe, and the reaction mixture was cooled to 23 °C. The resulting mixture was charged with a methanolic solution of sodium methoxide (1.0 M in MeOH, 40.0 μL , 0.040 mmol, 2.00 equiv). After 24 h, acetonitrile (800 μL) was added and the mixture was concentrated to 30% of the total volume (ca. 400 μL). Acetic acid (1.72 μL , 0.033 mmol, 2.00 eq) and DDQ (13.6 mg, 0.060 mmol, 3.00 equiv) were added sequentially, and the reaction mixture was sealed under an argon atmosphere. After 13 h, a solution of ascorbic acid (7 mg), citric acid (12.6 mg), and sodium hydroxide (9.4 mg) in H₂O (1 mL) were added to quench the excess oxidant (DDQ). The reaction mixture was diluted with saturated aqueous sodium bicarbonate solution (5 mL), and the resulting mixture was extracted with hexanes ($4 \times 5 \text{ mL}$). The combined organic layers were dried over anhydrous sodium sulfate, were filtered, and were concentrated under reduced pressure. Purification of the residue by flash chromatography (silica gel: diam. 0.5 cm, ht 5 cm; eluent: EtOAc:hexane [1:4]) afforded (-)-acylfulvene (**1**, 1.4 mg, 30%, 91% ee) as a yellow oil. (-)-Acylfulvene (**1**) was determined to be 91% ee by chiral HPLC analysis [Chirapak AD-H; 1.0 mL/min; 10% *i*PrOH in hexanes; t_{R} (major) = 8.30 min, t_{R} (minor) = 10.21 min]. For full characterization of (-)-acylfulvene (**1**), see the complete set of data presented above for the two-step procedure.



(-)-Irofulven (2):

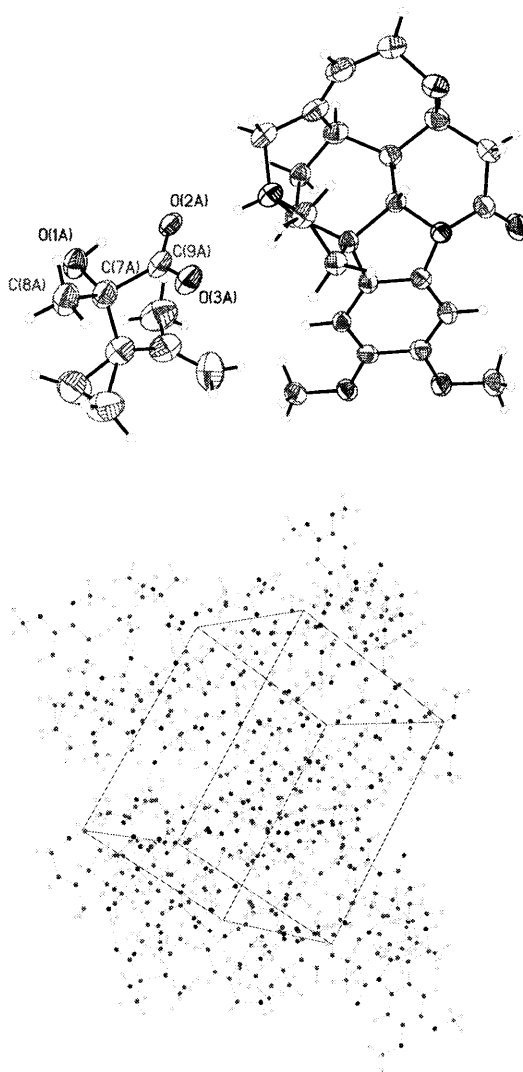
A solution of (-)-acylfulvene (**1**, 2.6 mg, 12 μmol , 1 equiv) in acetone (0.5 mL) was added to a solution of formaldehyde (37% wt. in H_2O , 35.0 μL , 0.44 mmol, 67.0 equiv) in a mixture of water (0.5 mL), acetone (1.0 mL), and aqueous hydrosulfuric acid (2.0 N, 0.5 mL) at 0 $^\circ\text{C}$. After 5 min, the reaction mixture was allowed to warm to 23 $^\circ\text{C}$. After 4 d, the reaction mixture was diluted with dichloromethane (5 mL), and saturated aqueous sodium bicarbonate solution (5 mL), and the layers were separated. The aqueous layer was extracted with dichloromethane (2 \times 5 mL), and the combined organic layers were washed sequentially with a saturated aqueous sodium bicarbonate solution (5 mL) and brine (5 mL). The organic layer was dried over anhydrous sodium sulfate, was filtered, and was further diluted by the addition of benzene (5 mL). The volatiles were removed and the total volume reduced (to approximately 1 mL) and the remaining orange solution was immediately¹³ purified by flash column chromatography (silica gel: diam. 1 cm, ht 5 cm; EtOAc-hexanes 1:1) to give (-)-irofulven (**4**, 1.1 mg, 35%, 92% ee, $[\alpha]_{\text{D}}^{20} = -512$ (c 0.03, EtOH)¹⁴) as an orange oil. Our synthetic (-)-irofulven (**4**) was determined to be 92% ee by chiral HPLC analysis [Chirapak AD-H; 1.5 mL/min; 20% i PrOH in hexanes; $t_{\text{R}}(\text{major}) = 4.88$ min, $t_{\text{R}}(\text{minor}) = 6.51$ min].

^1H NMR (400 MHz, CDCl_3) δ :	7.11 (br-s, 1H, $\text{CH}=\text{C}$), 4.66 (dd, $J = 11.6, 8.3$ Hz, 2H, CHOH), 3.91 (br-s, 1H, OH), 2.20 (s, 3H, CH_3), 2.16 (s, 3H, CH_3), 1.53-1.49 (m, 1H, CH_2CH_2), 1.39 (s, 3H, CH_3), 1.39-1.33 (m, 1H, CH_2CH_2), 1.11-1.07 (m, 1H, CH_2CH_2), 0.75-0.72 (m, 1H, CH_2CH_2).
^{13}C NMR (100.6 MHz, CDCl_3) δ :	198.3, 160.5, 142.4, 138.9, 135.0, 132.5, 127.1, 76.5, 56.6, 38.0, 27.8, 16.5, 14.6, 13.3, 9.8.
FTIR (neat) cm^{-1} :	3442 (br-m, O-H), 2920 (m, C-H), 1653 (m, C=O), 1593 (m), 1345 (m), 1280 (m).
HRMS (ESI):	calcd for $\text{C}_{15}\text{H}_{18}\text{O}_3$ $[\text{M}]^+$: 247.1329, found: 247.1331
TLC (hexanes:EtOAc 1:1) R_f :	0.38 (CAM, UV)

¹³ This is necessary to minimize bisacylfulvene formation; please see: Weinreb, S. M.; McMorris, T. C.; Anchel, M. *Tetrahedron Lett.* **1971**, 38, 3489 and McMorris, T. C.; Kelner, M. J.; Wang W.; Yu, J.; Estes, L. A.; Taetle, R. *J. Nat. Prod.* **1996**, 59, 896.

¹⁴ Our characterization data for irofulven was in agreement with those reported in McMorris, T. C.; Kelner, M. J.; Wang W.; Yu, J.; Estes, L. A.; Taetle, R. *J. Nat. Prod.* **1996**, 59, 896. For an optical rotation value reported for (-)-irofulven, see: $[\alpha]_{\text{D}}^{25} = -639$ (c 0.096, EtOH) in McMorris, T. C.; Kelner, M. J.; Wang W.; Yu, J.; Estes, L. A.; Taetle, R. *J. Nat. Prod.* **1996**, 59, 896. Our optical rotation measurements were conducted using absolute ethanol (Aldrich, 200 Proof 99.5%) and at 20 $^\circ\text{C}$ (pure samples, multiple readings). The enantiomeric excess of our synthetic (-)-irofulven was determined by HPLC analysis as described above.

Crystal Structure of (2*S*)-2-Hydroxy-2-(1-isopropenyl-cyclopropyl)-propionic acid-(*-*)-Brucine Complex.¹⁵



(2*S*)-2-Hydroxy-2-(1-isopropenyl-cyclopropyl)-propionic acid-(*-*)-Brucine Complex:

Lithium hydroxide (24 mg, 0.58 mmol, 5.0 equiv) was added to a solution of (*-*)-**87** (30 mg, 0.12 mmol, 1 equiv) in methanol (0.75 mL) and water (0.25 mL) at 23 °C. After 24 h, the volatiles were removed under reduced pressure and the resulting aqueous solution acidified to pH 3 by addition of aqueous hydrogen chloride solutions (1 N). The mixture was extracted with ethyl acetate (3 × 4 mL), and the combined organic layers were dried over anhydrous sodium sulfate and were concentrated under reduced pressure to afford (2*S*)-2-hydroxy-2-(1-isopropenyl-cyclopropyl)-propionic acid (**88**, 13.0 mg, 66%) as a white solid. (*-*)-Brucine (30 mg, 0.07 mmol, 1 eq) was added to a solution of (2*S*)-2-hydroxy-2-(1-isopropenyl-cyclopropyl)-propionic acid (**88**, 13.0 mg, 0.07 mmol, 1eq) in ethyl acetate (500 μ L). The resulting complex was crystallized by slow diffusion of hexanes into the ethyl acetate solution over 4 days at 23 °C.

¹⁵ Structural parameters for the carboxylic acid, **88**, salt with (*-*)-brucine are freely available from the Cambridge Crystallographic Data Center under CCDC-622286.

Table S1. Crystal data and structure refinement.

Identification code	05204	
Empirical formula	C ₃₂ H ₄₀ N ₂ O ₇	
Formula weight	564.66	
Temperature	100(2) K	
Wavelength	0.71073 Å	
Crystal system	Orthorhombic	
Space group	P2(1)2(1)2(1)	
Unit cell dimensions	a = 12.4406(13) Å	a = 90°.
	b = 13.6892(15) Å	b = 90°.
	c = 16.1340(17) Å	g = 90°.
Volume	2747.7(5) Å ³	
Z	4	
Density (calculated)	1.365 Mg/m ³	
Absorption coefficient	0.096 mm ⁻¹	
F(000)	1208	
Crystal size	0.30 x 0.25 x 0.20 mm ³	
Theta range for data collection	1.95 to 25.02°.	
Index ranges	-14<=h<=14, -16<=k<=16, -19<=l<=19	
Reflections collected	43545	
Independent reflections	2742 [R(int) = 0.0711]	
Completeness to theta = 25.02°	100.0 %	
Absorption correction	Semi-empirical from equivalents	
Max. and min. transmission	0.9810 and 0.9718	
Refinement method	Full-matrix least-squares on F ²	
Data / restraints / parameters	2742 / 409 / 456	
Goodness-of-fit on F ²	1.085	
Final R indices [I>2sigma(I)]	R1 = 0.0580, wR2 = 0.1512	
R indices (all data)	R1 = 0.0729, wR2 = 0.1677	
Absolute structure parameter	0(2)	
Largest diff. peak and hole	0.315 and -0.305 e.Å ⁻³	

Table S2. Atomic coordinates (x 10⁴) and equivalent isotropic displacement parameters (Å²x 10³). U(eq) is defined as one third of the trace of the orthogonalized U^{ij} tensor.

	x	y	z	U(eq)
N(1)	9473(3)	6082(3)	-2842(2)	35(1)
N(2)	10377(3)	6501(3)	-100(2)	30(1)
O(4)	12864(3)	5655(3)	-1324(2)	53(1)
O(5)	11097(3)	6283(3)	1188(2)	52(1)
O(6)	7161(2)	6624(3)	1702(2)	41(1)
O(7)	5981(2)	6243(2)	429(2)	35(1)
C(10)	9832(4)	7101(3)	-2656(3)	36(1)
C(11)	9278(4)	7360(3)	-1851(3)	31(1)
C(12)	9336(3)	6396(3)	-1356(2)	28(1)
C(13)	9040(4)	5636(3)	-2037(2)	30(1)
C(14)	9483(4)	4617(3)	-1903(3)	37(1)
C(15)	10718(4)	4687(3)	-1839(3)	41(1)
C(16)	11164(4)	5174(4)	-2606(3)	43(1)
C(17)	10339(4)	5470(4)	-3243(3)	41(1)
C(18)	12203(4)	5326(4)	-2707(4)	54(1)

C(19)	13005(5)	5051(5)	-2058(4)	64(2)
C(20)	10961(4)	5217(3)	-1021(3)	34(1)
C(21)	12135(4)	5262(4)	-731(3)	42(1)
C(22)	12226(3)	5957(4)	20(3)	38(1)
C(23)	11193(3)	6252(3)	433(3)	37(1)
C(24)	10490(3)	6250(3)	-992(2)	29(1)
C(25)	9267(3)	6519(3)	112(3)	30(1)
C(26)	8643(3)	6380(3)	-590(2)	28(1)
C(27)	7527(3)	6299(3)	-513(3)	29(1)
C(28)	7058(3)	6346(3)	264(3)	31(1)
C(29)	7714(4)	6538(3)	964(3)	33(1)
C(30)	8815(4)	6620(3)	891(3)	34(1)
C(31)	5311(3)	6010(4)	-250(3)	44(1)
C(32)	7805(4)	6867(5)	2409(3)	55(1)
C(1A)	5708(9)	5576(7)	-3063(6)	79(3)
C(2A)	5716(7)	6631(6)	-3133(5)	61(2)
C(3A)	5941(11)	7234(9)	-2519(7)	72(3)
C(5A)	4474(7)	7101(8)	-4286(7)	75(2)
C(6A)	4969(8)	8037(6)	-4086(6)	73(2)
C(4A)	5614(7)	7092(7)	-3969(5)	57(1)
C(7A)	6528(7)	6832(6)	-4593(5)	47(1)
O(1A)	6351(5)	5865(4)	-4901(3)	45(1)
C(8A)	6566(7)	7506(6)	-5339(4)	52(2)
C(9A)	7602(9)	6885(6)	-4123(8)	40(1)
O(2A)	8042(6)	6065(6)	-3985(4)	38(1)
O(3A)	7974(11)	7697(7)	-3939(8)	46(2)
C(1B)	5740(40)	6970(20)	-2524(16)	70(5)
C(2B)	5582(18)	7480(13)	-3296(11)	61(2)
C(3B)	5200(20)	8377(14)	-3388(17)	71(5)
C(5B)	4474(18)	6637(17)	-4436(17)	69(3)
C(6B)	4967(18)	5866(14)	-3945(15)	68(3)
C(4B)	5555(16)	6870(16)	-4052(11)	57(2)
C(7B)	6546(15)	6975(13)	-4633(11)	47(1)
O(1B)	6622(13)	6180(10)	-5207(9)	45(1)
C(8B)	6550(20)	7916(14)	-5138(13)	52(2)
C(9B)	7570(20)	7000(18)	-4090(20)	40(1)
O(2B)	7830(20)	6166(18)	-3806(14)	38(1)
O(3B)	7880(30)	7790(20)	-3800(30)	46(2)

Table S3. Bond lengths [Å] and angles [°].

N(1)-C(10)	1.496(6)	C(10)-C(11)	1.513(6)
N(1)-C(17)	1.510(6)	C(11)-C(12)	1.544(5)
N(1)-C(13)	1.532(5)	C(12)-C(26)	1.506(6)
N(2)-C(23)	1.373(6)	C(12)-C(13)	1.558(5)
N(2)-C(25)	1.423(5)	C(12)-C(24)	1.563(6)
N(2)-C(24)	1.487(5)	C(13)-C(14)	1.515(6)
O(4)-C(21)	1.423(6)	C(14)-C(15)	1.544(6)
O(4)-C(19)	1.456(6)	C(15)-C(16)	1.512(7)
O(5)-C(23)	1.224(6)	C(15)-C(20)	1.536(6)
O(6)-C(29)	1.380(5)	C(16)-C(18)	1.319(7)
O(6)-C(32)	1.433(6)	C(16)-C(17)	1.508(7)
O(7)-C(28)	1.374(5)	C(18)-C(19)	1.494(8)
O(7)-C(31)	1.413(5)	C(20)-C(24)	1.532(6)

C(20)-C(21)	1.535(7)	C(20)-C(15)-C(14)	106.4(4)
C(21)-C(22)	1.544(7)	C(18)-C(16)-C(17)	122.8(5)
C(22)-C(23)	1.503(6)	C(18)-C(16)-C(15)	122.0(5)
C(25)-C(30)	1.384(6)	C(17)-C(16)-C(15)	115.2(4)
C(25)-C(26)	1.386(6)	C(16)-C(17)-N(1)	110.0(4)
C(26)-C(27)	1.399(6)	C(16)-C(18)-C(19)	121.9(6)
C(27)-C(28)	1.383(6)	O(4)-C(19)-C(18)	110.3(4)
C(28)-C(29)	1.418(6)	C(24)-C(20)-C(21)	108.5(4)
C(29)-C(30)	1.379(6)	C(24)-C(20)-C(15)	112.8(4)
C(1A)-C(2A)	1.449(13)	C(21)-C(20)-C(15)	117.9(4)
C(2A)-C(3A)	1.319(14)	O(4)-C(21)-C(20)	114.6(4)
C(2A)-C(4A)	1.495(12)	O(4)-C(21)-C(22)	104.3(4)
C(5A)-C(6A)	1.458(13)	C(20)-C(21)-C(22)	109.5(4)
C(5A)-C(4A)	1.508(11)	C(23)-C(22)-C(21)	116.8(4)
C(6A)-C(4A)	1.534(12)	O(5)-C(23)-N(2)	122.8(4)
C(4A)-C(7A)	1.561(9)	O(5)-C(23)-C(22)	122.3(4)
C(7A)-O(1A)	1.431(8)	N(2)-C(23)-C(22)	114.9(4)
C(7A)-C(8A)	1.516(9)	N(2)-C(24)-C(20)	106.2(3)
C(7A)-C(9A)	1.538(9)	N(2)-C(24)-C(12)	104.3(3)
C(9A)-O(3A)	1.239(8)	C(20)-C(24)-C(12)	117.2(3)
C(9A)-O(2A)	1.270(8)	C(30)-C(25)-C(26)	122.0(4)
C(1B)-C(2B)	1.44(2)	C(30)-C(25)-N(2)	127.8(4)
C(2B)-C(3B)	1.326(19)	C(26)-C(25)-N(2)	110.2(4)
C(2B)-C(4B)	1.479(17)	C(25)-C(26)-C(27)	119.5(4)
C(5B)-C(6B)	1.45(2)	C(25)-C(26)-C(12)	110.4(3)
C(5B)-C(4B)	1.514(17)	C(27)-C(26)-C(12)	130.0(4)
C(6B)-C(4B)	1.57(2)	C(28)-C(27)-C(26)	119.8(4)
C(4B)-C(7B)	1.556(15)	O(7)-C(28)-C(27)	125.6(4)
C(7B)-O(1B)	1.432(15)	O(7)-C(28)-C(29)	115.2(4)
C(7B)-C(8B)	1.524(16)	C(27)-C(28)-C(29)	119.2(4)
C(7B)-C(9B)	1.543(15)	C(30)-C(29)-O(6)	124.2(4)
C(9B)-O(3B)	1.247(15)	C(30)-C(29)-C(28)	121.3(4)
C(9B)-O(2B)	1.274(16)	O(6)-C(29)-C(28)	114.6(4)
C(10)-N(1)-C(17)	113.0(4)	C(29)-C(30)-C(25)	118.2(4)
C(10)-N(1)-C(13)	107.8(3)	C(3A)-C(2A)-C(1A)	124.6(9)
C(17)-N(1)-C(13)	113.1(3)	C(3A)-C(2A)-C(4A)	115.5(8)
C(23)-N(2)-C(25)	124.9(4)	C(1A)-C(2A)-C(4A)	119.4(8)
C(23)-N(2)-C(24)	118.6(4)	C(6A)-C(5A)-C(4A)	62.3(6)
C(25)-N(2)-C(24)	109.1(3)	C(5A)-C(6A)-C(4A)	60.5(5)
C(21)-O(4)-C(19)	114.1(4)	C(2A)-C(4A)-C(5A)	113.0(7)
C(29)-O(6)-C(32)	115.3(3)	C(2A)-C(4A)-C(6A)	120.8(7)
C(28)-O(7)-C(31)	116.6(3)	C(5A)-C(4A)-C(6A)	57.3(6)
N(1)-C(10)-C(11)	104.8(3)	C(2A)-C(4A)-C(7A)	115.1(7)
C(10)-C(11)-C(12)	102.9(3)	C(5A)-C(4A)-C(7A)	117.9(7)
C(26)-C(12)-C(11)	114.2(3)	C(6A)-C(4A)-C(7A)	119.6(7)
C(26)-C(12)-C(13)	115.7(3)	O(1A)-C(7A)-C(8A)	107.0(6)
C(11)-C(12)-C(13)	101.2(3)	O(1A)-C(7A)-C(9A)	110.4(6)
C(26)-C(12)-C(24)	102.5(3)	C(8A)-C(7A)-C(9A)	109.6(7)
C(11)-C(12)-C(24)	110.3(3)	O(1A)-C(7A)-C(4A)	108.8(6)
C(13)-C(12)-C(24)	113.4(3)	C(8A)-C(7A)-C(4A)	113.3(7)
C(14)-C(13)-N(1)	111.1(4)	C(9A)-C(7A)-C(4A)	107.7(7)
C(14)-C(13)-C(12)	115.3(3)	O(3A)-C(9A)-O(2A)	126.1(8)
N(1)-C(13)-C(12)	104.4(3)	O(3A)-C(9A)-C(7A)	119.0(8)
C(13)-C(14)-C(15)	108.3(4)	O(2A)-C(9A)-C(7A)	114.8(6)
C(16)-C(15)-C(20)	115.0(4)	C(3B)-C(2B)-C(1B)	127(2)
C(16)-C(15)-C(14)	109.7(4)	C(3B)-C(2B)-C(4B)	115.0(17)

C(1B)-C(2B)-C(4B)	116.2(18)	C(8B)-C(7B)-C(9B)	106.4(15)
C(6B)-C(5B)-C(4B)	63.7(10)	O(1B)-C(7B)-C(4B)	111.8(14)
C(5B)-C(6B)-C(4B)	60.0(9)	C(8B)-C(7B)-C(4B)	113.7(16)
C(2B)-C(4B)-C(5B)	118.5(16)	C(9B)-C(7B)-C(4B)	108.2(17)
C(2B)-C(4B)-C(7B)	115.3(14)	O(3B)-C(9B)-O(2B)	124(2)
C(5B)-C(4B)-C(7B)	118.5(16)	O(3B)-C(9B)-C(7B)	120(2)
C(2B)-C(4B)-C(6B)	114.5(15)	O(2B)-C(9B)-C(7B)	113.3(17)
C(5B)-C(4B)-C(6B)	56.3(9)		
C(7B)-C(4B)-C(6B)	121.2(16)		
O(1B)-C(7B)-C(8B)	107.3(14)	Symmetry transformations used to generate equivalent atom	
O(1B)-C(7B)-C(9B)	109.3(15)		

Table S4. Anisotropic displacement parameters ($\text{\AA}^2 \times 10^3$). The anisotropic displacement factor exponent takes the form: $-2p^2 [h^2 a^{*2} U^{11} + \dots + 2 h k a^* b^* U^{12}]$

	U^{11}	U^{22}	U^{33}	U^{23}	U^{13}	U^{12}
N(1)	45(2)	30(2)	31(2)	1(2)	4(2)	0(2)
N(2)	30(2)	29(2)	32(2)	-2(2)	-1(2)	1(1)
O(4)	33(2)	69(2)	57(2)	-15(2)	5(2)	0(2)
O(5)	40(2)	82(3)	33(2)	-2(2)	-7(2)	3(2)
O(6)	33(2)	60(2)	30(2)	-6(1)	2(1)	0(2)
O(7)	28(1)	41(2)	38(2)	0(2)	-2(1)	-1(1)
C(10)	47(3)	28(2)	32(2)	1(2)	0(2)	-2(2)
C(11)	37(2)	23(2)	33(2)	3(2)	-4(2)	-1(2)
C(12)	31(2)	24(2)	30(2)	-1(2)	-3(2)	-2(2)
C(13)	35(2)	26(2)	29(2)	-1(2)	-2(2)	-2(2)
C(14)	47(3)	27(2)	36(2)	-5(2)	-5(2)	-1(2)
C(15)	46(3)	30(2)	46(3)	-5(2)	0(2)	6(2)
C(16)	50(3)	38(2)	41(3)	-12(2)	7(2)	4(2)
C(17)	51(3)	36(2)	35(2)	-6(2)	7(2)	-1(2)
C(18)	51(3)	60(3)	52(3)	-18(3)	12(3)	1(3)
C(19)	43(3)	90(5)	58(4)	-25(3)	8(3)	9(3)
C(20)	36(2)	26(2)	41(2)	-2(2)	-3(2)	3(2)
C(21)	38(2)	38(2)	50(3)	0(2)	-4(2)	6(2)
C(22)	29(2)	41(2)	42(3)	5(2)	-4(2)	-1(2)
C(23)	32(2)	38(2)	40(3)	0(2)	-6(2)	1(2)
C(24)	31(2)	26(2)	29(2)	-2(2)	-1(2)	1(2)
C(25)	29(2)	26(2)	36(2)	0(2)	-3(2)	-2(2)
C(26)	32(2)	23(2)	29(2)	0(2)	-4(2)	0(2)
C(27)	31(2)	25(2)	30(2)	-2(2)	-6(2)	1(2)
C(28)	27(2)	27(2)	39(2)	-2(2)	2(2)	1(2)
C(29)	35(2)	32(2)	33(2)	0(2)	1(2)	2(2)
C(30)	34(2)	37(2)	29(2)	0(2)	-5(2)	1(2)
C(31)	26(2)	59(3)	45(3)	-6(2)	0(2)	0(2)
C(32)	41(3)	91(4)	32(2)	-9(3)	-2(2)	1(3)
C(1A)	99(7)	66(4)	71(5)	5(4)	24(5)	3(5)
C(2A)	62(4)	61(3)	58(3)	-6(3)	13(3)	1(3)
C(3A)	76(7)	75(5)	64(4)	-2(4)	-14(5)	-19(5)
C(5A)	66(3)	80(4)	79(4)	2(4)	-3(3)	7(4)
C(6A)	83(4)	66(4)	71(4)	-2(3)	15(4)	15(3)
C(4A)	59(3)	57(3)	55(3)	-10(2)	0(2)	4(3)
C(7A)	61(2)	40(2)	38(2)	-5(2)	-6(2)	5(2)
O(1A)	60(3)	36(2)	39(3)	-2(2)	-8(2)	-5(2)
C(8A)	76(4)	38(3)	42(3)	-2(3)	-12(3)	3(4)

C(9A)	56(2)	37(2)	28(2)	-7(2)	1(2)	0(2)
O(2A)	48(4)	36(2)	28(3)	-10(2)	2(2)	5(2)
O(3A)	66(3)	36(2)	35(5)	-6(2)	0(3)	2(2)
C(1B)	77(11)	79(11)	54(5)	2(7)	19(9)	-14(10)
C(2B)	66(5)	59(5)	59(4)	-9(4)	7(4)	3(4)
C(3B)	68(10)	59(7)	87(11)	-20(6)	-19(10)	4(8)
C(5B)	65(4)	68(7)	75(6)	-9(6)	-11(5)	2(6)
C(6B)	65(7)	65(6)	72(7)	-5(5)	-12(6)	-8(5)
C(4B)	58(3)	57(4)	57(3)	-6(3)	-2(3)	4(4)
C(7B)	61(2)	40(2)	38(2)	-5(2)	-6(2)	5(2)
O(1B)	60(3)	36(2)	39(3)	-2(2)	-8(2)	-5(2)
C(8B)	76(4)	38(3)	42(3)	-2(3)	-12(3)	3(4)
C(9B)	56(2)	37(2)	28(2)	-7(2)	1(2)	0(2)
O(2B)	48(4)	36(2)	28(3)	-10(2)	2(2)	5(2)
O(3B)	66(3)	36(2)	35(5)	-6(2)	0(3)	2(2)

Table S5. Hydrogen coordinates ($\times 10^4$) and isotropic displacement parameters ($\text{\AA}^2 \times 10^3$) for.

	x	y	z	U(eq)
H(1N)	8940(30)	6160(40)	-3190(20)	42
H(10A)	9614	7554	-3104	43
H(10B)	10623	7130	-2592	43
H(11A)	8523	7559	-1947	37
H(11B)	9660	7893	-1559	37
H(13)	8239	5595	-2077	36
H(14A)	9279	4189	-2372	44
H(14B)	9183	4335	-1388	44
H(15)	11018	4010	-1804	49
H(17A)	10014	4879	-3493	49
H(17B)	10690	5848	-3690	49
H(18)	12449	5619	-3206	65
H(19A)	12912	4354	-1909	77
H(19B)	13741	5138	-2279	77
H(20)	10570	4841	-583	41
H(21)	12378	4593	-566	50
H(22A)	12688	5640	440	45
H(22B)	12599	6557	-165	45
H(24)	10998	6718	-1263	34
H(27)	7093	6211	-991	35
H(30)	9251	6743	1363	40
H(31A)	5337	6540	-658	65
H(31B)	4570	5925	-56	65
H(31C)	5560	5402	-508	65
H(32A)	8312	6336	2520	82
H(32B)	7339	6962	2892	82
H(32C)	8204	7471	2297	82
H(1A1)	6406	5316	-3237	118
H(1A2)	5142	5307	-3419	118
H(1A3)	5570	5390	-2486	118
H(3A1)	6113	6983	-1987	86
H(3A2)	5931	7920	-2610	86
H(5A1)	4360	6948	-4880	90
H(5A2)	3905	6858	-3911	90

H(6A1)	4716	8380	-3582	88
H(6A2)	5171	8470	-4551	88
H(10A)	6870(50)	5620(50)	-4630(40)	54
H(8A1)	7166	7317	-5698	78
H(8A2)	6666	8181	-5152	78
H(8A3)	5890	7454	-5648	78
H(1B1)	5490	7378	-2065	105
H(1B2)	6507	6827	-2452	105
H(1B3)	5334	6357	-2532	105
H(3B1)	4998	8748	-2915	86
H(3B2)	5125	8649	-3927	86
H(5B1)	3835	6966	-4200	83
H(5B2)	4450	6544	-5044	83
H(6B1)	5264	5294	-4244	81
H(6B2)	4648	5717	-3397	81
H(10B)	7210(70)	6050(160)	-4950(40)	54
H(8B1)	5904	7942	-5485	78
H(8B2)	7190	7933	-5491	78
H(8B3)	6557	8478	-4762	78

Chapter II.

Total Synthesis of the (–)-Agelastatin Alkaloids

Introduction and Background

The agelastatin alkaloids constitute an intriguing subset of the diverse pyrrole-imidazole family of marine alkaloids that are likely derived from the linear biogenetic precursors oroidin¹ (7), hymenidin² (8), and clathrocin³ (9, Figure 1). (-)-Agelastatins A (1) and B (2) were first isolated in 1993 from the Coral Sea sponge *Agelas dendromorpha* by Pietra, who successfully identified and chemically examined their unique tetracyclic structures.⁴ In 1998, Molinski isolated (-)-agelastatins C (3) and D (4) from the *Cymbastela* sp. of sponges native to the Indian Ocean.⁵ Recently, Al-Mourabit has reported the isolation of (-)-agelastatins E (5) and F (6) from the New Caledonian sponge *Agelas dendromorpha*.⁶ (-)-Agelastatin A (1) exhibits significant antitumor activity and inhibits osteopontin-mediated neoplastic transformation and metastasis in addition to slowing cancer cell proliferation by causing cells to accumulate in the G₂ phase of the cell cycle.⁷ (-)-Agelastatin A (1) also exhibits toxicity towards arthropods⁵ and selectively inhibits the glycogen synthase kinase-3 β , which is a potential target for the treatment of Alzheimer's disease and bipolar disorder.^{8,9}

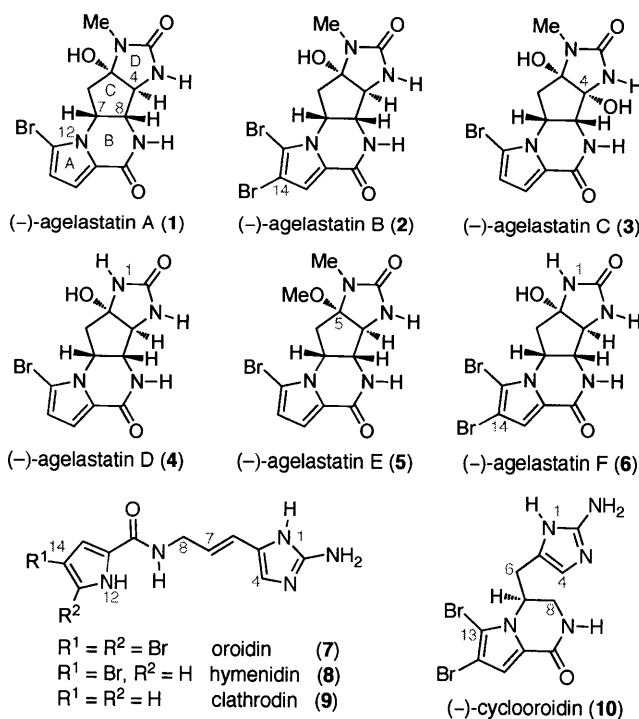
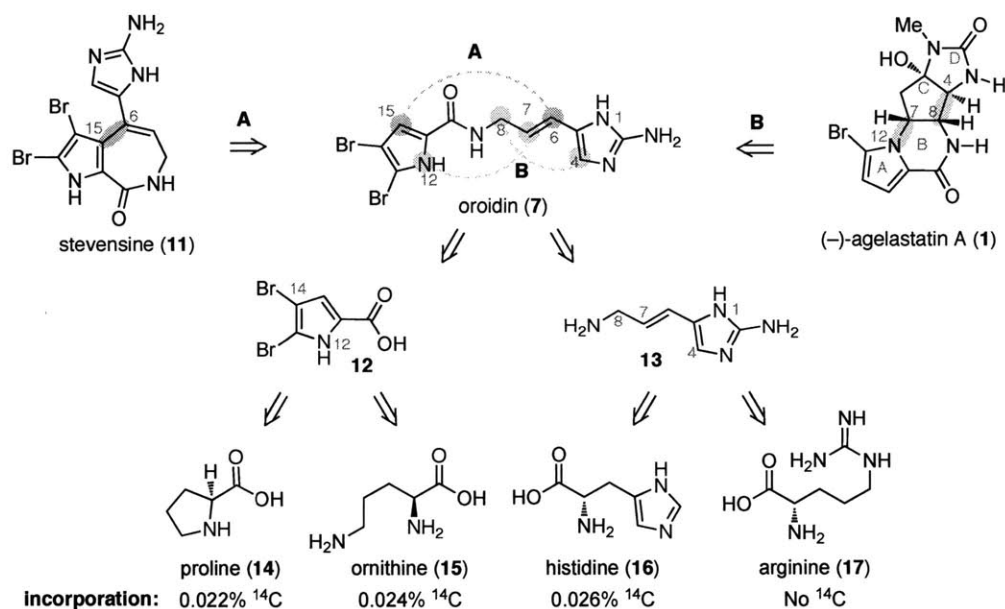


Figure 1. The molecular structures of all agelastatin alkaloids (1-6) and biogenetically related naturally occurring simple pyrrole-imidazole alkaloids (7-10).

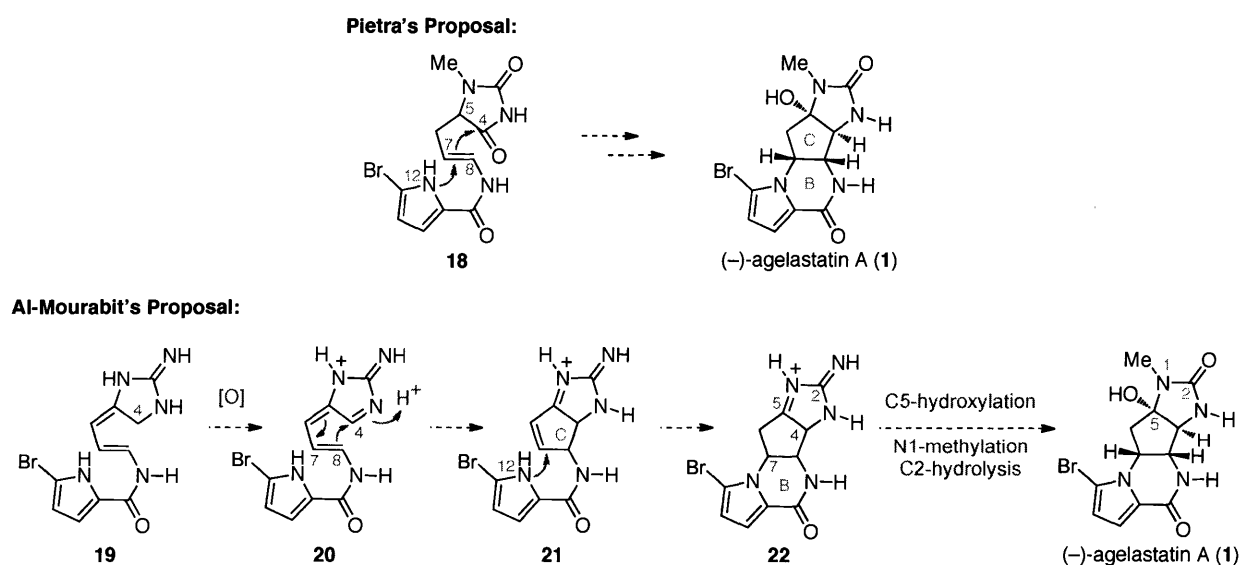
Investigations toward elucidating the metabolic pathways for the biogenesis of the diverse pyrrole-imidazole alkaloids have been limited due to the difficulty of establishing continuous cell lines of the marine invertebrates. However, Kerr has established primary cultures of the marine sponge *Teichaxinella morchella* and through feeding studies has demonstrated that histidine and ornithine (or proline) are the amino acid precursors for the related alkaloid stevensine (**11**, Scheme 1, Path A).¹⁰ This analysis suggests that stevensine (**11**) is derived from cyclization of the linear precursor oroidin (**7**) to afford the C6–C15 linkage. Oroidin (**7**) is likely derived from the condensation of dibromopyrrole **12** and aminoimidazole **13**. The dibromopyrrole **12** is derived from ornithine (**15**) or proline (**14**), and the aminoimidazole **13** is generated from histidine (**16**) through a sequence involving oxidative deamination, carboxylate reduction, and amination reactions. In addition to the feeding studies, this pathway is supported by the co-occurrence of **11**, **12**, and **13** in *Teichaxinella morchella*. Consequently, it is plausible that the marine sponge derived pyrrole-imidazole natural products, including the agelastatin alkaloids (Scheme 1, Path B), are biogenetically linked to similar precursors.¹¹



Scheme 1. Kerr's feeding studies that elucidate a plausible biosynthetic pathway for stevensine (**11**).

To date, the agelastatins are the only isolated pyrrole-imidazole alkaloids with C4–C8 and C7–N12 connectivities. There are currently two biosynthetic hypotheses for the formation of

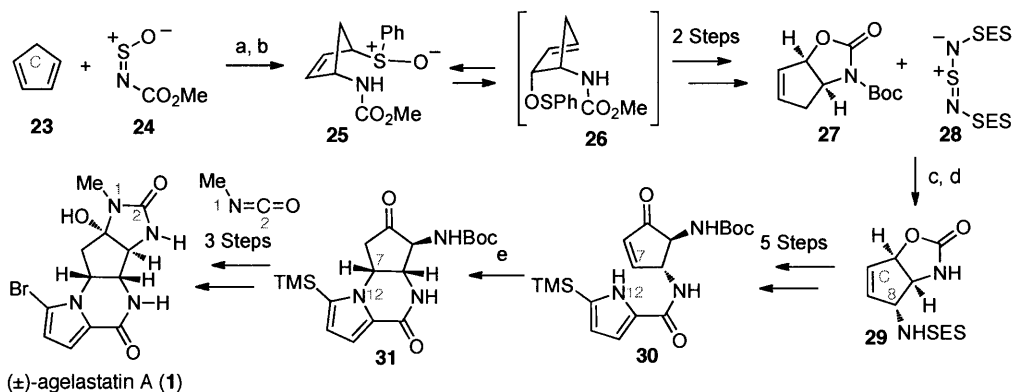
the agelastatins (Scheme 2).^{4a,11} Pietra has advanced the hypothesis that the linear precursor **18** undergoes an enzyme driven C8-attack of the C4-hydantoin followed by N12-addition to the C7-electrophile to afford the BC-ring system. Refunctionalization at the C4- and C5-centers then provides (-)-agelastatin A (**1**). Alternatively, Al-Mourabit has proposed that the linear aminoimidazole **19** initially undergoes C4-oxidation, which then proceeds through a Nazarov type cyclization to afford the C-ring **21** (Scheme 2). Conjugate addition of the pyrrolyl nitrogen to the C7-electrophile affords the B-ring **22**, which undergoes further elaboration to (-)-agelastatin A (**1**). Notably, both hypotheses suggest that the formation of the all carbon C-ring results from C8-nucleophilic trapping of a C4-electrophile. Furthermore, they suggest the formation of the C-ring prior to the B-ring and attribute stereochemical control to the action of biosynthetic enzymes.



Scheme 2. Previously reported biosynthetic pathways for the formation of (-)-agelastatin A (**1**).

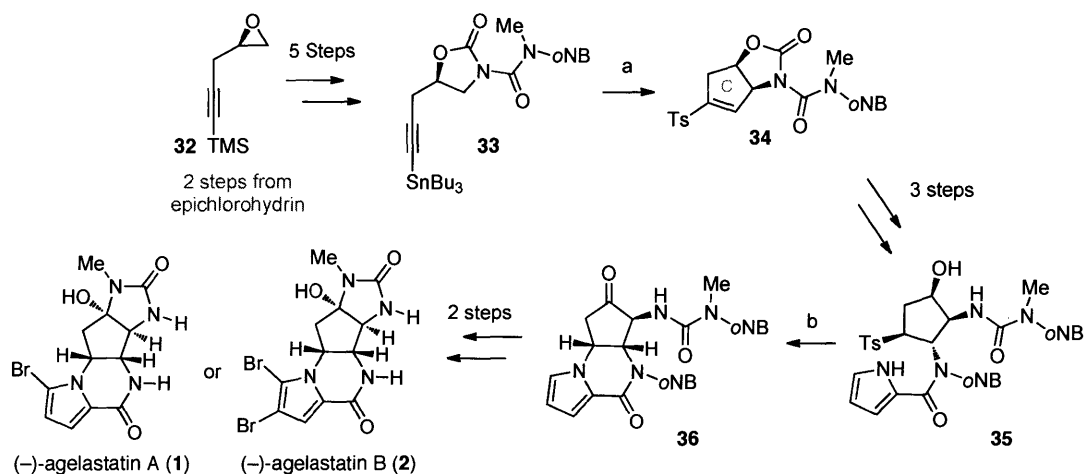
Review of Prior Syntheses of the Agelastatin Alkaloids. The remarkable biological activity and interesting molecular architecture of the agelastatins have prompted considerable efforts toward their total synthesis from 10 different research groups.¹² In 1999, Weinreb completed the first synthesis of racemic agelastatin A (**1**, Scheme 3).¹³ The hetero-Diels-Alder cycloaddition of cyclopentadiene (**23**) with *N*-sulfinyl methyl carbamate **24** afforded the equilibrium mixture **25** and **26**, which was carried on to the bicyclic oxizolidinone **27**. A Sharpless/Kresze allylic amination with sulfodiimide **28** then installed the C8-nitrogen **29**. Elaboration to the pyrrolyl

cyclopentenone **30** then set the stage for the formation of the N12–C7 bond via a conjugate addition reaction to afford tricycle **31**. A sequence involving bromination, Boc deprotection, and importantly addition of methyl isocyanate afforded the final target (\pm)-**1**. This first synthesis of racemic agelastatin A (**1**) was completed in 15 steps and approximately 7% overall yield.



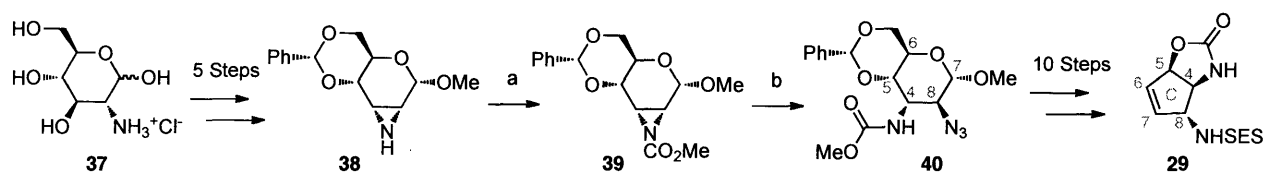
Scheme 3. Weinreb's first total synthesis of (\pm)-agelastatin A (**1**). Conditions: a) PhH, 0 °C. b) PhMgBr THF, –60 °C, 86% (2 steps). c) PhMe, 95 °C, 24 h; NaBH₄, MeOH. d) TFA, CH₂Cl₂, 86% (2 steps). e) CsCO₃, MeOH, 61%.

In 2002, Feldman reported the first enantioselective syntheses of (–)-agelastatin A (**1**) and (–)-agelastatin B (**2**) using a key alkylidenecarbene C–H insertion reaction (Scheme 4).¹⁴ Epoxide **32**, available in two steps from epichlorohydrin, was used to prepare the key oxazolidinone **33**. Their C–H insertion step involved treatment of **33** with PhI(CN)OTf followed by the addition of TolSO₂Na to afford the C-ring **34** in 34% yield. Elaboration to the cyclopentane **35** then set the stage for the formation of the N12–C7 bond via addition of the pyrrolyl nitrogen to the putative cyclopentenone to afford the B-ring **36** in 67% yield. Deprotection of the *o*-nitrobenzyl protecting groups then afforded des-bromoagelastatin, which was carried on to either (–)-agelastatin A (**1**) or (–)-agelastatin B (**2**) via selective mono- or dibromination. This first enantioselective synthesis of (–)-agelastatins A (**1**) was completed in 15 steps and approximately 3.6% overall yield with 94% ee.



Scheme 4. Feldman's first enantioselective total synthesis of (-)-agelastatins A (**1**) and (-)-agelastatins B (**2**). Conditions: a) $\text{PhI}(\text{CN})\text{OTf}$, CH_2Cl_2 , $-42\text{ }^\circ\text{C}$, 1h; ToISO_2Na , THF, $66\text{ }^\circ\text{C}$, 30 min, 34%. b) $(\text{COCl}_2)_2$, DMSO, Et_3N , CH_2Cl_2 , 67%.

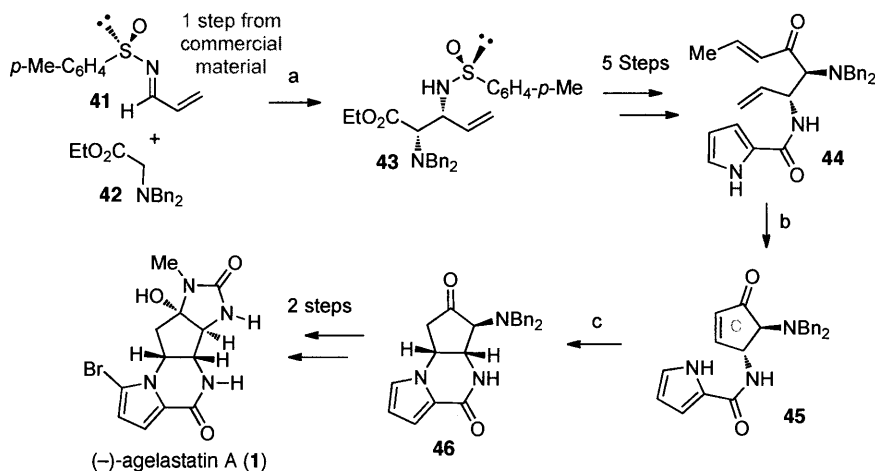
In 2003, Hale applied aziridine opening chemistry with the Hough and Richardson aziridine **38** toward the synthesis of (-)-**1** (Scheme 5).¹⁵ From aziridine **38**, carbonate formation followed by treatment with sodium azide selectively generated the aziridine opened product **40**. In 10 additional steps, **40** was converted to the bicyclic carbonate **29** that was an intermediate in Weinreb's synthesis as well (vide supra, Scheme 3). Hale then prepared (-)-agelastatin A (**1**) from **29** to complete their total synthesis in 26 total steps with approximately 0.06% overall yield.



Scheme 5. Hale's enantioselective total synthesis of (-)-agelastatins A (**1**). Conditions: a) $\text{MeOC}(\text{O})\text{Cl}$, pyr, CH_2Cl_2 , 86%. b) NaN_3 , NH_4Cl , DMF, $140\text{ }^\circ\text{C}$, 4h, 88%.

Davis' synthesis utilized a *N*-sulfinyl imine based methodology and ring-closing metathesis to efficiently secure (-)-agelastatin A (**1**, Scheme 6).¹⁶ Addition of amino ester **42** to the *N*-sulfinyl imine **41** afforded the diamino ester **43** in 73% yield as a single diastereomer. In five steps, **43** was converted to enone **44**, which was readily advanced to cyclopentenone **45** in 87% yield using the Hoveyda-Grubbs metathesis catalyst. With the C-ring secured, Davis

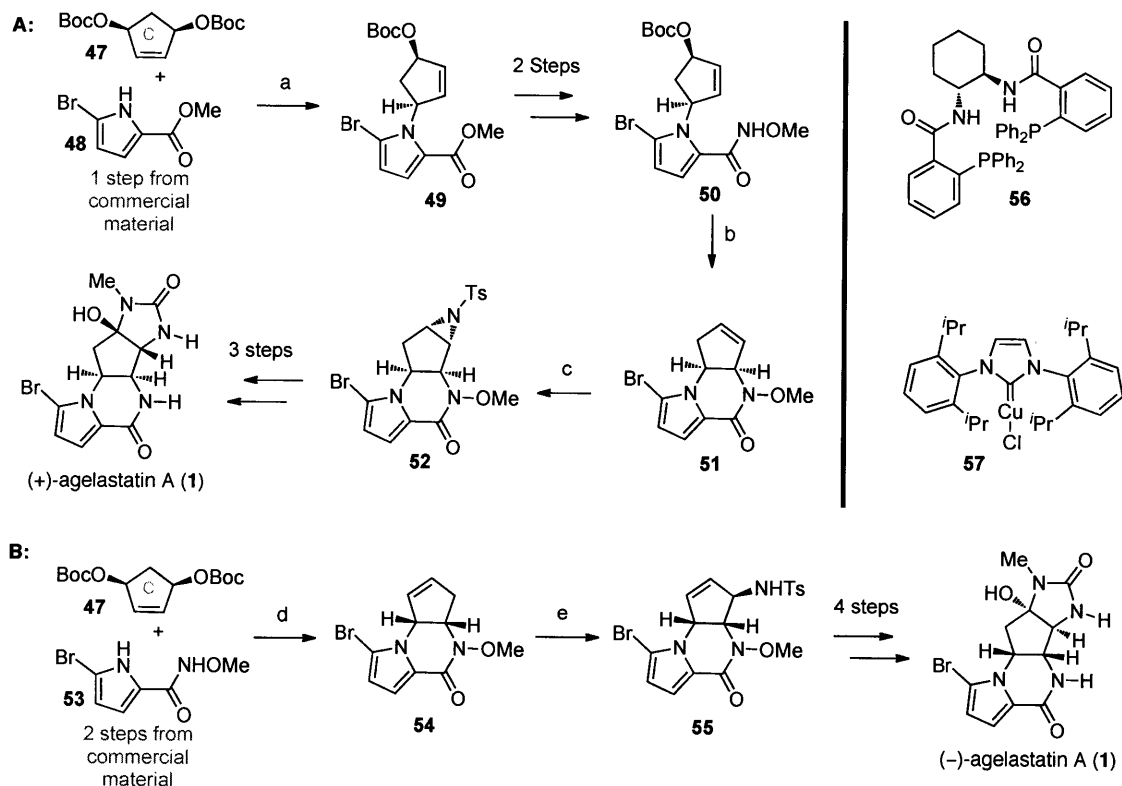
employed a Cs_2CO_3 mediated cyclization reaction to afford tricycle **46** in 66% yield with 22% recovered starting material **45**. Hydrogenative removal of the benzyl protecting groups, followed by in situ treatment with methyl isocyanate then generated des-bromoagelastatin, which was brominated to afford (-)-agelastatin A (**1**) in a total of 11 steps with approximately 15.7% overall yield.



Scheme 6. Davis' efficient enantioselective total synthesis of (-)-agelastatin A (**1**). Conditions: a) LDA, Et₂O, -78 °C, 30 min, 73%. b) Hoveyda-Grubbs catalyst, CH₂Cl₂, 45 °C, 12 h, 87%. c) Cs₂CO₃, MeOH, RT, 15 min, 66%.

Sequential palladium-catalyzed asymmetric allylic alkylation reactions were key to Trost's concise total synthesis of (+)-**1** and formal synthesis of (-)-**1** (Scheme 7).¹⁷ The union of cyclopentene **47** and pyrrole **48** was carried out with [Pd(C₃H₅)Cl]₂ in the presence of ligand **56** to generate **49** in 83% yield and 92% ee (Scheme 7, Path A). Conversion of the methyl ester **49** to methoxyamide **50** then set the stage for the second asymmetric allylic alkylation with Pd₂(dba)₃CHCl₃ and ligand **56** to afford tricycle **51** in 91% yield. An aziridination protocol, mediated by the copper *N*-heterocyclic carbene **57**, then afforded aziridine **52**, which was elaborated to (+)-agelastatin A (**1**) in a total of 9 steps in approximately 6.1% overall yield and 92% ee. Alternatively, Trost also reported the formal synthesis of (-)-**1** starting from pyrrole **53**. In a double asymmetric allylic alkylation process, tricycle **54** was generated directly in 82% yield and 97.5% ee using the same ligand **56** as above with Pd₂(dba)₃CHCl₃ (Scheme 7, Path B). A Sharpless/Kresze allylic amination then afforded allylic amine **55** in 43% yield. With only a

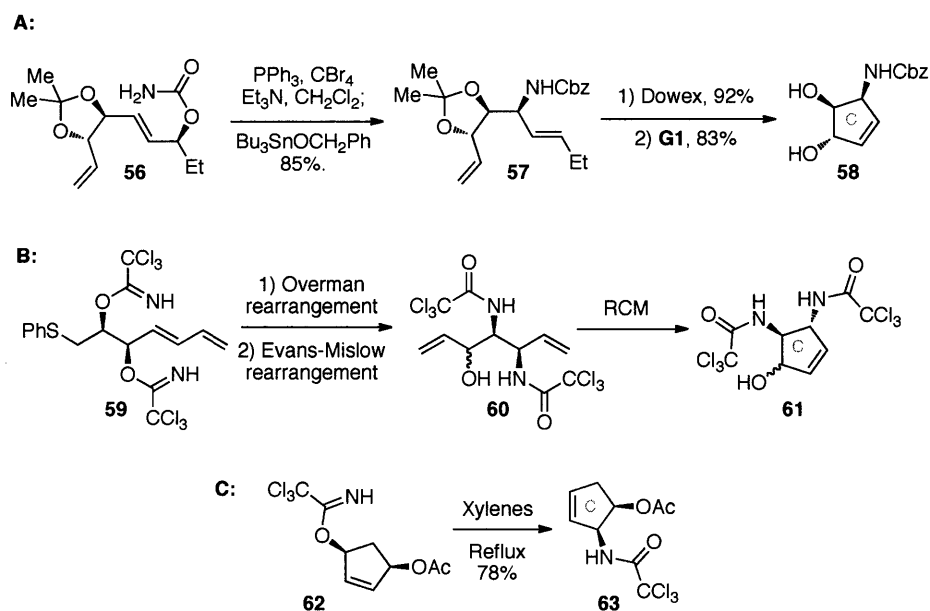
single step left to (-)-1, this formal synthesis would be completed in 8 steps with approximately 9.6% overall yield and 97.5% ee.



Scheme 7. Trost's efficient enantioselective total synthesis of (+)-agelastatin A (**1**, path A) and formal synthesis of (-)-agelastatin A (**1**, Path B). Conditions: a) $[\text{Pd}(\text{C}_3\text{H}_5\text{Cl})_2]$, **56**, Cs_2CO_3 , CH_2Cl_2 , RT, 3 h, 83%, 92% ee. b) $\text{Pd}_2(\text{dba})_3\text{CHCl}_3$, **56**, Cs_2CO_3 , CH_2Cl_2 , RT, 12 h, 91%. c) $\text{PhI}=\text{NTs}$, **57**, PhH, RT, 4 h, 52%. d) $\text{Pd}_2(\text{dba})_3\text{CHCl}_3$, **56**, AcOH, CH_2Cl_2 , RT, 6.5 h, 82%, 97.5% ee. e) $\text{TsN}=\text{S}=\text{NTs}$, PhMe, 100 °C, 40 h; MeOH, $(\text{MeO})_3\text{P}$, 43%.

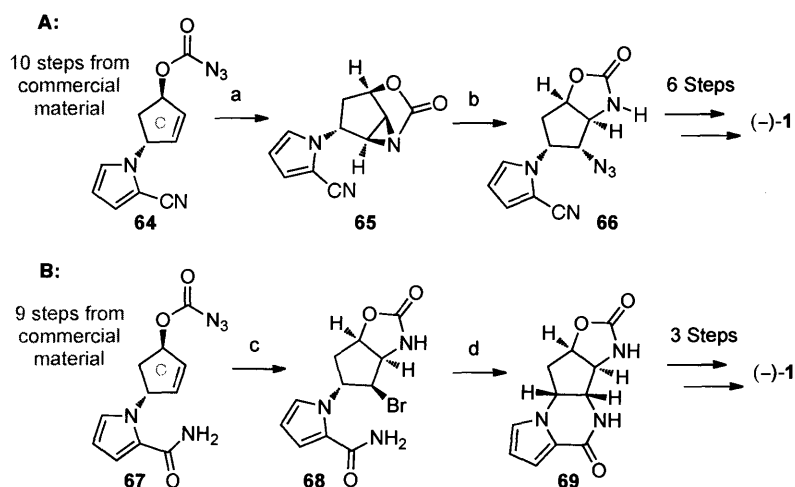
Ichikawa, Wardrop, and Chida each used sigmatropic rearrangement chemistry to secure the functionalized C-ring core of the agelastatins (Scheme 8). Ichikawa's sigmatropic rearrangement of an allyl cyanate, formed from amide **56**, afforded the amino diol **57** in 85% (Scheme 8, Path A).¹⁸ Removal of the acetonide protecting group followed by ring-closing metathesis with Grubbs' 1st generation metathesis catalyst (**G1**) afforded the cyclopentene **58**, which was carried on to (-)-1 in 27 steps with approximately 5.1% yield overall. Chida employed sequential Overman and Evans-Mislow rearrangements to afford the diamino alcohol **60** (Scheme 8, Path B).¹⁹ A ring-closing metathesis (RCM) reaction then afforded the C-ring **61**, which was advanced to (-)-agelastatin A (**1**) in a total of 23 steps and approximately 1.2%

overall yield. Finally, Wardrop employed and Overman rearrangement to secure the racemic amino alcohol **63**, which he used to prepare racemic agelastatin A (**1**) in 14 steps and approximately 8% overall yield.²⁰



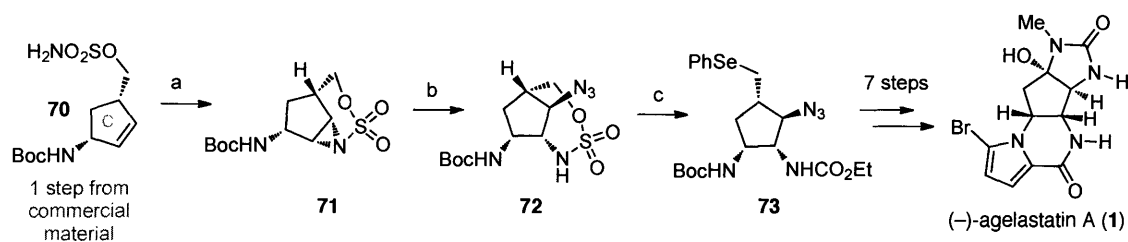
Scheme 8. Ichikawa's (Path A), Chida's (Path B), and Wardrops (Path C) total syntheses of agelastatin A (**1**) via sigmatropic rearrangement chemistry.

The interest in the field has continued with application of both aziridination, and radical aminobromination methodologies by Yoshimitsu (Scheme 9).²¹ Both nitrile **64** and amide **67** were prepared in >99% ee via a lipase mediated chiral resolution protocol followed by recrystallization. Upon heating at 160 °C in dichloromethane in a high-pressure steel tube, azidoformate **64** underwent aziridination to afford **65** in 92% yield (Scheme 9, Path A). Aziridine **65** was then treated with sodium azide to chemoselectively afford the ring-opened product **66** (63%), which was elaborated to (–)-**1** in 17 steps with approximately 1.4% overall yield. Yoshimitsu also developed a second route to (–)-**1** from amide **67** (Scheme 9, Path B). Subjection of **67** to FeBr₂ and Bu₄NBr afforded the aminobrominated product **68** in 68% yield. The B-ring was then formed through treatment of amide **68** with sodium hydride in dimethylformamide to afford the tetracycle **69** in 91% yield, which was carried on to (–)-**1** in 14 steps overall and approximately 1.8% yield.



Scheme 9. Yoshimitsu's total syntheses of (-)-agelastatin A (**1**) via aziridination (Path A) and radical aminobromination (Path B) strategies. Conditions: a) 160 °C, CH₂Cl₂, 92%. b) NaN₃, DMF, RT, 61%. c) FeBr₂, Bu₄NBr, EtOH, RT, 19 h, 68%. d) NaH, DMF, RT, 3.3 h, 91%.

Most recently, Du Bois reported an elegant solution to (-)-**1** employing his rhodium-catalyzed aziridination methodology.²² Sulfonamide **70**, readily available in 99% ee in one step from commercial material, was treated with Rh₂(esp)₂ (0.06 mol%), PhI(OAc)₂, and MgO to afford the aziridine **71** in 95% yield as a single diastereomer. Regioselective aziridine ring-opening with sodium azide afforded the oxathiazepane **72** in 71% yield. Displacement of the oxathiazepane C–O bond with sodium phenylselenide afforded cyclopentane **73**, which was elaborated to (-)-**1** in 11 steps and 15% overall yield. Notably, Du Bois prepared (-)-**1** on 270 mg scale in a single pass of the material.



Scheme 10. Du Bois' total synthesis of (-)-agelastatin A (**1**) via a Rhodium-catalyzed aziridination methodology. Conditions: a) Rh₂(esp)₂, PhI(OAc)₂, MgO, CH₂Cl₂, 10 h, 95%. b) NaN₃, ⁱPrOH, H₂O, 5 h, 71%. c) (EtO₂C)₂O, DMAP; Ph₂Se₂, NaBH₄, 15 min, 93%.

Interestingly, all of these syntheses share a common strategy whereby they initially introduce the C-ring followed by its elaboration to afford the desired tetracyclic framework. Additionally, none of the reported total syntheses evaluate existing hypotheses for plausible

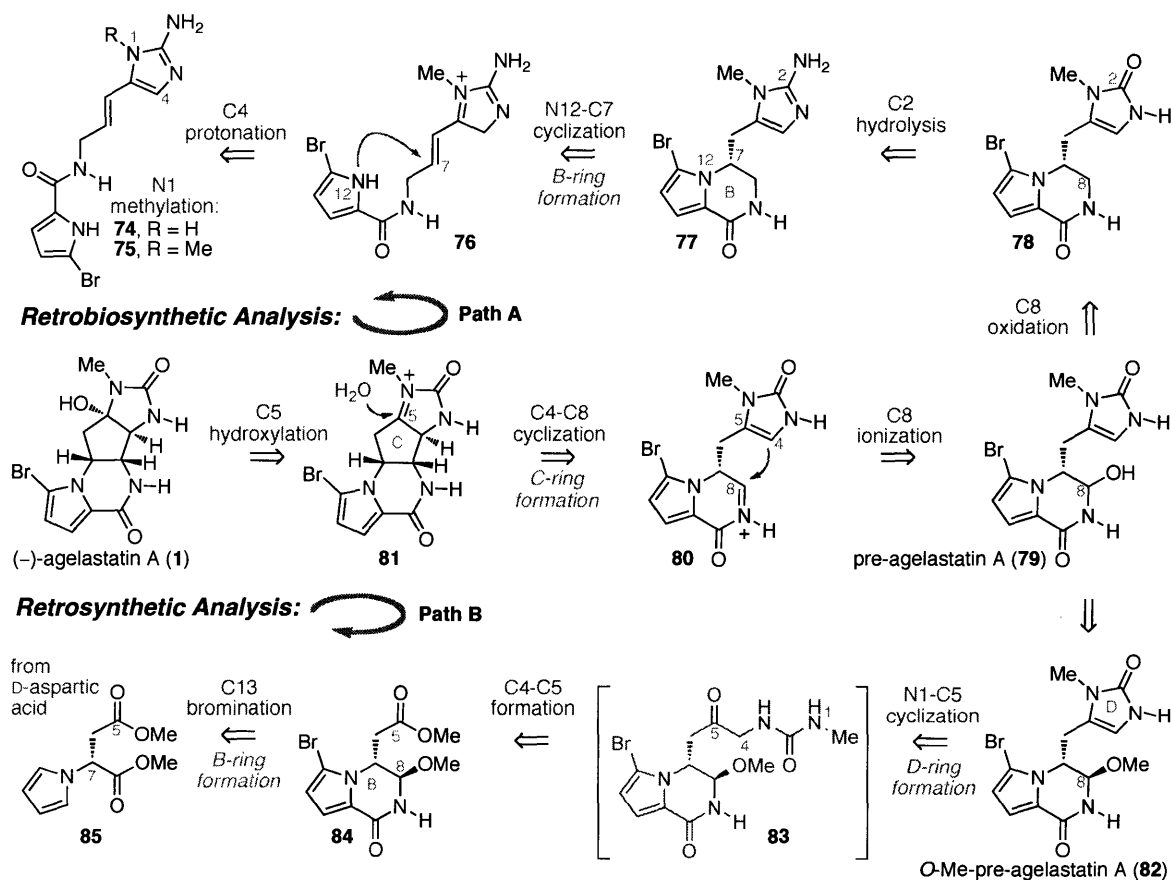
biosynthetic steps responsible for the generation of its intriguing molecular architecture, especially with respect to the C-ring formation. Furthermore, there are currently no total syntheses of agelastatins C (**3**), D (**4**), E (**5**), or F (**6**).

Results and Discussion

Herein, we report a biogenetically inspired and unified approach to the (–)-agelastatins alkaloids using a concise synthetic strategy empowered by the inherent chemistry of potential biosynthetic intermediates.²³ The fascinating molecular architecture of the agelastatins and our interest in evaluating our hypothesis for a biogenetically relevant C-ring formation that permits rapid introduction of three stereocenters motivated these studies. We envisioned an advanced-stage biosynthetic sequence distinct from the existing hypotheses (vide supra, Scheme 2) that relies on: 1) an electrophilic C8 and a nucleophilic C4 involved in C-ring formation, 2) introduction of the C-ring after the B-ring formation, and 3) substrate directed stereochemical control and use of inherent chemistry that is perhaps enhanced by the action of putative biosynthetic enzymes. The development of simplifying transforms²⁴ guided by our biosynthetic hypothesis is central to our synthetic approach to the agelastatins. This retrobiosynthetic factoring for the rapid generation of molecular complexity is in line with our group's ambitions of delving into the intricate interplay of chemistry and biology in order to explore subtle chemical reactivity in complex settings.²⁵

Our retrosynthetic factoring of (–)-agelastatin A (**1**) guided by our retrobiosynthetic analysis of **1** is illustrated in Scheme 11. Ionization of the C5-hydroxyl of **1** followed by the strategic disconnection of C4–C8 reveals the *N*-acyliminium ion **80** and clears three stereocenters and the all carbon C-ring. The mechanistic development of a transform linking **1** to **80** highlighted the significance of a versatile precursor pre-agelastatin A (**79**). Our biosynthetic hypothesis asserts that pre-agelastatin A (**79**) may be ionized to the C8-acyliminium ion allowing a 5-*exo*-trig cyclization followed by C5-hydroxylation, securing the C4-, C5-, and C8-stereocenters at the final stage of the biosynthesis (Scheme 11, Path A). We envisioned pre-agelastatin A (**79**) would result from C2-hydrolysis and C8-oxidation of the cyclooroidin analogue **77**, itself formed by C4-protonation of the linear precursor **75**, followed by C7-trapping

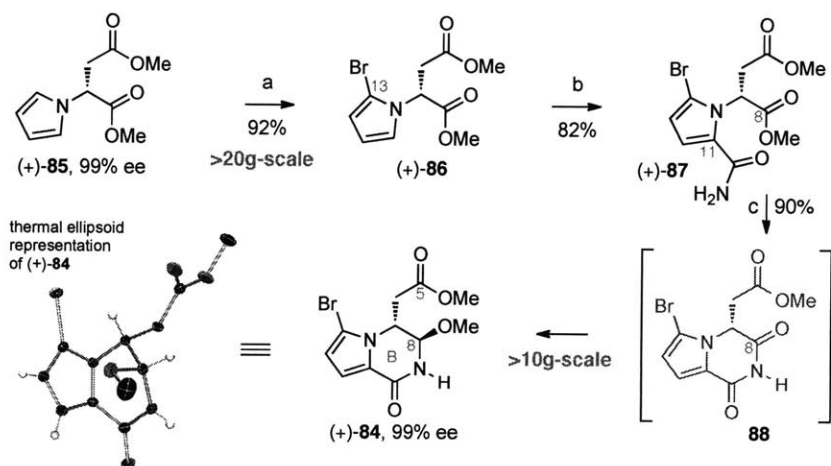
by the pyrrolyl-nitrogen (N12) via a 6-*exo*-trig cyclization.²⁶ Notably, this pathway would suggest a link between the agelastatins and the natural product cyclooroidin (**10**, Fig. 1),²⁷ and is consistent with Lindel's reported aqueous formic acid promoted conversion of oroidin (**7**) to **10**.²⁸ Inspired by the potential direct conversion of pre-agelastatin A (**79**) to (-)-agelastatin A (**1**), we targeted the related structure *O*-methyl-pre-agelastatin A (**82**) and envisioned its synthesis from readily available D-aspartic acid derivative **85** (Scheme 11, Path B).



Scheme 11. Our retrosynthetic analysis of (-)-agelastatin A (**1**, Path B) inspired by our biosynthetic hypothesis (Path A) that involves intermediacy of pre-agelastatin A (**79**) in a final stage formation of the C-ring and introduction of the C4-, C5-, and C8-stereochemistry (**79**→**1**).

Our convergent synthesis²⁹ for the targeted *O*-methyl-pre-agelastatin A (**82**) commenced with pyrrole (+)-**85** (Scheme 12), available in one step from commercially available bismethyl D-aspartic acid.³⁰ Exposure of pyrrole (+)-**85** to *N*-bromosuccinimide (NBS) in the presence of 2,6-di-*tert*-butyl-4-methylpyridine (DTBMP) afforded the bromopyrrole (+)-**86** in 92% yield with 99% ee. Treatment of bromopyrrole (+)-**86** with chlorosulfonyl isocyanate afforded amide

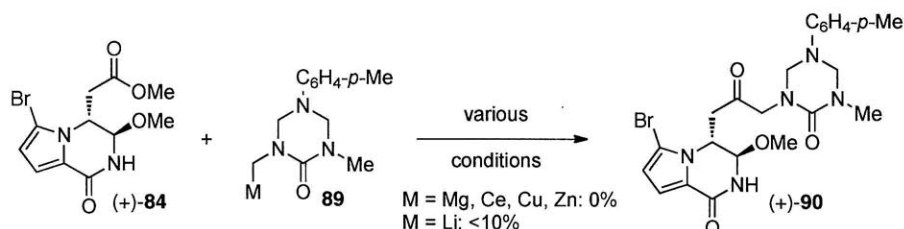
(+)-**87** (82%), which was treated sequentially with sodium borohydride followed by *p*-toluenesulfonic acid (TsOH) in methanol to generate bicycle (+)-**84** as a single diastereomer in 90% yield and 99% ee on greater than 10-gram scale. The conversion of (+)-**87** to bicycle (+)-**84** occurred via formation and immediate reduction of the imide intermediate **88**, preventing an undesired C7-epimerization. Interestingly, B-ring formation with the des-bromopyrrole derivative of **87** resulted in significant erosion of enantiomeric excess. This observation was consistent with our postulate that the C7-H bond would be forced to adopt a pseudo-equatorial conformation to minimize allylic strain between the C13-bromine and C6-methylene. In this conformation, deprotonation of the C7-methine is suppressed. The structure and relative stereochemistry of (+)-**84** was secured through X-ray crystallographic analysis, and its thermal ellipsoid representation illustrates that the C6-methylene and C8-methoxy group reside in pseudo-axial conformations (Scheme 12). Importantly, the use of the brominated pyrrole that is present in the final targets provided favorable chemical reactivity beneficial to our synthetic strategy.



Scheme 12. Decagram-scale synthesis of bicycle (+)-**84**. Conditions: a) NBS, DTBMP, THF, 92%. b) ClSO₂NCO, MeCN, 0 °C; Na(Hg), NaH₂PO₄, 82%. c) NaBH₄, MeOH, 0 °C; TsOH·H₂O, 23 °C, 90%.

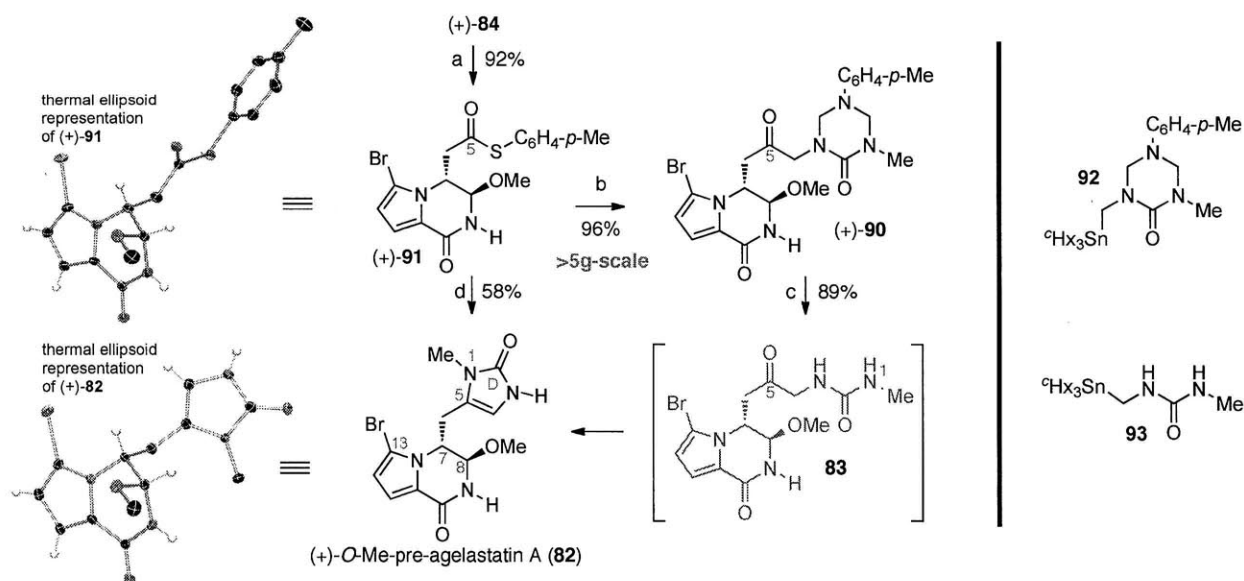
With the C5-ester (+)-**84** in hand, we developed a general approach for the introduction of the imidazolone substructures present in the targeted pre-agelastatin derivatives. Initially, we focused on the direct addition of metallated derivatives of triazone **89**^{31,32} to the C5-ester (+)-**84** (Scheme 13). Unfortunately, these strategies were plagued by either lack of reactivity (M = Mg, Cu, Ce, Zn), or the formation of byproducts associated with metal-halogen exchange, double

addition, and competing decomposition pathways ($M = \text{Li}$). Furthermore, these metallated triazone derivatives **89** were unstable at temperatures above 0 °C. Thus, it was necessary for us to develop a method for the C4–C5 bond formation using an activated derivative of the C5-ester (+)-**84** and a stable metallated triazone.



Scheme 13. Investigations of metallated triazone addition to the ester (+)-**84**.

We envisioned that the cross-coupling of thioester derivatives³³ with stannyltriazone and stannylurea derivatives would represent a versatile method for the rapid synthesis of substituted imidazolones. The thioester (+)-**91** was readily prepared in 92% yield through treatment of ester (+)-**84** with trimethylaluminum and 4-methylbenzenethiol in dichloromethane (Scheme 14). The structure of (+)-**91** was secured via X-ray crystallographic analysis, revealing the pseudo-equatorial C7–H bond.

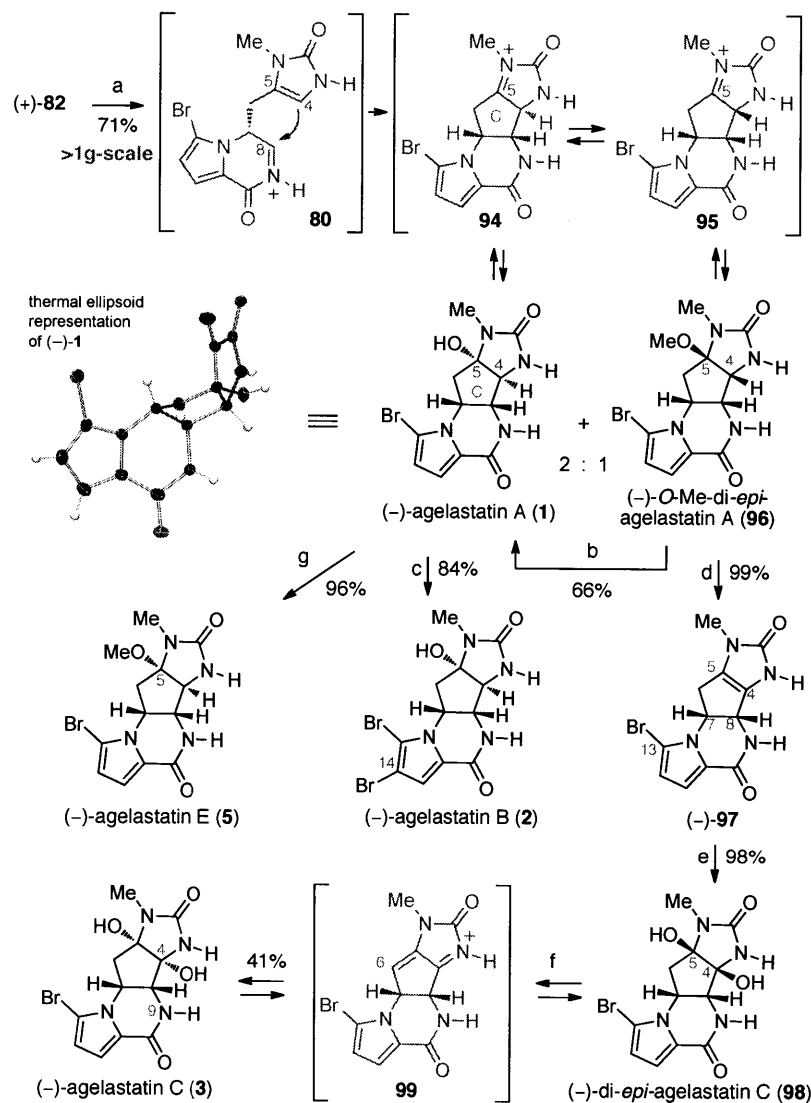


Scheme 14. Synthesis of the key intermediate (+)-*O*-methyl-pre-agelastatin A (**82**). Conditions: a) $\text{HSC}_6\text{H}_4\text{-}p\text{-Me}$, AlMe_3 , CH_2Cl_2 , 0 °C, 92%. b) **92**, CuTC , THF, 50 °C, 96%. c) HCl (0.5 N), MeOH, 23 °C, 89%. d) **93**, CuTC , THF, 50 °C; HCl (0.5 N), MeOH, 23 °C, 58%.

After significant experimentation, we found that the union of thioester (+)-**91** with the readily available stannyltriazone **92**³⁴ could be achieved in the presence of stoichiometric copper(I)-thiophene-2-carboxylate (CuTC) to efficiently give ketone (+)-**90** in 96% yield on greater than 5-gram scale (Scheme 14). Exposure of triazone (+)-**90** to methanolic hydrogen chloride unraveled the desired keto-urea **83**, which upon condensative cyclization provided the desired (+)-*O*-methyl-pre-agelastatin A (**82**) in 89% yield with 99% ee. The versatility of this new imidazolone annulation was highlighted in the union of thioester (+)-**91** and stannylurea **93** to afford (+)-*O*-methyl-pre-agelastatin A (**82**) without isolation of any intermediates. The structure of (+)-**82** was secured via X-ray crystallographic analysis, and its thermal ellipsoid representation illustrates that the C7-methylimidazolone and C8-methoxy group reside in a pseudo-axial conformations.

With (+)-*O*-methyl-pre-agelastatin A (**82**) in hand we proceeded to evaluate our biosynthetic hypothesis for the chemistry involved in the C-ring formation and rapid introduction of the C4-, C5-, and C8-stereocenters. Gratifyingly, exposure of (+)-**82** to methanesulfonic acid in water at 100 °C indeed provided (–)-agelastatin A (**1**, Scheme 15). Interestingly, (–)-agelastatin A (**1**) is formed as the major product along with (–)-*di-epi*-agelastatin A (not shown) as the minor stereoisomer (~2:1). Monitoring of this reaction by ¹H NMR revealed that (–)-*di-epi*-agelastatin A is the kinetic product, which equilibrates to the thermodynamically favored product (–)-agelastatin A (**1**). Careful analysis of the rate of solvolysis of each isomer revealed that the C5-hydroxyl of (–)-*di-epi*-agelastatin A ionizes at a significantly faster rate than the corresponding C5-hydroxyl of (–)-agelastatin A (**1**). This observation was key in the development of a simple procedure for preparative separation of (–)-agelastatin A (**1**) from the corresponding minor diastereomer. Upon complete consumption of the pre-agelastatin precursor, treatment with acidic methanol for 5 min efficiently converts (–)-*di-epi*-agelastatin A to (–)-*O*-methyl-*di-epi*-agelastatin A (**96**, Scheme 15). Under preparative conditions, our potentially biomimetic cyclization of (+)-**82** afforded (–)-agelastatin A (**1**) in 49% yield (1.4 g, 99% ee) along with (–)-*O*-methyl-*di-epi*-agelastatin A (**96**) in 22% yield (668 mg). Furthermore, resubmission of (–)-*O*-methyl-*di-epi*-agelastatin A (**96**) to the above protocol afforded a second batch of (–)-agelastatin A (**1**) in 66% yield (421 mg, 99% ee) along with recovered **96** (30%). The structure of (–)-**1** was secured through X-ray crystallographic analysis (Scheme 15). It

should be noted that this 5-(enolendo)-*exo*-trig³⁵ type of C-ring cyclization with an acyliminium ion is a rare and challenging reaction as evidenced by the paucity of relevant examples in the literature.³⁶



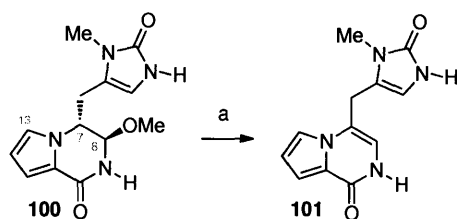
Scheme 15. Gram-scale synthesis of (-)-agelastatin A (1), and syntheses of (-)-agelastatin B (2), (-)-agelastatin C (3), and (-)-agelastatin E (5). Conditions: a) MeSO₃H, H₂O, 100 °C; MeOH, 49% (-)-1, 22% (-)-96. b) MeSO₃H, H₂O, 100 °C; MeOH, 66% (30% recovered (-)-96). c) NBS, DTBMP, THF, H₂O, 0 °C, 84%. d) pyr, 115 °C, 99%. e) DMDO, acetone, H₂O, 98%. f) Amberlyst® 15, H₂O, 100 °C, 5 d, 41% (42% recovered (-)-98). g) Amberlyst® 15, MeOH, 65 °C, 96%.

We then moved to address the synthesis of (-)-agelastatins B (2), C (3), and E (5, Scheme 15). Under optimal conditions treatment of (-)-agelastatin A (1) with NBS and DTBMP in a water–tetrahydrofuran solvent mixture afforded the natural product (-)-agelastatin B (2) in 84%

yield. We next turned our focus toward the installation of the C4-hydroxyl group present in (–)-agelastatin C (**3**). Importantly, (–)-*O*-methyl-di-*epi*-agelastatin A (**96**) served as a versatile precursor for the synthesis of (–)-agelastatin C (**3**, Scheme 15). Heating a solution of (–)-*O*-methyl-di-*epi*-agelastatin A (**96**) in pyridine afforded (–)-dehydroagelastatin A (**97**) in 99% yield.³⁷ As anticipated, treatment of (–)-**97** with dimethyldioxirane (DMDO) gave (–)-di-*epi*-agelastatin C (**98**, 98%) via oxidation on the convex face. Significantly, exposure of (–)-di-*epi*-agelastatin C (**98**) to acid (Amberlyst[®] 15) in water at 100 °C slowly afforded (–)-agelastatin C (**3**, 41%, along with 42% recovered **98**). We propose that this equilibration occurs via the intermediate **99**, which is consistent with our observations of deuterium incorporation at the C6-methylene using D₂O as solvent.³⁸ The newly isolated (–)-agelastatin E (**5**) was then prepared directly from (–)-agelastatin A (**1**, Scheme 15). According to a protocol previously described by Pietra,^{4b} (–)-agelastatin A (**1**) was treated with Amberlyst[®] 15 in methanol at 65 °C for 2 h to afford (–)-agelastatin E (**5**) in 96% yield.

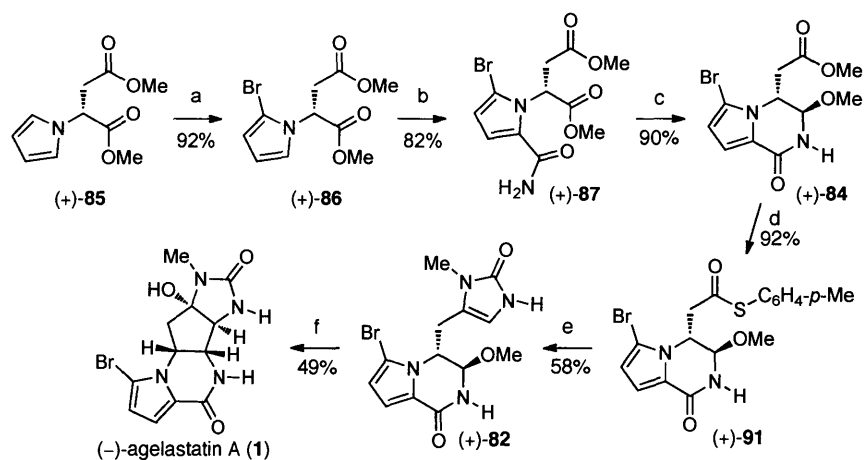
Our unified strategy for the C-ring formation utilizes the inherent chemistry of the pre-agelastatin intermediates for the generation of chemical complexity and stereochemical control to address the synthesis of the agelastatin alkaloids. Collectively, our observations hint at a plausible biosynthetic sequence for the formation of the agelastatins. For example, the stereochemical outcome for the key C-ring cyclization is controlled by the C7-methine to secure the desired thermodynamically favored C4-, C5-, and C8-stereocenters. Specifically, the C5-stereocenter is controlled by the C4-stereochemistry to give a *cis*-fused CD-ring system upon hydroxylation. It is feasible that the innate selectivity for this stereochemical outcome may perhaps be enhanced by the action of putative biosynthetic enzymes.

Furthermore, the C13-bromine that is present in all agelastatins is critical for the key C-ring cyclization. Treatment of the des-bromo derivative **100** under the cyclization conditions did not result in the desired C-ring formation, but rather gave the pyrrolopyrazinone **101** (Scheme 16). Thus, the allylic strain between the C13-bromine and C6-methylene that restricts the C7–H to a pseudo-equatorial conformation is essential for the formation of the agelastatins. Consequently, the C13-bromine is likely incorporated prior to C-ring formation in this plausible biosynthetic sequence. While our total syntheses do not in any way confirm our hypothesis for their biogenesis, it is gratifying to have chemical validation for our proposed mode and timing of bond and ring formations in this alkaloid family.



Scheme 16. Key observation concerning the biogenetically inspired C-ring synthesis. Conditions: a) MeSO₃H, H₂O, 100 °C, 20 min, 57%.

Conclusion



Scheme 17. Summary of our concise synthesis of (-)-agelastatin A (1). Conditions: a) NBS, DTBMP, THF, 92%. b) ClSO₂NCO, MeCN, 0 °C; Na(Hg), NaH₂PO₄, 82%. c) NaBH₄ MeOH, 0 °C; TsOH•H₂O, 23 °C, 90%. d) HSC₆H₄-*p*-Me, AlMe₃, CH₂Cl₂, 0 °C, 92%. e) **93**, CuTC, THF, 50 °C; HCl (0.5 N), MeOH, 23 °C, 58%. f) MeSO₃H, H₂O, 100 °C; MeOH, 49%.

We have completed the total syntheses of the agelastatin alkaloids through a highly concise and unifying strategy inspired by our biosynthetic hypothesis. Key features of our synthesis of the agelastatin alkaloids include: 1) the concise large scale enantioselective total synthesis of our proposed “pre-agelastatin” derivatives using a route from simple readily available starting materials, 2) the use of the bromopyrrole allylic strain, to prevent C7-epimerization, enabling access to key intermediates with >99% ee, 3) the rapid and versatile synthesis of imidazolone derivatives via a new [4+1] annulation strategy, 4) the validation of our planned 5-*exo*-trig advanced stage C-ring formation consistent with our hypothesis for their biogenesis, and 5) the verification of our plausible biogenetically relevant hypothesis for the

formation of (–)-agelastatin C (**3**) through oxidation of (–)-dehydroagelastatin A (**97**) followed by its equilibration. Our synthesis of (–)-agelastatin A (**1**) is summarized in Scheme 19 (7 steps, longest linear sequence). The overall efficiency of our strategy is evidenced by our preparation of a 1.4 gram batch of (–)-agelastatin A (**1**) in eight steps from commercial material in 22% overall yield through isolation of keto triazone (+)-**90**. With efficient access to the natural agelastatin alkaloids and related derivatives, mechanistic studies aimed at unlocking their chemical and biological mode of action are ongoing.

-
1. (a) Forenza, S.; Minale, L.; Riccio, R. Fattorusso, E. *J. Chem. Soc., Chem. Commun.* **1971**, 1129. (b) Garcia, E. E.; Benjamin, L. E.; Fryer, R. I. *J. Chem. Soc., Chem. Commun.* **1973**, 78.
 2. Kobayashi, J.; Ohizumi, H.; Hirata, Y. *Experientia*, **1986**, *42*, 1176.
 3. Morales, J. J.; Rodriguez, A. D. *J. Nat. Prod.* **1991**, *54*, 629.
 4. For initial isolation of agelastatin A and agelastatin B, see: (a) D'Ambrosio, M.; Guerriero, A.; Debitus, C.; Ribes, O.; Pusset, J.; Leroy, S.; Pietra, F. *J. Chem. Soc., Chem. Commun.* **1993**, 1305. For configurational and reactivity studies of agelastatin A, see: (b) D'Ambrosio, M.; Guerriero, A.; Chiasera, G.; Pietra, F. *Helv. Chim. Acta* **1994**, *77*, 1895. (c) D'Ambrosio, M.; Guerriero, A.; Ripamonti, M.; Debitus, C.; Waikedre, J.; Pietra, F. *Helv. Chim. Acta* **1996**, *79*, 727. For a later isolation and X-Ray crystallography analysis of agelastatin A, see: (d) Pettit, G. R.; Ducki, S.; Herald, D. L.; Doubek, D. L.; Schmidt, J. M.; Chapuis, J.-C. *Oncol. Res.* **2005**, *15*, 11.
 5. Hong, T. W.; Jimenez, D. R.; Molinski, T. F. *J. Nat. Prod.* **1998**, *61*, 158.
 6. Tilvi, S.; Moriou, C.; Martin, M.-T.; Gallard, J.-F.; Sorres, J.; Patel, K.; Petek, S.; Debitus, C.; Ermolenko L.; Al-Mourabit A. *J. Nat. Prod.* **2010**, Articles ASAP. DOI: 10.1021/np900539j.
 7. (a) Mason, C. K.; McFarlane, S.; Johnston, P. G.; Crowe, P.; Erwin, P. J.; Domostoj, M. M.; Campbell, F. C.; Manaviazar, S.; Hale, K. J.; El-Tanani, M. *Mol. Cancer Ther.* **2008**, *7*, 548. (b) Kapoor, S. *J. Cancer Res. Clin. Oncol.* **2008**, *134*, 927.

-
8. Meijer, L.; Thunnissen, A.-M. W. H.; White, A. W.; Garnier, M.; Nikolic, M.; Tsai, L. -H.; Walter, J.; Cleverley, K. E.; Salinas, P. C.; Wu, Y. -Z.; Biernat, J.; Mandelkow, E. -M.; Kim, S. -H.; Pettit, G. R. *Chem. Biol.* **2000**, *7*, 51.
 9. Hale, K. J.; Domostoj, M. M.; El-Tanani, M.; Campbell, F. C.; Mason, C. K. In *Strategies and Tactics in Organic Synthesis*; Harmata, M., Ed.; Elsevier Academic Press: London, 2005; Vol. 6, p 352-394.
 10. Andrade, P.; Willoughby, R.; Pomponi, S. A.; Kerr, R. G. *Tetrahedron Lett.* **1999**, *40*, 4775.
 11. Al-Mourabit, A.; Potier, P. *Eur. J. Org. Chem.* **2001**, 237.
 12. For reviews See: (a) Hoffmann, H.; Lindel, T. *Synthesis* **2003**, 1753. (b) Weinreb, S. M. *Nat. Prod. Rep.* **2007**, *24*, 931.
 13. (a) Anderson, G. T.; Chase, C. E.; Koh, Y.; Stien, D.; Weinreb, S. M. *J. Org. Chem.* **1998**, *63*, 7594. (b) Stien, D.; Anderson, G. T.; Chase, C. E.; Koh, Y.; Weinreb, S. M. *J. Am. Chem. Soc.* **1999**, *121*, 9574.
 14. (a) Feldman, K. S.; Saunders, J. C. *J. Am. Chem. Soc.* **2002**, *124*, 9060. (b) Feldman, K. S.; Saunders, J. C.; Wroblewski, M. L. *J. Org. Chem.* **2002**, *67*, 7096.
 15. (a) Hale, K. J.; Domostoj, M. M.; Tocher, D. A.; Irving, E.; Scheinmann, F. *Org. Lett.* **2003**, *5*, 2927. (b) Domostoj, M. M.; Irving, E.; Scheinmann, F.; Hale, K. J. *Org. Lett.* **2004**, *6*, 2615.
 16. (a) Davis, F. A.; Deng, J. *Org. Lett.* **2005**, *7*, 621. (b) Davis, F. A.; Zhang, Y.; Qiu, H. *Synth. Comm.* **2009**, *39*, 1914.
 17. (a) Trost, B. M.; Dong, G. *J. Am. Chem. Soc.* **2006**, *128*, 6054. (b) Trost, B. M.; Dong, G. *Chem. Eur. J.* **2009**, *15*, 6910.
 18. Ichikawa, Y.; Yamaoka, T.; Nakano, K.; Kotsuki, H. *Org. Lett.* **2007**, *9*, 2989.
 19. Hama, N.; Matsuda, T.; Sato, T.; Chida, N. *Org. Lett.* **2009**, *11*, 2687.
 20. Dickson, P. D.; Wardrop, D. J. *Org. Lett.* **2009**, *11*, 1341.
 21. (a) Yoshimitsu, T.; Ino, T.; Tanaka, T. *Org. Lett.* **2008**, *10*, 5457. (b) Yoshimitsu, T.; Ino, T.; Futamura, N.; Kamon, T.; Tanaka, T. *Org. Lett.* **2009**, *11*, 3402.
 22. When, P. M.; Du Bois, J. *Angew. Chem. Int. Ed.* **2009**, *48*, 3802.
 23. Movassaghi, M.; Siegel, D. S.; Han, S. "Total Synthesis of All (-)-Agelastatin Alkaloids." **2010**, *Manuscript in Preparation*.

-
24. Corey, E. J.; Cheng, X.-M. *The Logic of Chemical Synthesis*; John Wiley & Sons, Inc.: New York, 1995.
25. Kim, J.; Movassaghi, M. *Chem. Soc. Rev.* **2009**, *38*, 3035.
26. Alternative timing for the N1-methylation has been considered and may occur at any point up to pre-agelastatin A (**79**) for our proposed biogenesis of (–)-**1**.
27. Fattorusso, E.; Tagliatela-Scafati, O. *Tetrahedron Lett.* **2000**, *41*, 9917.
28. Pöverlein, C.; Breckle, G.; Lindel, T. *Org. Lett.* **2006**, *8*, 819.
29. While the yields and results in this chapter were obtained by me, they were greatly enabled through collaborative efforts with my colleague Sunkyun Han.
30. (+)-**85** is synthesized one step from commercial D-aspartic acid dimethyl ester in 84% (99% ee) on 17.9 gram scale. Please see the experimental section for details. For literature reference see: Jefford, C. W.; de Villedon de Naide, F.; Sienkiewicz, K. *Tetrahedron: Asymmetry* **1996**, *7*, 1069.
31. For literature references relevant to the formation of dipole stabilized lithiated amine derivatives see: (a) Hassel, T.; Seebach, D. *Helv. Chim. Acta* **1978**, *61*, 2237. (b) Beak, P.; Zajdel, W. *J. Chem. Rev.* **1984**, *84*, 471. (c) Beak, P.; Lee, W. K. *J. Org. Chem.* **1993**, *58*, 1109. (d) Sun, X.; Collum, D. B. *J. Am. Chem. Soc.* **2000**, *122*, 2459. (e) Pearson, W. H.; Stoy, P.; Mi, Y. *J. Org. Chem.* **2004**, *69*, 1919. (f) Pearson, W. H.; Lindbeck, A. C.; Kampf, J. W. *J. Am. Chem. Soc.* **1993**, *115*, 2622.
32. For the use of triazones as a protecting group for amines see: (a) Knapp, S.; Hale, J. J.; Bastos, M.; Gibson, F. S. *Tetrahedron Lett.* **1990**, *31*, 2109. (b) Knight, S. D.; Overman, L. E.; Pairedeau, G. *J. Am. Chem. Soc.* **1993**, *115*, 9293.
33. (a) Wittenberg, R.; Srogl, J.; Egi, M.; Liebeskind, L. S. *Org. Lett.* **2003**, *5*, 3033. For a recent review see: (b) Prokopová, H.; Kappe, C. O. *Angew. Chem. Int. Ed.* **2009**, *48*, 2276.
34. Stannyltriazone **92** was prepared in two steps from commercial material on 12.1 gram scale via lithiation of the corresponding triazone followed by trapping with tricyclohexylstannyl chloride. See experimental section for details.
35. Baldwin, J. E.; Lusch, M. J. *Tetrahedron* **1982**, *38*, 2939.
36. (a) Gramain, J.-C.; Remuson, R. *Heterocycles* **1989**, *29*, 1263. (b) Heaney, H.; Taha, M. O. *Tetrahedron Lett.*, **1998**, *39*, 3341.

-
37. For a previously described semi-synthesis of (-)-**97** from (-)-**5** via a similar protocol, see ref 4c.
38. Treatment of either (-)-*di-epi*-agelastatin C (**98**) or (-)-agelastatin C (**3**) with MeSO₃H (10 equiv) in D₂O at 100 °C for 3 d, afforded a 1:1 equilibrium mixture of (-)-*di-epi*-agelastatin C (**98**) and (-)-agelastatin C (**3**) with quantitative deuterium incorporation at the C6-methylene as indicated by ¹H NMR analysis.

Experimental Section

General Procedures. All reactions were performed in oven-dried or flame-dried round bottomed flasks or modified Schlenk (Kjeldahl shape) flasks. The flasks were fitted with rubber septa and reactions were conducted under a positive pressure of argon. Gas tight syringes equipped with stainless steel needles or cannulae were used to transfer air- and moisture-sensitive liquids. Where necessary (so noted), solutions were deoxygenated by argon purging for a minimum of 10 min. Flash column chromatography was performed as described by Still et al. using silica gel (60-Å pore size, 40–63 μm , 4–6% H_2O content, Zeochem).¹ Analytical thin-layer chromatography was performed using glass plates pre-coated with 0.25 mm 230–400 mesh silica gel impregnated with a fluorescent indicator (254 nm). Thin layer chromatography plates were visualized by exposure to ultraviolet light and/or by exposure to an ethanolic phosphomolybdic acid (PMA), an acidic solution of *p*-anisaldehyde (Anis), an aqueous solution of ceric ammonium molybdate (CAM), an aqueous solution of potassium permanganate (KMnO_4) or an ethanolic solution of ninhydrin followed by heating (<1 min) on a hot plate (~250 °C). Organic solutions were concentrated on Büchi R-200 rotary evaporators at ~10 torr (house vacuum) at 25–35 °C, then at ~0.5 torr (vacuum pump) unless otherwise indicated.

Materials. Commercial reagents and solvents were used as received with the following exceptions: dichloromethane, diethyl ether, tetrahydrofuran, acetonitrile, toluene, methanol, triethylamine, and pyridine were purchased from J.T. Baker (CycletainerTM) and were purified by the method of Grubbs et al. under positive argon pressure.² Copper thiophene 2-carboxylate (CuTC), a tan colored solid, was purchased from Matrix Inc. and was used as received. Chlorosulfonyl isocyanate was purchased from TCI and was used as received. Sodium Amalgam was freshly prepared before use.³ The molarity of *sec*-butyllithium solutions were determined by titration using diphenylacetic acid as an indicator (average of three determinations).⁴ The molarity of DMDO⁵ solutions were determined by titration using triphenylphosphine with ³¹P NMR analysis.

Instrumentation. Proton (¹H) and carbon (¹³C) nuclear magnetic resonance spectra were recorded with Varian inverse probe 500 INOVA and Varian 500 INOVA spectrometers. Proton nuclear magnetic resonance (¹H NMR) spectra are reported in parts per million on the δ scale and are referenced from the residual protium in the NMR solvent (CDCl_3 : δ 7.24, Toluene- d_8 : δ 7.09, 7.00, 6.98, 2.09; CHD_2OD : δ 3.31). Data is reported as follows: chemical shift [multiplicity (s = singlet, d = doublet, t = triplet, q = quartet, st = sextet, sp = septet, m = multiplet, app = apparent, br = broad), coupling constant(s) in Hertz, integration, assignment]. Carbon-13 nuclear magnetic resonance (¹³C NMR) spectra are reported in parts per million on the δ scale and are referenced from the carbon resonances of the solvent (CDCl_3 : δ 77.23, Toluene- d_8 : δ 137.86, 129.24, 128.33, 125.49, 20.40, CD_3OD : δ 49.15, Pyridine- d_5 : δ 150.35, 135.91, 123.87, DMSO- d_6 : δ 39.51). Data is reported as

¹ Still, W. C.; Kahn, M.; Mitra, A. *J. Org. Chem.* **1978**, *43*, 2923–2925.

² Pangborn, A. B.; Giardello, M. A.; Grubbs, R. H.; Rosen, R. K.; Timmers, F. J. *Organometallics* **1996**, *15*, 1518–1520.

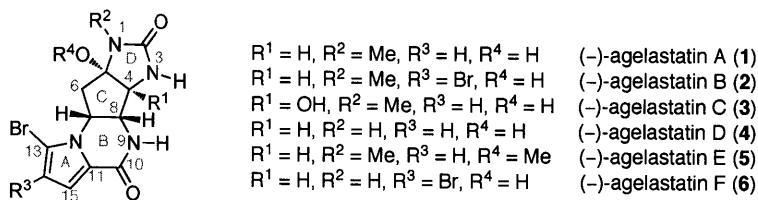
³ Sodium amalgam (5% wt) was prepared according to: Brasen, W. R.; Hauser, C. R. *Org. Synth.* **1954**, *34*, 56–57.

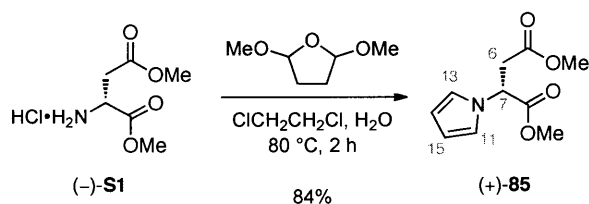
⁴ Kofron, W. G.; Baclawski, L. M. *J. Org. Chem.* **1976**, *41*, 1879–1880.

⁵ For the preparation of DMDO see: Murray, R. W.; Singh, M. *Org. Synth.* **1997**, *74*, 91–96.

follows: chemical shift. Infrared data (IR) were obtained with a Perkin-Elmer 2000 FTIR and are reported as follows: [frequency of absorption (cm^{-1}), intensity of absorption (s = strong, m = medium, w = weak, br = broad)]. Optical Rotation was recorded on a Jasco P-1010 Polarimeter (chloroform, Aldrich, Chromosolv Plus 99.9%; methanol, Aldrich, Chromosolv Plus 99.9%; pyridine, purified by the method of Grubbs et al.²). Chiral HPLC analysis was performed on an Agilent Technologies 1100 Series system. Semi-preparative HPLC was performed on a Waters system with the 1525 Binary HPLC Pump, 2489 UV/Vis Detector, SFO System Fluidics Organizer, and 2767 Sample Manager components. The structures of (-)-**1**, (+)-**82**, (+)-**84**, and (+)-**91** were obtained at the X-ray crystallography laboratory of the Department of Chemistry, Massachusetts Institute of Technology, with the assistance of Mr. Justin Kim. We are grateful to Dr. Li Li for obtaining the mass spectrometric data at the Department of Chemistry's Instrumentation Facility, Massachusetts Institute of Technology. High-resolution mass spectrometric data (HRMS) were recorded on a Bruker Daltonics APEXIV 4.7 Tesla FT-ICR-MS spectrometer using electrospray ion source (ESI) or direct analysis in real time (DART) ionization source.

Positional Numbering System. In assigning the ^1H and ^{13}C NMR data of all intermediates en route to our total synthesis of (-)-**1** through (-)-**6** we have employed a uniform numbering system consistent with that of the final targets.





(+)-(R)-Dimethyl-2-(1H-pyrrol-1-yl)succinate (85):⁶

To a solution of (–)-dimethyl D-aspartate hydrochloride⁷ (**S1**, 20.0 g, 101 mmol, 1 equiv) in water (153 ml) at 23 °C was added 1,2-dichloroethane (153 mL) via syringe followed by 2,5-dimethoxytetrahydrofuran (13.1 mL, 101 mmol, 1.00 equiv), and the resulting mixture was heated to 80 °C. After 2 h, the brown reaction mixture was cooled to 23 °C, and the aqueous layer was separated and was extracted with dichloromethane (3 × 150 mL). The combined organic layers were dried over anhydrous sodium sulfate and were concentrated under reduced pressure. The brown residue was purified by flash column chromatography (silica gel: diam. 6 cm, ht. 15 cm; eluent: 50% diethyl ether in hexanes) to afford pyrrole (+)-**85** (17.9 g, 84%) as colorless oil that was found to be 99% ee by chiral HPLC analysis [Welk-O (*S,S*); 3 mL/min; 2% isopropanol in hexanes; $t_R(\text{major}) = 4.5$ min, $t_R(\text{minor}) = 5.2$ min]. (+)-**85** could be stored for greater than a month as a solution frozen in benzene at –8 °C without any erosion of enantiomeric excess.

¹H NMR (500 MHz, CDCl₃, 21 °C): δ 6.69 (t, $J = 2.2$ Hz, 2H, C₁₁H, C₁₃H), 6.15 (t, $J = 2.1$ Hz, 2H, C₁₄H, C₁₅H), 5.11 (dd, $J = 7.9, 6.8$ Hz, 1H, C₇H), 3.71 (s, 3H, OCH₃), 3.66 (s, 3H, OCH₃), 3.26 (dd, $J = 16.8, 8.0$ Hz, 1H, C₆H_a), 2.92 (dd, $J = 16.7, 6.8$ Hz, 1H, C₆H_b).

¹³C NMR (125.8 MHz, CDCl₃, 21 °C): δ 170.4, 170.0, 120.1, 109.2, 57.8, 53.0, 52.2, 37.5.

FTIR (neat) cm⁻¹: 3643 (m), 3466 (m), 3103 (m), 2956 (s), 1739 (br-s), 1557 (w), 1490 (s), 729 (s).

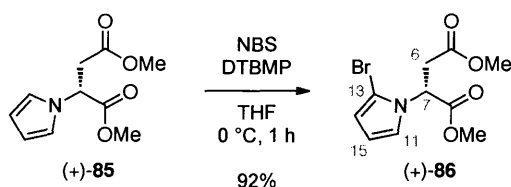
HRMS (DART) (m/z): calc'd for C₁₀H₁₄NNaO₄, [M+Na]⁺: 212.0917
found: 212.0911.

[α]_D²²: +71.3 (c 0.37, CHCl₃).

TLC (25% ethyl acetate in hexanes), R_f: 0.50 (CAM, UV).

⁶ For a previous report of the synthesis of (–)-**85** in 99% ee see: Jefford, C. W.; de Villedone de Naide, F.; Sienkiewicz, K. *Tetrahedron: Asymmetry* **1996**, *7*, 1069-1076.

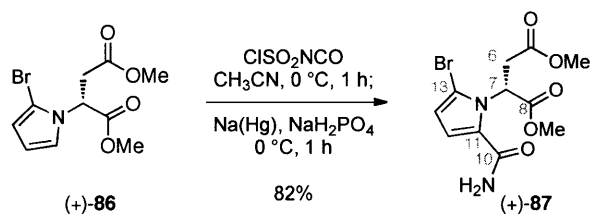
⁷ (–)-Dimethyl D-aspartate hydrochloride (**S1**) can be purchased from commercial sources. Alternatively, we prepared **S1** from (–)-D-aspartic acid in 99% yield on greater than 35 gram scale according to the following procedure: Gmeiner, P.; Feldman, P. L.; Chumoy, M. Y.; Rapoport, H. *J. Org. Chem.* **1990**, *55*, 3068-3074.



(+)-(R)-Dimethyl 2-(2-bromo-1H-pyrrol-1-yl)succinate (86):

N-Bromosuccinimide (NBS, 13.7 g, 77.0 mmol, 1.00 equiv) was added as solid in one portion to a solution of pyrrole (+)-**85** (16.2 g, 77.0 mmol, 1 equiv) and 2,6-di-*tert*-butyl-4-methylpyridine (DTBMP, 17.3 g, 84.0 mmol, 1.10 equiv) in tetrahydrofuran (385 mL) at 0 °C. After 1 h, the clear colorless reaction mixture was quenched with a mixture of saturated aqueous sodium thiosulfate solution and saturated aqueous sodium bicarbonate solution (1:1, 200 mL). The solution was diluted with ethyl acetate (800 mL) and water (800 mL), and the layers were separated. The aqueous layer was extracted with ethyl acetate (2 × 800 mL), and the combined organic layers were dried over anhydrous sodium sulfate and were concentrated under reduced pressure. The sample of the crude colorless residue was purified by flash column chromatography (silica gel: diam. 9 cm, ht. 17 cm; eluent: 10% ethyl acetate in hexanes) to afford (+)-**86** (20.6 g, 92%) as a colorless oil that was found to be 99% ee by chiral HPLC analysis [Welk-O (*R,R*); 3 mL/min; 2% isopropanol in hexanes; $t_{R(\text{major})}$ = 3.5 min, $t_{R(\text{minor})}$ = 4.1 min]. While neat (+)-**86** is sensitive toward long term storage, it could be stored for greater than a month as a solution frozen in benzene at -8 °C without any C₁₃→C₁₄ bromine migration.

¹ H NMR (500 MHz, CDCl ₃ , 21 °C):	δ 6.74 (ddd, J = 3.1, 1.9, 0.2 Hz, 1H, C ₁₁ H), 6.18-6.16 (m, 2H, C ₁₄ H, C ₁₅ H), 5.38 (t, J = 7.2 Hz, 1H, C ₇ H), 3.73 (s, 3H, OCH ₃), 3.67 (s, 3H, OCH ₃), 3.27 (dd, J = 16.8, 7.5 Hz, 1H, C ₆ H _a), 2.92 (dd, J = 16.8, 7.0 Hz, 1H, C ₆ H _b).
¹³ C NMR (125.8 MHz, CDCl ₃ , 21 °C):	δ 170.3, 169.8, 120.6, 111.7, 110.6, 102.1, 56.2, 53.3, 52.4, 37.2.
FTIR (neat) cm ⁻¹ :	3654 (w), 3468 (w), 3130 (m), 2954 (s), 1739 (br-s), 1437 (s), 1010 (s), 709 (s).
HRMS (ESI) (m/z):	calc'd for C ₁₀ H ₁₂ BrNNaO ₄ , [M+Na] ⁺ : 311.9842 found: 313.9847.
[α] _D ²² :	+65.9 (<i>c</i> 1.06, CHCl ₃).
TLC (25% ethyl acetate in hexanes) R _f :	0.42 (CAM, UV).



(+)-(R)-Dimethyl 2-(2-bromo-5-carbamoyl-1H-pyrrol-1-yl)succinate (87):

Chlorosulfonyl isocyanate (4.28 mL, 49.0 mmol, 1.05 equiv) was added slowly via syringe to a solution of bromopyrrole (+)-86 (13.6 g, 46.8 mmol, 1 equiv) in acetonitrile (235 mL) at 0 °C. After 1 h, anhydrous powdered sodium phosphate monobasic (28.2 g, 235 mmol, 5.00 equiv) followed by freshly prepared sodium amalgam (5%-Na, 110 g, 239 mmol, 5.11 equiv) were added as solids to the reaction mixture. After 1h, the reaction mixture was diluted with ethyl acetate (800 mL), and silica gel (400 mL) was added to the reaction mixture. The resulting slurry was filtered through a plug of silica gel (diam. 9 cm, ht. 8 cm; eluent: ethyl acetate). The filtrate was concentrated under reduced pressure, and the residue was purified by flash column chromatography (silica gel: diam. 9 cm, ht. 15 cm; eluent: 50% ethyl acetate in hexanes) to afford (+)-87 (12.7 g, 82%) as white solid. Pyrrole (+)-87 could be stored for greater than a month as a solution frozen in benzene at -8 °C. Exposure of (+)-87 to alcoholic solvents, namely methanol, or base results in rapid lactamization and erosion of enantiomeric excess.

$^1\text{H NMR}$ (500 MHz, CDCl_3 , 21 °C)⁸: δ 6.69 (br-d, $J = 3.9$ Hz, 1H, C_{15}H), 6.23 (d, $J = 4.1$ Hz, 1H, C_{14}H), 5.78 (br-s, 2H, N_9H_2), 5.78 (br-s, 1H, C_7H)⁹, 3.69 (s, 3H, OCH_3), 3.65 (s, 3H, OCH_3), 3.59 (br-d, $J = 14.4$ Hz, 1H, C_6H_a), 2.89 (br-dd, $J = 16.4, 6.3$ Hz, 1H, C_6H_b).

$^{13}\text{C NMR}$ (125.8 MHz, CDCl_3 , 21 °C)⁸: δ 171.2, 169.5, 162.5, 125.2, 115.1, 111.7, 111.7⁹, 56.8, 53.0, 52.3, 37.3.

FTIR (neat) cm^{-1} : 3359 (m), 3191 (m), 2953 (m), 1740 (s), 1660 (m), 1602 (m), 1534 (w), 1438 (s), 1413 (m), 1272 (m), 1011 (m), 751 (m).

HRMS (DART) (m/z): calc'd for $\text{C}_{11}\text{H}_{14}\text{BrN}_2\text{O}_5$, $[\text{M}+\text{H}]^+$: 333.0081
found: 333.0074.

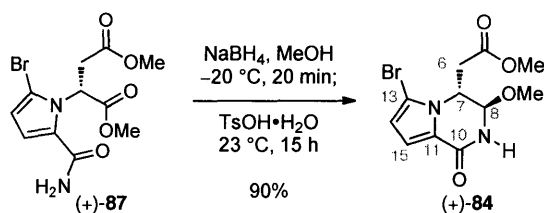
$[\alpha]_D^{22}$: +74.0 (c 1.25, CHCl_3).

M.p.: 45–49 °C.

TLC (33% in hexanes in ethyl acetate) R_f: 0.44 (CAM, UV).

⁸ Resonances at 21 °C are broadened due to rotamers.

⁹ Resonance is obscured due to line broadening. At higher temperature in toluene- d_6 the signals are resolved; however, rotamers persist for $^{13}\text{C NMR}$. $^1\text{H NMR}$ (500 MHz, Toluene- d_6 , 80 °C) δ 6.30 (br-s, 1H, C_7H), 6.27 (dd, $J = 4.1, 1.1$ Hz, 1H, C_{15}H), 6.01 (dd, $J = 4.1, 0.6$ Hz, 1H, C_{14}H), 5.40 (br-s, 2H, N_9H_2), 3.66 (dd, $J = 16.5, 6.7$ Hz, 1H, C_6H_a), 3.37 (s, 3H, OCH_3), 3.36 (s, 3H, OCH_3), 2.86 (dd, $J = 16.6, 6.5$ Hz, 1H, C_6H_b). $^{13}\text{C NMR}$ (125.8 MHz, Toluene- d_6 , 80 °C; Minor rotamer resonances denoted by *) δ 170.7, 169.2, 162.9, 126.8, 115.1*, 114.9*, 114.8, 114.6*, 112.2*, 112.0*, 111.6, 111.4*, 110.9 (br), 57.1 (br), 52.3, 52.1*, 51.7*, 51.5, 51.3*, 37.9*, 37.7, 37.5*.



(+)-Methyl-2-((3*R*,4*R*)-6-bromo-3-methoxy-1-oxo-1,2,3,4-tetrahydropyrrolo[1,2-*a*]pyrazin-4-yl)-acetate (84**):**

Anhydrous methanol (377 mL, precooled to $-20\text{ }^\circ\text{C}$) was added to a 2L flask charged with (+)-**87** (12.5 g, 37.7 mmol, 1 equiv) at $-20\text{ }^\circ\text{C}$ followed immediately by sodium borohydride (7.12 g, 188 mmol, 5.00 equiv) as a solid in one portion (Note: Significant gas evolution was observed. The internal temperature remained below $-10\text{ }^\circ\text{C}$). After 20 minutes, acetone (41.0 mL, 566 mmol, 15.0 equiv) was added slowly via syringe to the reaction mixture. After 10 min, the reaction mixture was diluted with methanol (1L, $-20\text{ }^\circ\text{C}$), and a solution of *p*-toluenesulfonic acid hydrate (TsOH \cdot H₂O, 43.0 g, 226 mmol, 6.00 equiv) in methanol (100 mL) was added slowly via cannula over a 10 min period, while maintaining an internal temperature of $-20\text{ }^\circ\text{C}$. The resulting mixture (pH = 3) was allowed to slowly warm to $23\text{ }^\circ\text{C}$. After 15 h, the reaction mixture was basified with saturated aqueous sodium bicarbonate solution (pH = 7) and was concentrated under reduced pressure to a volume of approximately 200 mL. The resulting mixture was partitioned between dichloromethane (750 mL) and saturated aqueous sodium bicarbonate solution (750 mL). The layers were separated, and the aqueous layer was extracted with dichloromethane (4 \times 750 mL). The combined organic layers were dried over anhydrous sodium sulfate, and were concentrated under reduced pressure to provide a white solid residue. This solid was purified by flash column chromatography (silica gel: diam. 5 cm, ht. 12 cm; eluent: 25% hexanes in ethyl acetate) to afford the bicycle (+)-**84** (10.8 g, 90%) as white crystalline solid that was found to be 99% ee by chiral HPLC analysis [Chiralpak AD-H; 0.54 mL/min; 21% isopropanol in hexanes; $t_R(\text{major}) = 16.2\text{ min}$, $t_R(\text{minor}) = 11.6\text{ min}$]. Crystals of the bicycle (+)-**84** suitable for X-ray diffraction were obtained from methanol. For a thermal ellipsoid representation of the bicycle (+)-**84** see page 123.

¹H NMR (500 MHz, CDCl₃, 21 $^\circ\text{C}$): δ 7.73 (br-d, $J = 4.4\text{ Hz}$, 1H, N₉H), 6.94 (d, $J = 4.1\text{ Hz}$, 1H, C₁₅H), 6.29 (d, $J = 4.1\text{ Hz}$, 1H, C₁₄H), 4.84 (dd, $J = 9.8, 3.5\text{ Hz}$, 1H, C₇H), 4.80 (dd, $J = 4.8, 1.5\text{ Hz}$, 1H, C₈H), 3.73 (s, 3H, OCH₃), 3.37 (s, 3H, OCH₃), 2.75 (dd, $J = 17.0, 10.8\text{ Hz}$, 1H, C₆H_a), 2.65 (dd, $J = 17.0, 3.6\text{ Hz}$, 1H, C₆H_b).

¹³C NMR (125.8 MHz, CDCl₃, 21 $^\circ\text{C}$): δ 170.2, 159.7, 123.5, 115.3, 113.2, 106.3, 84.7, 55.2, 53.6, 52.5, 36.6.

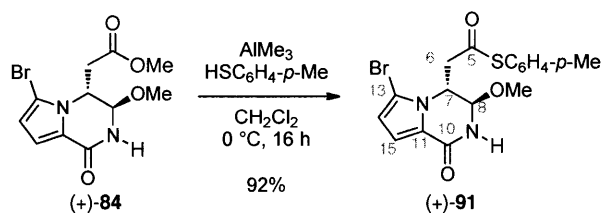
FTIR (neat) cm⁻¹: 3226 (br-m), 2952 (m), 1736 (s), 1669 (s), 1553 (m), 1423 (s), 1384 (w), 1319 (m), 1088 (m).

HRMS (ESI) (m/z): calc'd for C₁₁H₁₃BrN₂NaO₄, [M+Na]⁺: 317.0131, found: 317.0135.

[α]_D²²: +128.1 (c 0.61, CHCl₃).

M.p.: 156–157 $^\circ\text{C}$.

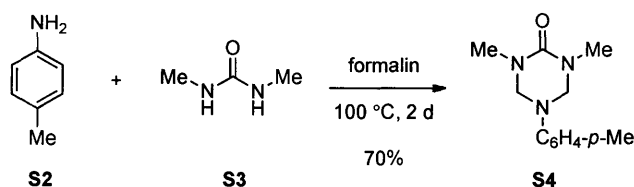
TLC (25% hexanes in ethyl acetate), R_f: 0.31 (CAM, UV).



(+)-*S-p*-Tolyl-2-((3*R*,4*R*)-6-bromo-3-methoxy-1-oxo-1,2,3,4-tetrahydropyrrolo[1,2-*a*]pyrazin-4-yl)ethanethioate (91):

Trimethyl aluminum (2 M in toluene, 30.7 mL, 61.5 mmol, 5.00 equiv) was added slowly via syringe to a solution of 4-methylbenzenethiol (7.80 g, 61.5 mmol, 5.00 equiv) in dichloromethane (123 mL) at 0 °C. After 40 min, a pre-cooled solution (0 °C) of bicycle (+)-**84** (3.90 g, 12.3 mmol, 1 equiv) in dichloromethane (90 mL) was added via cannula. After 16 h, the light yellow reaction mixture was diluted with saturated aqueous potassium sodium tartrate solution (360 mL) and saturated aqueous sodium bicarbonate solution (250 mL). After 1h, the layers were separated and the aqueous layer was extracted with dichloromethane (3 × 250 mL). The combined organic layers were dried over anhydrous sodium sulfate and were concentrated under reduced pressure to afford an opaque white oil. The residue was purified by flash column chromatography (silica gel: diam. 5 cm, ht. 14 cm; eluent: 50% ethyl acetate in hexanes) to afford thioester (+)-**91** (4.8 g, 92%) as white crystalline solid. Crystals of the thioester (+)-**91** suitable for X-ray diffraction were obtained from isopropanol. For a thermal ellipsoid representation of the thioester (+)-**91** see page 127.

$^1\text{H NMR}$ (500 MHz, CDCl_3 , 21 °C):	δ 8.01 (br-d, $J = 4.6$ Hz, 1H, N_9H), 7.30 (app-d, $J = 8.1$ Hz, 2H, $\text{SAr-}o\text{-H}$), 7.24 (d, $J = 7.9$ Hz, 2H, $\text{SAr-}m\text{-H}$), 6.95 (d, $J = 4.1$ Hz, 1H, C_{15}H), 6.30 (d, $J = 4.1$ Hz, 1H, C_{14}H), 4.89 (app-dd, $J = 10.4, 3.5$ Hz, 1H, C_7H), 4.79 (dd, $J = 4.8, 1.5$ Hz, 1H, C_8H), 3.33 (s, 3H, OCH_3), 3.09 (dd, $J = 16.6, 10.5$ Hz, 1H, C_6H_a), 2.98 (dd, $J = 16.6, 3.5$ Hz, 1H, C_6H_b), 2.37 (s, 3H, SArCH_3).
$^{13}\text{C NMR}$ (125.8 MHz, CDCl_3 , 21 °C):	δ 194.9, 159.9, 140.6, 134.6, 130.5, 123.5, 123.0, 115.4, 113.2, 106.4, 83.6, 55.3, 53.7, 45.1, 21.6.
FTIR (neat) cm^{-1} :	3216 (s), 3094 (m), 2931 (s), 2248 (w), 1670 (br-s), 1553 (s), 1423 (s), 1318 (s), 1087 (s), 733 (s).
HRMS (DART) (m/z):	calc'd for $\text{C}_{17}\text{H}_{18}\text{BrN}_2\text{O}_3\text{S}$, $[\text{M}+\text{H}]^+$: 409.0216, found: 409.0212.
$[\alpha]_D^{22}$:	+97.8 (c 0.3, CHCl_3).
M.p.:	133–135 °C (dec.).
TLC (25% hexanes in ethyl acetate), R_f :	0.42 (CAM, UV).



1,3-Dimethyl-5-(*p*-tolyl)-1,3,5-triazinan-2-one (S4):

p-Toluidine (S2, 12.2 g, 113 mmol, 1.00 equiv) was added as a solid to a solution of *N,N*-dimethylurea (S3, 10.0 g, 113 mmol, 1 equiv) in formalin (37% wt in water, 18.4 ml, 227 mmol, 2.00 equiv) at 23 °C, and the resulting suspension was heated to 100 °C. After 2 d, the reaction mixture was allowed to cool to 23 °C, and was partitioned between dichloromethane (500 mL) and water (500 mL). The layers were separated, and the aqueous layer was extracted with dichloromethane (3 × 100 mL). The combined organic layers were dried over anhydrous sodium sulfate, and were concentrated under reduced pressure. The solid residue was purified by crystallization from hot hexanes to afford triazone S4 (17.4 g, 70%) as a tan crystalline solid.

¹H NMR (500 MHz, CDCl₃, 21 °C): δ 7.06 (d, *J* = 8.5 Hz, 2H, NAr-*o*-H), 6.89 (d, *J* = 8.5 Hz, 2H, NAr-*m*-H), 4.60 (s, 4H, NCH₂N, NCH₂N), 2.85 (s, 6H, NCH₃, NCH₃), 2.27 (s, 3H, NArCH₃).

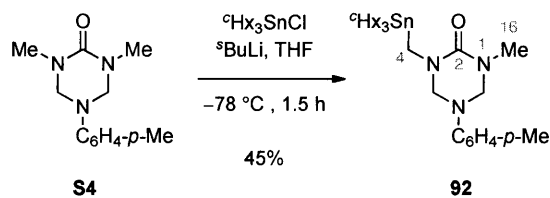
¹³C NMR (125.8 MHz, CDCl₃, 21 °C): 155.9, 145.6, 132.0, 129.7, 119.2, 67.1, 32.1, 20.4.

FTIR (neat) cm⁻¹: 3029 (s), 2872 (s), 1638 (s), 1513 (s), 1451 (m), 1403 (m), 1294 (m), 1197 (m), 1093 (w).

HRMS (ESI) (*m/z*): calc'd for C₁₂H₁₇N₃NaO, [M+Na]⁺: 242.1264, found: 242.1275.

M.p.: 79–82 °C.

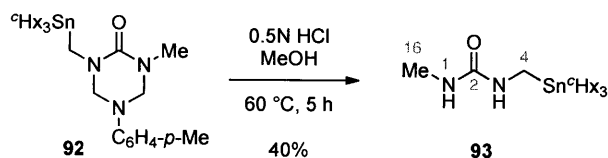
TLC (10% ethyl acetate in hexanes), R_f: 0.80 (CAM, UV).



1-Methyl-5-(*p*-tolyl)-3-((tricyclohexylstannyl)methyl)-1,3,5-triazinan-2-one (92):

To a solution of triazone **S4** (10.0 g, 46.0 mmol, 1 equiv) in tetrahydrofuran (400 mL) at -78 °C was added *sec*-butyllithium (1.4 M in cyclohexane, 34.5 mL, 48.0 mmol, 1.05 equiv) rapidly via cannula. After 10 min, the resulting bright orange mixture was added via cannula over a 15 min period to a solution of tricyclohexyltin chloride (20.3 g, 50.0 mmol, 1.10 equiv) in tetrahydrofuran (400 mL) at -78 °C. After 1.5 h, saturated aqueous ammonium chloride solution (100 mL) was added via syringe, and the resulting mixture was concentrated under reduced pressure. The residue was partitioned between dichloromethane (800 mL) and water (800 mL). The layers were separated, and the organic layer was washed with brine (800 mL), was dried over anhydrous sodium sulfate, and was concentrated under reduced pressure. The crude residue adsorbed onto silica gel was purified by flash column chromatography (silica gel: diam. 6 cm, ht. 15 cm; eluent: hexanes then 10% ethyl acetate in hexanes) to afford stannyltriazone **92** (12.1 g, 45%) as a white solid.

^1H NMR (500 MHz, CDCl_3 , 21 °C):	δ 7.07 (dd, $J = 8.7, 0.7$ Hz, 2H, NAr- <i>o</i> -H), 6.89 (d, $J = 8.5$ Hz, 2H, NAr- <i>m</i> -H), 4.60 (s, 2H, NCH_2N), 4.58 (s, 2H, NCH_2N), 2.85 (s, 3H, NCH_3), 2.78 (t, $J = 12.2$ Hz, 2H, NCH_2Sn), 2.27 (s, 3H, NAr CH_3), 1.82-1.74 (m, 6H, ^tHx), 1.65-1.56 (m, 9H, ^cHx), 1.52-1.13 (m, 18H, ^cHx).
^{13}C NMR (125.8 MHz, CDCl_3 , 21 °C):	δ 156.3, 146.1, 132.2, 130.0, 119.5, 69.2, 67.3, 32.7, 32.3, 29.5, 28.7, 27.9, 27.4, 20.8.
FTIR (neat) cm^{-1} :	2915 (s), 2844 (s), 1636 (s), 1515 (s), 1444 (s), 1407 (m), 1299 (s), 1201 (m), 991 (m).
HRMS (DART) (m/z):	calc'd for $\text{C}_{30}\text{H}_{50}\text{N}_3\text{OSn}$, $[\text{M}+\text{H}]^+$: 588.2987, found: 588.2982.
M.p.:	59–62 °C.
TLC (15% ethyl acetate in hexanes), R_f :	0.20 (CAM, UV).



1-Methyl-3-((tricyclohexylstannyl)methyl)urea (93):

Aqueous hydrochloric acid solution (0.5 N, 2.30 mL, 1.15 mmol, 2.00 equiv) was added via syringe to a solution of stannyltriazone **92** (338 mg, 0.576 mmol, 1 equiv) in methanol (11.5 mL) at 23 °C, and the resulting mixture was heated to 60 °C. After 5 h, the reaction mixture was allowed to cool to 23 °C, and was neutralized with saturated aqueous sodium bicarbonate solution (4 mL). The resulting mixture was concentrated under reduced pressure, and the residue was partitioned between dichloromethane (50 mL) and water (50 mL). The layers were separated, and the aqueous layer was extracted with dichloromethane (2 × 50 mL). The combined organic layers were dried over anhydrous sodium sulfate and were concentrated under reduced pressure. The crude residue was purified by flash column chromatography (silica gel: diam. 2.5 cm, ht. 15 cm; eluent: 15% ethyl acetate in dichloromethane) to afford stannylurea **93** (104 mg, 40%) as a white crystalline solid.

$^1\text{H NMR}$ (500 MHz, CDCl_3 , 21 °C): δ 4.63 (br-s, 1H, NH), 4.33 (br-s, 1H, NH), 2.77 (br-d, $J = 4.6$ Hz, C_{16}H_3), 2.75-2.65 (m, 2H, C_4H_2), 1.85-1.74 (m, 6H, $^{\circ}\text{Hx}$), 1.70-1.44 (m, 18H, $^{\circ}\text{Hx}$), 1.36-1.16 (m, 9H, $^{\circ}\text{Hx}$).

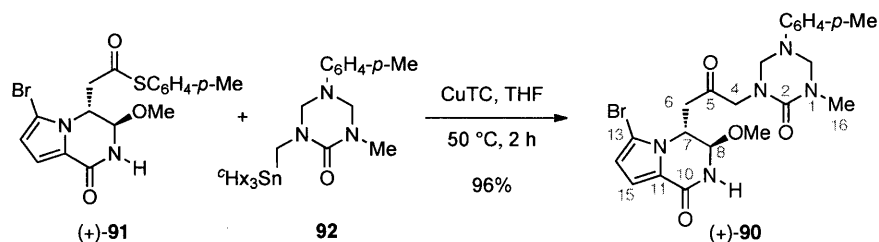
$^{13}\text{C NMR}$ (125.8 MHz, CDCl_3 , 21 °C): δ 160.7, 32.5, 29.3, 27.5, 27.2, 26.9, 22.3.

FTIR (neat) cm^{-1} : 3357 (br-m), 2912 (s), 2842 (s), 1628 (s), 1580 (s), 1442 (m), 1279 (m), 1167 (w).

HRMS (ESI) (m/z): calc'd for $\text{C}_{21}\text{H}_{40}\text{N}_2\text{NaOSn}$, $[\text{M}+\text{Na}]^+$: 479.2068, found: 479.2056.

M.p.: 144–148 °C.

TLC (15% ethyl acetate in dichloromethane), R_f : 0.25 (CAM, UV).



(+)-(3*R*,4*R*)-6-Bromo-3-methoxy-4-(3-(3-methyl-2-oxo-5-(*p*-tolyl)-1,3,5-triazinan-1-yl)-2-oxopropyl)-3,4-dihydropyrrolo[1,2-*a*]pyrazin-1(2*H*)-one (90):

A flask was charged with thioester (+)-**91** (5.70 g, 13.9 mmol, 1 equiv), stannyltriazone **92** (9.80 g, 16.8 mmol, 1.20 equiv), and copper thiophene 2-carboxylate (CuTC, 4.00 g, 21.0 mmol 1.50 equiv) at 23 °C and placed under an argon atmosphere. Anhydrous tetrahydrofuran (140 mL) was added via syringe, and the entire reaction mixture was degassed thoroughly by passage of a stream of argon. After the reaction mixture was heated to 50 °C for 2 h, the resulting brown reaction mixture was allowed to cool to 23 °C, was diluted with ethyl acetate (500 mL), and was filtered through a plug of celite with ethyl acetate as eluent (3 × 200 mL). The resulting green filtrate was washed with ~5% aqueous ammonium hydroxide solution (4 × 600 mL), and brine (400 mL). The resulting light yellow organic layer was dried over anhydrous sodium sulfate and was concentrated under reduced pressure. The residue was purified by flash column chromatography (silica gel: diam. 5 cm, ht. 14 cm; eluent: 5% methanol in ethyl acetate then 10% methanol in ethyl acetate) and was lyophilized from benzene to afford ketone (+)-**90** (6.7 g, 96%) as a light tan solid.

¹H NMR (500 MHz, CDCl₃, 21 °C):

δ 7.04 (dd, *J* = 8.6, 0.6 Hz, 2H, NAr-*o*-H), 6.93 (d, *J* = 4.0 Hz, 1H, C₁₅H), 6.89 (d, *J* = 8.5 Hz, 2H, NAr-*m*-H), 6.55 (d, *J* = 4.6 Hz, 1H, N₉H), 6.26 (d, *J* = 4.1 Hz, 1H, C₁₄H), 4.85 (ddd, *J* = 11.2, 2.8, 1.4 Hz, 1H, C₇H), 4.81 (d, *J* = 11.6 Hz, 1H, NCH₂N), 4.71 (d, *J* = 12.0 Hz, 1H, NCH₂N), 4.66 (dd, *J* = 11.7, 1.3 Hz, 1H, NCH₂N), 4.63-4.60 (m, 2H, C₈H, NCH₂N), 3.92 (d, *J* = 17.7 Hz, 1H, C₄H_a), 3.85 (d, *J* = 17.7 Hz, 1H, C₄H_b) 3.33 (s, 3H, OCH₃), 2.92 (s, 3H, C₁₆H₃), 2.79 (dd, *J* = 17.9, 11.2 Hz, 1H, C₆H_a), 2.39 (dd, *J* = 17.9, 2.9 Hz, 1H, C₆H_b), 2.23 (s, 3H, NArCH₃).

¹³C NMR (125.8 MHz, CDCl₃, 21 °C):

δ 204.4, 159.5, 155.8, 145.4, 132.7, 130.1, 123.6, 119.4, 114.7, 112.7, 105.7, 83.4, 67.8, 66.8, 55.6, 55.0, 52.7, 41.1, 32.2, 20.7.

FTIR (neat) cm⁻¹:

3248 (m), 2921 (m), 1724, (m), 1667 (s), 1640 (s), 1514 (s), 1422 (s), 1316 (s), 1087 (m).

HRMS (ESI) (*m/z*):

calc'd for C₂₂H₂₆BrN₅NaO₄, [M+Na]⁺: 526.1060, found: 526.1063.

[α]_D²²:

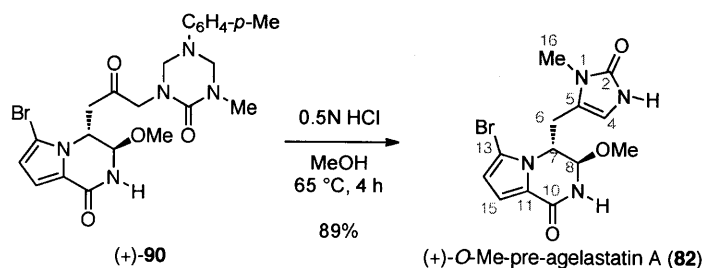
+81.1 (c 0.62, CHCl₃).

M.p.:

101–105 °C.

TLC (5% methanol in ethyl acetate), *R*_f:

0.20 (CAM, UV).



(+)-*O*-Methyl-pre-agelastatin A (82):

Aqueous hydrochloric acid solution (0.5 N, 23.8 mL, 11.9 mmol, 2.00 equiv) was added via syringe to a solution of ketone (+)-**90** (3.00 g, 5.90 mmol, 1 equiv) in methanol (1.18 L) at 23 °C, and the entire reaction mixture was degassed thoroughly by passage of a stream of argon. After the reaction mixture was heated to 65 °C for 4 h, the light pink reaction mixture was allowed to cool to 23 °C, and was concentrated to approximately 250 mL volume under reduced pressure. The resulting solution was basified to pH = 8 by the addition of a 5% aqueous ammonium hydroxide in methanol solution and the reaction mixture became a clear light orange color. A silica gel (50 mL) slurry in a 1% aqueous ammonium hydroxide in methanol solution (75 mL) was added and the resulting mixture was concentrated to dryness under reduced pressure. The crude residue adsorbed onto silica gel was purified by flash column chromatography (silica gel: diam. 5 cm, ht. 15 cm; eluent: 9% methanol, 1% ammonium hydroxide in chloroform to 13.5% methanol, 1.5% ammonium hydroxide in chloroform) to afford (+)-*O*-methyl-pre-agelastatin A (**82**, 1.87 g, 89%) as a light tan solid that was found to be 99% ee by chiral HPLC analysis [Chiralcel OD-H; 0.8 mL/min; 35% isopropanol in hexanes; $t_R(\text{major}) = 14.9$ min, $t_R(\text{minor}) = 12.1$ min]. Crystals of (+)-*O*-methyl-pre-agelastatin A (**82**) suitable for X-ray diffraction were obtained from methanol. For a thermal ellipsoid representation of (+)-*O*-methyl-pre-agelastatin A (**82**) see page 132. (+)-*O*-Methyl-pre-agelastatin A (**82**) is best used immediately in the following step; however, it could be stored as a dry solid at –8 °C under an argon atmosphere, or as a suspension frozen in benzene at –8 °C under an argon atmosphere for greater than a month. (+)-*O*-Methyl-pre-agelastatin A (**82**) is sparingly soluble in organic solvents, methanol, and water.

$^1\text{H NMR}$ (500 MHz, CD_3OD , 21 °C): δ 6.90 (dd, $J = 4.1, 0.4$ Hz, 1H, C_{15}H), 6.27 (d, $J = 4.1$ Hz, 1H, C_{14}H), 5.97 (t, $J = 0.7$ Hz, 1H, C_4H), 4.76 (d, $J = 1.6$ Hz, 1H, C_8H), 4.54 (ddd, $J = 8.4, 6.1, 1.5$ Hz, 1H, C_7H), 3.35 (s, 3H, OCH_3), 3.14 (s, 3H, C_{16}H_3), 2.95 (ddd, $J = 15.4, 6.0, 0.8$ Hz, 1H, C_6H_a), 2.78 (ddd, $J = 15.4, 8.5, 0.8$ Hz, 1H, C_6H_b).

$^{13}\text{C NMR}$ (125.8 MHz, CD_3OD , 21 °C): δ 161.2, 156.1, 124.5, 120.2, 116.1, 113.5, 108.8, 108.5, 84.9, 58.0, 55.2, 29.5, 27.7.

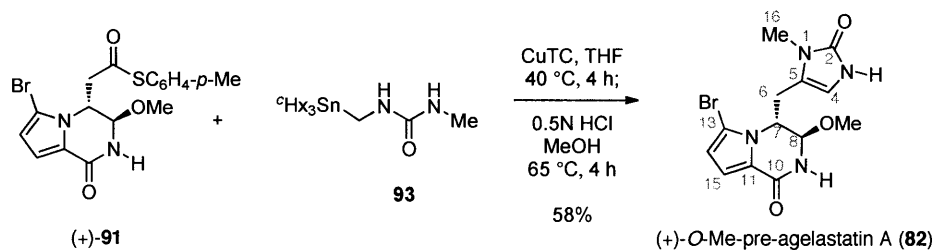
FTIR (neat) cm^{-1} : 3227 (br-m), 2936 (w), 1666 (s), 1552 (m), 1460 (w), 1421 (m), 1386 (w), 1319 (m), 1085 (m).

HRMS (ESI) (m/z): calcd for $\text{C}_{13}\text{H}_{15}\text{BrN}_4\text{NaO}_3$, $[\text{M}+\text{Na}]^+$: 377.0220, found: 377.0221.

$[\alpha]_D^{22}$: +248.7 (c 0.032, methanol).

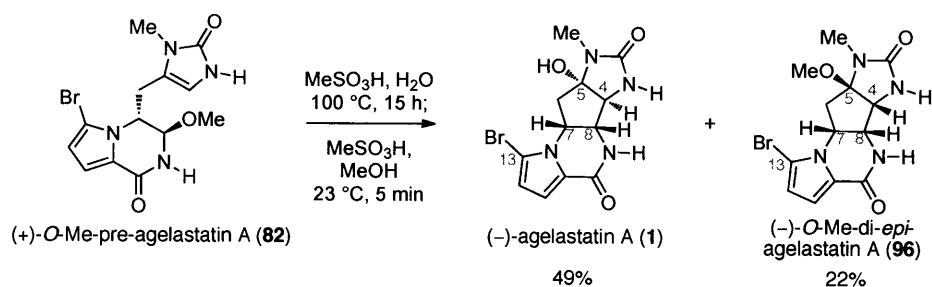
M.p.: 157-161 °C (dec.).

TLC (18% methanol, 2% ammonium hydroxide in chloroform), R_f : 0.40 (CAM, UV).



Direct synthesis of (+)-*O*-methyl-pre-agelastatin A (19):

Anhydrous tetrahydrofuran (1 mL) was added via syringe to a flask charged with (+)-**91** (20.0 mg, 49.0 μmol , 1 equiv), urea **93** (67.0 mg, 147 μmol , 3.00 equiv), and copper thiophene 2-carboxylate (CuTC, 23.3 mg, 123 μmol , 2.50 equiv) at 23 $^\circ\text{C}$ and under an argon atmosphere. The entire reaction mixture was degassed thoroughly by passage of a stream of argon, and the mixture was heated to 40 $^\circ\text{C}$. After 4 h, the reaction mixture was allowed to cool to 23 $^\circ\text{C}$, was diluted with methanol (7 mL), and was filtered through a plug of celite with methanol washings (3×1 mL). Aqueous hydrochloric acid solution (0.5 N, 196 μL , 98.0 μmol , 2.00 equiv) was added to the filtrate, and the resulting mixture was heated to 65 $^\circ\text{C}$. After 4 h, the reaction mixture was allowed to cool to 23 $^\circ\text{C}$ and was basified to pH = 8 by the addition of a 5% aqueous ammonium hydroxide in methanol solution. The resulting mixture was concentrated under reduced pressure, and the crude residue adsorbed onto silica gel was purified by flash column chromatography (silica gel: diam. 1.5 cm, ht. 10 cm; eluent: 10% methanol in dichloromethane to 15% methanol in dichloromethane) to afford (+)-*O*-methyl-pre-agelastatin A (**82**, 10.0 mg, 58%) as a tan solid that was found to be 99% ee by chiral HPLC analysis [Chiralcel OD-H; 0.8 mL/min; 35% isopropanol in hexanes; t_{R} (major) = 14.9 min, t_{R} (minor) = 12.1 min]. See page 108 for full characterization data.



(-)-Agelastatin A (1) and (-)-*O*-methyl-di-*epi*-agelastatin A (96):

A solution of methanesulfonic acid (10.9 mL, 168 mmol, 20.0 equiv) in water (100 mL) was added slowly via syringe to a solution of (+)-*O*-methyl-pre-agelastatin A (**82**, 2.97 g, 8.39 mmol, 1 equiv) in water (1.68 L) at 23 °C. The entire reaction mixture was degassed thoroughly by passage of a stream of argon, and the mixture was heated to 100 °C. After 15 h, the reaction mixture was allowed to cool to 23 °C and was basified to pH = 8 by addition of 5% aqueous ammonium hydroxide solution. The resulting mixture was concentrated under reduced pressure. The crude residue was dissolved in methanol (839 mL) and the resulting mixture was acidified to pH = 2 by the addition of a solution of 5% methanesulfonic acid in methanol (20 mL). After 5 min, the reaction mixture was basified to pH = 8 by addition of 5% aqueous ammonium hydroxide solution. The resulting mixture was concentrated under reduced pressure, and the crude residue adsorbed onto silica gel was purified by flash column chromatography (silica gel: diam. 7 cm, ht. 14 cm; eluent: 9% methanol, 1.0% ammonium hydroxide in chloroform to 13.5% methanol, 1.5% ammonium hydroxide in chloroform) to afford (-)-agelastatin A (**1**, 1.40 g, 49%) as a tan solid that was found to be 99% ee by chiral HPLC analysis [Chiralpak AD-H; 0.53 mL/min; 10% isopropanol in hexanes; $t_R(\text{major}) = 40.0$ min, $t_R(\text{minor}) = 24.5$ min]. (-)-*O*-Methyl-di-*epi*-agelastatin A (**96**, 668 mg, 22%) was also isolated as light tan solid. (-)-Agelastatin A (**1**) is sparingly soluble in organic solvents, methanol, and water. Crystals of (-)-agelastatin A (**1**) suitable for X-ray diffraction were obtained from methanol. For a thermal ellipsoid representation of (-)-agelastatin A (**1**) see page 137.

(-)-agelastatin A (1):

$^1\text{H NMR}$ (500 MHz, CD_3OD , 21 °C): δ 6.92 (d, $J = 4.0$ Hz, 1H, C_{15}H), 6.33 (d, $J = 4.1$ Hz, 1H, C_{14}H), 4.60 (app-dt, $J = 11.9, 6.0$ Hz, 1H, C_7H), 4.09 (d, $J = 5.4$ Hz, 1H, C_8H), 3.88 (s, 1H, C_4H), 2.81 (s, 3H, C_{16}H_3), 2.65 (dd, $J = 13.1, 6.3$ Hz, 1H, C_6H), 2.10 (app-t, $J = 12.7$ Hz, 1H, C_6H).

$^{13}\text{C NMR}$ (125.8 MHz, CD_3OD , 21 °C): δ 161.6, 161.2, 124.3, 116.2, 113.9, 107.4, 95.8, 67.5, 62.3, 54.5, 40.1, 24.4.

FTIR (neat) cm^{-1} : 3269 (m), 2921 (w), 1651 (s), 1552 (w), 1423 (m), 1378 (w), 1090 (w), 746 (w).

HRMS (ESI) (m/z): calc'd for $\text{C}_{12}\text{H}_{13}\text{BrN}_4\text{NaO}_3$, $[\text{M}+\text{Na}]^+$: 363.0063, found: 363.0073.

$[\alpha]_{\text{D}}^{22}$: -87.6 (c 0.10, methanol).¹⁰

¹⁰ Optical rotations from naturally occurring samples of (-)-agelastatin A (**1**). $[\alpha]_{\text{D}} = -59.3$ (c 0.13, methanol), Hong, T. W.; Jimenez, D. R.; Molinski, T. F. *J. Nat. Prod.* **1998**, *61*, 158–161. $[\alpha]_{\text{D}}^{26} = -88.9$ (c 0.09, chloroform), Pettit, G. R.; Ducki, S.; Herald, D. L.; Doubek, D. L.; Schmidt, J. M.; Chapuis, J.-C. *Oncol. Res.* **2005**, *15*, 11–20. $[\alpha]_{\text{D}}^{25} = -58.5$ (c 0.21, methanol), Tilvi, S.; Moriou, C.; Martin, M.-T.; Gallard, J.-F.; Sorres, J.; Patel, K.; Petek, S.; Debitus, C.; Ermolenko, L.; Al-Mourabit, A. *J. Nat. Prod.* Article ASAP,

M.p.: 213–215 °C (dec.).

TLC (18% methanol, 2% ammonium hydroxide in chloroform), R_f: 0.34 (CAM, UV).

(–)-O-methyl-di-epi-agelastatin A (96):

¹H NMR (500 MHz, CD₃OD, 21 °C): δ 6.90 (d, *J* = 4.1 Hz, 1H, C₁₅H), 6.33 (d, *J* = 4.1 Hz, 1H, C₁₄H), 4.95 (ddd, *J* = 10.4, 7.2, 5.1 Hz, 1H, C₇H), 4.42 (app-t, *J* = 5.4 Hz, 1H, C₈H), 4.22 (d, *J* = 5.9 Hz, 1H, C₄H), 3.13 (s, 3H, OCH₃), 2.69 (s, 3H, NCH₃), 2.53 (dd, *J* = 13.4, 7.1 Hz, 1H, C₆H), 2.32 (dd, *J* = 13.5, 10.5 Hz, 1H, C₆H).

¹³C NMR (125.8 MHz, CD₃OD, 21 °C): δ 162.4, 161.6, 124.9, 116.3, 114.3, 107.2, 100.1, 59.3, 58.6, 55.1, 49.9, 42.2, 24.9.

FTIR (neat) cm⁻¹: 3374 (m), 2951 (w), 1703 (s), 1659 (s), 1552 (m), 1424 (m), 1346 (w).

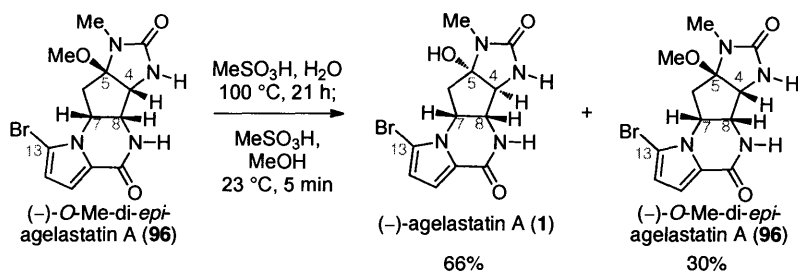
HRMS (ESI) (*m/z*): calc'd for C₁₃H₁₅BrN₄NaO₃, [M+Na]⁺: 377.0220, found: 377.0220.

[α]_D²²: –70.0 (c 0.042, methanol).

M.p.: 205–208 °C.

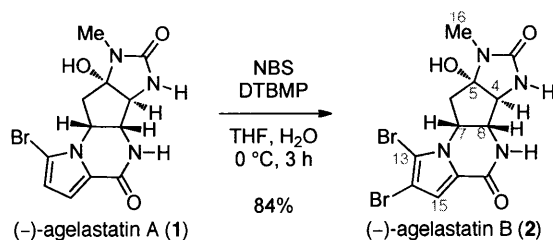
TLC (18% methanol, 2% ammonium hydroxide in chloroform), R_f: 0.60 (CAM, UV).

Publication Date (Web): February 17, 2010. DOI: 10.1021/np900539j. Optical rotations from synthetic samples of (–)-agelastatin A (**1**). [α]_D²⁰ = –65.5 (c 0.5, methanol), Feldman, K. S.; Saunders, J. C. *J. Am. Chem. Soc.* **2002**, *124*, 9060-9061. [α]_D = –84.2 (c 1, methanol), Domostoj, M. M.; Irving, E.; Scheinmann, F.; Hale, K. J. *Org. Lett.* **2004**, *6*, 2615-2618. [α]_D²⁰ = –62.2 (c 0.18, methanol), Davis, F. A.; Deng, J. *Org. Lett.* **2005**, *7*, 621-623. (+)-Agelastatin A, [α]_D = +53.2 (c 0.13, methanol), Trost, B. M.; Dong, G. *J. Am. Chem. Soc.* **2006**, *128*, 6054-6055. [α]_D¹⁴ = –83.8 (c 0.21, methanol), Ichikawa, Y.; Yamaoka, T.; Nakano, K.; Kotsuki, H. *Org. Lett.* **2007**, *9*, 2989-2992. [α]_D²⁰ = –64.4 (c 0.15, methanol), Yoshimitsu, T.; Ino, T.; Tanaka, T. *Org. Lett.* **2008**, *10*, 5457-5460. [α]_D²³ = –83.4 (c 0.93, methanol), Hama, N.; Matsuda, T.; Sato, T.; Chida, N. *Org. Lett.* **2009**, *11*, 2687–2690. [α]_D²³ = –87.0 (c 1.1, methanol), When, P. M.; Du Bois, J. *Angew. Chem. Int. Ed.* **2009**, *48*, 3802-3805.



Equilibration of (-)-*O*-methyl-di-*epi*-agelastatin A (96**) to (-)-agelastatin A (**1**):**

A solution of methanesulfonic acid (613 μL , 9.44 mmol, 5.00 equiv) in water (10 mL) was added slowly via syringe to a solution of (-)-*O*-methyl-di-*epi*-agelastatin A (**96**, 668 mg, 1.89 mmol, 1 equiv) in water (378 mL) at 23 $^\circ\text{C}$. The entire reaction mixture was degassed thoroughly by passage of a stream of argon and was heated to 100 $^\circ\text{C}$. After 21 h, the reaction mixture was allowed to cool to 23 $^\circ\text{C}$ and was basified to pH = 8 by addition of 5% aqueous ammonium hydroxide solution. The resulting mixture was concentrated under reduced pressure. The crude residue was dissolved in methanol (378 mL) and the resulting mixture was acidified to pH = 2 by the addition of a solution of 5% methanesulfonic acid in methanol (20 mL). After 5 min, the reaction mixture was basified to pH = 8 by addition of 5% aqueous ammonium hydroxide solution. The resulting mixture was concentrated under reduced pressure, and the crude residue adsorbed onto silica gel was purified by flash column chromatography (silica gel: diam. 4 cm, ht. 14 cm; eluent: 9% methanol, 1.0% ammonium hydroxide in chloroform to 13.5% methanol, 1.5% ammonium hydroxide in chloroform) to afford (-)-agelastatin A (**1**, 421 mg, 66%) as a tan solid. (-)-*O*-Methyl-di-*epi*-agelastatin A (**96**, 200 mg, 30%) was also isolated as a light tan solid. See pages 110 and 111 for full characterization data.



(-)-Agelastatin B (2):

N-Bromosuccinimide (NBS, 5.0 mg, 28 μmol , 1.1 equiv) was added as a solid in one portion to a solution of (-)-agelastatin A (**1**, 9.1 mg, 27 μmol , 1 equiv) and 2,6-di-*tert*-butyl-4-methylpyridine (DTBMP, 8.3 mg, 41 μmol , 1.5 equiv) in water (500 μL) and tetrahydrofuran (1.00 mL) at 0 $^\circ\text{C}$. After 2 h, a mixture of saturated aqueous sodium thiosulfate solution and saturated aqueous sodium bicarbonate solution (1:1, 100 μL ,) was added, and the resulting mixture was purified directly by flash column chromatography (silica gel: diam. 1.5 cm, ht. 9 cm; eluent: 9% methanol, 1.0% ammonium hydroxide in chloroform to 13.5% methanol, 1.3% ammonium hydroxide in chloroform) to afford (-)-agelastatin B (**2**, 9.4 mg, 84%) as a white crystalline solid that was found to be 99% ee by chiral HPLC analysis [Chiralpak AD-H; 0.53 mL/min; 10% isopropanol in hexanes; t_{R} (major) = 27.7 min, t_{R} (minor) = 21.1 min]. (-)-Agelastatin B (**2**) is sparingly soluble in organic solvents, methanol, and water.

$^1\text{H NMR}$ (500 MHz, CD_3OD , 21 $^\circ\text{C}$): δ 6.97 (s, 1H, C_{15}H), 4.60 (app-dt, $J = 12.0, 6.0$ Hz, 1H, C_7H), 4.11 (d, $J = 5.4$ Hz, 1H, C_8H), 3.88 (s, 1H, C_4H), 2.81 (s, 3H, C_{16}H_3), 2.68 (dd, $J = 13.1, 6.5$ Hz, 1H, C_6H_a), 2.12 (app-t, $J = 12.6$ Hz, 1H, C_6H_b).

$^{13}\text{C NMR}$ (125.8 MHz, CD_3OD , 21 $^\circ\text{C}$): δ 161.5, 160.2, 124.9, 117.1, 108.9, 101.8, 95.7, 67.5, 62.2, 55.5, 40.0, 24.4.

FTIR (neat) cm^{-1} : 3219 (m), 2919 (m), 1639 (s), 1548 (m), 1497 (m), 1403 (m), 1360 (m).

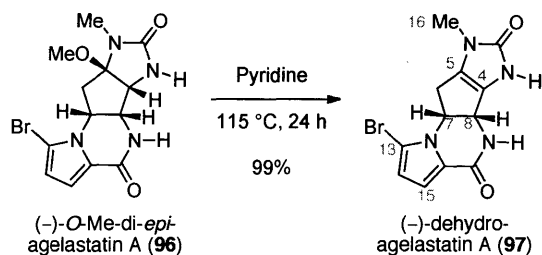
HRMS (ESI) (m/z): calc'd for $\text{C}_{12}\text{H}_{13}\text{Br}_2\text{N}_4\text{O}_3$, $[\text{M}+\text{H}]^+$: 418.9349, found: 418.9343.

$[\alpha]_{\text{D}}^{22}$: -60.6 (c 0.018, methanol).¹¹

M.p.: 211–214 $^\circ\text{C}$ (dec.).

TLC (18% methanol, 2% ammonium hydroxide in chloroform), R_f : 0.25 (CAM, UV).

¹¹ $[\alpha]_{\text{D}}^{20} = -60.3$ (c 0.50, methanol), Feldman, K. S.; Saunders, J. C. *J. Am. Chem. Soc.* **2002**, *124*, 9060-9061.



(-)-Dehydroagelastatin A (97):¹²

A solution of (-)-*O*-methyl-di-*epi*-agelastatin A (**96**, 11.6 mg, 32.8 μmol , 1 equiv) in pyridine (3.28 mL) sealed under an argon atmosphere was heated to 115 $^\circ\text{C}$. After 24 h, the resulting mixture was allowed to cool to 23 $^\circ\text{C}$, and was concentrated under reduced pressure. The residue was purified by flash column chromatography (silica gel: diam. 1.5 cm, ht. 8 cm; eluent: 9% methanol, 1% ammonium hydroxide in chloroform) to afford (-)-dehydroagelastatin A (**97**, 10.9 mg, 99%) as a light tan solid that was found to be 99% ee by chiral HPLC analysis [Chiralcel OD-H; 0.8 mL/min; 35% isopropanol in hexanes; t_{R} (major) = 53.8 min, t_{R} (minor) = 62.8 min]. (-)-dehydroagelastatin A (**97**) is sparingly soluble in organic solvents, methanol, and water.

^1H NMR (500 MHz, CD_3OD , 21 $^\circ\text{C}$): δ 6.91 (d, J = 4.0 Hz, 1H, C_{15}H), 6.39 (d, J = 4.1 Hz, 1H, C_{14}H), 5.34 (app-q, J = 7.1 Hz, 1H, C_7H), 5.10 (dd, J = 6.7, 1.6 Hz, 1H, C_8H), 3.48 (dd, J = 14.4, 7.4 Hz, 1H, C_6H_a), 3.22 (s, 3H, C_{16}H_3), 2.63 (ddd, J = 14.4, 7.2, 1.8 Hz, 1H, C_6H_b).

^{13}C NMR (125.8 MHz, CD_3OD , 21 $^\circ\text{C}$): δ 160.0, 158.5, 127.5, 124.0, 120.3, 116.0, 114.2, 107.2, 57.1, 53.1, 32.4, 29.1.

FTIR (neat) cm^{-1} : 3209 (br-m), 2924 (w), 1691 (s), 1657 (s), 1555 (m), 1427 (m), 1375 (w), 1323 (w).

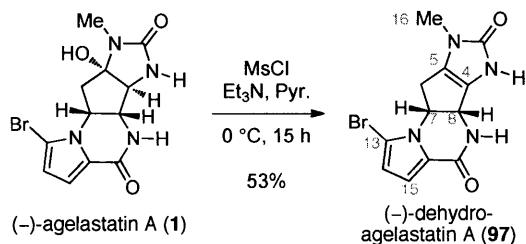
HRMS (ESI) (m/z): calc'd for $\text{C}_{12}\text{H}_{12}\text{BrN}_4\text{O}_2$, $[\text{M}+\text{H}]^+$: 323.0138, found: 323.0144.

$[\alpha]_{\text{D}}^{22}$: -765.9 (c 0.07, methanol).

M.p.: 219-222 $^\circ\text{C}$ (dec.).

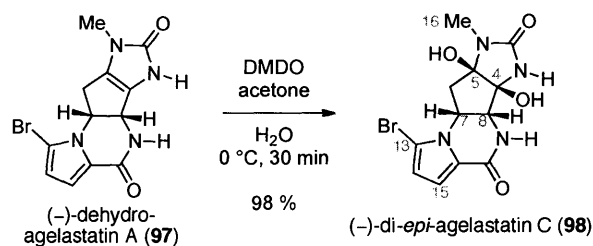
TLC (18% methanol, 2% ammonium hydroxide in chloroform), R_f : 0.30 (CAM, UV).

¹² For a previous report of the synthesis of (-)-dehydroagelastatin A (**97**) see: D'Ambrosio, M.; Guerriero, A.; Ripamonti, M.; Debitus, C.; Waikedre, J.; Pietra, F. *Helv. Chim. Acta* **1996**, *79*, 727-735.



Alternate synthesis of (-)-dehydroagelastatin A (97):

Methanesulfonyl chloride (MsCl, 45.5 μL , 588 μmol , 1.00 equiv) was added to a solution of (-)-agelastatin A (**1**, 200 mg, 588 μmol , 1 equiv) and triethylamine (164 μL , 1.18 mmol, 2.00 equiv) in pyridine (2.94 mL) at 0 $^\circ\text{C}$ under an argon atmosphere. After 15 h, the dark orange reaction mixture was purified directly by flash column chromatography (silica gel: diam. 2.5 cm, ht. 10 cm; eluent: 9% methanol, 1% ammonium hydroxide in chloroform to 13.5% methanol, 1.5% ammonium hydroxide in chloroform) to afford (-)-dehydroagelastatin A (**97**, 100 mg, 53%) as a light tan solid that was found to be 99% ee by chiral HPLC analysis [Chiralcel OD-H; 0.8 mL/min; 35% isopropanol in hexanes; $t_{\text{R}}(\text{major}) = 53.8$ min, $t_{\text{R}}(\text{minor}) = 62.8$ min]. See page 114 for full characterization data. (-)-Agelastatin A (**1**, 80 mg, 40%) was also recovered from the reaction mixture.



(-)-Di-epi-agelastatin C (98):

Freshly prepared dimethyldioxirane (DMDO, 0.108 M in acetone, 2.16 mL, 233 μmol , 1.00 equiv) was added via syringe to a solution of (-)-dehydroagelastatin A (**97**, 75.0 mg, 233 μmol , 1 equiv) in acetone (2.3 mL) and water (2.3 mL) at 0 $^\circ\text{C}$. After 30 min, the reaction mixture was concentrated under reduced pressure to afford (-)-di-epi-agelastatin C (**98**, 81.5 mg, 98%) as a white solid. (-)-di-epi-agelastatin C (**98**) is sparingly soluble in organic, methanol, and water, and is sensitive to base.

^1H NMR (500 MHz, CD_3OD , 21 $^\circ\text{C}$): δ 6.89 (d, $J = 4.1$ Hz, 1H, C₁₅H), 6.33 (d, $J = 4.0$ Hz, 1H, C₁₄H), 5.05-5.00 (m, 1H, C₇H), 4.23 (d, $J = 5.8$ Hz, 1H, C₈H), 2.72 (s, 3H, C₁₆H₃), 2.56 (ddd, $J = 13.6, 6.8, 1.0$ Hz, 1H, C₆H_a), 2.40 (dd, $J = 13.7, 10.0$ Hz, 1H, C₆H_b).

^{13}C NMR (125.8 MHz, CD_3OD , 21 $^\circ\text{C}$): δ 161.2, 159.9, 124.6, 116.3, 114.4, 107.1, 94.0, 92.5, 64.3, 54.2, 42.7, 25.0.

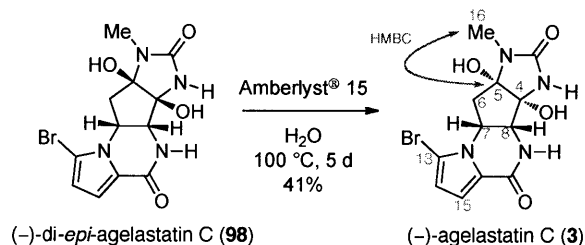
FTIR (neat) cm^{-1} : 3335 (br-s), 2922 (m), 2851 (m), 1691 (s), 1658 (s), 1553 (m), 1424 (m), 1337 (w), 1127 (w).

HRMS (ESI) (m/z): calc'd for $\text{C}_{12}\text{H}_{13}\text{BrN}_4\text{NaO}_4$, $[\text{M}+\text{Na}]^+$: 379.0012, found: 379.0024.

$[\alpha]_{\text{D}}^{22}$: -89.1 (c 0.011, methanol).

M.p.: 190-194 $^\circ\text{C}$ (dec.).

TLC (18% methanol, 2% ammonium hydroxide in chloroform), R_f : 0.21 (CAM, UV).



(-)-Agelastatin C (3):

Amberlyst[®] 15 (400 mg) was added to a solution of (-)-di-epi-agelastatin C (**98**, 10.0 mg, 28.0 μmol , 1 equiv) in water (14 mL) at 23 $^\circ\text{C}$. The entire reaction mixture was degassed thoroughly by passage of a stream of argon and the reaction mixture was heated to 100 $^\circ\text{C}$. After 5 d, the light yellow hot reaction mixture was filtered through a plug of cotton, and the filtered resin beads were washed with hot water ($3 \times 1\text{ mL}$). The filtrate was allowed to cool to 23 $^\circ\text{C}$ and was concentrated under reduced pressure to approximately 1 mL volume. The resulting mixture was purified directly by semi-preparative HPLC [Grace Vydac semi-preparative HPLC column, C18, monomeric 120 \AA ; 10.0 mL/min; 15% acetonitrile and 0.1% trifluoroacetic acid in water; $t_{\text{R}}(\mathbf{98}) = 4.3\text{ min}$, $t_{\text{R}}(\mathbf{3}) = 5.2\text{ min}$] to afford (-)-agelastatin C (**3**, 4.1 mg, 41%) as a white solid. (-)-Agelastatin C (**3**) is sparingly soluble in organic solvents, methanol, and water, and is sensitive to base. (-)-Di-epi-agelastatin C (**98**, 4.2 mg, 42%) was also isolated from the reaction mixture. Treatment of either (-)-di-epi-agelastatin C (**31**) or (-)-agelastatin C (**3**) with methanesulfonic acid (10 equiv) in D_2O at 100 $^\circ\text{C}$ for 3 d afforded a 1:1 equilibrium mixture of (-)-**3** and (-)-**98** with quantitative deuterium incorporation at the C6-, C14-, and C15-centers as indicated by ^1H NMR analysis.

^1H NMR (500 MHz, CD_3OD , 21 $^\circ\text{C}$): δ 6.92 (d, $J = 4.1\text{ Hz}$, 1H, C₁₅H), 6.34 (d, $J = 4.1\text{ Hz}$, 1H, C₁₄H), 4.57 (ddd, $J = 11.9, 6.8, 5.2\text{ Hz}$, 1H, C₇H), 4.19 (d, $J = 5.2\text{ Hz}$, 1H, C₈H), 2.79 (s, 3H, C₁₆H₃), 2.68 (dd, $J = 13.3, 6.9\text{ Hz}$, 1H, C₆H_a), 2.05 (dd, $J = 13.3, 11.9\text{ Hz}$, 1H, C₆H_b).

^{13}C NMR (125.8 MHz, CD_3OD , 21 $^\circ\text{C}$): δ 160.4, 159.8, 124.1, 116.3, 114.1, 107.5, 93.9, 90.0, 62.1, 52.1, 41.1, 24.6.

FTIR (neat) cm^{-1} : 3311 (br-s), 2921 (w), 1679 (s), 1642 (s), 1554 (m), 1425 (s), 1335 (w), 1273 (w), 1206 (m), 1184 (m), 1129 (m), 742 (w).

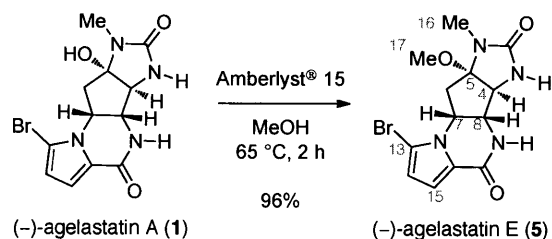
HRMS (ESI) (m/z): calc'd for $\text{C}_{12}\text{H}_{14}\text{BrN}_4\text{O}_4$, $[\text{M}+\text{H}]^+$: 357.0193, found: 357.0199.

$[\alpha]_{\text{D}}^{22}$: -26.9 (c 0.125, methanol).¹³

TLC (18% methanol, 2% ammonium hydroxide in chloroform), R_f : 0.21 (CAM, UV).

HMBC correlations (500 MHz, CD_3OD , 21 $^\circ\text{C}$) additional data: C2-H16, C4-H6_a, C4-H8, C5-H6_a, C5-H6_b, C5-H8, **C5-H16**, C6-H7, C6-H8, C7-H6_a, C7-H6_b, C7-H8, C7-H14, C7-H15, C8-H6_a, C8-H7, C10-H14, C10-H15, C11-H7, C11-H14, C11-H15, C13-H7, C13-H14, C13-H15, C14-H15, C15-H14. Key correlations are shown in bold.

¹³ $[\alpha]_{\text{D}} = -5$ (c 0.06, methanol), Hong, T. W.; Jimenez, D. R.; Molinski, T. F. *J. Nat. Prod.* **1998**, *61*, 158–161.



(-)-Agelastatin E (5):¹⁴

Amberlyst[®] 15 (25.0 mg) was added to a solution of (-)-agelastatin A (**1**, 10.0 mg, 29.4 μmol , 1 equiv) in methanol (5.8 mL) at 23 $^\circ\text{C}$, and the resulting mixture was heated to 65 $^\circ\text{C}$. After 2 h, the reaction mixture was filtered through a plug of cotton, and the filtrate was concentrated to afford (-)-agelastatin E (**5**, 10.0 mg, 96%) as a light tan solid. (-)-Agelastatin E (**5**) was sparingly soluble in organic solvents, methanol, and water.

¹H NMR (500 MHz, CD₃OD, 21 $^\circ\text{C}$): δ 6.91 (d, $J = 4.0$ Hz, 1H, C₁₅H), 6.33 (d, $J = 4.1$ Hz, 1H, C₁₄H), 4.62 (app-dt, $J = 11.9, 6.1$ Hz, 1H, C₇H), 4.12 (d, $J = 5.6$ Hz, 1H, C₈H), 4.09 (s, 1H, C₄H), 3.18 (s, 1H, C₁₇H₃), 2.79 (s, 3H, C₁₆H₃), 2.66 (dd, $J = 13.2, 6.5$ Hz, 1H, C₆H_a), 2.14 (app-t, $J = 12.7$ Hz, 1H, C₆H_b).

¹³C NMR (125.8 MHz, CD₃OD, 21 $^\circ\text{C}$): δ 161.9, 161.1, 124.2, 116.2, 114.0, 107.5, 100.2, 62.1, 61.2, 53.9, 50.8, 39.3, 24.7.

FTIR (neat) cm⁻¹: 3239 (br-m), 2927 (m), 1703 (s), 1659 (s), 1552 (m), 1425 (s), 1377 (w), 1302 (w), 1198 (w), 1103 (m).

HRMS (DART) (m/z): calc'd for C₁₃H₁₄BrN₄O₃, [M-H]⁻: 353.0255, found: 353.0254.

[α]_D²²: -63.4 (c 0.054, methanol).¹⁵

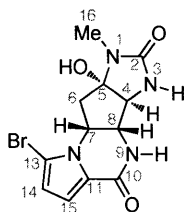
M.p.: 186–190 $^\circ\text{C}$ (dec.).

TLC (18% methanol, 2% ammonium hydroxide in chloroform), R_f: 0.60 (CAM, UV).

¹⁴ For a previous report of the semi-synthesis of (-)-agelastatin E (**5**) see: D'Ambrosio, M.; Guerriero, A.; Chiasera, G.; Pietra, F. *Helv. Chim. Acta* **1994**, *77*, 1895-1902.

¹⁵ [α]_D²⁵ = -28 (c 0.09, methanol), Tilvi, S.; Moriou, C.; Martin, M.-T.; Gallard, J.-F.; Sorres, J.; Patel, K.; Petek, S.; Debitus, C.; Ermolenko, L.; Al-Mourabit, A. *J. Nat. Prod.* Article ASAP, Publication Date (Web): February 17, 2010. DOI: 10.1021/np900539j.

Table S1. Comparison of our data for (-)-agelastatin A (1) with literature:



(-)-agelastatin A (1)

Assignment	Pietra's Report ¹⁶ ¹ H NMR, 300 MHz, CD ₃ OD	Du Bois' Report ¹⁷ ¹ H NMR, 400 MHz, CD ₃ OD	This Work ¹⁸ ¹ H NMR, 500 MHz, CD ₃ OD
C4	3.89 (br-s, 1H)	3.87 (br-s, 1H)	3.88 (s, 1H)
C6'	2.65 (br-dd, <i>J</i> = 12.9, 6.6 Hz, 1H)	2.64 (dd, <i>J</i> = 12.8, 6.4 Hz, 1H)	2.65 (dd, <i>J</i> = 13.1, 6.3 Hz, 1H)
C6''	2.10 (br-t, <i>J</i> = 12.3, 12.9, Hz, 1H)	2.09 (dd, <i>J</i> = 12.8, 12.4 Hz, 1H)	2.10 (app-t, <i>J</i> = 12.7 Hz, 1H)
C7	4.60 (m, <i>J</i> = 12.3, 6.6, 5.4 Hz, 1H)	4.59 (dt, <i>J</i> = 12.0, 6.0 Hz, 1H)	4.60 (app-dt, <i>J</i> = 11.9, 6.0 Hz, 1H)
C8	4.09 (br-d, <i>J</i> = 5.4 Hz, 1H)	4.08 (d, <i>J</i> = 5.6 Hz, 1H)	4.09 (d, <i>J</i> = 5.4 Hz, 1H)
C14	6.33 (d, <i>J</i> = 4.2 Hz, 1H)	6.32 (d, <i>J</i> = 4.0 Hz, 1H)	6.33 (d, <i>J</i> = 4.1 Hz, 1H)
C15	6.92 (br-d, <i>J</i> = 4.2 Hz, 1H)	6.90 (d, <i>J</i> = 4.0 Hz, 1H)	6.92 (d, <i>J</i> = 4.0 Hz, 1H)
C16	2.81 (s, 3H)	2.80 (s, 3H)	2.81 (s, 3H)

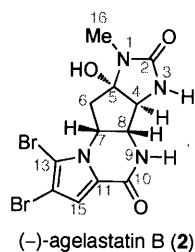
Assignment	Pietra's Report ¹⁶ ¹³ C NMR, 75 MHz, CD ₃ OD	Du Bois' Report ¹⁷ ¹³ C NMR, 125 MHz, CD ₃ OD	This Work ¹⁸ ¹³ C NMR, 125.8 MHz, CD ₃ OD
C2	163.00	161.4	161.6
C4	68.98	67.4	67.5
C5	97.24	95.6	95.8
C6	41.58	40.0	40.1
C7	55.96	54.4	54.5
C8	63.76	62.2	62.3
C10	162.65	161.1	161.2
C11	125.71	124.1	124.3
C13	108.80	107.3	107.4
C14	115.37	113.8	113.9
C15	117.59	116.0	116.2
C16	25.79	24.2	24.4

¹⁶ The reference points for the residual protium and carbon resonances of the NMR solvent were not provided. D'Ambrosio, M.; Guerriero, A.; Debitus, C.; Ribes, O.; Pusset, J.; Leroy, S.; Pietra, F. *J. Chem. Soc., Chem. Commun.* **1993**, 1305-1306.

¹⁷ The reference points for the residual protium and carbon resonances of the NMR solvent were not provided. When, P. M.: Du Bois, J. *Angew. Chem. Int. Ed.* **2009**, *48*, 3802-3805.

¹⁸ In this report, the NMR spectra are referenced from the residual protium resonance, CHD₂OD: δ 3.31, and carbon resonance, CD₃OD: δ 49.15.

Table S2. Comparison of our data for (-)-Agelastatin B (2) with literature:



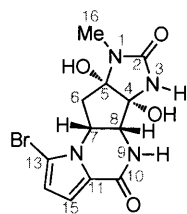
Assignment	Feldman's Report ¹⁹ ¹ H NMR, 300 MHz, CD ₃ OD	This Work ¹⁸ ¹ H NMR, 500 MHz, CD ₃ OD
C4	3.88 (s, 1H)	3.88 (s, 1H)
C6'	2.68 (dd, <i>J</i> = 13.1, 6.5 Hz, 1H)	2.68 (dd, <i>J</i> = 13.1, 6.5 Hz, 1H)
C6''	2.12 (t, <i>J</i> = 12.6 Hz, 1H)	2.12 (app-t, <i>J</i> = 12.6 Hz, 1H)
C7	4.60 (dt, <i>J</i> = 11.8, 6.0 Hz, 1H)	4.60 (app-dt, <i>J</i> = 12.0, 6.0 Hz, 1H)
C8	4.11 (d, <i>J</i> = 5.5 Hz, 1H)	4.11 (d, <i>J</i> = 5.4 Hz, 1H)
C15	6.96 (s, 1H)	6.97 (s, 1H)
C16	2.81 (s, 3H)	2.81 (s, 3H)

Assignment	Feldman's Report ¹⁹ ¹³ C NMR, 75 MHz, CD ₃ OD	This Work ¹⁸ ¹³ C NMR, 125.8 MHz, CD ₃ OD
C2	161.4	161.5
C4	67.6	67.5
C5	95.6	95.7
C6	40.0	40.0
C7	55.5	55.5
C8	62.1	62.2
C10	159.6	160.2
C11	111.0	124.9 ²⁰
C13	108.6	108.9
C14	101.8	101.8
C15	117.0	117.1
C16	24.2	24.4

¹⁹ The reference point for the residual proton of the NMR solvent was not provided. The ¹³C NMR spectrum is referenced from the carbon resonance, CD₃OD: δ 49.00. Feldman, K. S.; Saunders, J. C. *J. Am. Chem. Soc.* **2002**, *124*, 9060-9061.

²⁰ The C11 ¹³C NMR resonance is reassigned to δ 124.9.

Table S3. Comparison of our data for (-)-Agelastatin C (3) with literature:



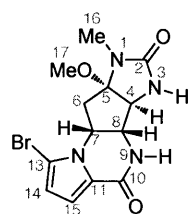
(-)-agelastatin C (3)

Assignment	Molinski's Report ²¹ ¹ H NMR, CD ₃ OD	This Work ¹⁸ ¹ H NMR, 500 MHz, CD ₃ OD
C6a	2.68 (dd, <i>J</i> = 13.3, 6.7 Hz, 1H)	2.68 (dd, <i>J</i> = 13.3, 6.9 Hz, 1H)
C6b	2.05 (dd, <i>J</i> = 13.3, 11.9 Hz, 1H)	2.05 (dd, <i>J</i> = 13.3, 11.9 Hz, 1H)
C7	4.56 (m, <i>J</i> = 11.9, 6.7, 5.1 Hz, 1H)	4.57 (ddd, <i>J</i> = 11.9, 6.8, 5.2 Hz, 1H)
C8	4.19 (d, <i>J</i> = 5.1 Hz, 1H)	4.19 (d, <i>J</i> = 5.2 Hz, 1H)
C14	6.33 (d, <i>J</i> = 4.1 Hz, 1H)	6.34 (d, <i>J</i> = 4.1 Hz, 1H)
C15	6.92 (d, <i>J</i> = 4.1 Hz, 1H)	6.92 (d, <i>J</i> = 4.1 Hz, 1H)
C16	2.78 (s, 3H)	2.79 (s, 3H)

Assignment	Molinski's Report ²¹ ¹³ C NMR, CD ₃ OD	This Work ¹⁸ ¹³ C NMR, 125.8 MHz, CD ₃ OD
C2	160.26	160.4
C4	89.85	90.0
C5	93.78	93.9
C6	40.96	41.1
C7	51.97	52.1
C8	61.91	62.1
C10	159.61	159.8
C11	124.00	124.1
C13	107.29	107.5
C14	113.90	114.1
C15	116.11	116.3
C16	24.47	24.6

²¹ The reference points for the residual protium and carbon resonances of the NMR solvent and the magnetic field strength were not provided. Hong, T. W.; Jimenez, D. R.; Molinski, T. F. *J. Nat. Prod.* **1998**, *61*, 158-161.

Table S4. Comparison of our data for (-)-agelastatin E (5) with literature:



(-)-agelastatin E (5)

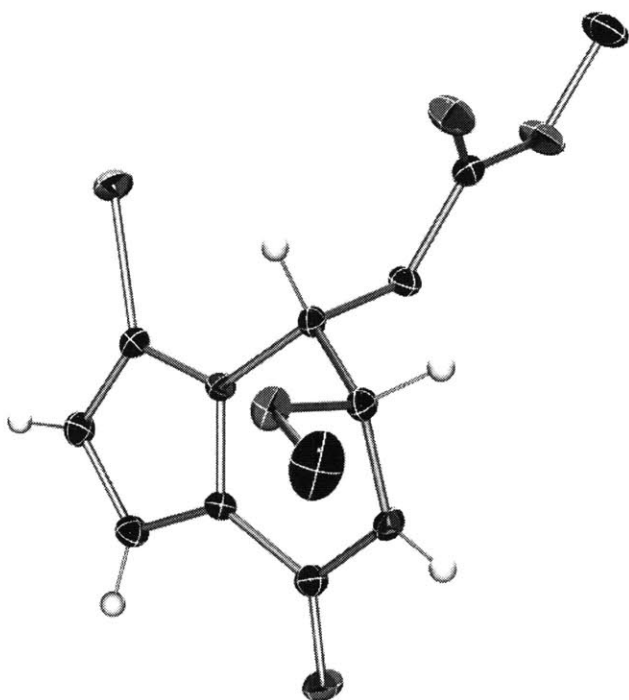
Assignment	Al-Mourabit's Report ²² ¹ H NMR, 600 MHz, CD ₃ OD	This Work ¹⁸ ¹ H NMR, 500 MHz, CD ₃ OD
C4	4.08 (br-s, 1H)	4.09 (s, 1H)
C6'	2.66 (dd, <i>J</i> = 12.9, 6.6 Hz, 1H)	2.66 (dd, <i>J</i> = 13.2, 6.5 Hz, 1H)
C6''	2.14 (br-t, <i>J</i> = 12.9, Hz, 1H)	2.14 (app-t, <i>J</i> = 12.7 Hz, 1H)
C7	4.62 (m, <i>J</i> = 12.6, 6.6 Hz, 1H)	4.62 (app-dt, <i>J</i> = 11.9, 6.1 Hz, 1H)
C8	4.11 (d, <i>J</i> = 5.4 Hz, 1H)	4.12 (d, <i>J</i> = 5.6 Hz, 1H)
C14	6.32 (d, <i>J</i> = 4.1 Hz, 1H)	6.33 (d, <i>J</i> = 4.1 Hz, 1H)
C15	6.91 (d, <i>J</i> = 4.1 Hz, 1H)	6.91 (d, <i>J</i> = 4.0 Hz, 1H)
C16	2.78 (s, 3H)	2.79 (s, 3H)
C17	3.18 (s, 3H)	3.18 (s, 3H)

Assignment	Al-Mourabit's Report ²² ¹³ C NMR, 150.8 MHz, CD ₃ OD	This Work ¹⁸ ¹³ C NMR, 125.8 MHz, CD ₃ OD
C2	162.2	161.9
C4	61.2	61.2
C5	101.0	100.2
C6	39.3	39.3
C7	53.9	53.9
C8	62.2	62.1
C10	161.2	161.1
C11	124.2	124.2
C13	107.4	107.5
C14	114.0	114.0
C15	116.2	116.2
C16	24.7	24.7
C17	50.8	50.8

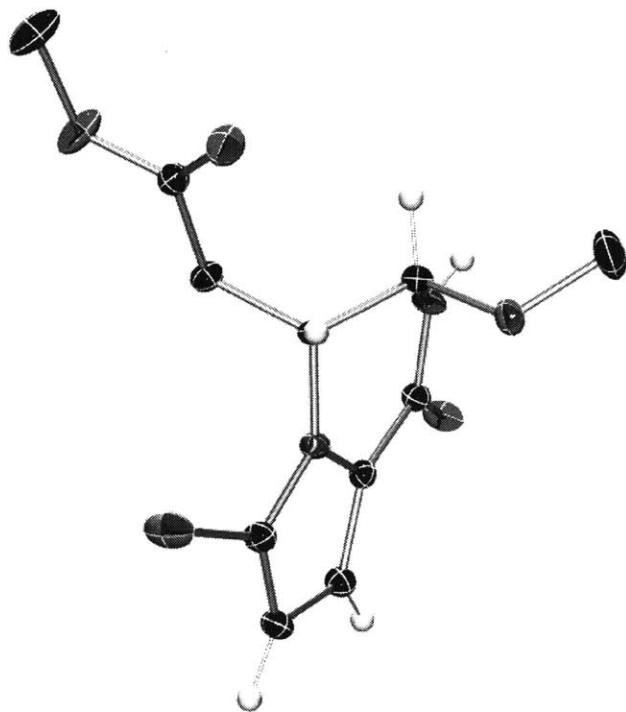
²² The NMR spectra are referenced from the residual protium resonance, CHD₂OD: δ 3.32, and carbon resonance, CD₃OD: δ 49.0. Tilvi, S.; Moriou, C.; Martin, M.-T.; Gallard, J.-F.; Sorres, J.; Patel, K.; Petek, S.; Debitus, C.; Ermolenko, L.; Al-Mourabit, A. *J. Nat. Prod.* Article ASAP, Publication Date (Web): February 17, 2010. DOI: 10.1021/np900539j.

Crystal Structure of Bicycle (+)-84

View 1:



View 2:



View 3:

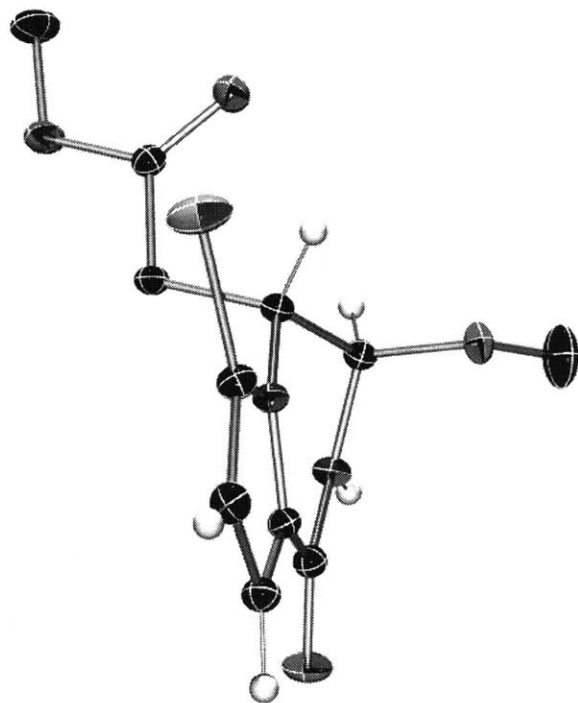


Table S5. Crystal data and structure refinement for bicycle (+)-**84**.

Identification code	10011	
Empirical formula	C11 H13 Br N2 O4	
Formula weight	317.14	
Temperature	100(2) K	
Wavelength	0.71073 Å	
Crystal system	Orthorhombic	
Space group	P2(1)2(1)2(1)	
Unit cell dimensions	a = 8.4061(9) Å	a = 90°.
	b = 9.2037(10) Å	b = 90°.
	c = 17.3522(18) Å	g = 90°.
Volume	1342.5(2) Å ³	
Z	4	
Density (calculated)	1.569 Mg/m ³	
Absorption coefficient	3.070 mm ⁻¹	
F(000)	640	
Crystal size	0.35 x 0.20 x 0.15 mm ³	
Theta range for data collection	2.35 to 29.56°.	
Index ranges	-11<=h<=11, -12<=k<=12, -24<=l<=24	
Reflections collected	35594	
Independent reflections	3764 [R(int) = 0.0403]	
Completeness to theta = 29.56°	100.0 %	
Absorption correction	None	
Max. and min. transmission	0.6559 and 0.4129	
Refinement method	Full-matrix least-squares on F ²	
Data / restraints / parameters	3764 / 155 / 168	
Goodness-of-fit on F ²	1.030	
Final R indices [I>2sigma(I)]	R1 = 0.0224, wR2 = 0.0556	
R indices (all data)	R1 = 0.0241, wR2 = 0.0561	
Absolute structure parameter	0.009(6)	
Largest diff. peak and hole	0.646 and -0.476 e.Å ⁻³	

Table S6. Atomic coordinates (x 10⁴) and equivalent isotropic displacement parameters (Å²x 10³) for bicycle (+)-**84**. U(eq) is defined as one third of the trace of the orthogonalized U^{ij} tensor.

	x	y	z	U(eq)
Br(1)	4530(1)	12344(1)	7612(1)	25(1)
O(3)	-588(2)	11005(1)	7596(1)	22(1)
O(1)	3784(1)	7512(2)	5030(1)	21(1)
C(11)	4314(2)	9440(2)	5895(1)	13(1)
C(8)	1060(2)	10016(2)	5919(1)	13(1)
C(13)	4913(2)	11063(2)	6798(1)	15(1)
O(2)	1136(2)	11236(1)	5425(1)	18(1)
C(6)	1639(2)	9434(2)	7331(1)	15(1)
N(9)	1681(2)	8707(2)	5561(1)	15(1)
C(7)	1994(2)	10421(2)	6642(1)	12(1)
C(10)	3270(2)	8482(2)	5451(1)	14(1)

N(12)	3685(2)	10368(2)	6443(1)	13(1)
C(5)	194(2)	9954(2)	7768(1)	15(1)
O(4)	-98(2)	9125(1)	8382(1)	26(1)
C(14)	6335(2)	10625(2)	6477(1)	16(1)
C(16)	-1439(3)	9579(2)	8850(1)	30(1)
C(15)	5961(2)	9584(2)	5907(1)	15(1)
C(17)	16(3)	11172(3)	4806(1)	35(1)

Table S7. Bond lengths [Å] and angles [°] for bicycle (+)-**84**.

Br(1)-C(13)	1.8667(16)	O(2)-C(8)-C(7)	106.33(13)
O(3)-C(5)	1.2064(19)	N(9)-C(8)-C(7)	111.66(13)
O(1)-C(10)	1.232(2)	N(12)-C(13)-C(14)	109.66(14)
C(11)-N(12)	1.384(2)	N(12)-C(13)-Br(1)	120.57(12)
C(11)-C(15)	1.390(2)	C(14)-C(13)-Br(1)	129.74(12)
C(11)-C(10)	1.463(2)	C(8)-O(2)-C(17)	113.14(14)
C(8)-O(2)	1.4135(19)	C(5)-C(6)-C(7)	111.19(13)
C(8)-N(9)	1.452(2)	C(10)-N(9)-C(8)	122.51(14)
C(8)-C(7)	1.525(2)	N(12)-C(7)-C(8)	107.35(13)
C(13)-N(12)	1.362(2)	N(12)-C(7)-C(6)	110.72(13)
C(13)-C(14)	1.379(2)	C(8)-C(7)-C(6)	113.40(13)
O(2)-C(17)	1.430(2)	O(1)-C(10)-N(9)	122.42(15)
C(6)-C(5)	1.510(2)	O(1)-C(10)-C(11)	122.61(15)
C(6)-C(7)	1.532(2)	N(9)-C(10)-C(11)	114.93(14)
N(9)-C(10)	1.366(2)	C(13)-N(12)-C(11)	108.15(13)
C(7)-N(12)	1.463(2)	C(13)-N(12)-C(7)	127.87(14)
C(5)-O(4)	1.3321(19)	C(11)-N(12)-C(7)	123.63(13)
O(4)-C(16)	1.452(2)	O(3)-C(5)-O(4)	123.83(16)
C(14)-C(15)	1.413(2)	O(3)-C(5)-C(6)	124.62(15)
		O(4)-C(5)-C(6)	111.54(14)
N(12)-C(11)-C(15)	108.14(14)	C(5)-O(4)-C(16)	115.14(14)
N(12)-C(11)-C(10)	120.30(14)	C(13)-C(14)-C(15)	106.74(15)
C(15)-C(11)-C(10)	131.49(15)	C(11)-C(15)-C(14)	107.28(14)
O(2)-C(8)-N(9)	112.54(14)		

Symmetry transformations used to generate equivalent atoms:

Table S8. Anisotropic displacement parameters ($\text{Å}^2 \times 10^3$) for bicycle (+)-**84**. The anisotropic displacement factor exponent takes the form: $-2p^2 [h^2 a^{*2} U^{11} + \dots + 2 h k a^* b^* U^{12}]$

	U ¹¹	U ²²	U ³³	U ²³	U ¹³	U ¹²
Br(1)	21(1)	28(1)	27(1)	-16(1)	3(1)	-7(1)
O(3)	21(1)	25(1)	21(1)	4(1)	4(1)	8(1)
O(1)	16(1)	22(1)	25(1)	-11(1)	1(1)	1(1)
C(11)	13(1)	14(1)	12(1)	-1(1)	1(1)	1(1)
C(8)	12(1)	13(1)	15(1)	-1(1)	0(1)	0(1)
C(13)	15(1)	15(1)	15(1)	-3(1)	0(1)	-2(1)

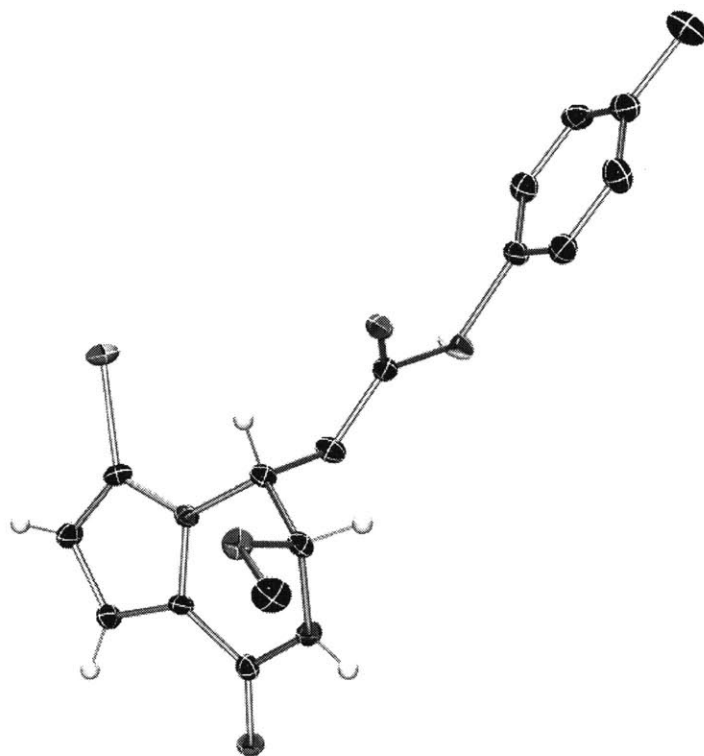
O(2)	20(1)	17(1)	17(1)	4(1)	-5(1)	0(1)
C(6)	15(1)	14(1)	16(1)	0(1)	3(1)	2(1)
N(9)	11(1)	15(1)	19(1)	-5(1)	-1(1)	-1(1)
C(7)	10(1)	12(1)	14(1)	-1(1)	1(1)	-1(1)
C(10)	14(1)	15(1)	14(1)	-1(1)	0(1)	0(1)
N(12)	11(1)	14(1)	14(1)	-2(1)	1(1)	0(1)
C(5)	16(1)	14(1)	14(1)	-2(1)	0(1)	-2(1)
O(4)	33(1)	20(1)	24(1)	6(1)	16(1)	8(1)
C(14)	13(1)	18(1)	17(1)	-1(1)	-2(1)	-2(1)
C(16)	36(1)	23(1)	29(1)	2(1)	20(1)	3(1)
C(15)	13(1)	17(1)	16(1)	-1(1)	1(1)	1(1)
C(17)	38(1)	37(1)	28(1)	12(1)	-18(1)	-7(1)

Table S9. Hydrogen coordinates ($\times 10^4$) and isotropic displacement parameters ($\text{\AA}^2 \times 10^{-3}$) for bicycle (+)-**84**.

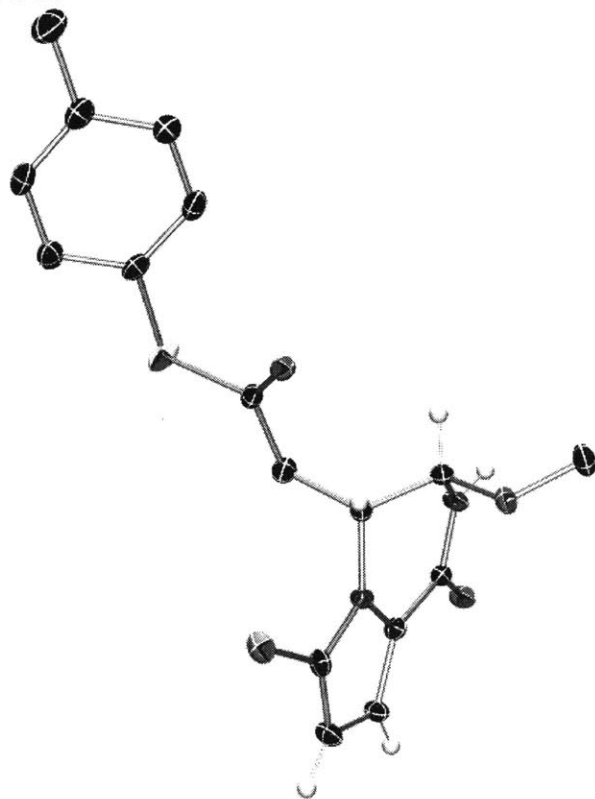
	x	y	z	U(eq)
H(8)	-75	9846	6065	16
H(6A)	1454	8430	7148	18
H(6B)	2569	9420	7681	18
H(9)	1070(20)	8200(20)	5292(12)	18
H(7)	1718	11442	6786	14
H(14)	7367	10959	6613	20
H(16A)	-1233	10550	9060	44
H(16B)	-1588	8890	9275	44
H(16C)	-2402	9605	8532	44
H(15)	6697	9077	5590	18
H(17A)	261	10338	4475	52
H(17B)	79	12068	4503	52
H(17C)	-1060	11065	5016	52

Crystal Structure of Thioester (+)-91

View 1:



View 2:



View 3:

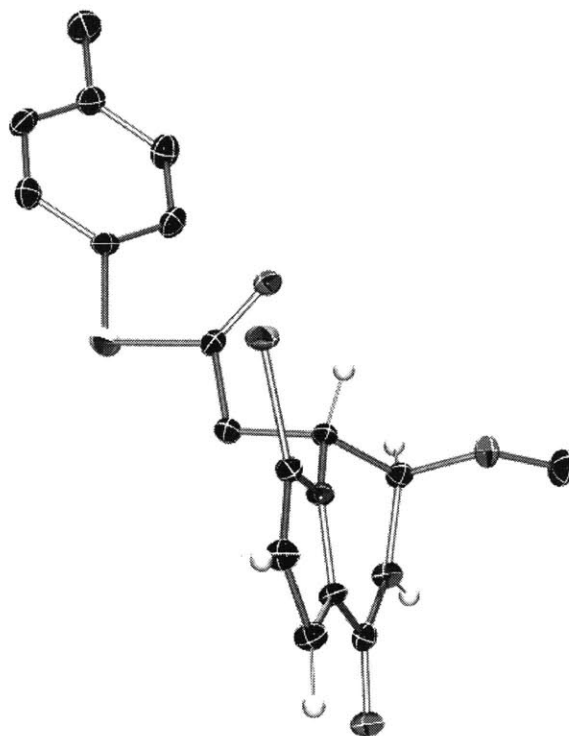


Table S10. Crystal data and structure refinement for thioester (+)-**91**.

Identification code	10013	
Empirical formula	C ₁₇ H ₁₇ Br N ₂ O ₃ S	
Formula weight	409.30	
Temperature	100(2) K	
Wavelength	0.71073 Å	
Crystal system	Monoclinic	
Space group	P2(1)	
Unit cell dimensions	a = 9.2556(9) Å	a = 90°.
	b = 8.0917(8) Å	b = 91.799(2)°.
	c = 11.7613(12) Å	g = 90°.
Volume	880.41(15) Å ³	
Z	2	
Density (calculated)	1.544 Mg/m ³	
Absorption coefficient	2.470 mm ⁻¹	
F(000)	416	
Crystal size	0.35 x 0.35 x 0.15 mm ³	
Theta range for data collection	1.73 to 29.13°.	
Index ranges	-12 ≤ h ≤ 12, -10 ≤ k ≤ 11, -16 ≤ l ≤ 16	
Reflections collected	19103	
Independent reflections	4583 [R(int) = 0.0383]	
Completeness to theta = 29.13°	99.9 %	
Absorption correction	None	
Max. and min. transmission	0.7082 and 0.4785	
Refinement method	Full-matrix least-squares on F ²	
Data / restraints / parameters	4583 / 203 / 222	
Goodness-of-fit on F ²	1.008	
Final R indices [I > 2σ(I)]	R1 = 0.0251, wR2 = 0.0560	
R indices (all data)	R1 = 0.0282, wR2 = 0.0570	
Absolute structure parameter	0.014(5)	
Largest diff. peak and hole	0.519 and -0.232 e.Å ⁻³	

Table S11. Atomic coordinates (x 10⁴) and equivalent isotropic displacement parameters (Å²x 10³) for thioester (+)-**91**. U(eq) is defined as one third of the trace of the orthogonalized U^{ij} tensor.

	x	y	z	U(eq)
Br(1)	135(1)	9493(1)	3768(1)	20(1)
S(1)	3998(1)	4712(1)	5370(1)	26(1)
O(3)	1618(1)	4293(2)	4073(1)	17(1)
C(5)	2720(2)	5054(2)	4221(2)	15(1)
C(7)	2125(2)	6816(2)	2470(2)	14(1)
C(19)	2830(2)	1758(3)	7926(2)	22(1)
C(17)	3282(2)	3004(3)	6116(2)	18(1)
C(22)	2870(2)	1547(3)	5576(2)	21(1)
C(18)	3263(2)	3118(3)	7301(2)	21(1)
C(6)	3212(2)	6452(3)	3461(2)	18(1)
C(20)	2403(2)	297(3)	7410(2)	22(1)

C(23)	1951(3)	-1187(3)	8091(2)	33(1)
C(21)	2420(2)	214(3)	6216(2)	25(1)
O(1)	4980(2)	8576(2)	117(1)	18(1)
O(2)	1148(2)	5943(2)	706(1)	19(1)
C(11)	3137(2)	9187(2)	1394(2)	14(1)
N(12)	2177(2)	8549(2)	2165(1)	14(1)
C(13)	1509(2)	9849(2)	2670(2)	16(1)
C(16)	1114(2)	4835(3)	-239(2)	26(1)
N(9)	3697(2)	6443(2)	833(2)	16(1)
C(10)	4007(2)	8076(2)	723(2)	15(1)
C(8)	2425(2)	5821(2)	1393(2)	15(1)
C(15)	3040(2)	10894(3)	1419(2)	17(1)
C(14)	2000(2)	11308(3)	2229(2)	18(1)

Table S12. Bond lengths [\AA] and angles [$^\circ$] for thioester (+)-**91**.

Br(1)-C(13)	1.8635(17)	N(12)-C(7)-C(6)	110.21(16)
S(1)-C(17)	1.776(2)	C(8)-C(7)-C(6)	113.14(17)
S(1)-C(5)	1.789(2)	C(20)-C(19)-C(18)	121.9(2)
O(3)-C(5)	1.199(2)	C(22)-C(17)-C(18)	120.05(19)
C(5)-C(6)	1.521(3)	C(22)-C(17)-S(1)	122.48(16)
C(7)-N(12)	1.448(3)	C(18)-C(17)-S(1)	117.23(17)
C(7)-C(8)	1.533(3)	C(17)-C(22)-C(21)	119.72(19)
C(7)-C(6)	1.544(3)	C(19)-C(18)-C(17)	119.3(2)
C(19)-C(20)	1.381(3)	C(5)-C(6)-C(7)	112.71(16)
C(19)-C(18)	1.390(3)	C(19)-C(20)-C(21)	117.9(2)
C(17)-C(22)	1.387(3)	C(19)-C(20)-C(23)	121.89(19)
C(17)-C(18)	1.397(3)	C(21)-C(20)-C(23)	120.2(2)
C(22)-C(21)	1.387(3)	C(22)-C(21)-C(20)	121.2(2)
C(20)-C(21)	1.406(3)	C(8)-O(2)-C(16)	113.47(15)
C(20)-C(23)	1.510(3)	C(15)-C(11)-N(12)	108.31(16)
O(1)-C(10)	1.235(2)	C(15)-C(11)-C(10)	131.64(17)
O(2)-C(8)	1.414(2)	N(12)-C(11)-C(10)	120.04(17)
O(2)-C(16)	1.427(2)	C(13)-N(12)-C(11)	107.77(15)
C(11)-C(15)	1.385(3)	C(13)-N(12)-C(7)	128.29(16)
C(11)-N(12)	1.389(2)	C(11)-N(12)-C(7)	123.21(16)
C(11)-C(10)	1.456(2)	N(12)-C(13)-C(14)	109.77(16)
N(12)-C(13)	1.365(2)	N(12)-C(13)-Br(1)	120.69(14)
C(13)-C(14)	1.373(3)	C(14)-C(13)-Br(1)	129.53(15)
N(9)-C(10)	1.358(3)	C(10)-N(9)-C(8)	123.69(17)
N(9)-C(8)	1.457(2)	O(1)-C(10)-N(9)	122.22(18)
C(15)-C(14)	1.416(3)	O(1)-C(10)-C(11)	122.47(18)
		N(9)-C(10)-C(11)	115.29(17)
C(17)-S(1)-C(5)	104.18(9)	O(2)-C(8)-N(9)	112.99(15)
O(3)-C(5)-C(6)	124.42(18)	O(2)-C(8)-C(7)	105.37(15)
O(3)-C(5)-S(1)	124.72(15)	N(9)-C(8)-C(7)	111.24(16)
C(6)-C(5)-S(1)	110.86(14)	C(11)-C(15)-C(14)	107.20(18)
N(12)-C(7)-C(8)	107.21(15)	C(13)-C(14)-C(15)	106.95(19)

Symmetry transformations used to generate equivalent atoms:

Table S13. Anisotropic displacement parameters ($\text{\AA}^2 \times 10^3$) for thioester (+)-**91**. The anisotropic displacement factor exponent takes the form: $-2p^2 [h^2 a^{*2} U^{11} + \dots + 2 h k a^* b^* U^{12}]$

	U ¹¹	U ²²	U ³³	U ²³	U ¹³	U ¹²
Br(1)	18(1)	24(1)	19(1)	-3(1)	8(1)	-4(1)
S(1)	20(1)	35(1)	24(1)	13(1)	-7(1)	-8(1)
O(3)	19(1)	16(1)	15(1)	2(1)	2(1)	0(1)
C(5)	17(1)	18(1)	12(1)	1(1)	1(1)	2(1)
C(7)	16(1)	12(1)	13(1)	1(1)	1(1)	-3(1)
C(19)	21(1)	30(1)	13(1)	3(1)	2(1)	2(1)
C(17)	12(1)	23(1)	17(1)	8(1)	-1(1)	1(1)
C(22)	22(1)	27(1)	14(1)	2(1)	-1(1)	6(1)
C(18)	20(1)	23(1)	18(1)	0(1)	-4(1)	2(1)
C(6)	19(1)	18(1)	17(1)	2(1)	-1(1)	-6(1)
C(20)	19(1)	28(1)	19(1)	6(1)	-1(1)	3(1)
C(23)	38(1)	32(1)	27(1)	10(1)	-2(1)	-8(1)
C(21)	31(1)	21(1)	21(1)	1(1)	-4(1)	2(1)
O(1)	20(1)	15(1)	19(1)	1(1)	7(1)	-1(1)
O(2)	21(1)	19(1)	16(1)	-4(1)	-3(1)	0(1)
C(11)	16(1)	14(1)	12(1)	2(1)	3(1)	-1(1)
N(12)	15(1)	12(1)	15(1)	1(1)	2(1)	-2(1)
C(13)	14(1)	20(1)	13(1)	-3(1)	3(1)	-2(1)
C(16)	33(1)	26(2)	18(1)	-7(1)	-2(1)	-3(1)
N(9)	19(1)	12(1)	18(1)	-1(1)	5(1)	0(1)
C(10)	17(1)	14(1)	13(1)	0(1)	-1(1)	2(1)
C(8)	19(1)	12(1)	15(1)	2(1)	1(1)	-2(1)
C(15)	22(1)	11(1)	18(1)	0(1)	4(1)	0(1)
C(14)	20(1)	14(1)	20(1)	-3(1)	5(1)	1(1)

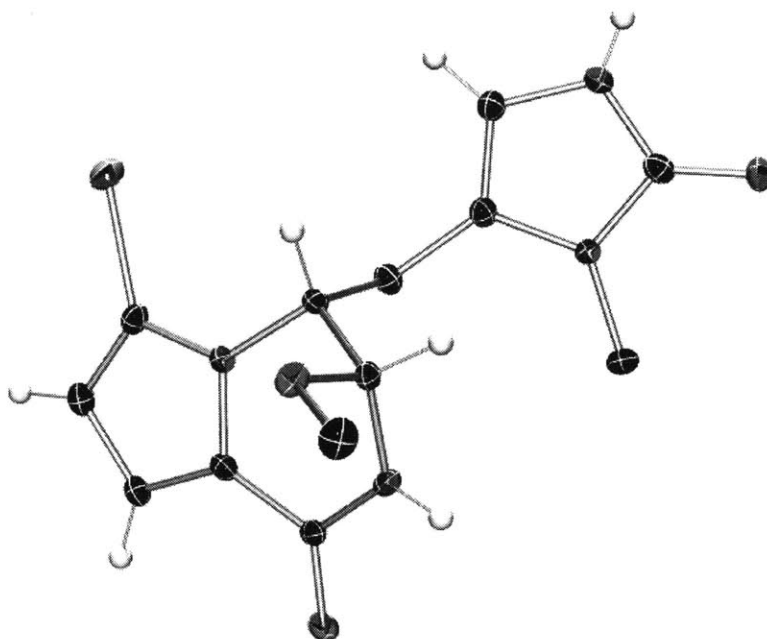
Table S14. Hydrogen coordinates ($\times 10^4$) and isotropic displacement parameters ($\text{\AA}^2 \times 10^3$) for thioester (+)-**91**.

	x	y	z	U(eq)
H(7)	1129	6547	2719	17
H(19)	2827	1836	8732	26
H(22)	2896	1463	4772	25
H(18)	3544	4114	7674	25
H(6A)	4158	6159	3146	22
H(6B)	3347	7464	3925	22
H(23A)	2805	-1851	8298	49
H(23B)	1270	-1858	7633	49
H(23C)	1485	-817	8783	49

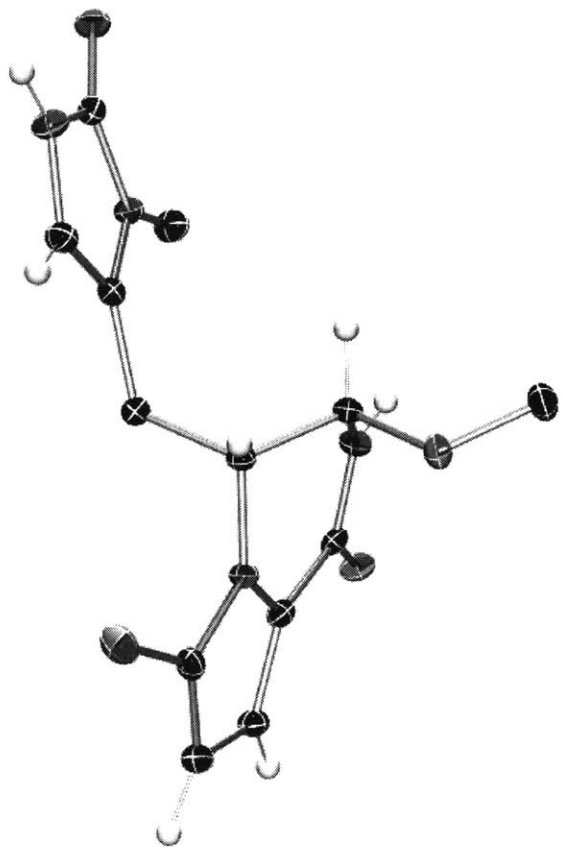
H(21)	2118	-773	5842	30
H(16A)	1943	5053	-715	38
H(16B)	216	4999	-688	38
H(16C)	1159	3694	38	38
H(9)	4120(20)	5750(30)	416(17)	19
H(8)	2588	4638	1605	18
H(15)	3573	11647	975	20
H(14)	1699	12389	2428	21

Crystal Structure of (+)-O-Methyl-pre-agelastatin A (82)

View 1:



View 2:



View 3:

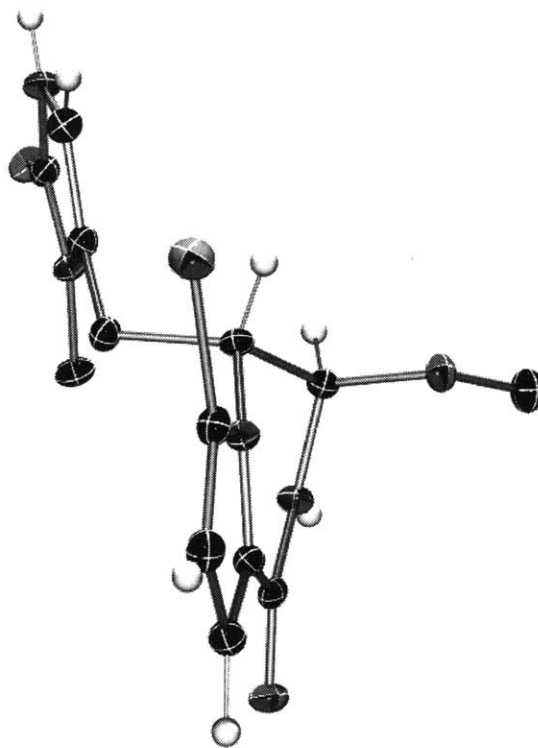


Table S15. Crystal data and structure refinement for (+)-*O*-methyl-pre-agelastatin A (**82**).

Identification code	10012	
Empirical formula	C ₁₄ H ₁₉ Br N ₄ O ₄	
Formula weight	387.24	
Temperature	100(2) K	
Wavelength	0.71073 Å	
Crystal system	Orthorhombic	
Space group	P2(1)2(1)2(1)	
Unit cell dimensions	a = 10.3843(11) Å	a = 90°.
	b = 10.7461(11) Å	b = 90°.
	c = 14.0947(15) Å	g = 90°.
Volume	1572.8(3) Å ³	
Z	4	
Density (calculated)	1.635 Mg/m ³	
Absorption coefficient	2.640 mm ⁻¹	
F(000)	792	
Crystal size	0.49 x 0.20 x 0.18 mm ³	
Theta range for data collection	2.38 to 29.56°.	
Index ranges	-14<=h<=14, -14<=k<=14, -19<=l<=19	
Reflections collected	31959	
Independent reflections	4413 [R(int) = 0.0524]	
Completeness to theta = 29.56°	100.0 %	
Absorption correction	None	
Max. and min. transmission	0.6479 and 0.3578	
Refinement method	Full-matrix least-squares on F ²	
Data / restraints / parameters	4413 / 199 / 220	
Goodness-of-fit on F ²	1.016	
Final R indices [I>2sigma(I)]	R1 = 0.0276, wR2 = 0.0618	
R indices (all data)	R1 = 0.0327, wR2 = 0.0635	
Absolute structure parameter	-0.007(6)	
Largest diff. peak and hole	0.598 and -0.372 e.Å ⁻³	

Table S16. Atomic coordinates (x 10⁴) and equivalent isotropic displacement parameters (Å²x 10³) for (+)-*O*-methyl-pre-agelastatin A (**82**). U(eq) is defined as one third of the trace of the orthogonalized U^{ij} tensor.

	x	y	z	U(eq)
Br(1)	159(1)	5727(1)	8694(1)	19(1)
C(7)	299(2)	8579(2)	9501(1)	12(1)
O(1)	3736(1)	10457(1)	9284(1)	17(1)
N(9)	1768(2)	10252(2)	9958(1)	14(1)
C(13)	1556(2)	6821(2)	8716(2)	14(1)
C(4)	-2779(2)	9358(2)	8879(1)	16(1)
N(1)	-1764(2)	11168(2)	8930(1)	13(1)
O(2)	-3553(2)	12482(1)	9115(1)	18(1)
O(3)	1132(1)	8682(1)	11052(1)	16(1)
C(17)	1400(2)	9361(2)	11909(1)	20(1)

N(3)	-3662(2)	10316(2)	8998(1)	16(1)
C(15)	3436(2)	7809(2)	8539(1)	15(1)
C(8)	740(2)	9455(2)	10295(1)	12(1)
N(12)	1452(2)	7949(2)	9159(1)	12(1)
C(6)	-325(2)	9256(2)	8651(1)	15(1)
C(10)	2770(2)	9819(2)	9433(1)	12(1)
C(2)	-3051(2)	11429(2)	9029(1)	15(1)
C(16)	-794(2)	12148(2)	8888(2)	18(1)
C(11)	2611(2)	8564(2)	9047(1)	13(1)
C(5)	-1592(2)	9867(2)	8832(1)	14(1)
C(14)	2771(2)	6692(2)	8339(1)	16(1)
O(1S)	9175(2)	1656(2)	1844(1)	27(1)
C(1S)	7951(2)	1693(2)	1404(2)	24(1)

Table S17. Bond lengths [Å] and angles [°] for (+)-*O*-methyl-pre-agelastatin A (**82**).

Br(1)-C(13)	1.8678(19)	N(12)-C(13)-Br(1)	120.24(15)
C(7)-N(12)	1.457(2)	C(14)-C(13)-Br(1)	129.98(16)
C(7)-C(8)	1.532(3)	C(5)-C(4)-N(3)	107.96(19)
C(7)-C(6)	1.545(3)	C(2)-N(1)-C(5)	109.55(17)
O(1)-C(10)	1.234(2)	C(2)-N(1)-C(16)	121.94(17)
N(9)-C(10)	1.359(3)	C(5)-N(1)-C(16)	128.43(17)
N(9)-C(8)	1.448(3)	C(8)-O(3)-C(17)	113.06(15)
C(13)-N(12)	1.368(2)	C(2)-N(3)-C(4)	110.46(17)
C(13)-C(14)	1.375(3)	C(11)-C(15)-C(14)	107.40(18)
C(4)-C(5)	1.350(3)	O(3)-C(8)-N(9)	112.48(16)
C(4)-N(3)	1.388(3)	O(3)-C(8)-C(7)	106.02(15)
N(1)-C(2)	1.372(3)	N(9)-C(8)-C(7)	110.20(15)
N(1)-C(5)	1.416(3)	C(13)-N(12)-C(11)	107.54(17)
N(1)-C(16)	1.459(3)	C(13)-N(12)-C(7)	128.87(17)
O(2)-C(2)	1.252(3)	C(11)-N(12)-C(7)	122.15(16)
O(3)-C(8)	1.413(2)	C(5)-C(6)-C(7)	116.37(16)
O(3)-C(17)	1.439(2)	O(1)-C(10)-N(9)	121.63(19)
N(3)-C(2)	1.355(3)	O(1)-C(10)-C(11)	122.74(19)
C(15)-C(11)	1.380(3)	N(9)-C(10)-C(11)	115.62(18)
C(15)-C(14)	1.413(3)	O(2)-C(2)-N(3)	127.34(19)
N(12)-C(11)	1.382(3)	O(2)-C(2)-N(1)	126.9(2)
C(6)-C(5)	1.492(3)	N(3)-C(2)-N(1)	105.78(17)
C(10)-C(11)	1.464(3)	C(15)-C(11)-N(12)	108.65(18)
O(1S)-C(1S)	1.415(3)	C(15)-C(11)-C(10)	131.65(19)
		N(12)-C(11)-C(10)	119.69(18)
N(12)-C(7)-C(8)	106.31(16)	C(4)-C(5)-N(1)	106.24(18)
N(12)-C(7)-C(6)	107.86(14)	C(4)-C(5)-C(6)	129.41(19)
C(8)-C(7)-C(6)	113.71(16)	N(1)-C(5)-C(6)	124.23(18)
C(10)-N(9)-C(8)	122.66(17)	C(13)-C(14)-C(15)	106.60(18)
N(12)-C(13)-C(14)	109.78(18)		

Symmetry transformations used to generate equivalent atoms:

Table S18. Anisotropic displacement parameters ($\text{\AA}^2 \times 10^3$) for (+)-*O*-methyl-pre-agelastatin A (**82**). The anisotropic displacement factor exponent takes the form: $-2p^2 [h^2 a^{*2} U^{11} + \dots + 2 h k a^* b^* U^{12}]$

	U ¹¹	U ²²	U ³³	U ²³	U ¹³	U ¹²
Br(1)	22(1)	15(1)	20(1)	-4(1)	1(1)	-4(1)
C(7)	10(1)	12(1)	14(1)	-2(1)	1(1)	0(1)
O(1)	11(1)	18(1)	23(1)	2(1)	2(1)	0(1)
N(9)	14(1)	10(1)	17(1)	-2(1)	2(1)	-2(1)
C(13)	18(1)	12(1)	14(1)	-2(1)	-2(1)	0(1)
C(4)	16(1)	14(1)	17(1)	-2(1)	0(1)	1(1)
N(1)	11(1)	11(1)	17(1)	-2(1)	-1(1)	0(1)
O(2)	17(1)	14(1)	24(1)	-4(1)	-1(1)	4(1)
O(3)	20(1)	15(1)	12(1)	0(1)	-2(1)	-1(1)
C(17)	27(1)	21(1)	14(1)	-2(1)	-3(1)	1(1)
N(3)	11(1)	16(1)	21(1)	1(1)	2(1)	0(1)
C(15)	13(1)	16(1)	15(1)	0(1)	2(1)	3(1)
C(8)	12(1)	11(1)	13(1)	-1(1)	1(1)	1(1)
N(12)	11(1)	12(1)	14(1)	-1(1)	1(1)	1(1)
C(6)	14(1)	16(1)	14(1)	-1(1)	-1(1)	2(1)
C(10)	11(1)	12(1)	15(1)	4(1)	-3(1)	0(1)
C(2)	12(1)	19(1)	13(1)	-2(1)	-1(1)	1(1)
C(16)	14(1)	16(1)	25(1)	-3(1)	-1(1)	-3(1)
C(11)	11(1)	15(1)	13(1)	2(1)	0(1)	1(1)
C(5)	14(1)	14(1)	13(1)	-2(1)	-1(1)	1(1)
C(14)	17(1)	16(1)	16(1)	-1(1)	0(1)	4(1)
O(1S)	19(1)	29(1)	32(1)	6(1)	5(1)	-2(1)
C(1S)	27(1)	19(1)	25(1)	4(1)	-2(1)	-2(1)

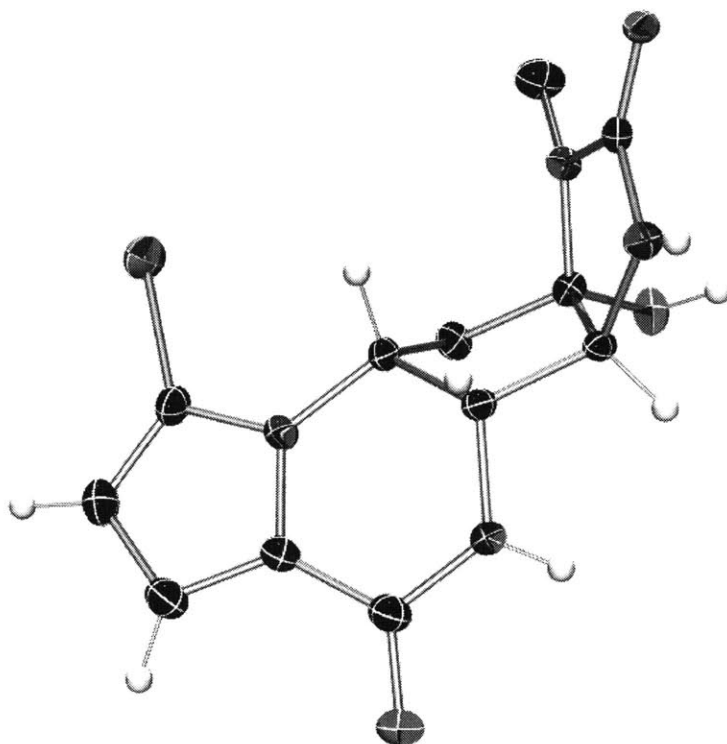
Table S19. Hydrogen coordinates ($\times 10^4$) and isotropic displacement parameters ($\text{\AA}^2 \times 10^3$) for (+)-*O*-methyl-pre-agelastatin A (**82**).

	x	y	z	U(eq)
H(7)	-318	7952	9764	14
H(9)	1820(20)	10950(16)	10199(16)	16
H(4)	-2976	8497	8837	19
H(17A)	2117	9936	11799	31
H(17B)	1631	8777	12415	31
H(17C)	634	9834	12097	31
H(3)	-4461(16)	10210(20)	9060(17)	19
H(15)	4294	8004	8358	18
H(8)	-3	9980	10504	15
H(6A)	284	9898	8423	17
H(6B)	-440	8646	8131	17

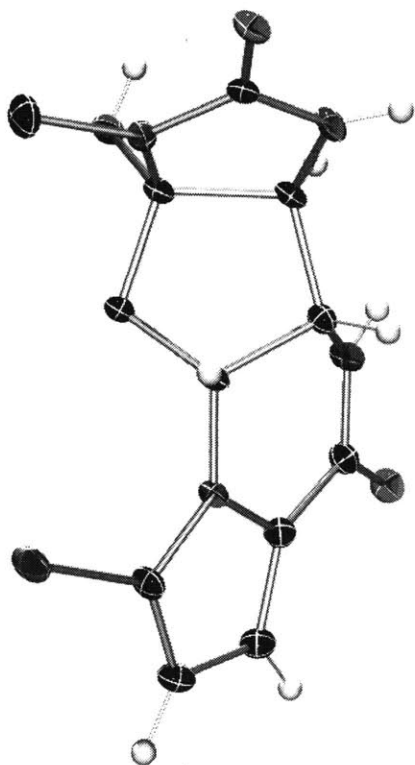
H(16A)	-1189	12947	9057	27
H(16B)	-443	12197	8244	27
H(16C)	-99	11960	9336	27
H(14)	3098	5989	8009	20
H(101)	9730(20)	1980(20)	1516(16)	32
H(1S1)	7284	1498	1873	36
H(1S2)	7921	1080	890	36
H(1S3)	7799	2526	1145	36

Crystal Structure of (-)-Agelastatin A (1)

View 1:



View 2:



View 3:

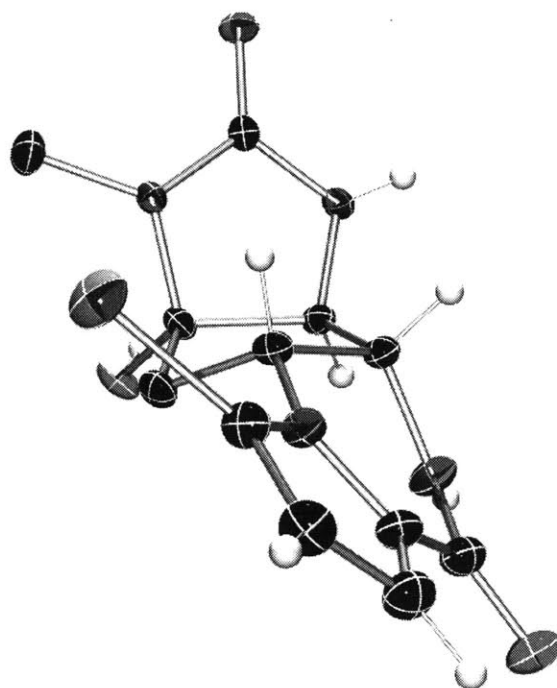


Table S20. Crystal data and structure refinement for (–)-agelastatin A (**1**).

Identification code	10026	
Empirical formula	C ₁₂ H ₁₆ Br N ₄ O _{4.50}	
Formula weight	368.20	
Temperature	100(2) K	
Wavelength	0.71073 Å	
Crystal system	Monoclinic	
Space group	P2(1)	
Unit cell dimensions	a = 13.5873(14) Å	a = 90°.
	b = 6.9161(7) Å	b = 98.786(2)°.
	c = 15.7114(17) Å	g = 90°.
Volume	1459.1(3) Å ³	
Z	4	
Density (calculated)	1.676 Mg/m ³	
Absorption coefficient	2.844 mm ⁻¹	
F(000)	748	
Crystal size	0.48 x 0.25 x 0.04 mm ³	
Theta range for data collection	1.31 to 30.03°.	
Index ranges	-19<=h<=19, -9<=k<=9, -22<=l<=21	
Reflections collected	39133	
Independent reflections	8508 [R(int) = 0.0524]	
Completeness to theta = 30.03°	99.9 %	
Absorption correction	None	
Max. and min. transmission	0.8947 and 0.3422	
Refinement method	Full-matrix least-squares on F ²	
Data / restraints / parameters	8508 / 402 / 426	
Goodness-of-fit on F ²	1.017	
Final R indices [I>2sigma(I)]	R1 = 0.0346, wR2 = 0.0795	
R indices (all data)	R1 = 0.0437, wR2 = 0.0829	
Absolute structure parameter	0.015(5)	
Largest diff. peak and hole	0.875 and -0.490 e.Å ⁻³	

Table S22. Atomic coordinates (x 10⁴) and equivalent isotropic displacement parameters (Å²x 10³) for (–)-agelastatin A (**1**). U(eq) is defined as one third of the trace of the orthogonalized U^{ij} tensor.

	x	y	z	U(eq)
Br(1A)	10024(1)	9800(1)	4181(1)	20(1)
O(1A)	7655(1)	2032(3)	3166(1)	19(1)
O(2A)	5380(1)	12339(3)	4193(1)	15(1)
O(3A)	6575(1)	7489(3)	5834(1)	16(1)
N(1A)	6544(2)	10312(3)	4960(1)	13(1)
N(3A)	5476(2)	9051(3)	3910(2)	16(1)
N(9A)	6925(1)	4729(4)	3601(1)	16(1)
N(12A)	8666(1)	6765(3)	3693(1)	13(1)
C(2A)	5761(2)	10700(4)	4338(2)	13(1)
C(4A)	6100(2)	7438(4)	4214(2)	13(1)
C(5A)	6771(2)	8256(4)	5039(2)	13(1)

C(6A)	7840(2)	7741(4)	4947(2)	14(1)
C(7A)	7830(2)	7787(4)	3976(2)	12(1)
C(8A)	6834(2)	6839(3)	3592(2)	13(1)
C(10A)	7700(2)	3773(4)	3354(2)	15(1)
C(11A)	8604(2)	4898(4)	3361(2)	14(1)
C(13A)	9618(2)	7390(4)	3713(2)	15(1)
C(14A)	10170(2)	5986(4)	3382(2)	16(1)
C(15A)	9532(2)	4414(3)	3163(2)	16(1)
C(16A)	7030(2)	11771(4)	5551(2)	20(1)
Br(1B)	677(1)	1059(1)	-861(1)	30(1)
O(1B)	3160(2)	8724(3)	175(1)	28(1)
O(2B)	3843(1)	-1576(3)	2515(1)	17(1)
O(3B)	1898(1)	3202(3)	2824(1)	22(1)
N(1B)	2475(2)	446(3)	2140(1)	15(1)
N(3B)	3984(2)	1698(3)	2274(2)	16(1)
N(9B)	3293(2)	6008(4)	988(2)	21(1)
N(12B)	1965(2)	4066(3)	-199(2)	18(1)
C(2B)	3473(2)	41(4)	2325(2)	14(1)
C(4B)	3345(2)	3314(4)	2009(2)	14(1)
C(5B)	2286(2)	2529(4)	2096(2)	15(1)
C(6B)	1615(2)	3162(4)	1279(2)	18(1)
C(7B)	2307(2)	3044(4)	598(2)	16(1)
C(8B)	3300(2)	3896(4)	1057(2)	15(1)
C(10B)	2944(2)	6983(4)	254(2)	22(1)
C(11B)	2275(2)	5912(4)	-382(2)	20(1)
C(13B)	1303(2)	3459(4)	-886(2)	20(1)
C(14B)	1190(2)	4839(5)	-1516(2)	25(1)
C(15B)	1809(2)	6408(4)	-1198(2)	25(1)
C(16B)	1704(2)	-950(4)	2232(2)	26(1)
O(1W)	5937(1)	1920(3)	1936(2)	27(1)
O(2W)	3590(2)	477(4)	8668(2)	47(1)
O(3W)	4605(2)	3913(5)	9290(2)	59(1)

Table S23. Bond lengths [Å] and angles [°] for (–)-agelastatin A (**1**).

Br(1A)-C(13A)	1.870(3)	N(12A)-C(7A)	1.464(3)
O(1A)-C(10A)	1.239(3)	C(4A)-C(8A)	1.556(3)
O(2A)-C(2A)	1.252(3)	C(4A)-C(5A)	1.571(3)
O(3A)-C(5A)	1.419(3)	C(5A)-C(6A)	1.524(3)
N(1A)-C(2A)	1.357(3)	C(6A)-C(7A)	1.523(3)
N(1A)-C(5A)	1.456(3)	C(7A)-C(8A)	1.541(3)
N(1A)-C(16A)	1.459(3)	C(10A)-C(11A)	1.453(3)
N(3A)-C(2A)	1.350(3)	C(11A)-C(15A)	1.385(3)
N(3A)-C(4A)	1.438(3)	C(13A)-C(14A)	1.376(4)
N(9A)-C(10A)	1.350(3)	C(14A)-C(15A)	1.401(4)
N(9A)-C(8A)	1.465(3)	Br(1B)-C(13B)	1.868(3)
N(12A)-C(13A)	1.360(3)	O(1B)-C(10B)	1.251(3)
N(12A)-C(11A)	1.391(3)	O(2B)-C(2B)	1.244(3)

O(3B)-C(5B)	1.410(3)	O(1A)-C(10A)-C(11A)	122.2(2)
N(1B)-C(2B)	1.372(3)	N(9A)-C(10A)-C(11A)	115.5(2)
N(1B)-C(16B)	1.447(3)	C(15A)-C(11A)-N(12A)	107.7(2)
N(1B)-C(5B)	1.463(3)	C(15A)-C(11A)-C(10A)	131.8(3)
N(3B)-C(2B)	1.349(3)	N(12A)-C(11A)-C(10A)	120.2(2)
N(3B)-C(4B)	1.437(3)	N(12A)-C(13A)-C(14A)	109.8(2)
N(9B)-C(10B)	1.357(4)	N(12A)-C(13A)-Br(1A)	120.95(18)
N(9B)-C(8B)	1.465(3)	C(14A)-C(13A)-Br(1A)	129.24(18)
N(12B)-C(13B)	1.361(3)	C(13A)-C(14A)-C(15A)	106.8(2)
N(12B)-C(11B)	1.388(4)	C(11A)-C(15A)-C(14A)	107.9(2)
N(12B)-C(7B)	1.452(3)	C(2B)-N(1B)-C(16B)	123.3(2)
C(4B)-C(8B)	1.541(4)	C(2B)-N(1B)-C(5B)	111.8(2)
C(4B)-C(5B)	1.563(3)	C(16B)-N(1B)-C(5B)	122.5(2)
C(5B)-C(6B)	1.521(4)	C(2B)-N(3B)-C(4B)	112.60(19)
C(6B)-C(7B)	1.530(3)	C(10B)-N(9B)-C(8B)	123.8(2)
C(7B)-C(8B)	1.546(3)	C(13B)-N(12B)-C(11B)	107.7(2)
C(10B)-C(11B)	1.448(4)	C(13B)-N(12B)-C(7B)	128.2(2)
C(11B)-C(15B)	1.384(4)	C(11B)-N(12B)-C(7B)	124.0(2)
C(13B)-C(14B)	1.367(4)	O(2B)-C(2B)-N(3B)	125.8(2)
C(14B)-C(15B)	1.416(4)	O(2B)-C(2B)-N(1B)	125.8(2)
		N(3B)-C(2B)-N(1B)	108.4(2)
C(2A)-N(1A)-C(5A)	112.7(2)	N(3B)-C(4B)-C(8B)	114.7(2)
C(2A)-N(1A)-C(16A)	123.4(2)	N(3B)-C(4B)-C(5B)	103.2(2)
C(5A)-N(1A)-C(16A)	123.5(2)	C(8B)-C(4B)-C(5B)	106.0(2)
C(2A)-N(3A)-C(4A)	112.4(2)	O(3B)-C(5B)-N(1B)	111.8(2)
C(10A)-N(9A)-C(8A)	123.6(2)	O(3B)-C(5B)-C(6B)	109.9(2)
C(13A)-N(12A)-C(11A)	107.9(2)	N(1B)-C(5B)-C(6B)	113.7(2)
C(13A)-N(12A)-C(7A)	128.3(2)	O(3B)-C(5B)-C(4B)	114.8(2)
C(11A)-N(12A)-C(7A)	123.82(19)	N(1B)-C(5B)-C(4B)	100.89(19)
O(2A)-C(2A)-N(3A)	126.5(2)	C(6B)-C(5B)-C(4B)	105.5(2)
O(2A)-C(2A)-N(1A)	124.5(2)	C(5B)-C(6B)-C(7B)	102.81(19)
N(3A)-C(2A)-N(1A)	109.0(2)	N(12B)-C(7B)-C(6B)	115.4(2)
N(3A)-C(4A)-C(8A)	113.5(2)	N(12B)-C(7B)-C(8B)	111.0(2)
N(3A)-C(4A)-C(5A)	103.5(2)	C(6B)-C(7B)-C(8B)	103.9(2)
C(8A)-C(4A)-C(5A)	105.46(18)	N(9B)-C(8B)-C(4B)	109.3(2)
O(3A)-C(5A)-N(1A)	111.9(2)	N(9B)-C(8B)-C(7B)	110.5(2)
O(3A)-C(5A)-C(6A)	107.80(19)	C(4B)-C(8B)-C(7B)	104.8(2)
N(1A)-C(5A)-C(6A)	114.4(2)	O(1B)-C(10B)-N(9B)	120.4(3)
O(3A)-C(5A)-C(4A)	115.33(19)	O(1B)-C(10B)-C(11B)	123.8(3)
N(1A)-C(5A)-C(4A)	101.15(19)	N(9B)-C(10B)-C(11B)	115.7(3)
C(6A)-C(5A)-C(4A)	106.22(19)	C(15B)-C(11B)-N(12B)	108.0(2)
C(7A)-C(6A)-C(5A)	103.11(19)	C(15B)-C(11B)-C(10B)	131.6(3)
N(12A)-C(7A)-C(6A)	113.87(19)	N(12B)-C(11B)-C(10B)	120.4(2)
N(12A)-C(7A)-C(8A)	110.6(2)	N(12B)-C(13B)-C(14B)	110.2(3)
C(6A)-C(7A)-C(8A)	104.85(19)	N(12B)-C(13B)-Br(1B)	120.4(2)
N(9A)-C(8A)-C(7A)	110.6(2)	C(14B)-C(13B)-Br(1B)	129.4(2)
N(9A)-C(8A)-C(4A)	108.67(19)	C(13B)-C(14B)-C(15B)	106.6(2)
C(7A)-C(8A)-C(4A)	104.47(19)	C(11B)-C(15B)-C(14B)	107.4(3)
O(1A)-C(10A)-N(9A)	122.2(2)		

Symmetry transformations used to generate equivalent atoms:

Table S24. Anisotropic displacement parameters ($\text{\AA}^2 \times 10^3$) for (–)-agelastatin A (**1**). The anisotropic displacement factor exponent takes the form: $-2p^2 [h^2 a^{*2} U^{11} + \dots + 2 h k a^* b^* U^{12}]$

	U ¹¹	U ²²	U ³³	U ²³	U ¹³	U ¹²
Br(1A)	13(1)	17(1)	30(1)	-5(1)	4(1)	-5(1)
O(1A)	20(1)	12(1)	25(1)	-2(1)	2(1)	0(1)
O(2A)	10(1)	13(1)	21(1)	2(1)	2(1)	1(1)
O(3A)	12(1)	22(1)	14(1)	4(1)	2(1)	0(1)
N(1A)	12(1)	13(1)	14(1)	-2(1)	1(1)	0(1)
N(3A)	11(1)	13(1)	22(1)	-1(1)	-4(1)	2(1)
N(9A)	12(1)	10(1)	25(1)	-1(1)	4(1)	-4(1)
N(12A)	10(1)	12(1)	16(1)	0(1)	2(1)	0(1)
C(2A)	8(1)	17(1)	14(1)	-1(1)	4(1)	0(1)
C(4A)	8(1)	14(1)	17(1)	2(1)	1(1)	1(1)
C(5A)	9(1)	13(1)	17(1)	0(1)	2(1)	1(1)
C(6A)	9(1)	16(1)	15(1)	-1(1)	2(1)	1(1)
C(7A)	9(1)	10(1)	18(1)	0(1)	2(1)	0(1)
C(8A)	11(1)	11(1)	16(1)	0(1)	1(1)	0(1)
C(10A)	14(1)	15(1)	16(1)	2(1)	0(1)	1(1)
C(11A)	15(1)	12(1)	16(1)	0(1)	3(1)	2(1)
C(13A)	12(1)	14(1)	20(1)	0(1)	2(1)	-4(1)
C(14A)	13(1)	17(1)	20(1)	3(1)	5(1)	3(1)
C(15A)	16(1)	13(1)	19(1)	1(1)	5(1)	2(1)
C(16A)	19(1)	16(1)	24(1)	-5(1)	-3(1)	-2(1)
Br(1B)	29(1)	26(1)	29(1)	-1(1)	-9(1)	-9(1)
O(1B)	38(1)	17(1)	29(1)	3(1)	1(1)	-3(1)
O(2B)	17(1)	14(1)	20(1)	0(1)	-2(1)	2(1)
O(3B)	16(1)	32(1)	18(1)	-3(1)	2(1)	8(1)
N(1B)	10(1)	16(1)	18(1)	2(1)	1(1)	1(1)
N(3B)	10(1)	17(1)	22(1)	0(1)	0(1)	1(1)
N(9B)	28(1)	14(1)	18(1)	0(1)	-2(1)	-4(1)
N(12B)	19(1)	17(1)	17(1)	2(1)	-2(1)	0(1)
C(2B)	13(1)	18(1)	11(1)	-1(1)	2(1)	-1(1)
C(4B)	13(1)	12(1)	17(1)	0(1)	0(1)	0(1)
C(5B)	11(1)	16(1)	17(1)	-3(1)	2(1)	2(1)
C(6B)	12(1)	21(1)	20(1)	2(1)	-1(1)	3(1)
C(7B)	16(1)	14(1)	15(1)	0(1)	-2(1)	1(1)
C(8B)	15(1)	12(1)	17(1)	0(1)	0(1)	0(1)
C(10B)	25(1)	18(1)	22(1)	2(1)	4(1)	2(1)
C(11B)	23(1)	16(1)	20(1)	2(1)	2(1)	2(1)
C(13B)	20(1)	21(1)	19(1)	-3(1)	-2(1)	-1(1)
C(14B)	26(1)	30(1)	18(1)	0(1)	-2(1)	0(1)
C(15B)	29(1)	23(2)	22(1)	4(1)	4(1)	2(1)
C(16B)	17(1)	23(1)	38(2)	5(1)	4(1)	-5(1)
O(1W)	16(1)	29(1)	36(1)	-3(1)	4(1)	-4(1)

O(2W)	68(2)	37(1)	39(2)	1(1)	17(1)	-4(1)
O(3W)	58(2)	52(2)	70(2)	14(2)	17(2)	4(2)

Table S25. Hydrogen coordinates ($\times 10^4$) and isotropic displacement parameters ($\text{\AA}^2 \times 10^3$) for (–)-agelastatin A (**1**).

	x	y	z	U(eq)
H(3A)	5979(14)	7400(50)	5910(20)	24
H(3C)	5030(18)	8970(50)	3485(14)	19
H(9A)	6394(16)	4140(40)	3660(20)	19
H(4A)	5695	6311	4359	16
H(6A1)	8314	8702	5242	16
H(6A2)	8020	6441	5184	16
H(7A)	7831	9163	3780	15
H(8A)	6601	7324	2996	15
H(14A)	10852	6068	3316	20
H(15A)	9704	3226	2921	19
H(16A)	6673	13002	5450	31
H(16B)	7720	11939	5453	31
H(16C)	7023	11354	6146	31
H(3B)	2340(20)	2970(50)	3263(17)	33
H(3D)	4624(13)	1690(40)	2343(19)	20
H(9B)	3540(20)	6620(40)	1443(15)	25
H(4B)	3520	4449	2396	17
H(6B1)	1369	4497	1334	22
H(6B2)	1039	2280	1140	22
H(7B)	2412	1653	463	19
H(8B)	3876	3338	813	18
H(14B)	776	4761	-2060	30
H(15B)	1889	7585	-1492	30
H(16D)	2007	-2223	2361	39
H(16E)	1234	-1018	1694	39
H(16F)	1351	-553	2702	39
H(1WB)	5980(30)	3100(30)	1780(20)	40
H(1WA)	6400(20)	1660(50)	2325(18)	40
H(2WA)	3980(30)	1650(50)	8790(30)	70
H(2WB)	3620(30)	90(60)	9199(16)	70
H(3WA)	4290(30)	4630(70)	8840(30)	89
H(3WB)	5240(15)	4070(80)	9230(30)	89

Appendix A.

Spectra for Chapter I

exp1 s2pu1

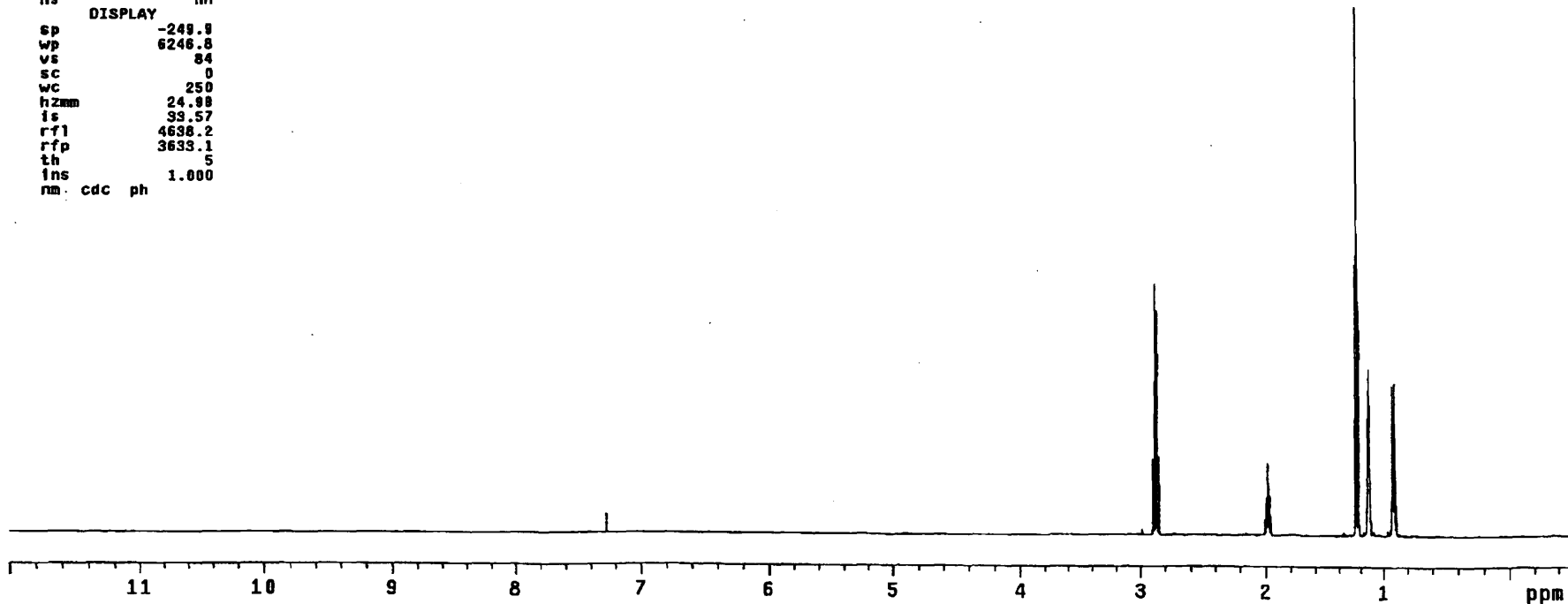
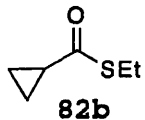
DEC. & VT
dfrq 125.674
dn C13
dpwr 34
dof 1498.1
dm nnn
dam w
dmf 10000

ACQUISITION
sfrq 499.749
tn H1
at 3.277
np 65536
sw 9998.8
fb not used
bs 1
tpwr 56
pw 8.2
d1 5.000
tor 1498.1
nt 16
ct 16
alock n
gain not used

PROCESSING
wtfile
proc ft
fn 65536
math r
werr
wexp
wbs
wnt

FLAGS
l1 n
l2 n
dp y
hs nn

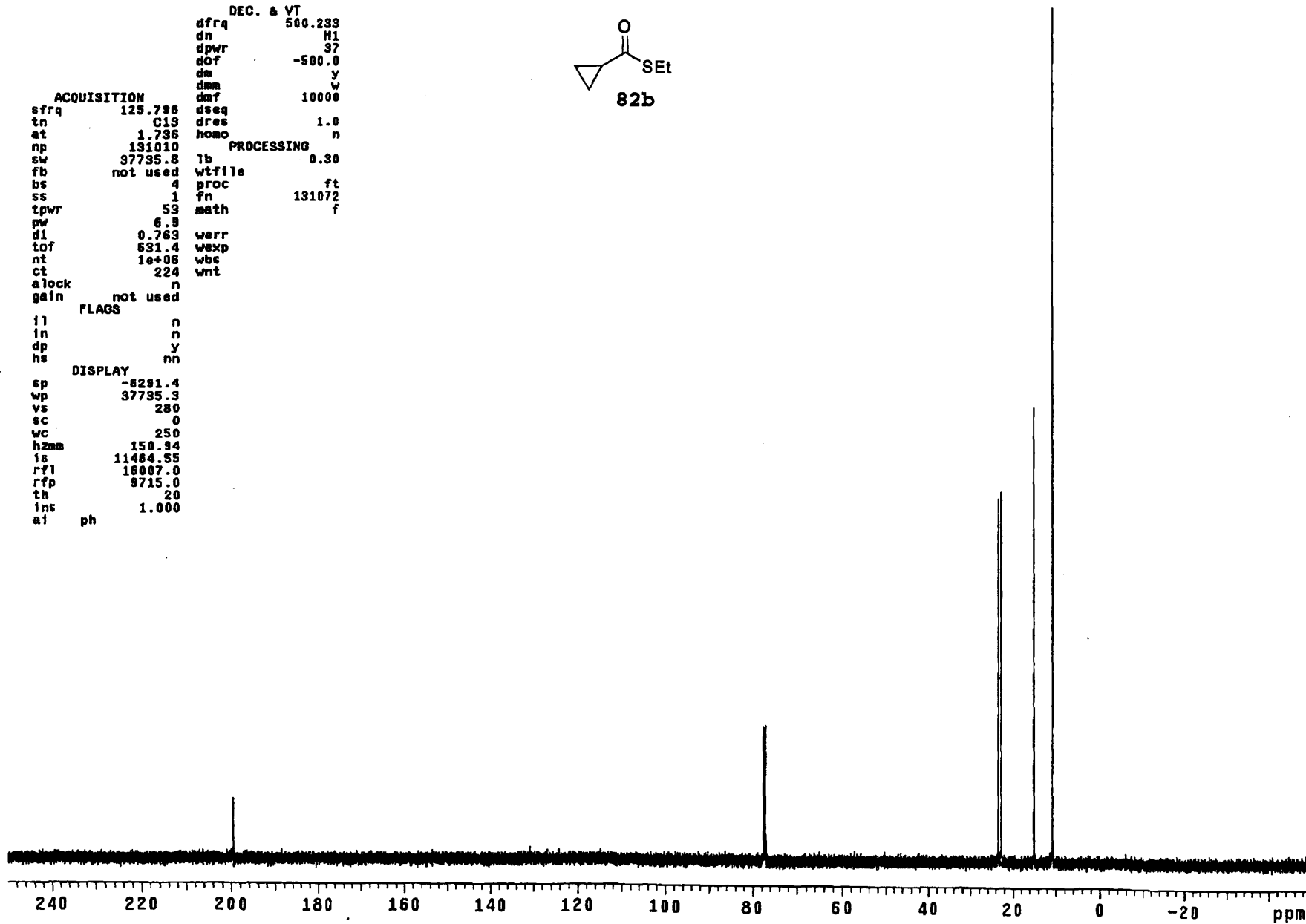
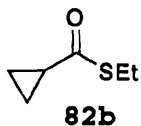
DISPLAY
sp -249.9
wp 6246.8
vs 84
sc 0
wc 250
hzmm 24.98
ls 93.57
rfl 4638.2
rfp 3633.1
th 5
ins 1.000
nm cdc ph

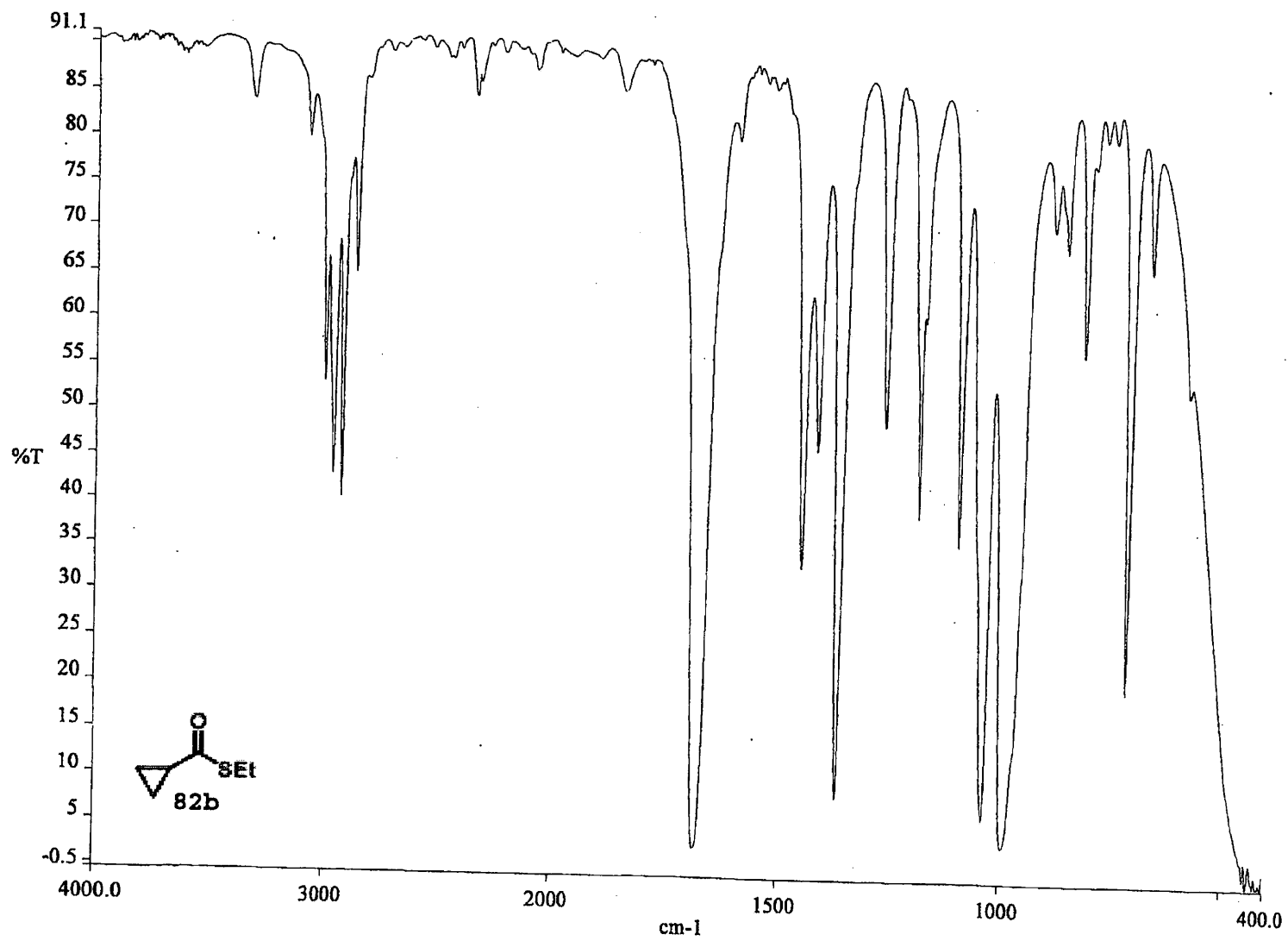


exp1 s2pu1

DEC. & VT
dfrq 500.233
dn H1
dpwr 37
dof -500.0
dm y
dmm w
dmf 10000
dseq
dres 1.0
homo n
PROCESSING
lb 0.30
wtfile
proc ft
fn 131072
math f
werr
wexp
wbs
wnt

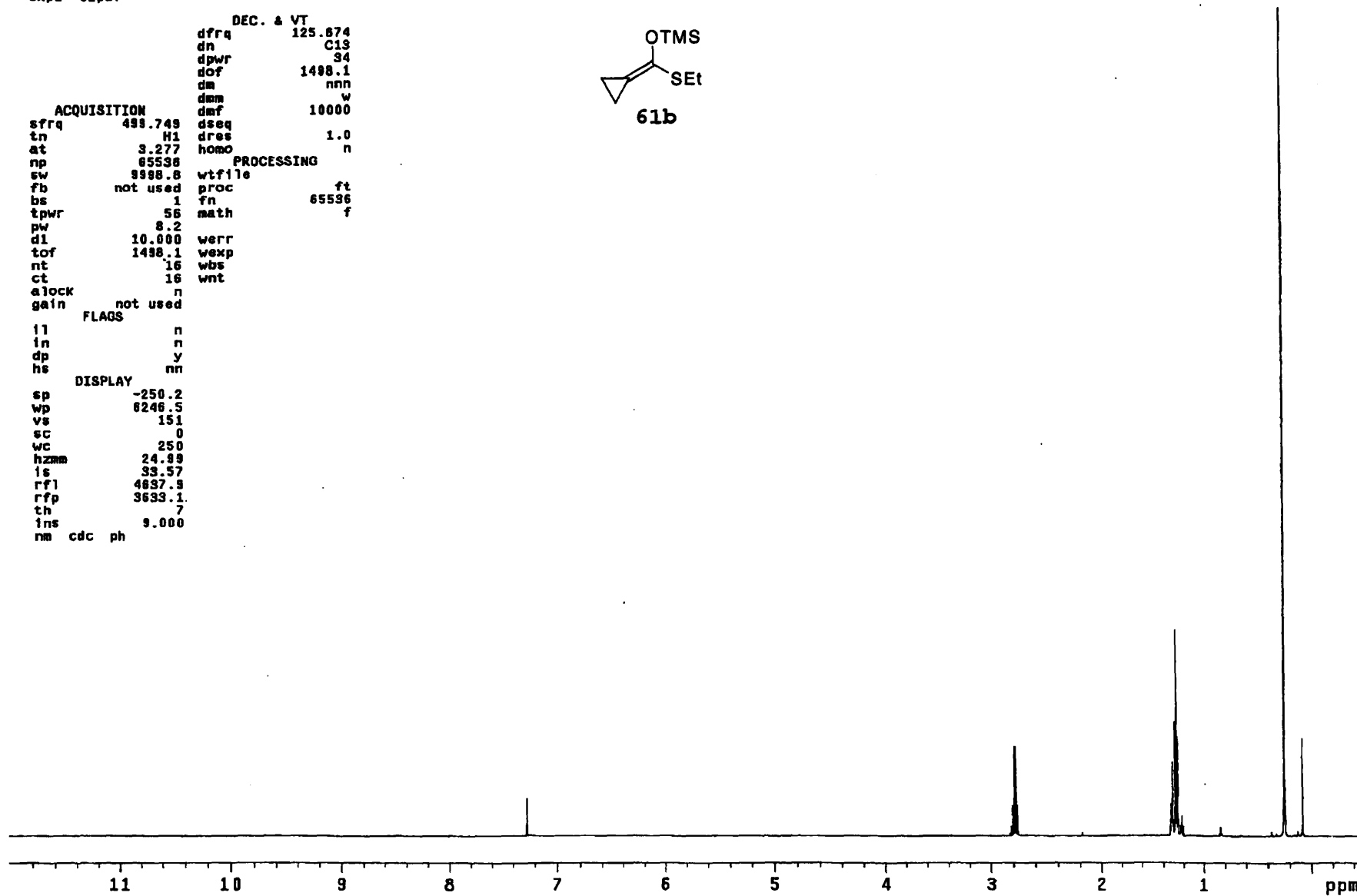
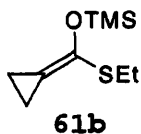
ACQUISITION
sfrq 125.796
tn C13
at 1.736
np 131010
sw 37735.8
fb not used
bs 4
ss 1
tpwr 53
pw 6.8
d1 0.763
tof 631.4
nt 1e+06
ct 224
alock n
gain not used
FLAGS
il n
in n
dp y
hs nn
DISPLAY
sp -8291.4
wp 37735.3
vs 280
sc 0
wc 250
hzma 150.94
is 11484.55
rf1 16007.0
rfp 9715.0
th 20
int 1.000
at ph





exp1 s2pul

```
DEC. & VT
dfrq      125.874
dn        C13
dpwr      34
dof       1498.1
dm        nnn
dm        w
dmf       10000
ACQUISITION
sfrq      499.749
tn        H1
at        3.277
np        65536
sw        9988.8
fb        not used
bs        1
tpwr      56
pw        8.2
dl        10.000
tof       1498.1
nt        16
ct        16
clock     n
gain      not used
          FLAGS
il        n
in        n
dp        y
hs        nn
          DISPLAY
sp        -250.2
wp        6246.5
vs        151
sc        0
wc        250
hzmm      24.89
ls        33.57
rf1       4637.9
rfp       3633.1
th        7
ins       9.000
nm cdc ph
```



exp1 s2pu1

DEC. & VT
dfrq 500.233
dn H1
dpwr 37
dof -500.0
dm y
dmm w
dmf 10000

ACQUISITION

sfrq 125.796
tn C13
at 1.736
np 131010
sw 37735.8
fb not used
bs 4
ss 1
tpwr 53
pw 6.9
d1 0.763
tof 631.4
nt 1e+06
ct 0
alock n
gain not used

PROCESSING

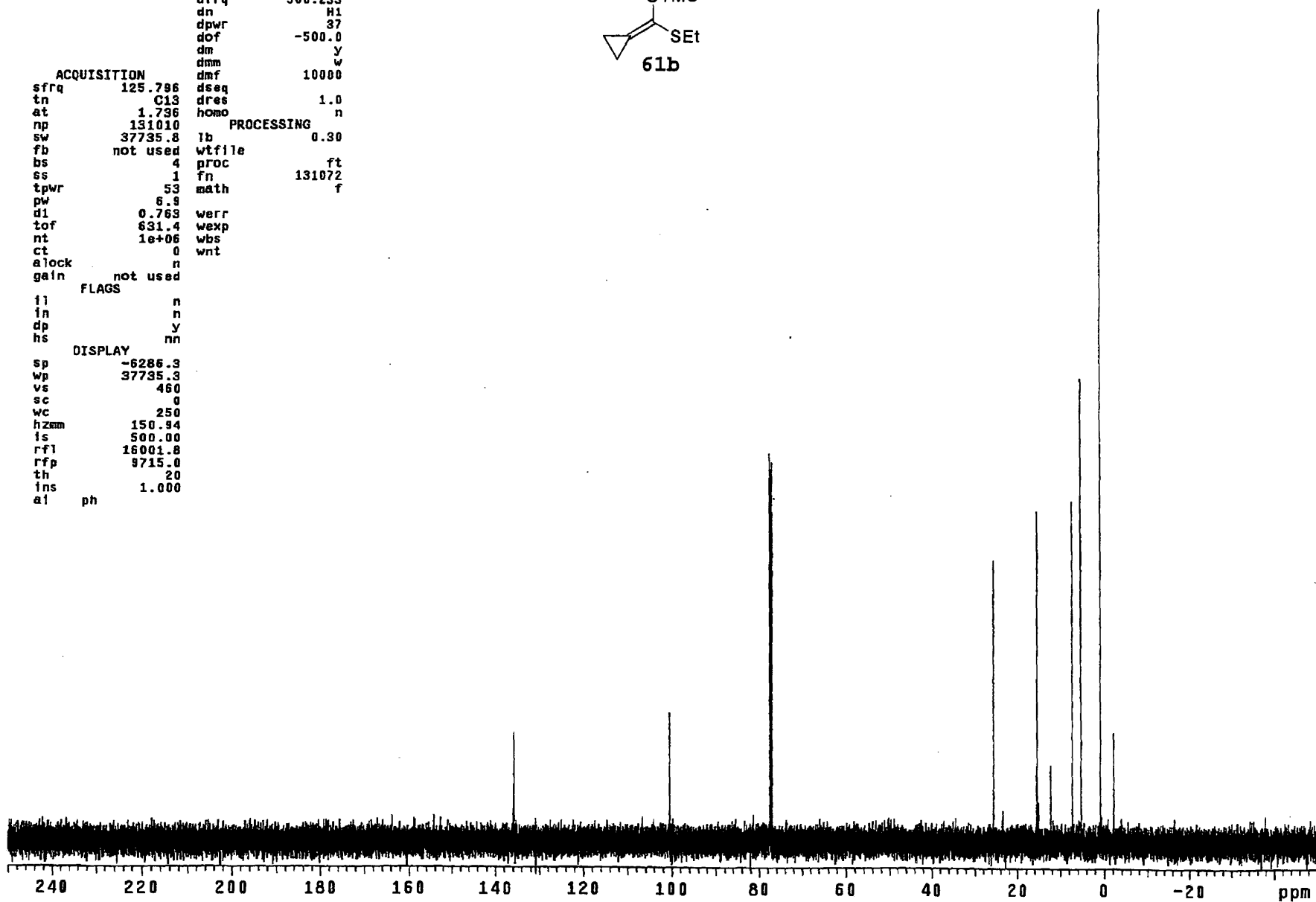
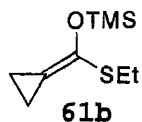
lb 0.30
wtfile
proc ft
fn 131072
math f
werr
wexp
wbs
wnt

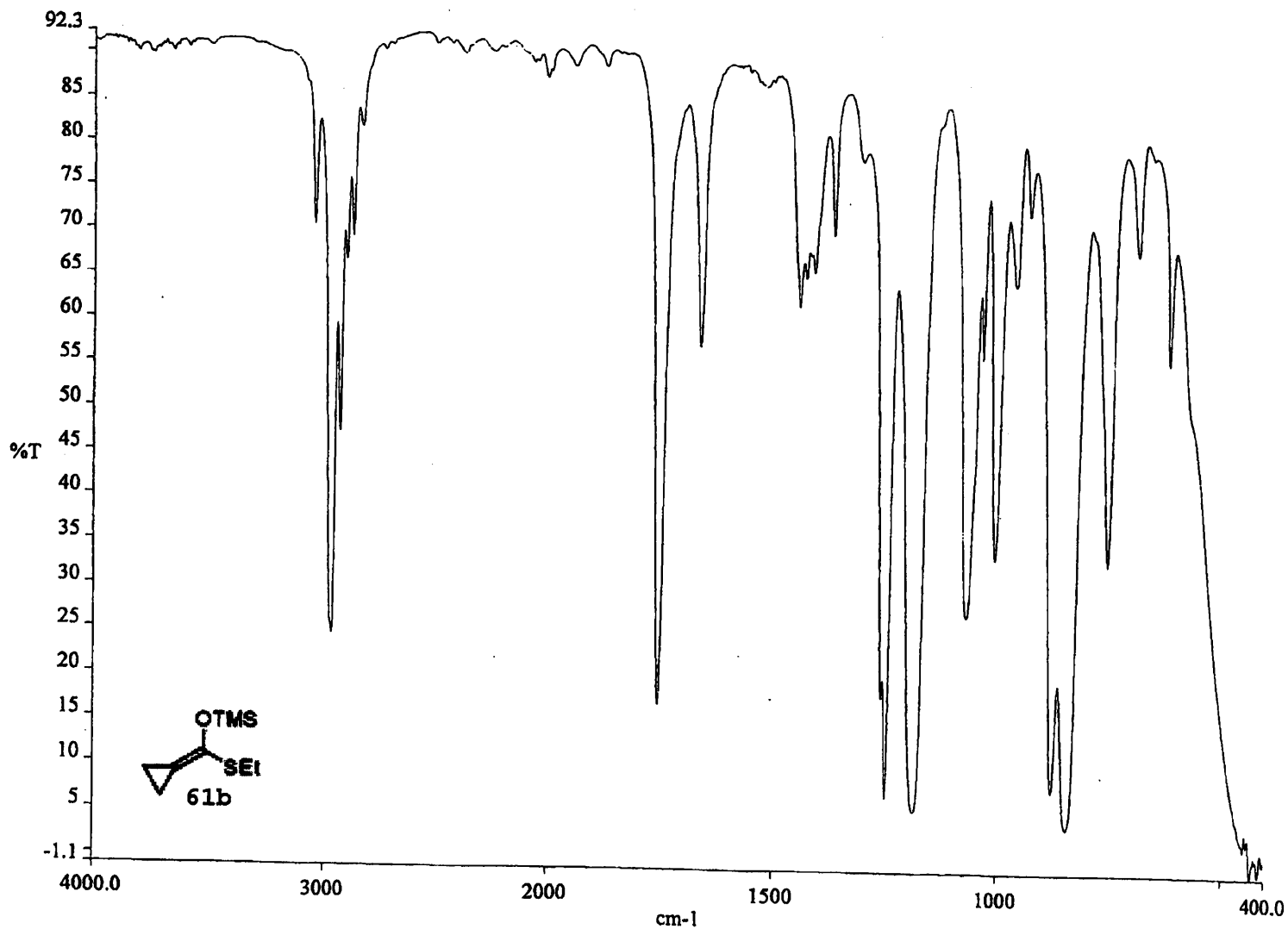
FLAGS

fl n
fn n
dp y
hs nn

DISPLAY

sp -6286.3
wp 37735.3
vs 460
sc 0
wc 250
hzmm 150.94
fs 500.00
rf1 16001.8
rfp 9715.0
th 20
ins 1.000
al ph





exp1 s2pu1

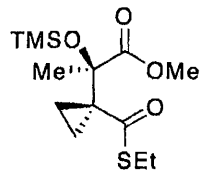
DEC. & VT
dfrq 125.674
dn C13
dpwr 34
dof 1498.1
dm nnn
dmm w
dmf 10000

ACQUISITION
sfrq 499.749
in H1
at 3.277
np 65536
sw 9998.8
fb not used
bs 1
tpwr 56
pw 8.2
d1 20.000
tof 1498.1
nt 16
ct 16
alock n
gain not used

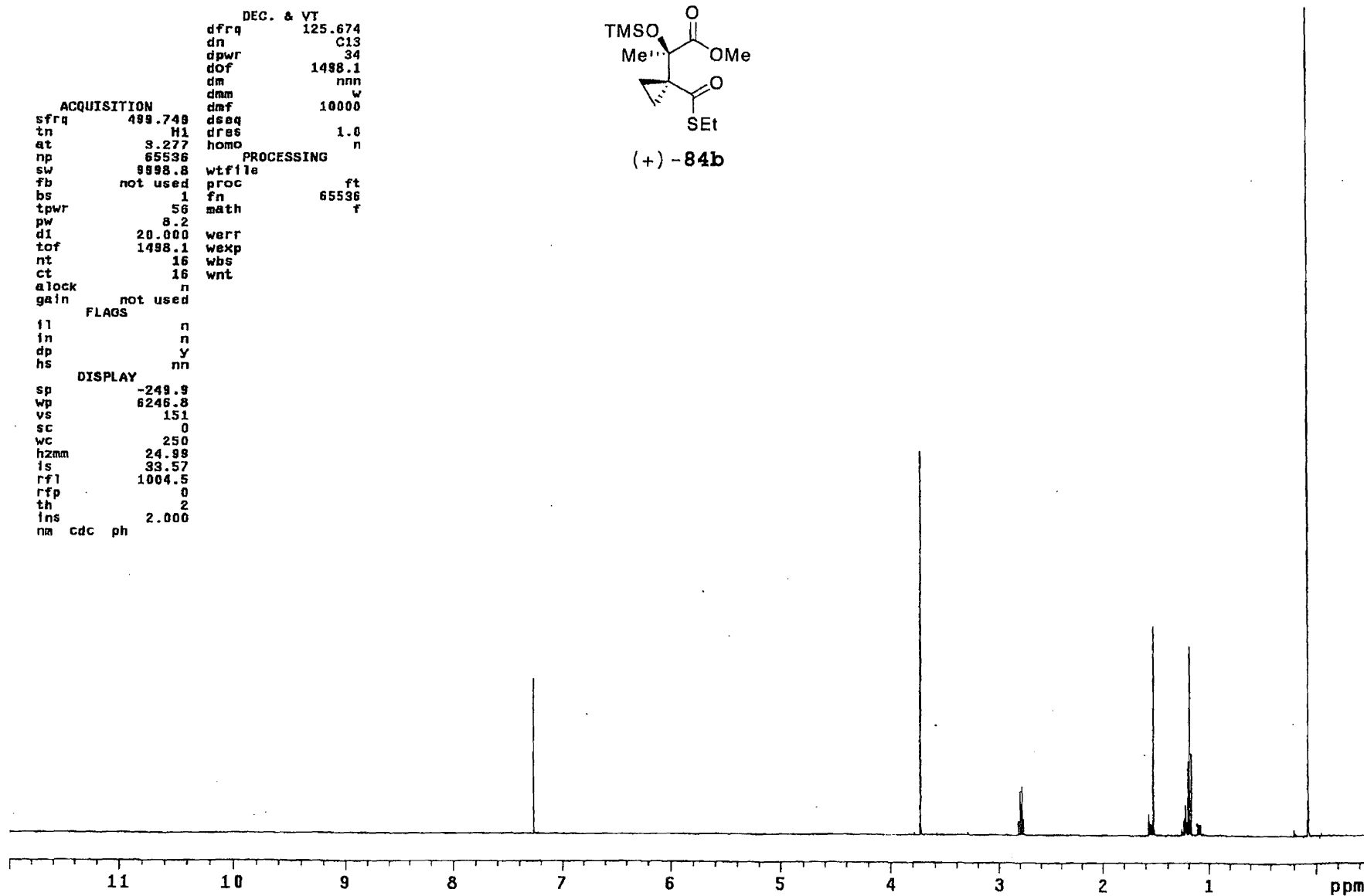
PROCESSING
wtfile
proc ft
fn 65536
math f

FLAGS
ll n
in n
dp y
hs nn

DISPLAY
sp -249.9
wp 8246.8
vs 151
sc 0
wc 250
hzmm 24.98
is 33.57
rfl 1004.5
rfp 0
th 2
ins 2.000
nm cdc ph



(+)-84b



exp1 s2pu1

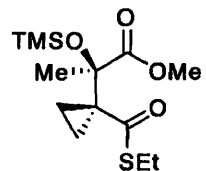
DEC. & VT
dfrq 500.299
dn H1
dpwr 37
dof -500.0
dm y
dam w
dmf 10000

ACQUISITION
sfrq 125.786 dseq
tn C13 dres 1.0
at 1.736 homo n
np 131010 PROCESSING
sw 37735.8 lb 0.30
fb not used wtfile
bs 4 proc ft
ss 1 fn 131072
tpwr 53 math f
pw 5.8
d1 0.763 werr
tof 631.4 wexp
nt 1e+06 wbs
ct 1108 wnt

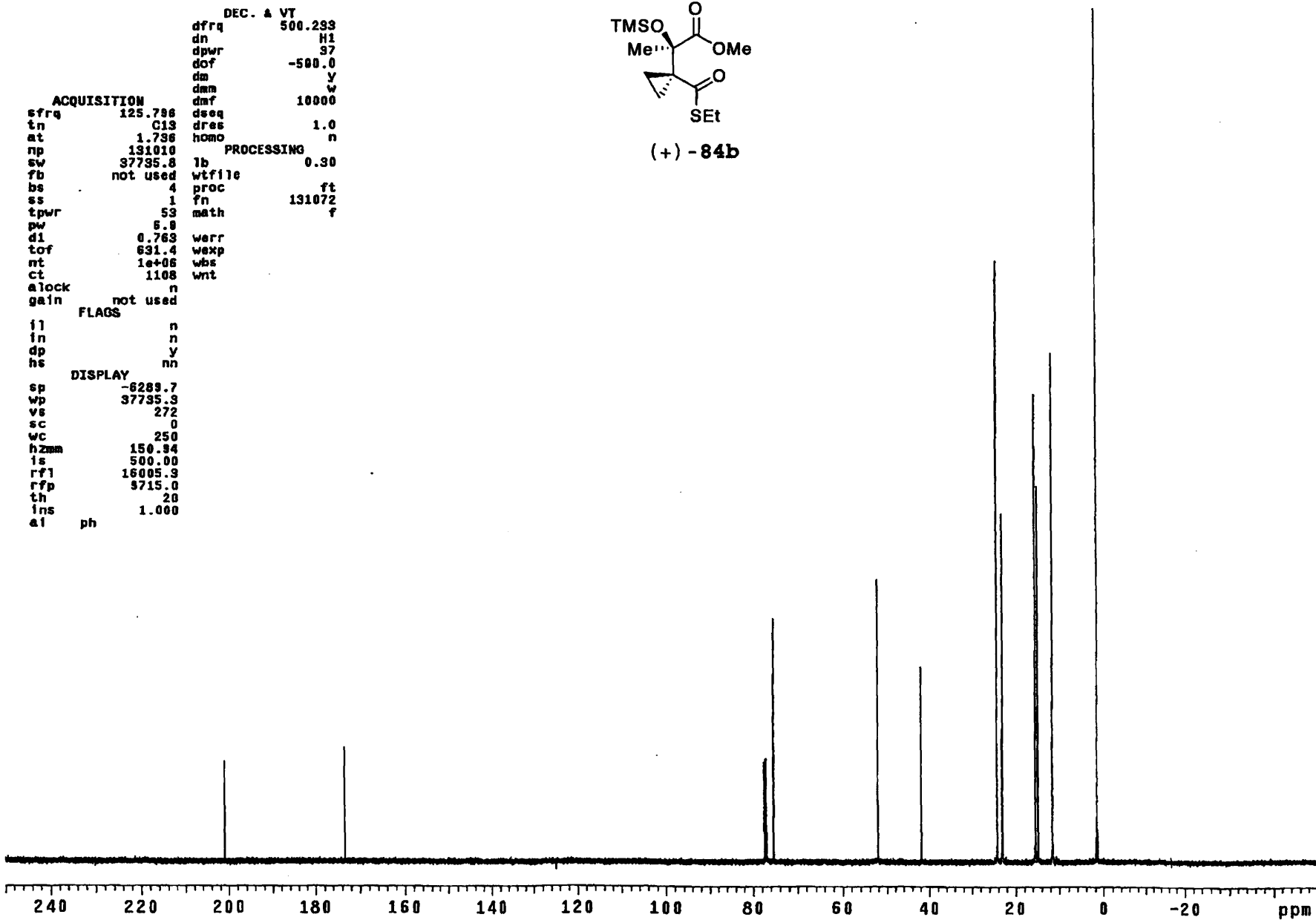
alock n
gain not used

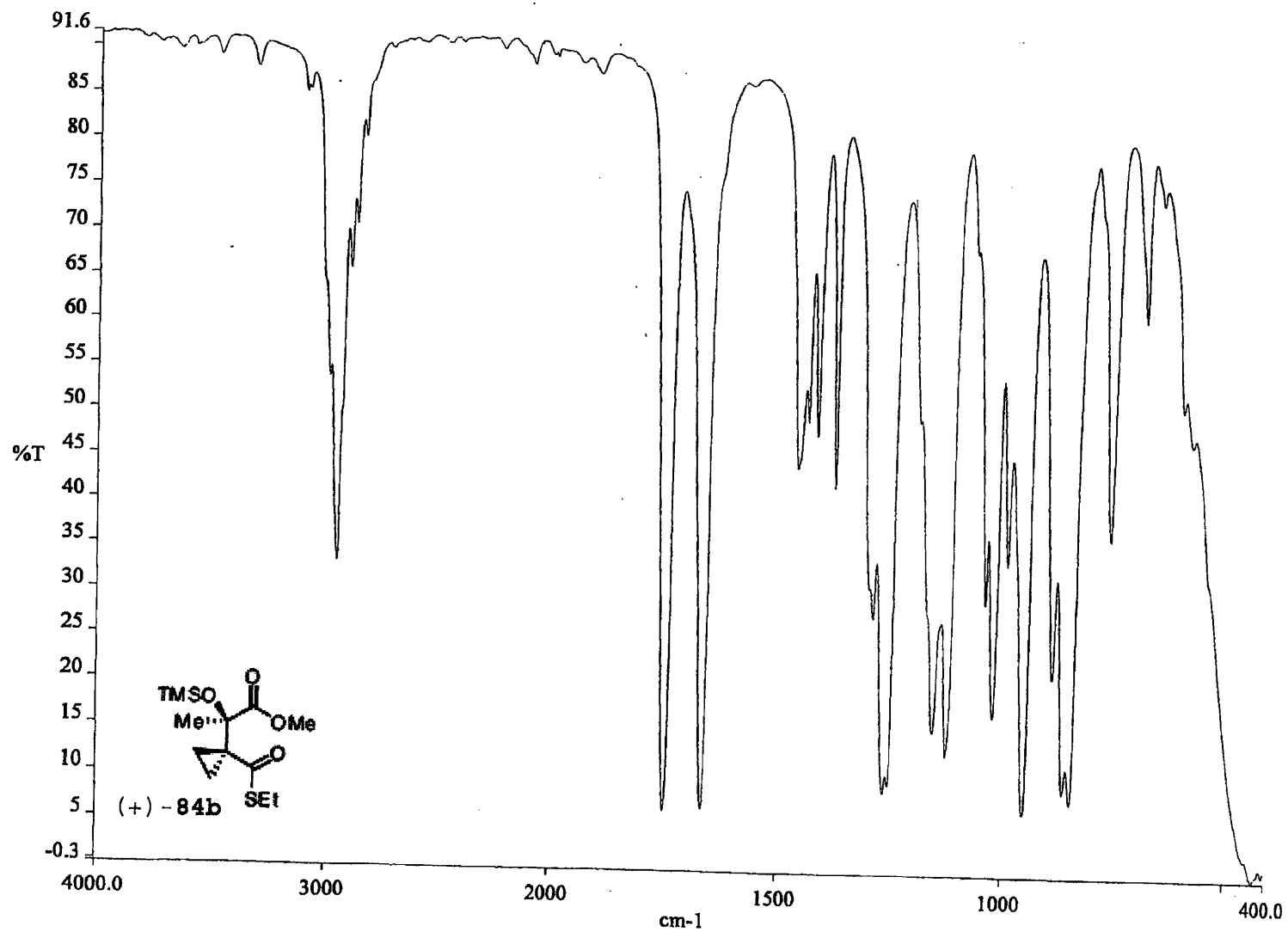
FLAGS
fl n
in n
dp y
hs nn

DISPLAY
sp -6289.7
wp 37735.3
vs 272
sc 0
wc 250
hzmm 150.94
is 500.00
rf1 16005.3
rfp 3715.0
th 20
ins 1.000
af ph



(+) -84b

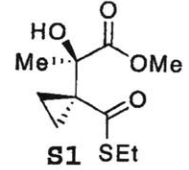




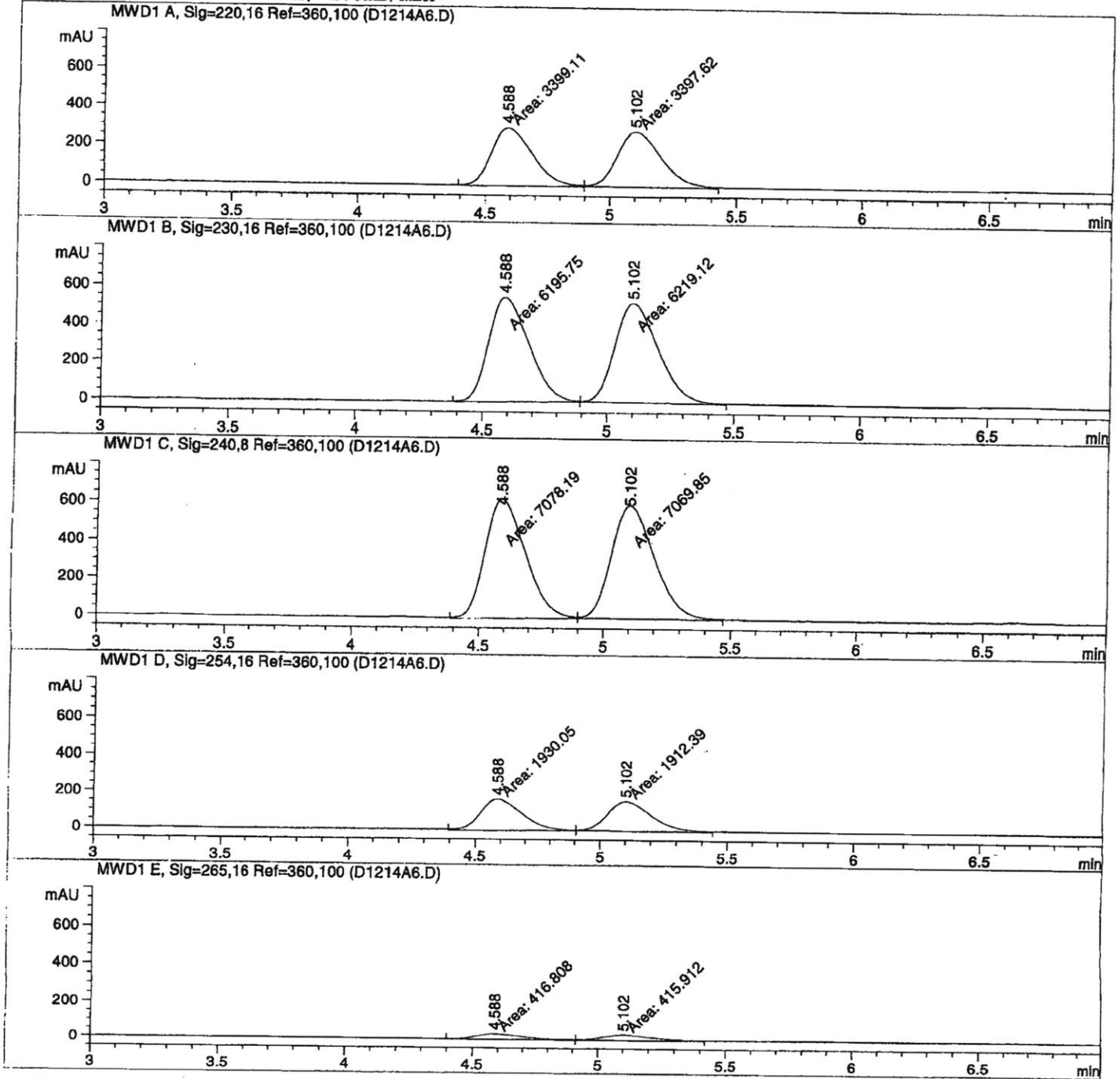
```

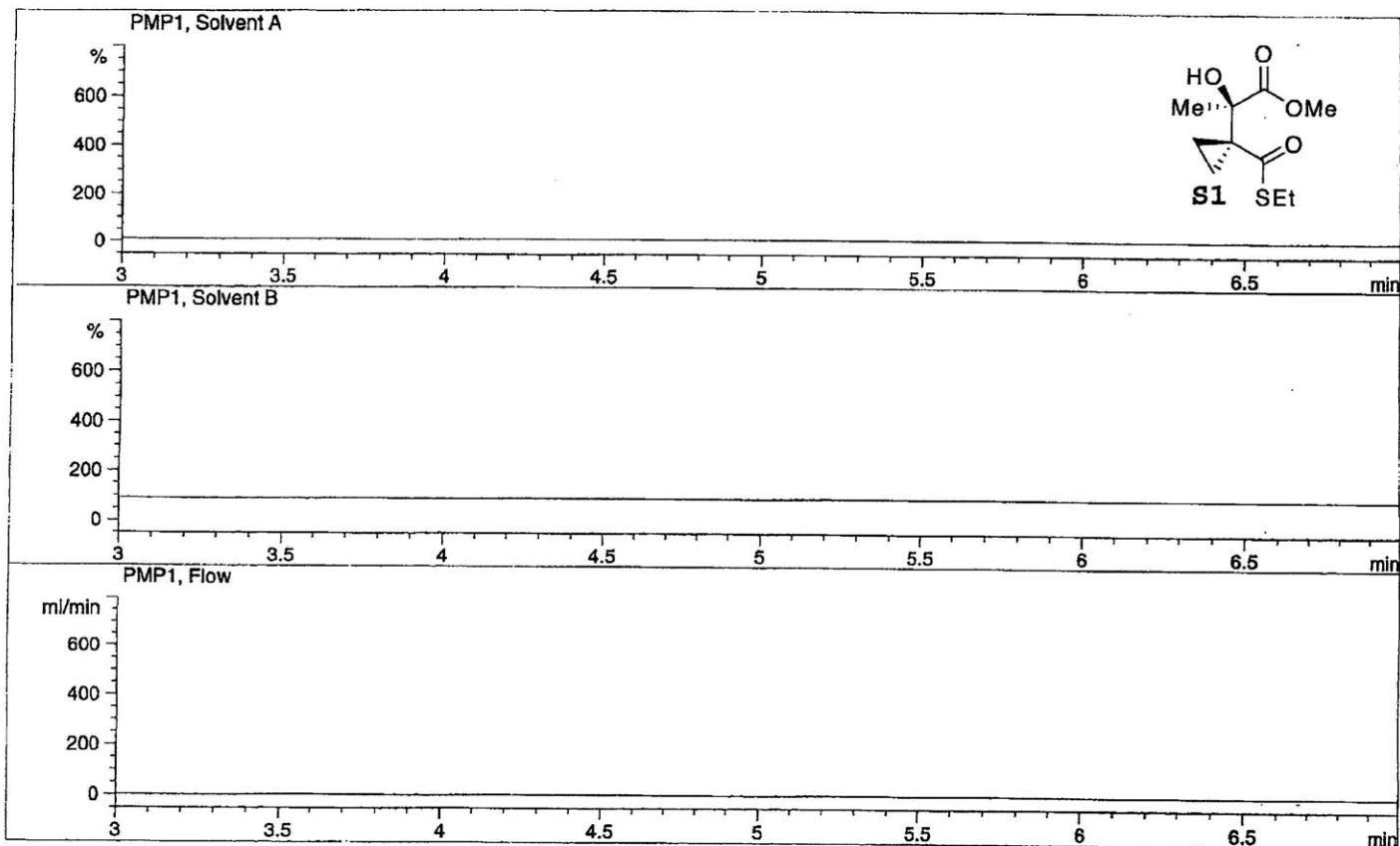
=====
Injection Date   :                               Seq. Line :    2
Sample Name     :                               Location  : Vial 91
Acq. Operator   :                               Inj       :    1
                                                    Inj Volume: 1 µl

Acq. Method    :
Last changed   :
Analysis Method:
Last changed   :
  
```



Zorbax CN; 1.0% iPrOH-hex; 1.0mL/min





=====
 Area Percent Report
 =====

Sorted By : Signal
 Multiplier : 1.0000
 Dilution : 1.0000
 Use Multiplier & Dilution Factor with ISTDs

Signal 1: MWD1 A, Sig=220,16 Ref=360,100

Peak #	RetTime [min]	Type	Width [min]	Area [mAU*s]	Height [mAU]	Area %
1	4.588	MM	0.1896	3399.11206	298.79694	50.0110
2	5.102	MM	0.1992	3397.62256	284.23749	49.9890

Totals : 6796.73462 583.03442

Results obtained with enhanced integrator!

Signal 2: MWD1 B, Sig=230,16 Ref=360,100

Peak #	RetTime [min]	Type	Width [min]	Area [mAU*s]	Height [mAU]	Area %
1	4.588	MM	0.1867	6195.75098	553.00427	49.9059
2	5.102	MM	0.1972	6219.11719	525.51385	50.0941

Totals : 1.24149e4 1078.51813

Results obtained with enhanced integrator!

Signal 3: MWD1 C, Sig=240,8 Ref=360,100

Peak #	RetTime [min]	Type	Width [min]	Area [mAU*s]	Height [mAU]	Area %
1	4.588	MM	0.1882	7078.19482	626.99695	50.0295
2	5.102	MM	0.1979	7069.85059	595.39844	49.9705

Totals : 1.41480e4 1222.39539

Results obtained with enhanced integrator!

Signal 4: MWD1 D, Sig=254,16 Ref=360,100

Peak #	RetTime [min]	Type	Width [min]	Area [mAU*s]	Height [mAU]	Area %
1	4.588	MM	0.1918	1930.04724	167.68768	50.2297
2	5.102	MM	0.2014	1912.39209	158.27319	49.7703

Totals : 3842.43933 325.96088

Results obtained with enhanced integrator!

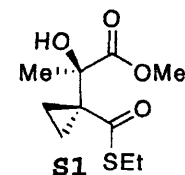
Signal 5: MWD1 E, Sig=265,16 Ref=360,100

Peak #	RetTime [min]	Type	Width [min]	Area [mAU*s]	Height [mAU]	Area %
1	4.588	MM	0.2159	416.80847	32.17342	50.0538
2	5.102	MM	0.2246	415.91214	30.85807	49.9462

Totals : 832.72061 63.03149

Results obtained with enhanced integrator!

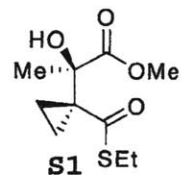
=====
*** End of Report ***



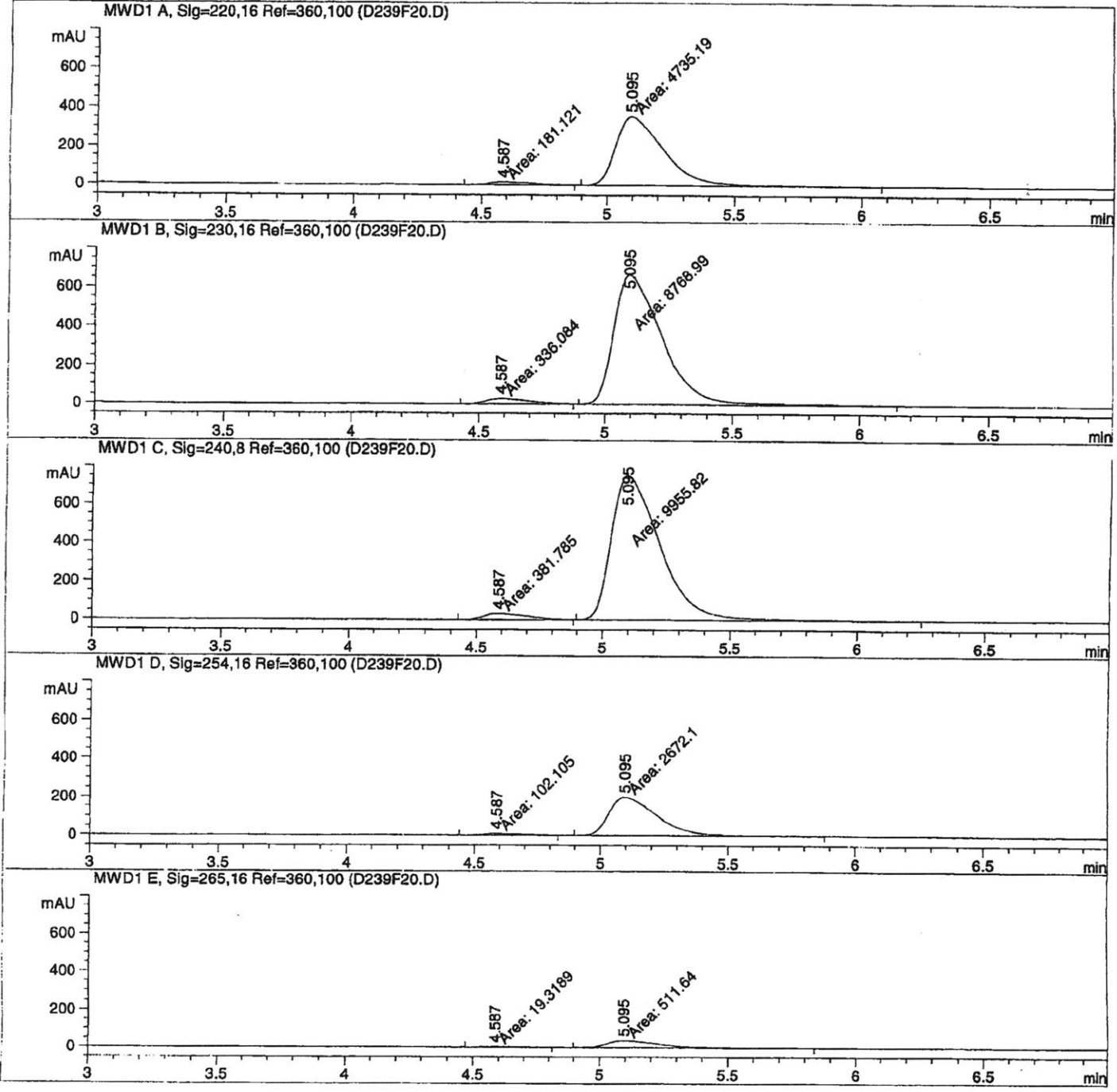
```

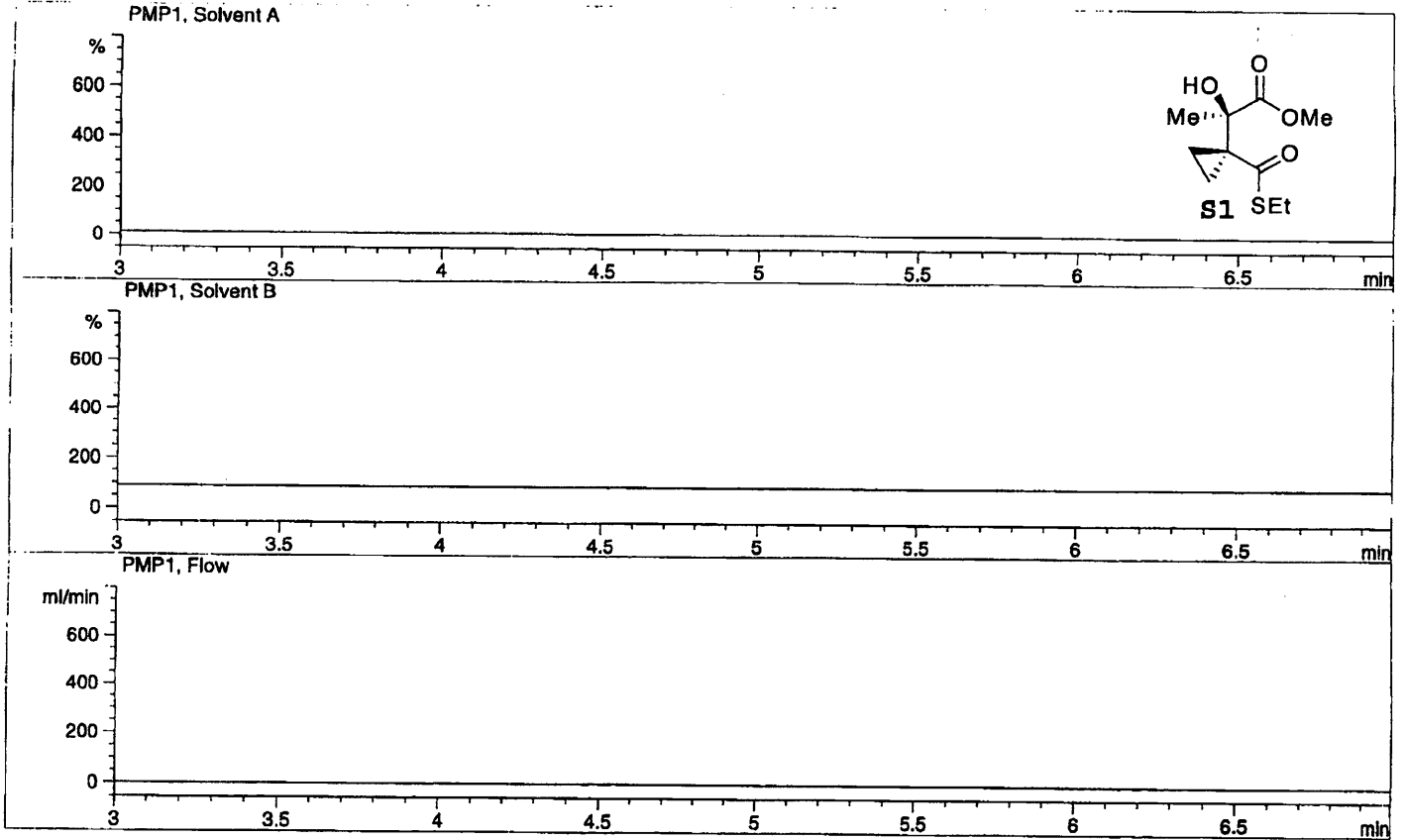
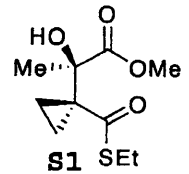
=====
Injection Date :                               Seq. Line :    1
Sample Name    :                               Location  : Vial 91
Acq. Operator  :                               Inj       :    1
                                                    Inj Volume: 1 µl

Acq. Method   :
Last changed  :
Analysis Method :
Last changed  :
  
```



Zorbax CN; 1.0%iPrOH-hex; 1.0mL/min





=====
 Area Percent Report
 =====

Sorted By : Signal
 Multiplier : 1.0000
 Dilution : 1.0000
 Use Multiplier & Dilution Factor with ISTDs

Signal 1: MWD1 A, Sig=220,16 Ref=360,100

Peak #	RetTime [min]	Type	Width [min]	Area [mAU*s]	Height [mAU]	Area %
1	4.587	MM	0.1984	181.12068	15.21405	3.6841
2	5.095	MM	0.2209	4735.18701	357.24994	96.3159

Totals : 4916.30769 372.46399

Results obtained with enhanced integrator!

Signal 2: MWD1 B, Sig=230,16 Ref=360,100

Peak #	RetTime [min]	Type	Width [min]	Area [mAU*s]	Height [mAU]	Area %
1	4.587	MM	0.1964	336.08368	28.51702	3.6912
2	5.095	MM	0.2197	8768.99316	665.32880	96.3088

Totals : 9105.07684 693.84582

Results obtained with enhanced integrator!

Signal 3: MWD1 C, Sig=240,8 Ref=360,100

Peak #	RetTime [min]	Type	Width [min]	Area [mAU*s]	Height [mAU]	Area %
1	4.587	MM	0.1971	381.78519	32.28540	3.6932
2	5.095	MM	0.2201	9955.81836	753.86084	96.3068

Totals : 1.03376e4 786.14624

Results obtained with enhanced integrator!

Signal 4: MWD1 D, Sig=254,16 Ref=360,100

Peak #	RetTime [min]	Type	Width [min]	Area [mAU*s]	Height [mAU]	Area %
1	4.587	MM	0.1951	102.10541	8.72269	3.6805
2	5.095	MM	0.2212	2672.10400	201.31873	96.3195

Totals : 2774.20941 210.04141

Results obtained with enhanced integrator!

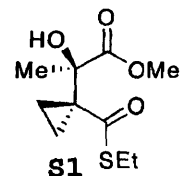
Signal 5: MWD1 E, Sig=265,16 Ref=360,100

Peak #	RetTime [min]	Type	Width [min]	Area [mAU*s]	Height [mAU]	Area %
1	4.587	MM	0.1958	19.31890	1.64459	3.6385
2	5.095	MM	0.2330	511.64023	36.59689	96.3615

Totals : 530.95913 38.24148

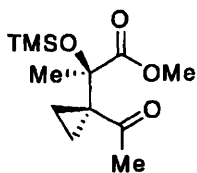
Results obtained with enhanced integrator!

=====
*** End of Report ***



exp1 s2pu1

DEC. & VT
dfrq 125.785
dn C13
dpwr 37
dof 0
da nnn
dam c
daf 10000



(+) -86

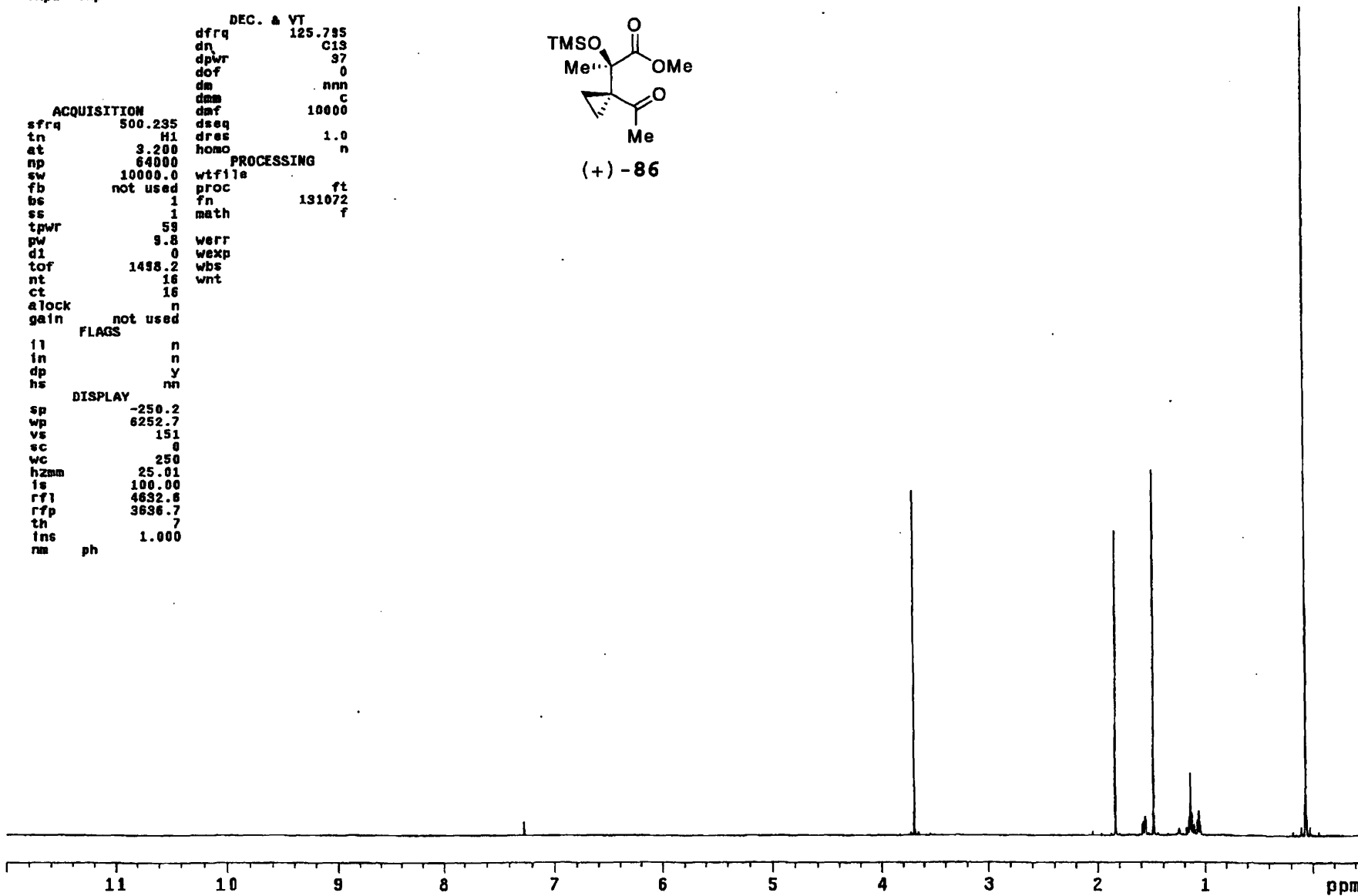
ACQUISITION
sfrq 500.235
tn H1
at 3.200
np 64000
sw 10000.0
fb not used
bs 1
ss 1
tpwr 59
pw 9.8
d1 0
tof 1438.2
nt 16
ct 16
alock n
gain not used

PROCESSING
wifile
proc ft
fn 131072
math f

weff
wexp
wbs
wnt

FLAGS
ll n
in n
dp y
hs nn

DISPLAY
sp -250.2
wp 6252.7
vs 151
sc 0
wc 250
hzmm 25.01
fs 100.00
rf1 4632.6
rfp 3636.7
th 7
ins 1.000
nm ph



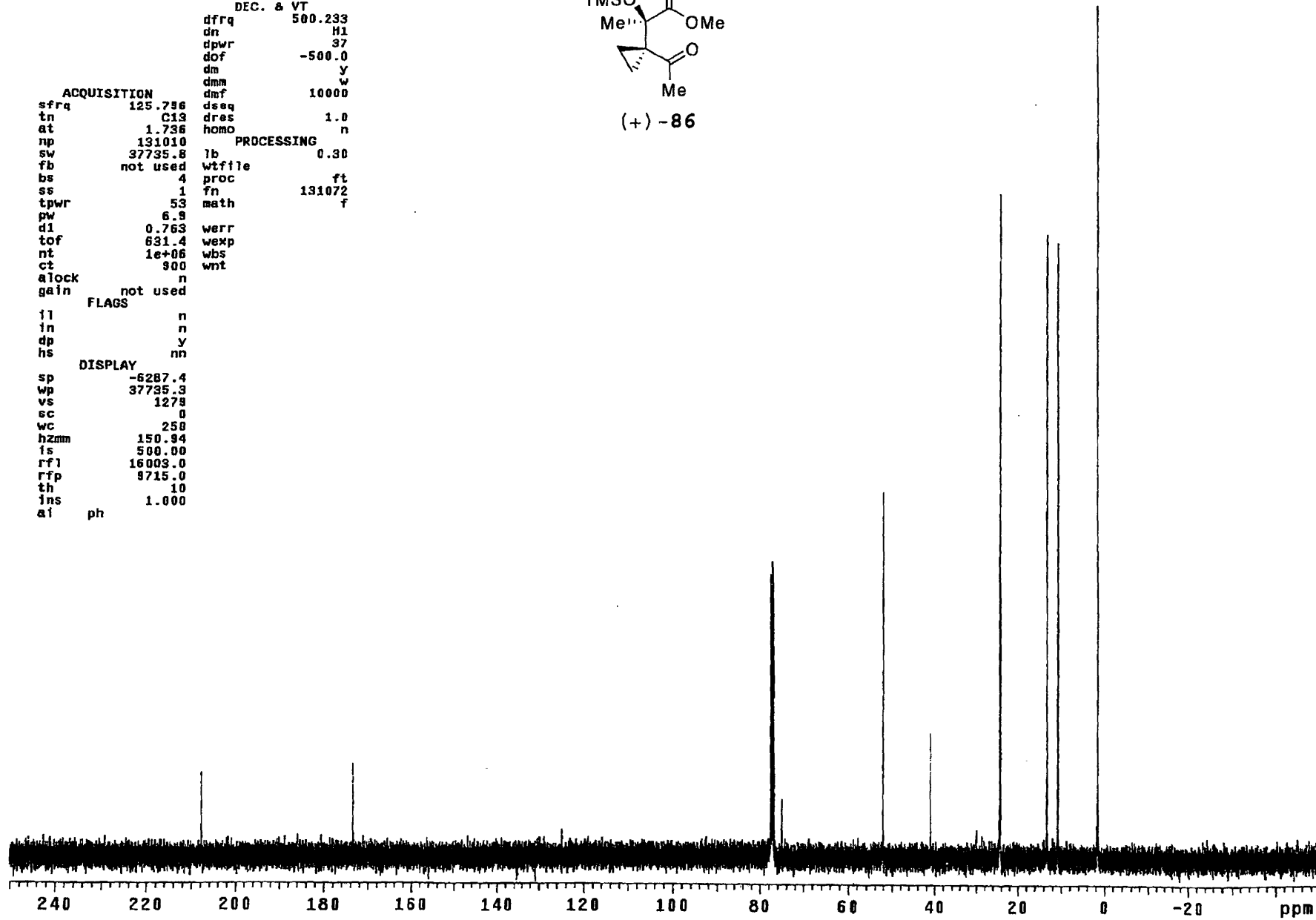
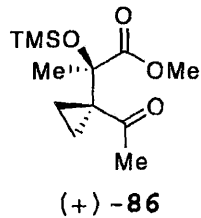
exp1 s2pu1

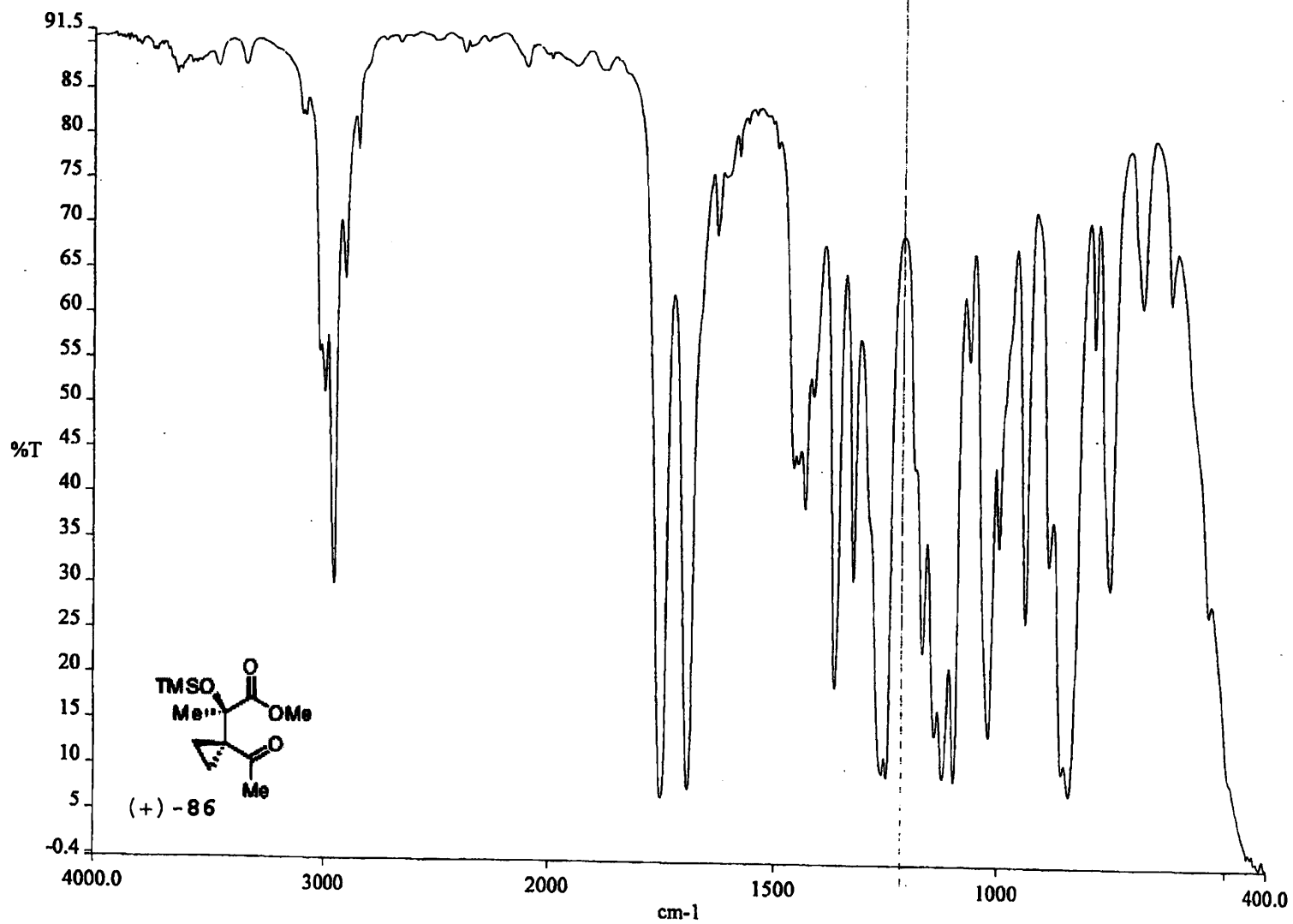
```
DEC. & VT
dfrq 500.233
dn H1
dpwr 37
dof -500.0
dm y
dmm w
dmf 10000

ACQUISITION
sfrq 125.736 dseq
tn C13 dres 1.0
at 1.736 homo n
np 131010
sw 37735.8 lb 0.30
fb not used wtfile
bs 4 proc ft
ss 1 fn 131072
tpwr 53 math f
pw 6.9
d1 0.763 werr
tof 631.4 wexp
nt 1e+06 wbs
ct 900 wnt
alock n
gain not used

FLAGS
fl n
fn n
dp y
hs nn

DISPLAY
sp -6287.4
wp 37735.3
vs 1279
sc 0
wc 250
hzmm 150.94
fs 500.00
rf1 16003.0
rfp 9715.0
th 10
ins 1.000
ai ph
```





exp1 s2pu1

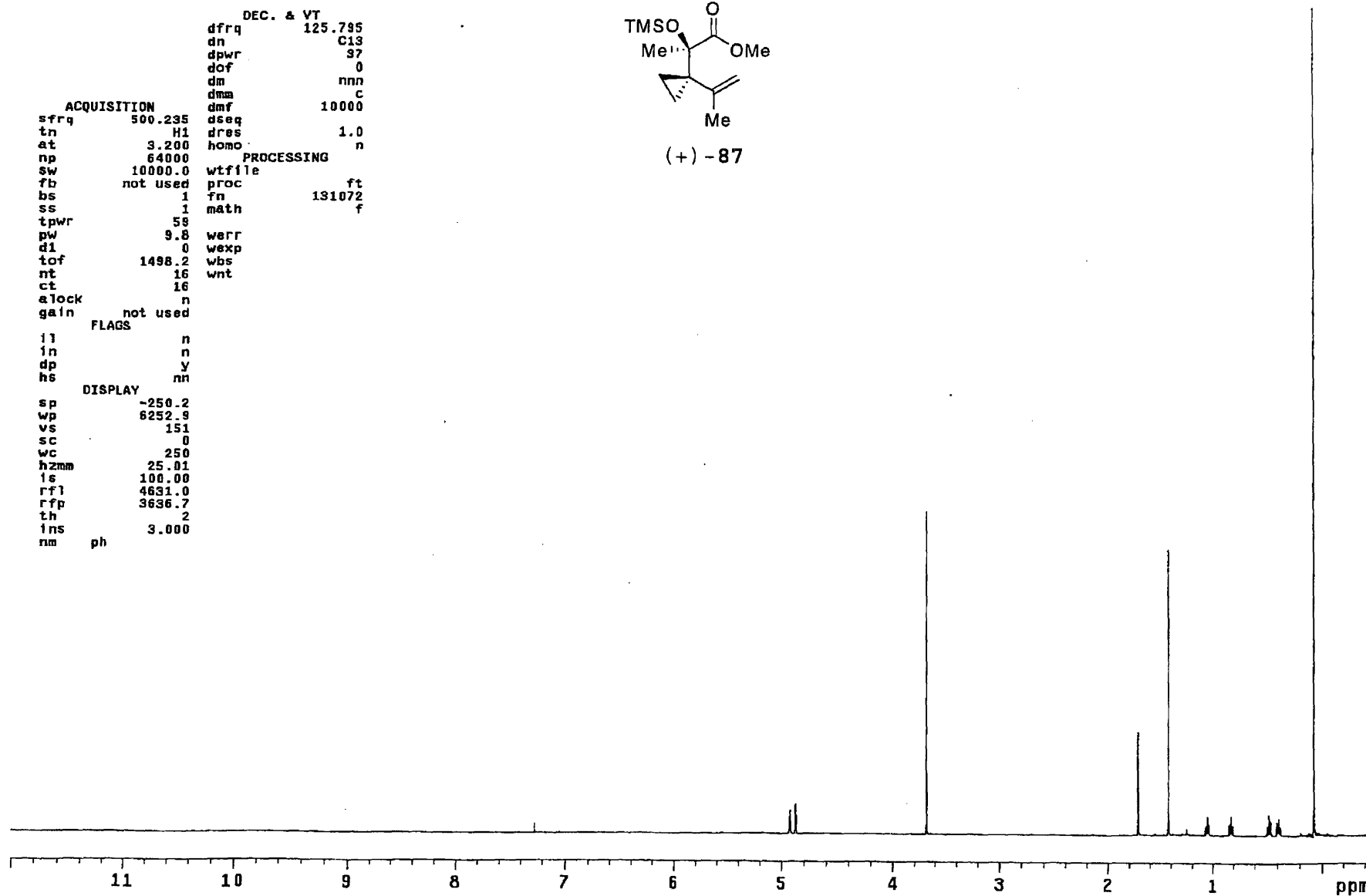
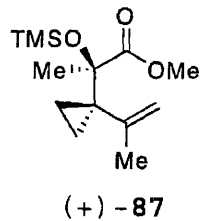
DEC. & VT
dfrq 125.795
dn C13
dpwr 37
dof 0
dm nnn
dma c
dmf 10000
dseq 1.0
dres n
homo n

ACQUISITION
sfrq 500.235
tn H1
at 3.200
np 64000
sw 10000.0
fb not used
bs 1
ss 1
tpwr 58
pw 9.8
d1 0
tof 1498.2
nt 16
ct 16
clock n
gain not used

PROCESSING
wtfile ft
proc 131072
fn f
math

FLAGS
ll n
in n
dp y
hs nn

DISPLAY
sp -250.2
wp 6252.9
vs 151
sc 0
wc 250
hzmm 25.01
ls 100.00
rfl 4631.0
rfp 3636.7
th 2
ins 3.000
nm ph



exp1 s2pul

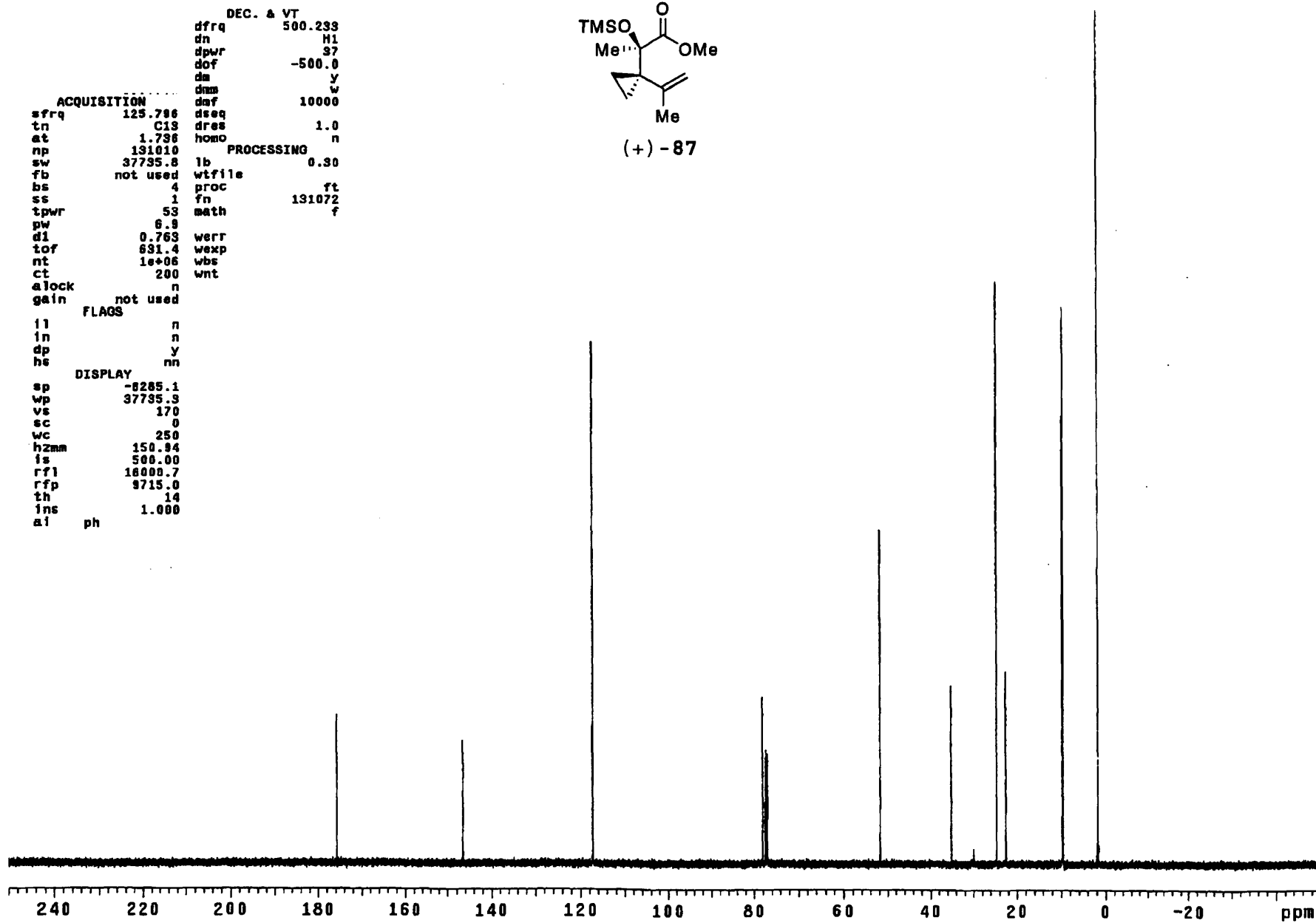
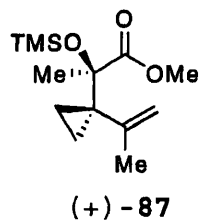
DEC. & VT
dfrq 500.233
dn H1
dpwr 37
dof -500.0
da y
dmm w
dof 10000

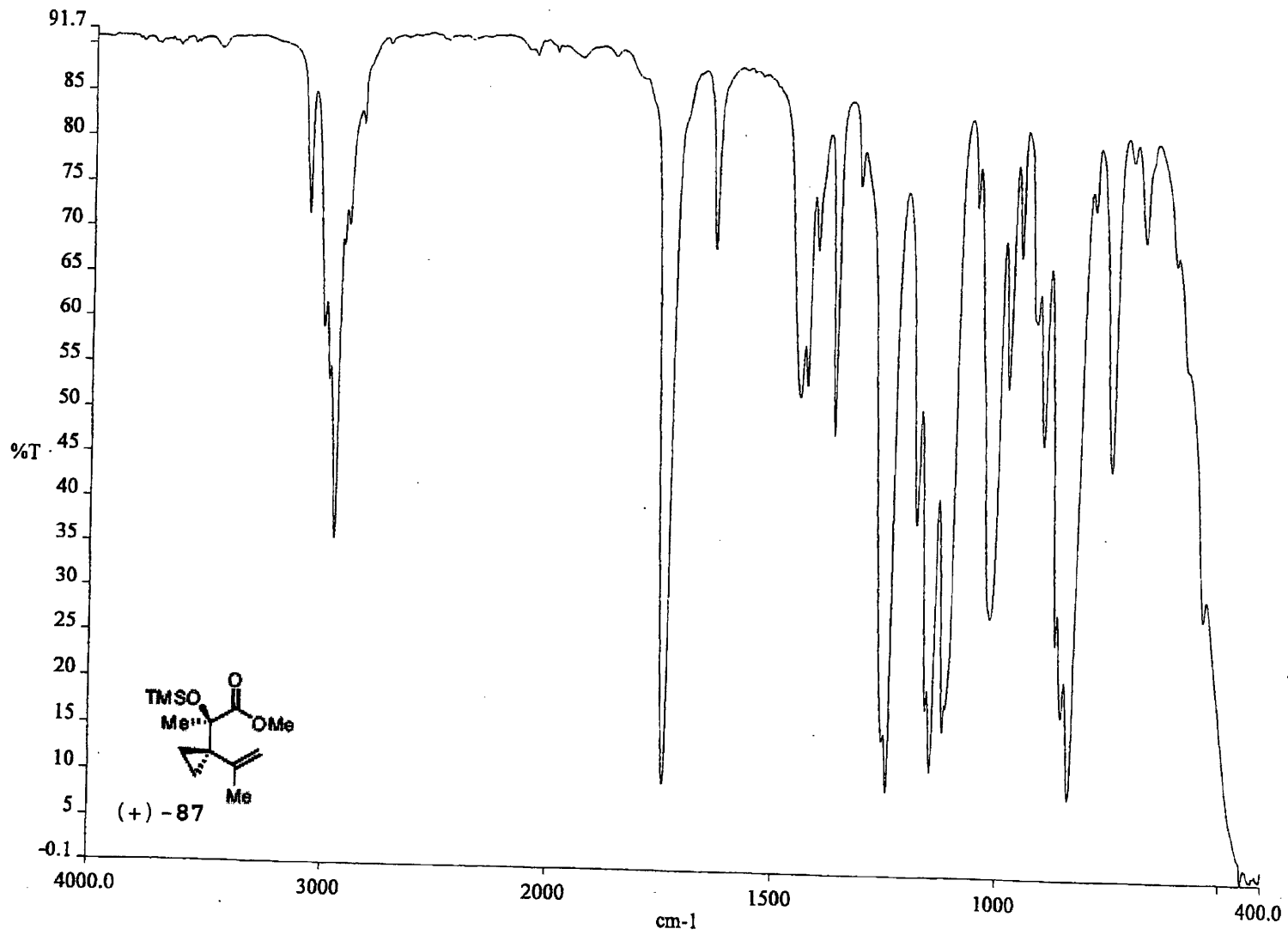
ACQUISITION
sfrq 125.786
tn C13
at 1.736
np 131010
sw 37735.8
fb not used
bs 4
ss 1
tpwr 53
pw 6.9
d1 0.763
tof 631.4
nt 1e+06
ct 200
alock n
gain not used

PROCESSING
dseq 1.0
dres n
lbr 0.30
wtfile
proc ft
fn 131072
math f

FLAGS
ll n
ln n
dp y
hs nn

DISPLAY
sp -8285.1
wp 37735.3
vs 170
sc 0
wc 250
hzmm 150.94
is 500.00
rfl 16000.7
rfp 9715.0
th 14
ins 1.000
al ph





exp803 s2pu1

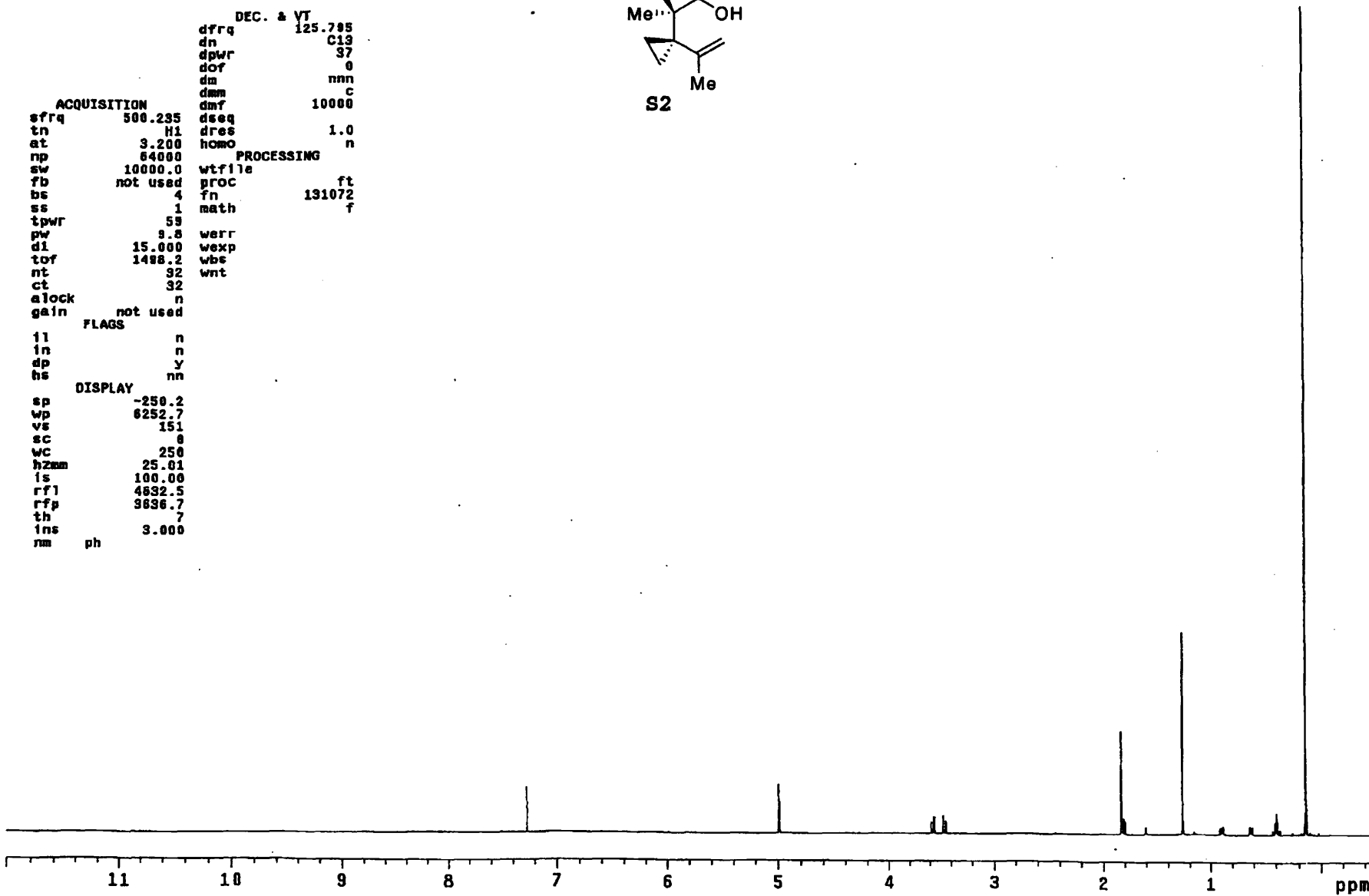
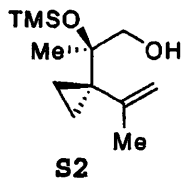
DEC. & VT
dfrq 125.785
dn C13
dpwr 37
dof 0
dm nnn
dam c
dmf 10000

ACQUISITION
sfrq 500.235
tn H1
at 3.200
np 64000
sw 10000.0
fb not used
bs 4
ss 1
tpwr 58
pw 9.8
d1 15.000
tof 1488.2
nt 32
ct 32
alock n
gain not used

PROCESSING
wtfile
proc ft
fn 131072
math f

FLAGS
ll n
in n
dp y
hs nn

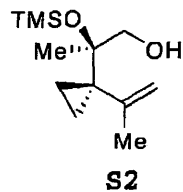
DISPLAY
sp -250.2
wp 6252.7
vs 151
sc 0
wc 250
hzmm 25.01
is 100.00
rf1 4632.5
rfp 3636.7
th 7
ins 3.000
nm ph



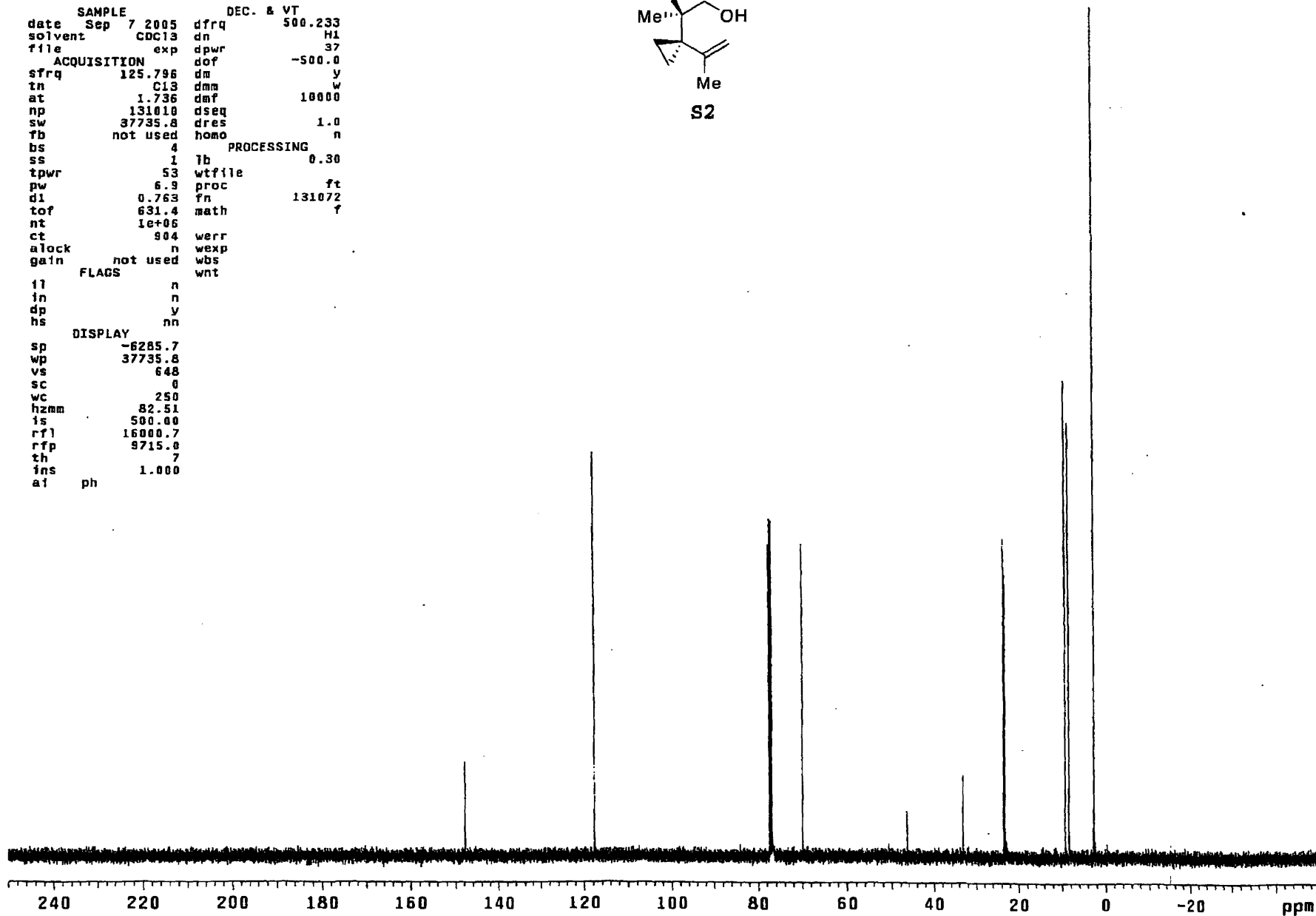
```

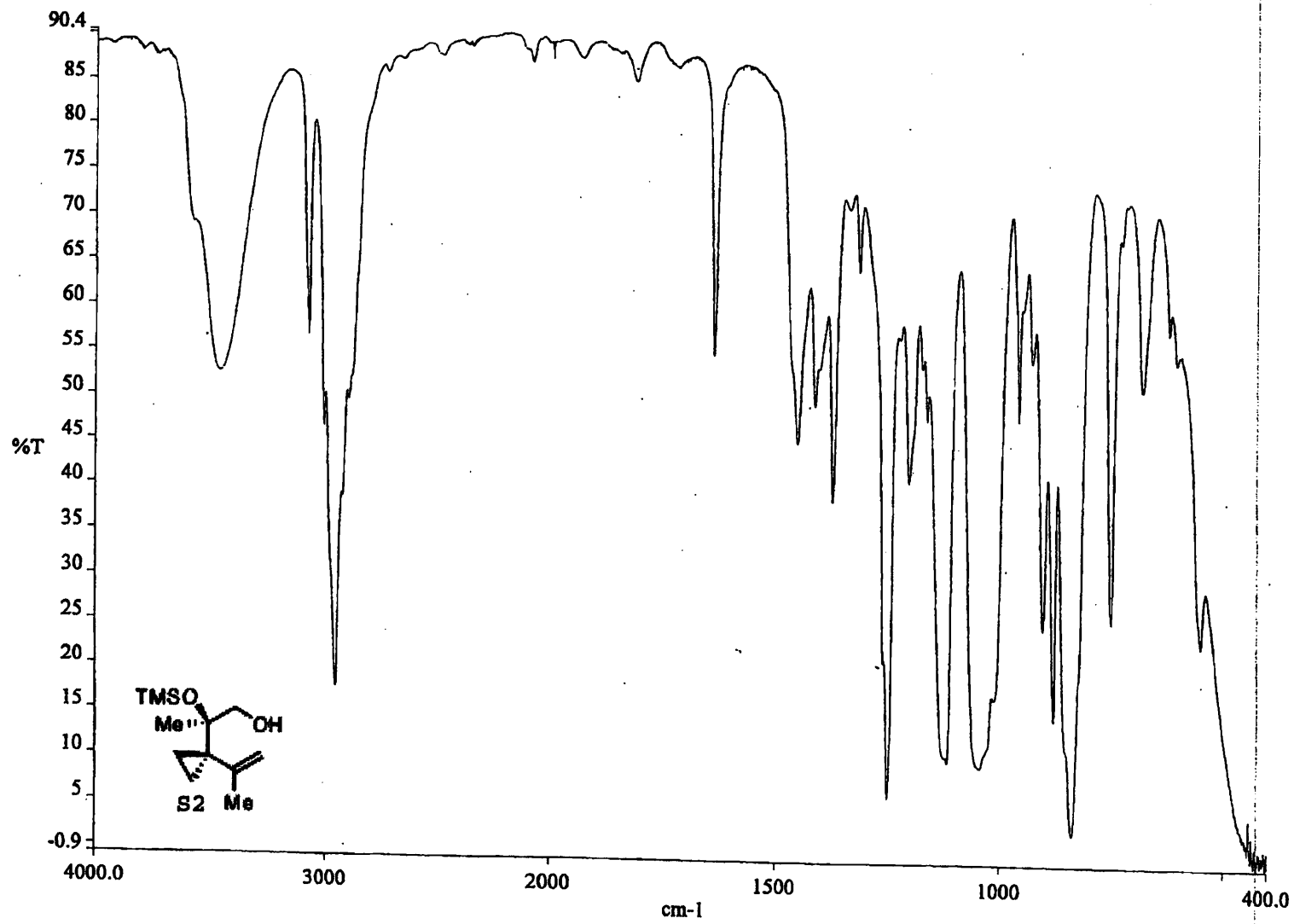
expl s2pu1
SAMPLE          DEC. & VT
date Sep 7 2005 dfrq      500.233
solvent CDCl3     dn       H1
file exp dpwr       37
ACQUISITION    dof      -500.0
sfrq 125.796 dm       y
tn C13 dmm          w
at 1.736 dmf       10000
np 131010 dseq
sw 37735.8 dres     1.0
fb not used homo   n
bs 4
ss 1 PROCESSING
tpwr 53 fb 0.30
pw 6.9 wtfile
dl 0.763 fn
tof 631.4 fn 131072
nt 1e+05 math f
ct 904 werr
alock n wexp
gain not used wbs
        FLAGS wnt
il n
in n
dp y
hs nn
DISPLAY
sp -6285.7
wp 37735.8
vs 648
sc 0
wc 250
hzmm 82.51
is 500.00
rfl 16000.7
rfp 9715.8
th 7
ins 1.000
ai ph

```



166

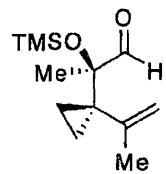




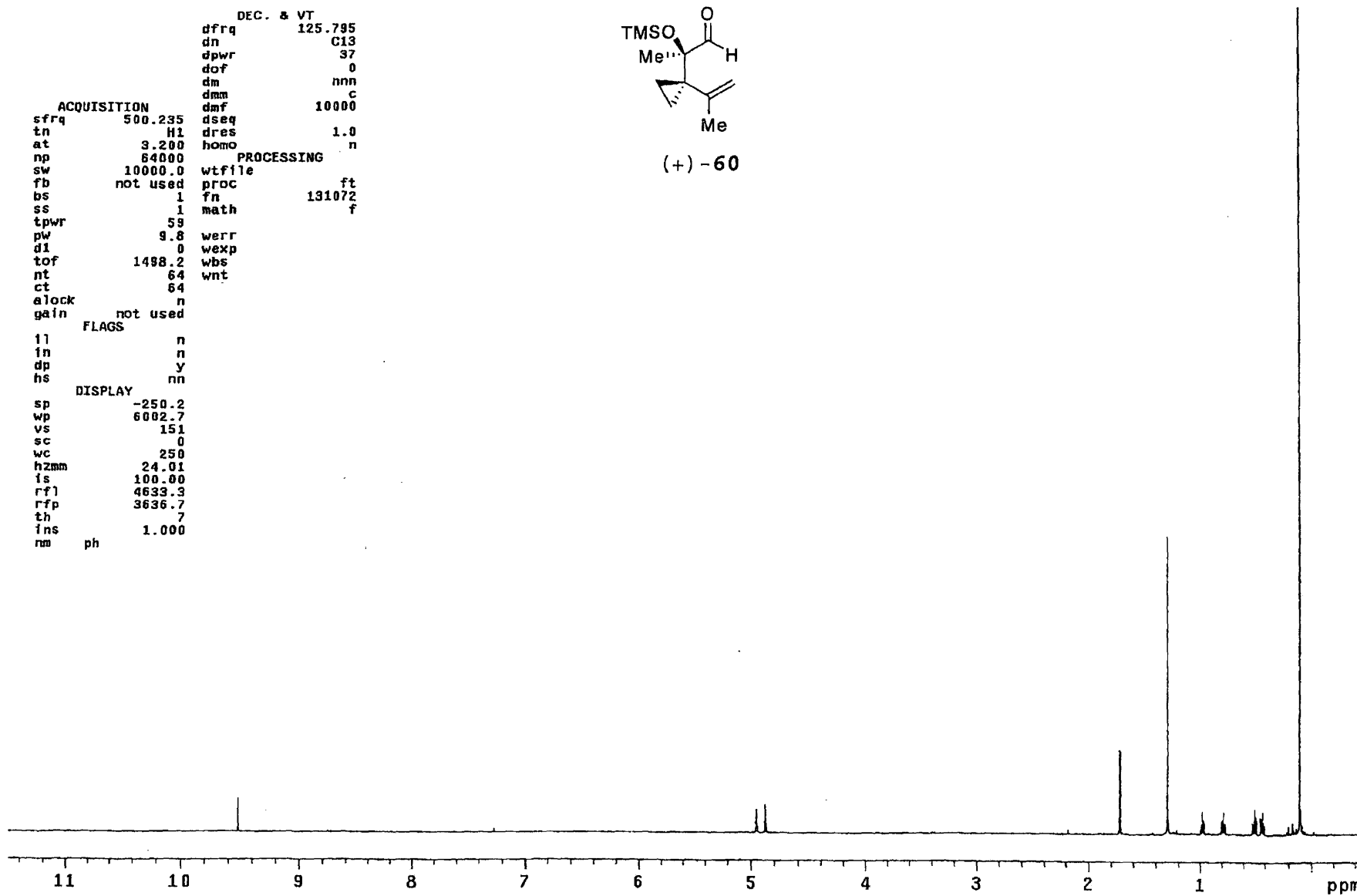
exp1 s2pu1

```
DEC. & VT
dfrq      125.795
dn        C13
dpwr      37
dof       0
dm        nnn
dmm       c
dmf       10000
ACQUISITION
sfrq      500.235
in        H1
at        3.200
np        64000
sw        10000.0
fb        not used
bs        1
ss        1
tpwr      59
pw        9.8
d1        0
tof       1498.2
nt        64
ct        64
alock     n
gain      not used
          FLAGS
ll        n
in        n
dp        y
hs        nn
          DISPLAY
sp        -250.2
wp        6002.7
vs        151
sc        0
wc        250
hzmm      24.01
is        100.00
rfl       4633.3
rfp       3636.7
th        7
ins       1.000
nm        ph
```

```
PROCESsing
wtfile
proc      ft
fn        131072
math      f
```

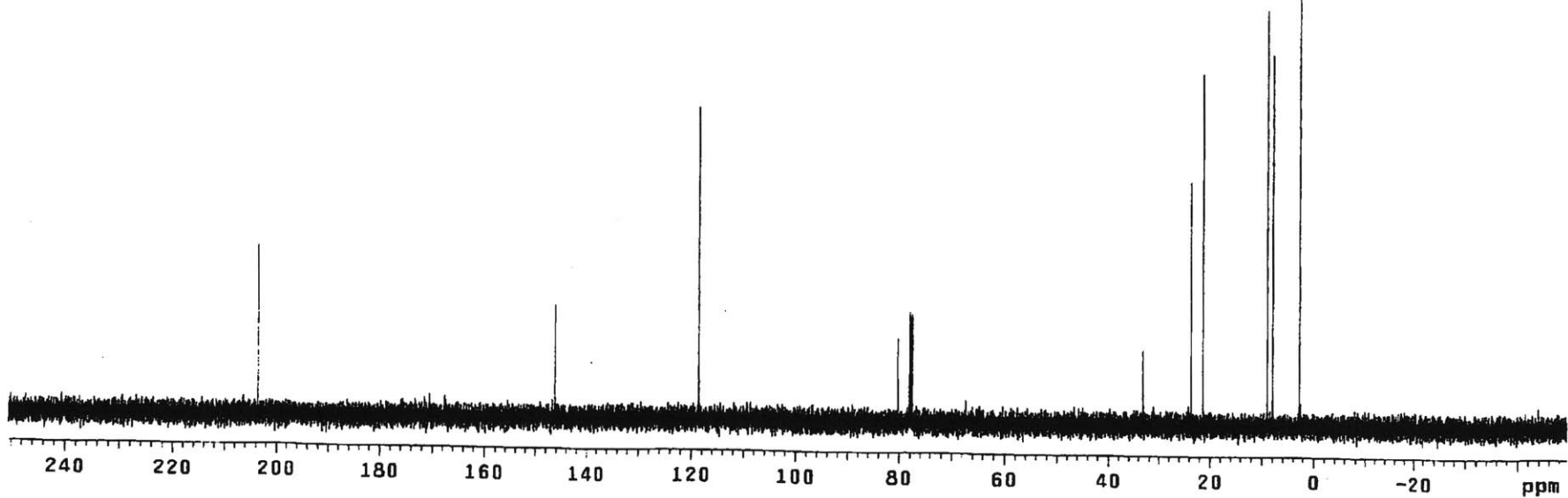
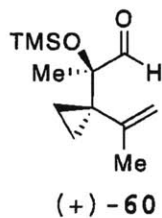


(+)-60

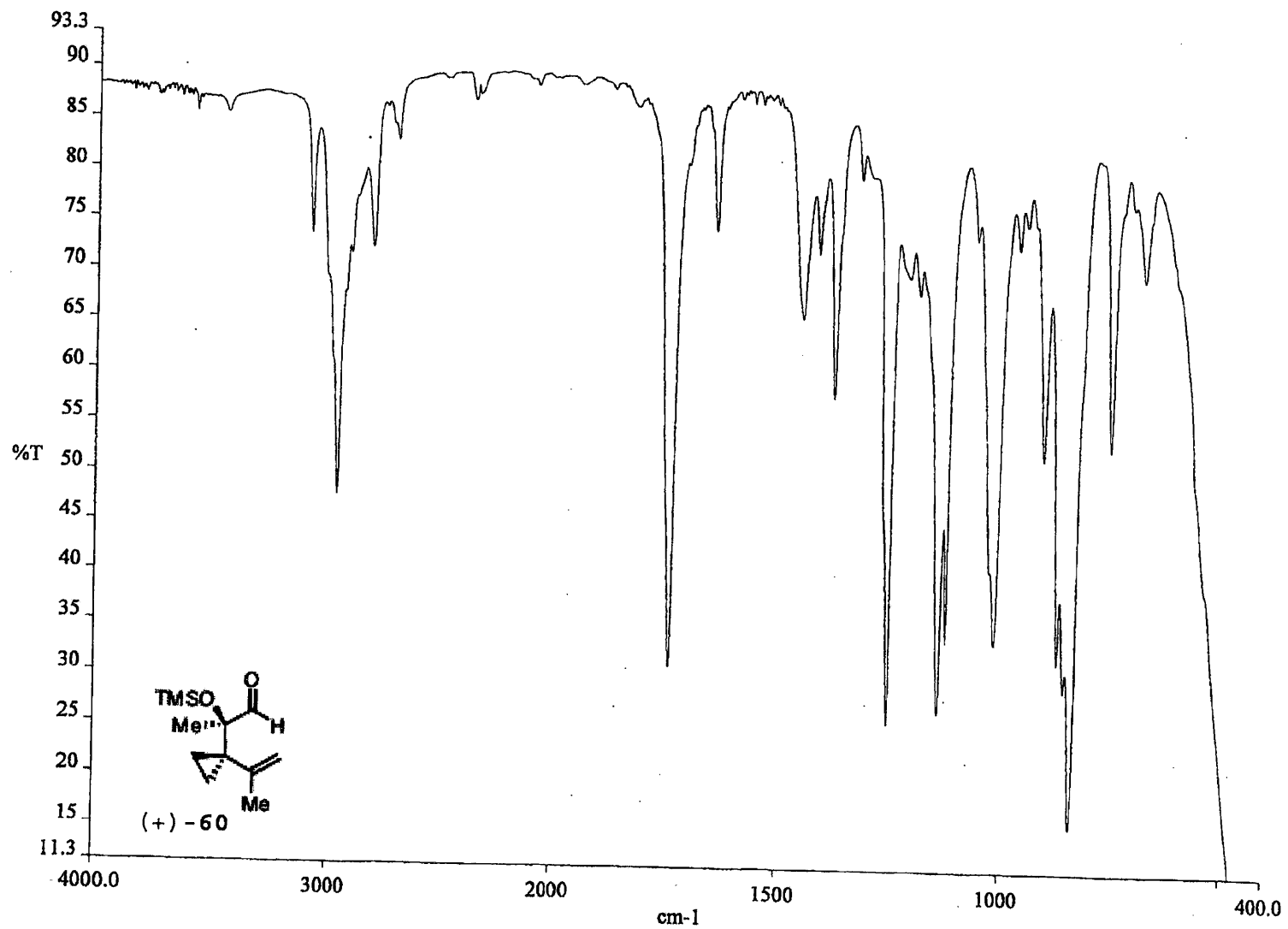


exp2 s2pu1

SAMPLE		DEC. & VT	
date	Nov 1 2005	dfrq	500.233
solvent	CDCl3	dn	H1
file	exp	dpwr	37
ACQUISITION			
sfrq	125.796	dot	-500.0
tn	C13	dm	y
at	1.736	dmm	w
np	131010	dsmf	10000
sw	37735.8	dseq	
fb	not used	dres	1.0
bs	4	homo	n
PROCESSING			
ss	1	lb	0.30
tpwr	53	wtfile	
pw	6.9	proc	ft
d1	0.763	fn	131072
tof	631.4	math	f
nt	1e+07		
ct	12	werr	
alock	not used	wexp	
gain	not used	wbs	
FLAGS		wnt	
il	n		
in	n		
dp	y		
hs	nn		
DISPLAY			
sp	-6225.8		
wp	37735.8		
vs	121		
sc	0		
wc	250		
hzmm	10.91		
is	500.00		
rfl	15911.8		
rfp	9686.0		
th	20		
ins	1.000		
al	ph		



170



exp60 s2pu1

DEC. & VT
dfrq 125.795
dn C13
dpwr 37
dof 0
dn nnn
dms c
dmf 10000
dseq
dres 1.0
homo n

ACQUISITION

sfrq 500.235
tn H1
at 3.200
np 64000
sw 10000.0
fb not used
bs 1
sc 1
tpwr 58
pw 8.8
d1 0
tof 1498.2
nt 16
ct 16
alock n
gain not used

PROCESSING

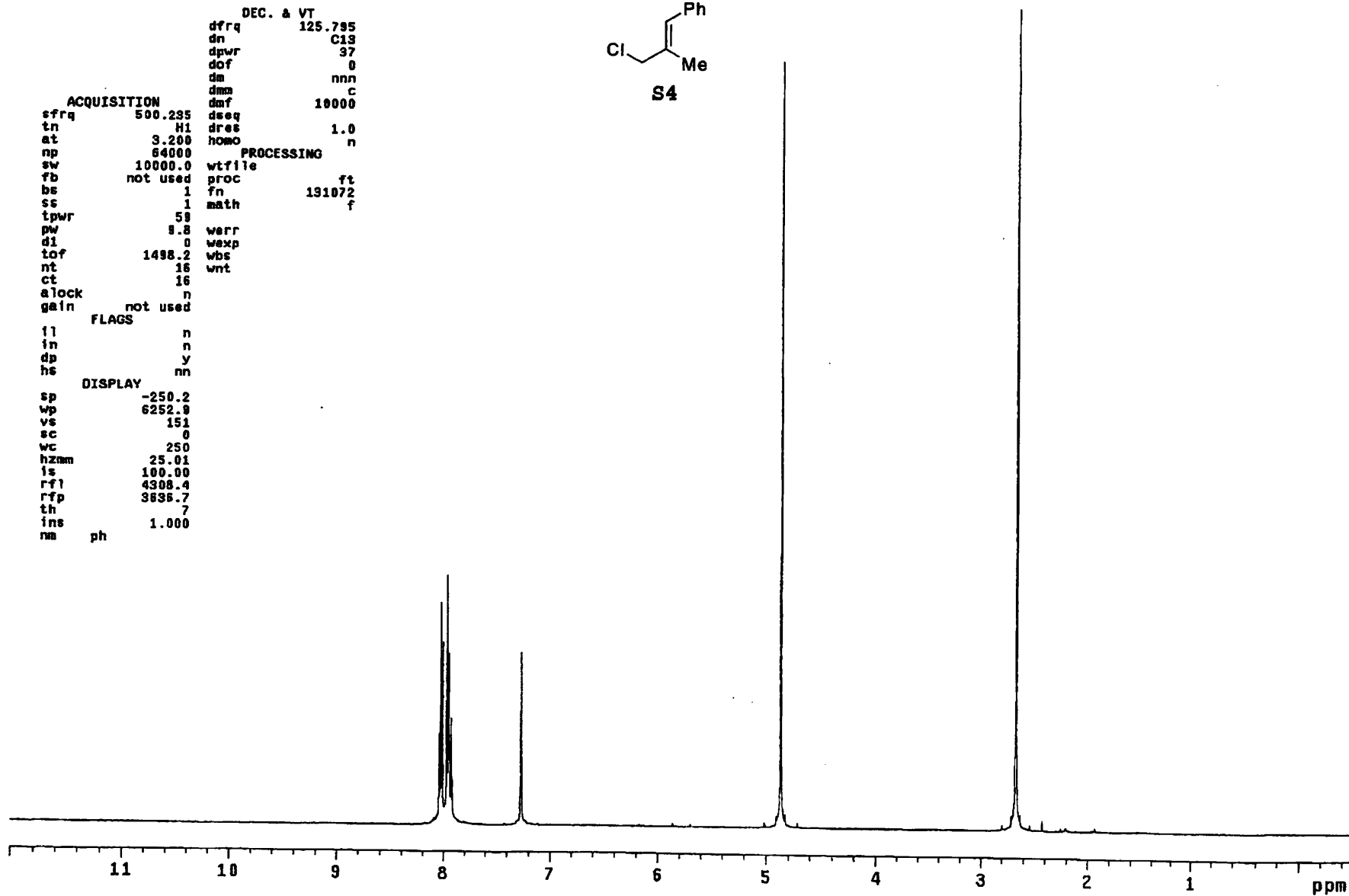
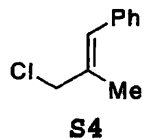
wtfile
proc ft
fn 191072
math f

FLAGS

fl n
in n
dp y
hs nn

DISPLAY

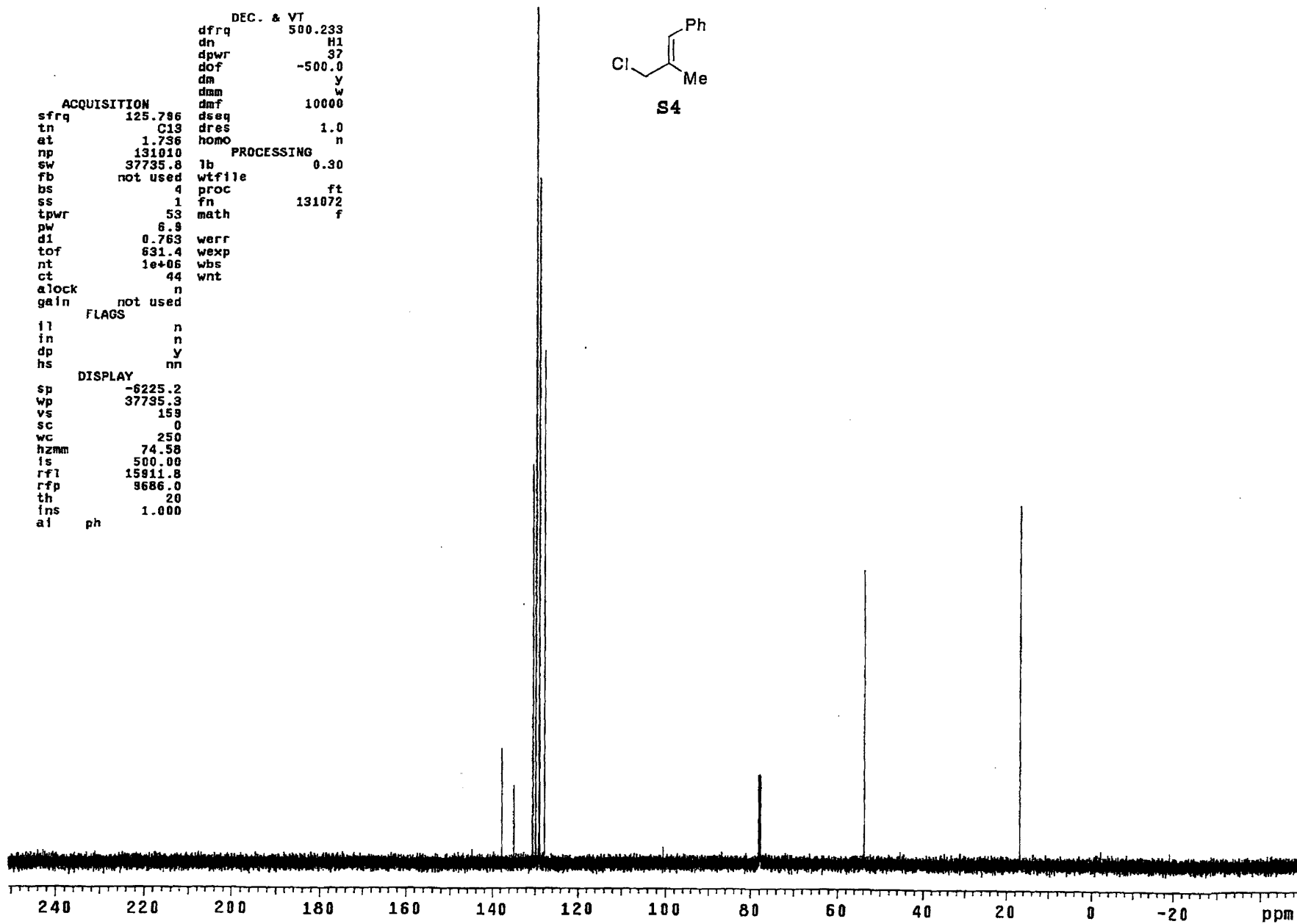
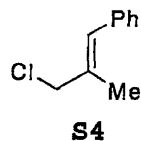
sp -250.2
wp 6252.9
vs 151
sc 0
wc 250
hznm 25.01
fs 100.00
rfl 4308.4
rfp 3636.7
th 7
ins 1.000
nm ph

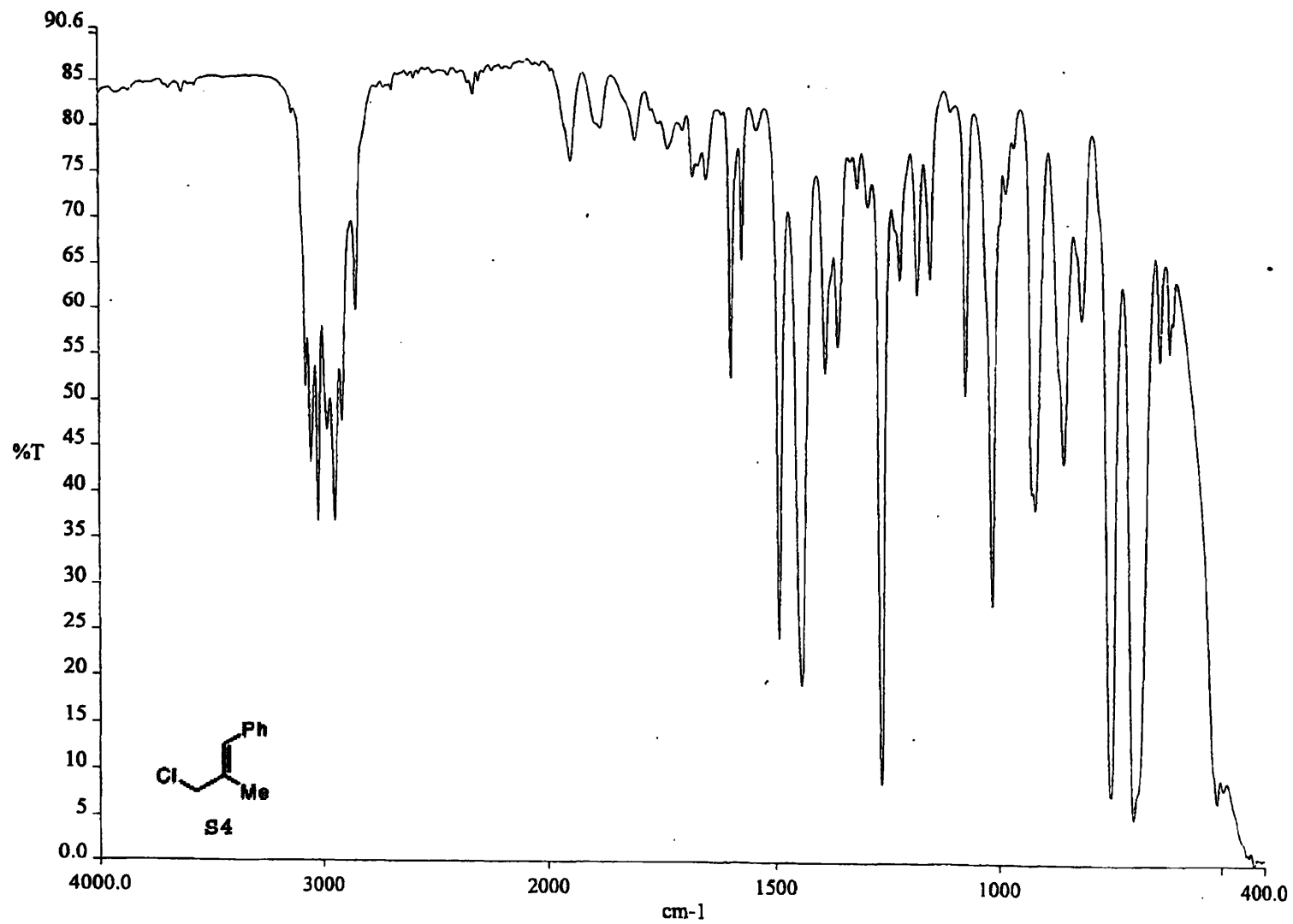


exp60 s2pu1

```
DEC. & VT
dfrq 500.233
dn H1
dpwr 37
dof -500.0
dm y
dmm w
dmf 10000
ACQUISITION
sfrq 125.786
tn C13
at 1.736
np 131010
sw 37735.8
fb not used
bs 4
ss 1
tpwr 53
pw 6.9
d1 0.763
tof 631.4
nt 1e+06
ct 44
alock n
gain not used
FLAGS
il n
in n
dp Y
hs nn
DISPLAY
sp -6225.2
wp 37735.3
vs 159
sc 0
wc 250
hzmm 74.58
ls 500.00
rfl 15911.8
rfp 9686.0
th 20
ins 1.000
al ph
```

```
PROCESSING
lb 0.30
wtfile
proc ft
fn 131072
math f
```





exp2 s2pul

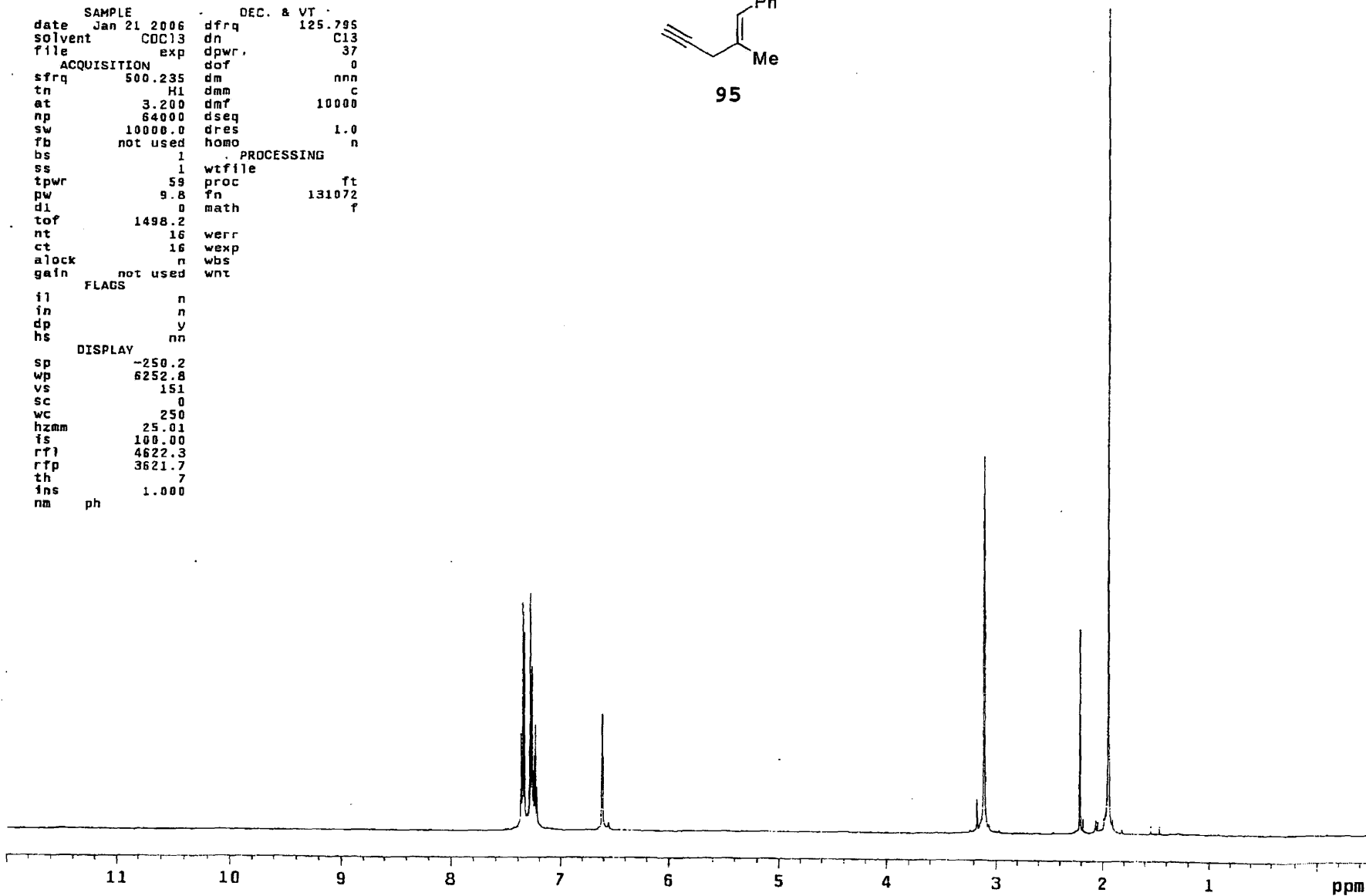
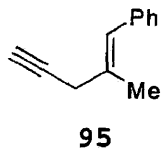
```

SAMPLE
date Jan 21 2006 dfrq 125.795
solvent CDCl3 dn C13
file exp dpwr 37
ACQUISITION dof 0
sfrq 500.235 dm nnn
tn H1 dmm c
at 3.200 dmf 10000
np 64000 dseq
sw 10000.0 dres 1.0
fb not used homo n
bs 1 . PROCESSING
ss 1 wtfile
tpwr 59 proc Ft
pw 9.8 fn 131072
dl 0 math f
tof 1498.2
nt 16 werr
ct 16 wexp
alock n wbs
gain not used wnt

FLAGS
il n
in n
dp y
hs nn

DISPLAY
sp -250.2
wp 6252.8
vs 151
sc 0
wc 250
hzmm 25.01
fs 100.00
rfi 4622.3
rfp 3621.7
th 7
fns 1.000
nm ph

```

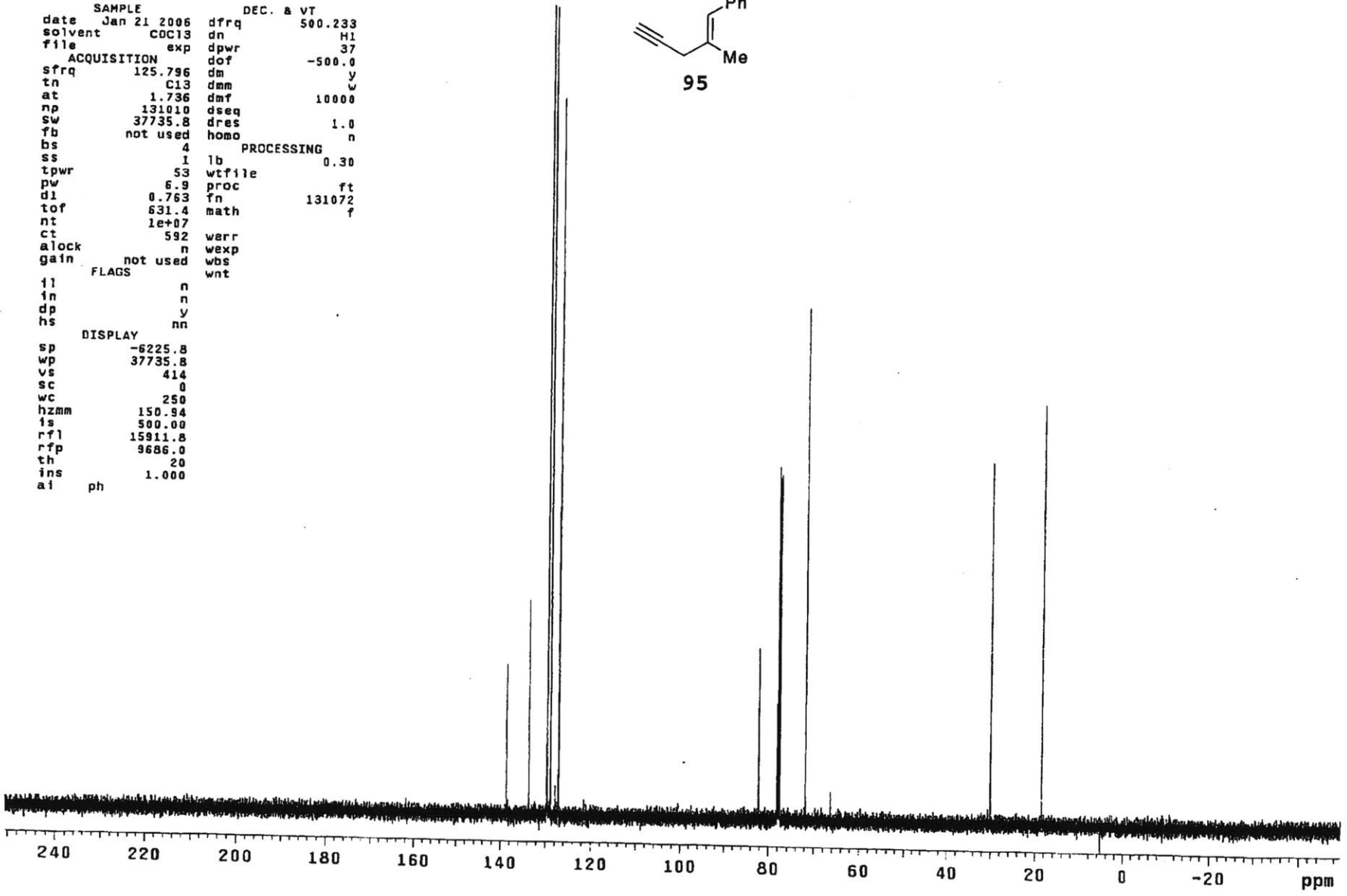
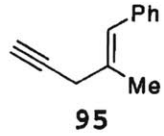


174

exp2 s2pu1

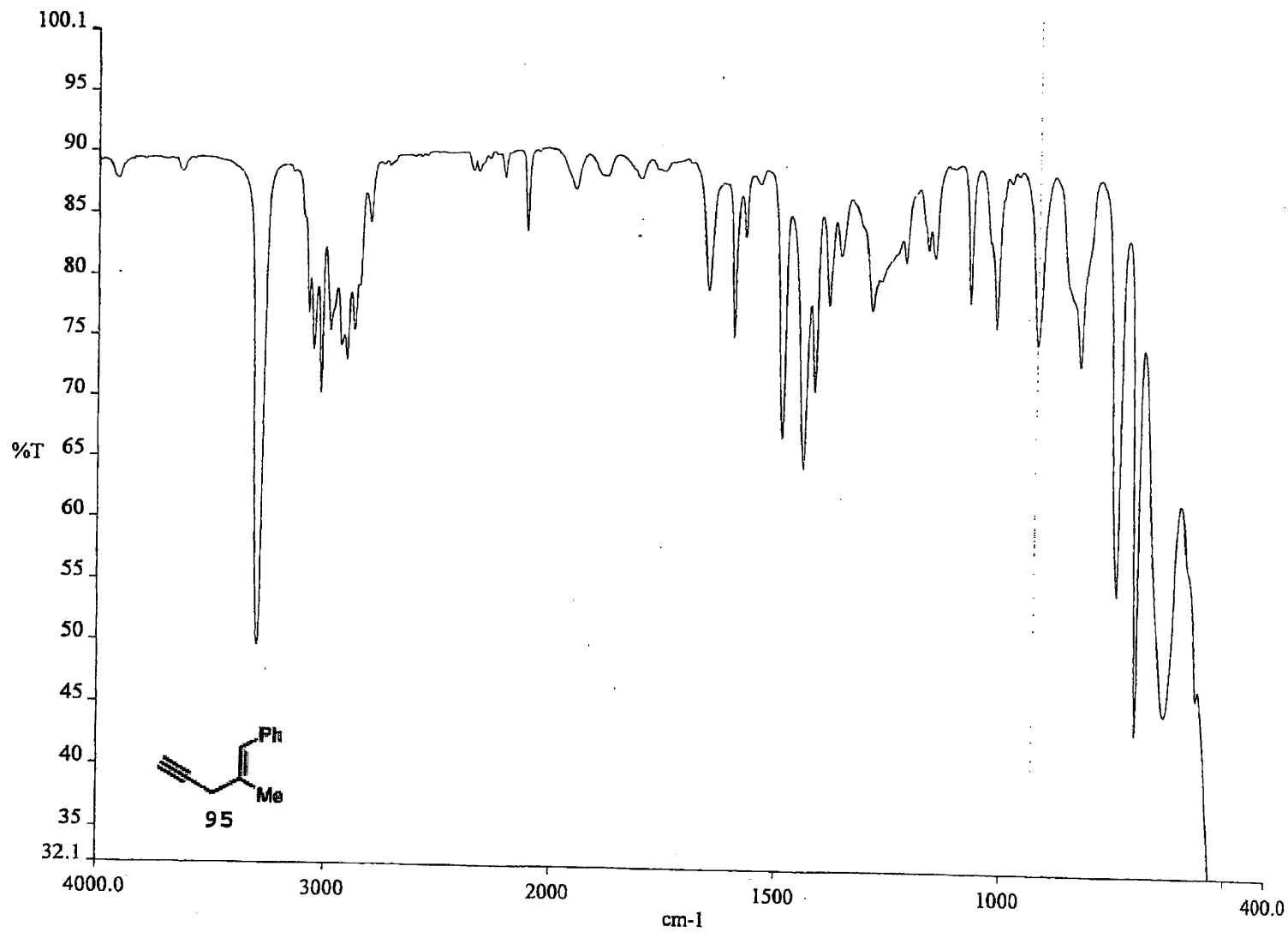
```
SAMPLE          DEC. & VT
date Jan 21 2006 dfrq      500.233
solvent COC13     dn        H1
file      exp     dpwr      37
ACQUISITION     dof      -500.0
sfrq      125.796 dm        y
tn         C13    dmm       w
at         1.736 dmf      10000
np         131010 dseq
sw         37735.8 dres      1.0
fb         not used homo      n
bs         4      PROCESSING
ss         1      lb        0.30
tpwr      53     wtfile
pw         6.9   proc
d1         0.763 fn        131072
tof        631.4 math
nt         1e+07
ct         592   warr
alock     n     wexp
gain     not used wbs
          FLAGS  wnt

          n
          n
          y
          nn
DISPLAY
sp        -6225.8
wp        37735.8
vs        414
sc         0
wc        250
hzmm      150.94
is        500.00
rfl       15911.8
rfp       9686.0
th         20
ins       1.000
al        ph
```



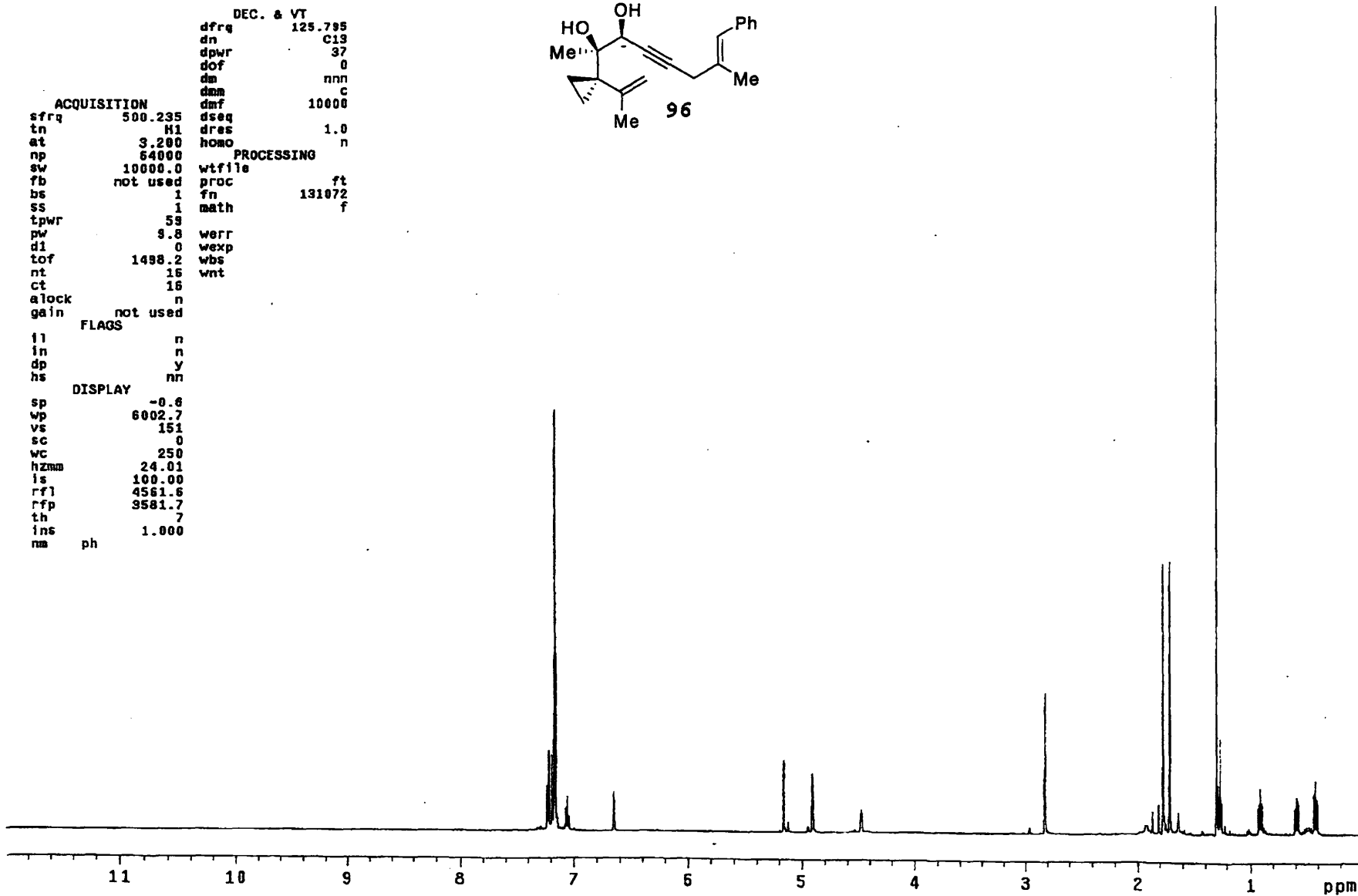
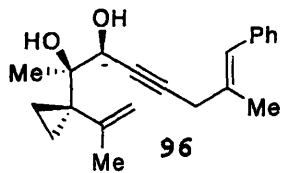
175

176



exp1 s2pu1

```
DEC. & VT
dfrq 125.795
dn C13
dpwr 37
dof 0
dm nnn
dmm c
dmf 10000
ACQUISITION
sfrq 500.235
tn H1
at 3.200
np 64000
sw 10000.0
fb not used
bs 1
ss 1
tpwr 59
pw 9.8
di 0
tof 1498.2
nt 16
ct 16
atlock n
gain not used
FLAGS
ll n
ln n
dp y
hs nn
DISPLAY
sp -0.8
wp 6002.7
vs 151
sc 0
wc 250
hzmm 24.01
ls 100.00
rfl 4561.6
rfp 9581.7
th 7
ins 1.000
nm ph
```



177

exp1 s2pu1

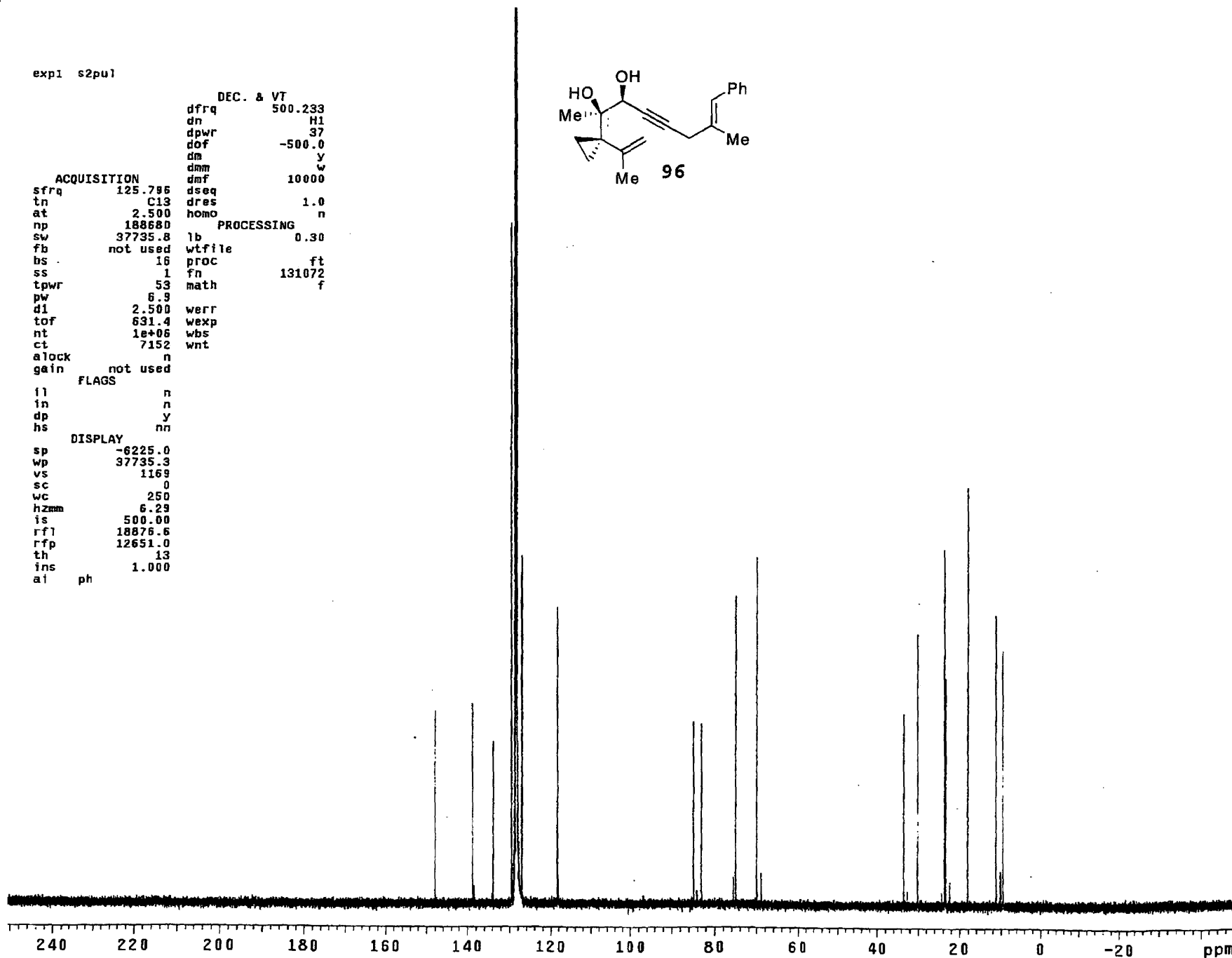
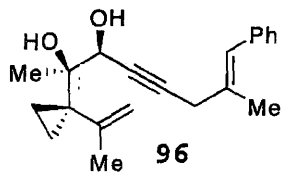
DEC. & VT
dfrq 500.233
dn H1
dpwr 37
dof -500.0
dm y
dmm w
dmf 10000

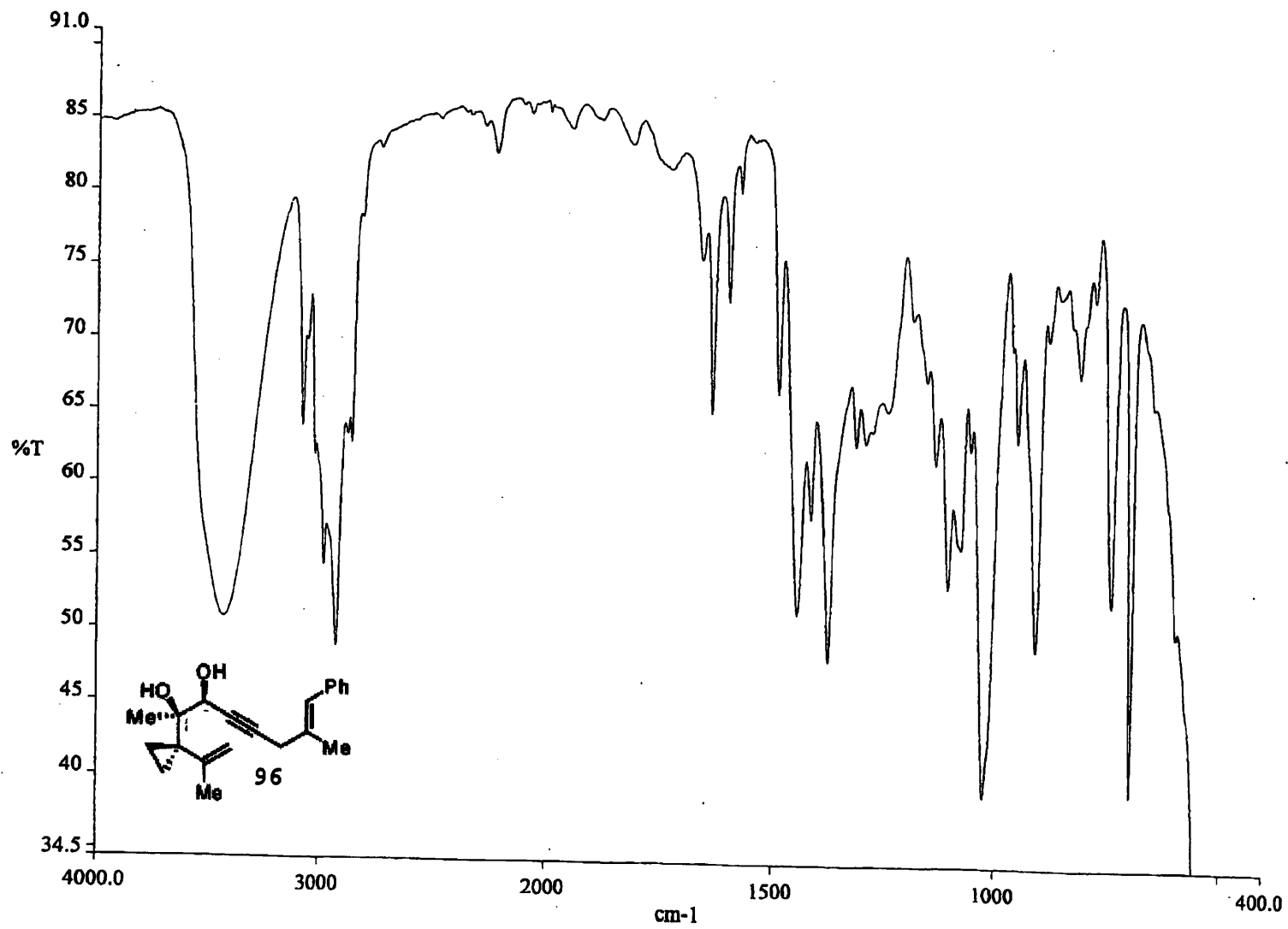
ACQUISITION
sfrq 125.796
tn C13
at 2.500
np 188680
sw 37735.8
fb not used
bs 16
ss 1
tpwr 53
pw 6.9
d1 2.500
tof 631.4
nt 1e+06
ct 7152
alock n
gain not used

PROCESSING
lb 0.30
wtfile
proc ft
fn 131072
math f

FLAGS
il n
in n
dp y
hs nn

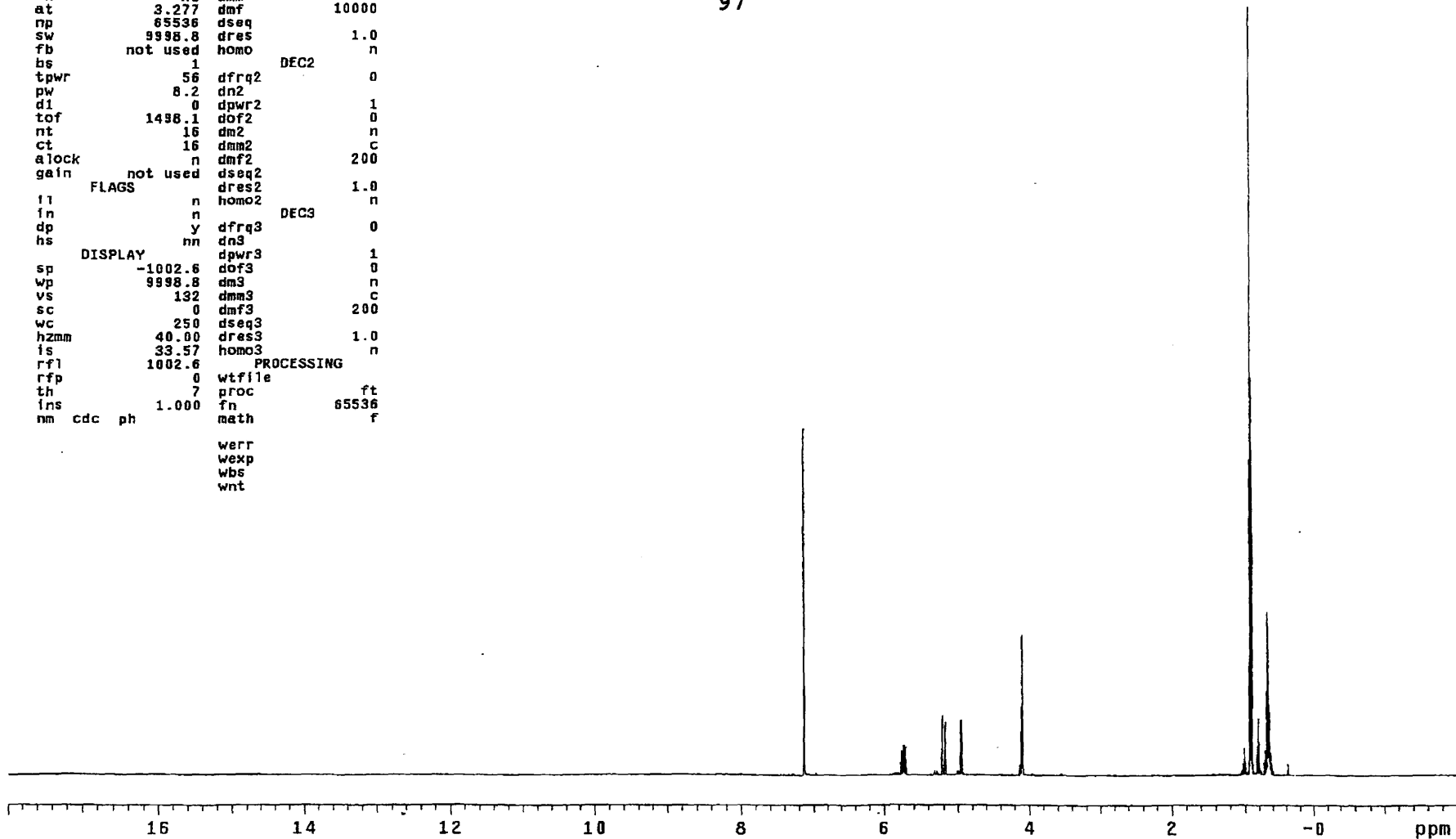
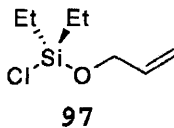
DISPLAY
sp -6225.0
wp 37735.3
vs 1169
sc 0
wc 250
hzmm 6.29
is 500.00
rfl 18876.6
rfp 12651.0
th 13
ins 1.000
ai ph





exp10 s2pu1

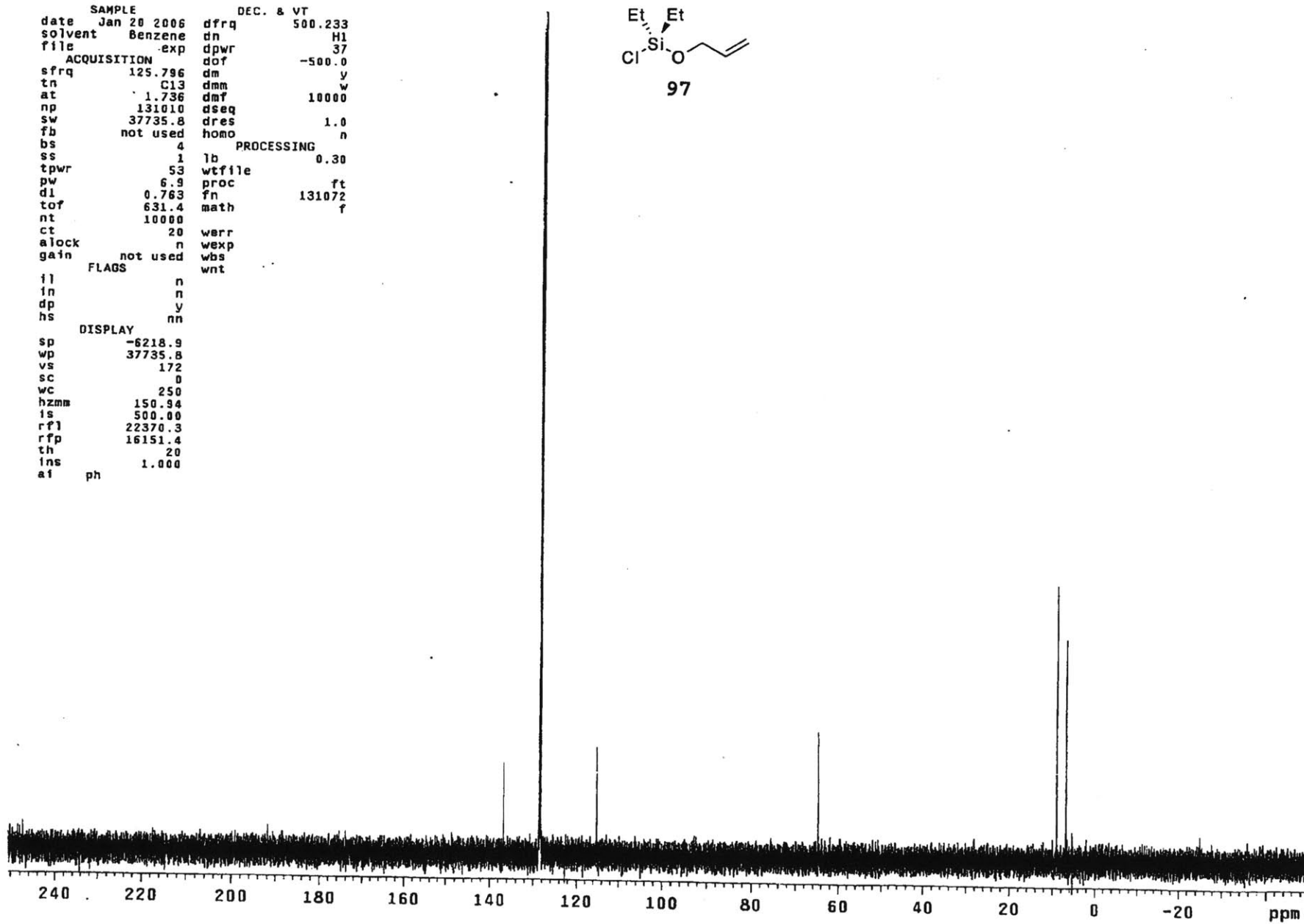
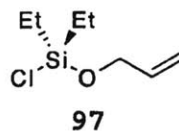
date	Oct 30 2005	dfrq	125.674
solvent	Benzene	dn	C13
file	exp	dpwr	34
ACQUISITION		dof	1498.1
sfrq	499.749	dm	nnn
tn	H1	dmm	w
at	3.277	dof	10000
np	65536	dseq	
sw	9998.8	dres	1.0
fb	not used	homo	n
bs	1	DEC2	
tpwr	56	dfrq2	0
pw	8.2	dn2	
d1	0	dpwr2	1
tof	1498.1	dof2	0
nt	16	dm2	n
ct	16	dmm2	c
alock	n	dof2	200
gain	not used	dseq2	
FLAGS		dres2	1.0
ii	n	homo2	n
in	n	DEC3	
dp	y	dfrq3	0
hs	nn	dn3	
DISPLAY		dpwr3	1
sp	-1002.6	dof3	0
wp	9998.8	dm3	n
vs	132	dmm3	c
sc	0	dof3	200
wc	250	dseq3	
hzmm	40.00	dres3	1.0
is	33.57	homo3	n
rfl	1002.6	PROCESSING	
rfp	0	wtfile	ft
th	7	proc	65536
ins	1.000	fn	f
nm	cdc ph	math	
		werr	
		wexp	
		wbs	
		wnt	



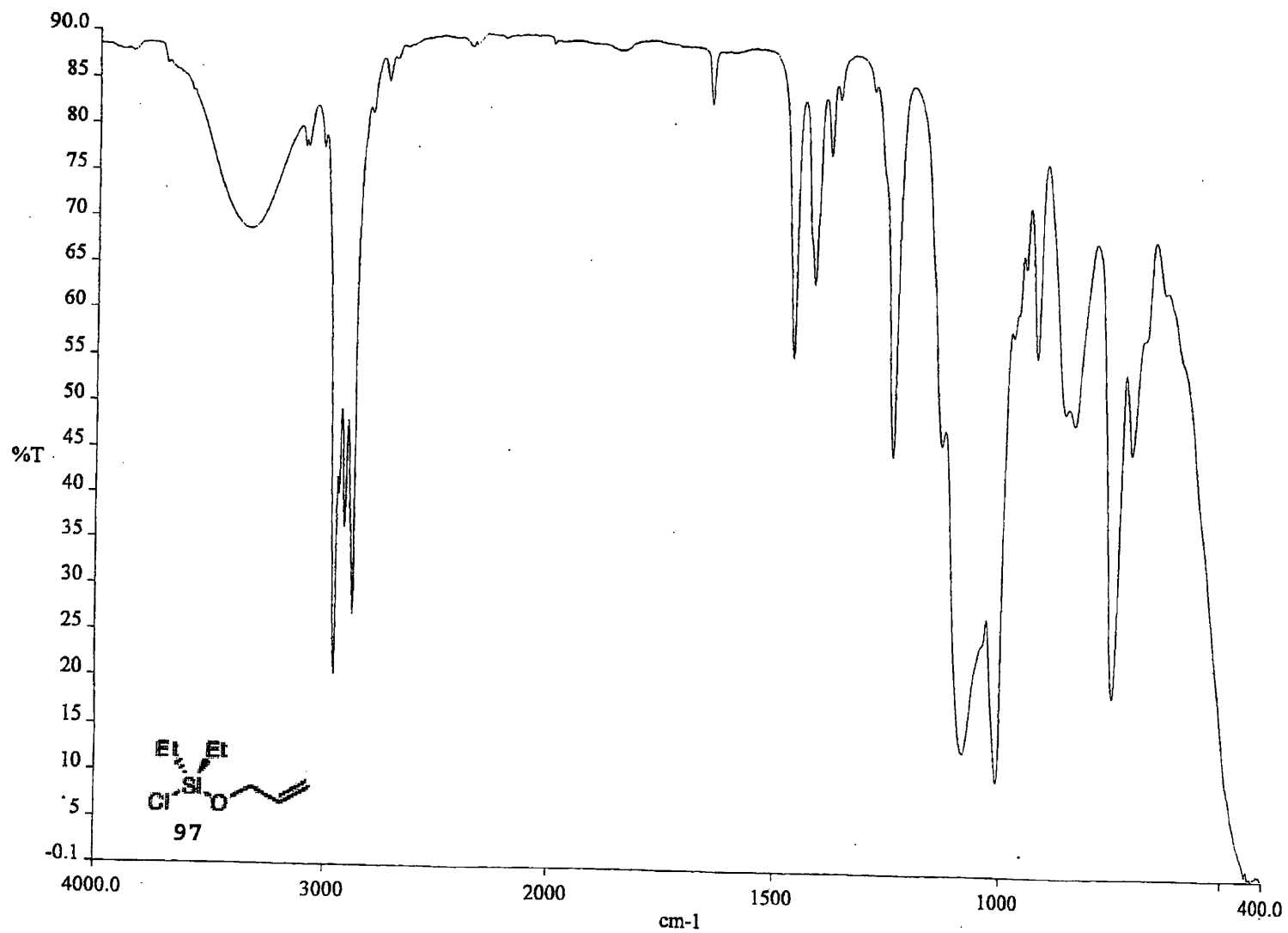
180

exp2 s2pu1

```
SAMPLE          DEC. & VT
date Jan 20 2006 dfrq 500.233
solvent Benzene  dn      H1
file          exp  dpwr   37
ACQUISITION    dof     -500.0
sfrq 125.796   dm      y
tn    C13      dmm     w
at    1.736    dmf     10000
np    131010   dseq
sw    37735.8 dres     1.0
fb    not used homo    n
bs    4        PROCESSING
ss    1        lb      0.30
tpwr  53      wtfile
pw    6.9     proc    ft
dl    0.763   fn      131072
tof   631.4   math    f
nt    10000
ct    20      werr
alock n        wexp
gain  not used wbs
      FLAGS    wnt
il    n
in    n
dp    y
hs    nn
DISPLAY
sp    -6218.9
wp    37735.8
vs    172
sc    0
wc    250
hzmm  150.94
is    500.00
rf1   22370.3
rfp   16151.4
th    20
ins   1.000
a1    ph
```

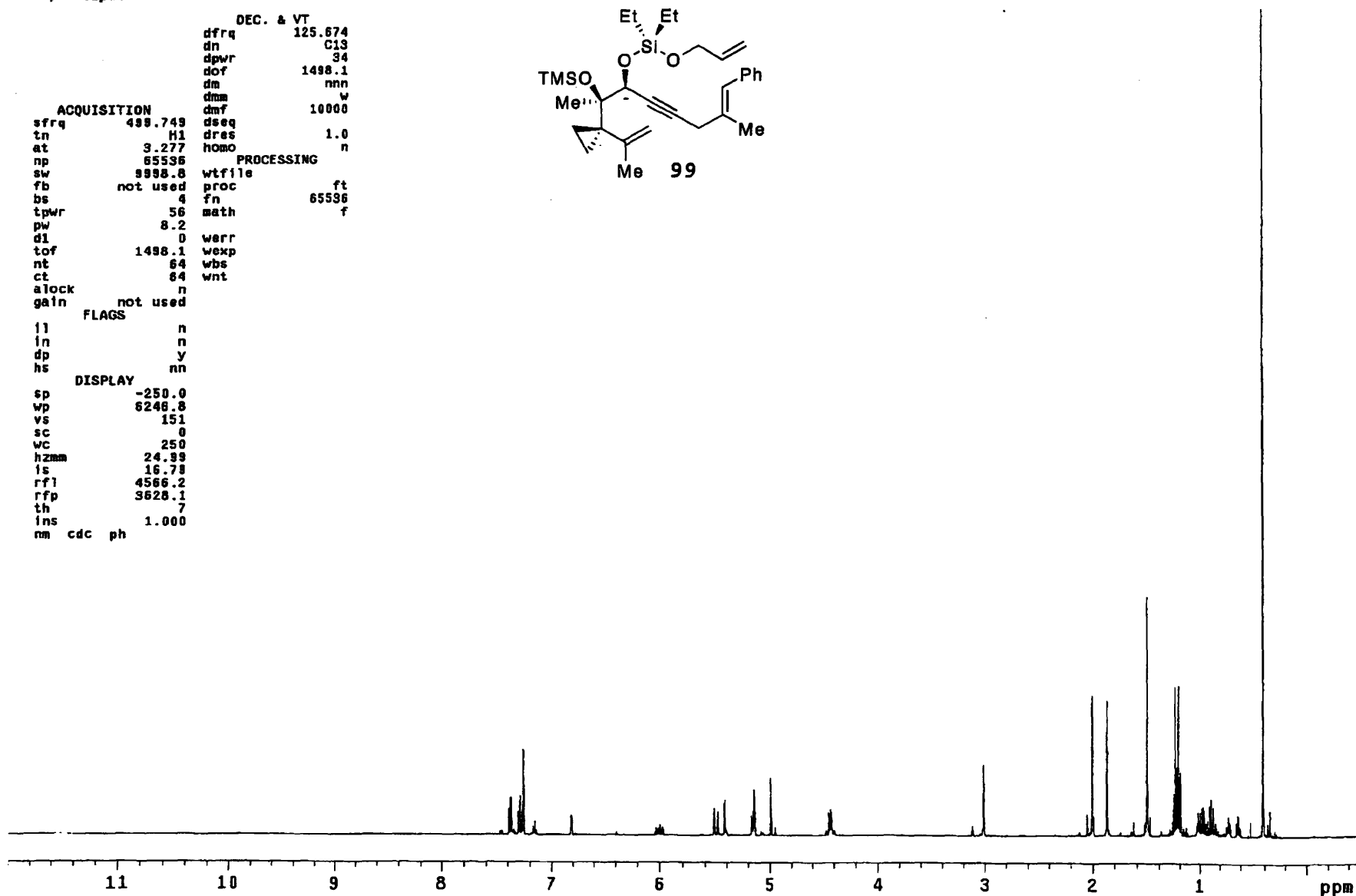
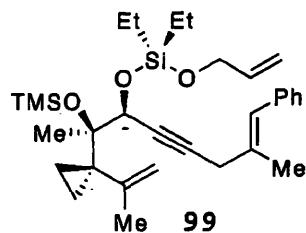


181



exp1 s2pu1

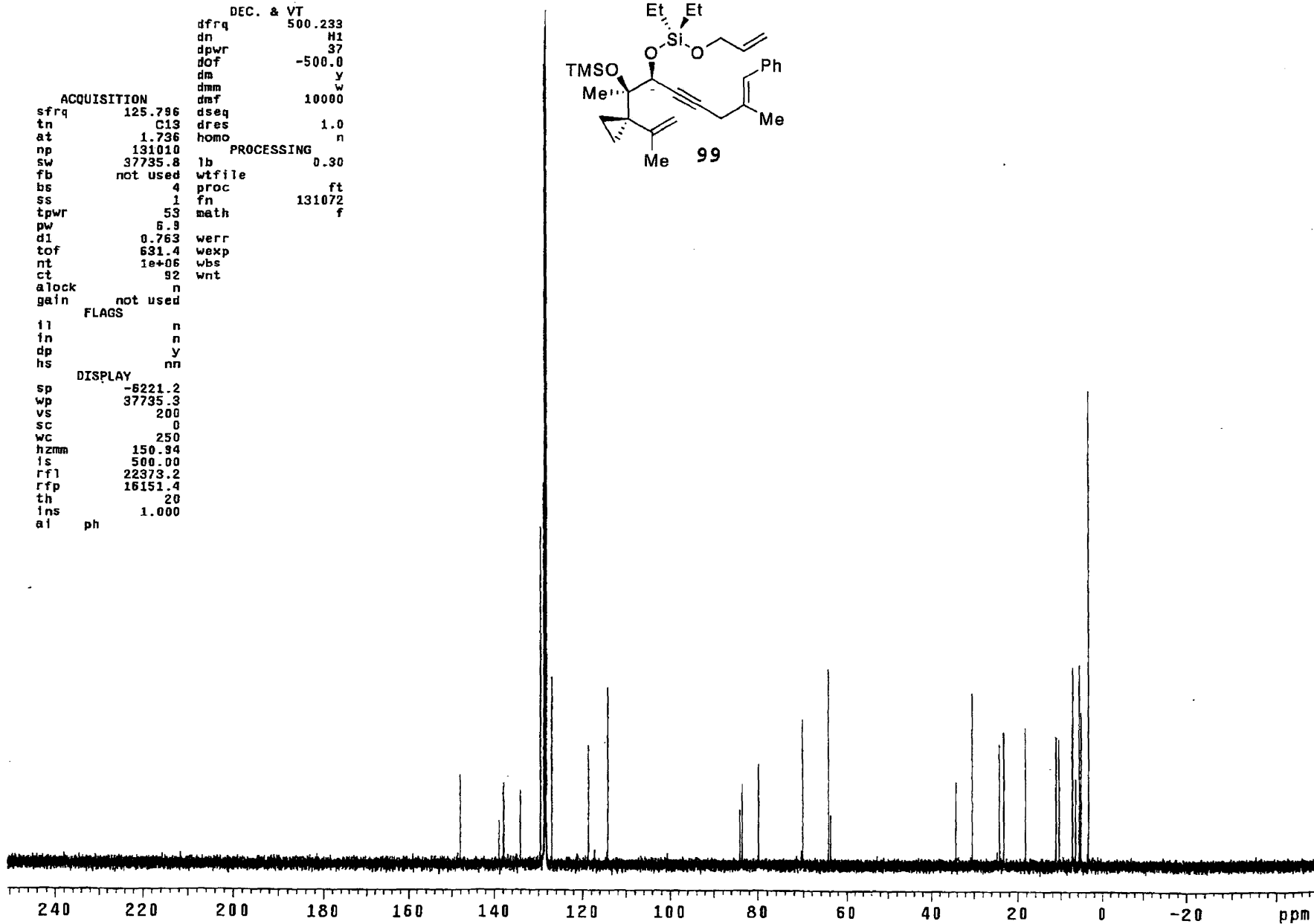
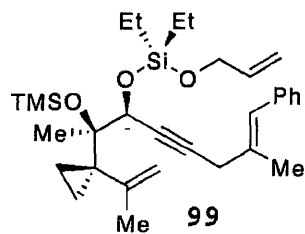
```
DEC. & VT
dfrq 125.674
dn C13
dpwr 34
dof 1498.1
dm nnn
dmm w
dmf 10000
dseq 1.0
dres n
homo n
PROCESSING
wtfile ft
proc 65596
fn f
math f
werr
wexp
wbs
wnt
ACQUISITION
sfrq 499.749
tn H1
at 3.277
np 65596
sw 9998.8
fb not used
bs 4
tpwr 56
pw 8.2
dl 0
tof 1498.1
nt 64
ct 64
alock n
gain not used
FLAGS
ll n
in n
dp y
hs nn
DISPLAY
sp -250.0
wp 6246.8
vs 151
sc 0
wc 250
hzmm 24.99
is 16.79
rf1 4566.2
rfp 3626.1
th 7
ins 1.000
nm cdc ph
```

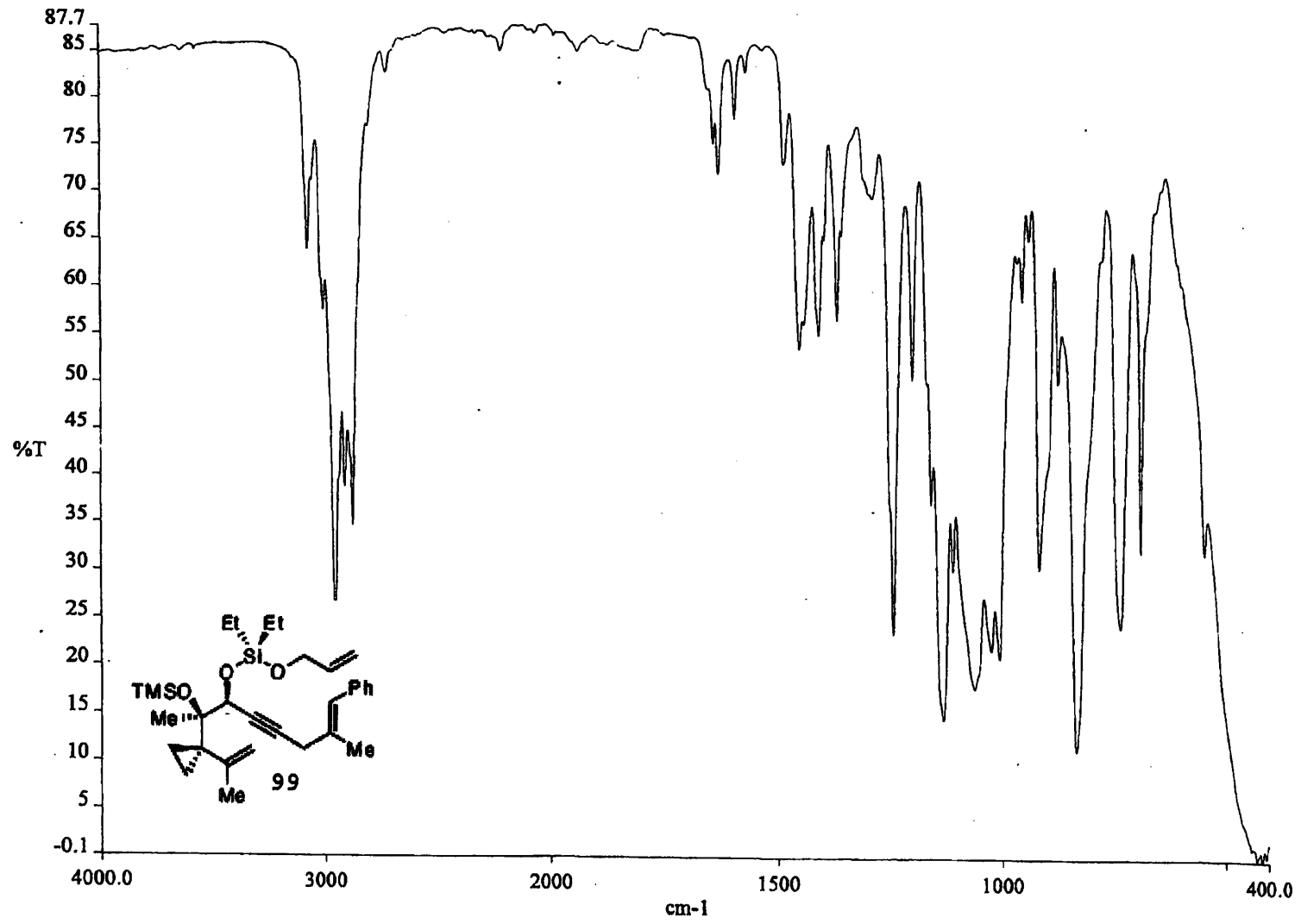


exp1 s2pu1

```
DEC. & VT
dfrq 500.233
dn H1
dpwr 37
dof -500.0
dm y
dmm w
dmf 10000
ACQUISITION
sfrq 125.796
tn C13
at 1.736
np 131010
sw 37735.8
fb not used
bs 4
ss 1
tpwr 53
pw 5.9
d1 0.763
tof 631.4
nt 1e+06
ct 92
alock n
gain not used
FLAGS
il n
in n
dp y
hs nn
DISPLAY
sp -6221.2
wp 37735.3
vs 200
sc 0
wc 250
hzmm 150.94
is 500.00
rfl 22373.2
rfp 16151.4
th 20
ins 1.000
ai ph
```

```
PROCESSING
lb 0.30
wtfile
proc ft
fn 131072
math f
werr
wexp
wbs
wnt
```





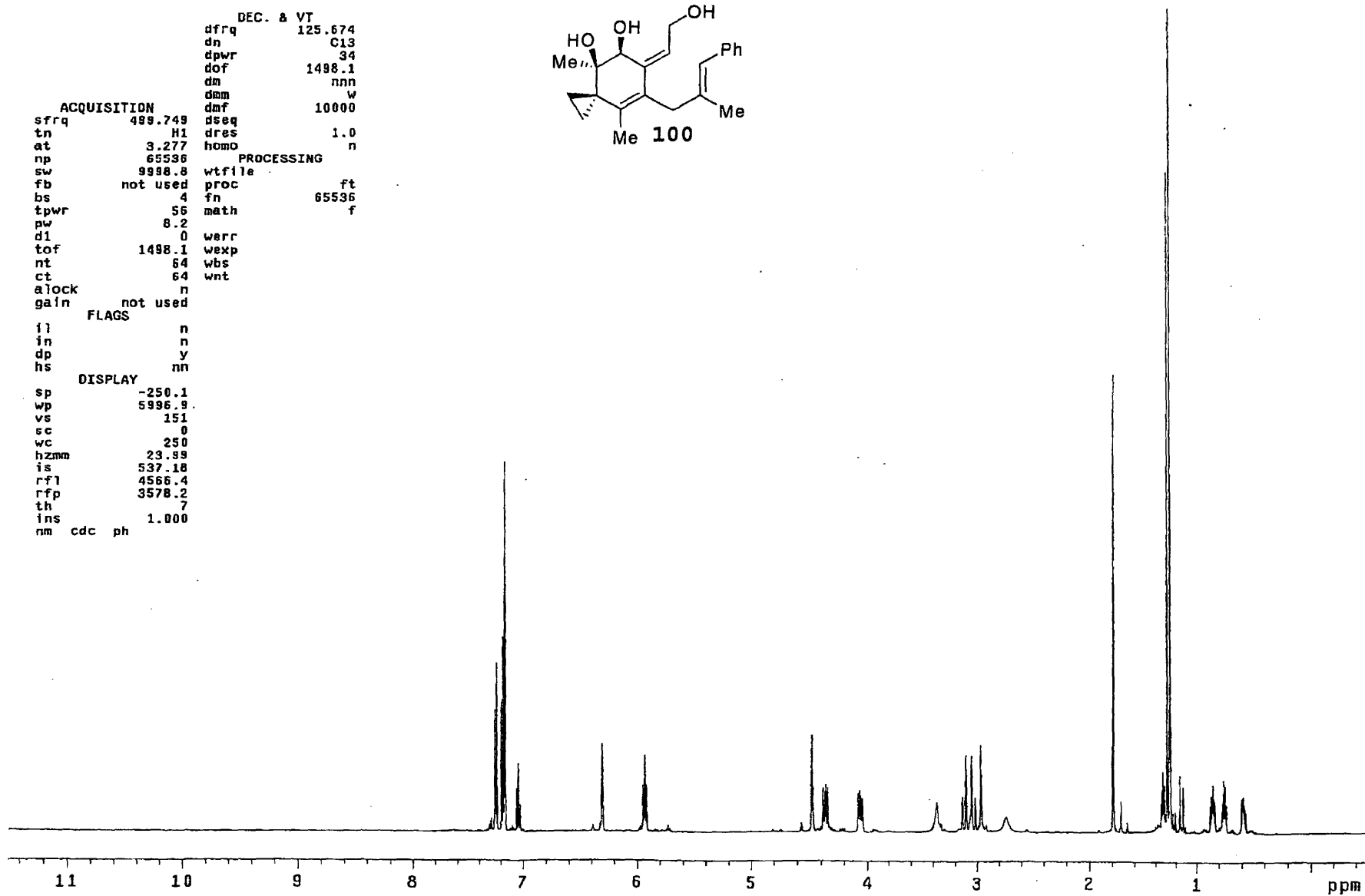
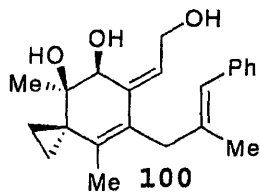
exp1 s2pu1

DEC. & VT
dfrq 125.674
dn C13
dpwr 34
dof 1498.1
dm nnn
dmm w
dmf 10000
dsbg
tn H1 dres 1.0
at 3.277 homo n

ACQUISITION
sfrq 489.749 dsbg
tn H1 dres 1.0
at 3.277 homo n
np 65536
sw 9998.8 wfile
fb not used proc ft
bs 4 fn 65536
tpwr 56 math f
pw 8.2
d1 0 werr
tof 1498.1 wexp
nt 64 wbs
ct 64 wnt
alock n
gain not used

PROCESSING
wfile
proc ft
fn 65536
math f
werr
wexp
wbs
wnt

FLAGS
il n
in n
dp y
hs nn
DISPLAY
sp -250.1
wp 5996.9
vs 151
sc 0
wc 250
hzmm 23.99
is 537.18
rf1 4566.4
rfp 3578.2
th 7
ins 1.000
nm cdc ph



exp1 s2pu1

DEC. & VT

dfreq 500.233
dn H1
dpwr 37
dof -500.0
dm y
dmm w
dmf 10000

ACQUISITION

sfrq 125.786
in C13
at 1.736
np 131010
sw 37735.8
fb not used
bs 4
ss 1
tpwr 53
pw 6.9
d1 0.763
tof 631.4
nt 1e+06
ct 372
alock n
gain not used

PROCESSING

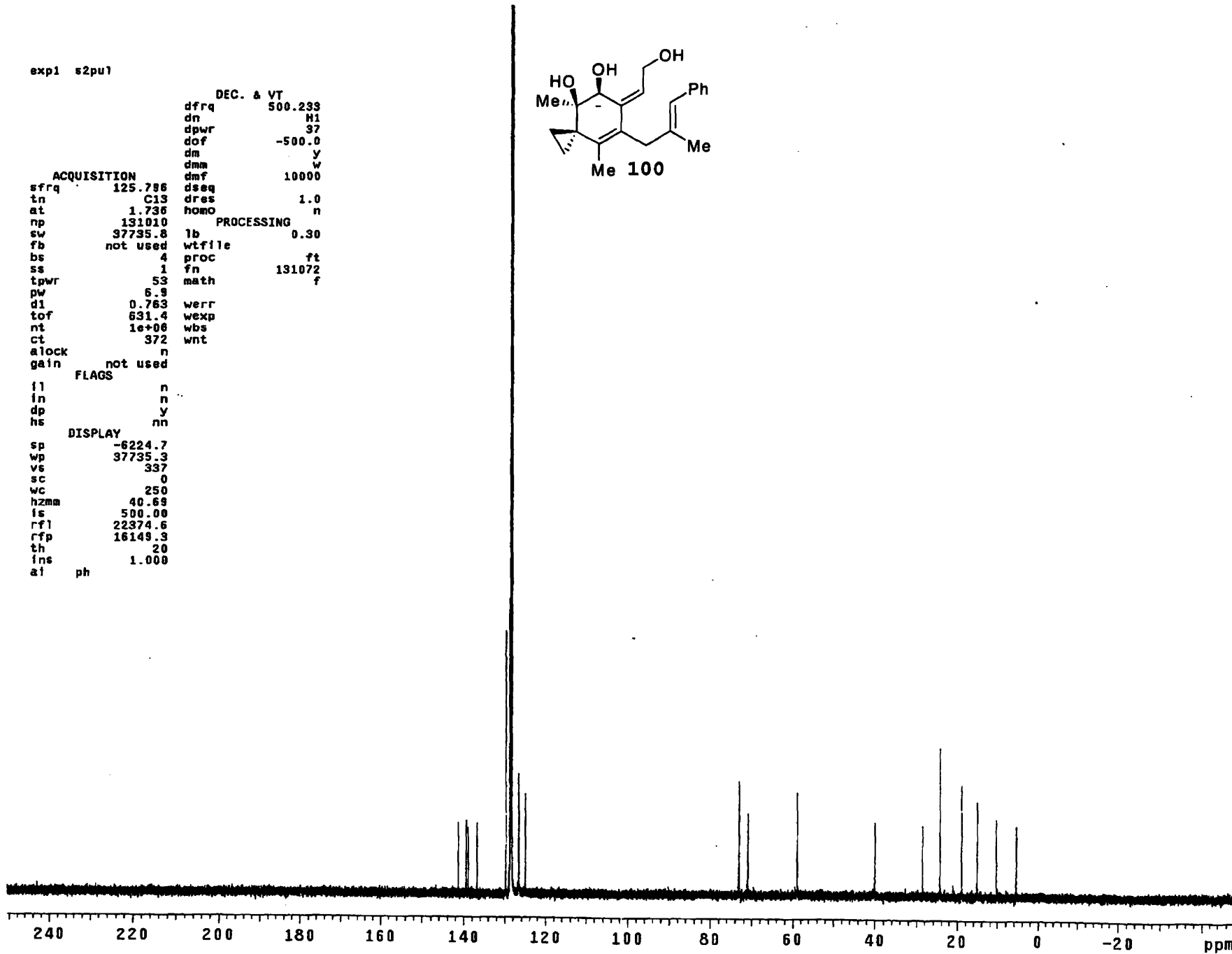
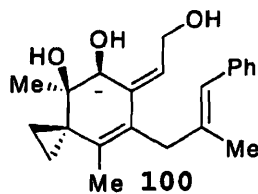
lb 0.30
wtfile
proc ft
fn 131072
math f

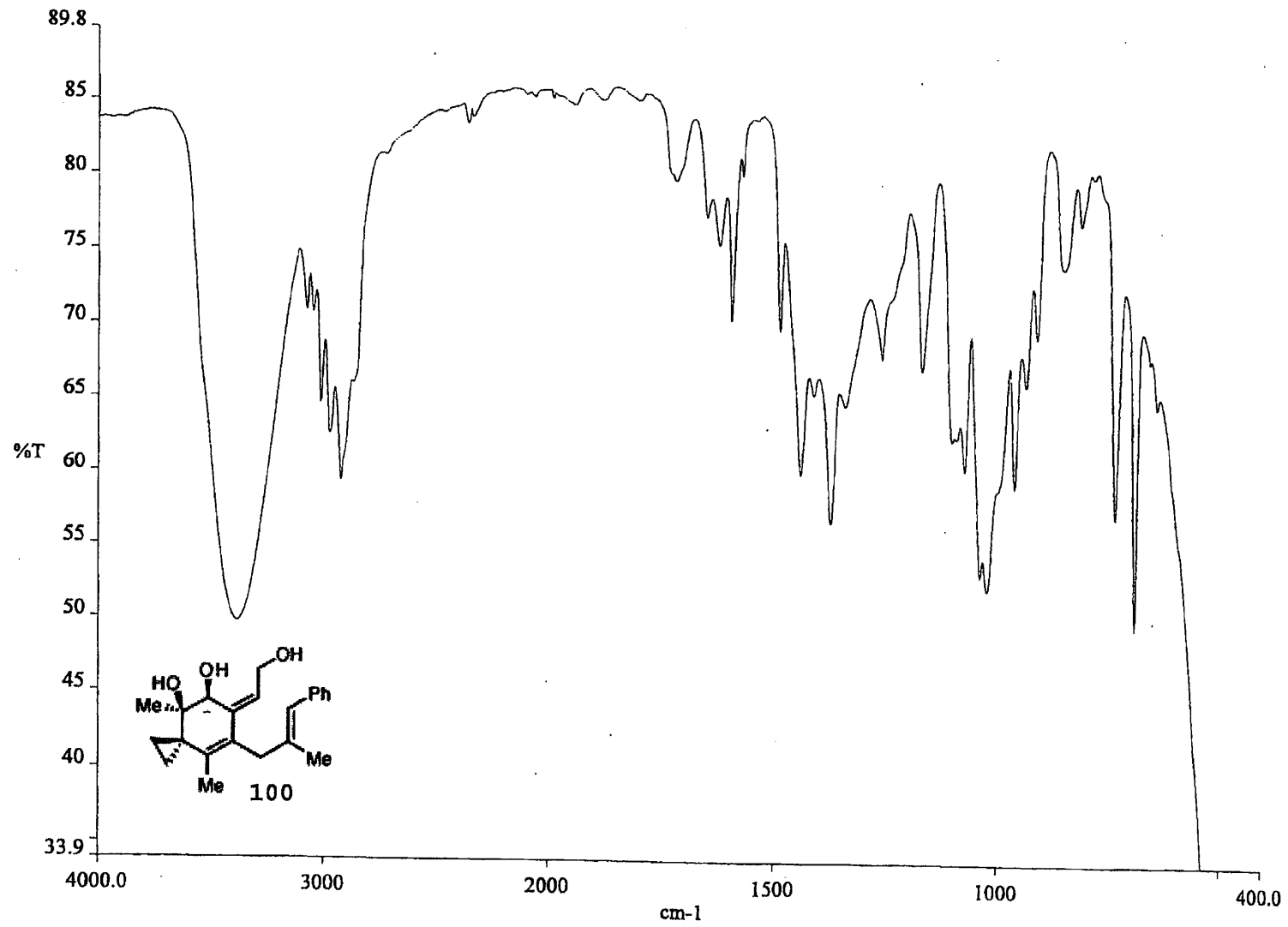
FLAGS

fl n
in n
dp y
hs nn

DISPLAY

sp -6224.7
wp 37735.3
vs 337
sc 0
wc 250
hzmm 40.69
fs 500.00
rfl 22374.6
rfp 16149.3
th 20
ins 1.000
at ph





exp1 s2pu1

DEC. & VT
dfrq 125.785
dn C13
dpwr 97
dof 0
dm nnn
dmm c
dmf 10000
dseq
dres 1.0
homo n

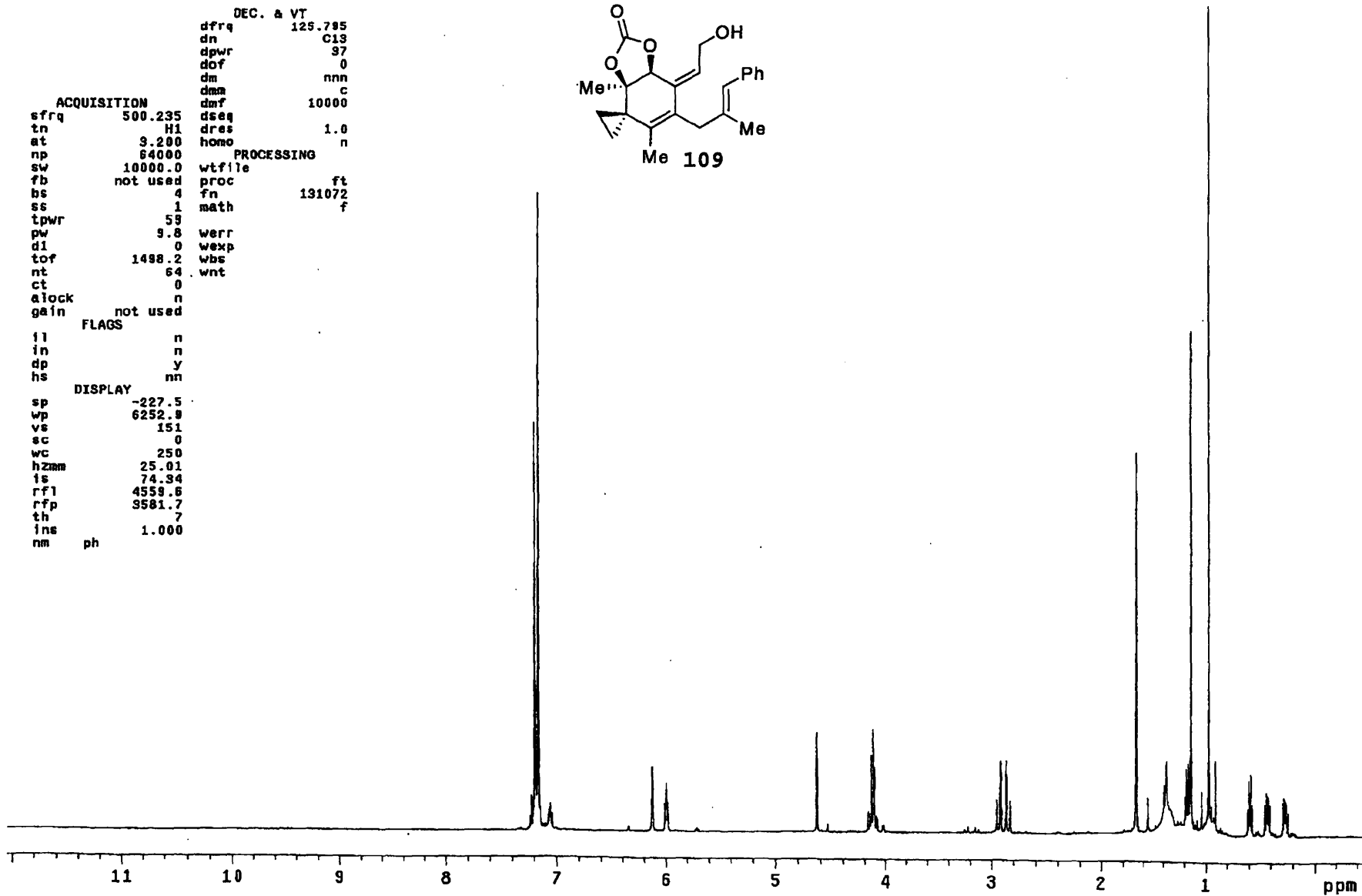
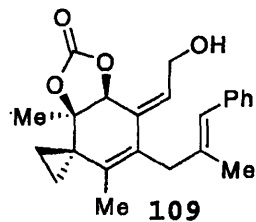
ACQUISITION

sfrq 500.235
tn H1
at 3.200
np 64000
sw 10000.0
fb not used
bs 4
ss 1
tpwr 59
pw 9.8
d1 0
tof 1498.2
nt 64
ct 0
alock n
gain not used

PROCESSING
wtfile
proc ft
fn 131072
math f

FLAGS
fl n
in n
dp y
hs nn

DISPLAY
sp -227.5
wp 6252.9
vs 151
sc 0
wc 250
hzm 25.01
ts 74.34
rf1 4559.6
rfp 3581.7
th 7
ins 1.000
nm ph



exp1 s2pu1

DEC. & VT

dfrq 500.233
dn H1
dpwr 37
dof -500.0
dm y
dmm w
dmf 10000
dseq
dn C13
dres 1.0
homo n

ACQUISITION

sfrq 125.796
tn
at 1.736
np 131010
sw 37735.8
fb not used
bs 4
ss 1
tpwr 53
pw 6.8
d1 0.763
tof 631.4
nt 1e+06
ct 0
alock n
gain not used

PROCESSING

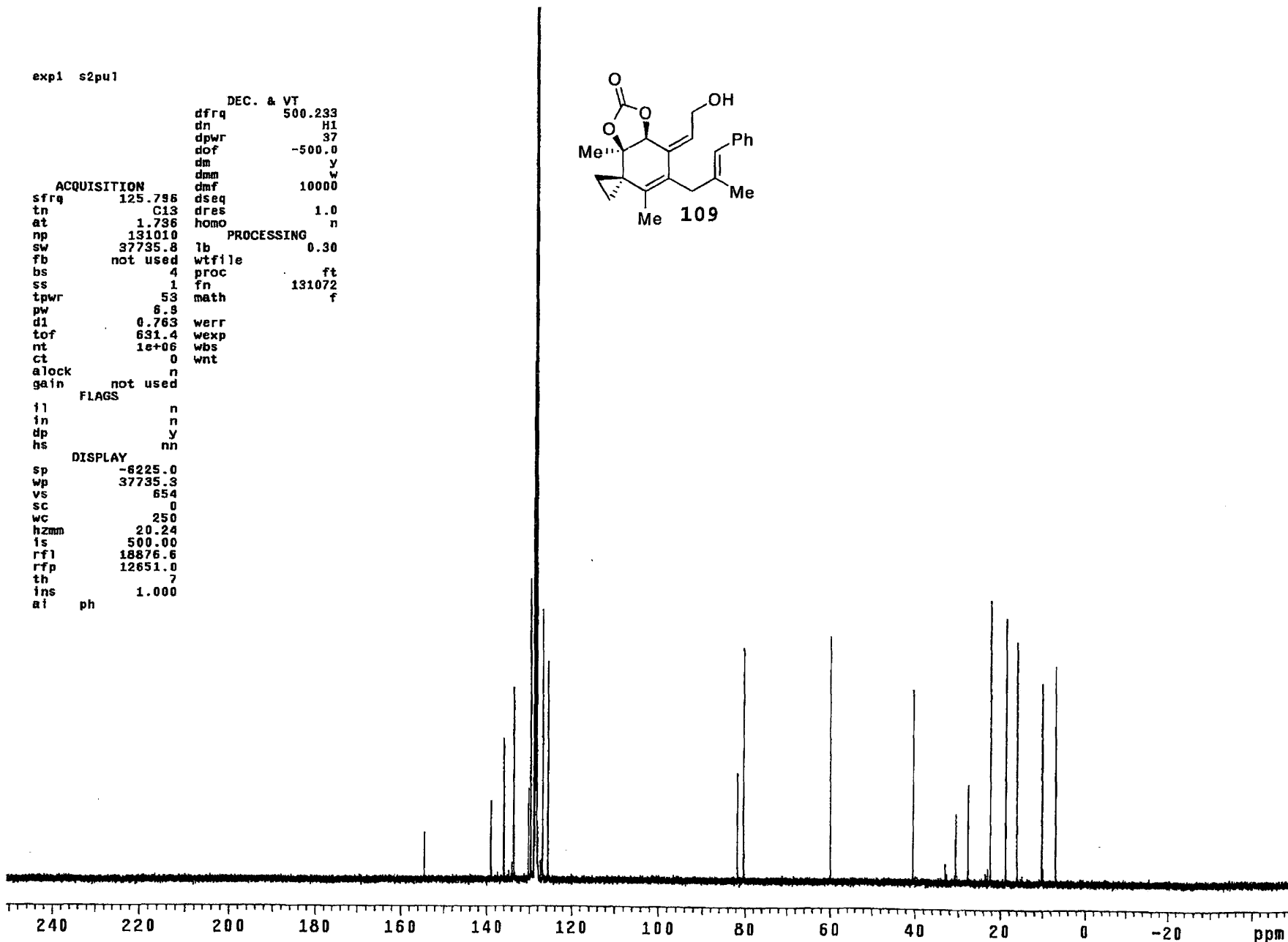
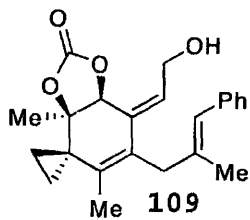
lb 0.30
wtfile
proc ft
fn 131072
math f
werr
wexp
wbs
wnt

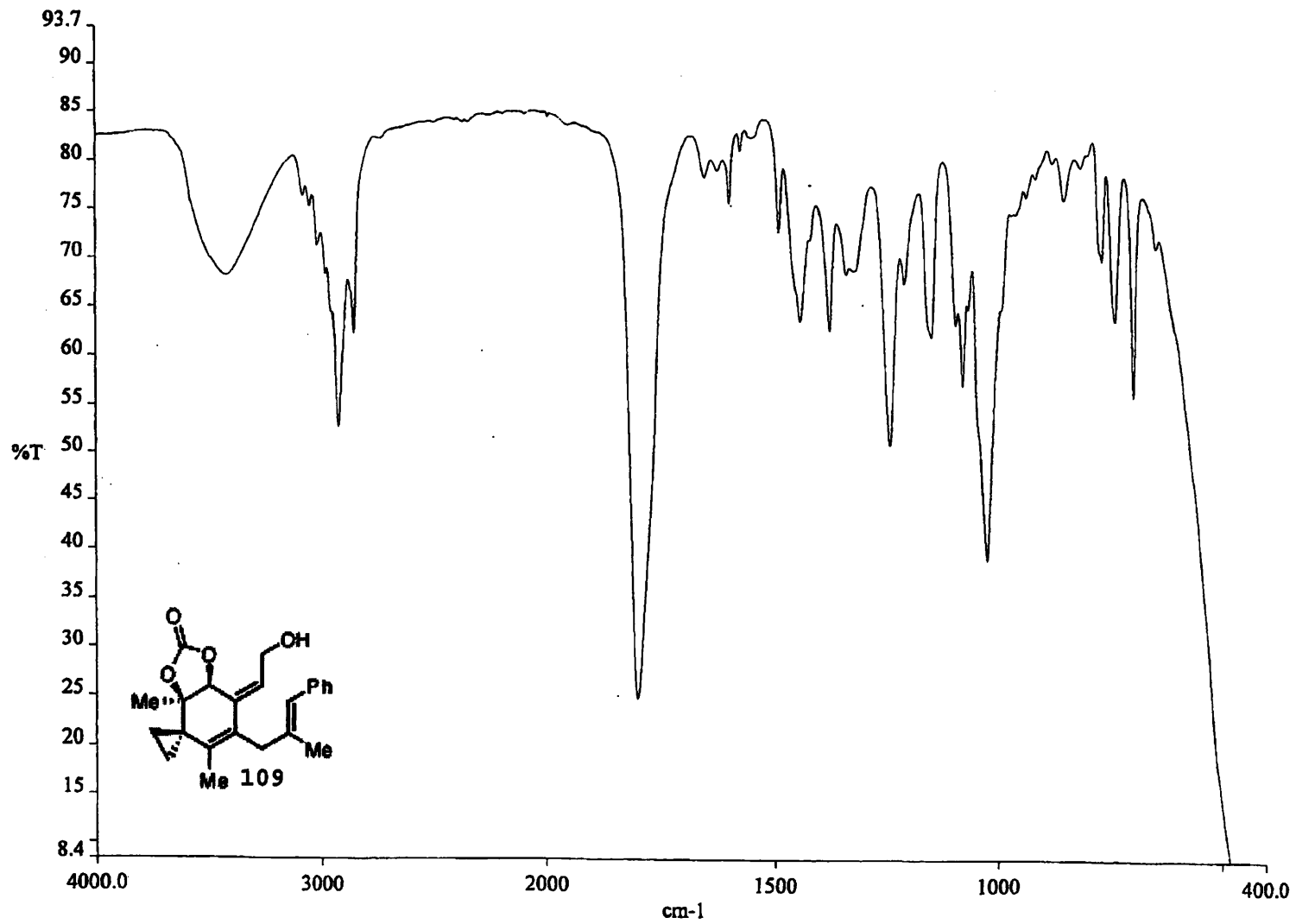
FLAGS

fl n
in n
dp y
hs nn

DISPLAY

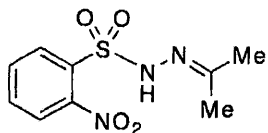
sp -6225.0
wp 37735.3
vs 654
sc 0
wc 250
hzmm 20.24
is 500.00
rfl 18876.6
rfp 12651.0
th 7
ins 1.000
ai ph



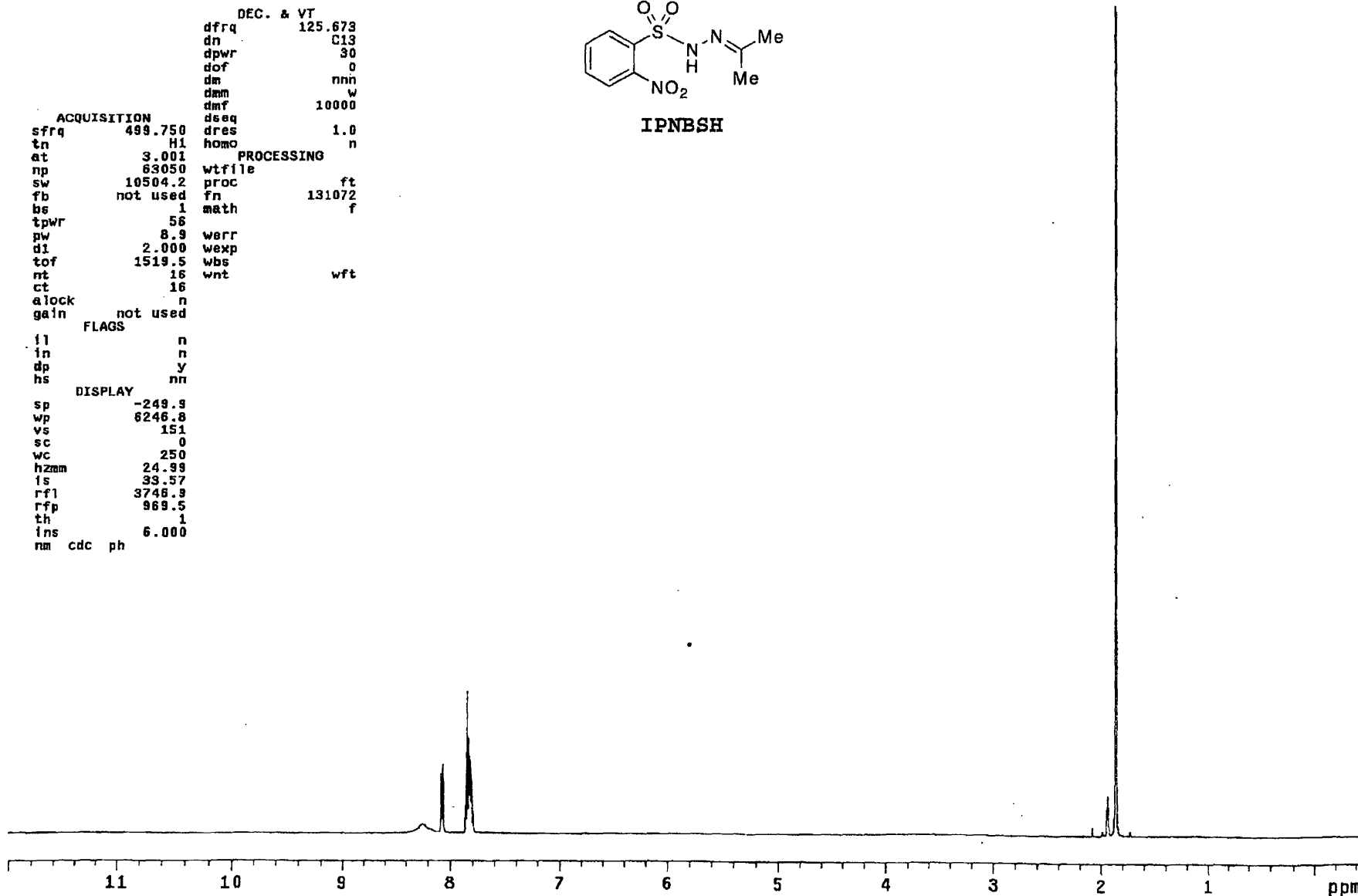


exp1 s2pu1

```
DEC. & VT
dfrq 125.673
dn C13
dpwr 30
dof 0
dm nnn
dmm w
dmf 10000
ACQUISITION
sfrq 499.750
tn H1
at 3.001
np 63050
sw 10504.2
fb not used
bs 1
tpwr 56
pw 8.9
di 2.000
tof 1519.5
nt 16
ct 16
alock n
gain not used
FLAGS
il n
in n
dp y
hs nn
DISPLAY
sp -249.9
wp 6246.8
vs 151
sc 0
wc 250
hzmm 24.99
is 33.57
rf1 3748.9
rfp 969.5
th 1
ins 6.000
nm cdc ph
```



IPNBSH

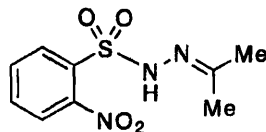


exp2 s2pu1

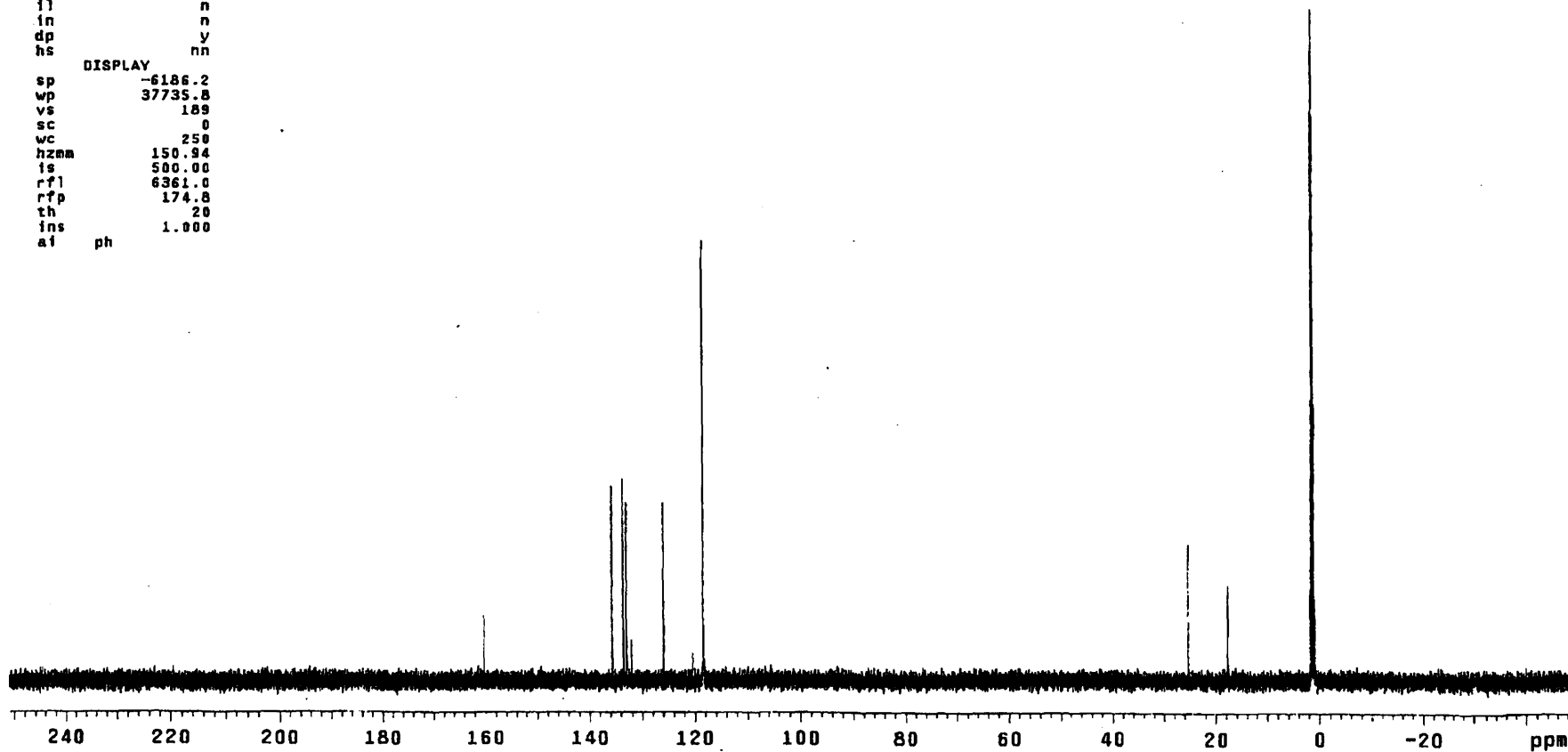
```
SAHPLK DEC. & VT
date Jan 20 2006 dfrq 500.236
solvent acetonitri- dn H1
file le dpwr 37
ACQUISITION dof -500.0
sfrq 125.796 dm y
tn C13 dmm w
at 1.736 dmf 10000
np 131010 dseq
sw 37735.8 dres 1.0
fb not used homo n
bs 4 PROCESSING lb 0.30
ss 1 wtfile
tpwr 53 proc ft
pw 6.9 fn 131072
dl 0.763 math f
tof 631.4
nt 1e+06 werr
ct 84 wexp
alock n wbs
gain not used wnt

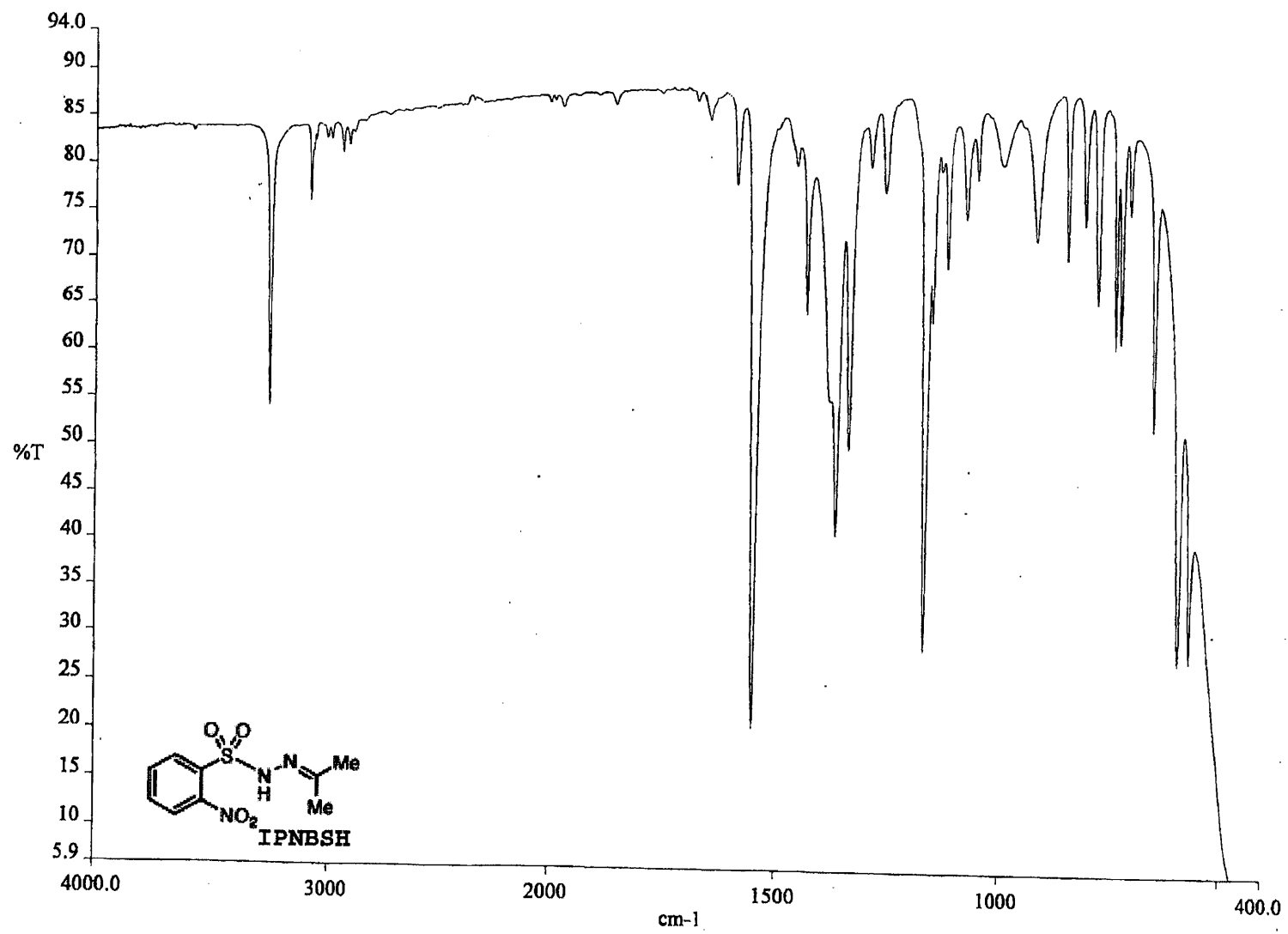
FLAGS
il n
in n
dp y
hs nn

DISPLAY
sp -6186.2
wp 37735.8
vs 189
sc 0
wc 250
hzma 150.94
is 500.00
rf1 6361.0
rfp 174.8
th 20
ins 1.000
ai ph
```



IPNBSH





exp1 s2pu1

DEC. & VT
 dfrq 125.674
 dn C13
 dpwr 34
 dof 1498.1
 dm nnn
 dsm w
 dmf 10000

ACQUISITION

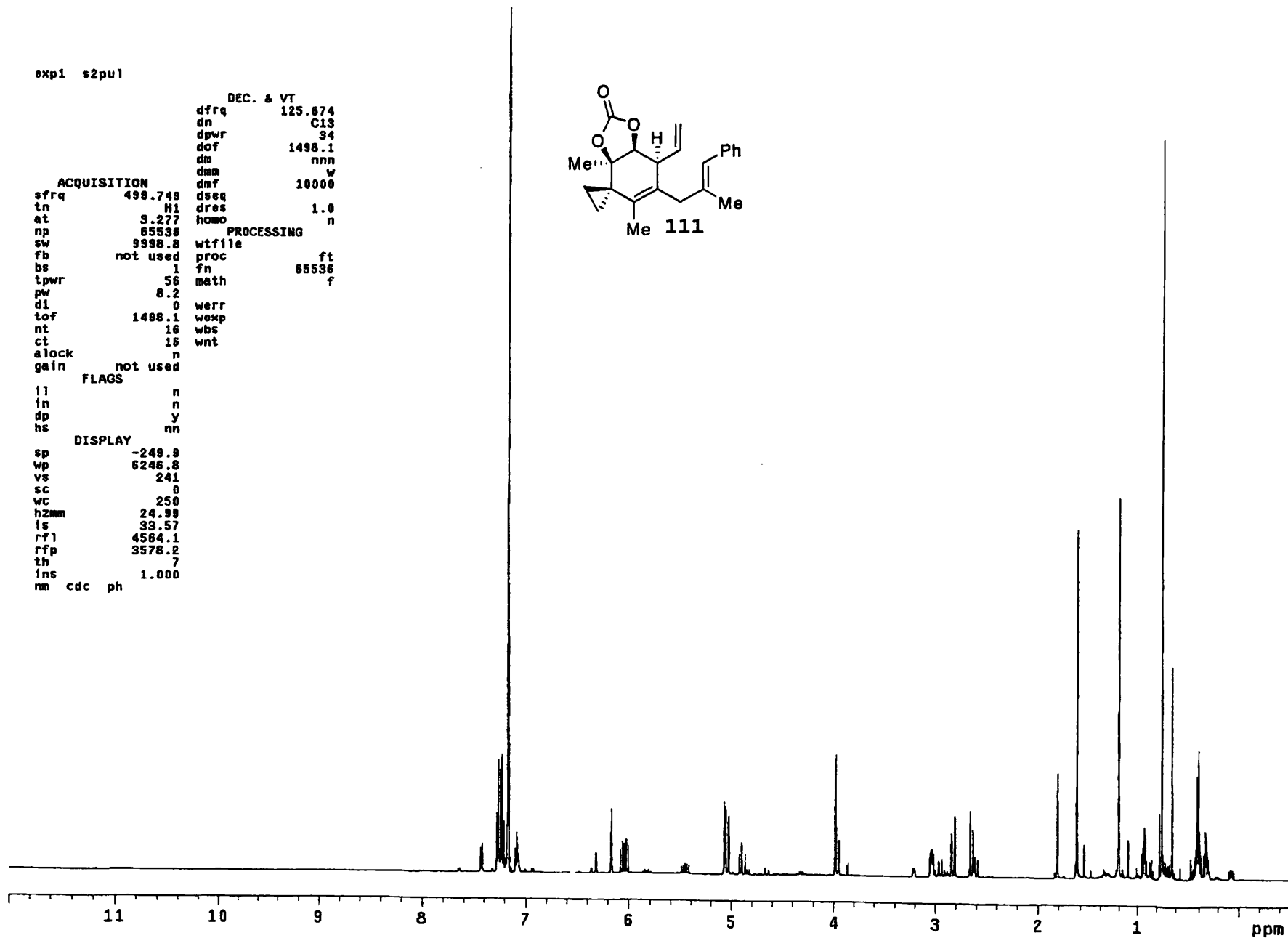
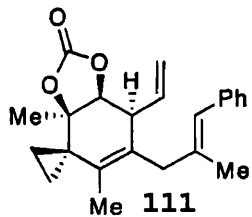
sfrq 498.748 dseq
 tn H1 dres 1.0
 at 3.277 homo n
 np 65536 PROCESSING
 sw 9998.8 wtf1e
 fb not used proc ft
 bs 1 fn 85536
 tpwr 56 math f
 pw 8.2
 dl 0 werr
 tof 1498.1 wexp
 nt 16 wbs
 ct 15 wnt
 alock n
 gain not used

FLAGS

ll n
 in n
 dp y
 hs nn

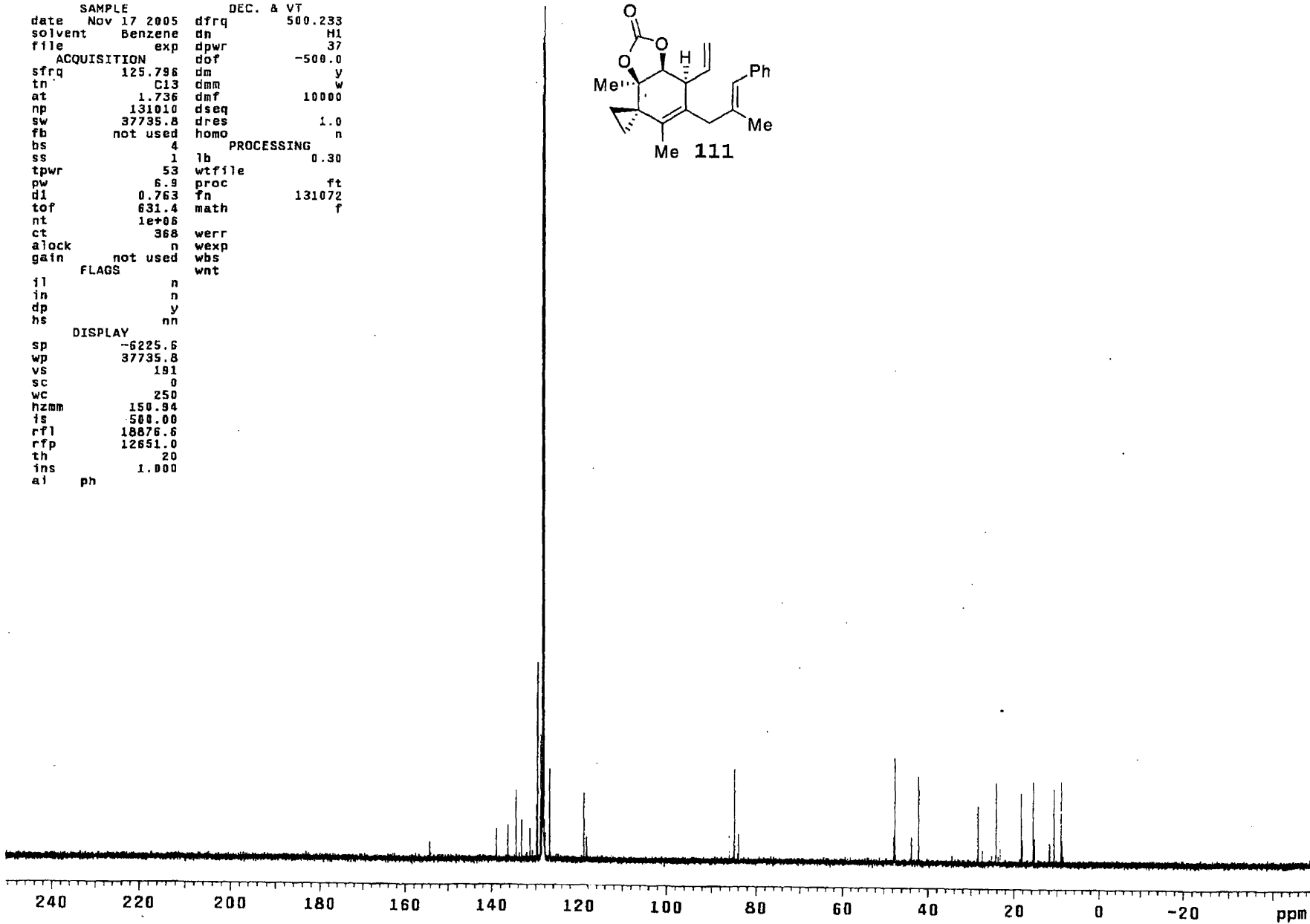
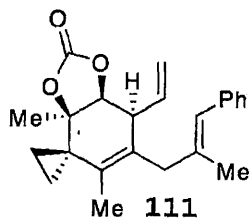
DISPLAY

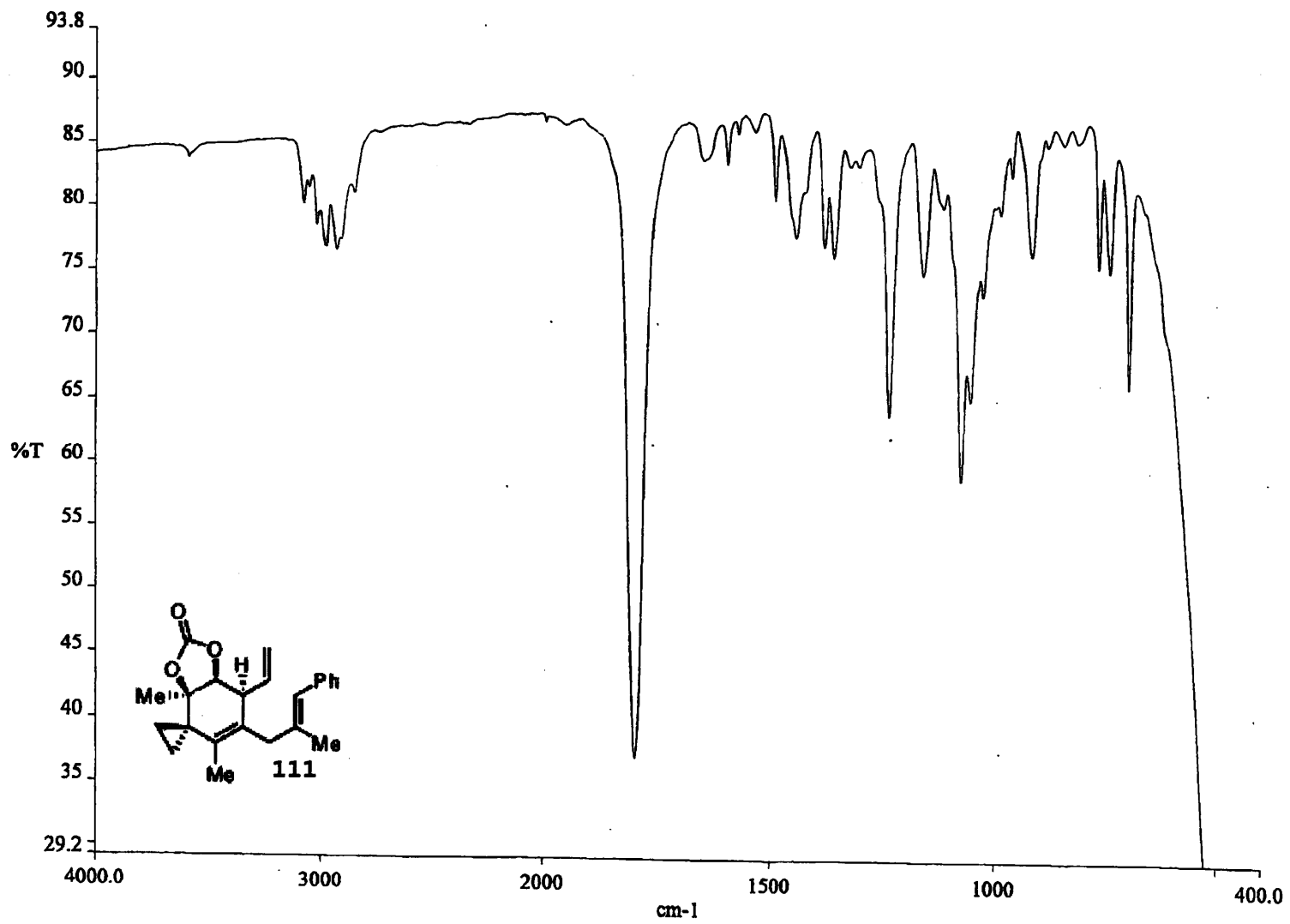
sp -249.8
 wp 6246.8
 vs 241
 sc 0
 wc 250
 hzmm 24.99
 ls 33.57
 rfl 4584.1
 rfp 3578.2
 th 7
 ins 1.000
 nm cdc ph

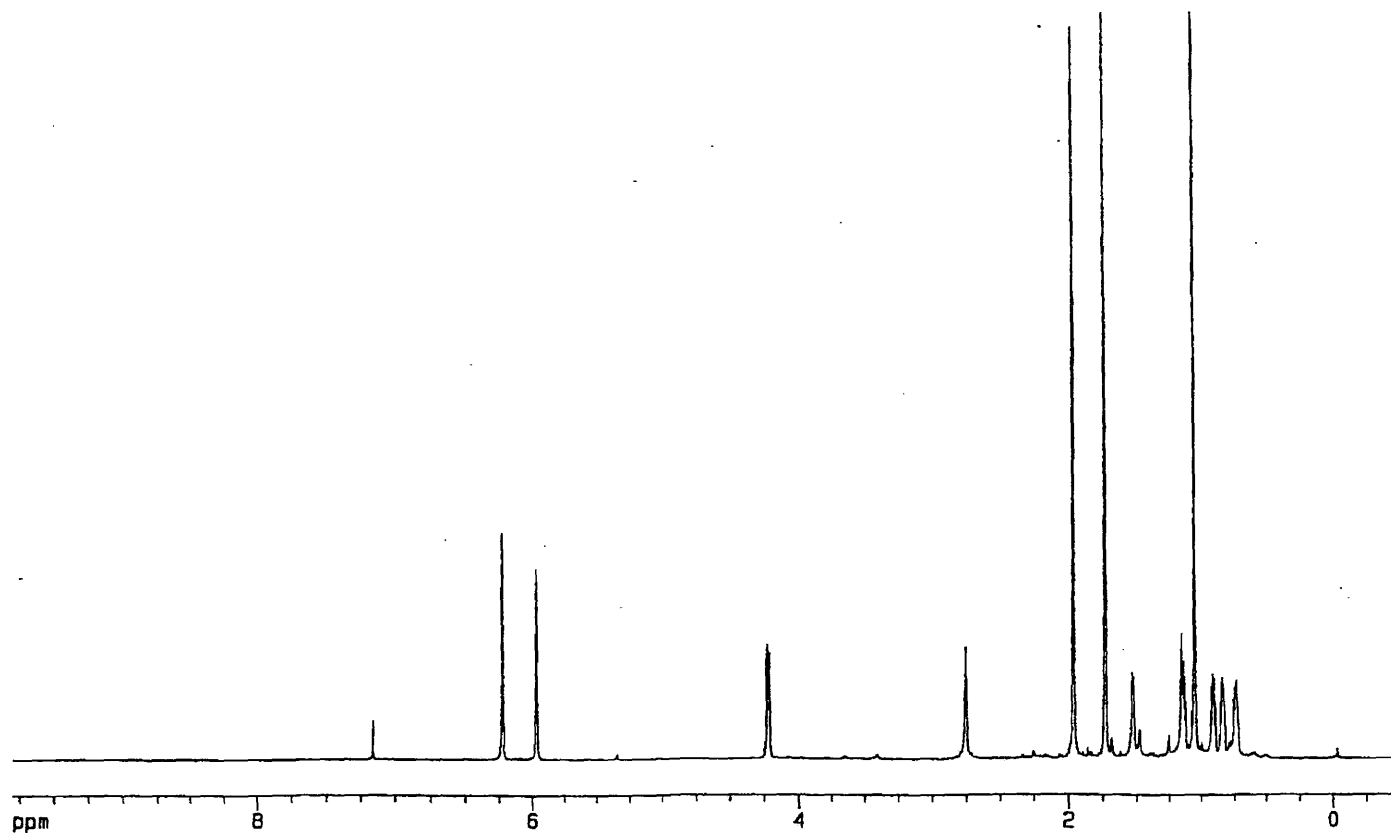
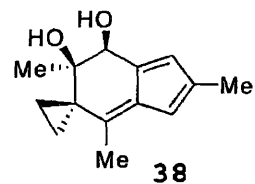


exp2 s2pu1

```
SAMPLE          DEC. & VT
date Nov 17 2005 dfrq      500.233
solvent Benzene  dn        H1
file exp        dpwr      37
ACQUISITION     dof      -500.0
sfrq 125.796    dm        y
tn    C13       dmm       w
at    1.736     dmf      10000
np    131010    dseq
sw    37735.8   dres      1.0
fb    not used homo      n
bs    4         PROCESSING
ss    1         lb        0.30
tpwr  53       wtfile
pw    6.9      proc      ft
dl    0.763    fn        131072
tof   631.4    math      f
nt    1e+06
ct    368     werr
alock not used wexp
gain  not used wbs
      FLAGS    wnt
il    n
in    n
dp    y
hs    nn
DISPLAY
sp    -6225.6
wp    37735.8
vs    191
sc    0
wc    250
hzmm  150.94
is    -500.00
rfl   18876.6
rfp   12651.0
th    20
ins   1.000
aj    ph
```







Current Data Parameters

NAME
EXPNO 1
PROCNO 1

F2 - Acquisition Parameters

Date_ 20060206
Time 12.05
INSTRUM spect
PROBHD 5 mm CPTCI 1H/
PULPROG zg30
TD 65536
SOLVENT CDCl3
NS 8
DS 0
SWH 8992.806 Hz
FIDRES 0.137219 Hz
AQ 3.6439073 sec
RG 22.6
DW 55.600 usec
DE 6.00 usec
TE 298.0 K
D1 1.0000000 sec
MCREST 0.0000000 sec
MCMRK 0.0150000 sec

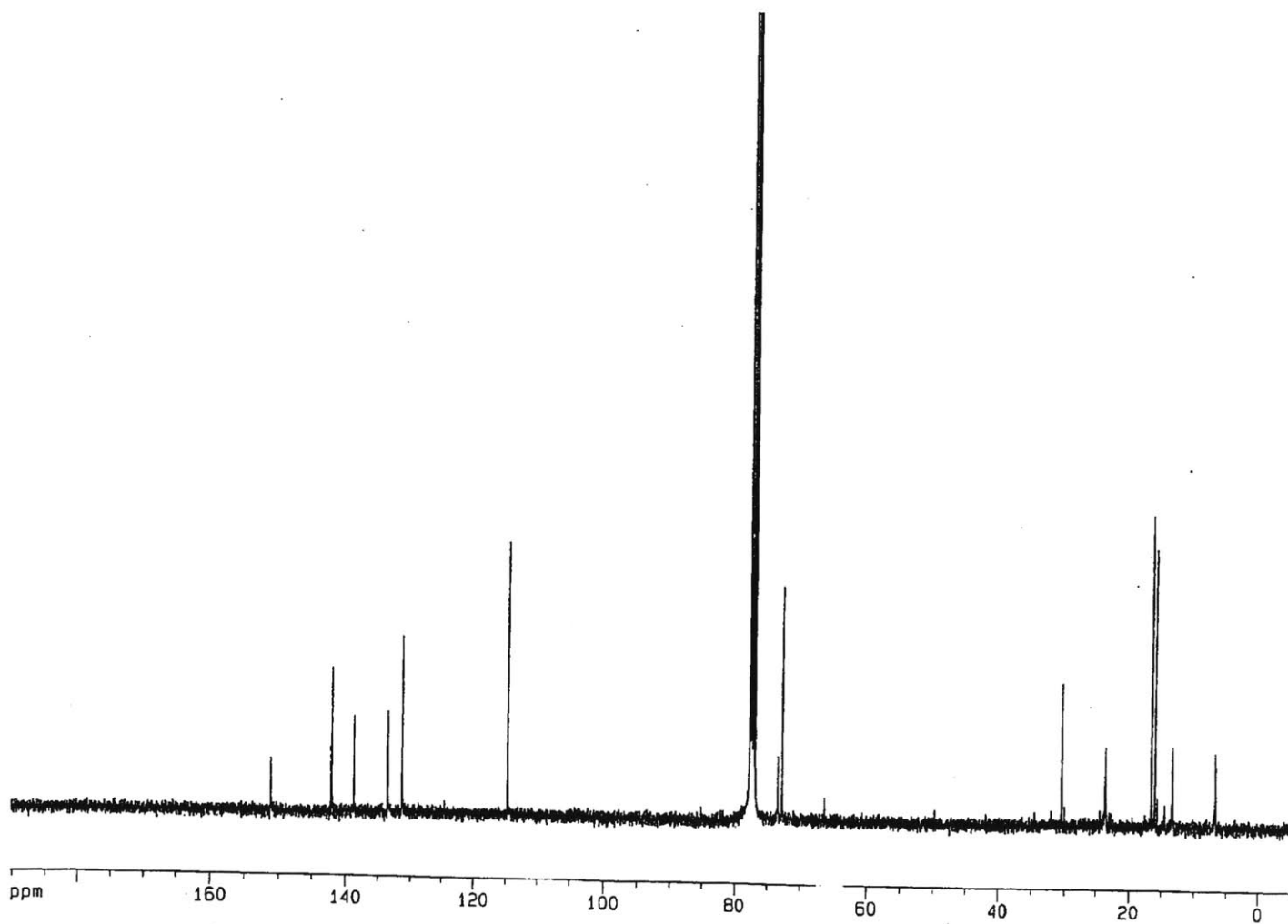
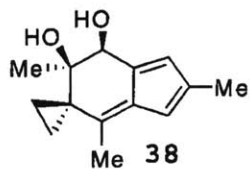
===== CHANNEL f1 =====
NUC1 1H
P1 10.00 usec
PL1 0.60 dB
SFO1 600.1314635 MHz

F2 - Processing parameters

SI 32768
SF 600.1300773 MHz
WDW EM
SSB 0
LB 0.30 Hz
GB 0
PC 1.00

1D NMR plot parameters

CX 20.00 cm
CY 13.02 cm
F1P 10.000 ppm
F1 6001.30 Hz
F2P -0.500 ppm
F2 -300.07 Hz
PPMCM 0.52500 ppm/cm
HZCM 315.06830 Hz/cm



Current Data Parameters

NAME
EXPNO 2
PROCNO 1

F2 - Acquisition Parameters

Date_ 20060205
Time 11.58
INSTRUM spect
PROBHD 5mm BBO BB-1
PULPROG zgpg30
TD 65536
SOLVENT CDCl₃
NS 17365
DS 4
SWH 24875.621 Hz
FIDRES 0.379572 Hz
AQ 1.3173236 sec
RG 1448.2
DW 20.100 usec
DE 6.00 usec
TE 300.0 K
D1 2.0000000 sec
d11 0.0300000 sec
d12 0.0002000 sec

===== CHANNEL f1 =====

NUC1 13C
P1 15.25 usec
PL1 3.00 dB
SFO1 100.6237959 MHz

===== CHANNEL f2 =====

CPDPRG2 waltz16
NUC2 1H
PCPD2 107.50 usec
PL2 0.00 dB
PL12 24.00 dB
PL13 24.00 dB
SFO2 400.1316005 MHz

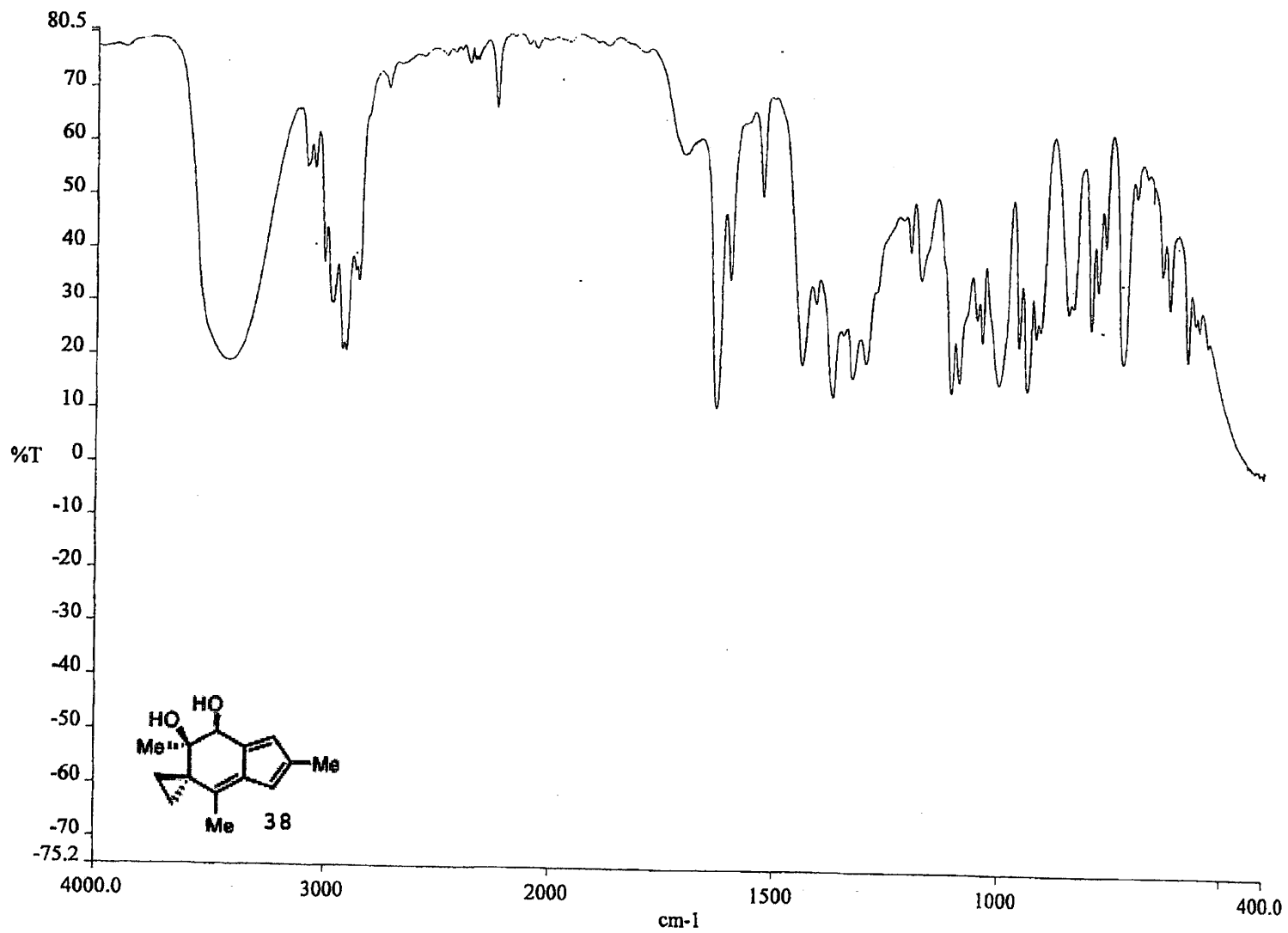
F2 - Processing parameters

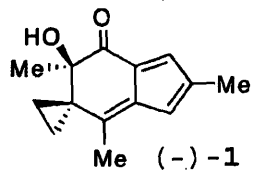
SI 32768
SF 100.6127290 MHz
WDW EM
SSB 0
LB 1.00 Hz
GB 0
PC 1.40

1D NMR plot parameters

CX 20.00 cm
F1P 190.288 ppm
F1 19145.36 Hz
F2P -6.043 ppm
F2 -508.01 Hz
PPMCH 9.81654 ppm/cm
HZCH 987.66852 Hz/cm

200





Current Data Parameters

NAME
EXPNO 1
PROCNO 1

F2 - Acquisition Parameters

Date_ 20060206
Time 19.53
INSTRUM spect
PROBHD 5mm 880 BB-1
PULPROG zg30
TD 65536
SOLVENT C606
NS 16
DS 2
SWH 8278.146 Hz
FIDRES 0.126314 Hz
AQ 3.9584243 sec
RG 287.4
DW 60.400 usec
DE 6.00 usec
TE 300.0 K
D1 1.0000000 sec

===== CHANNEL f1 =====

NUC1 1H
P1 7.90 usec
PL1 0.00 dB
SFO1 400.1324710 MHz

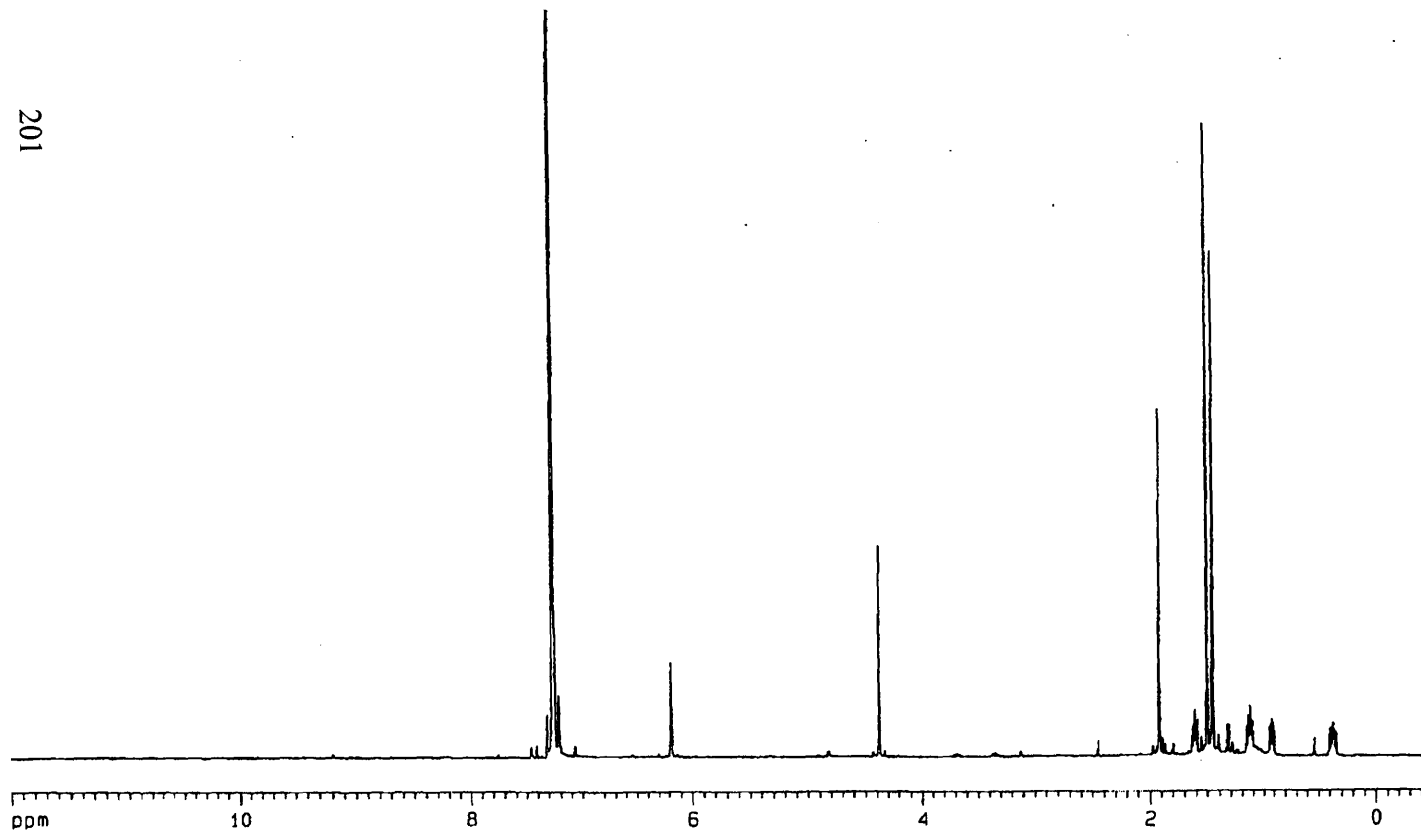
F2 - Processing parameters

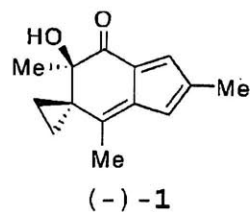
SI 32768
SF 400.1300000 MHz
WDW EM
SSB 0
LB 0.30 Hz
GB 0
PC 1.00

1D NMR plot parameters

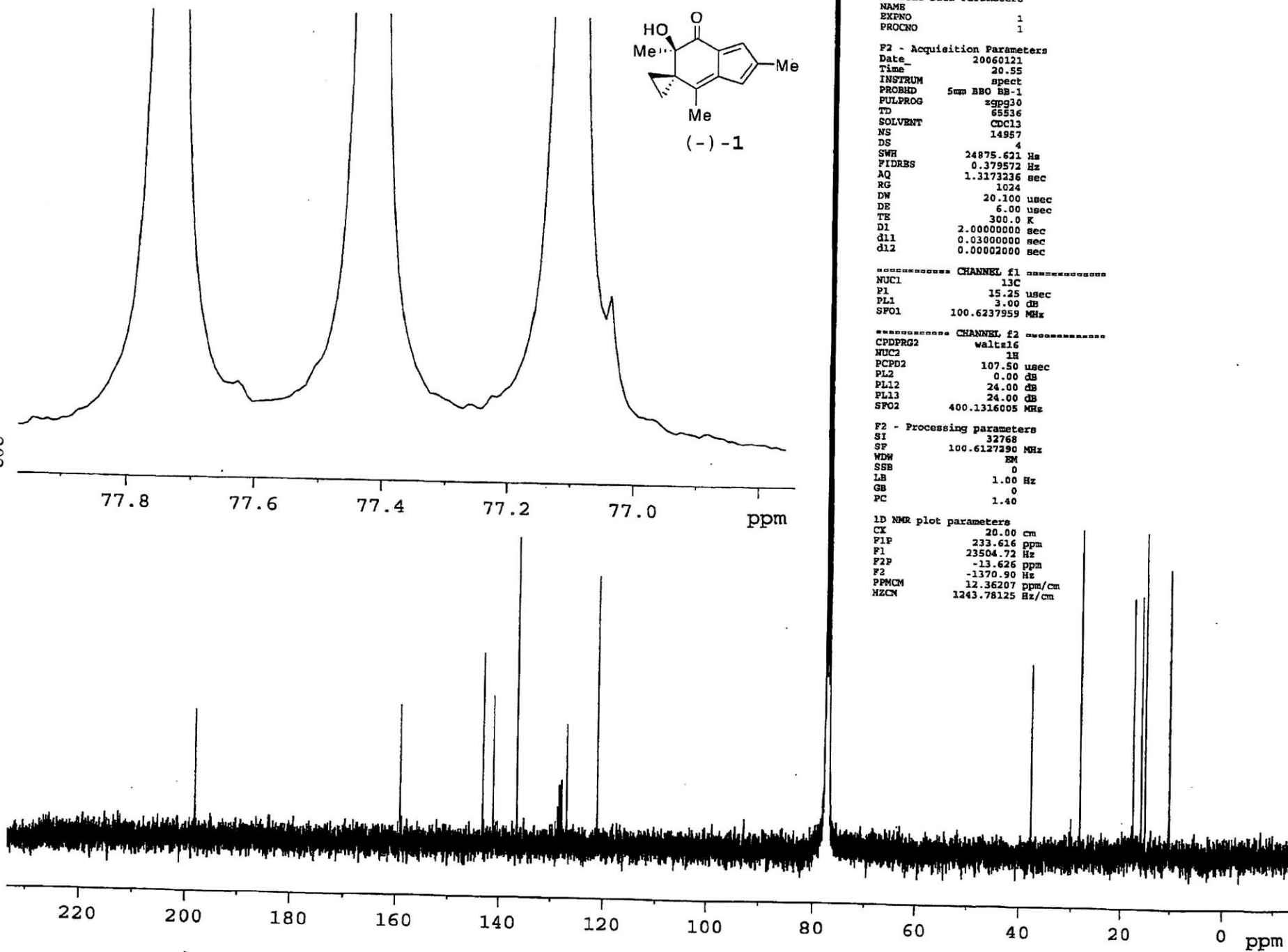
CX 20.00 cm
F1P 12.012 ppm
F1 4806.17 Hz
F2P -0.503 ppm
F2 -201.07 Hz
PPMCM 0.62570 ppm/cm
HZCM 250.36191 Hz/cm

201





202



Current Data Parameters

NAME
 EXENO 1
 PROCNO 1

F2 - Acquisition Parameters

Date_ 20060121
 Time 20.55
 INSTRUM spect
 PROBRD 5mm BBO BB-1
 FULPROG zgpg30
 TD 65536
 SOLVENT CDCl3
 NS 14957
 DS 4
 SWH 24875.621 Hz
 FIDRES 0.379572 Hz
 AQ 1.3172236 sec
 RG 1024
 DW 20.100 usec
 DE 6.00 usec
 TE 300.0 K
 D1 2.0000000 sec
 d11 0.0300000 sec
 d12 0.0000200 sec

===== CHANNEL f1 =====

NUC1 13C
 P1 15.25 usec
 PL1 3.00 dB
 SFO1 100.6237959 MHz

===== CHANNEL f2 =====

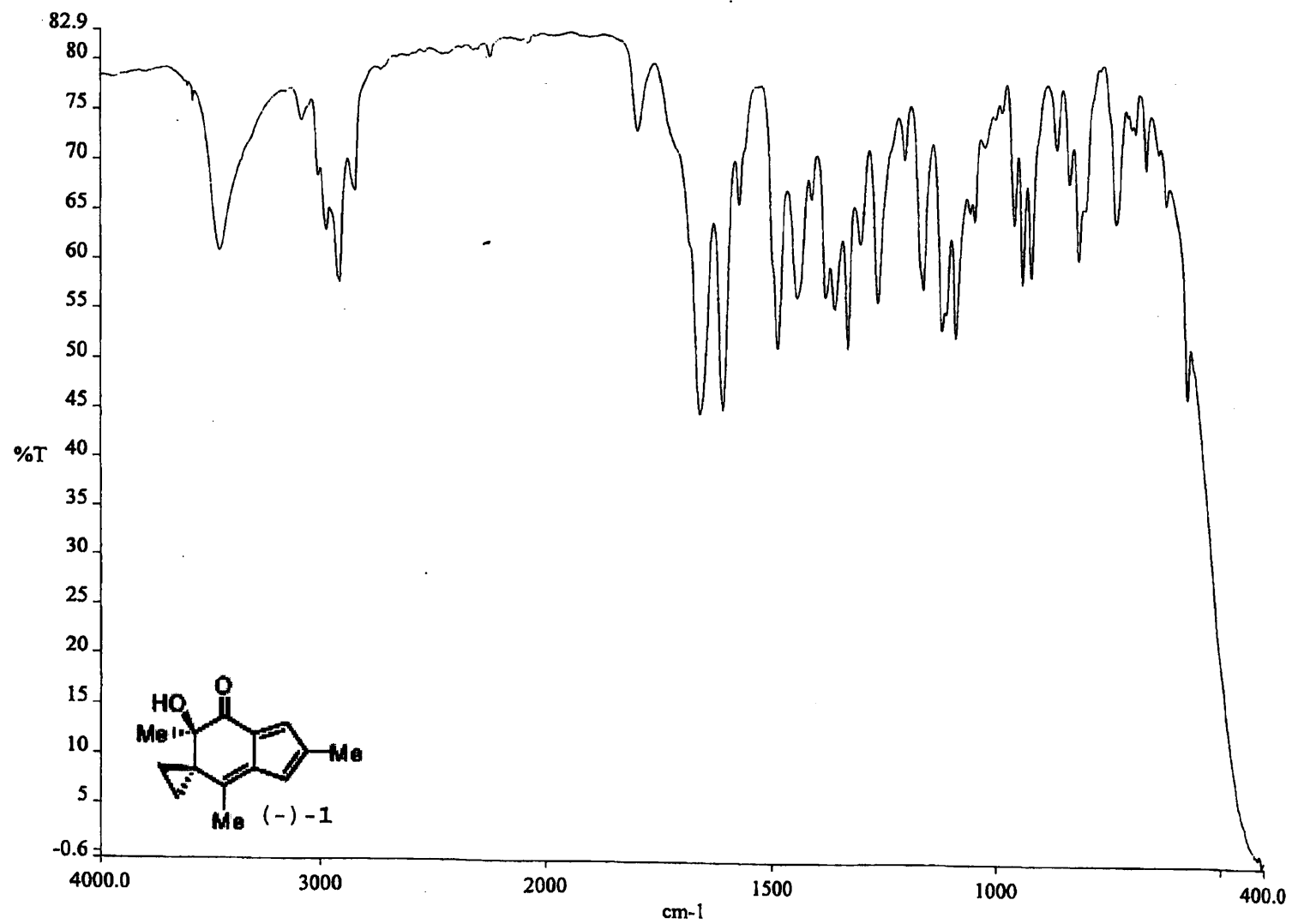
CDPRG2 waltz16
 NUC2 1H
 PCPD2 107.50 usec
 PL2 0.00 dB
 PLL2 24.00 dB
 PLL3 24.00 dB
 SFO2 400.1316005 MHz

F2 - Processing parameters

S1 32768
 SF 100.6127290 MHz
 WDW EM
 SSB 0
 LB 1.00 Hz
 GB 0
 PC 1.40

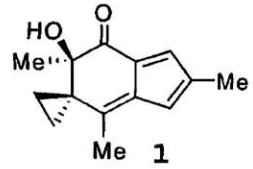
1D NMR plot parameters

CX 20.00 cm
 F1P 233.616 ppm
 F1 23504.72 Hz
 F2P -13.626 ppm
 F2 -1370.90 Hz
 PPMCM 12.36207 ppm/cm
 HZCM 1243.78125 Hz/cm

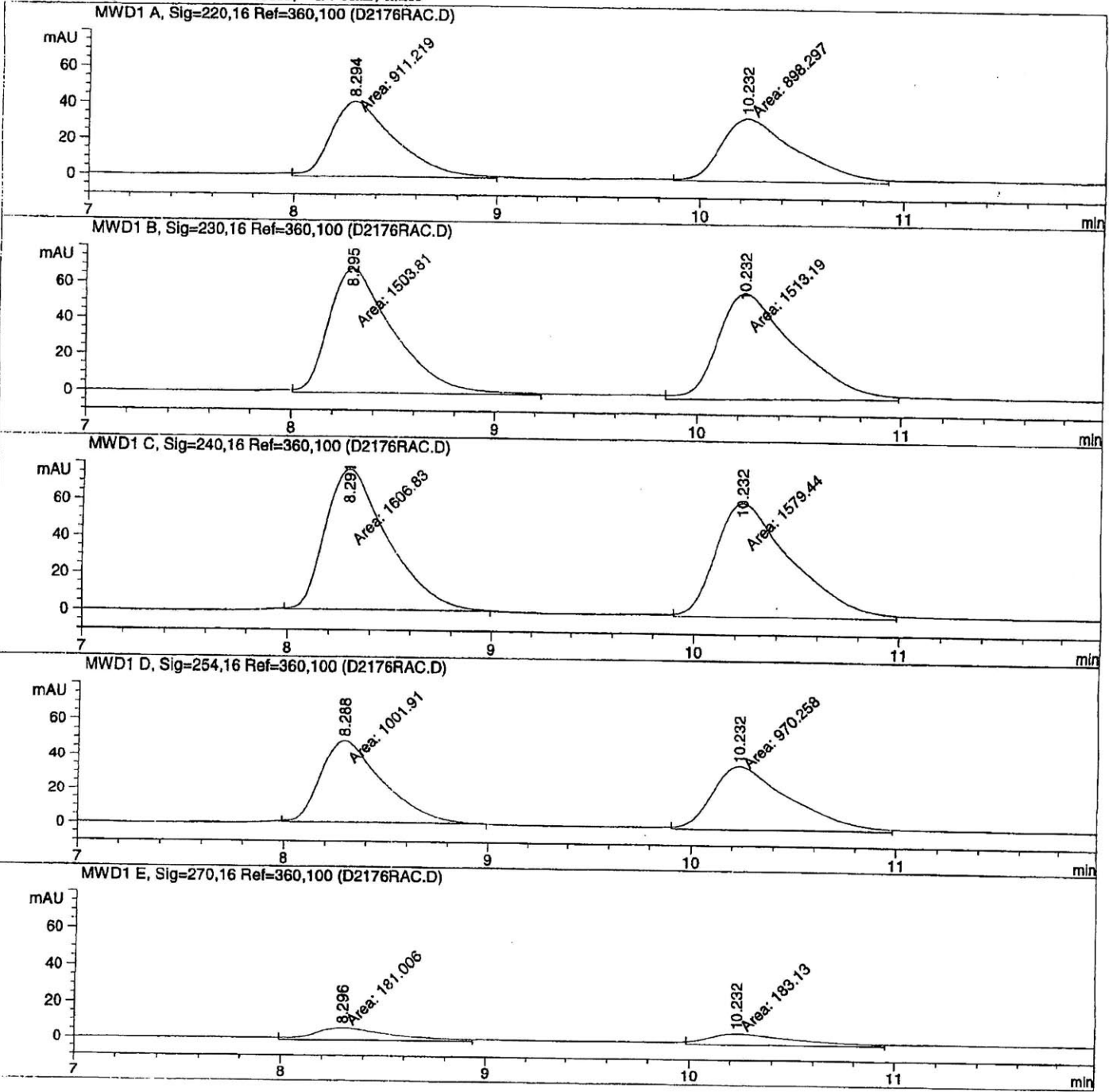


```

=====
Injection Date   :                               Seq. Line :    1
Sample Name     :                               Location  : Vial 91
Acq. Operator   :                               Inj       :    1
                                                    Inj Volume: 1 µl
Acq. Method     :
Last changed    :
Analysis Method  :
Last changed    :
  
```

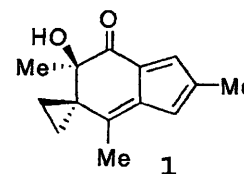


Zorbax CN; 1.0% iPrOH-hex; 1.0mL/min



=====
 Area Percent Report
 =====

Sorted By : Signal
 Multiplier : 1.0000
 Dilution : 1.0000
 Use Multiplier & Dilution Factor with ISTDs



Signal 1: MWD1 A, Sig=220,16 Ref=360,100

Peak #	RetTime [min]	Type	Width [min]	Area [mAU*s]	Height [mAU]	Area %
1	8.294	MM	0.3635	911.21899	41.78366	50.3570
2	10.232	MM	0.4289	898.29730	34.90594	49.6430

Totals : 1809.51630 76.68960

Results obtained with enhanced integrator!

Signal 2: MWD1 B, Sig=230,16 Ref=360,100

Peak #	RetTime [min]	Type	Width [min]	Area [mAU*s]	Height [mAU]	Area %
1	8.295	MM	0.3657	1503.81494	68.54411	49.8446
2	10.232	MM	0.4320	1513.18909	58.38517	50.1554

Totals : 3017.00403 126.92929

Results obtained with enhanced integrator!

Signal 3: MWD1 C, Sig=240,16 Ref=360,100

Peak #	RetTime [min]	Type	Width [min]	Area [mAU*s]	Height [mAU]	Area %
1	8.291	MM	0.3521	1606.82849	76.06040	50.4298
2	10.232	MM	0.4278	1579.44067	61.52729	49.5702

Totals : 3186.26917 137.58769

Results obtained with enhanced integrator!

Signal 4: MWD1 D, Sig=254,16 Ref=360,100

Peak #	RetTime [min]	Type	Width [min]	Area [mAU*s]	Height [mAU]	Area %
1	8.288	MM	0.3491	1001.91046	47.83171	50.8025
2	10.232	MM	0.4357	970.25781	37.11912	49.1975

Totals : 1972.16827 84.95083

Results obtained with enhanced integrator!

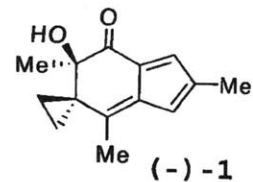
Signal 5: MWD1 E, Sig=270,16 Ref=360,100

Peak #	RetTime [min]	Type	Width [min]	Area [mAU*s]	Height [mAU]	Area %
1	8.296	MM	0.4375	181.00645	6.89578	49.7084
2	10.232	MM	0.4941	183.12990	6.17725	50.2916

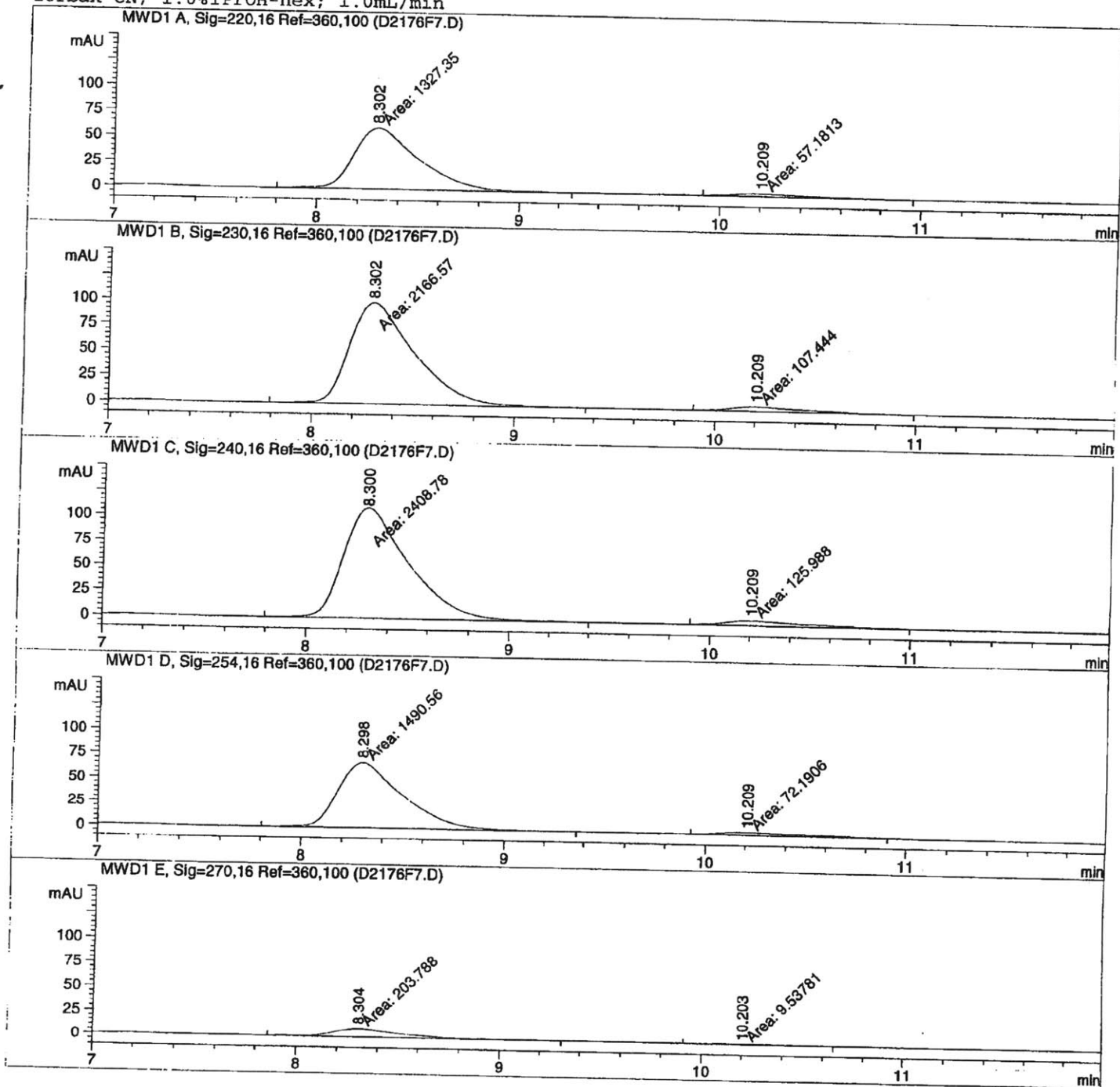
Totals : 364.13635 13.07303

```

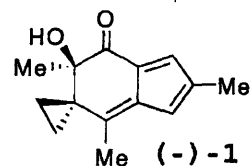
=====
Injection Date :                               Seq. Line :    1
Sample Name   :                               Location  : Vial 91
Acq. Operator :                               Inj       :    1
                                                    Inj Volume: 1 µl
Acq. Method   :
Last changed  :
Analysis Method :
Last changed  :
  
```



Zorbax CN; 1.0% iPrOH-hex; 1.0mL/min



=====
 Area Percent Report
 =====



Sorted By : Signal
 Multiplier : 1.0000
 Dilution : 1.0000
 Use Multiplier & Dilution Factor with ISTDs

Signal 1: MWD1 A, Sig=220,16 Ref=360,100

Peak #	RetTime [min]	Type	Width [min]	Area [mAU*s]	Height [mAU]	Area %
1	8.302	MM	0.3690	1327.35315	59.95131	95.8700
2	10.209	MM	0.3880	57.18126	2.45643	4.1300

Totals : 1384.53440 62.40774

Results obtained with enhanced integrator!

Signal 2: MWD1 B, Sig=230,16 Ref=360,100

Peak #	RetTime [min]	Type	Width [min]	Area [mAU*s]	Height [mAU]	Area %
1	8.302	MM	0.3658	2166.57349	98.70364	95.2752
2	10.209	MM	0.4169	107.44352	4.29493	4.7248

Totals : 2274.01701 102.99857

Results obtained with enhanced integrator!

Signal 3: MWD1 C, Sig=240,16 Ref=360,100

Peak #	RetTime [min]	Type	Width [min]	Area [mAU*s]	Height [mAU]	Area %
1	8.300	MM	0.3678	2408.77856	109.15147	95.0296
2	10.209	MM	0.4560	125.98849	4.60503	4.9704

Totals : 2534.76705 113.75651

Results obtained with enhanced integrator!

Signal 4: MWD1 D, Sig=254,16 Ref=360,100

Peak #	RetTime [min]	Type	Width [min]	Area [mAU*s]	Height [mAU]	Area %
1	8.298	MM	0.3686	1490.56372	67.39674	95.3806
2	10.209	MM	0.4593	72.19061	2.61948	4.6194

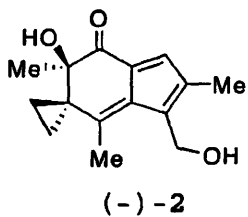
Totals : 1562.75433 70.01622

Results obtained with enhanced integrator!

Signal 5: MWD1 E, Sig=270,16 Ref=360,100

Peak #	RetTime [min]	Type	Width [min]	Area [mAU*s]	Height [mAU]	Area %
1	8.304	MM	0.3836	203.78841	8.85333	95.5290
2	10.203	MM	0.3813	9.53781	4.16884e-1	4.4710

Totals : 213.32622 9.27021



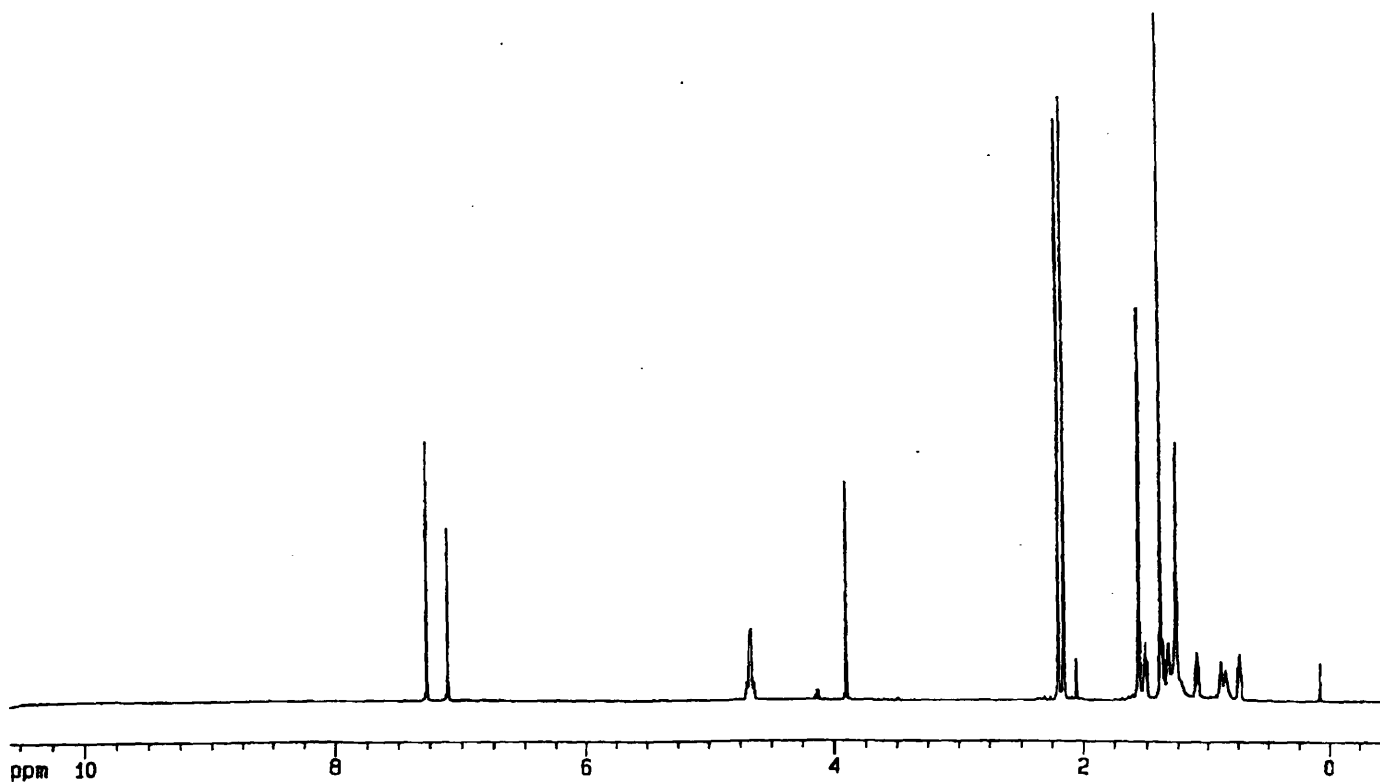
Current Data Parameters
 NAME
 EXPNO 1
 PROCNO 1

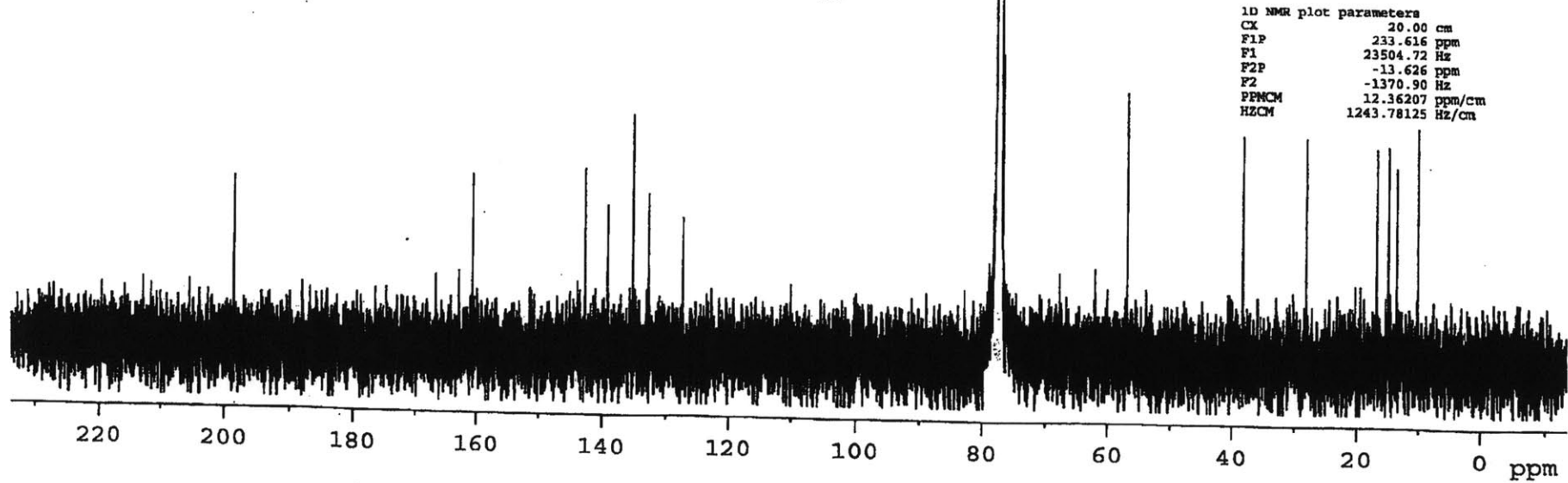
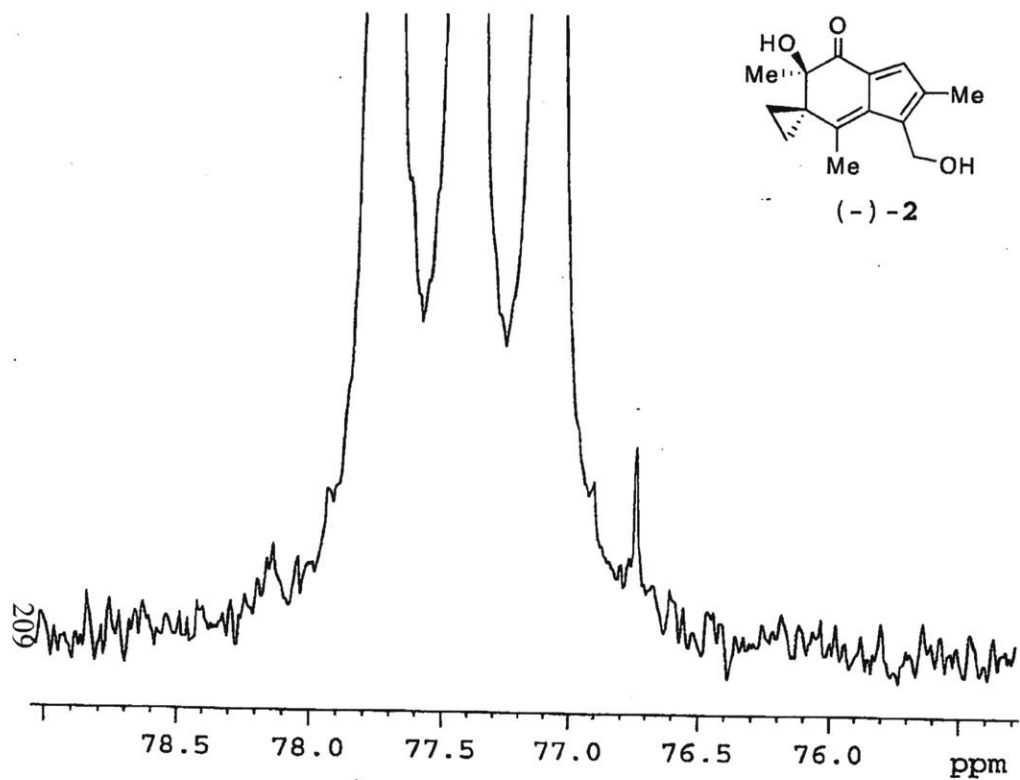
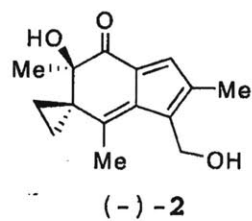
F2 - Acquisition Parameters
 Date_ 20060123
 Time 13.01
 INSTRUM spect
 PROBHD 5 mm CPTCI 1H/
 PULPROG zg30
 TD 65536
 SOLVENT CDCl3
 NS 16
 DS 0
 SWH 7936.508 Hz
 FIDRES 0.121102 Hz
 AQ 4.1288805 sec
 RG 28.5
 DN 63.000 usec
 DE 6.00 usec
 TE 298.0 K
 D1 1.0000000 sec
 MCREST 0.0000000 sec
 MCMRK 0.01500000 sec

----- CHANNEL f1 -----
 NUC1 1H
 P1 8.00 usec
 PL1 -4.00 dB
 SFO1 600.1323934 MHz

F2 - Processing parameters
 SI 32768
 SF 600.1300114 MHz
 WDW EM
 SSB 0
 LB 0.30 Hz
 GB 0
 PC 1.00

1D NMR plot parameters
 CX 20.00 cm
 CY 9.86 cm
 F1P 10.800 ppm
 F1 6481.40 Hz
 F2P -0.500 ppm
 F2 -300.07 Hz
 PPMCH 0.56500 ppm/cm
 HZCM 339.07346 Hz/cm





```

Current Data Parameters
NAME
EXPNO 1
PROCNO 1

F2 - Acquisition Parameters
Date_ 20060124
Time 8.53
INSTRUM spect
PROBHD 5mm BBO BB-1
PULPROG zgpg30
TD 65536
SOLVENT CDCl3
NS 13967
DS 4
SWH 24875.621 Hz
FIDRES 0.379572 Hz
AQ 1.3173236 sec
RG 16384
DW 20.100 usec
DE 6.00 usec
TE 300.0 K
D1 2.00000000 sec
d11 0.03000000 sec
d12 0.00002000 sec

```

```

----- CHANNEL f1 -----
NUC1 13C
P1 15.25 usec
PL1 3.00 dB
SFO1 100.6237959 MHz

```

```

----- CHANNEL f2 -----
CPDPRG2 waltz16
NUC2 1H
PCPD2 107.50 usec
PL2 0.00 dB
PL12 24.00 dB
PL13 24.00 dB
SFO2 400.1316005 MHz

```

```

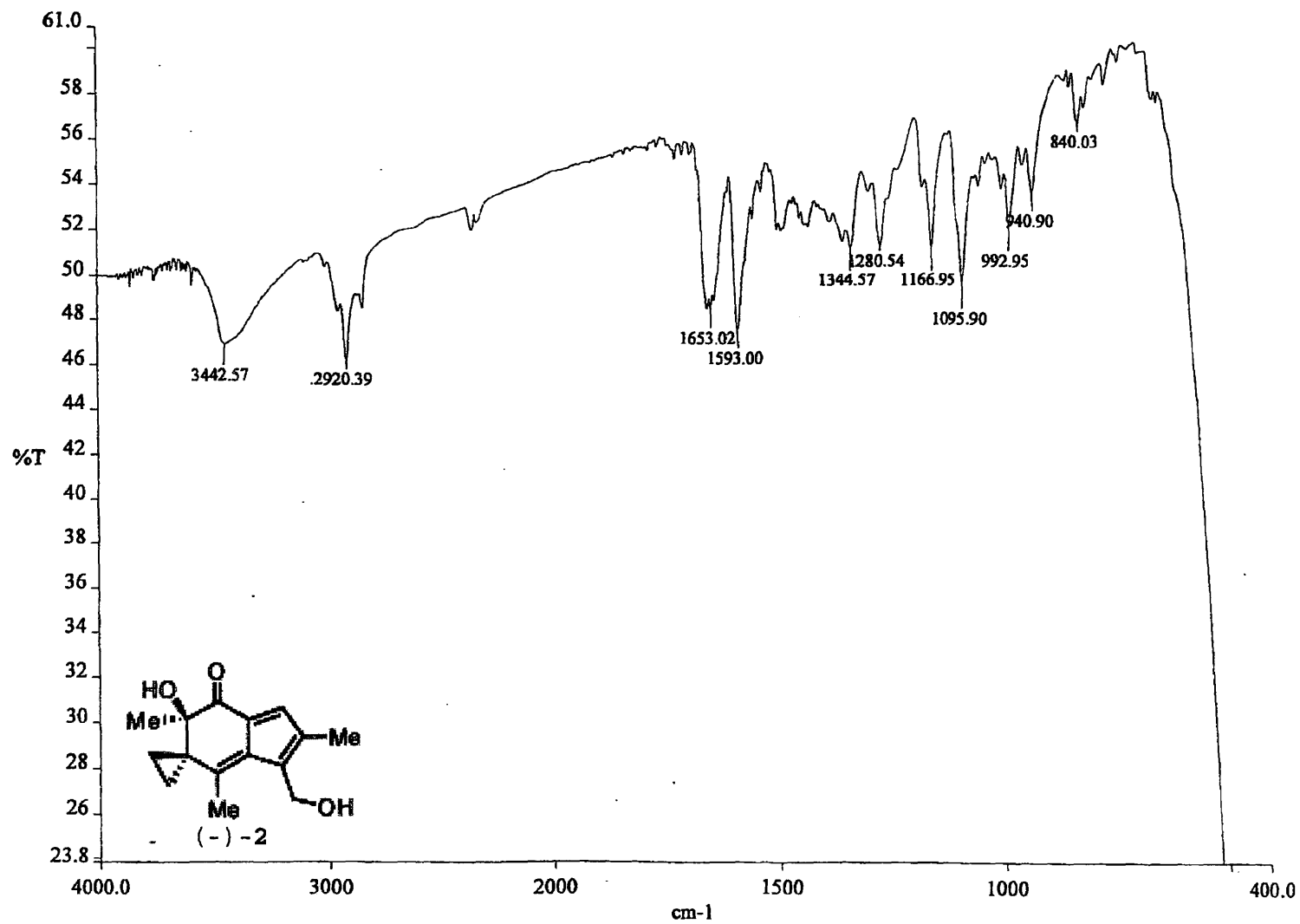
F2 - Processing parameters
SI 32768
SF 100.6127290 MHz
WDW EM
SSB 0
LB 1.00 Hz
GB 0
PC 1.40

```

```

1D NMR plot parameters
CX 20.00 cm
F1P 233.616 ppm
F1 23504.72 Hz
F2P -13.626 ppm
F2 -1370.90 Hz
PPMCM 12.36207 ppm/cm
HZCM 1243.78125 Hz/cm

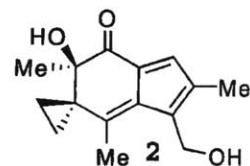
```



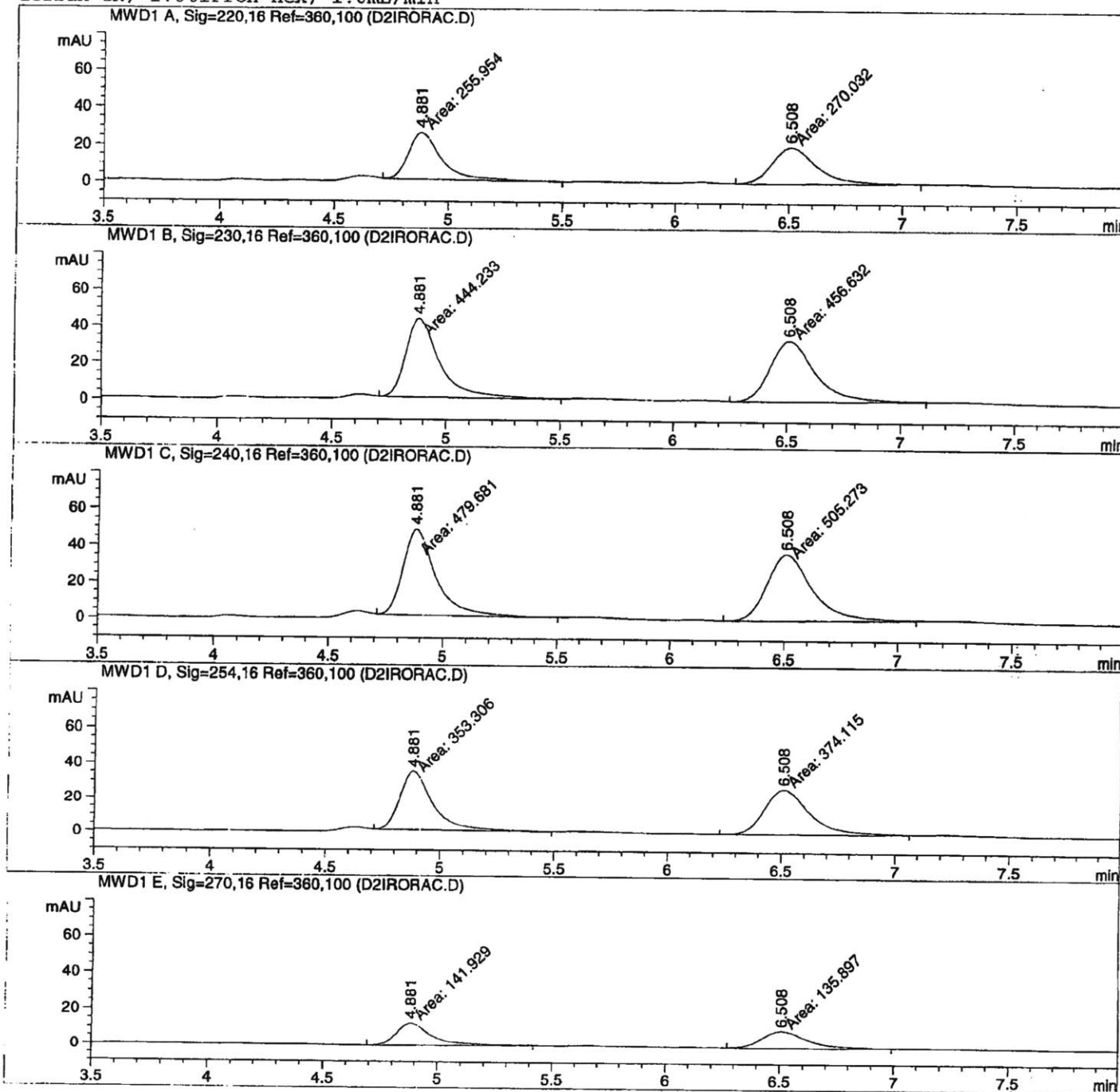
```

=====
Injection Date :                               Seq. Line :    1
Sample Name    :                               Location  : Vial 91
Acq. Operator  :                               Inj       :    1
                                                    Inj Volume: 1 µl

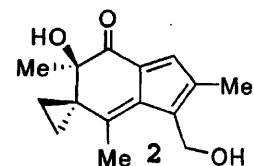
Acq. Method   :
Last changed  :
Analysis Method :
Last changed  :
  
```



Zorbax CN; 1.0% iPrOH-hex; 1.0mL/min



=====
 Area Percent Report
 =====



Sorted By : Signal
 Multiplier : 1.0000
 Dilution : 1.0000
 Use Multiplier & Dilution Factor with ISTDs

Signal 1: MWD1 A, Sig=220,16 Ref=360,100

Peak #	RetTime [min]	Type	Width [min]	Area [mAU*s]	Height [mAU]	Area %
1	4.881	MM	0.1691	255.95450	25.22759	48.6618
2	6.508	MM	0.2286	270.03177	19.68349	51.3382

Totals : 525.98627 44.91107

Results obtained with enhanced integrator!

Signal 2: MWD1 B, Sig=230,16 Ref=360,100

Peak #	RetTime [min]	Type	Width [min]	Area [mAU*s]	Height [mAU]	Area %
1	4.881	MM	0.1724	444.23315	42.93738	49.3118
2	6.508	MM	0.2301	456.63242	33.07205	50.6882

Totals : 900.86557 76.00943

Results obtained with enhanced integrator!

Signal 3: MWD1 C, Sig=240,16 Ref=360,100

Peak #	RetTime [min]	Type	Width [min]	Area [mAU*s]	Height [mAU]	Area %
1	4.881	MM	0.1700	479.68124	47.03773	48.7008
2	6.508	MM	0.2305	505.27335	36.53200	51.2992

Totals : 984.95459 83.56973

Results obtained with enhanced integrator!

Signal 4: MWD1 D, Sig=254,16 Ref=360,100

Peak #	RetTime [min]	Type	Width [min]	Area [mAU*s]	Height [mAU]	Area %
1	4.881	MM	0.1703	353.30612	34.58545	48.5697
2	6.508	MM	0.2314	374.11542	26.94118	51.4303

Totals : 727.42154 61.52663

Results obtained with enhanced integrator!

Signal 5: MWD1 E, Sig=270,16 Ref=360,100

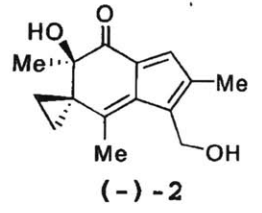
Peak #	RetTime [min]	Type	Width [min]	Area [mAU*s]	Height [mAU]	Area %
1	4.881	MM	0.1827	141.92921	12.94412	51.0856
2	6.508	MM	0.2336	135.89722	9.69631	48.9144

Totals : 277.82643 22.64043

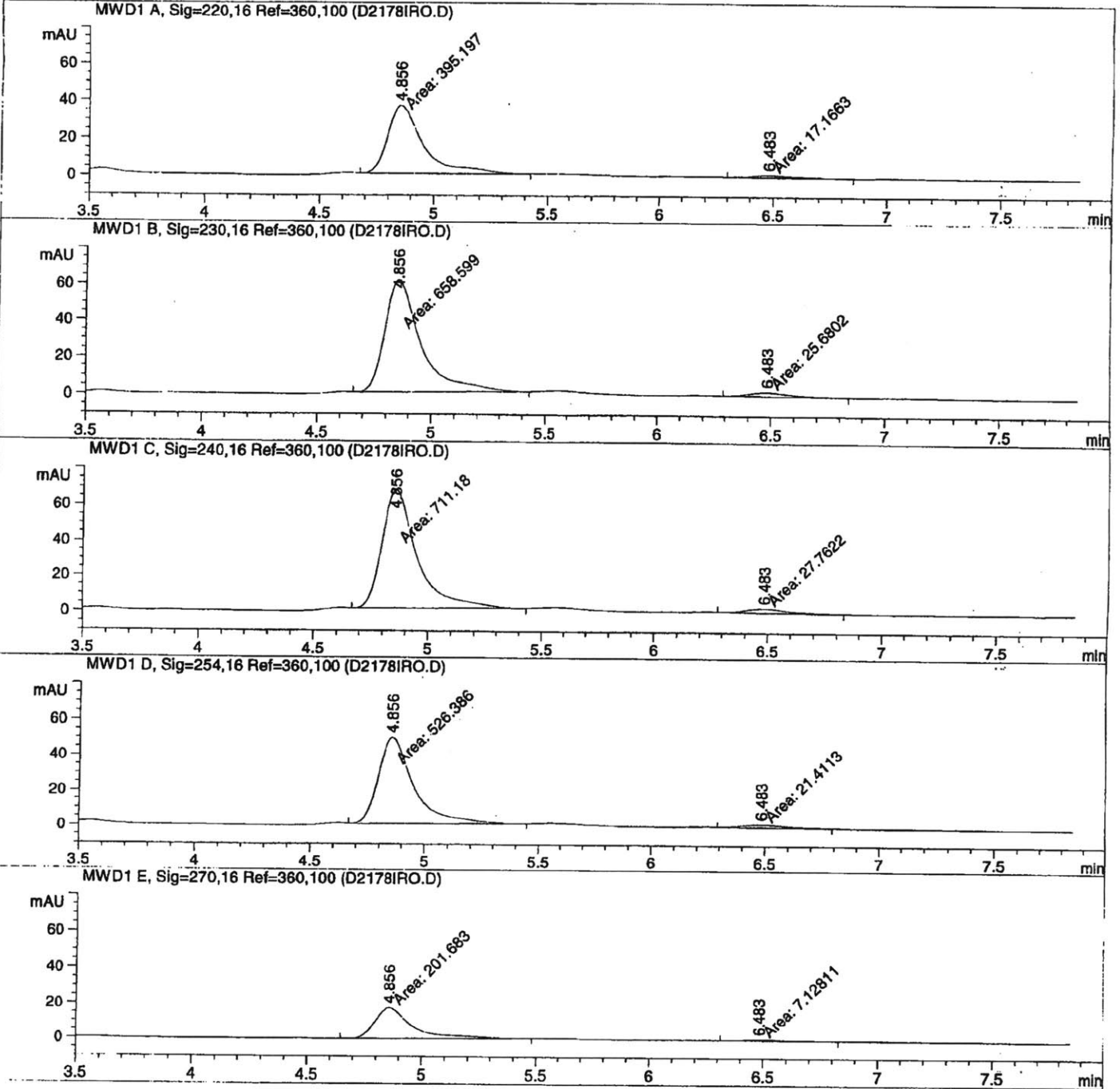

```

=====
Injection Date   :                               Seq. Line :    1
Sample Name     :                               Location  : Vial 91
Acq. Operator   :                               Inj       :    1
                                                    Inj Volume: 1 µl

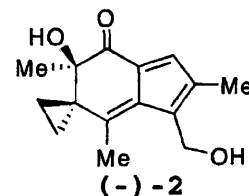
Acq. Method    :
Last changed   :
Analysis Method:
Last changed   :
  
```



Zorbax CN; 1.0% iPrOH-hex; 1.0mL/min



=====
 Area Percent Report
 =====



Sorted By : Signal
 Multiplier : 1.0000
 Dilution : 1.0000
 Use Multiplier & Dilution Factor with ISTDs

Signal 1: MWD1 A, Sig=220,16 Ref=360,100

Peak #	RetTime [min]	Type	Width [min]	Area [mAU*s]	Height [mAU]	Area %
1	4.856	MM	0.1823	395.19705	36.14056	95.8371
2	6.483	MM	0.2388	17.16626	1.19831	4.1629

Totals : 412.36331 37.33887

Results obtained with enhanced integrator!

Signal 2: MWD1 B, Sig=230,16 Ref=360,100

Peak #	RetTime [min]	Type	Width [min]	Area [mAU*s]	Height [mAU]	Area %
1	4.856	MM	0.1798	658.59857	61.06145	96.2471
2	6.483	MM	0.2199	25.68021	1.94622	3.7529

Totals : 684.27878 63.00767

Results obtained with enhanced integrator!

Signal 3: MWD1 C, Sig=240,16 Ref=360,100

Peak #	RetTime [min]	Type	Width [min]	Area [mAU*s]	Height [mAU]	Area %
1	4.856	MM	0.1770	711.18018	66.97616	96.2430
2	6.483	MM	0.2160	27.76224	2.14248	3.7570

Totals : 738.94242 69.11864

Results obtained with enhanced integrator!

Signal 4: MWD1 D, Sig=254,16 Ref=360,100

Peak #	RetTime [min]	Type	Width [min]	Area [mAU*s]	Height [mAU]	Area %
1	4.856	MM	0.1777	526.38641	49.36498	96.0914
2	6.483	MM	0.2169	21.41133	1.64554	3.9086

Totals : 547.79775 51.01052

Results obtained with enhanced integrator!

Signal 5: MWD1 E, Sig=270,16 Ref=360,100

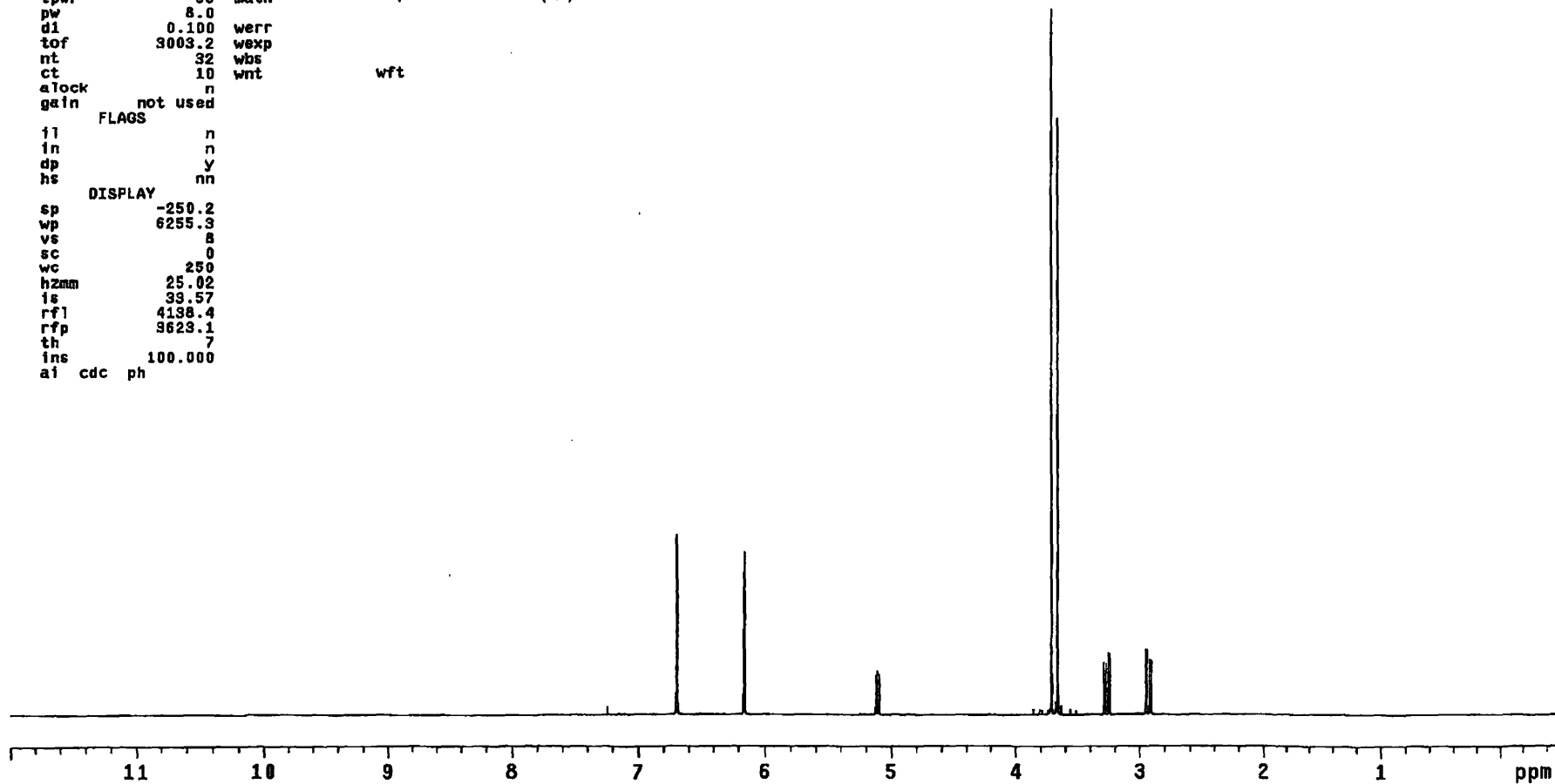
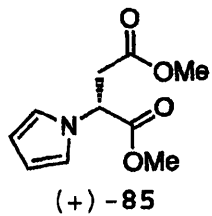
Peak #	RetTime [min]	Type	Width [min]	Area [mAU*s]	Height [mAU]	Area %
1	4.856	MM	0.1871	201.68265	17.96253	96.5863
2	6.483	MM	0.2061	7.12811	5.76507e-1	3.4137

Totals : 208.81076 18.53904

Appendix B.

Spectra for Chapter II

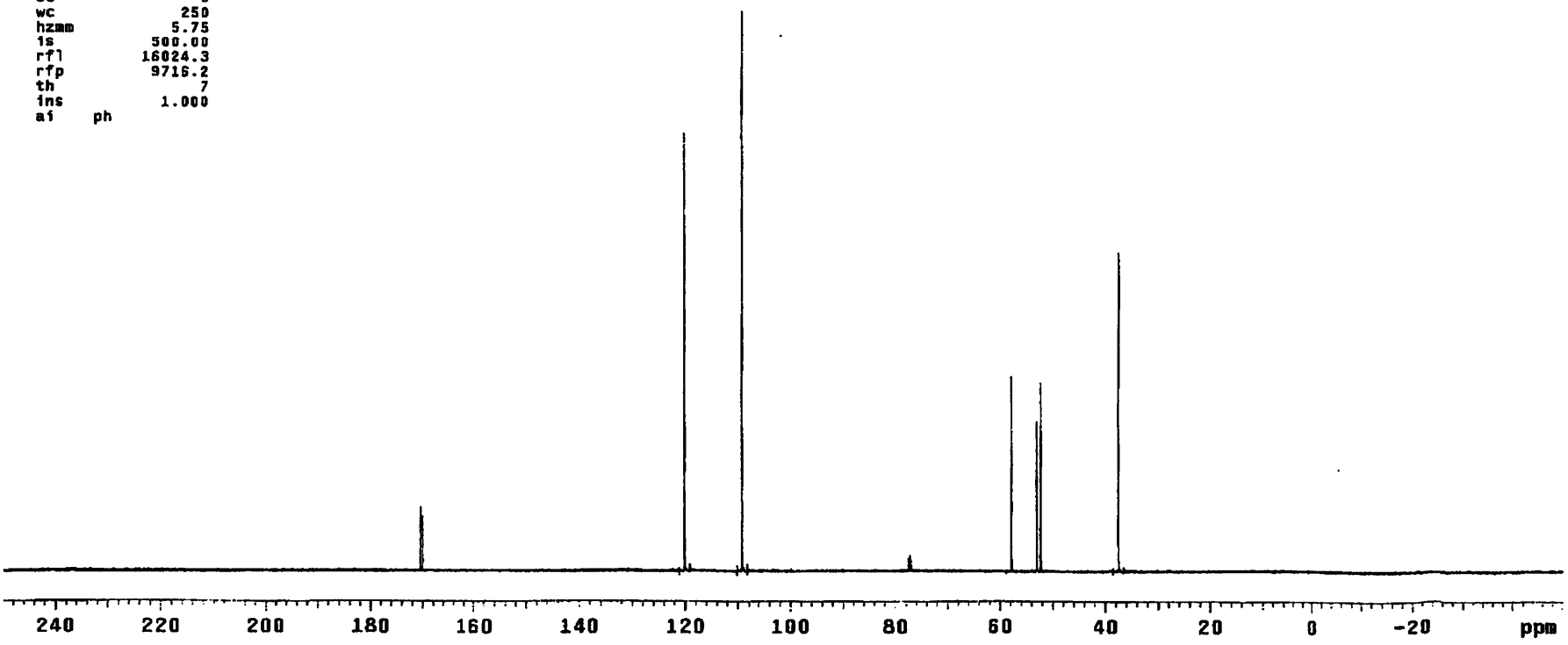
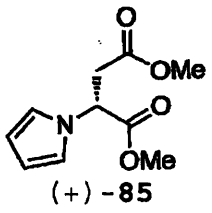
		DEC. & VT	
		dfrq	125.845
		dn	C13
		dpwr	30
		dof	0
		dm	nnn
		dmm	C
		dmf	200
ACQUISITION		dseq	
sfrq	500.435	dres	1.0
tn	H1	homo	n
at	4.999		
np	120102	PROCESSING	
sw	12012.0	wtfile	
fb	not used	proc	ft
bs	2	fn	262144
tpwr	56	math	f
pw	8.0		
d1	0.100	werr	
tof	3003.2	wexp	
nt	32	wbs	
ct	10	wnt	wft
alock	n		
gain	not used		
FLAGS			
fl	n		
in	n		
dp	y		
hs	nn		
DISPLAY			
sp	-250.2		
wp	6255.3		
vs	8		
sc	0		
wc	250		
hzmm	25.02		
is	39.57		
rf1	4198.4		
rfp	3623.1		
th	7		
ins	100.000		
ai	cdc	ph	



```

DEC. & VT
dfrq 500.229
dn H1
dpwr 38
dof -500.0
dm y
at 1.738 dmf 10000
np 131010 dseq
sw 37735.8 dres 1.0
fb not used homo n
bs 2
ss 1 lb PROCESSING 0.38
tpwr 53 wtfile
pw 6.9 proc ft
dl 0.763 fn 131072
tof 831.4 math f
nt 1000
ct 32 werr
alock n wexp
gain not used wbs
FLAGS wnt
il n
in n
dp y
hs nn
DISPLAY
sp -6308.1
wp 37735.8
vs 21
sc 0
wc 250
hzmm 5.75
ts 500.00
rfl 16024.3
rfp 9716.2
th 7
ins 1.000
ai ph

```

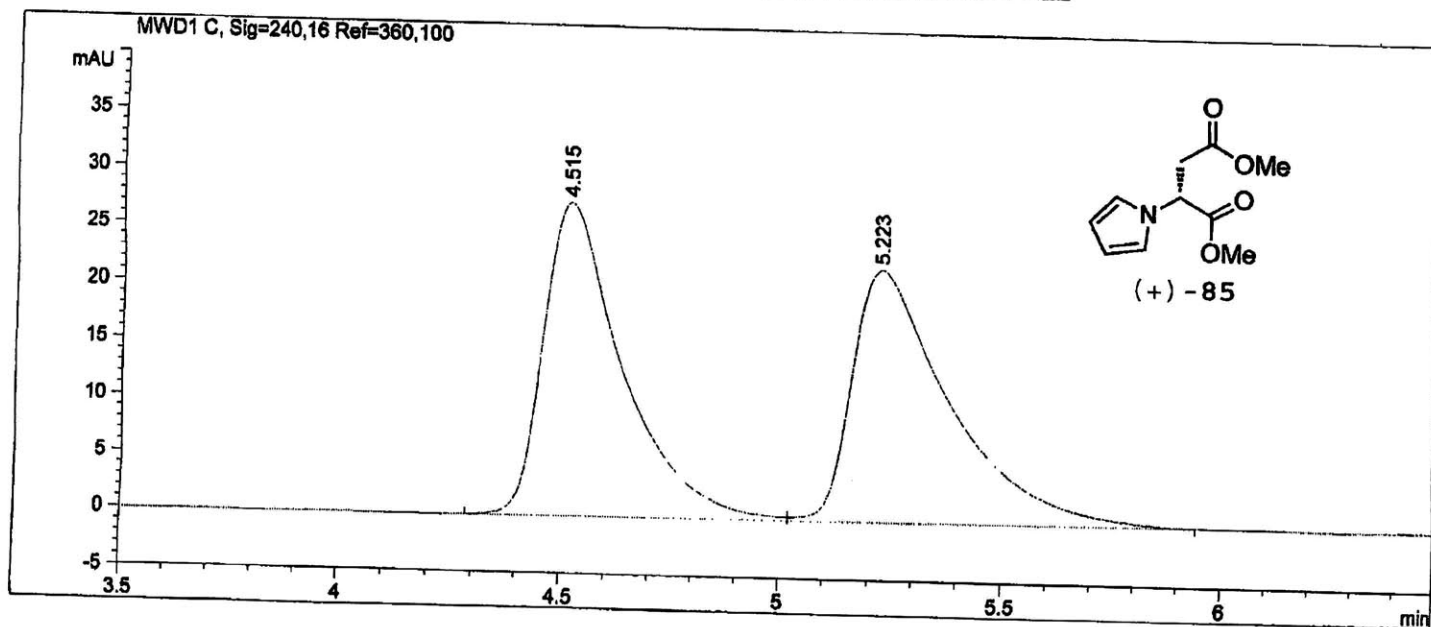


217

```

=====
Injection Date :                               Seq. Line : 1
Sample Name   :                               Location  : Vial 73
Acq. Operator :                               Inj       : 1
                                                    Inj Volume: 1 µl
Acq. Method   :
Last changed  :
Analysis Method :
Last changed  :
=====

```



=====
Area Percent Report
=====

```

Sorted By      : Signal
Multiplier    : 1.0000
Dilution      : 1.0000
Use Multiplier & Dilution Factor with ISTDs

```

Signal 1: MWD1 C, Sig=240,16 Ref=360,100

Peak #	RetTime [min]	Type	Width [min]	Area [mAU*s]	Height [mAU]	Area %
1	4.515	BV	0.1810	342.47797	27.56392	50.0382
2	5.223	VB	0.2221	341.95474	22.15433	49.9618

Totals : 684.43271 49.71825

Results obtained with enhanced integrator!

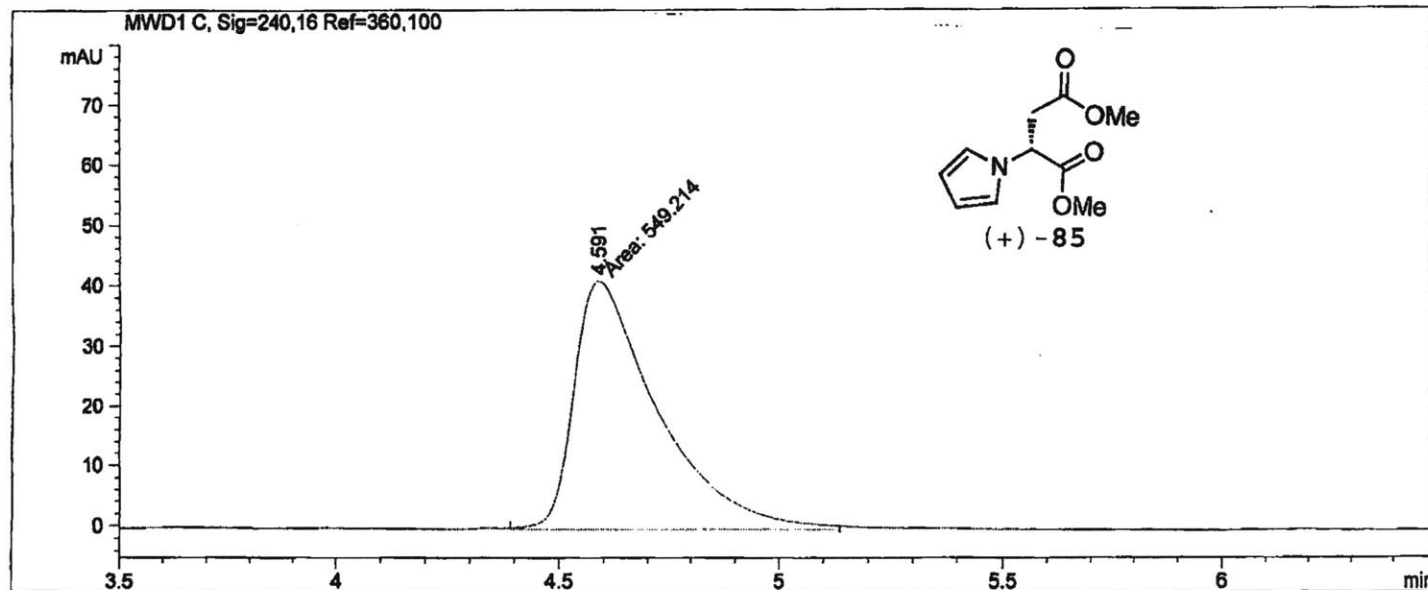
=====
*** End of Report ***

```

=====
Injection Date   :                               Seq. Line :    1
Sample Name     :                               Location  : Vial 91
Acq. Operator   :                               Inj       :    1
                                           Inj Volume: 1 µl

Acq. Method     :
Last changed    :
Analysis Method :
Last changed    :
=====

```



=====
Area Percent Report
=====

```

Sorted By       :      Signal
Multiplier      :      1.0000
Dilution        :      1.0000
Use Multiplier & Dilution Factor with ISTDs

```

Signal 1: MWD1 C, Sig=240,16 Ref=360,100

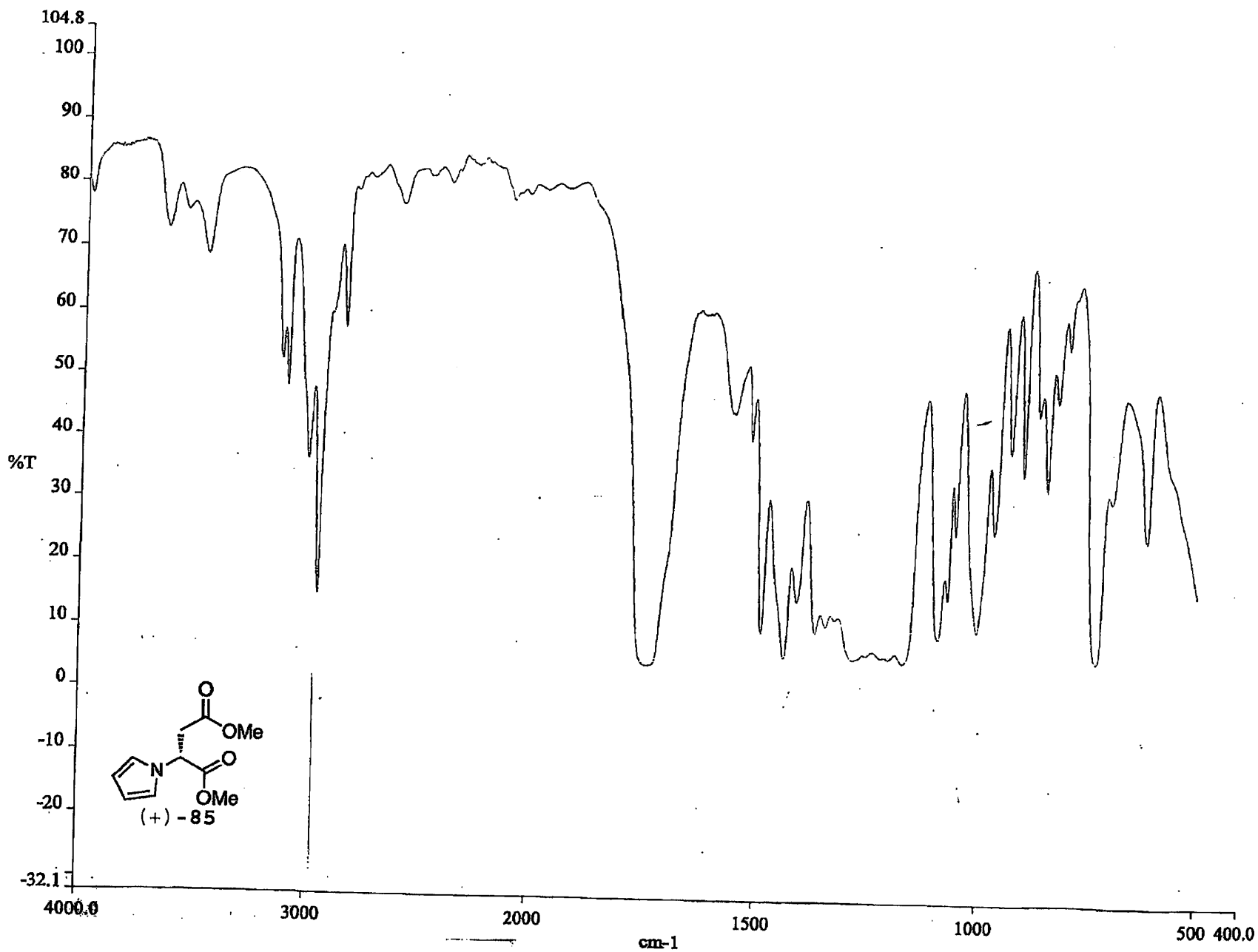
Peak #	RetTime [min]	Type	Width [min]	Area [mAU*s]	Height [mAU]	Area %
1	4.591	MM	0.2209	549.21417	41.44402	100.0000

Totals : 549.21417 41.44402

Results obtained with enhanced integrator!

=====
*** End of Report ***

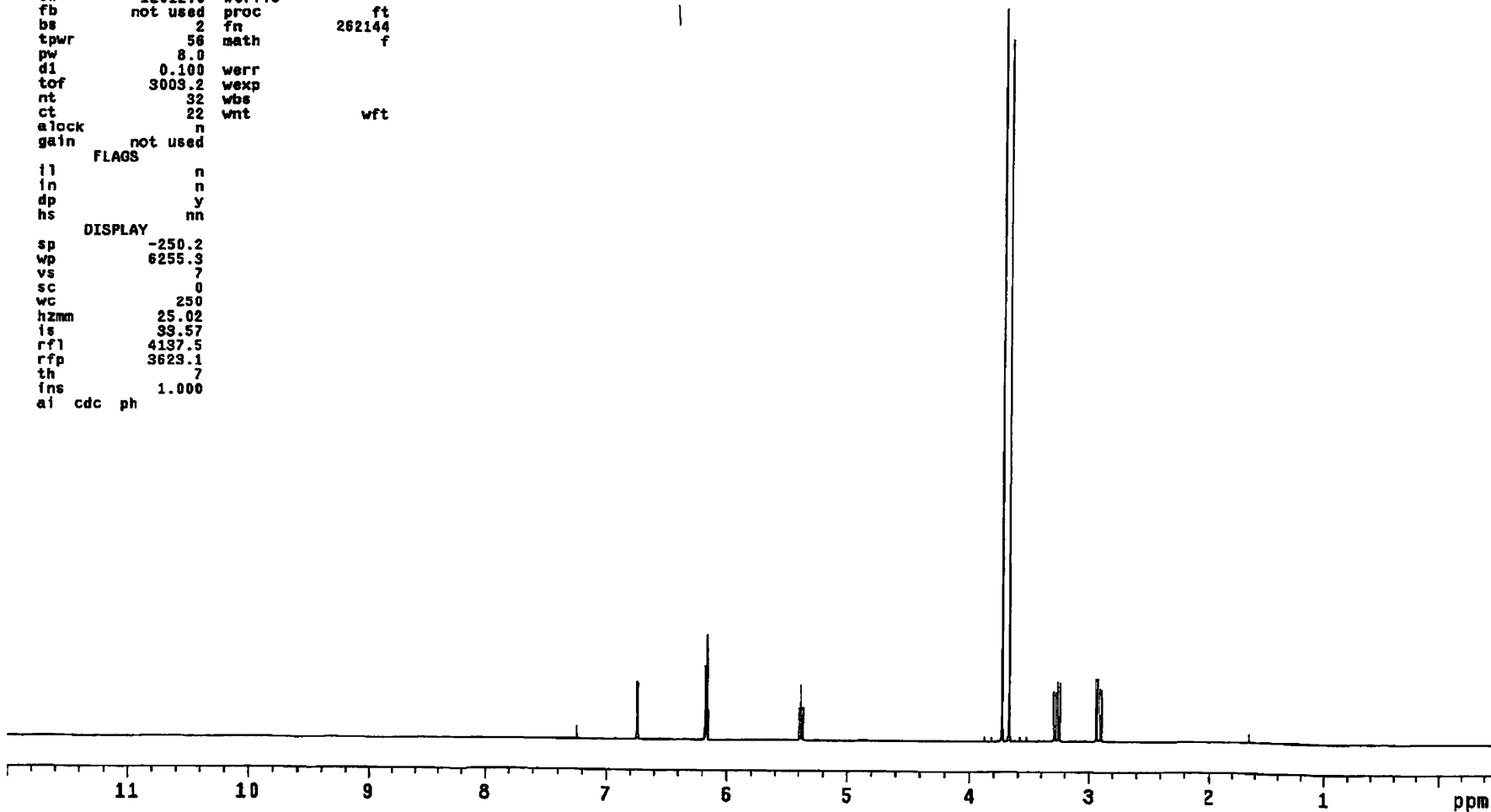
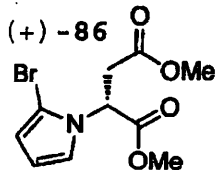
220




```

DEC. & VT
dfrq 125.845
dn C13
dpwr 30
dof 0
dm nnn
dmm c
dm7 200
ACQUISITION
sfrq 500.495
tn H1
at 4.989
np 120102
sw 12012.0
fb not used
bs 2
tpwr 56
pw 8.0
d1 0.100
tof 3009.2
nt 32
ct 22
alock n
gain not used
FLAGS
f1 n
in n
dp y
hs nn
DISPLAY
sp -250.2
wp 6255.3
vs 7
sc 0
wc 250
hzmm 25.02
is 39.57
rf1 4137.5
rfp 3629.1
th 7
fns 1.000
ai cdc ph
PROCESSING
wtfile
proc ft
fn 262144
math f
werr
wexp
wbs
wnt wft

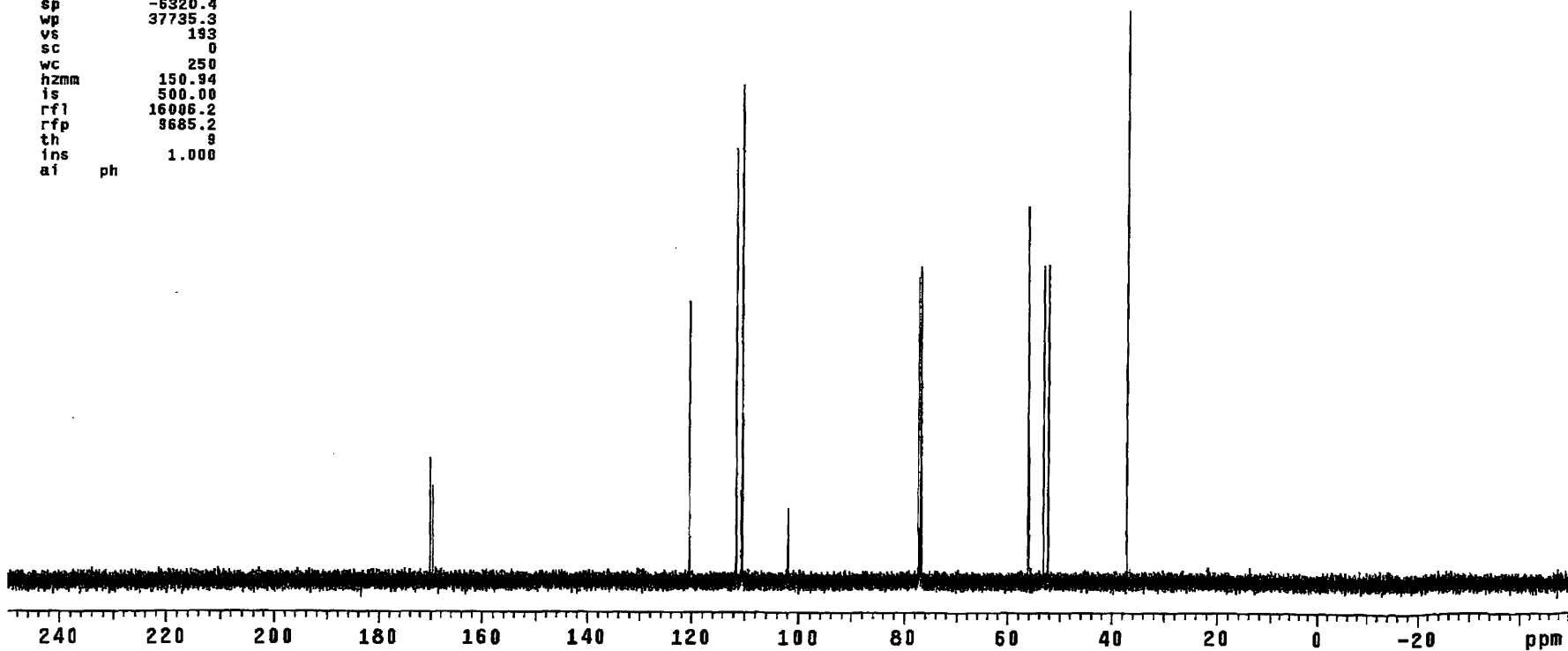
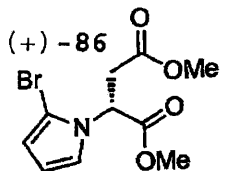
```



```

DEC. & VT
dfrq 500.229
dn H1
dpwr 38
dof -500.0
dm y
dmm w
dmf 10000
dseq 1.0
dres n
homo
ACQUISITION
sfrq 125.795
tn C13
at 1.736
np 131010
sw 37735.8
fb not used
bs 4
ss 1
tpwr 53
pw 6.9
dl 0.763
tof 631.4
nt 1e+06
ct 100
alock n
gain not used
FLAGS
il n
in n
dp y
hs nn
DISPLAY
sp -6320.4
wp 37735.3
vs 193
sc 0
wc 250
hzmm 150.94
ls 500.00
rf1 16006.2
rfp 9685.2
th 8
ins 1.000
ai ph
PROCESSING
fb 0.30
wtfile
proc ft
fn 131072
math f
werr
wexp
wbs
wnt

```



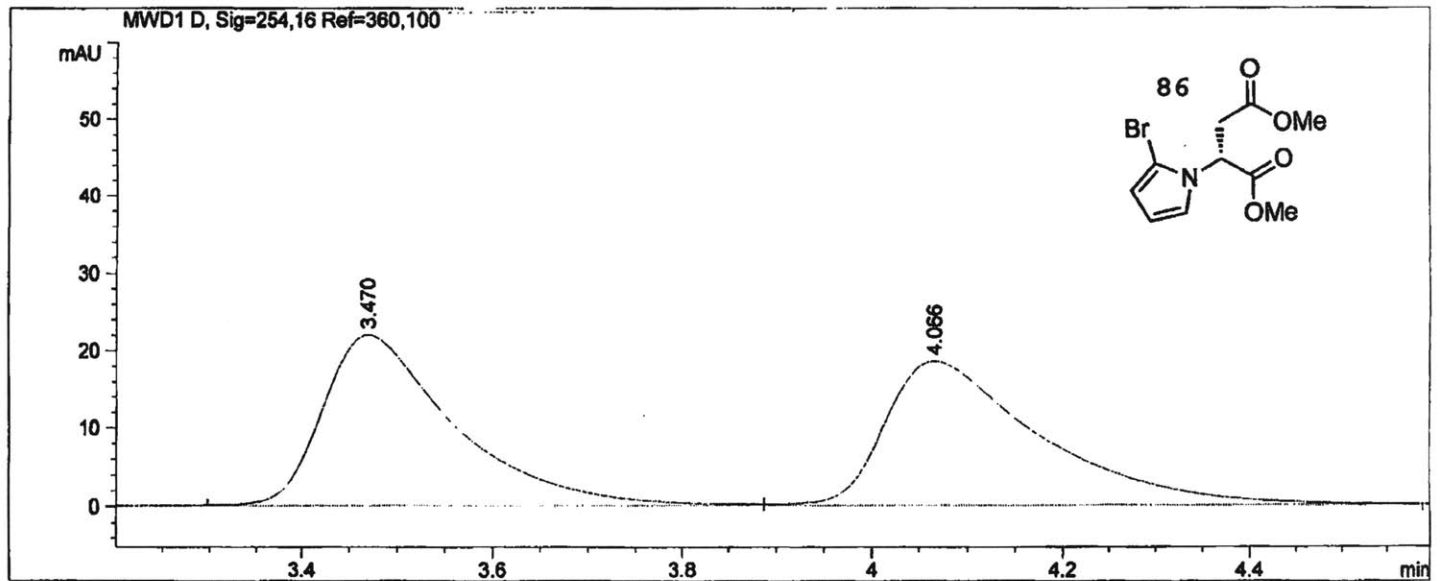
```

=====
Injection Date   :                               Seq. Line :    1
Sample Name     :                               Location  : Vial 74
Acq. Operator   :                               Inj       :    1
                                           Inj Volume: 1 µl

Acq. Method     :
Last changed    :

Analysis Method :
Last changed    :
=====

```



=====
Area Percent Report
=====

```

Sorted By      :      Signal
Multiplier     :      1.0000
Dilution      :      1.0000
Use Multiplier & Dilution Factor with ISTDs

```

Signal 1: MWD1 D, Sig=254,16 Ref=360,100

Peak #	RetTime [min]	Type	Width [min]	Area [mAU*s]	Height [mAU]	Area %
1	3.470	BV	0.1392	209.35068	21.96089	49.9378
2	4.066	VB	0.1622	209.87196	18.52020	50.0622

Totals : 419.22264 40.48109

Results obtained with enhanced integrator!

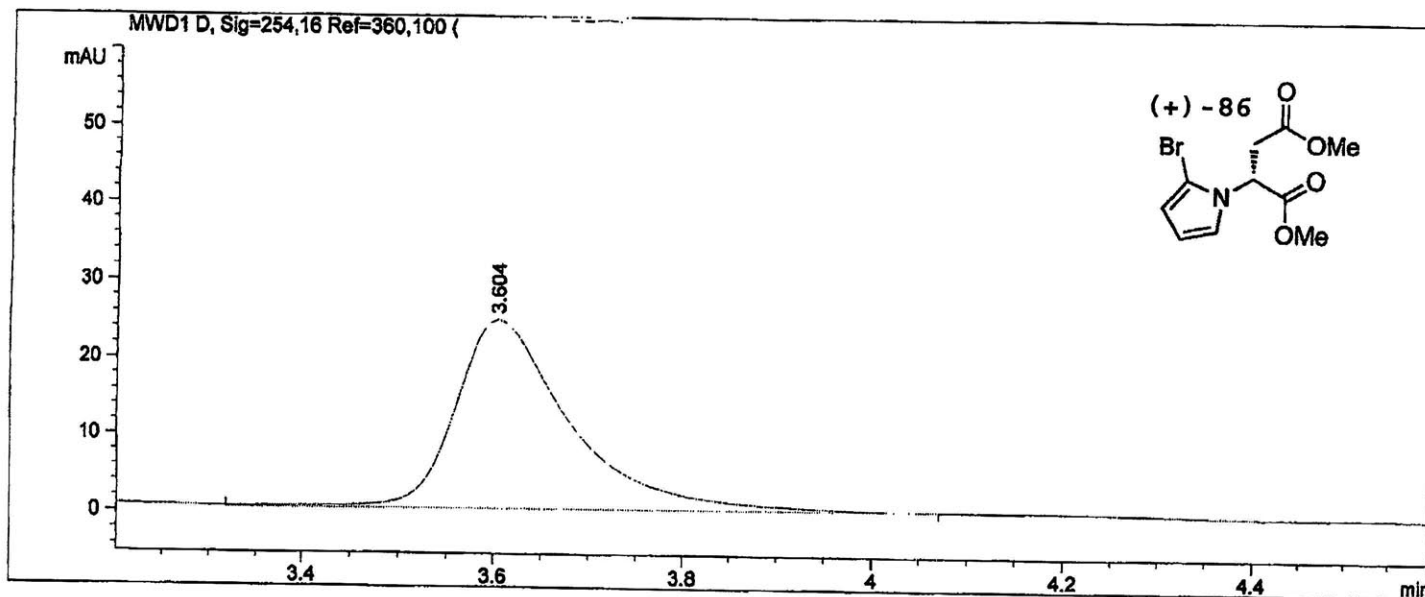
=====
*** End of Report ***

```

=====
Injection Date   :                               Seq. Line :    1
Sample Name     :                               Location  : Vial 91
Acq. Operator   :                               Inj       :    1
                                                    Inj Volume: 1 µl

Acq. Method    :
Last changed   :
Analysis Method:
Last changed   :
=====

```



```

=====
                          Area Percent Report
=====

```

```

Sorted By      :      Signal
Multiplier     :      1.0000
Dilution       :      1.0000
Use Multiplier & Dilution Factor with ISTDs

```

Signal 1: MWD1 D, Sig=254,16 Ref=360,100

Peak #	RetTime [min]	Type	Width [min]	Area [mAU*s]	Height [mAU]	Area %
1	3.604	VP	0.1247	207.81982	24.56680	100.0000

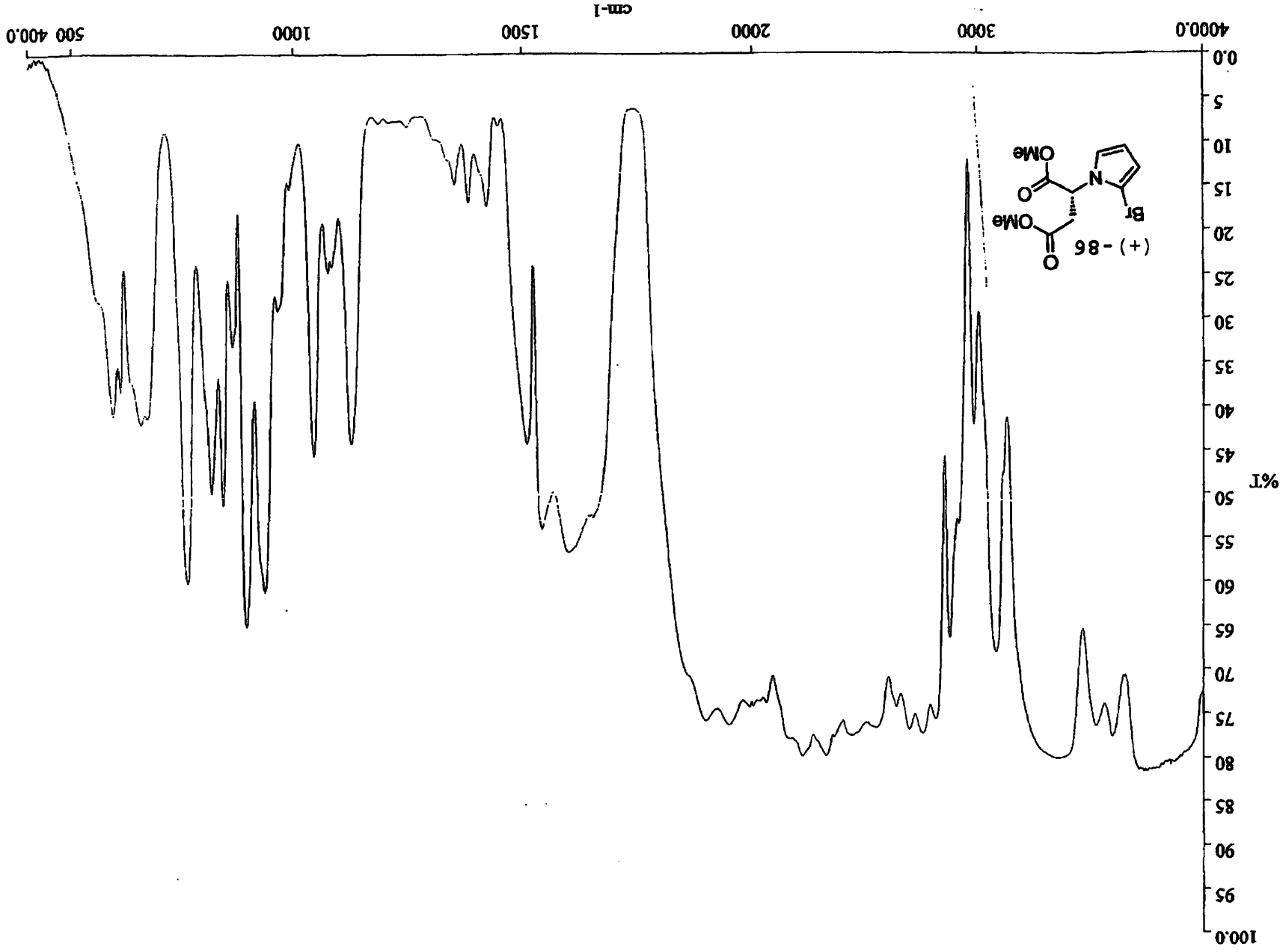
Totals : 207.81982 24.56680

Results obtained with enhanced integrator!

```

=====
*** End of Report ***

```



```

DEC. & VT      125.845
dfrq           C13
dn             30
dpwr          0
dof           nnn
dm            c
dmm           200
dmf           1.0
dseq         homo
dres         n
dwtfile      ft
dproc        262144
dfn          f
dmath        wft

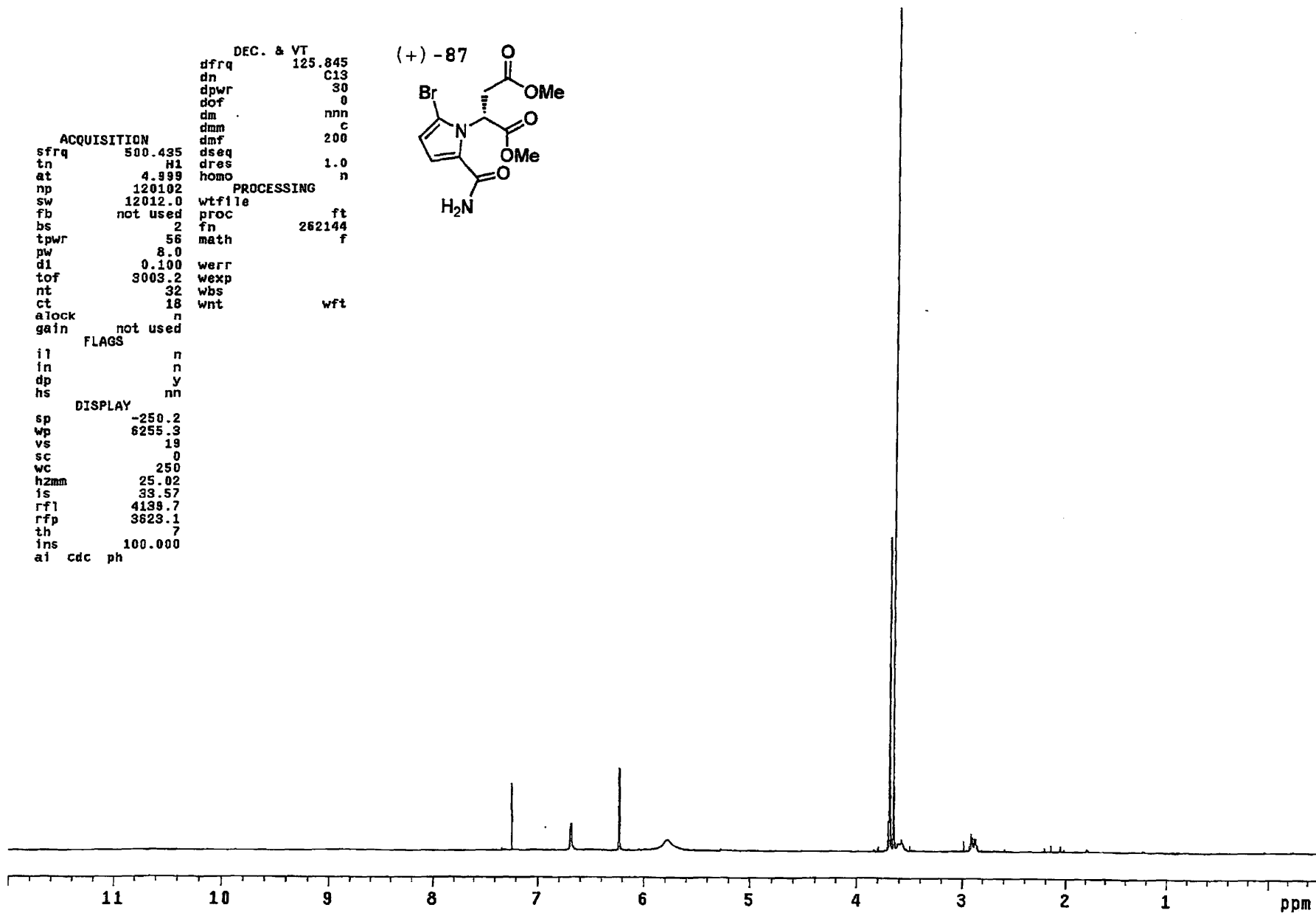
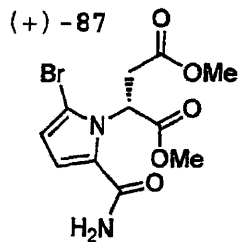
ACQUISITION
sfrq         500.435
tn           H1
at           4.999
np           120102
sw           12012.0
fb           not used
bs           2
tpwr         56
pw           8.0
d1           0.100
tof          3003.2
nt           32
ct           18
alock        n
gain         not used

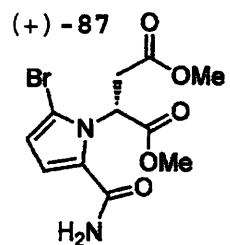
PROCESSING
werr
wexp
wbs
wnt

FLAGS
il           n
in           n
dp           y
hs           nn

DISPLAY
sp           -250.2
wp           6255.3
vs           19
sc           0
wc           250
hzmm         25.02
is           33.57
rfl          4138.7
rfp          3623.1
th           7
ins          100.000
ai cdc ph

```

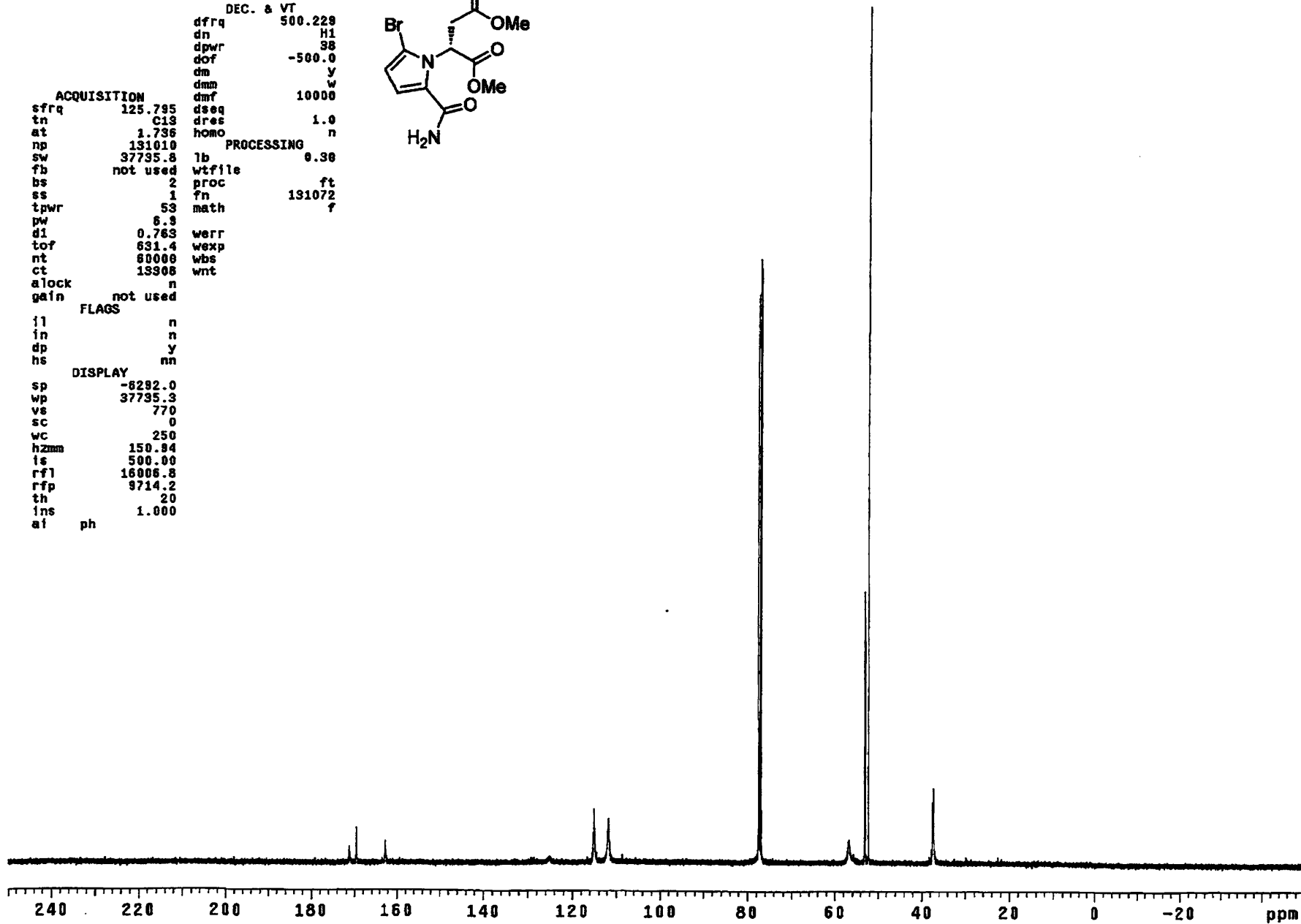


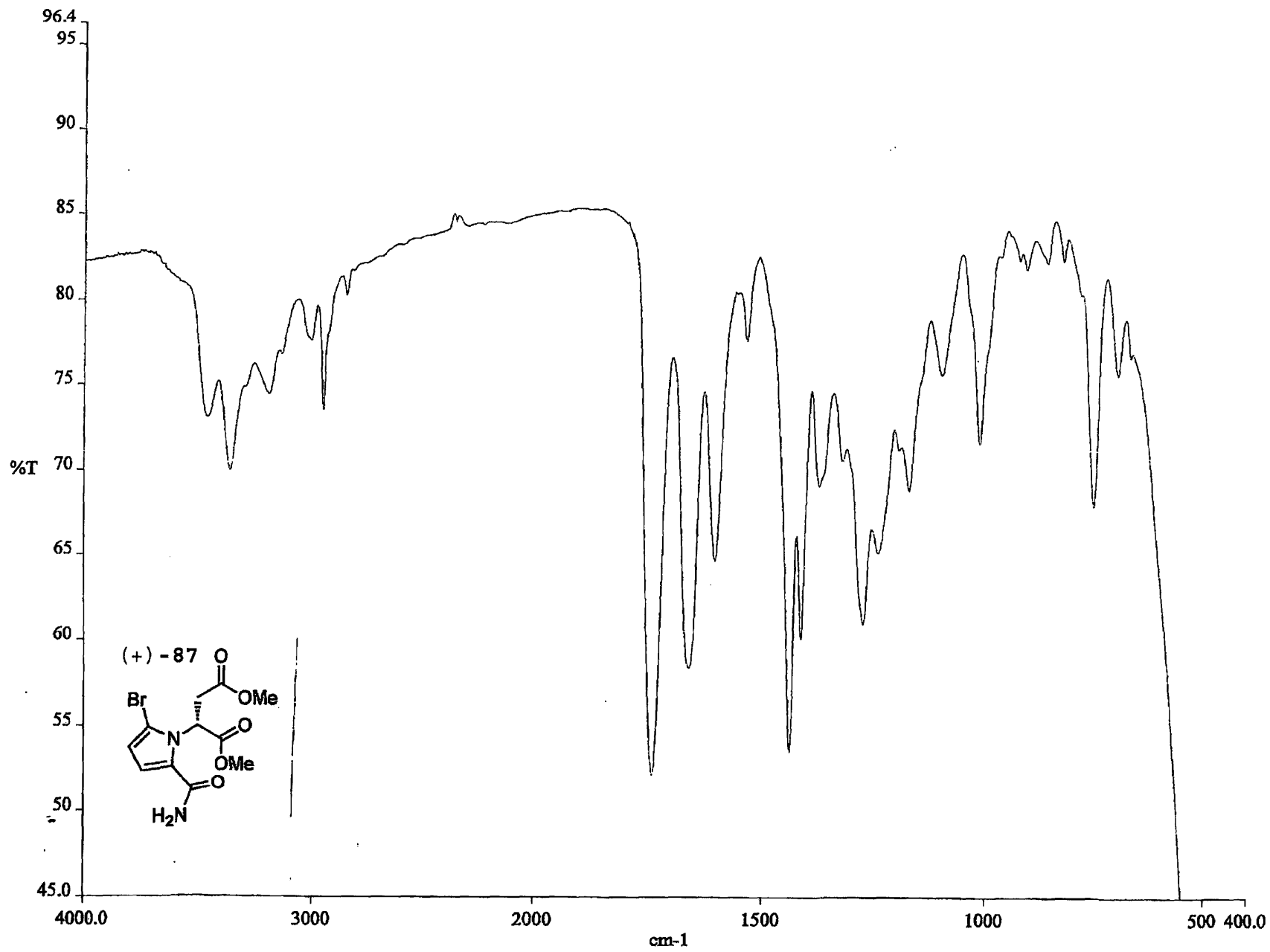


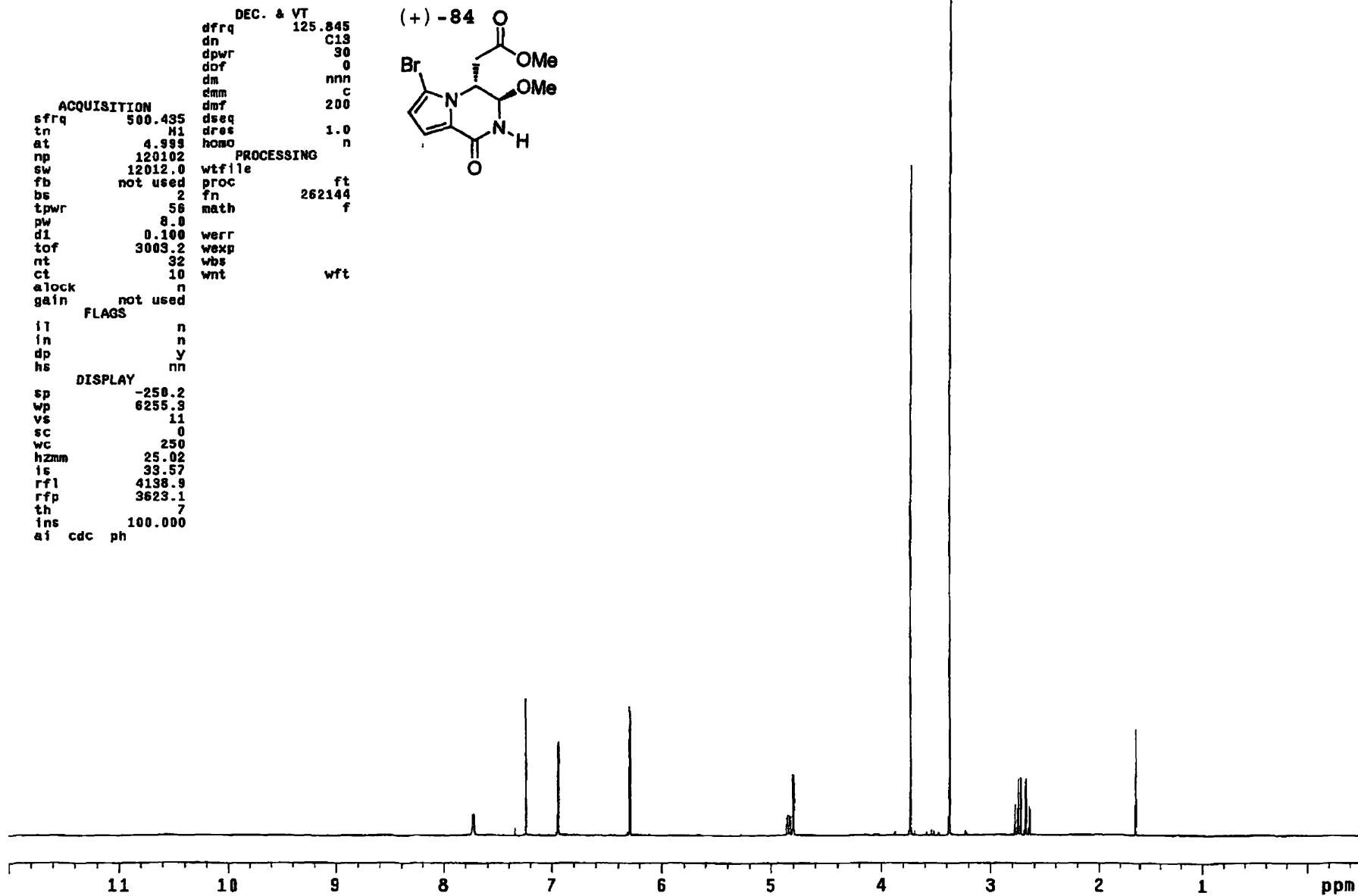
```

DEC. & VT      500.229
dfrq           H1
dn             38
dpwr          -500.0
dof           y
dm            w
dmm           10000
dmf           1.0
dseq         homo
dres         1.0
dres         n
PROCESSING
lb           0.30
wtfile
proc        ft
fn          131072
math        f
werr
wexp
wbs
wnt

ACQUISITION
sfrq        125.795
tn          C13
at          1.736
np          131010
sw          37735.8
fb          not used
bs          2
ss          1
tpwr        53
pw          8.9
d1          0.763
tof         631.4
nt          80000
ct          13308
alock       n
gain        not used
FLAGS
il          n
in          n
dp          y
hs          nn
DISPLAY
sp          -8282.0
wp          37735.3
vs          770
sc          0
wc          250
hzmm       150.84
is          500.00
rfl        16006.8
rfp        9714.2
th          20
ins        1.000
ai         ph
  
```



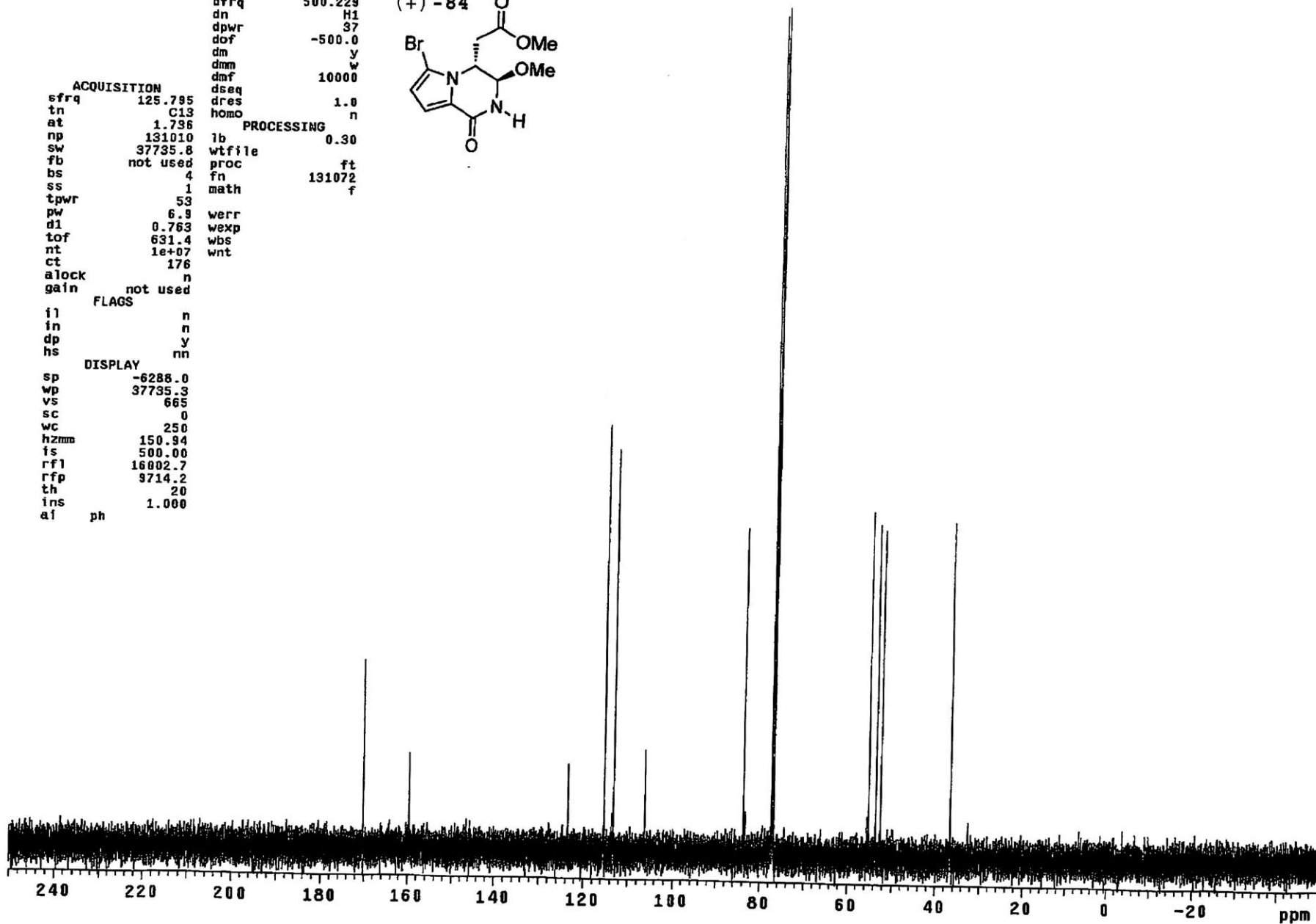
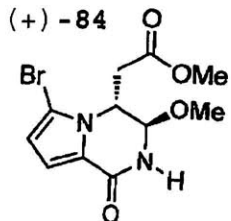




```

DEC. & VT
dfrq 500.229
dn H1
dpwr 37
dof -500.0
dm y
dmm w
dmf 10000
dseq
dres 1.0
homo n
ACQUISITION
sfrq 125.795
tn C13
at 1.796
np 131010
sw 37735.8
fb not used
bs 4
ss 1
tpwr 53
pw 6.9
d1 0.763
tof 631.4
nt 1e+07
ct 176
alock n
gain not used
FLAGS
ij n
in n
dp y
hs nn
DISPLAY
sp -6288.0
wp 37735.3
vs 665
sc 0
wc 250
hzmm 150.94
fs 500.00
rf1 16802.7
rfp 3714.2
th 20
ins 1.000
af ph
PROCESSING
lb 0.30
wtfile
proc ft
fn 131072
math f
werr
wexp
wbs
wnt

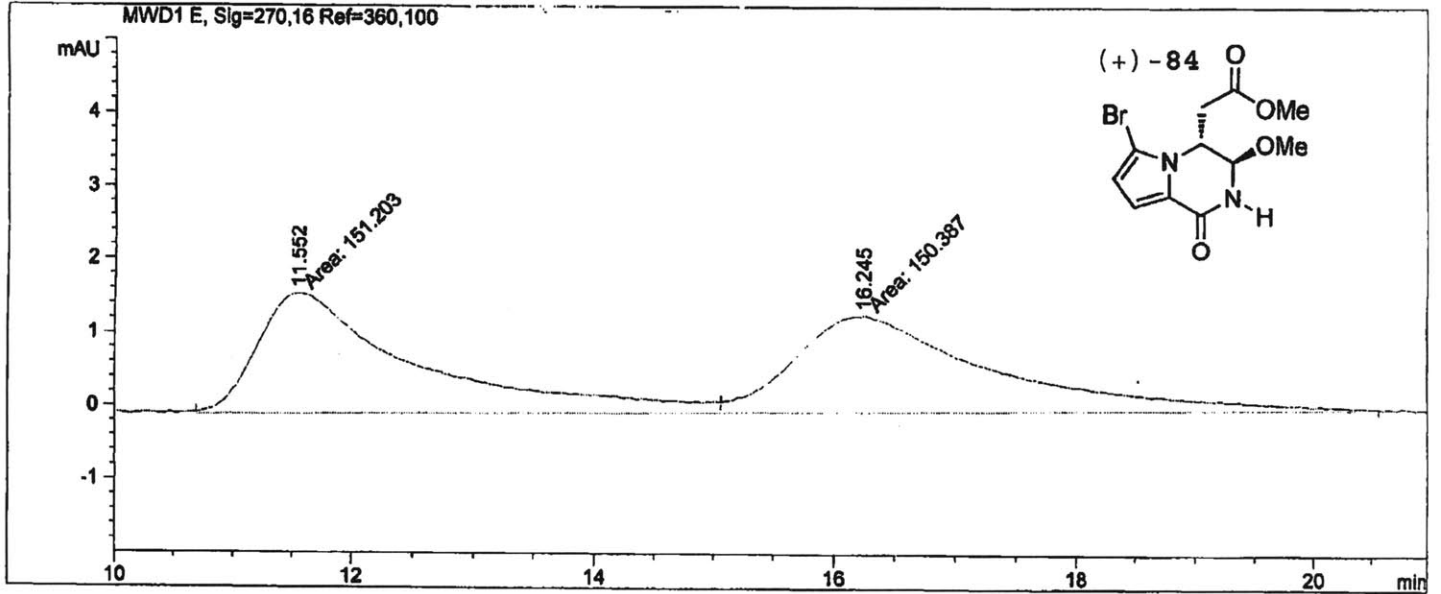
```



```

=====
Injection Date   :                               Seq. Line :    1
Sample Name     :                               Location  : Vial 91
Acq. Operator   :                               Inj       :    1
                                                    Inj Volume: 1 µl
Acq. Method     :
Last changed    :
Analysis Method :
Last changed    :
=====

```



=====
Area Percent Report
=====

```

Sorted By      :      Signal
Multiplier     :      1.0000
Dilution       :      1.0000
Use Multiplier & Dilution Factor with ISTDs

```

Signal 1: MWD1 E, Sig=270,16 Ref=360,100

Peak #	RetTime [min]	Type	Width [min]	Area [mAU*s]	Height [mAU]	Area %
1	11.552	MF	1.5397	151.20343	1.63667	50.1354
2	16.245	FM	1.9061	150.38686	1.31497	49.8646

Totals : 301.59029 2.95164

Results obtained with enhanced integrator!

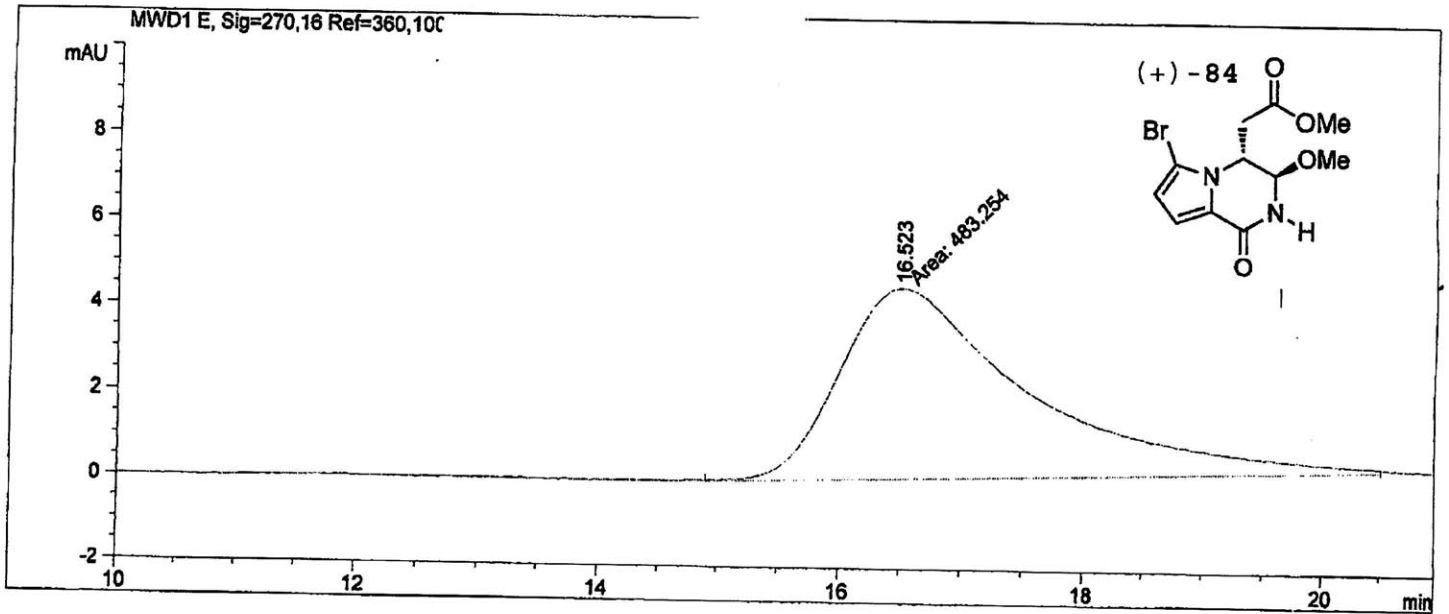
=====
*** End of Report ***

```

=====
Injection Date   :                               Seq. Line :    1
Sample Name     :                               Location  : Vial 91
Acq. Operator   :                               Inj       :    1
                                                    Inj Volume: 1 µl

Acq. Method    :
Last changed   :
Analysis Method:
Last changed   :
=====

```



=====
Area Percent Report
=====

```

Sorted By      :      Signal
Multiplier     :      1.0000
Dilution       :      1.0000
Use Multiplier & Dilution Factor with ISTDs

```

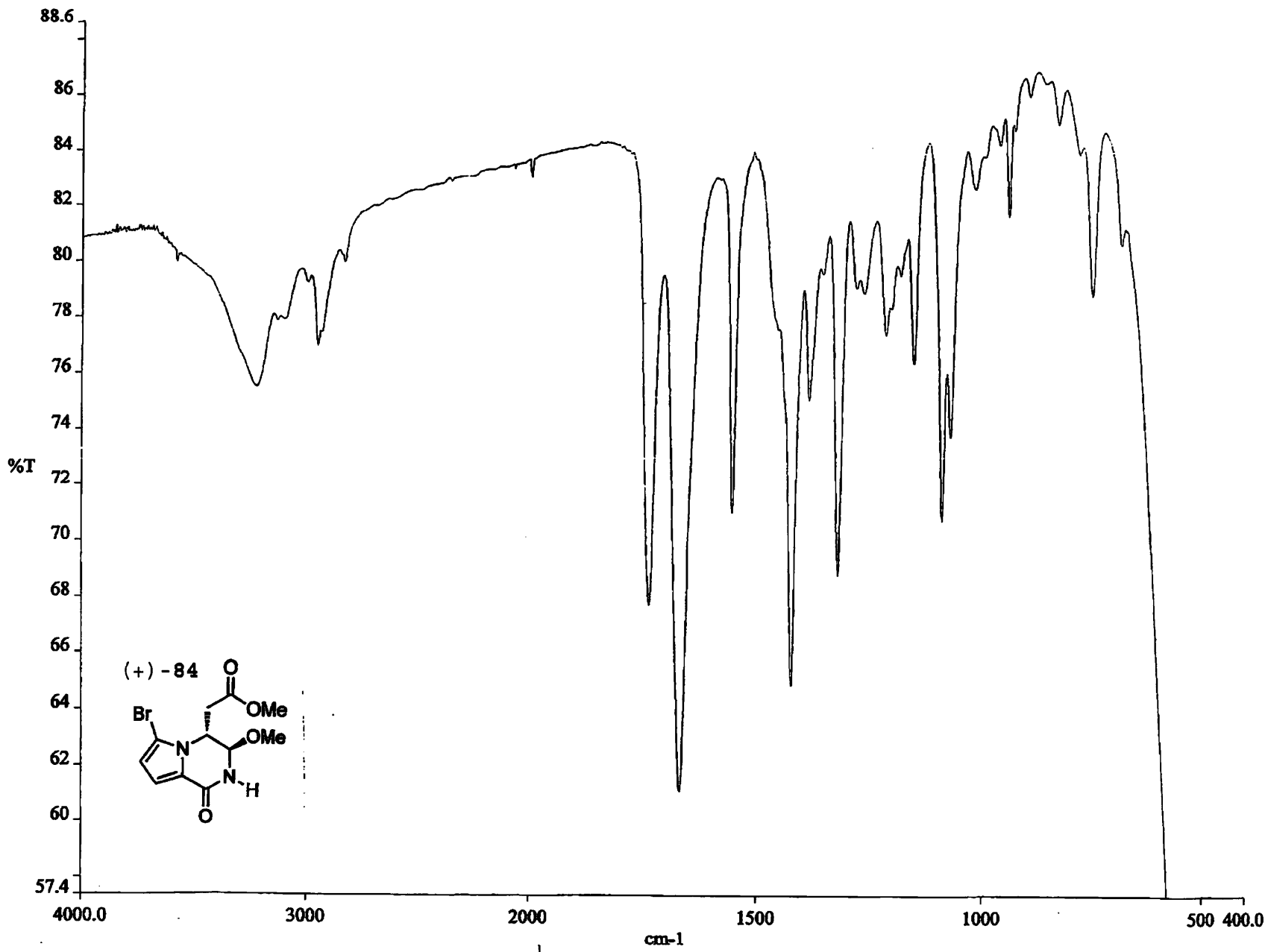
Signal 1: MWD1 E, Sig=270,16 Ref=360,100

Peak #	RetTime [min]	Type	Width [min]	Area [mAU*s]	Height [mAU]	Area %
1	16.523	MM	1.8067	483.25354	4.45788	100.0000

Totals : 483.25354 4.45788

Results obtained with enhanced integrator!

=====
*** End of Report ***



```

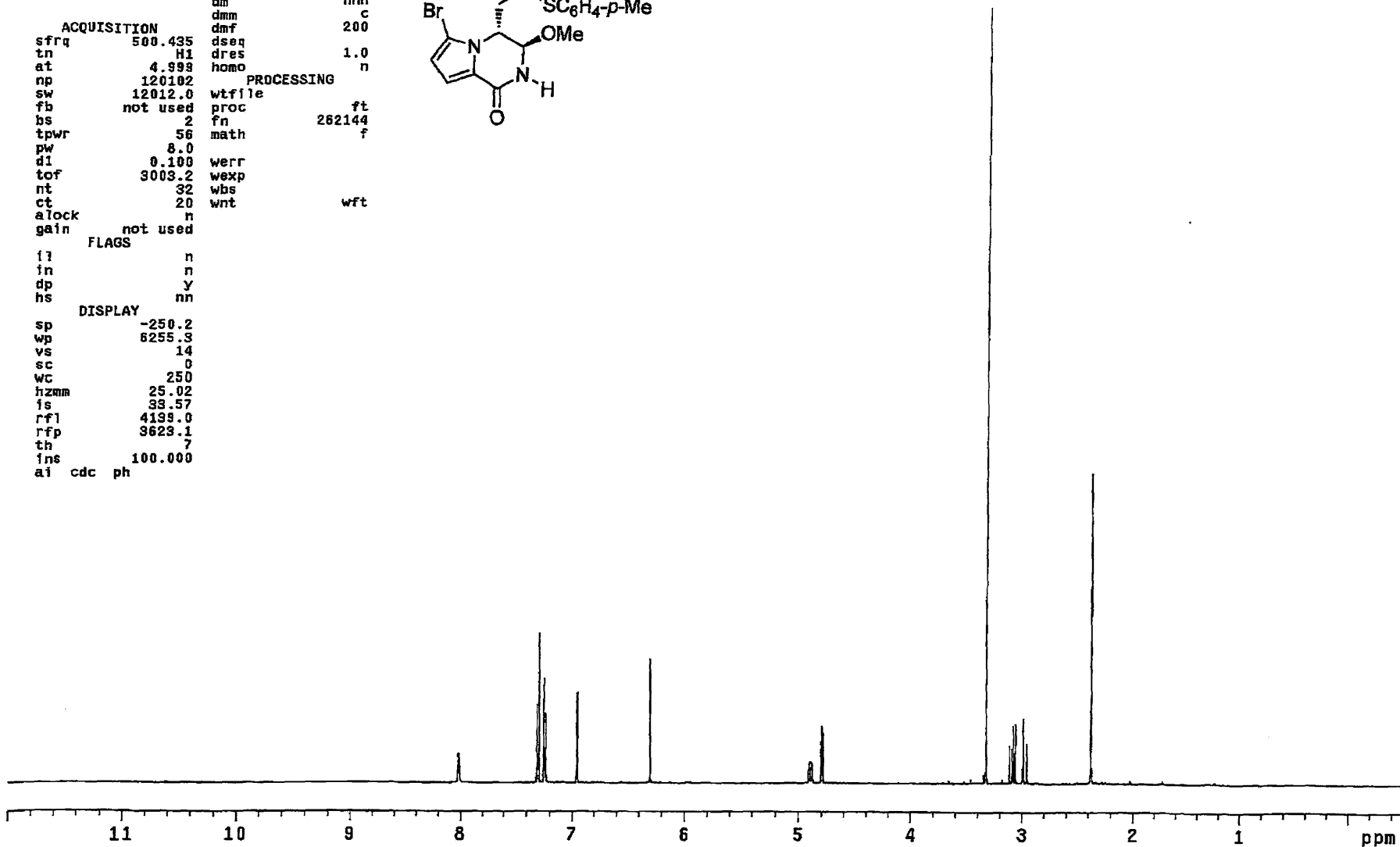
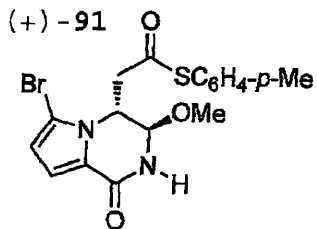
DEC. & VT      125.845
dfrq          C13
dn            30
dpwr         0
dof          0
dm           nnn
dmm          c
dmf         200
ACQUISITION
sfrq        500.435
tn          H1
at          4.999
np         120102
sw         12012.0
fb         not used
bs          2
tpwr        56
pw          8.0
d1          0.100
tof        3003.2
nt          32
ct          20
atock       n
gain        not used
          FLAGS
il          n
in          n
dp          y
hs          nn
          DISPLAY
sp         -250.2
wp         6255.3
vs         14
sc          0
wc         250
hzmm       25.02
is         33.57
rfl        4139.0
rfp        3623.1
th          7
ins        100.000
a1 cdc ph

```

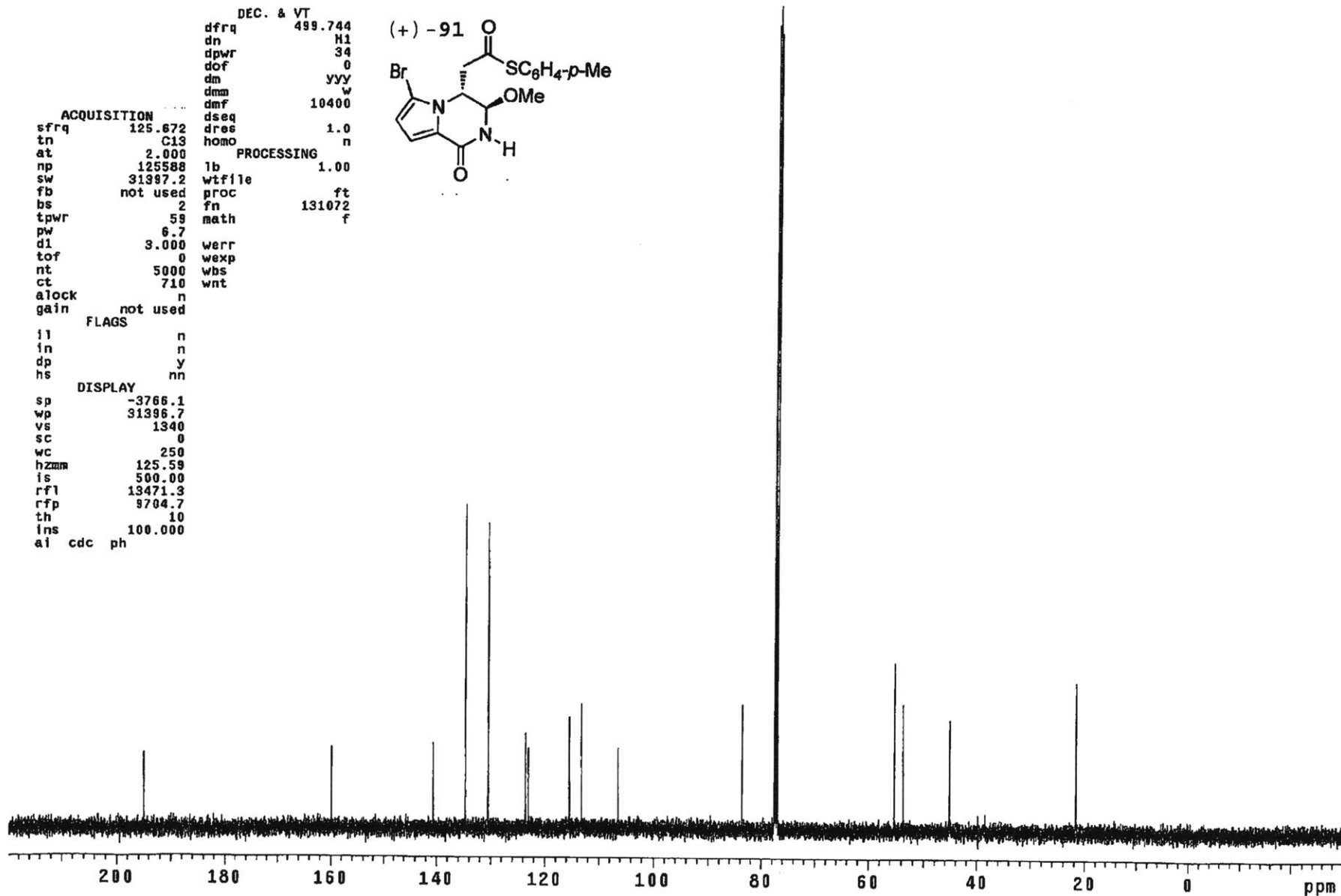
```

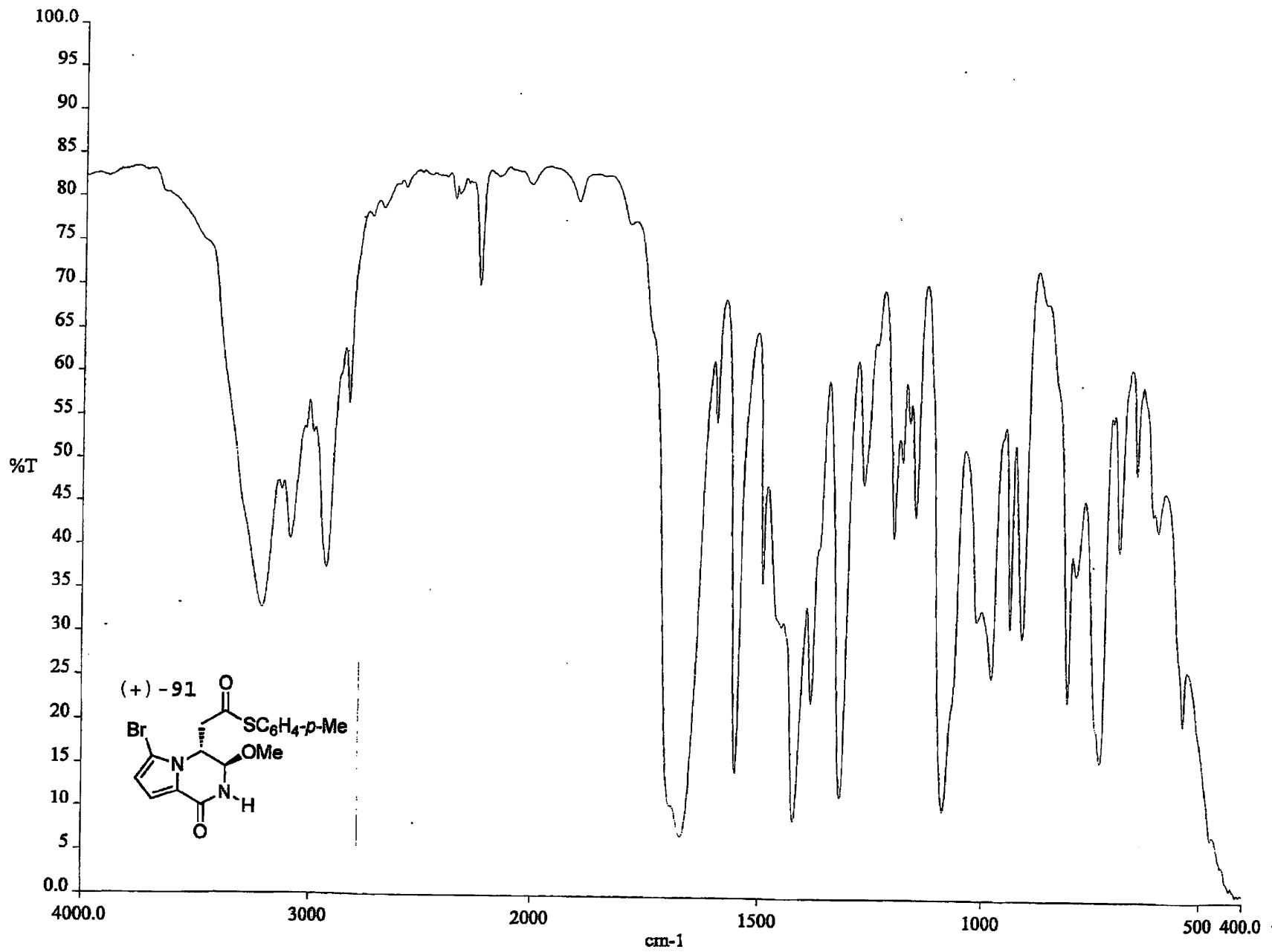
dseq         1.0
dres         n
homo         n
PROCESSING
wtfile
proc         ft
fn          262144
math         f
werr
wexp
wbs
wnt          wft

```



235






```

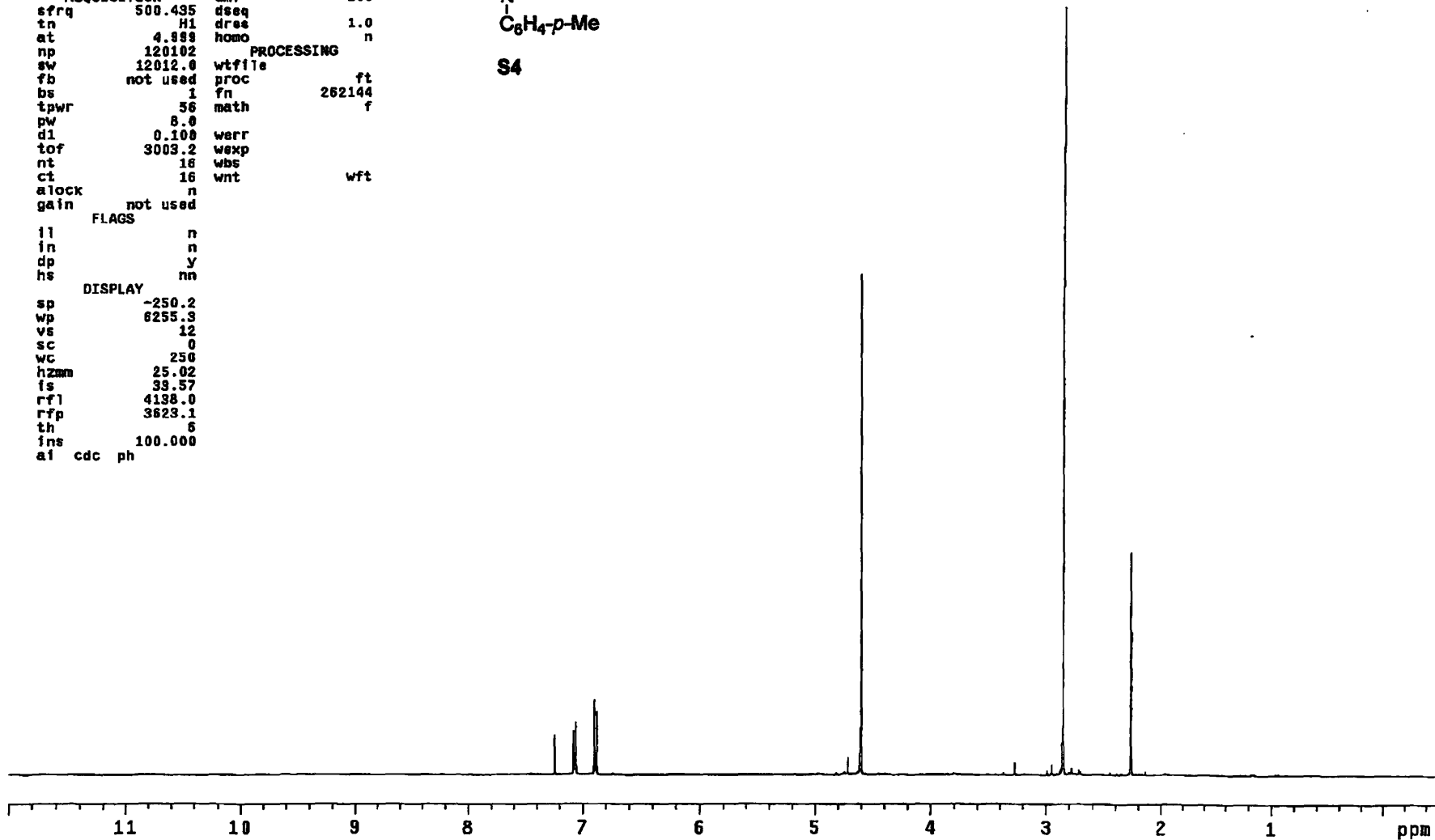
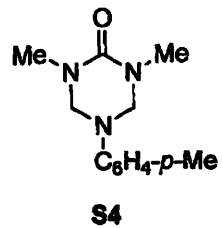
DEC. & VT
dfrq      125.845
dn        C13
dpwr      30
dof       0
dm        nnn
dmm       c
dmf       200
ACQUISITION
sfrq     500.435
tn       H1
at       4.888
np       120102
sw       12012.0
fb       not used
bs       1
tpwr     56
pw       8.0
d1       0.100
tof      3003.2
nt       16
ct       16
alock    n
gain     not used
        FLAGS
il       n
in       n
dp       y
hs       nn
        DISPLAY
sp       -250.2
wp       6255.3
vs       12
sc       0
wc       250
hzmm     25.02
fs       33.57
rfl      4138.0
rfp      3623.1
th       6
fns      100.000
al cdc ph

```

```

PROCESSING
wtfile
proc     ft
fn       262144
math     f
werr
wexp
wbs
wnt      wft

```



```

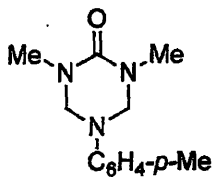
DEC. & VT
dfrq      500.229
dn        H1
dpwr      38
dof       -500.0
dm        Y
dmm       W
dmf       10000
ACQUISITION
sfrq      125.795
tn        C13
at        1.736
np        131010
sw        37735.8
fb        not used
bs        4
ss        1
tpwr      53
pw        8.9
d1        0.763
tof       631.4
nt        1e+08
ct        12
alock     n
gain      not used
FLAGS
il        n
in        n
dp        Y
hs        nn
DISPLAY
sp        -8332.3
wp        37735.3
vs        25
sc        0
wc        250
hzmm      150.94
is        500.00
rfl       16047.1
rfp       9714.2
th        20
ins       1.000
af        ph

```

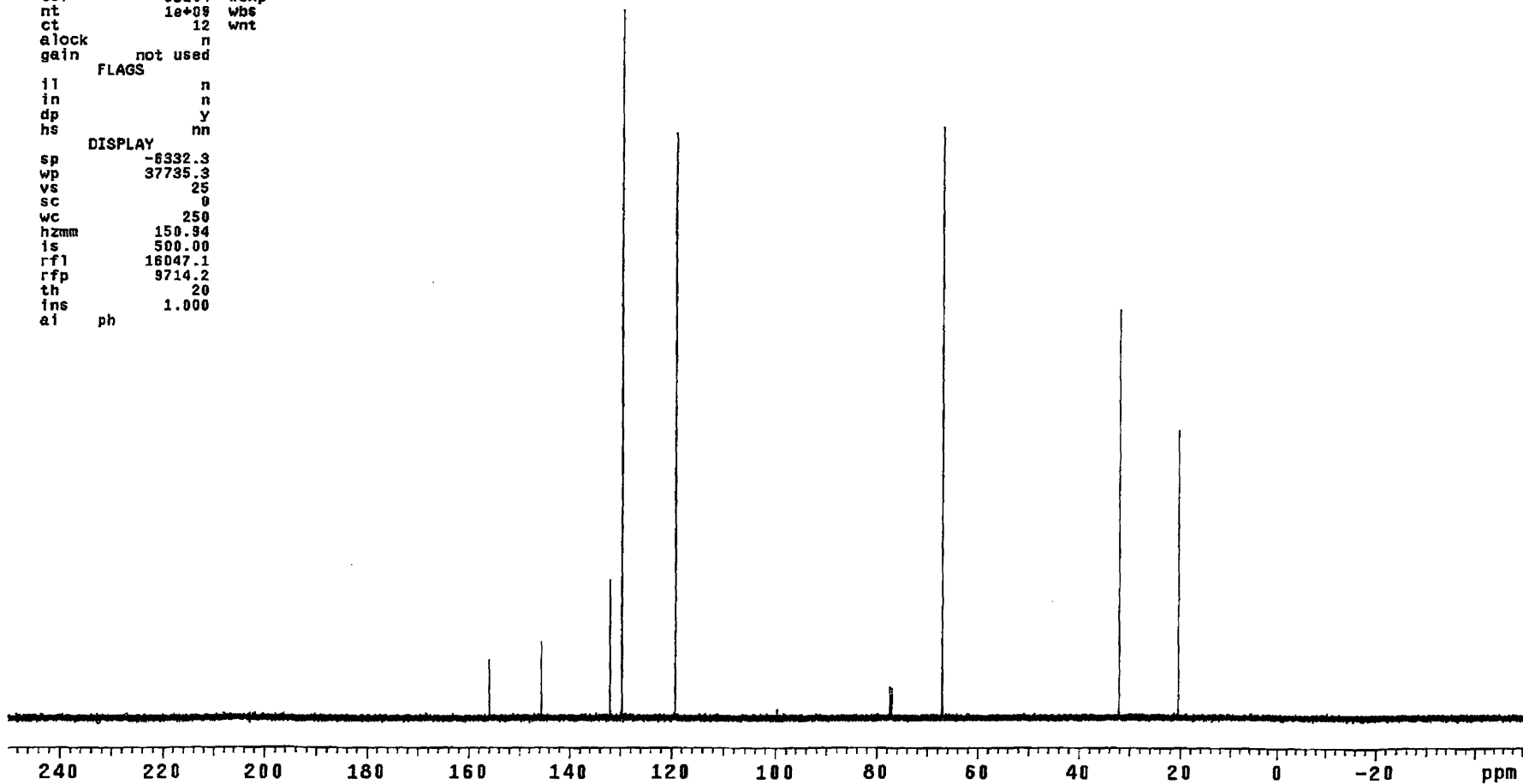
```

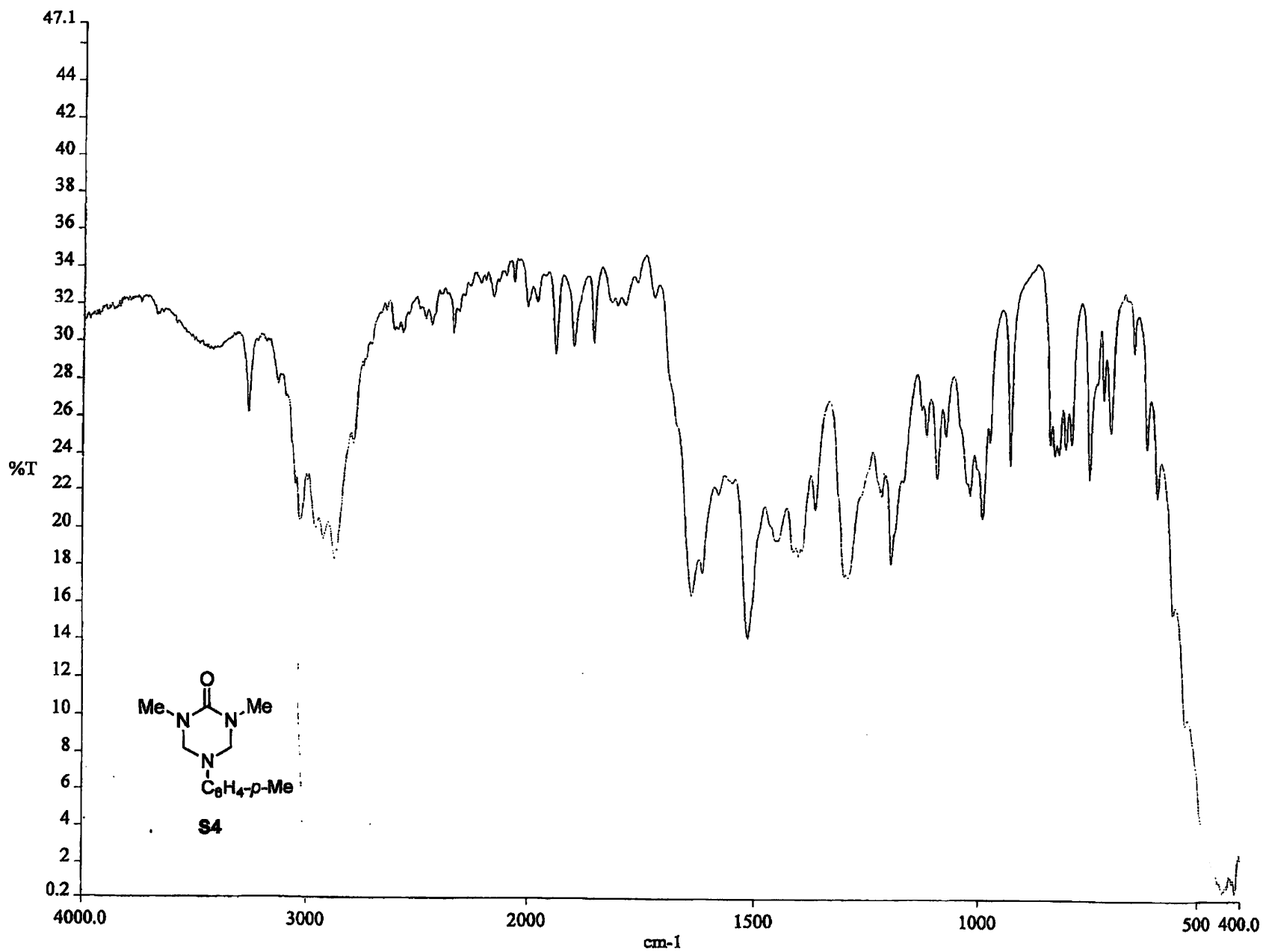
dseq      1.0
dres      n
homo      n
PROCESSING
lb        0.30
wtfile
proc      ft
fn        131072
math      f

```



S4

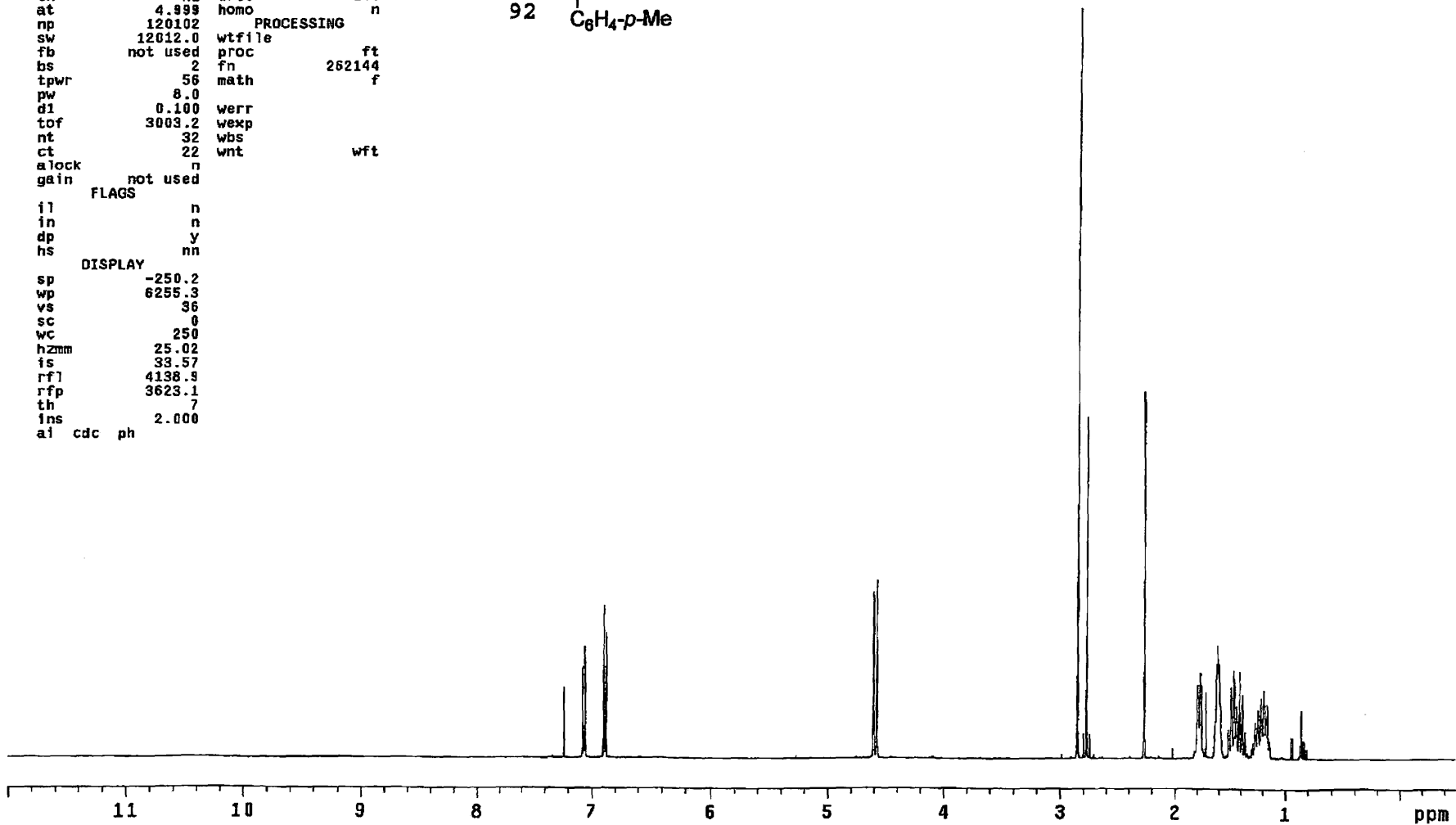
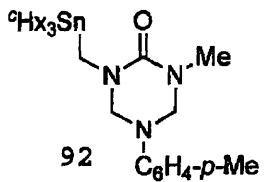




```

DEC. & VT
dfrq      125.845
dn        C13
dpwr      30
dof       0
dm        nnn
dmm       c
dmf       200
ACQUISITION
sfrq      500.435
tn        H1
at        4.999
np        120102
sw        12012.0
fb        not used
bs        2
tpwr      56
pw        8.0
d1        0.100
tof       3003.2
nt        32
ct        22
alock     n
gain      not used
          FLAGS
il        n
in        n
dp        Y
hs        nn
          DISPLAY
sp        -250.2
wp        6255.3
vs        36
sc        0
wc        250
hzmm      25.02
is        33.57
rfl       4138.9
rfp       3623.1
th        7
ins       2.000
ai cdc ph
PROCESSING
wtfile
proc      ft
fn        262144
math      f
werr
wexp
wbs
wnt       wft

```



```

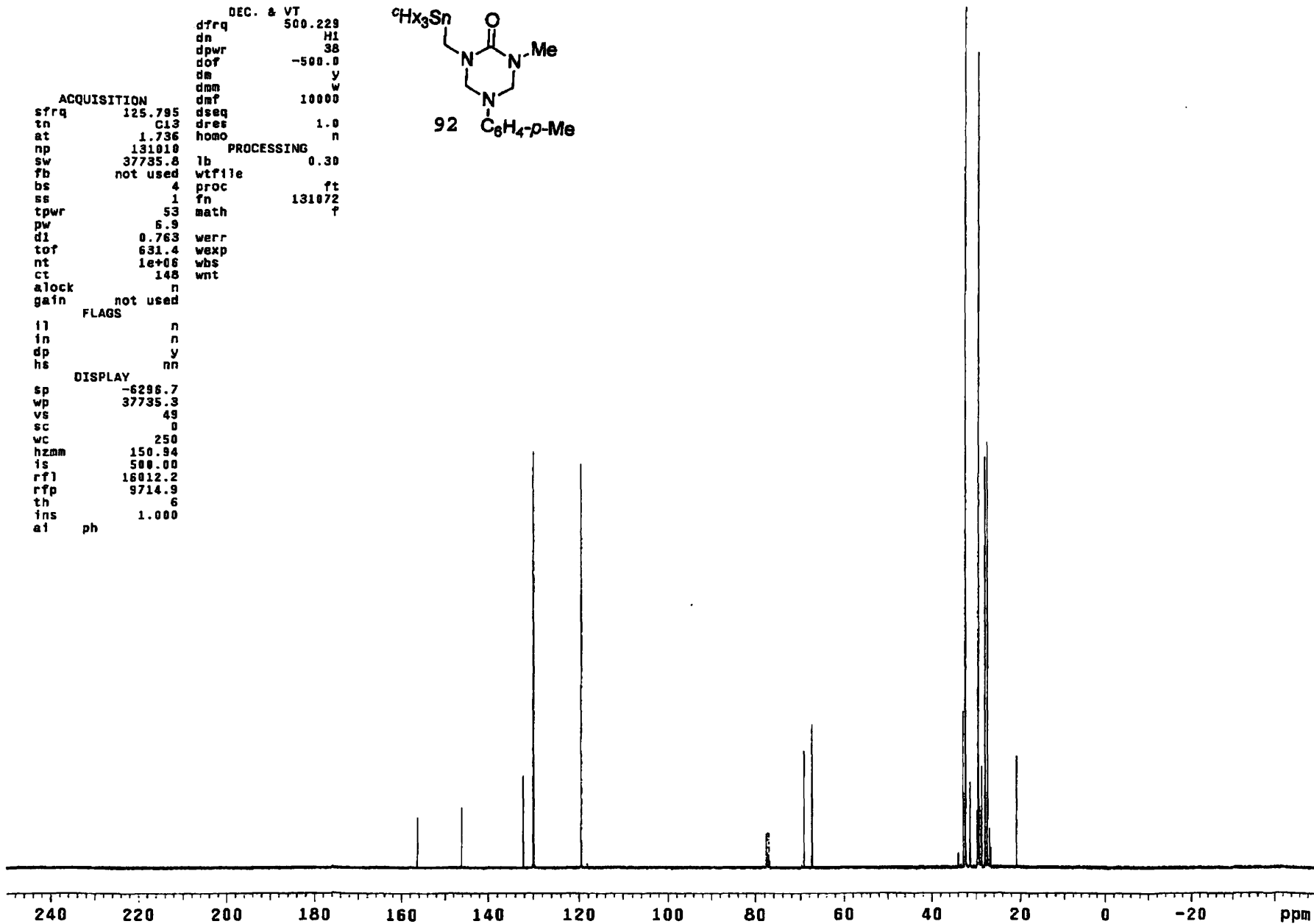
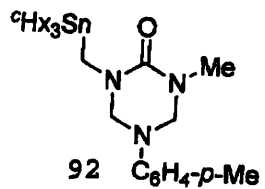
DEC. & VT
dfrq      500.229
dn        H1
dpwr      38
dof       -500.0
dm        y
dmm       w
dmf       10000
ACQUISITION
sfrq     125.795
tn       C13
at       1.736
np       131010
sw       37735.8
fb       not used
bs       4
ss       1
tpwr     53
pw       5.9
d1       0.763
tof      631.4
nt       1e+06
ct       148
alock    n
gain     not used
  FLAGS
  fl     n
  in     n
  dp     y
  hs     nn
  DISPLAY
sp      -6296.7
wp      37735.3
vs      49
sc      0
wc      250
hzmm    150.94
is      500.00
rfl     16012.2
rfp     9714.9
th      6
ins     1.000
ai      ph

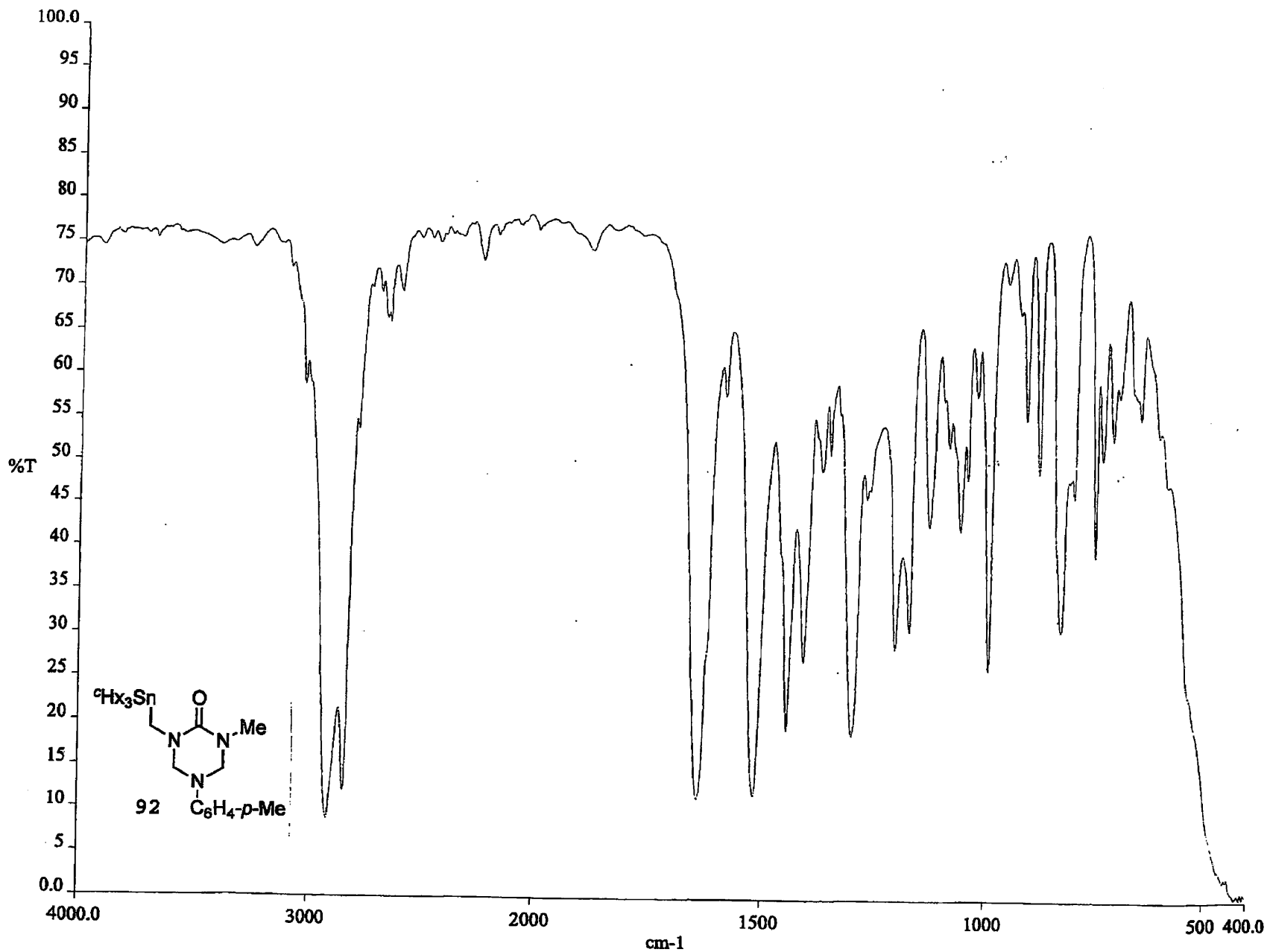
```

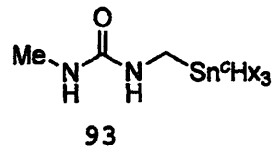
```

dseq      1.0
dres      n
homo      n
PROCESSING
lb        0.30
wtfile
proc      ft
fn        131072
math      ?

```



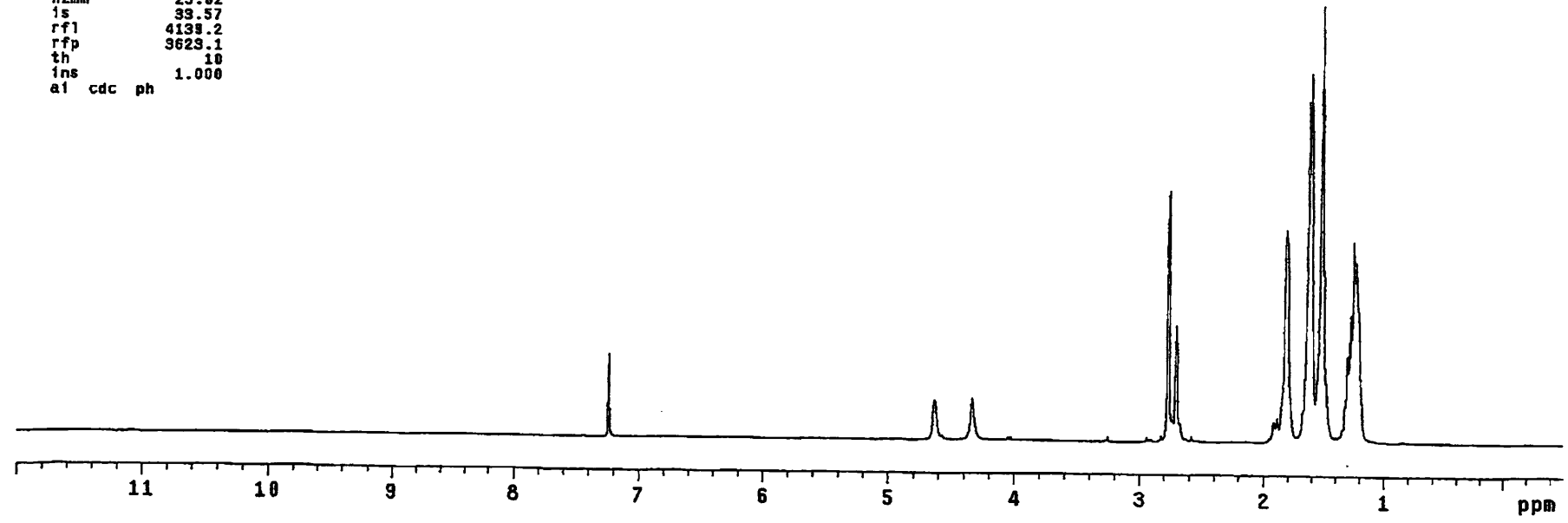




```

DEC. & VT
dfrq      125.845
dn         C13
dpwr       30
dof        0
dm         nnn
dmm        c
dmf        200
ACQUISITION
sfrq      500.435
tn         H1
at         4.888
np         120102
sw         12012.0
fb         not used
bs         1
tpwr       56
pw         8.0
d1         0.100
tof        3009.2
nt         16
ct         18
alock      n
gain       not used
          FLAGS
il         n
in         n
dp         y
hs         nn
          DISPLAY
sp         -250.2
wp         6255.3
vs         111
sc         0
wc         250
hzmm       25.02
is         39.57
rf1        4139.2
rfp        3623.1
th         10
ins        1.000
al cdc ph
          PROCESSING
wtfile
proc       ft
fn         262144
math       f
werr
wexp
wbs
wnt        wft

```



```

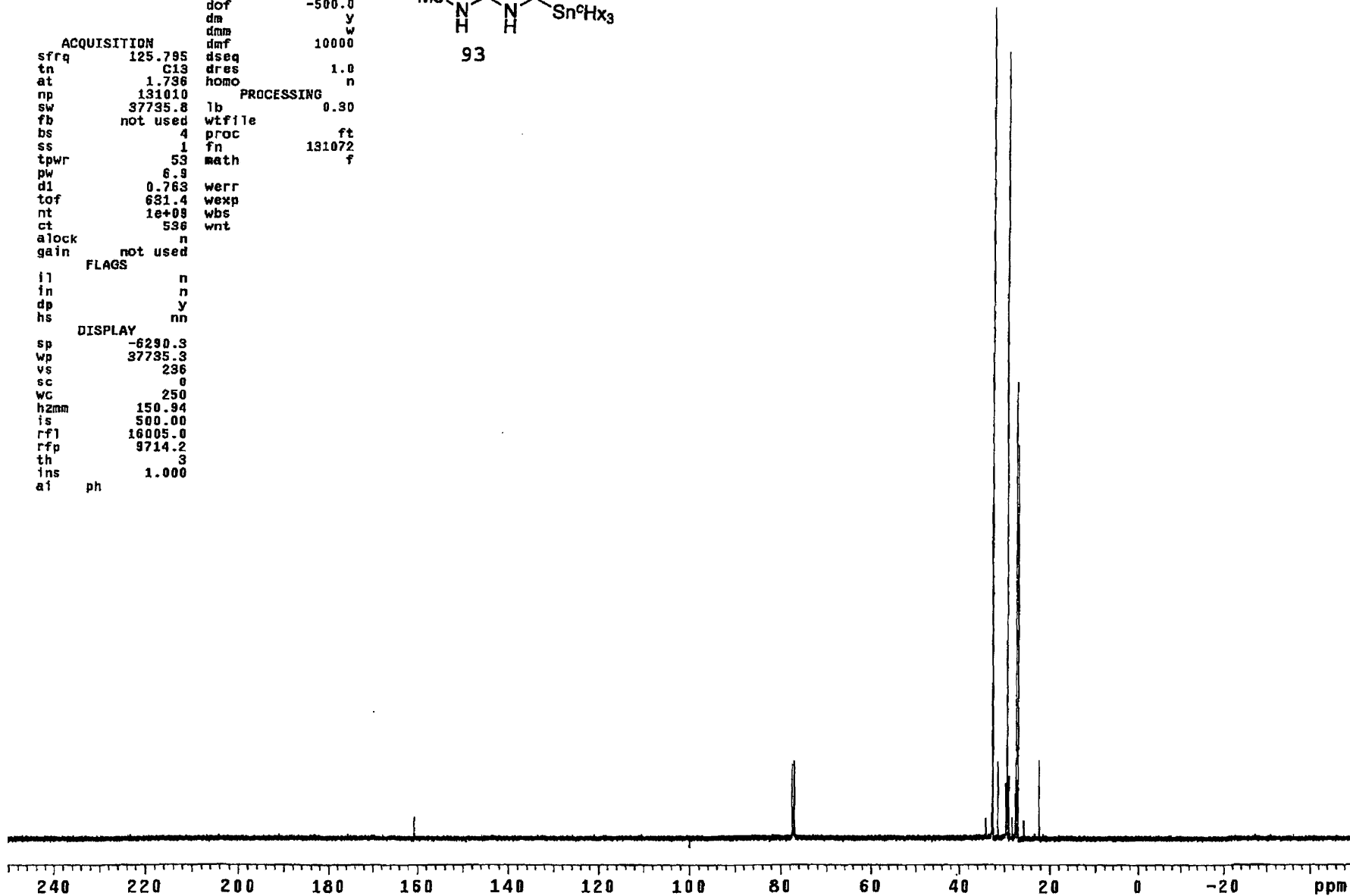
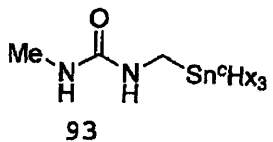
DEC. & VT
dfrq      500.229
dn        H1
dpwr      38
dof       -500.0
dm        y
dmb       w
dmf       10000
ACQUISITION
sfrq      125.795
tn        C13
at        1.736
np        131010
sw        37735.8
fb        not used
bs        4
ss        1
tpwr      53
pw        6.9
d1        0.763
tof       631.4
nt        1e+08
ct        536
alock     n
gain      not used
          FLAGS
il        n
in        n
dp        y
hs        nn
          DISPLAY
sp        -6290.3
wp        37735.3
vs        236
sc        0
wc        250
h2mm     150.94
is        500.00
rf1      16005.0
rfp      9714.2
th        3
ins      1.000
ai        ph

```

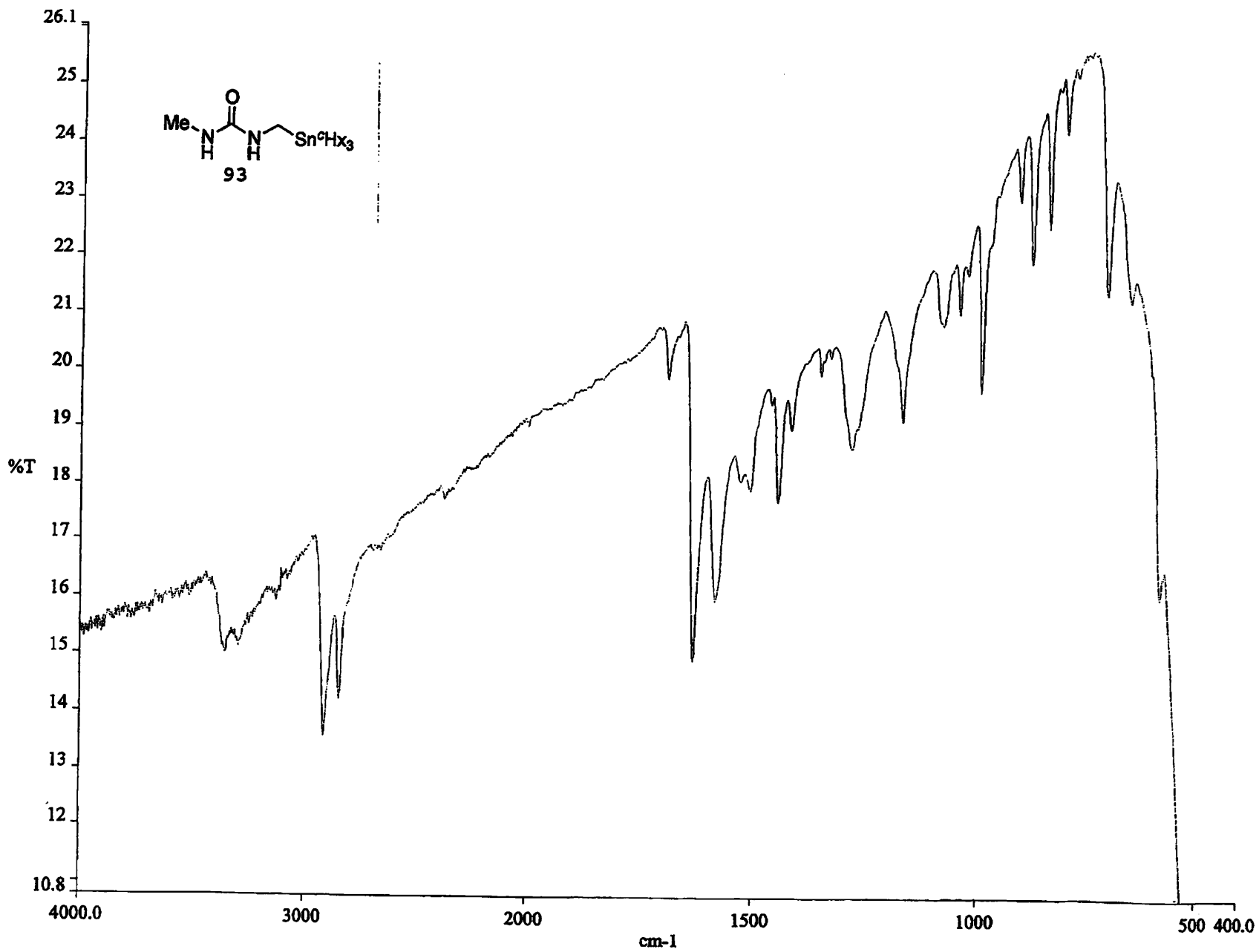
```

          PROCESSING
lb        0.30
wtfile
proc      ft
fn        131072
math      f
werr
wexp
wbs
wnt

```



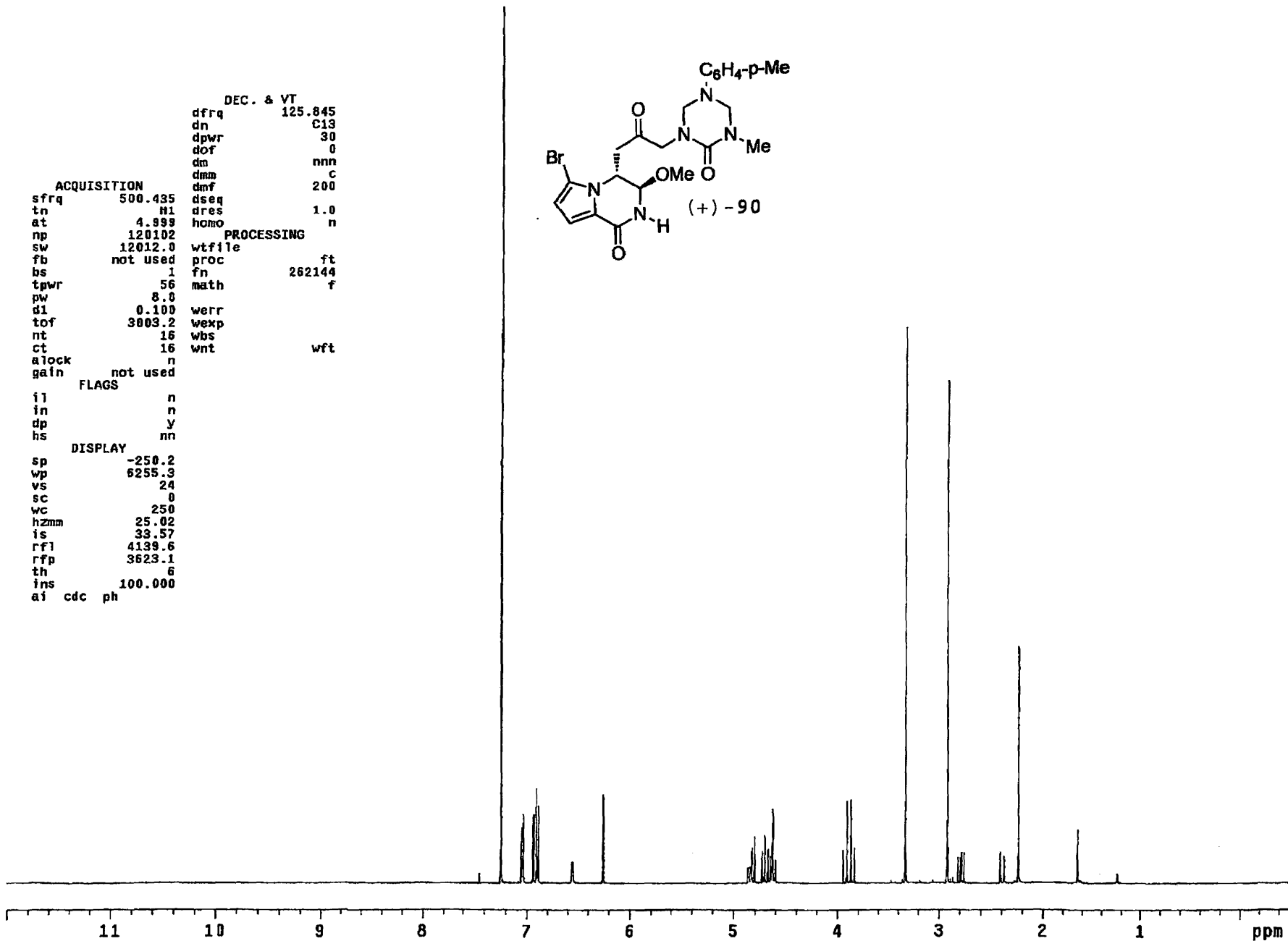
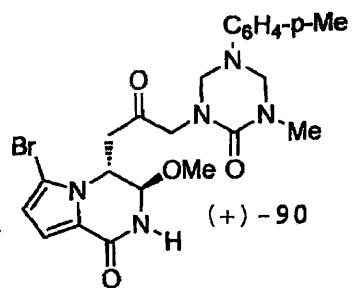
245



```

DEC. & VT      125.845
dfrq           C13
dn             30
dpwr          0
dof           nnn
dm            c
dmm          200
dmf
sfrq          500.435
t1            H1
at           4.999
np           120102
sw           12012.0
fb           not used
bs            1
tpwr         56
pw           8.0
d1           0.100
tof          3003.2
nt           16
ct           16
alock        n
gain         not used
ACQUISITION
sfrq          500.435
t1            H1
at           4.999
np           120102
sw           12012.0
fb           not used
bs            1
tpwr         56
pw           8.0
d1           0.100
tof          3003.2
nt           16
ct           16
alock        n
gain         not used
PROCESSING
wtfile
proc         ft
fn           262144
math         f
werr
wexp
wbs
wnt          wft
FLAGS
i1           n
in           n
dp           y
hs           nn
DISPLAY
sp           -250.2
wp           6255.3
vs           24
sc           0
wc           250
hzmm        25.02
is           33.57
rf1         4139.6
rfp         3623.1
th           6
ins         100.000
ai cdc ph

```



```

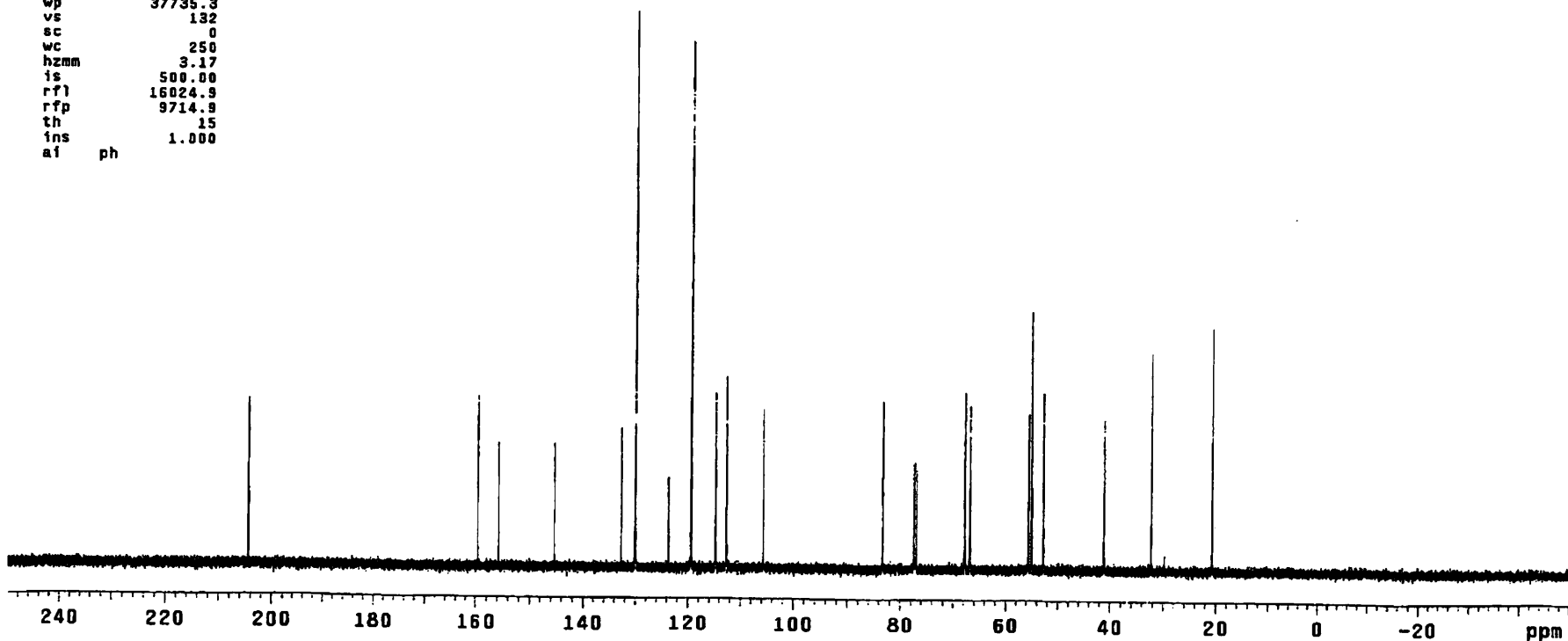
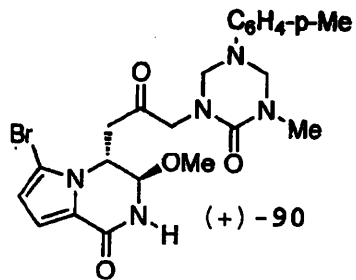
DEC. & VT
dfrq 500.228
dn H1
dpwr 38
dof -500.0
dm y
dmn w
dmf 10000
dseq
dres 1.0
homo n
PROCESSING
lb 0.30
wtfile
proc ft
fn 131072
math f
werr
wexp
wbs
wnt

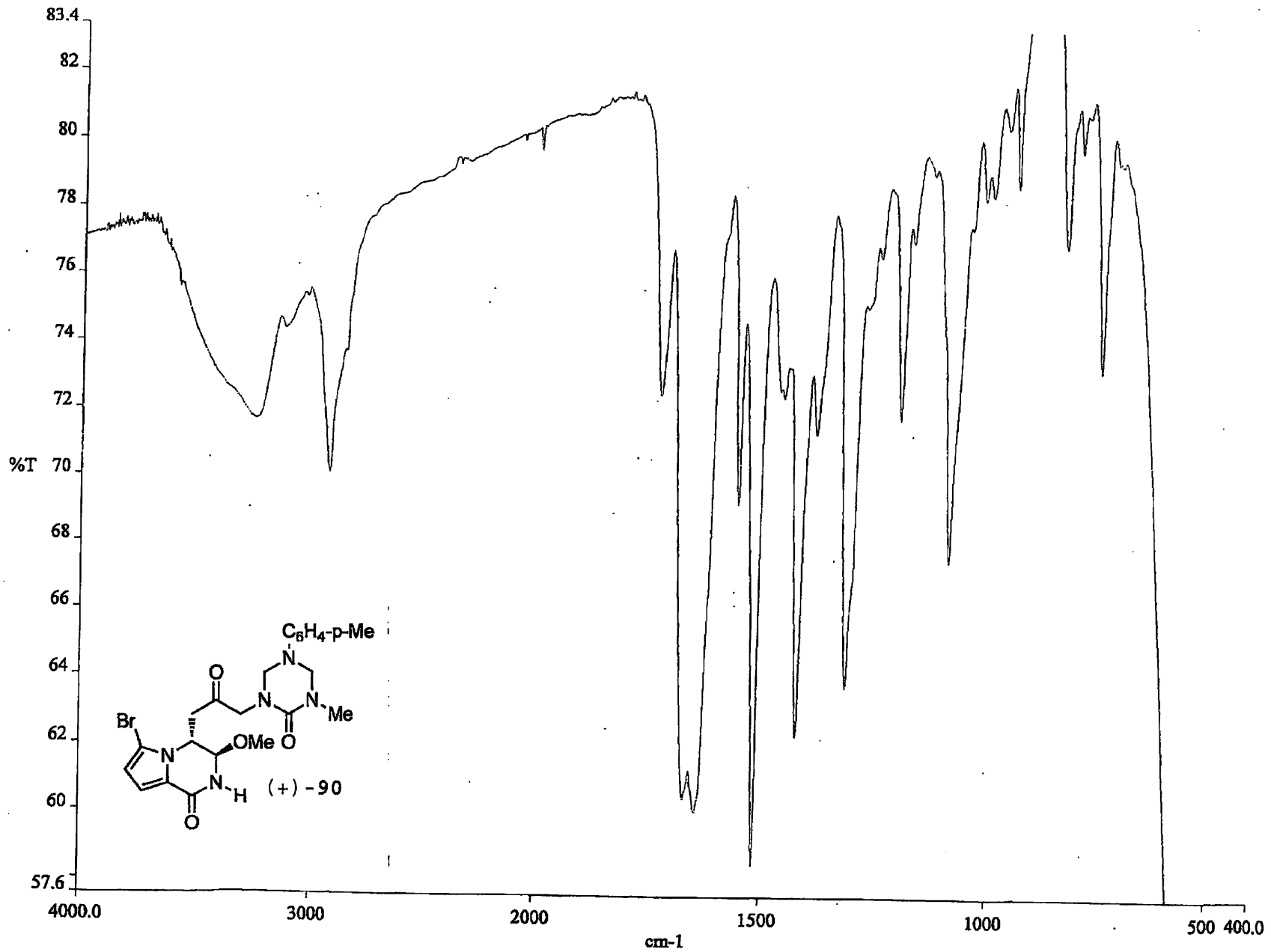
ACQUISITION
sfrq 125.795
tn C13
at 1.736
np 131010
sw 37735.8
fb not used
bs 4
ss 1
tpwr 53
pw 6.9
di 0.763
tof 631.4
nt 1e+09
ct 60
alock n
gain 60

FLAGS
fl n
in n
dp v
hs nn

DISPLAY
sp -6389.4
wp 37735.3
vs 132
sc 0
wc 250
hzmn 3.17
is 500.00
rf 16024.9
rfp 9714.9
th 15
ins 1.000
af ph

```

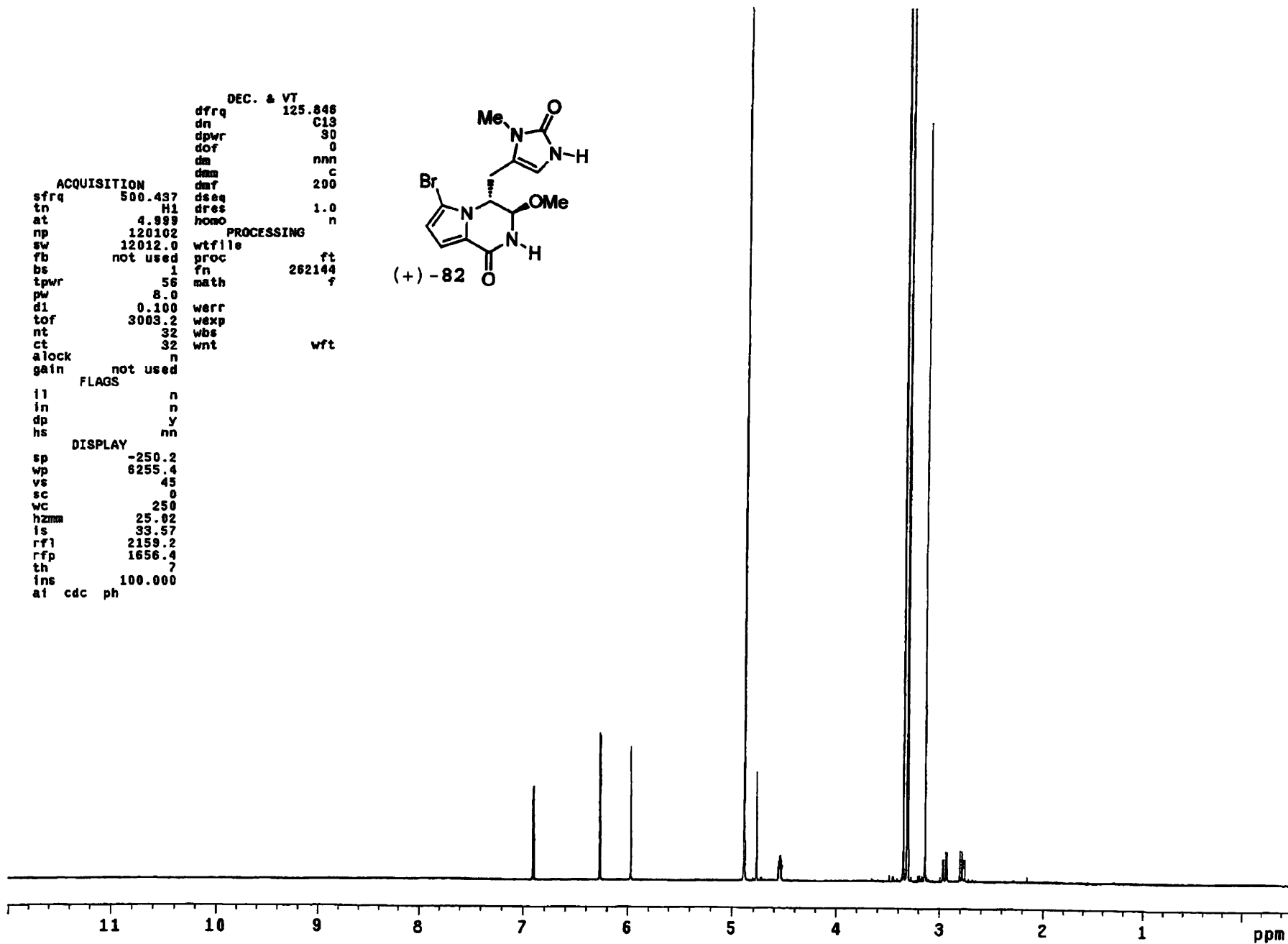
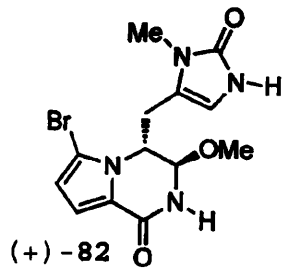




```

DEC. & VT
dfrq      125.846
dn         C13
dpwr       30
dof        0
dm         nnn
dmm        c
dmf        200
ACQUISITION
sfrq      500.437
tn        H1
at        4.999
np        120102
sw        12012.0
fb        not used
bs        1
tpwr      56
pw        8.0
d1        0.100
tof       3003.2
nt        32
ct        32
alock     n
gain      not used
          FLAGS
il        n
in        n
dp        y
hs        nn
          DISPLAY
sp        -250.2
wp        9255.4
vs        45
sc        0
wc        250
hzmm      25.02
is        33.57
rfl       2159.2
rfp       1656.4
th        7
ins       100.000
af cdc ph
          PROCESSING
wtfile
proc      ft
fn        262144
math      f
          wft
werr
wexp
wbs
wnt

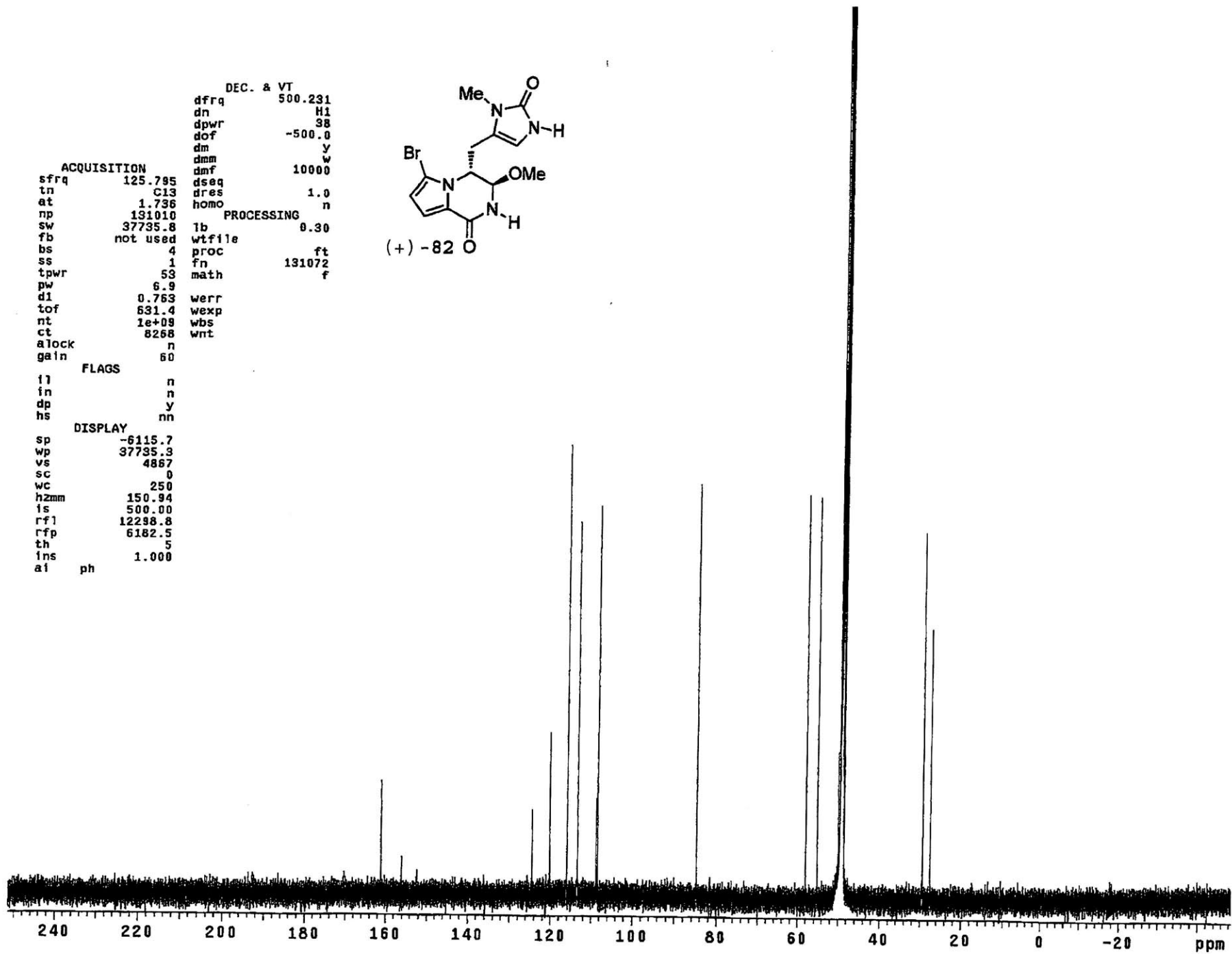
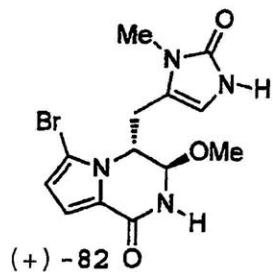
```



```

DEC. & VT
dfrq 500.231
dn Hi
dpwr 38
dof -500.0
dm y
dmm w
dmf 10000
dseq
dres 1.0
homo n
ACQUISITION
sfrq 125.795
tn C13
at 1.736
np 131010
sw 37735.8
fb not used
bs 4
ss 1
tpwr 53
pw 6.9
d1 0.763
tof 531.4
nt 1e+09
ct 8268
alock n
gain 60
PROCESSING
lb 0.30
wtfile
proc ft
fn 131072
f
werr
wexp
wbs
wnt
FLAGS
il n
in n
dp y
hs nn
DISPLAY
sp -6115.7
wp 37735.3
vs 4867
sc 0
wc 250
hzmm 150.94
ls 500.00
rf1 12298.8
rfp 6182.5
th 5
ins 1.000
ai ph

```

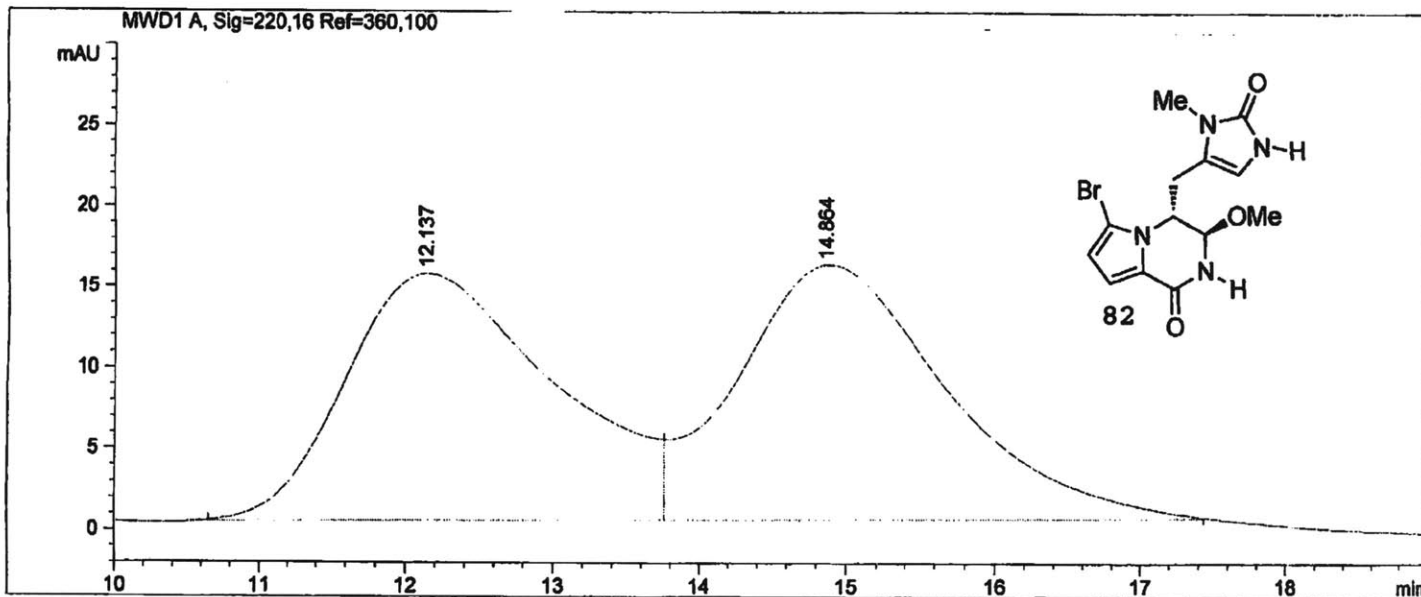


```

=====
Injection Date :                               Seq. Line :    1
Sample Name   :                               Location  : Vial 61
Acq. Operator :                               Inj       :    1
                                           Inj Volume: 1 µl

Acq. Method   :
Last changed  :
Analysis Method :
Last changed  :
=====

```



=====
Area Percent Report
=====

```

Sorted By      :      Signal
Multiplier     :      1.0000
Dilution       :      1.0000
Use Multiplier & Dilution Factor with ISTDs

```

Signal 1: MWD1 A, Sig=220,16 Ref=360,100

Peak #	RetTime [min]	Type	Width [min]	Area [mAU*s]	Height [mAU]	Area %
1	12.137	BV	1.1608	1499.41431	15.28030	49.0828
2	14.864	VB	1.1626	1555.45105	15.82612	50.9172

Totals : 3054.86536 31.10642

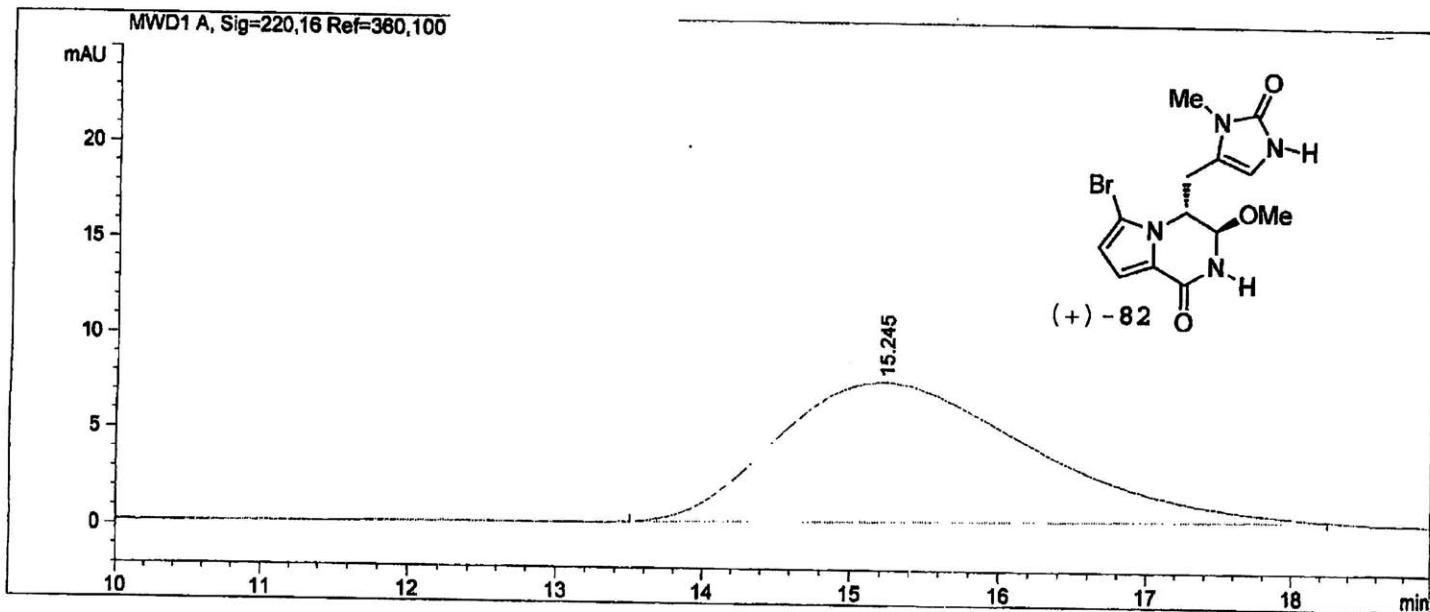
Results obtained with enhanced integrator!

=====
*** End of Report ***

```

=====
Injection Date   :                               Seq. Line :    1
Sample Name     :                               Location  : Vial 91
Acq. Operator   :                               Inj       :    1
                                                    Inj Volume: 1 µl
Acq. Method    :
Last changed   :
Analysis Method :
Last changed   :
=====

```



=====
Area Percent Report
=====

```

Sorted By      :      Signal
Multiplier    :      1.0000
Dilution      :      1.0000
Use Multiplier & Dilution Factor with ISTDs

```

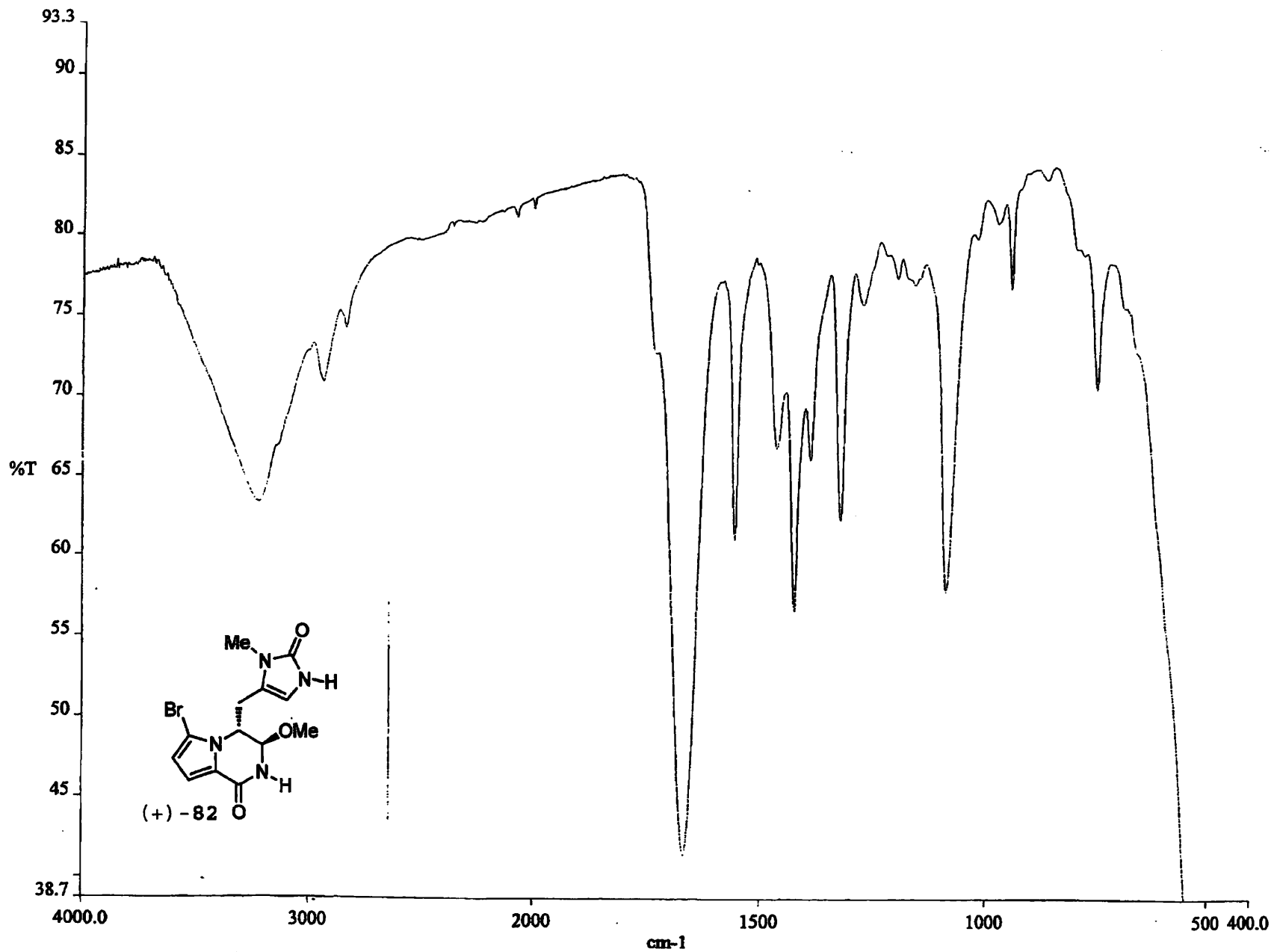
Signal 1: MWD1 A, Sig=220,16 Ref=360,100

Peak #	RetTime [min]	Type	Width [min]	Area [mAU*s]	Height [mAU]	Area %
1	15.245	PB	1.4033	875.68500	7.33223	100.0000

Totals : 875.68500 7.33223

Results obtained with enhanced integrator!

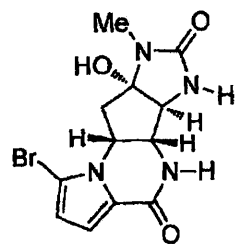
=====
*** End of Report ***



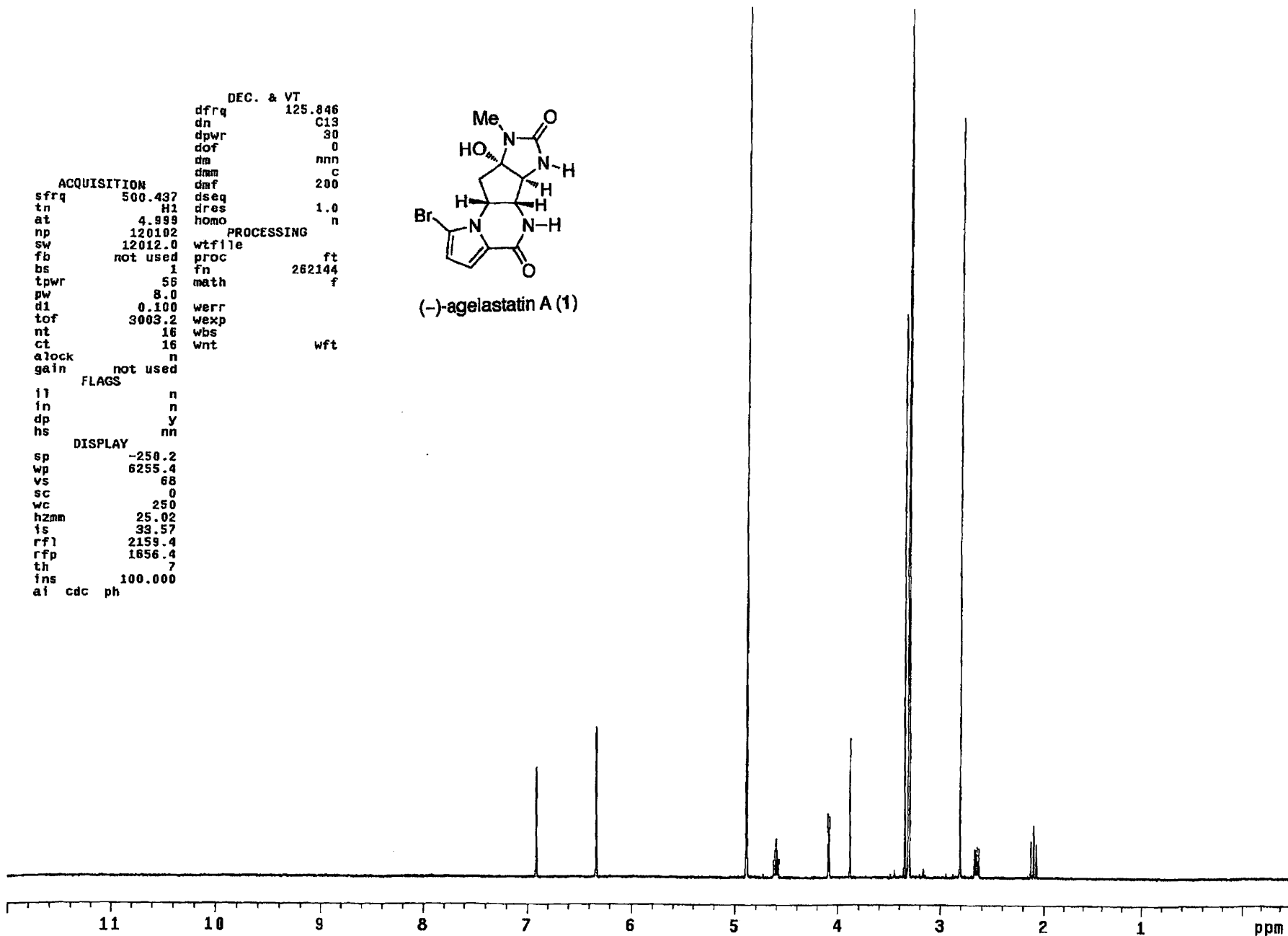
```

DEC. & VT
dfrq      125.846
dn        C13
dpwr      30
dof       0
dm        nnn
dmm       C
dmf       200
ACQUISITION
sfrq      500.437
tn        H1
at        4.999
np        120102
sw        12012.0
fb        not used
bs        1
tpwr      56
pw        8.0
dl        0.100
tof       3003.2
nt        16
ct        16
alock     n
gain      not used
          FLAGS
i1        n
in        n
dp        y
hs        nn
          DISPLAY
sp        -250.2
wp        6255.4
vs        68
sc        0
wc        250
hzmm      25.02
is        33.57
rfl       2159.4
rfp       1656.4
th        7
ins       100.000
ai cdc ph
          PROCESSING
dseq      1.0
dres      n
homo      n
wtfile    ft
proc      fn
          262144
fn        f
math      f
werr      wexp
wbs       wnt
          wft

```



(-)-agelastatin A (1)



```

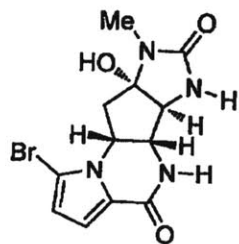
DEC. & VT      dfrq      500.231
                dn         H1
                dpwr       38
                dof       -500.0
                dm         y
                dmm        w
                dmf       10000
ACQUISITION    sfrq      125.795
                tn        C13
                at        1.736
                np        131010
                sw        37735.8
                fb        not used
                bs         4
                ss         1
                tpwr      53
                pw         6.9
                dl        0.763
                tof       631.4
                nt        1e+09
                ct        21180
                alock     n
                gain      60
                FLAGS
                il        n
                in        n
                dp        y
                hs        nn
                DISPLAY
                sp        -6115.7
                wp        37735.3
                vs        7283
                sc         0
                wc        250
                hzmm      5.16
                is        500.00
                rfl       12298.8
                rfp       6182.5
                th         10
                ins       1.000
                ai        ph

```

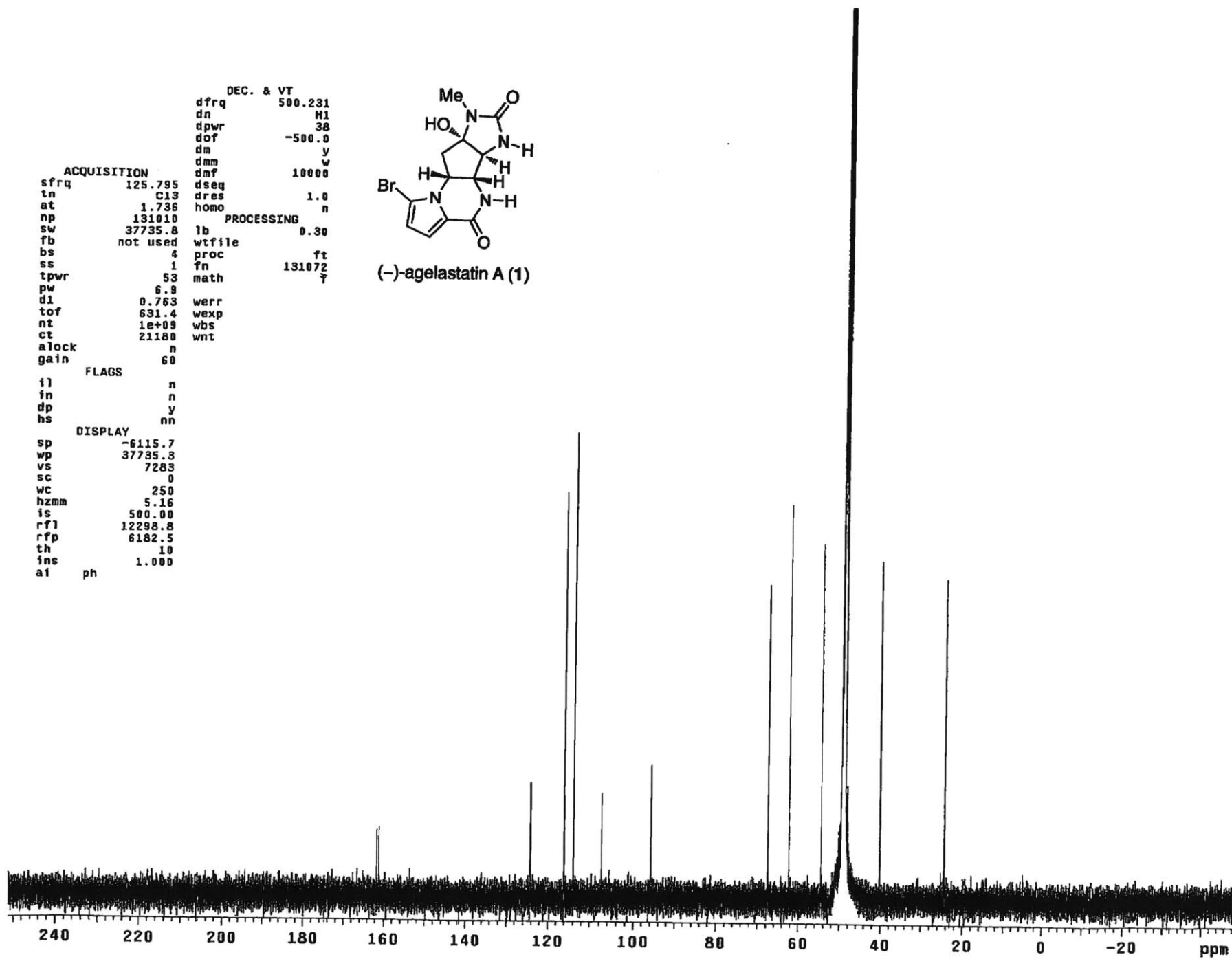
```

                dseq      1.0
                dres      n
                homo      n
PROCESSING      lb        0.30
                wtfile
                proc      ft
                fn        131072
                math      7

```



(-)-agelastatin A (1)

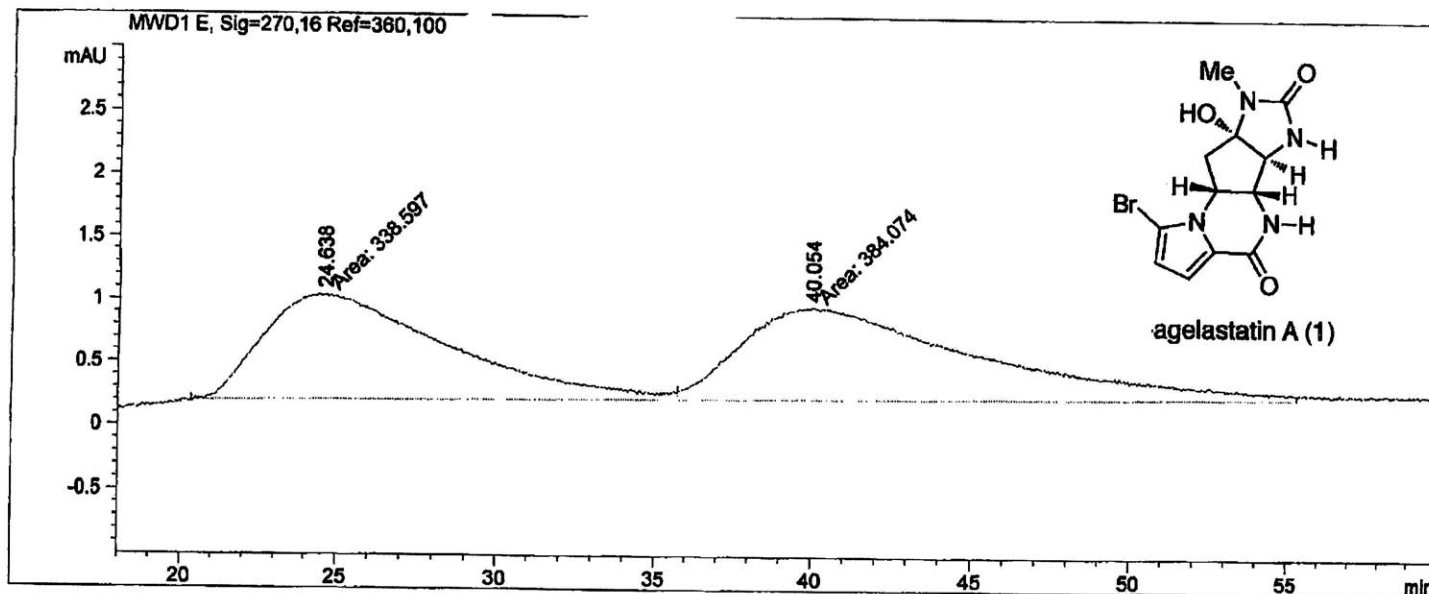


```

=====
Injection Date   :                               Seq. Line :    1
Sample Name     :                               Location  : Vial 91
Acq. Operator   :                               Inj       :    1
                                                    Inj Volume: 5 µl

Acq. Method    :
Last changed   :
Analysis Method:
Last changed   :
=====

```



=====
Area Percent Report
=====

```

Sorted By      :      Signal
Multiplier     :      1.0000
Dilution       :      1.0000
Use Multiplier & Dilution Factor with ISTDs

```

Signal 1: MWD1 E, Sig=270,16 Ref=360,100

Peak #	RetTime [min]	Type	Width [min]	Area [mAU*s]	Height [mAU]	Area %
1	24.638	MF	6.6959	338.59686	8.42801e-1	46.8535
2	40.054	FM	8.6223	384.07428	7.42408e-1	53.1465

Totals : 722.67114 1.58521

Results obtained with enhanced integrator!

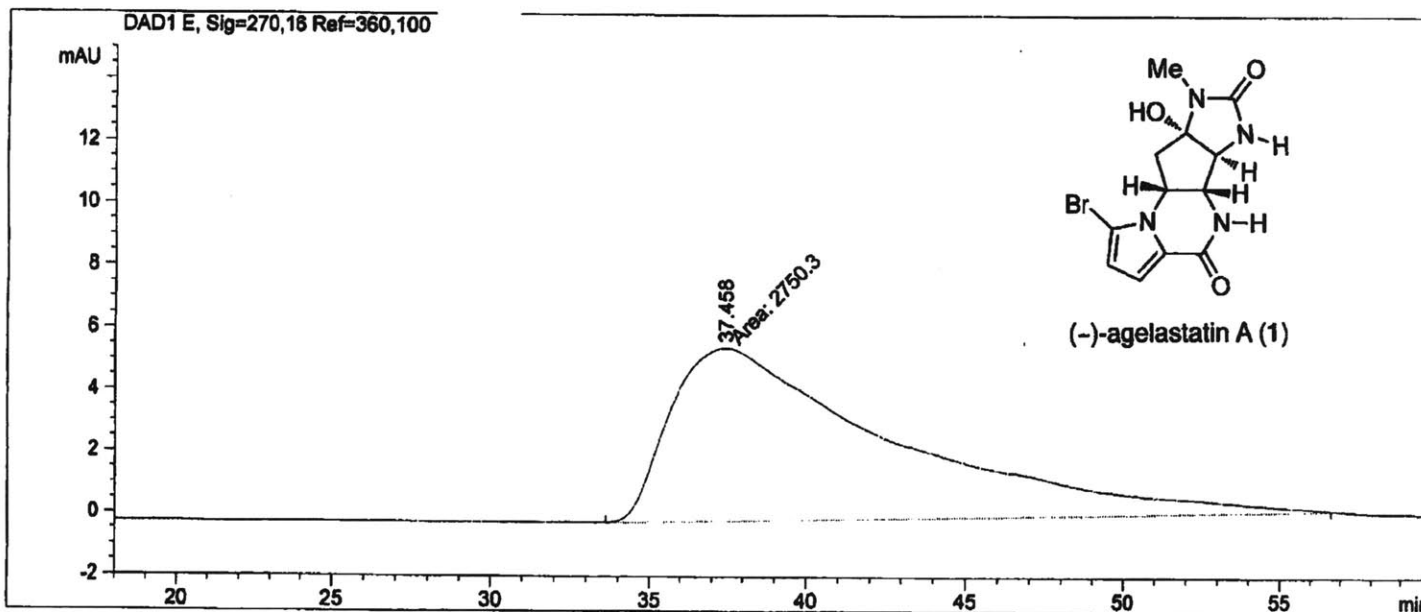
=====
*** End of Report ***

```

=====
Injection Date   :                               Seq. Line :    1
Sample Name     :                               Location  : Vial 91
Acq. Operator   :                               Inj       :    1
                                                    Inj Volume: 1 µl

Acq. Method    :
Last changed   :
Analysis Method:
Last changed   :
=====

```



```

=====
                          Area Percent Report
=====

```

```

Sorted By      :      Signal
Multiplier     :      1.0000
Dilution       :      1.0000
Use Multiplier & Dilution Factor with ISTDs

```

Signal 1: DAD1 E, Sig=270,16 Ref=360,100

Peak #	RetTime [min]	Type	Width [min]	Area [mAU*s]	Height [mAU]	Area %
1	37.458	MM	8.1336	2750.29980	5.63566	100.0000

Totals : 2750.29980 5.63566

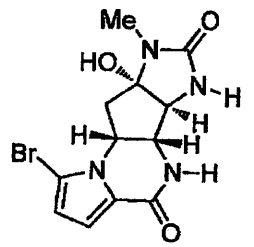
Results obtained with enhanced integrator!

```

=====
*** End of Report ***
=====

```

90.7
90
89
88
87
86
85
84
83
82
81
80
79
78
77
76
75
74
73
72
71
70
69
67.8



(-)-agelastatin A (1)

%T

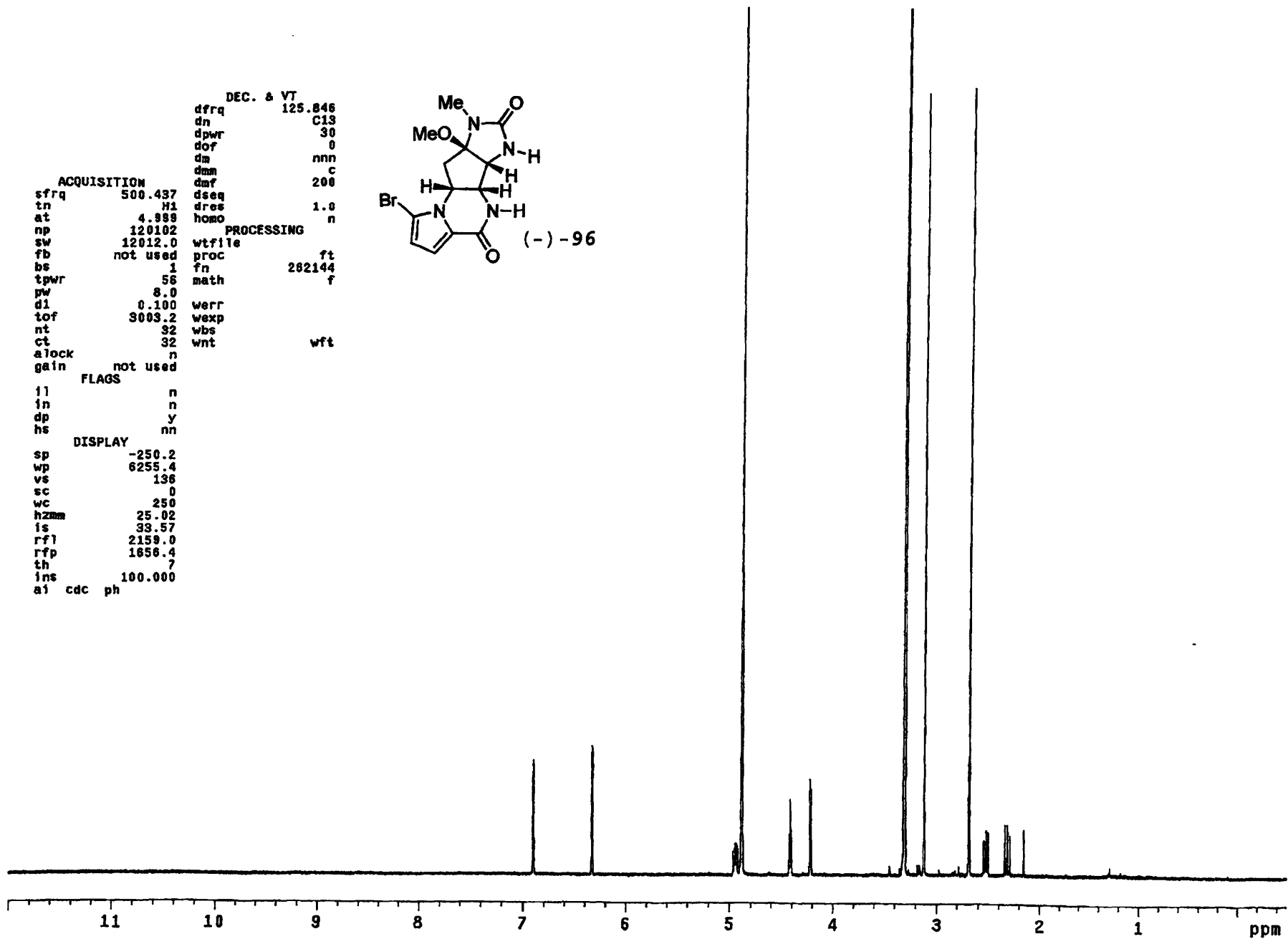
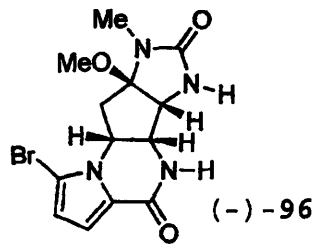
cm-1

4000.0 3000 2000 1500 1000 500 400.0

```

DEC. & VT      125.846
dfrq           C13
dn             30
dpwr           0
dof           nnn
dm            c
dmm           200
dmf
ACQUISITION   500.437
sfrq          H1
tn            4.988
at           120102
np           12012.0
sw           not used
fb           1
bs           56
tpwr         8.0
pw           0.100
d1           3003.2
tof          32
nt           32
ct           32
alock        not used
gain         not used
          FLAGS
          ll      n
          in      n
          dp      y
          hs      nn
          DISPLAY
          sp      -250.2
          wp      6255.4
          vs      136
          sc      0
          wc      250
          hzmm    25.02
          is      33.57
          rfl     2159.0
          rfp     1656.4
          th      7
          ins     100.000
          al cdc ph
          wtfile
          proc    ft
          fn      262144
          math    f
          werr
          wexp
          wbs
          wnt     wft

```



```

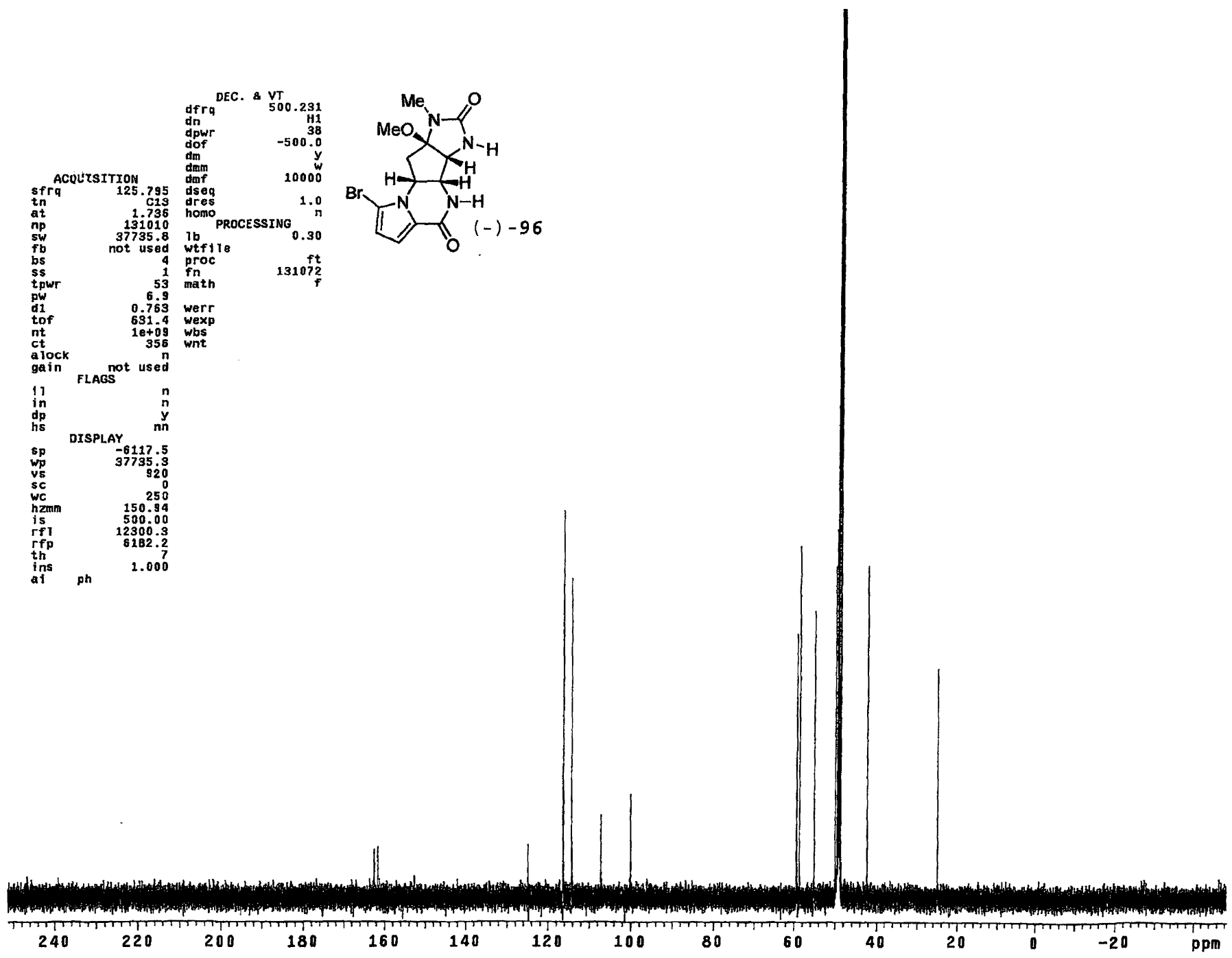
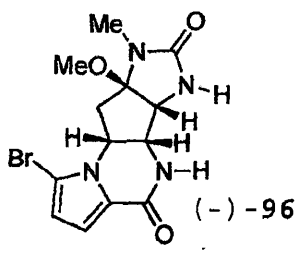
DEC. & VT
dfrq 500.231
dn H1
dpwr 38
dof -500.0
dm y
dmm w
dmf 10000
ACQUISITION
sfrq 125.795 dseq
tn C13 dres
at 1.736 homo
np 131010
sw 37735.8
fb not used
bs 4
ss 1
tpwr 53
pw 6.9
d1 0.763 werr
tof 631.4 wexp
nt 1e+09 wbs
ct 356 wnt
alock n
gain not used
FLAGS
f1 n
in n
dp y
hs nn
DISPLAY
sp -6117.5
wp 37735.3
vs 820
sc 0
wc 250
hzmm 150.84
is 500.00
rfl 12300.3
rfp 8182.2
th 7
ins 1.000
al ph

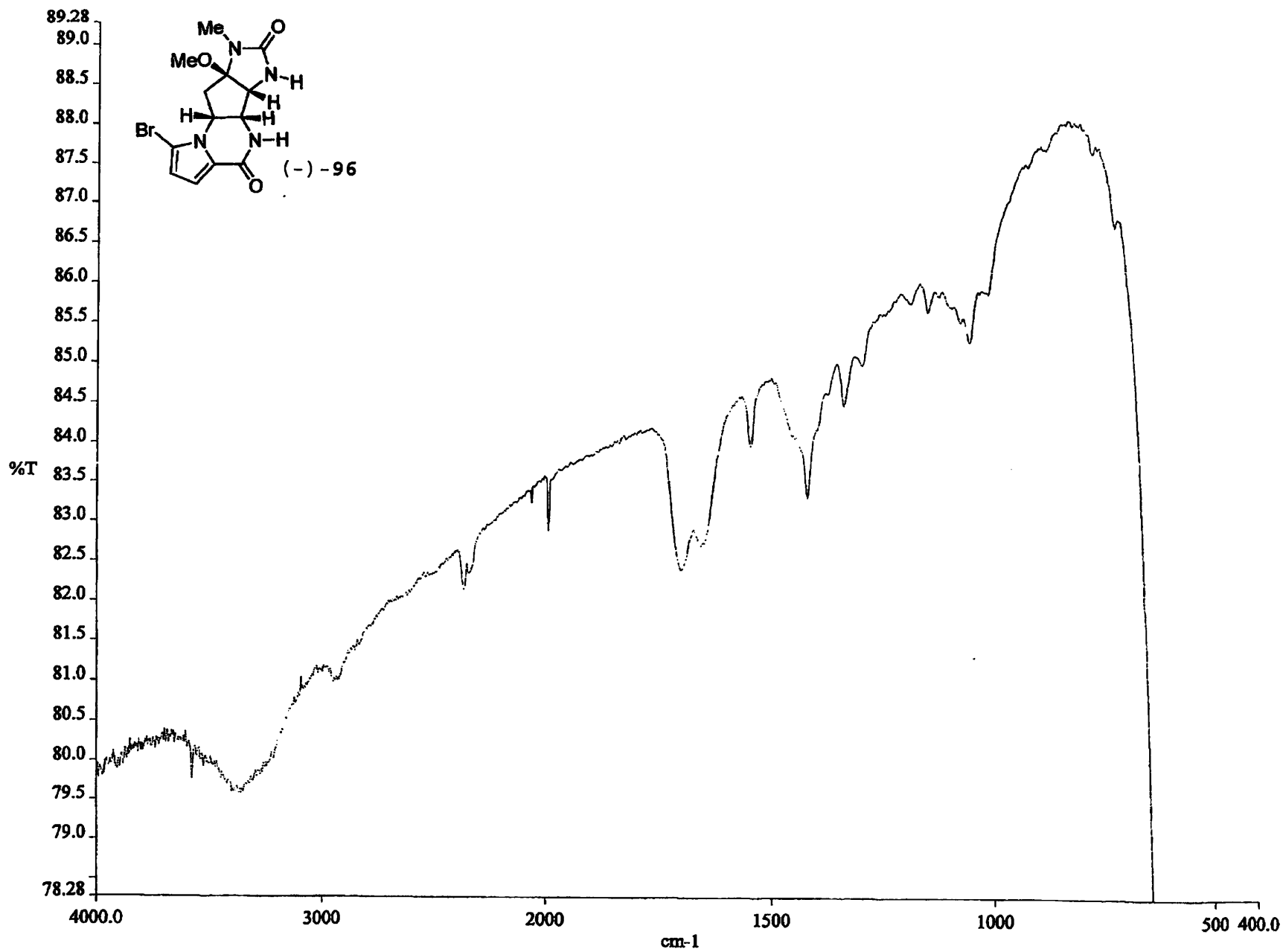
```

```

PROCESSING
lb 0.30
wfile
proc ft
fn 131072
math f

```

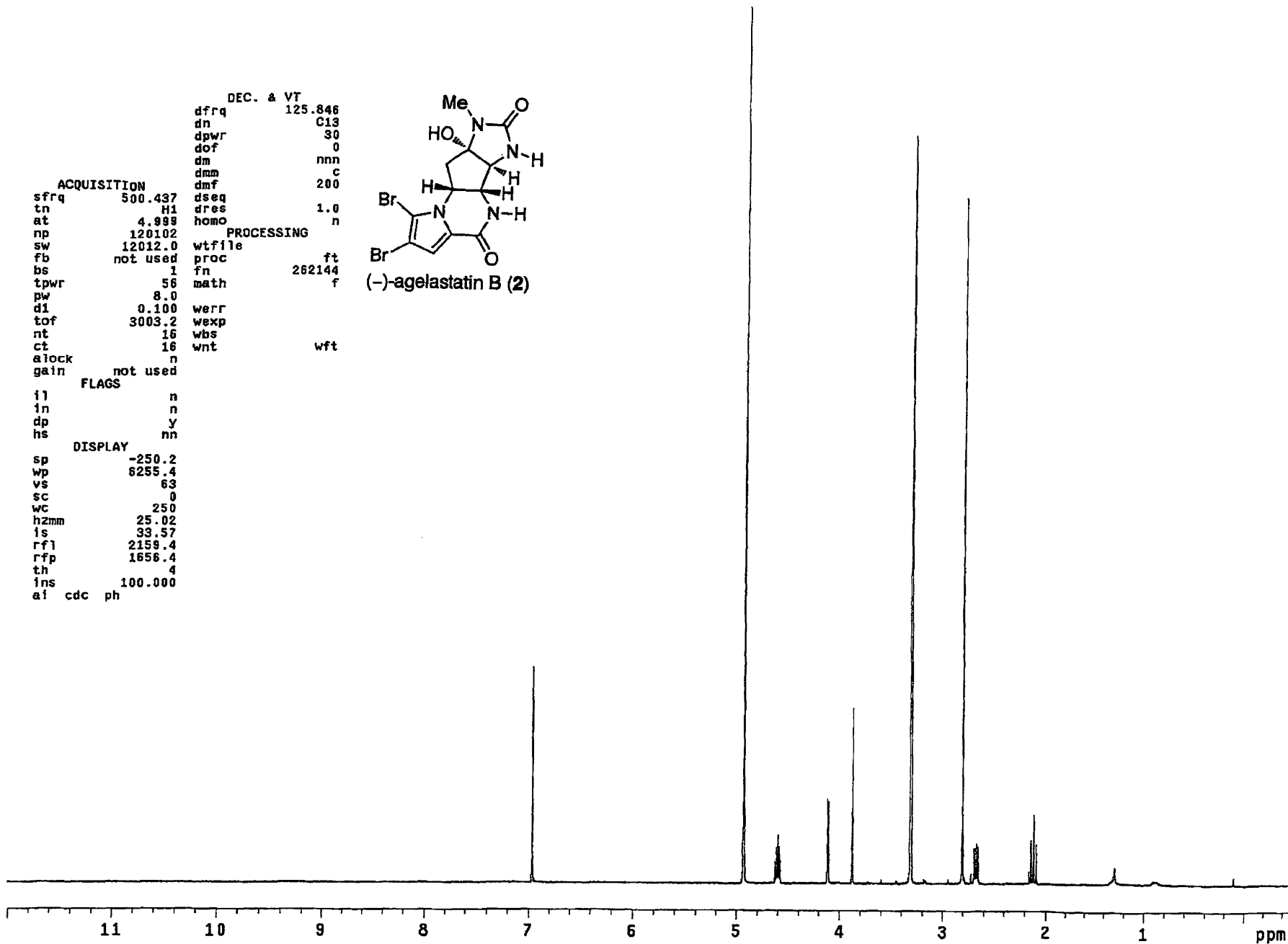
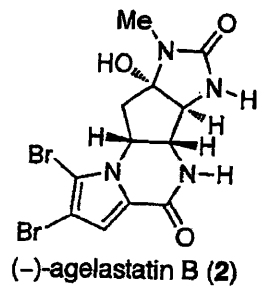




```

DEC. & VT
dfrq 125.846
dn C13
dpwr 30
dof 0
dm nnn
dmm c
dmf 200
dseq
dres 1.0
homo n
ACQUISITION
sfrq 500.437
tn H1
at 4.899
np 120102
sw 12012.0
fb not used
bs 1
tpwr 56
pw 8.0
d1 0.100
tof 3003.2
nt 16
ct 16
atlock n
gain not used
PROCESSING
wtfile ft
proc 262144
fn f
math f
werr
wexp
wbs
wnt wft
FLAGS
il n
in n
dp y
hs nn
DISPLAY
sp -250.2
wp 6255.4
vs 63
sc 0
wc 250
hzmm 25.02
is 33.57
rfl 2159.4
rfp 1656.4
tn 4
ins 100.000
ai cdc ph

```



```

ACQUISITION
sfrq 125.795
tn C13
at 1.736
np 131010
sw 37735.8
fb not used
bs 4
ss 1
tpwr 53
pw 6.9
d1 0.763
tof 631.4
nt 1e+09
ct 16156
alock n
gain 60

DEC. & VT
dfrq 500.231
dn H1
dpwr 38
dof -500.0
dm y
dmm w
dmf 10000
dseq 1.0
dres n
homo n

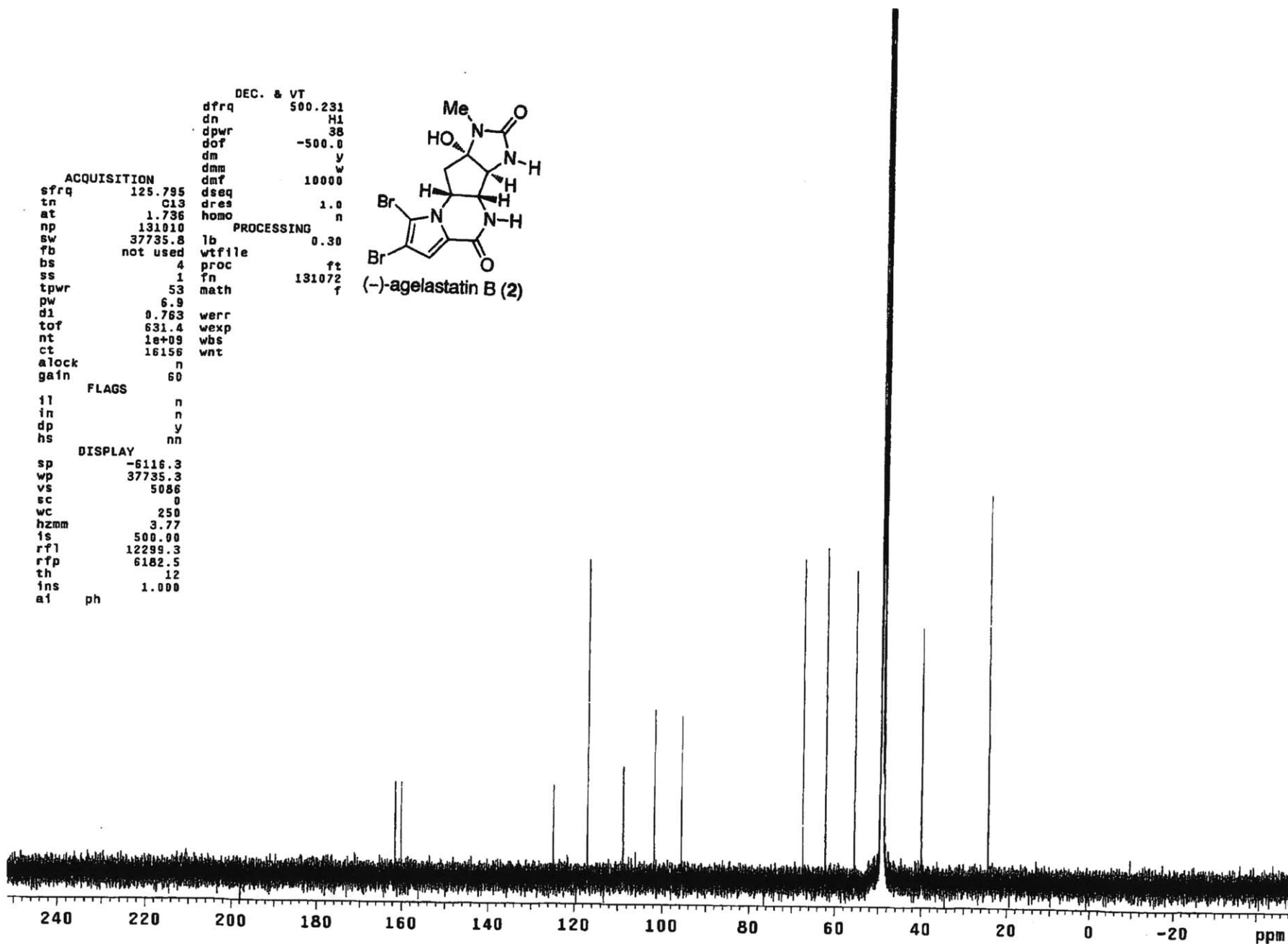
PROCESSING
lb 0.30
wtfile
proc ft
fn 131072
math f

werr
wexp
wbs
wnt

FLAGS
ll n
in n
dp y
hs nn

DISPLAY
sp -6116.3
wp 37735.3
vs 5086
sc 0
wc 250
hzmm 3.77
fs 500.00
rf1 12299.3
rfp 6182.5
th 12
ins 1.000
a1 ph

```



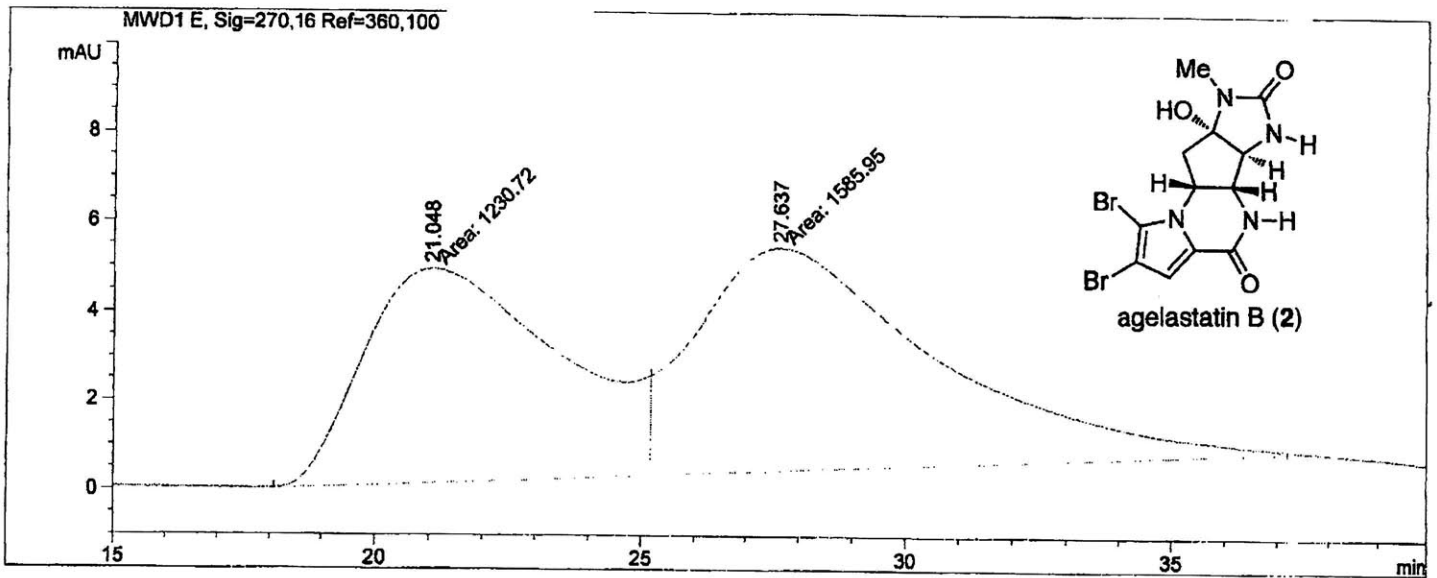
```

=====
Injection Date :                               Seq. Line : 1
Sample Name   :                               Location  : Vial 79
Acq. Operator :                               Inj       : 1
                                           Inj Volume: 3 µl

Acq. Method   :
Last changed  :

Analysis Method :
Last changed  :
=====

```



=====
Area Percent Report
=====

```

Sorted By      : Signal
Multiplier    : 1.0000
Dilution      : 1.0000
Use Multiplier & Dilution Factor with ISTDs

```

Signal 1: MWD1 E, Sig=270,16 Ref=360,100

Peak #	RetTime [min]	Type	Width [min]	Area [mAU*s]	Height [mAU]	Area %
1	21.048	MF	4.2737	1230.71851	4.79959	43.6941
2	27.637	FM	5.2827	1585.95435	5.00365	56.3059

Totals : 2816.67285 9.80324

Results obtained with enhanced integrator!

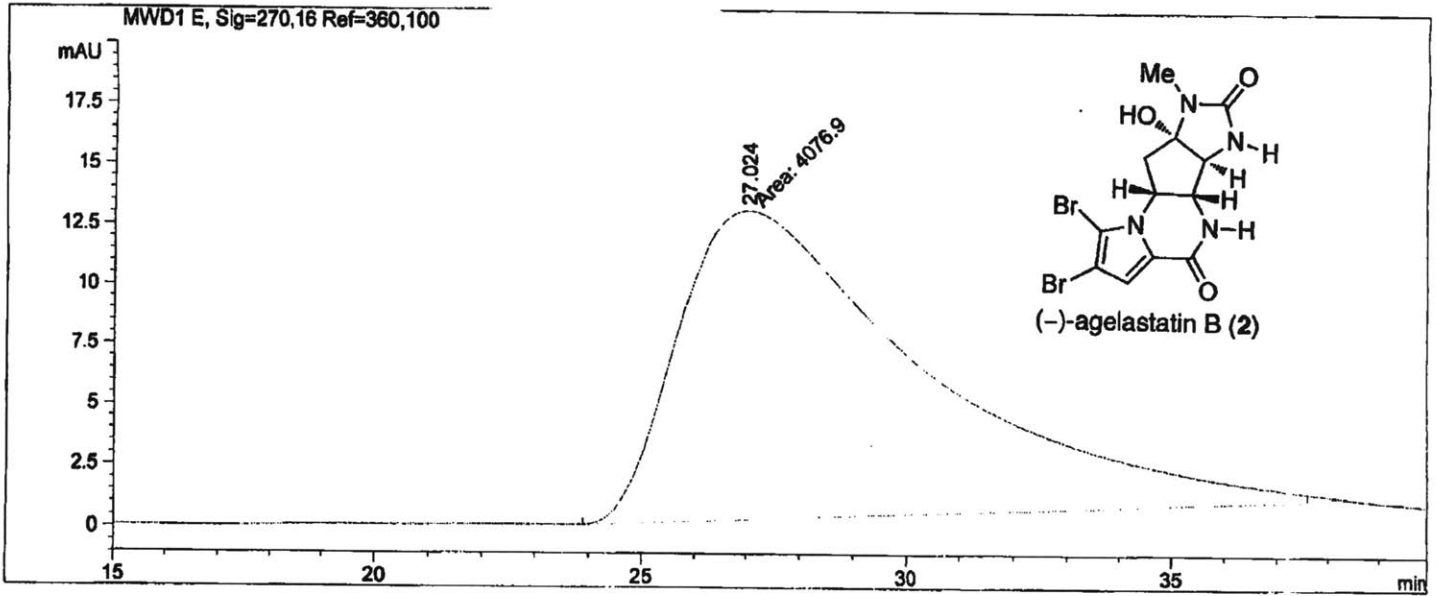
=====
*** End of Report ***

```

=====
Injection Date   :                               Seq. Line :    1
Sample Name     :                               Location  : Vial 80
Acq. Operator   :                               Inj       :    1
                                                    Inj Volume: 5 µl

Acq. Method    :
Last changed   :
Analysis Method:
Last changed   :
=====

```



```

=====
                          Area Percent Report
=====

```

```

Sorted By      :      Signal
Multiplier     :      1.0000
Dilution       :      1.0000
Use Multiplier & Dilution Factor with ISTDs

```

Signal 1: MWD1 E, Sig=270,16 Ref=360,100

Peak #	RetTime [min]	Type	Width [min]	Area [mAU*s]	Height [mAU]	Area %
1	27.024	MM	5.3130	4076.89722	12.78911	100.0000

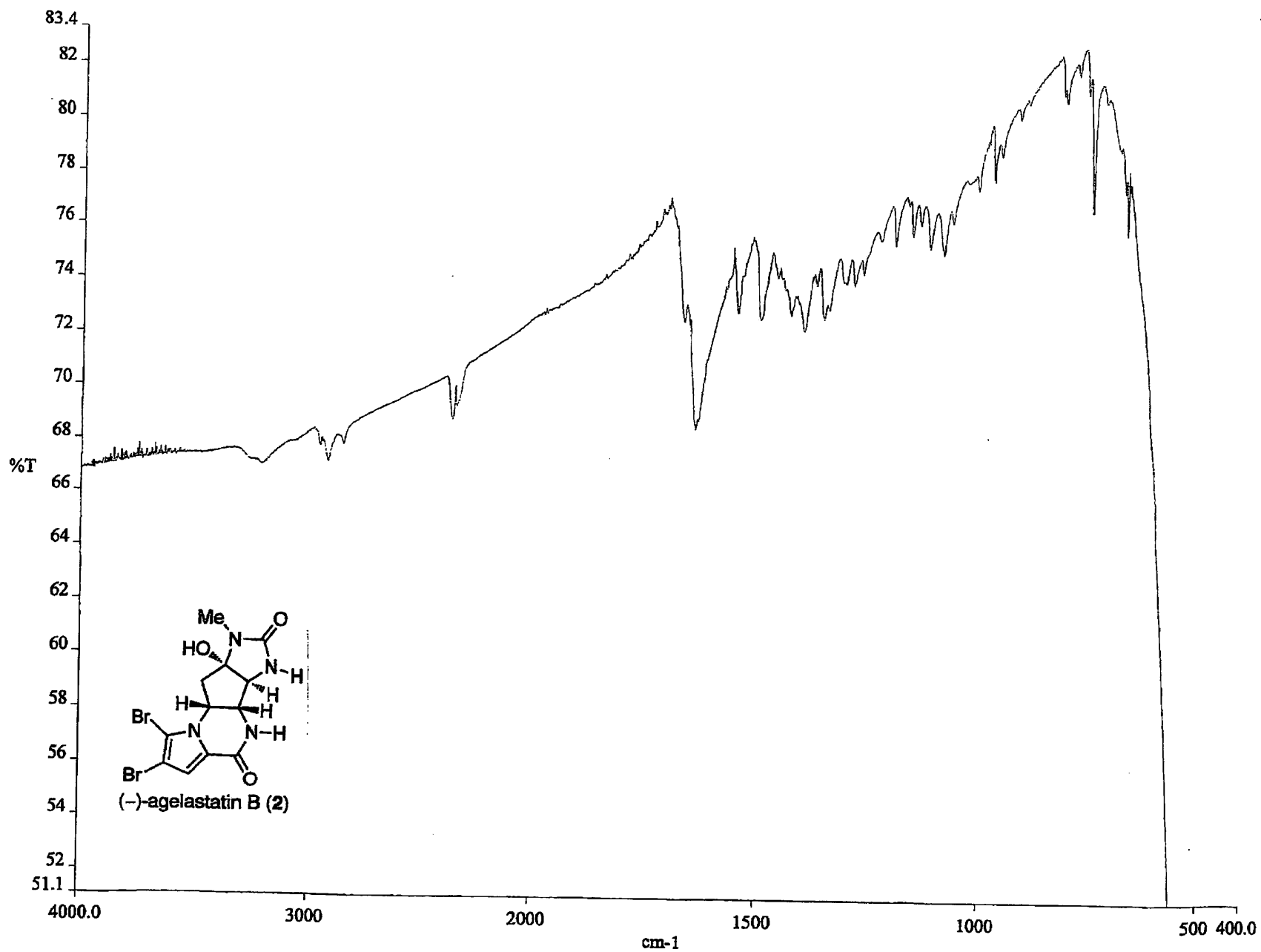
Totals : 4076.89722 12.78911

Results obtained with enhanced integrator!

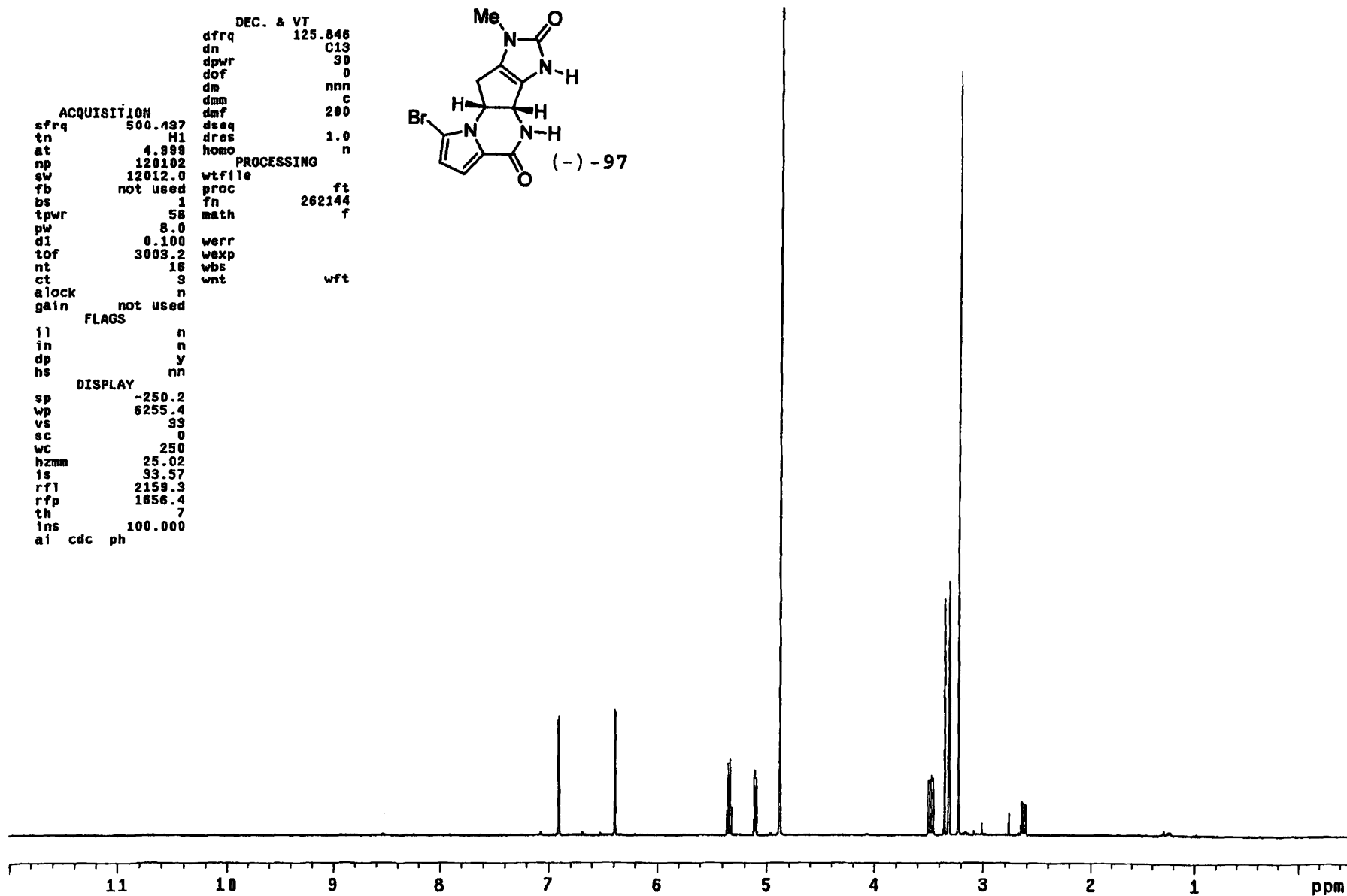
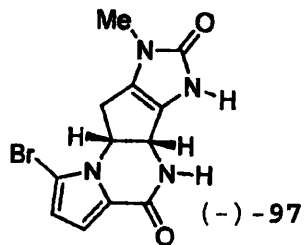
```

=====
*** End of Report ***

```



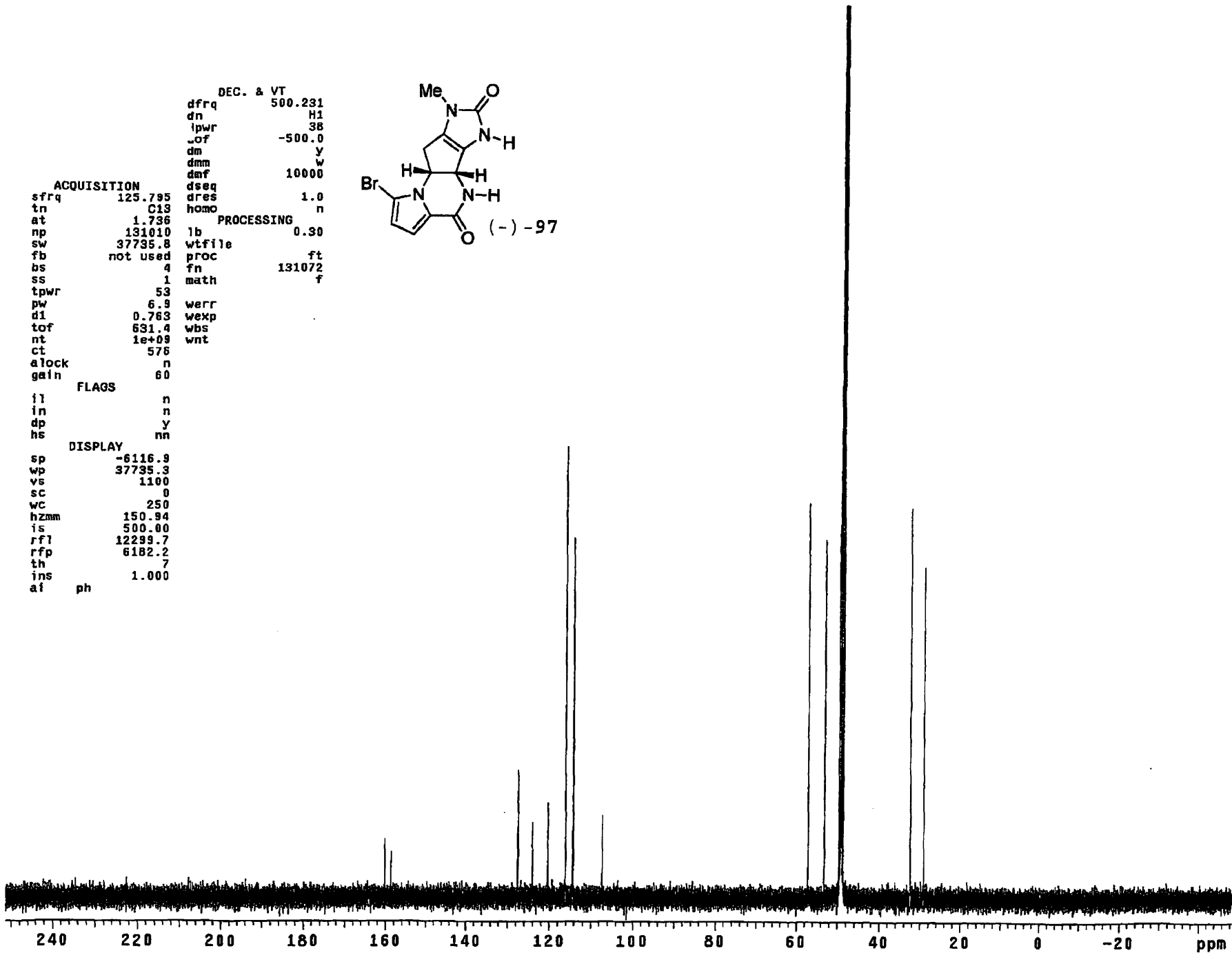
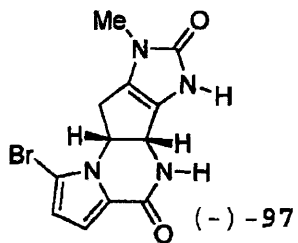
		DEC. & VT	
	dfrq	125.848	
	dn	C13	
	dpwr	30	
	dof	0	
	dm	nnn	
	dmm	c	
	dmf	200	
ACQUISITION			
sfrq	500.437		
tn	H1		
at	4.999	dseq	1.0
np	120102	dres	n
sw	12012.0	hom	
fb	not used	wtfile	
bs	1	proc	ft
tpwr	56	fn	262144
pw	8.0	math	f
d1	0.100		
tof	3003.2	werr	
nt	16	wexp	
ct	9	wbs	
alock	n	wnt	wft
gain	not used		
	FLAGS		
il	n		
in	n		
dp	y		
hs	nn		
	DISPLAY		
sp	-250.2		
wp	6255.4		
vs	33		
sc	0		
wc	250		
hzmm	25.02		
ls	33.57		
rfl	2159.3		
rff	1656.4		
th	7		
ins	100.000		
ai	cdc ph		



```

DEC. & VT
dfrq 500.231
dn H1
lpwr 38
lof -500.0
dm y
dmm w
dmf 10000
dseq
dres 1.0
homo n
ACQUISITION
sfrq 125.795
tn C13
at 1.736
np 131010
sw 37735.8
fb not used
bs 4
ss 1
tpwr 53
pw 6.9
dl 0.763
tof 631.4
nt 1e+09
ct 576
alock n
gain 60
        FLAGS
        ii n
        in n
        dp y
        hs nn
        DISPLAY
sp -6116.9
wp 37735.3
vs 1100
sc 0
wc 250
hzmm 150.94
is 500.00
rf1 12299.7
rfp 6182.2
th 7
ins 1.000
af ph
        PROCESSING
lb 0.30
wtfile
proc ft
fn 131072
math f
werr
wexp
wbs
wnt

```

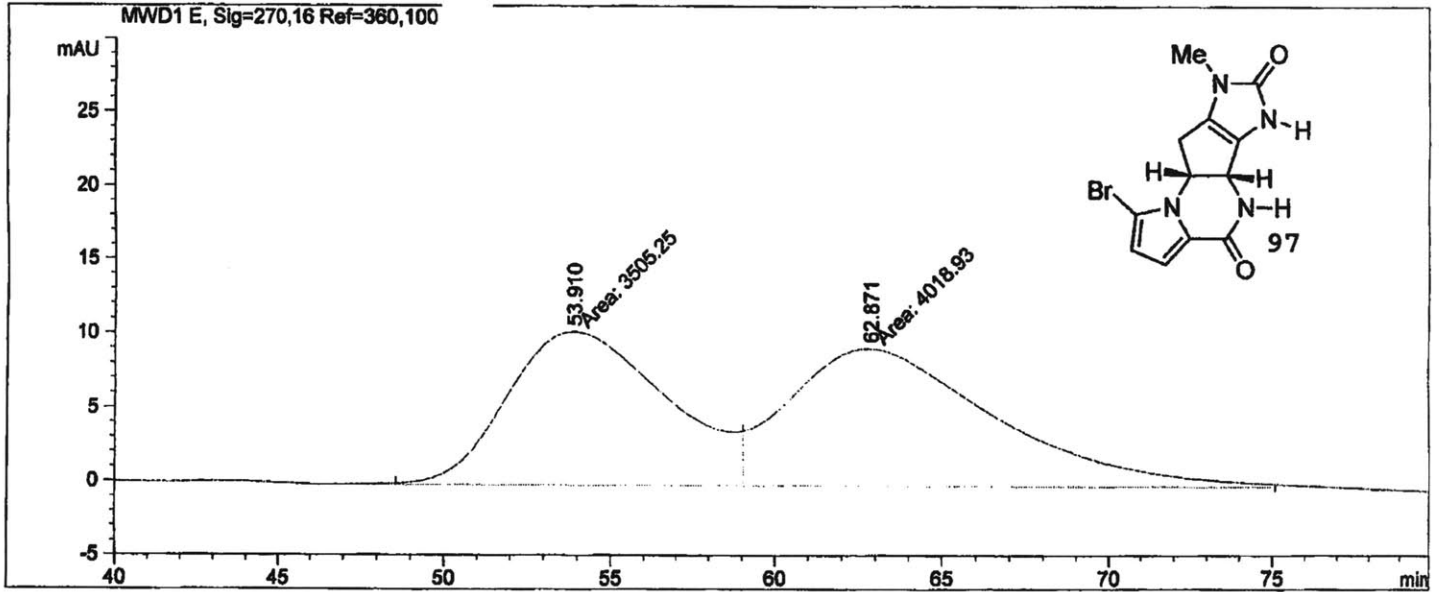



```

=====
Injection Date   :                               Seq. Line :    1
Sample Name     :                               Location  : Vial 91
Acq. Operator   :                               Inj       :    1
                                                    Inj Volume: 1 µl

Acq. Method    :
Last changed   :
Analysis Method:
Last changed   :
=====

```



=====
Area Percent Report
=====

```

Sorted By      :      Signal
Multiplier     :      1.0000
Dilution       :      1.0000
Use Multiplier & Dilution Factor with ISTDs

```

Signal 1: MWD1 E, Sig=270,16 Ref=360,100

Peak #	RetTime [min]	Type	Width [min]	Area [mAU*s]	Height [mAU]	Area %
1	53.910	MF	5.6060	3505.24609	10.42107	46.5865
2	62.871	FM	7.1602	4018.92529	9.35472	53.4135

Totals : 7524.17139 19.77579

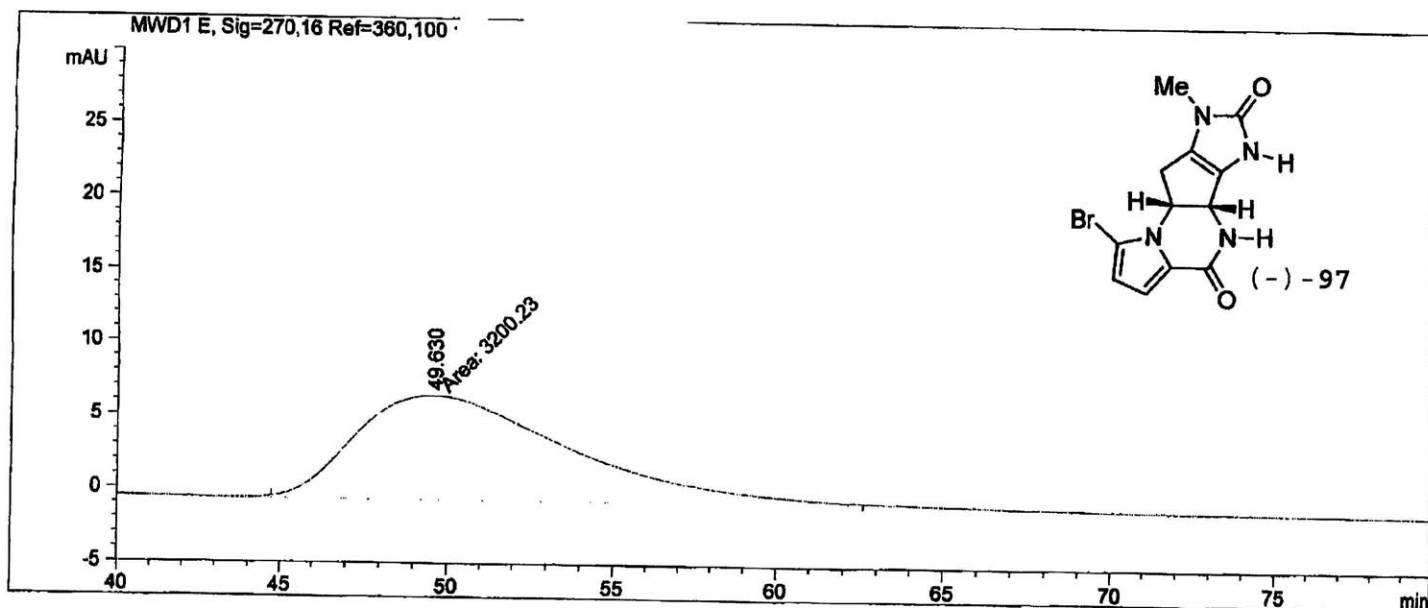
Results obtained with enhanced integrator!

=====
*** End of Report ***

```

=====
Injection Date   :                               Seq. Line :    1
Sample Name     :                               Location  : Vial 91
Acq. Operator   :                               Inj       :    1
                                                    Inj Volume: 1 µl
Acq. Method     :
Last changed    :
Analysis Method :
Last changed    :
=====

```



=====
Area Percent Report
=====

```

Sorted By      :      Signal
Multiplier    :      1.0000
Dilution      :      1.0000
Use Multiplier & Dilution Factor with ISTDs

```

Signal 1: MWD1 E, Sig=270,16 Ref=360,100

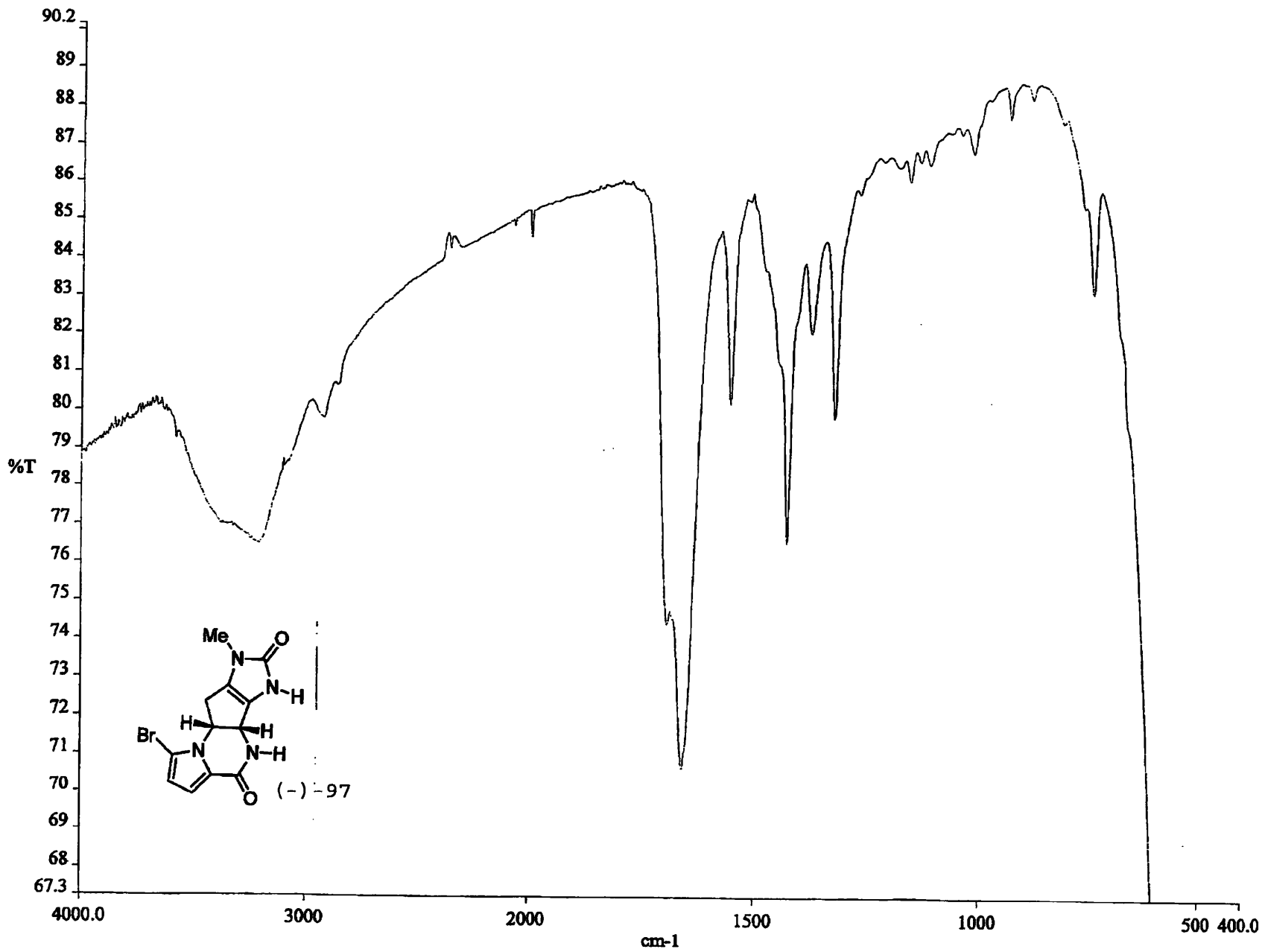
Peak #	RetTime [min]	Type	Width [min]	Area [mAU*s]	Height [mAU]	Area %
1	49.630	MM	7.4872	3200.22583	7.12375	100.0000

Totals : 3200.22583 7.12375

Results obtained with enhanced integrator!

=====
*** End of Report ***

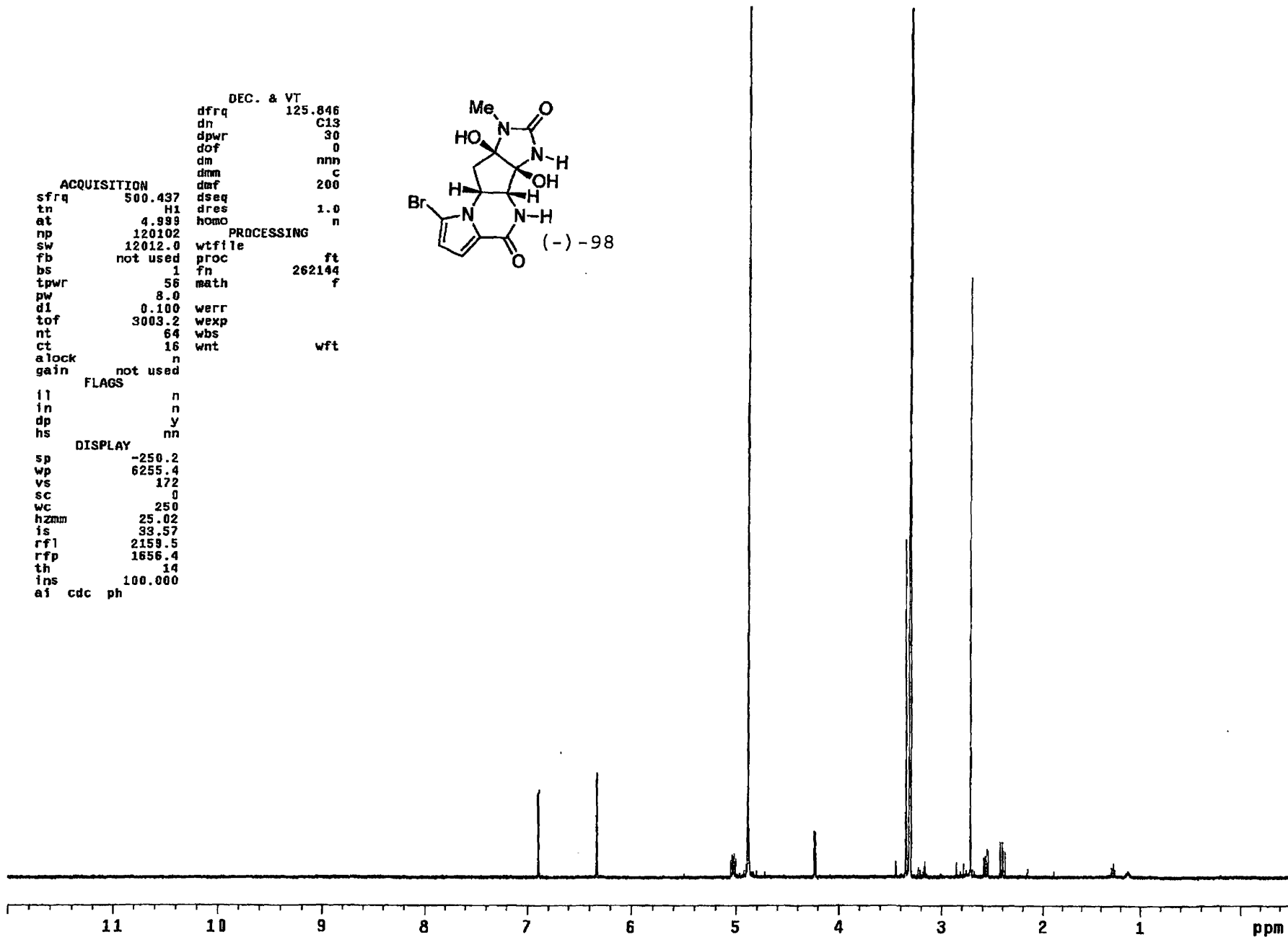
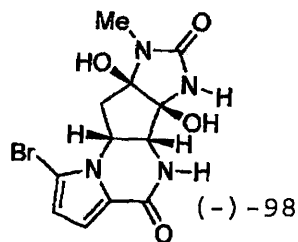
271



```

DEC. & VT
dfrq 125.846
dn C13
dpwr 30
dof 0
dm nnn
dmm C
dmf 200
ACQUISITION
sfrq 500.437
tn H1
at 4.988
np 120102
sw 12012.0
fb not used
bs 1
tpwr 56
pw 8.0
d1 0.100
tof 3003.2
nt 64
ct 16
alock n
gain not used
PROCESSING
wfile
proc ft
fn 262144
math f
werr
wexp
wbs
wnt wft
FLAGS
il n
in n
dp y
hs nn
DISPLAY
sp -250.2
wp 6255.4
vs 172
sc 0
wc 250
hzmm 25.02
is 33.57
rfl 2159.5
rfp 1656.4
th 14
ins 100.000
af cdc ph

```



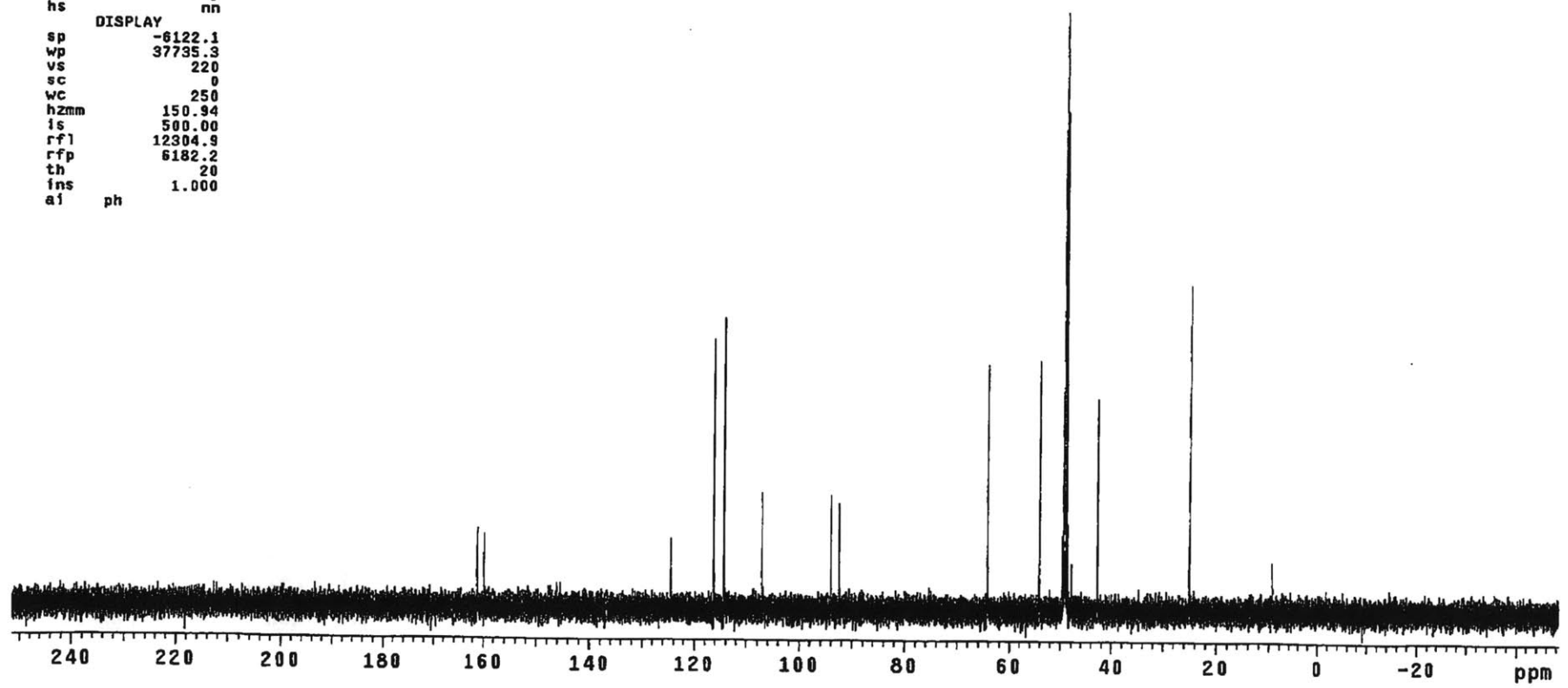
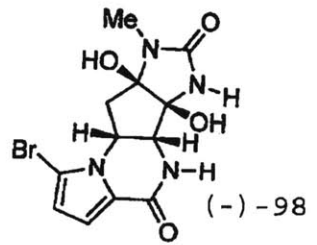
DEC. & VT
 dfrq 500.231
 dn H1
 dpwr 38
 dof -500.0
 dm y
 dmm w
 dmf 10000
 dseq
 dres 1.0
 homo n

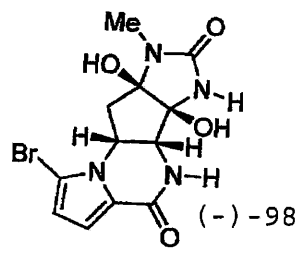
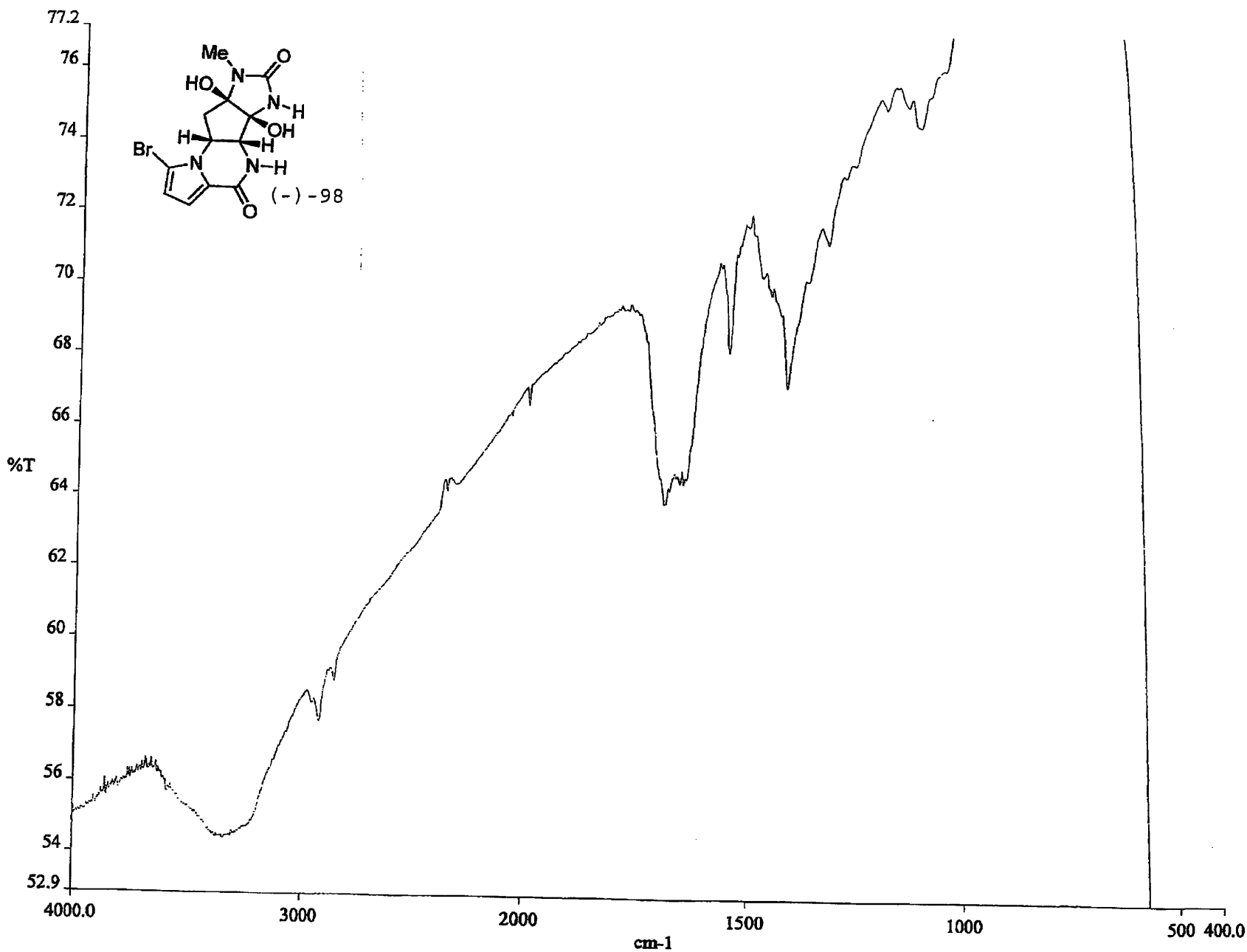
ACQUISITION
 sfrq 125.795
 tn C13
 at 1.736
 np 131010
 sw 37735.8
 fb not used
 bs 4
 ss 1
 tpwr 53
 pw 6.9
 dl 0.763
 tof 631.4
 nt 1e+09
 ct 24
 a lock n
 gain 60

PROCESSING
 lb 0.30
 wtfile
 proc ft
 fn 131072
 math f
 werr
 wexp
 wbs
 wnt

FLAGS
 il n
 in n
 dp y
 hs nn

DISPLAY
 sp -6122.1
 wp 37735.3
 vs 220
 sc 0
 wc 250
 hzmm 150.94
 is 500.00
 rfl 12304.9
 rfp 6182.2
 th 20
 ins 1.000
 al ph





274

```

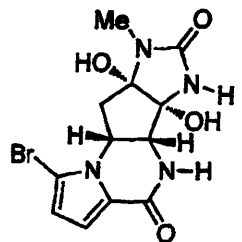
DEC. & VT
dfrq 125.846
dn C13
dpwr 30
dof 0
dm nnn
dmm c
dmf 200
ACQUISITION
sfrq 500.437
tn H1
at 4.989
np 120102
sw 12012.0
fb not used
bs 1
tpwr 58
pw 8.0
d1 0.100
tof 3003.2
nt 64
ct 33
alock n
gain not used
FLAGS
il n
in n
dp y
hs nn
DISPLAY
sp -250.2
wp 6255.4
vs 51
sc 0
wc 250
h2mm 25.02
is 33.57
rfl 2159.2
rfp 1658.4
th 3
ins 100.000
ai cdc ph

```

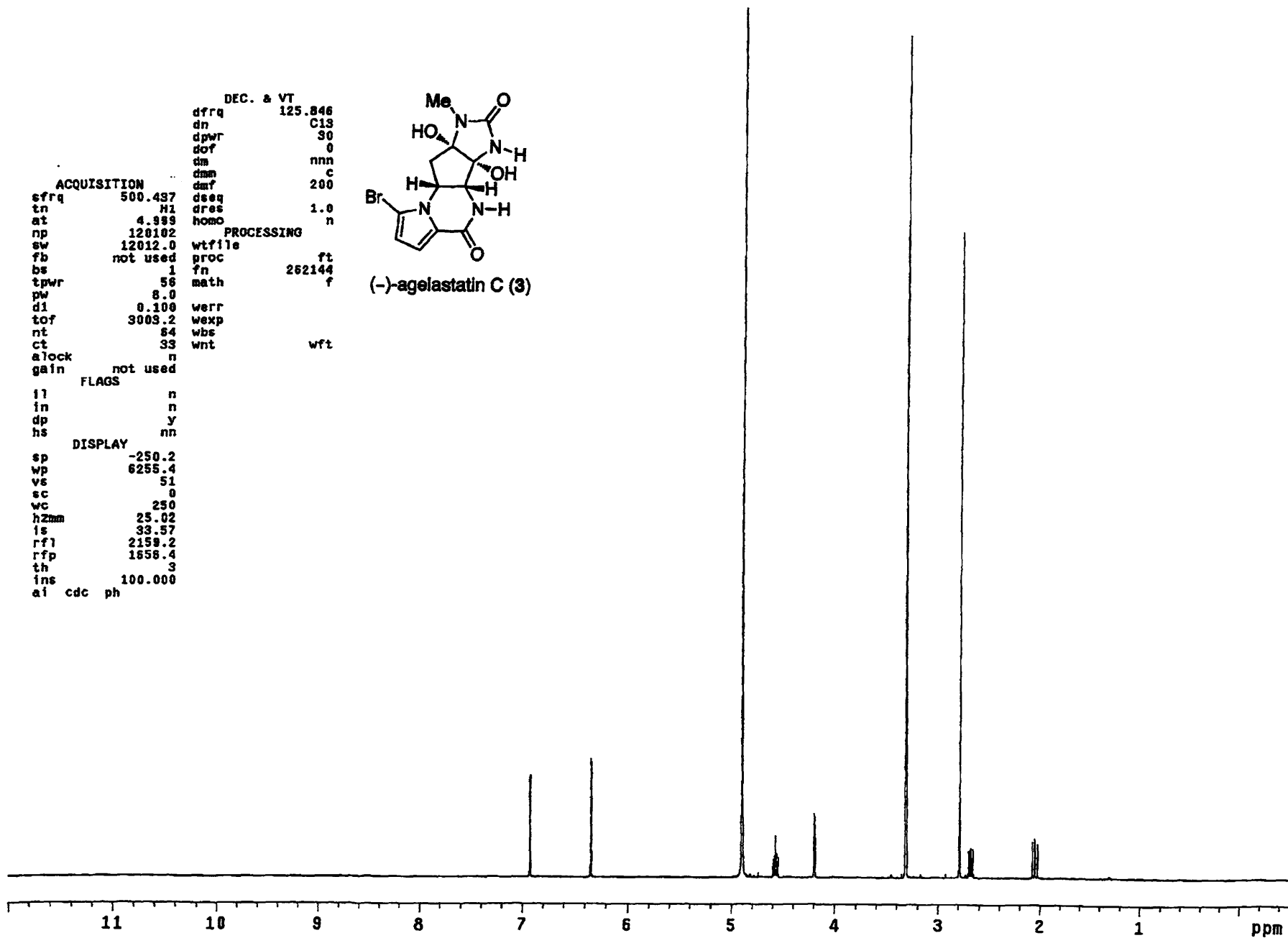
```

dseq dres 1.0
homo n
PROCESSING
wtfile
proc ft
fn 262144
math f
werr
wexp
wbs
wnt wft

```



(-)-agelastatin C (3)



```

ACQUISITION
sfrq 125.795
tn C13
at 1.736
np 131010
sw 37735.8
fb not used
bs 4
ss 1
tpwr 53
pw 6.9
dl 0.763
tof 631.4
nt 1e+08
ct 20820
alock n
gain 60

FLAGS
il n
in n
dp y
hs nn

DISPLAY
sp -6116.4
wp 37735.3
vs 5122
sc 0
wc 250
hzm 150.94
is 500.00
rf1 12299.2
rfp 6182.2
th 7
ins 1.000
al ph

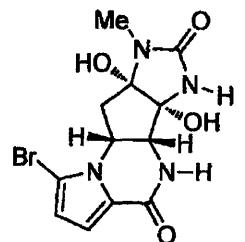
```

```

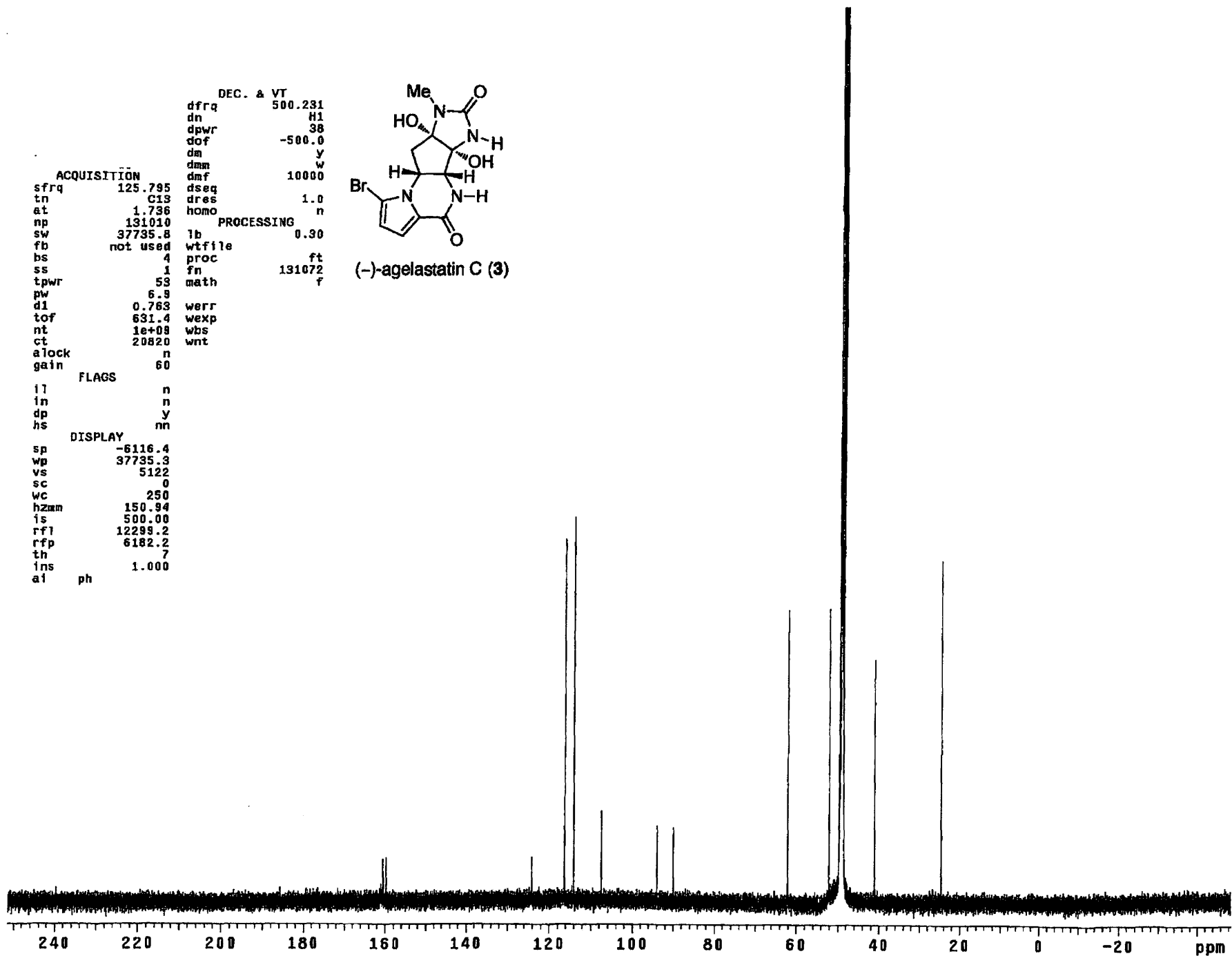
DEC. & VT
dffq 500.231
dn H1
dpwr 38
dof -500.0
dm y
dmm w
dmf 10000
dseq
dres 1.0
homo n

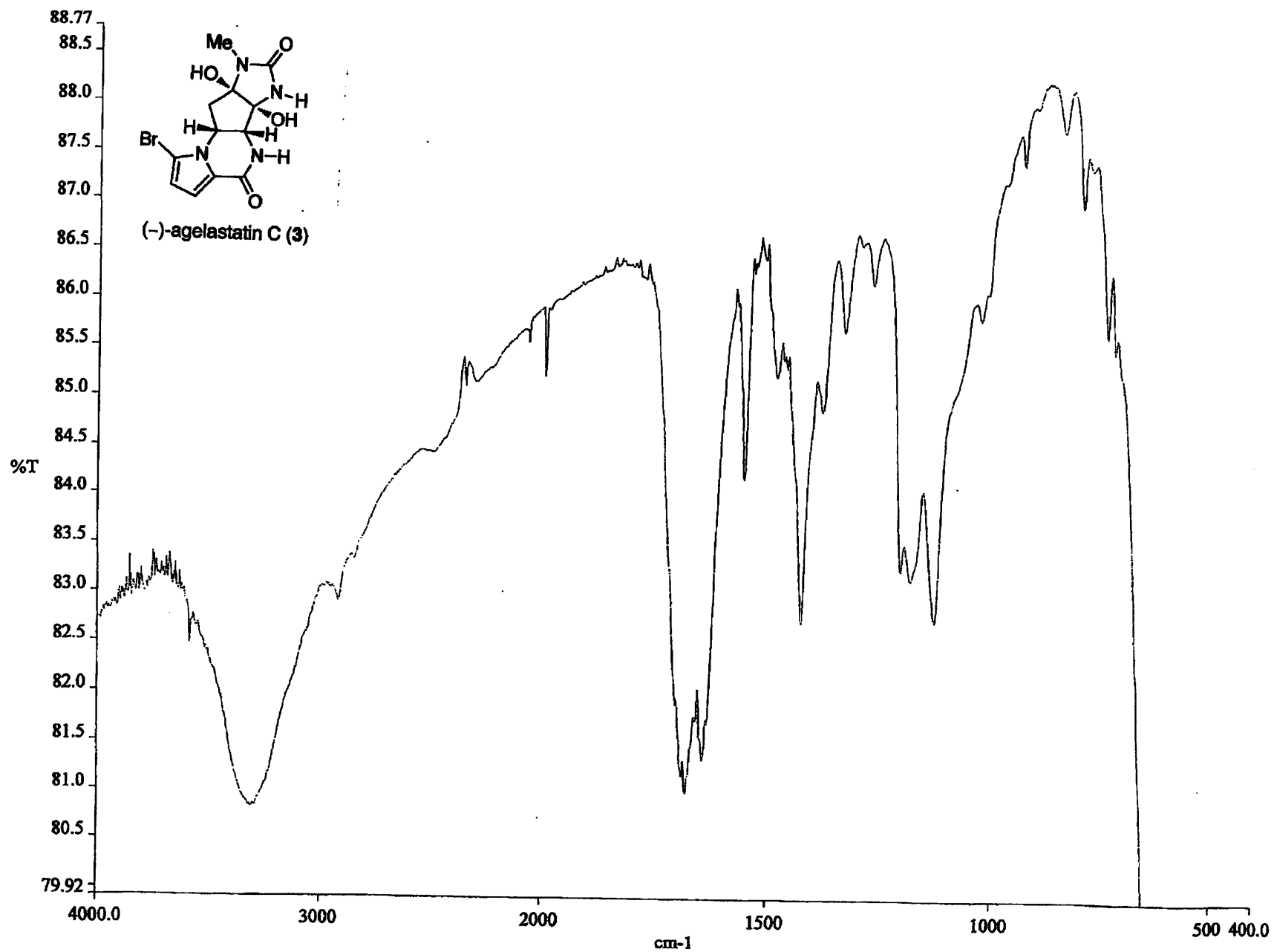
PROCESSING
lb 0.30
wtfile
proc ft
fn 131072
math f
werr
wexp
wbs
wnt

```



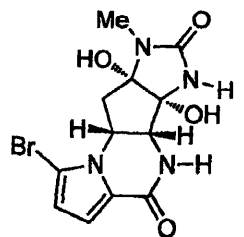
(-)-agelastatin C (3)



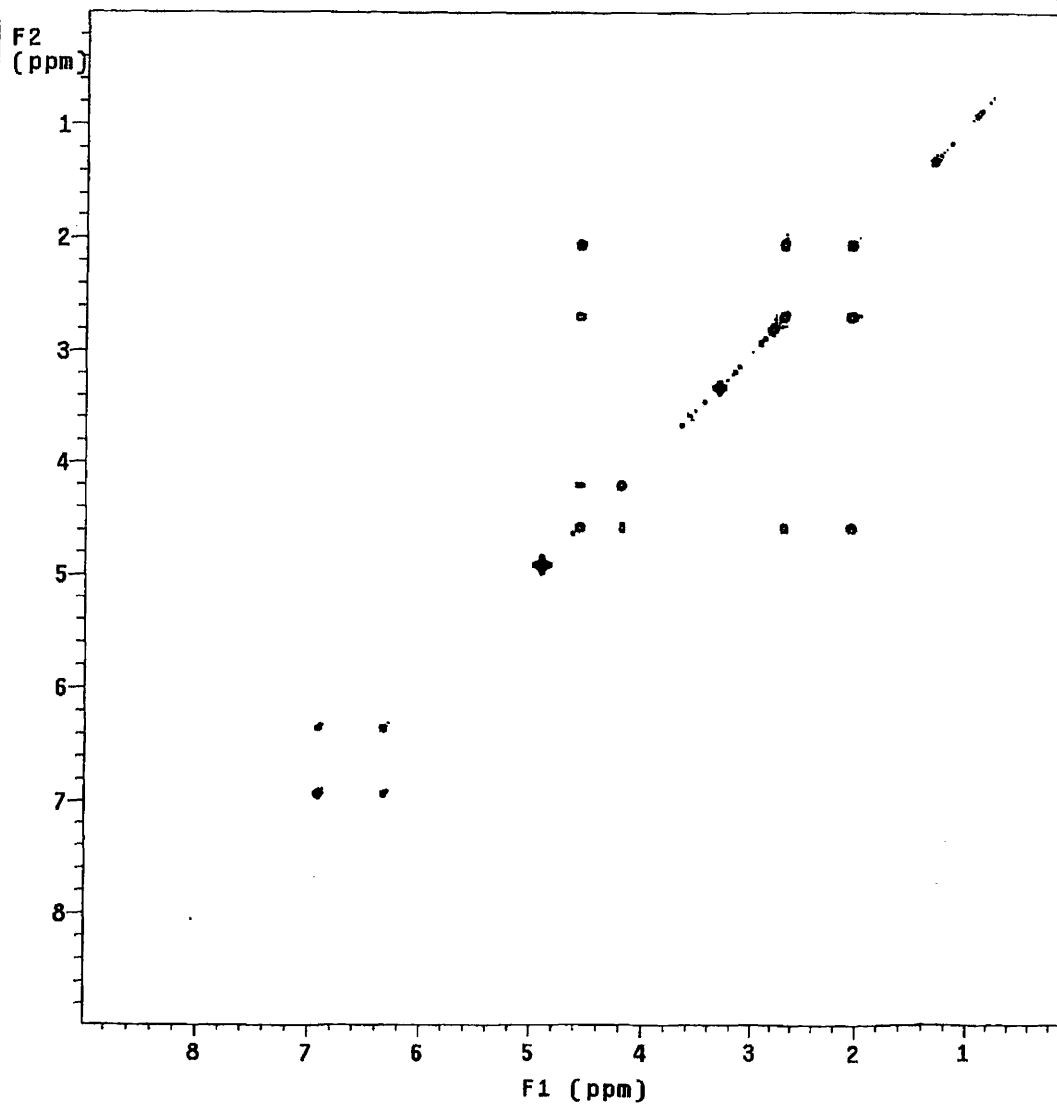


exp3 gCOSY

	hs	nn
solvent	CD3OD	n
sample	undefined	hsglv1
ACQUISITION		SPECIAL
sw	4490.3	temp not used
at	0.228	gain 58
np	2048	spin 0
fb	not used	F2 PROCESSING
ss	16	sb -0.114
d1	1.000	sbs not used
nt	23	fn 2048
2D ACQUISITION	F1 PROCESSING	
sw1	4490.3	sb1 -0.057
n1	128	sbs1 not used
TRANSMITTER	proc1	lp
tn	H1	fn1 2048
sfrq	499.746	DISPLAY
tof	-252.5	sp 4.6
tpwr	56	wp 4486.0
pw	9.200	sp1 0.6
GRADIENTS	wp1 4486.0	
gzlv11	2000	rfl -0.2
gt1	0.001000	rfp 0
gstab	0.000500	rfl1 3.8
DECOUPLER	rfp1	0
dn	C13	PLOT
dm	nnn	wc 138.9
		sc 0
		wc2 138.9
		sc2 0
		vs 322
		th 2
	al cdc av	

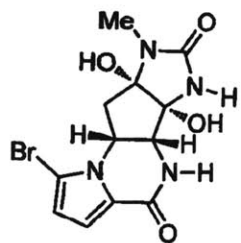


(-)-agelastatin C (3)

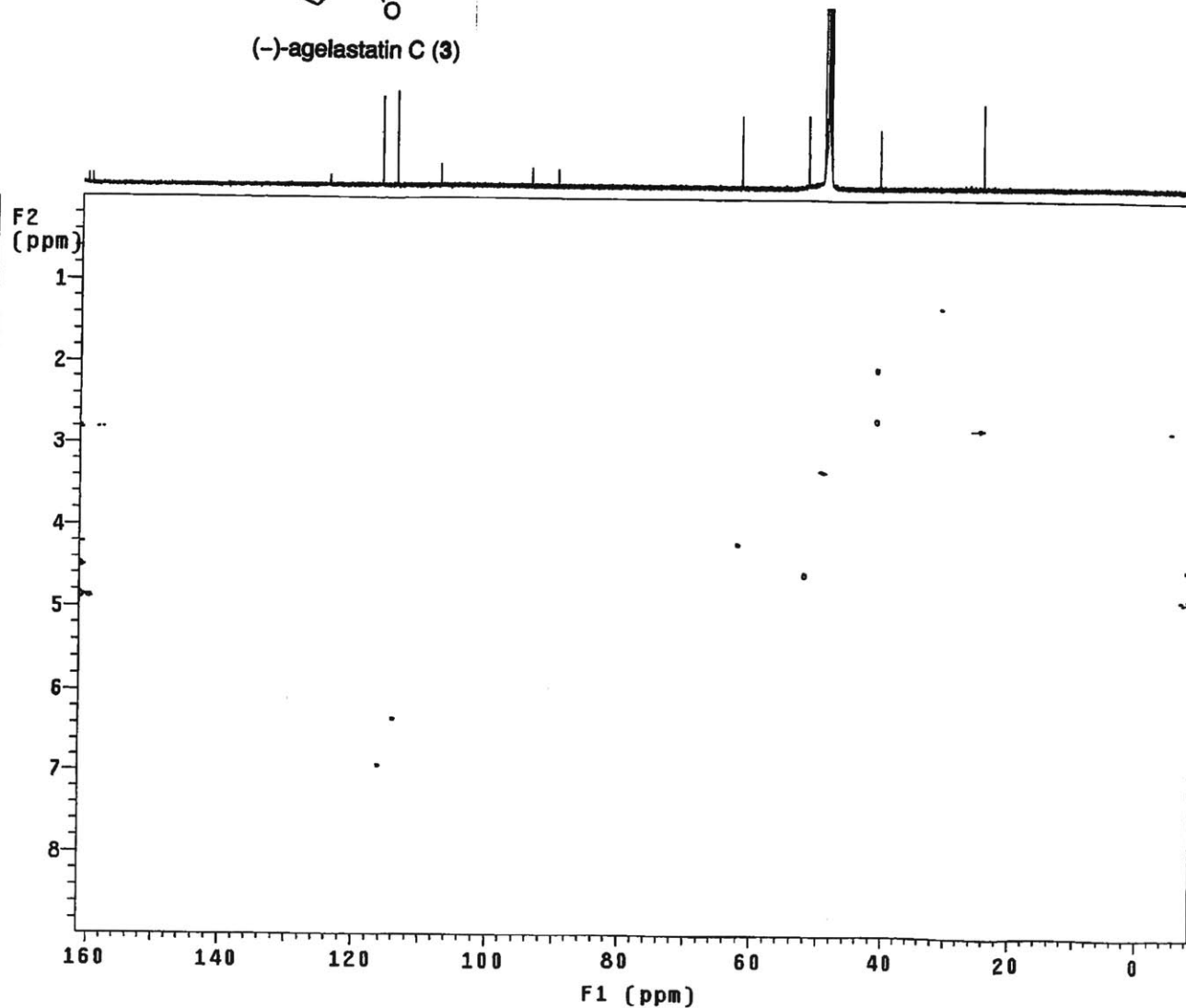


exp4 HSQC

solvent	CD300	hs	n	ACQUISITION	ARRAYS	phase
sample	undefined	sspul	n	array	arraydim	512
ACQUISITION		PFgflg	y			
sw	4490.3	hsglv1	2000	1	phase	1
at	0.150	SPECIAL		1		2
np	1348	temp	not used	2		
fb	not used	gain	52			
ss	256	spin	0			
d1	1.000	PRESATURATION				
nt	37	satmode	n			
2D ACQUISITION		satpwr	0			
sw1	21361.8	satdly	0			
n1	256	satfrq	0			
phase	arrayed	F2 PROCESSING				
TRANSMITTER		gf	0.105			
tn	H1	gfs	not used			
sfrq	499.746	fn	2048			
tof	-252.5	F1 PROCESSING				
tpwr	56	sb1	-0.024			
pw	9.200	sbs1	-0.024			
DECOUPLER		proci	1p			
dn	C13	fn1	2048			
dof	-2514.8	DISPLAY				
dm	nny	sp	5.1			
dmm	ccg	wp	4486.0			
dmf	32200	sp1	-1064.1			
dpwr	53	wp1	21341.0			
pwlv1	59	rfl	3167.7			
pw	18.000	rfp	3168.4			
HSQC		rfl1	15417.0			
j1xh	140.0	rfp1	14332.1			
null	0.350	PLOT				
nullflg	n	wc	170.0			
mult	2	sc	0			
		wc2	110.0			
		sc2	0			
		vs	322			
		th	2			
		ai	cdc pn			

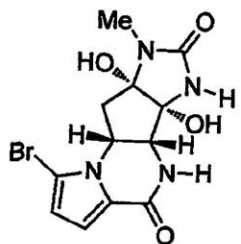


(-)-agelastatin C (3)

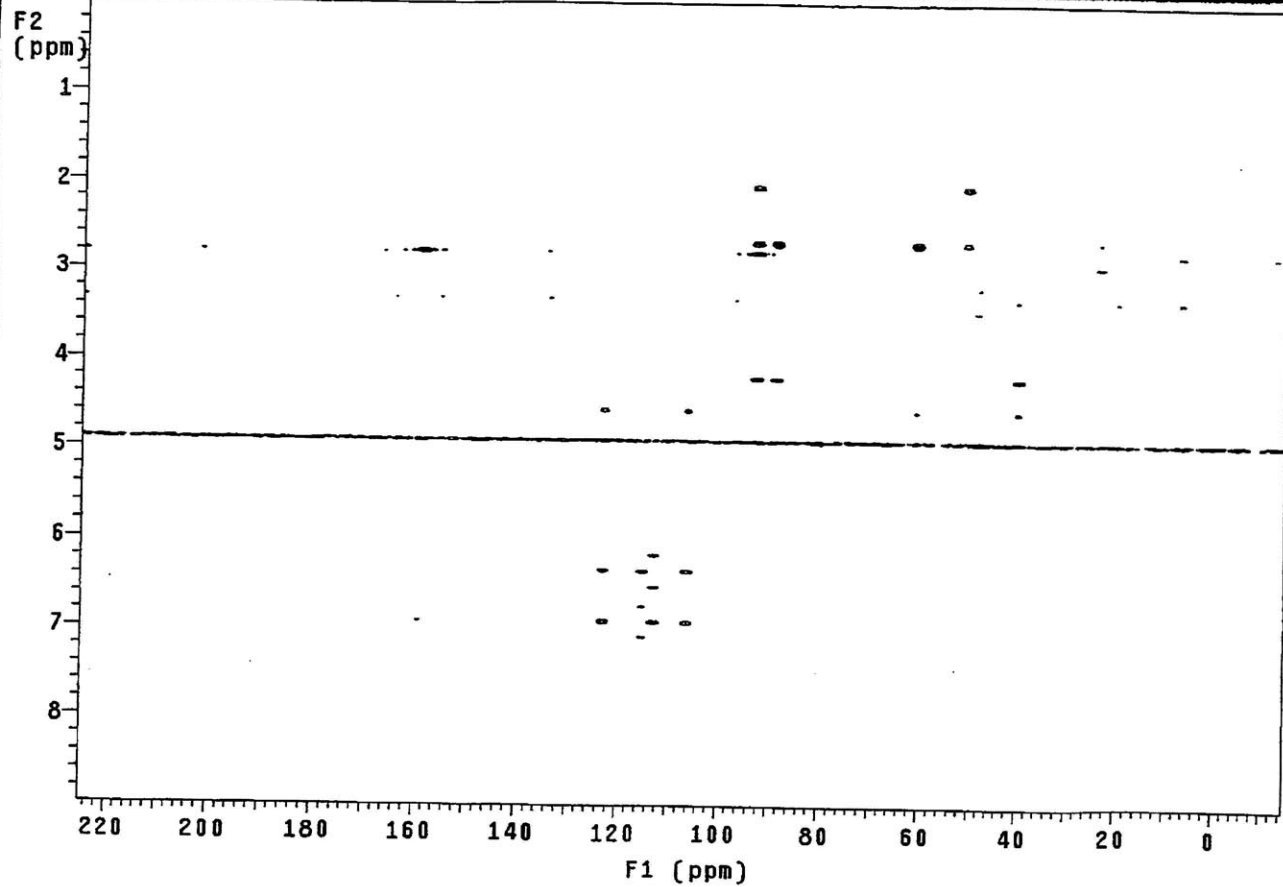


exp5 HMBC

		FLAGS	ACQUISITION ARRAYS
solvent	CD3OD	hs	n
sample	undefined	sspul	n
ACQUISITION		PFGflg	n
sw	4480.3	hsglv1	2000
at	0.228	SPECIAL	1
np	2048	temp	not used
fb	not used	gain	52
ss	32	spin	0
d1	1.000	PRESATURATION	
nt	40	satmode	n
2D ACQUISITION		satpwr	0
sw1	30154.5	satdly	0
ni	256	satfrq	0
phase	arrayed	F2 PROCESSING	
TRANSMITTER		sb	0.114
tn	H1	sbs	not used
sfrq	499.746	fn	2048
tof	-252.5	F1 PROCESSING	
tpwr	56	sbi	0.004
pw	9.200	sbs1	not used
DECOUPLER		fn1	2048
dn	C13	sp	4.6
dof	1255.1	wp	4486.0
dm		nnn	-1853.5
dmm	ccc	wp1	30125.1
dmf	32200	rf1	-0.2
dpwr	53	rfp	0
pwxlv1	59	rf11	1882.9
pwx	18.000	rfp1	0
HMBC			
j1xh	140.0	PLOT	
jnxh	8.0	wc	170.0
		sc	0
		wc2	110.0
		sc2	0
		vs	322
		th	2
		ai	cdc av



(-)-agelastatin C (3)



```

DEC. & VT      125.846
dfrq           C13
dn             30
dpwr           0
dof           nnn
da            c
dmm           200
daf           1.0
dseq          n
dres          homo
dwt           262144
dwt           f

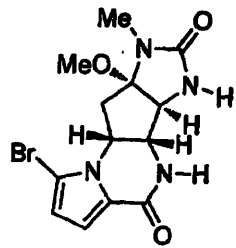
ACQUISITION
sfrq          500.437
tn            H1
at            4.889
np            120102
sw            12012.0
fb            not used
bs            1
tpwr         56
pw            8.0
d1            0.100
tof          3003.2
nt            18
ct            16
atlock       n
gain         not used

PROCESSING
wtfile
proc         ft
fn           262144
math         f
werr
wexp
wbs
wnt          wft

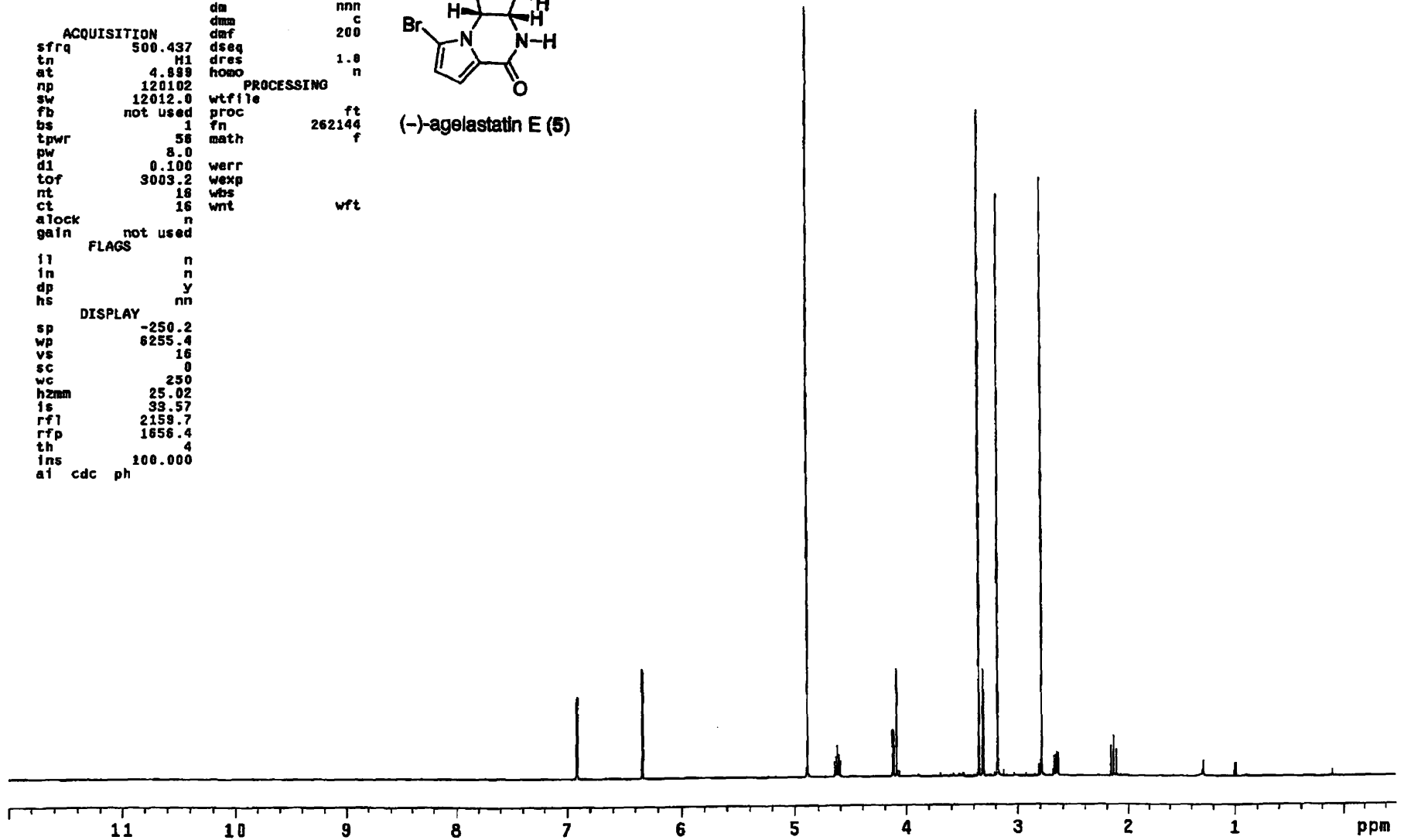
FLAGS
il           n
in           n
dp           y
hs           nn

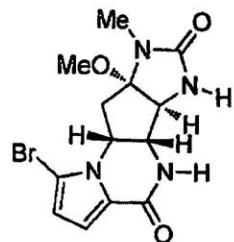
DISPLAY
sp           -250.2
wp           6255.4
vs           16
sc           0
wc           250
h2mm        25.02
is           39.57
rf1          2159.7
rfp          1656.4
th           4
ins          100.000
al          cdc ph

```



(-)-agelastatin E (5)





(-)-agelastatin E (5)

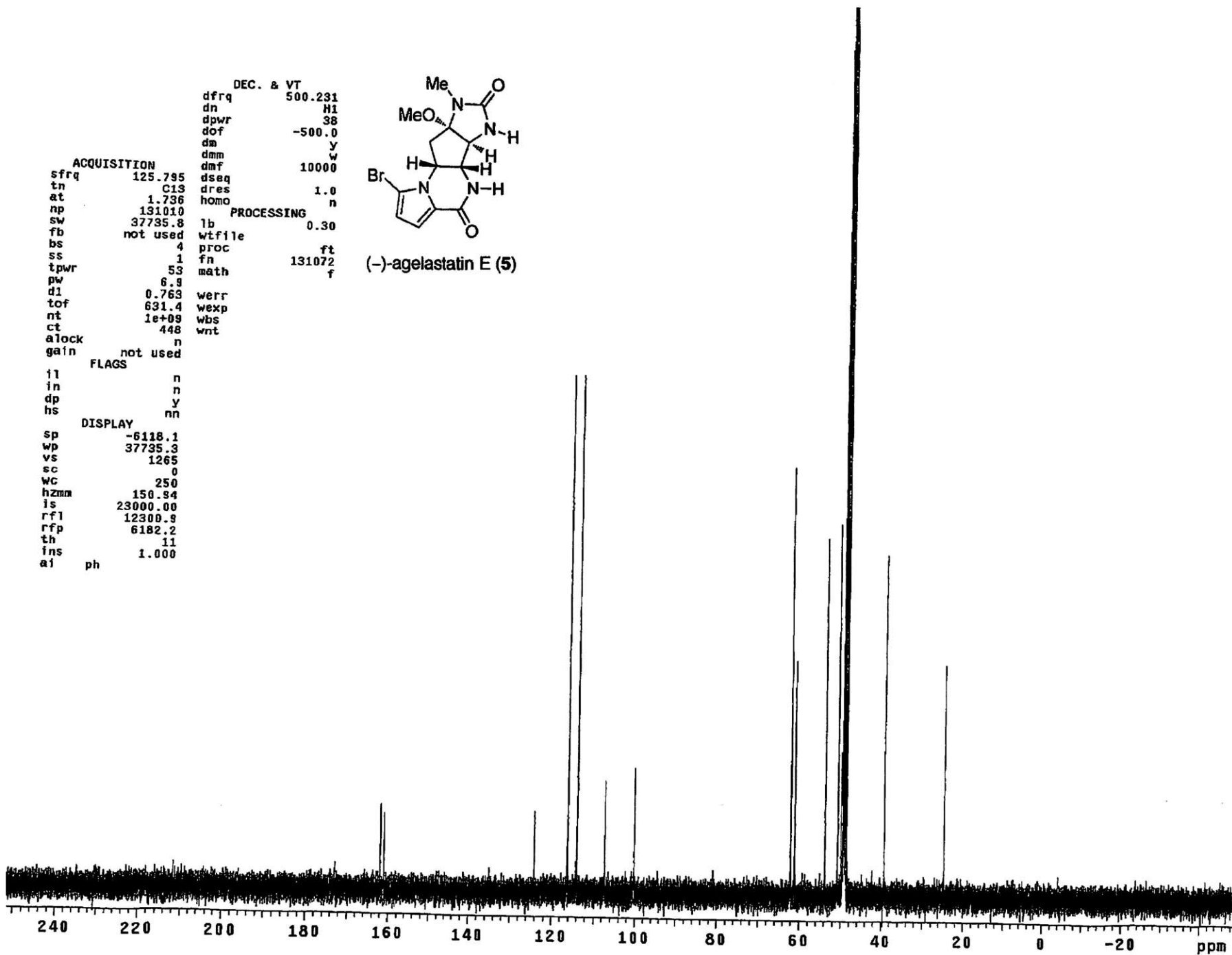
```

DEC. & VT
dfrq      500.231
dn        H1
dpwr      38
dof       -500.0
dm        y
dmm       w
dmf       10000
dseq      1.0
dres      1.0
homo      n
PROCESSING
lb        0.30
wtfile
proc     ft
fn       131072
math     f

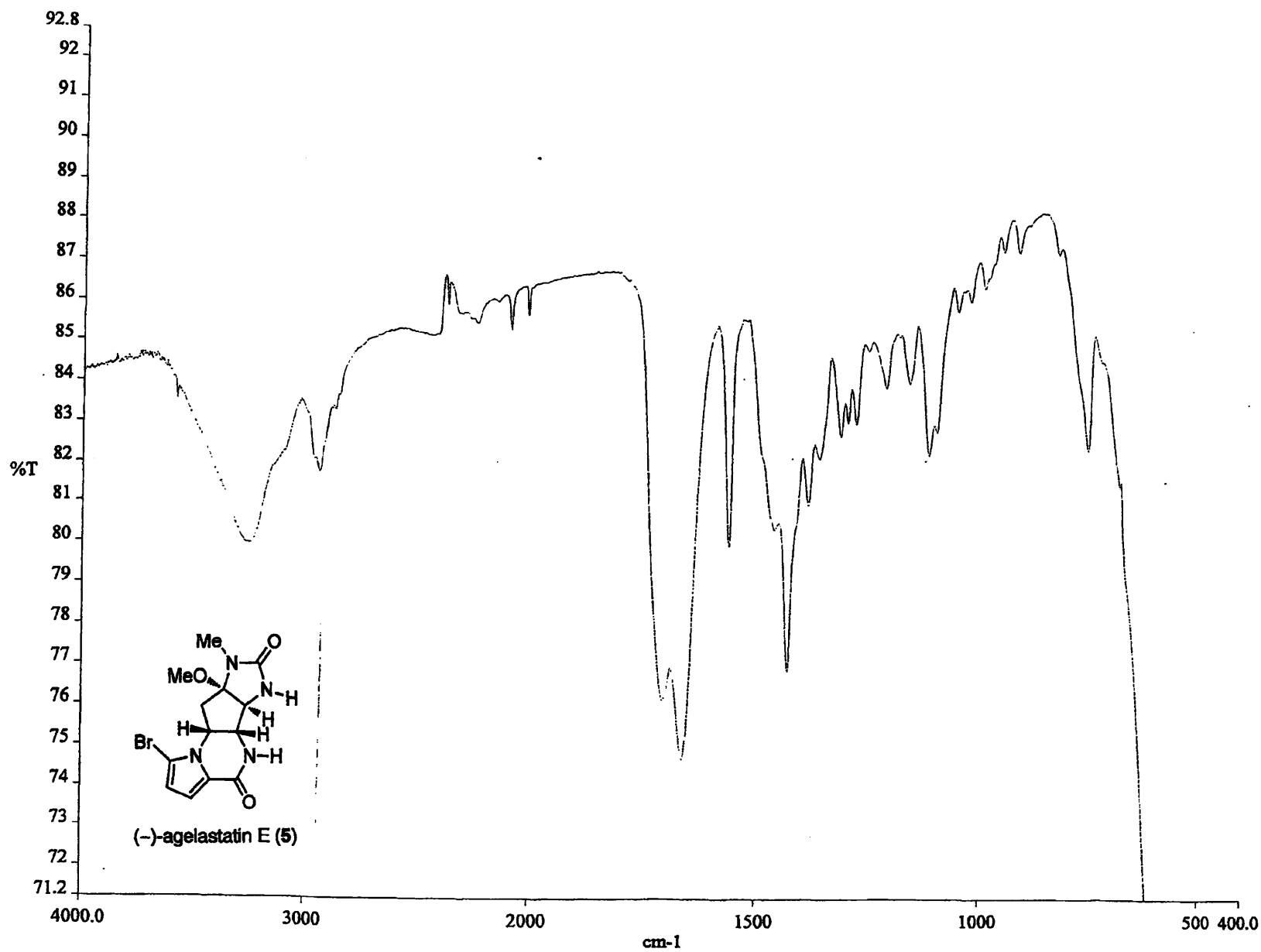
ACQUISITION
sfrq     125.795
tn       C13
at       1.736
np       131010
sw       37735.8
fb       not used
bs       4
ss       1
tpwr     53
pw       6.9
d1       0.763
tof      631.4
nt       1e+09
ct       448
alock    n
gain     not used

FLAGS
il       n
in       n
dp       y
hs       nn

DISPLAY
sp       -6118.1
wp       37735.3
vs       1265
sc       0
wc       250
hzmm    150.94
is       23000.00
rfl     12300.9
rfp     6182.2
th       11
fns     1.000
ai      ph
  
```



283



Dustin S. Siegel

Massachusetts Institute of Technology, Department of Chemistry
77 Massachusetts Avenue, 18-243, Cambridge, MA 02139
Lab: (617) 324-0394, dsiegel@mit.edu

PERSONAL: Born December 16, 1980.

EDUCATION:

2004-Present **Massachusetts Institute of Technology**, Cambridge, MA
Ph.D. candidate, Organic Chemistry
Cumulative Graduate GPA: 4.9 / 5.0
Advisor: Associate Professor Mohammad Movassaghi

1999-2003 **University of California, San Diego**, San Diego, CA
Degree: B.S. Chemistry, *Cum Laude* / Departmental Honors with High Distinction
Major GPA: 3.77/4.00 *Cumulative GPA: 3.61/4.00*
Advisor: Professor Clifford P. Kubiak

PROFESSIONAL EXPERIENCE:

2004-Present **Massachusetts Institute of Technology**, Cambridge, MA
Department of Chemistry, *Advisor:* Associate Professor Mohammad Movassaghi
Graduate Research Assistant

- The total synthesis of the (–)-agelastatin alkaloids.
- The enantioselective total synthesis of (–)-acylfulvene and (–)-irofulven.

2003-2004 **ChemBridge Research Laboratories**, Rancho Bernardo, CA
Research Associate

- Development of small molecules for medicinal chemistry.

2002-2003 **University of California, San Diego**, San Diego, CA
Department of Chemistry, *Advisor:* Professor Clifford P. Kubiak
Undergraduate Research Assistant

- Development of charge transfer complexes for application in molecular electronics.

HONORS AND ACTIVITIES:

2009 Award for Outstanding Teaching at MIT.
2009 Guest lecturer for two lectures of an advanced organic chemistry class at MIT.
2006 Sigma-Aldrich Graduate Student Innovation Award.
2006 Gordon Research Conference Travel Grant.
2006 *SYNLETT* Star Journal Award, for academic excellence.
2006 Guest lecturer for one lecture of a graduate synthetic organic chemistry class at MIT.
2003 President of the American Chemical Society Student Affiliates at UCSD.
2002 California Institute for Telecommunications and Information Technology Fellowship.
2002 American Chemical Society Student Affiliates Undergraduate Summer Research Fellowship.

PUBLICATIONS:

- Movassaghi, M.; Siegel, D. S.; Sunkyu, H. "Total Synthesis of All (-)-Agelastatin Alkaloids." **2010**, *Manuscript in Preparation*.
- Siegel, D. S.; Piizzi, G.; Piersanti, G.; Movassaghi, M. "Enantioselective Total Synthesis of (-)-Acylfulvene and (-)-Irofulven." *J. Org. Chem.* **2009**, *74*, 9292-9304.
- Movassaghi, M.; Piizzi, G.; Siegel, D. S.; Piersanti, G. "Observations in the Synthesis of the Core of the Antitumor Illudins via an Enyne Ring Closing Metathesis Cascade." *Tetrahedron Lett.* **2009**, *50*, 5489-5492.
- Movassaghi, M.; Piizzi, G.; Siegel, D. S.; Piersanti, G. "Enantioselective Total Synthesis of (-)-Acylfulvene and (-)-Irofulven." *Angew. Chem. Int. Ed.* **2006**, *45*, 5859-5863.
- Stires, J. C.; Kasibhatla, B. S.; Siegel, D.; Kwong, J. C.; Caballero, J. B.; Labonte, A. P.; Reifenberger, R. G.; Datta, S.; Kubiak, C. P. "Conducting molecular nanostructures assembled from charge-transfer complexes grafted onto silicon surfaces." *Proc. SPIE Int. Soc. Opt. Eng.* **2003**, *5223*, 85-90.

PRESENTATIONS:

- "Enantioselective Total Synthesis of (-)-Acylfulvene and (-)-Irofulven." MIT Graduate Student Research Symposium (Boston, MA, May 2008)
- "Enantioselective Total Synthesis of (-)-Acylfulvene and (-)-Irofulven." ACS National Meeting Boston (Boston, MA, August 2007)
- "Enantioselective Total Synthesis of (-)-Acylfulvene and (-)-Irofulven." Aldrich Graduate Student Innovation Award Symposium (Milwaukee, WI, August 2006)
- "Enantioselective Total Synthesis of (-)-Acylfulvene and (-)-Irofulven." Gordon Research Conference; Stereochemistry (Newport, RI, June 2006)

TEACHING EXPERIENCE:

- | | |
|------|--|
| 2008 | One semester of teaching assistantship as head TA for an advanced organic chemistry class at MIT (Professors M. Movassaghi, and S. L. Buchwald). |
| 2007 | One semester of teaching assistantship for an advanced organic chemistry class at MIT (Professors M. Movassaghi, and S. L. Buchwald). |
| 2005 | One semester of teaching assistantship for an advanced synthetic organic chemistry graduate level class at MIT (Professor M. Movassaghi). |
| 2005 | One semester of teaching assistantship as head TA for an organic chemistry graduate class at MIT (Professor S. O'Connor, and Dr. K. Berkowski). |
| 2004 | One semester of teaching assistantship for a laboratory chemistry class at MIT (Dr. J. Schrenk). |

REFERENCES:

Mohammad Movassaghi, Ph.D.

Associate Professor of Chemistry
Massachusetts Institute of Technology
Department of Chemistry
77 Massachusetts Avenue, 18-292
Cambridge, MA 02139
(617) 253-3986
movassag@mit.edu

Rick L. Danheiser, Ph.D.

Arthur C. Cope Professor of Chemistry
Massachusetts Institute of Technology
Department of Chemistry
77 Massachusetts Avenue, 18-298
Cambridge, MA 02139
(617) 253-1842
danheiser@mit.edu

Clifford P. Kubiak, Ph.D.

Harold C. Urey Professor of Chemistry
University of California, San Diego
Department of Chemistry and
Biochemistry
La Jolla, CA 92093-0358
(858) 822-2665
ckubiak@ucsd.edu